

**SYNTHETIC STUDIES IN THE SELECTIVE
FUNCTIONALIZATION OF UNSATURATED COMPOUNDS:
FROM INITIAL APPLICATIONS IN MEDICINAL CHEMISTRY TO
GENERAL APPLICATIONS IN UNACTIVATED SYSTEMS**

by

LIELA ANTOINETTE BAYEH

DISSERTATION

Presented to the Faculty of the Graduate School of Biomedical Sciences

The University of Texas Southwestern Medical Center

In Partial Fulfillment of the Requirements

For the Degree of

DOCTOR OF PHILOSOPHY

The University of Texas Southwestern Medical Center

Dallas, Texas

December 2016

To my father, Albert Bayeh

ACKNOWLEDGEMENTS

I would like to acknowledge all of the people who have made the last five years of my life that much more rewarding and enjoyable. While the list may be too extensive to write out in detail, I have been fortunate to have colleagues, professors, friends, and family lend their support to me throughout this process. To all of these people I am eternally grateful.

First, I'd like to extend my gratitude to all of my committee members: Professors Joseph Ready, Jef DeBrabander and Cho Chen. I have benefitted greatly throughout the years from all of our scientific discussions and I thank them for allowing me to drop by their offices on random occasions with questions. Their guidance and continued support throughout my time at UT Southwestern will always be remembered.

I would also like to thank all of my fellow lab members throughout the years. Not only did they make the day-to-day lab work more meaningful and engaging, but also their attendance to all of my practice talks, presentations, and paper editing sessions was always greatly appreciated. In particular I'd like to thank Dr. Hongli Bao, Dr. Phong Le, Aaron Nash, Chris Sleet and my good friend Melissa Moss. Working alongside Hongli was beneficial to my training in so many ways during my first two years in the lab, and for that I am grateful to her. Phong was a wonderful colleague to work alongside in the lab on my last research project and was instrumental in helping me get this work to the finish line. Aaron, Chris and Melissa have not only been wonderful colleagues to work with these last five years, but also great friends and confidants. I wish them all the best in their future careers and will miss our lunches.

To my family members who have been nothing but supportive throughout this time: my mother Mary Bayeh, my siblings Alex, William, Madeleine and Samuel, my grandparents, fondly referred to as Mamaw and Papaw, and my extended family. For several years now they have allowed me to sacrifice my time with them in order to fully pursue my career. I'd like to particularly thank my mother who knows no limits when it comes to sacrificing for her children. She has been one of my biggest cheerleaders and has always encouraged me to pursue my dreams. I am grateful to my oldest brother, Alex, for always setting the bar high and then commending me when I somehow manage to raise it higher. This continued friendly competition and mutual support for one another has sustained my intellectual drive at times when nothing else did.

Likewise, I thank Derich Romero for being such a supportive and understanding boyfriend these last five years and being sympathetic of the perpetual student. From his uncanny ability to keep me calm and collected when preparing for stressful presentations, to his unrelenting encouragement as I followed my dreams, Derich has been a constant source of light in my life. I will always appreciate the sacrifices he has made for me.

Last, but certainly not least, I would like to thank my advisor, Uttam Tambar, who has been nothing short of an ideal mentor these last five years. His never-ending enthusiasm for all things chemistry has not only galvanized my own love for this field, but also taught me that chemistry can be both a profession and hobby. Throughout the years I have also grown more confident in my ability to develop new ideas; this self-assurance is a direct result of Uttam's openness to letting his students explore interesting novel ideas in the lab. His phrase "I'll never tell you not to run a reaction" has been truly prolific in this respect.

During the five years that I have worked with Uttam, he has been nothing short of kind and generous to his students. I appreciate the innumerable hours of time he's taken to personally assist me with the countless presentations and projects I've undertaken. Through these interactions I have learned so much and grown to admire him as both a mentor and friend. I consider myself truly fortunate to have been afforded the opportunity to conduct my graduate studies in Uttam's lab as one of his first graduate students and look forward to seeing the many great things his lab will do in the future.

**SYNTHETIC STUDIES IN THE SELECTIVE FUNCTIONALIZATION OF
UNSATURATED COMPOUNDS: FROM INITIAL APPLICATIONS IN
MEDICINAL CHEMISTRY TO GENERAL APPLICATIONS IN
UNACTIVATED SYSTEMS**

Liela Antoinette Bayeh Ph.D.

The University of Texas Southwestern Medical Center, 2016

Uttam Krishan Tambar, Ph.D.

Medicinal chemistry and reaction development have influenced one another in the field of organic chemistry. The synthesis of therapeutic small molecules often requires the use of practical synthetic methodologies, while reaction development is frequently inspired by the demands of medicinal chemistry.

First the development of small molecule inhibitors of hypoxia inducible factors, which are heterodimeric transcription factors that have been implicated in a number of cancer environments, will be discussed. Two scaffolds have been designed and evaluated for their ability to selectively bind within the binding domain of the hypoxia inducible factor-2 α isoform and inhibit heterodimerization, with the most potent agonist exhibiting a half maximal inhibitory concentration value of 23 nanomolar. Inspired by the stereospecific mode of action exhibited by the diaryl-tetrazolo-tetrahydropyrimidine-based scaffold of hypoxia inducible factor-2 antagonists, a potential co-catalyst system for the asymmetric synthesis of these derivatives has been identified, utilizing a synergistic combination of a cinchona alkaloid-based primary amine and acid catalysts. While the enantioselectivity of this reaction as it currently stands remains modest, these products can be isolated in up to 96:4 enantiomeric ratio through recrystallization efforts.

Secondly, the development of a series of general and efficient methods for the synthesis of functionalized olefin products from simple unsaturated systems will be described. Unfunctionalized olefins and dienes are ideal substrates for chemical synthesis due to their low cost and ease of availability. However they present a variety of challenges when attempting to selectively differentiate between sterically and electronically similar carbon-hydrogen bonds. The processes described herein exploit the ability of sulfurimide and sulfurdiimide reagents to undergo hetero-ene reactions with terminal and internal olefins as well as [4+2] couplings with dienes. These reactions result in reactive intermediates that are utilized in a host of chemical transformations, including [2,3]-rearrangements to generate allylic amines and alcohols, Grignard coupling to generate linear and branched alkylated products, and aminoarylation chemistry. Most notably, a regio- diastereo- and enantioselective synthesis of multifunctional allylic sulfinimides from internal olefins is discussed.

TABLE OF CONTENTS

Dedication	ii
Acknowledgements	iii
Abstract	v
Table of Contents	vii
List of Figures	xii
List of Schemes	xxii
List of Tables	xxiv
List of Abbreviations	xxvi

CHAPTER ONE: The Development of Allosteric Inhibitors of HIF-2 α 1

1.1 Background	1
1.1.1 Introduction.....	1
1.1.2 The HIF Family of Transcription Factors	2
1.2 Synthesis and Evaluation of Scaffold I Small Molecule Inhibitors	3
1.2.1 Initial Screening for HIF-2 α Inhibition	3
1.2.2 Library Synthesis of Scaffold I Analogues	4
1.2.3 Analysis of Inhibitory Activity of Scaffold I Analogues.....	8
1.2.4 Conclusions	16
1.3 Progress Toward a Stereoselective Synthesis of Scaffold II Small Molecule Disruptors of HIF-2 α	16
1.3.1 Identification of Scaffold II Allosteric Inhibitors of HIF-2 α ...	16
1.3.2 Strategy for the Enantioselective Synthesis of Scaffold II Analogues	18
1.3.3 Progress Toward an Asymmetric Tandem Aza-Michael	

Addition/Cyclocondensation	20
1.3.4 Conclusions	23
1.4 Experimental	23
1.4.1 Methods and Materials	23
1.4.2 Preparative Procedures	24
1.5 References	61
APPENDIX ONE: Spectra Relevant to Chapter One	66
APPENDIX TWO: HPLC Traces Relevant to Chapter One	84
CHAPTER TWO: An Allylic Alkylation of Unsaturated Terminal Olefins with Grignard Reagents	86
2.1 Background	86
2.1.1 Introduction.....	86
2.1.2 Stabilized Carbon Nucleophiles for the Selective Allylic Alkylation of Terminal Olefins	87
2.1.3 Allylic C–H Alkylation of Unactivated Olefins with Trifluoromethane Donors	91
2.1.4 Conclusions	93
2.2 Development and Scope of an Allylic Alkylation of Unactivated Olefins with Grignard Reagents	94
2.2.1 Choice of Oxidant and Optimization	94
2.2.2 Grignard and Olefin Scope of the Allylic Alkylation	97

2.2.3 Application of This Strategy Toward the Synthesis of Polyenes	99
2.2.4 Mechanistic Studies	101
2.2.5 Conclusions	104
2.3 Experimental Section	105
2.3.1 Materials and Methods	105
2.3.2 Preparative Procedures	105
2.4 References	124
APPENDIX THREE: Spectra Relevant to Chapter Two	128
CHAPTER THREE: The Development of a Regio- and Diastereoselective Aminoarylation of Simple Dienes	157
3.1 Background	157
3.1.1 Introduction.....	157
3.1.2 Catalytic Telomerization of Dienes with Amines.....	158
3.1.3 Heck's Palladium-Catalyzed Aminoarylation of Dienes.....	159
3.1.4 Palladium-Catalyzed Heteroannulation to Vinyl Heterocycles	160
3.1.5 Conclusions	161
3.2 The Development of a Regio- and Diastereoselective Aminoarylation of Unactivated 1,3-Dienes.....	162
3.2.1 An Alternative Strategy for Carboamination	162
3.2.2 Optimization of the Aminoarylation of 1,3-Butadiene	163

3.2.3 Scope of Grignard Reagents and 1,3-Dienes	165
3.2.4 Initial Studies Toward an Enantioselective Aminoarylation of Dienes	170
3.2.5 Conclusions	172
3.3 Experimental Section	172
3.3.1 Materials and Methods	172
3.3.2 Preparative Procedures	173
3.4 References	190
APPENDIX FOUR: Spectra Relevant to Chapter Three.....	193
APPENDIX FIVE: HPLC Traces Relevant to Chapter Three	228
CHAPTER FOUR: The Development of a General, Highly Selective Method for the Allylic Functionalization of Unactivated Internal Olefins.....	230
4.1 Background	230
4.1.1 Introduction	230
4.1.2 Asymmetric Kharasch-Sosnovsky Reaction with Unactivated Cycloalkenes.....	232
4.1.3 Asymmetric Allylic Amination of Unactivated Cycloalkenes	236
4.1.4 Enantioselective Heck Reaction with Unactivated Cycloalkenes	238
4.1.5 Enantioselective Ene Reactions of Glyoxylates	240

4.1.6 Enantioselective Allylic Alkylation of Unactivated Olefins with Donor/Acceptor Stabilized Carbenoids	242
4.1.7 Conclusions	244
4.2 The Development of a Catalytic Highly Selective Allylic Oxidation of Unactivated Internal Olefins	245
4.2.1 Strategy and Choice of Oxidant	245
4.2.2 Optimization of a Catalytic Enantioselective Hetero-Ene Reaction with Cis-5-Decene	247
4.2.3 Substrate Scope and Trends in Regioselectivity	252
4.2.4 Mechanistic Insight Into the Catalytic Asymmetric Allylic Oxidation of Unfunctionalized Olefins	258
4.2.5 Stereospecific Diversification of Allylic Sulfinimides	264
4.2.6 Conclusions	265
4.3 Experimental Section	266
4.3.1 Materials and Methods	266
4.3.2 Preparative Procedures	267
4.4 References	309
APPENDIX SIX: Spectra Relevant to Chapter Four	315
APPENDIX SEVEN: HPLC Traces Relevant to Chapter Four	372
APPENDIX EIGHT: Crystallography Data Relevant to Chapters One and Four	386

LIST OF FIGURES

CHAPTER ONE

Figure 1.1.1	HIF	2
Figure 1.1.2	Structure of HIF-2 α Cavity	3
Figure 1.2.1	Co-Crystal Structure of 1.3p and 1.3q	11
Figure 1.3.1	Scaffold I/Scaffold II Comparison	17
Figure 1.3.2	Comparison of 1.3q and 1.32 Bound Within HIF-2 α	18

APPENDIX ONE

Figure A1.1	¹ H NMR (400 MHz, Acetone- <i>d</i> ₆) of compound 1.4a	67
Figure A1.2	¹³ C NMR (100 MHz, Acetone- <i>d</i> ₆) of compound 1.4a	67
Figure A1.3	¹ H NMR (400 MHz, Acetone- <i>d</i> ₆) of compound 1.4b	68
Figure A1.4	¹³ C NMR (100 MHz, Acetone- <i>d</i> ₆) of compound 1.4b	68
Figure A1.5	¹ H NMR (400 MHz, Acetone- <i>d</i> ₆) of compound 1.4c	69
Figure A1.6	¹³ C NMR (100 MHz, Acetone- <i>d</i> ₆) of compound 1.4c	69
Figure A1.7	¹ H NMR (400 MHz, Acetone- <i>d</i> ₆) of compound 1.4d	70
Figure A1.8	¹³ C NMR (100 MHz, Acetone- <i>d</i> ₆) of compound 1.4d	70
Figure A1.9	¹ H NMR (400 MHz, Acetone- <i>d</i> ₆) of compound 1.4e	71
Figure A1.10	¹³ C NMR (100 MHz, Acetone- <i>d</i> ₆) of compound 1.4e	71
Figure A1.11	¹ H NMR (400 MHz, Acetone- <i>d</i> ₆) of compound 1.4f	72
Figure A1.12	¹³ C NMR (100 MHz, Acetone- <i>d</i> ₆) of compound 1.4f	72
Figure A1.13	¹ H NMR (400 MHz, Acetone- <i>d</i> ₆) of compound 1.4g	73
Figure A1.14	¹³ C NMR (100 MHz, Acetone- <i>d</i> ₆) of compound 1.4g	73
Figure A1.15	¹ H NMR (400 MHz, Acetone- <i>d</i> ₆) of compound 1.4h	74
Figure A1.16	¹³ C NMR (100 MHz, Acetone- <i>d</i> ₆) of compound 1.4h	74
Figure A1.17	¹ H NMR (400 MHz, Acetone- <i>d</i> ₆) of compound 1.4i	75
Figure A1.18	¹³ C NMR (100 MHz, Acetone- <i>d</i> ₆) of compound 1.4i	75

Figure A1.19	^1H NMR (400 MHz, Acetone- d_6) of compound 1.6	76
Figure A1.20	^{13}C NMR (100 MHz, Acetone- d_6) of compound 1.6	76
Figure A1.21	^1H NMR (400 MHz, Acetone- d_6) of compound S1	77
Figure A1.22	^{13}C NMR (100 MHz, Acetone- d_6) of compound S1	77
Figure A1.23	^1H NMR (400 MHz, Acetone- d_6) of compound 1.11	78
Figure A1.24	^1H NMR (400 MHz, Acetone- d_6) of compound 1.21	79
Figure A1.25	^{13}C NMR (100 MHz, Acetone- d_6) of compound 1.21	79
Figure A1.26	^1H NMR (400 MHz, Acetone- d_6) of compound 1.23	80
Figure A1.27	^{13}C NMR (100 MHz, Acetone- d_6) of compound 1.23	80
Figure A1.28	^1H NMR (400 MHz, Acetone- d_6) of compound 1.29	81
Figure A1.29	^{13}C NMR (100 MHz, Acetone- d_6) of compound 1.29	81
Figure A1.30	^1H NMR (400 MHz, DMSO- d_6) of compound 1.39	82
Figure A1.31	^{13}C NMR (100 MHz, DMSO- d_6) of compound 1.39	82
Figure A1.32	^1H NMR (500 MHz, CDCl_3) of compound 1.40	83
Figure A1.33	^{13}C NMR (100 MHz, CDCl_3) of compound 1.40	83

APPENDIX TWO

Figure A2.1	HPLC traces of compound 1.40	85
Figure A2.2	HPLC traces of compound 1.39	85

CHAPTER TWO

Figure 2.1.1	Liu's Proposed Transition State (2.13)	93
--------------	---	----

APPENDIX THREE

Figure A3.1	^1H NMR (400 MHz, CDCl_3) of compound 2.18	129
Figure A3.2	^{13}C NMR (100 MHz, CDCl_3) of compound 2.18	129

Figure A3.3	^1H NMR (500 MHz, CDCl_3) of compound 2.21a	130
Figure A3.4	^{13}C NMR (100 MHz, CDCl_3) of compound 2.21a	130
Figure A3.5	^1H NMR (500 MHz, C_6D_6) of compound 2.21a	131
Figure A3.6	^1H NMR (400 MHz, CDCl_3) of compound 2.21b	132
Figure A3.7	^{13}C NMR (100 MHz, CDCl_3) of compound 2.21b	132
Figure A3.8	^1H NMR (400 MHz, CDCl_3) of compound 2.21c	133
Figure A3.9	^{13}C NMR (100 MHz, CDCl_3) of compound 2.21c	133
Figure A3.10	^1H NMR (400 MHz, CDCl_3) of compound 2.21d	134
Figure A3.11	^{13}C NMR (100 MHz, CDCl_3) of compound 2.21d	134
Figure A3.12	^1H NMR (400 MHz, CDCl_3) of compound 2.21e	135
Figure A3.13	^{13}C NMR (100 MHz, CDCl_3) of compound 2.21e	135
Figure A3.14	^1H NMR (400 MHz, CDCl_3) of compound 2.21f	136
Figure A3.15	^{13}C NMR (100 MHz, CDCl_3) of compound 2.21f	136
Figure A3.16	^1H NMR (500 MHz, CDCl_3) of compound 2.21g	137
Figure A3.17	^{13}C NMR (125 MHz, CDCl_3) of compound 2.21g	137
Figure A3.18	^1H NMR (500 MHz, CDCl_3) of compound 2.21h	138
Figure A3.19	^{13}C NMR (125 MHz, CDCl_3) of compound 2.21h	138
Figure A3.20	^1H NMR (500 MHz, CDCl_3) of compound 2.21i	139
Figure A3.21	^{13}C NMR (125 MHz, CDCl_3) of compound 2.21i	139
Figure A3.22	^1H NMR (500 MHz, CDCl_3) of compound 2.21l	140
Figure A3.23	^{13}C NMR (125 MHz, CDCl_3) of compound 2.21l	140
Figure A3.24	^1H NMR (500 MHz, CDCl_3) of compound 2.21m	141
Figure A3.25	^{13}C NMR (100 MHz, CDCl_3) of compound 2.21m	141
Figure A3.26	^1H NMR (500 MHz, CDCl_3) of compound 2.21n	142
Figure A3.27	^{13}C NMR (125 MHz, CDCl_3) of compound 2.21n	142
Figure A3.28	^1H NMR (500 MHz, CDCl_3) of compound 2.21o	143
Figure A3.29	^{13}C NMR (125 MHz, CDCl_3) of compound 2.21o	143
Figure A3.30	^1H NMR (500 MHz, CDCl_3) of compound 2.21p	144
Figure A3.31	^{13}C NMR (125 MHz, CDCl_3) of compound 2.21p	144
Figure A3.32	^1H NMR (500 MHz, CDCl_3) of compound 2.21q	145

Figure A3.33	^{13}C NMR (125 MHz, CDCl_3) of compound 2.21q	145
Figure A3.34	^1H NMR (500 MHz, CDCl_3) of compound 2.21r	146
Figure A3.35	^{13}C NMR (125 MHz, CDCl_3) of compound 2.21r	146
Figure A3.36	^1H NMR (500 MHz, CDCl_3) of compound 2.21s	147
Figure A3.37	^{13}C NMR (125 MHz, CDCl_3) of compound 2.21s	147
Figure A3.38	^1H NMR (500 MHz, CDCl_3) of compound 2.21t	148
Figure A3.39	^{13}C NMR (100 MHz, CDCl_3) of compound 2.2t	148
Figure A3.40	^1H NMR (400 MHz, CDCl_3) of compound 2.24	149
Figure A3.41	^{13}C NMR (100 MHz, CDCl_3) of compound 2.24	149
Figure A3.42	^1H NMR (400 MHz, CDCl_3) of compound 2.26	150
Figure A3.43	^{13}C NMR (100 MHz, CDCl_3) of compound 2.26	150
Figure A3.44	^1H NMR (500 MHz, CDCl_3) of compound 2.27	151
Figure A3.45	^{13}C NMR (125 MHz, CDCl_3) of compound 2.27	151
Figure A3.46	^1H NMR (500 MHz, CDCl_3) of compound 2.28	152
Figure A3.47	^{13}C NMR (125 MHz, CDCl_3) of compound 2.28	152
Figure A3.48	^1H NMR (500 MHz, CDCl_3) of compound 2.29a	153
Figure A3.49	^{13}C NMR (125 MHz, CDCl_3) of compound 2.29a	153
Figure A3.50	^1H NMR (500 MHz, CDCl_3) of compound 2.29b	154
Figure A3.51	^{13}C NMR (125 MHz, CDCl_3) of compound 2.29b	154
Figure A3.52	^1H NMR (500 MHz, CDCl_3) of compound 2.29c	155
Figure A3.53	^{13}C NMR (125 MHz, CDCl_3) of compound 2.29c	155
Figure A3.54	^1H NMR (500 MHz, CDCl_3) of compound 2.29d	156
Figure A3.55	^{13}C NMR (125 MHz, CDCl_3) of compound 2.29d	156

APPENDIX FOUR

Figure A4.1	^1H NMR (400 MHz, CDCl_3) of compound 3.11a	194
Figure A4.2	^{13}C NMR (100 MHz, CDCl_3) of compound 3.11a	194
Figure A4.3	^1H NMR (500 MHz, CDCl_3) of compound 3.14a	195
Figure A4.4	^{13}C NMR (100 MHz, CDCl_3) of compound 3.14a	195

Figure A4.5	^1H NMR (500 MHz, CDCl_3) of compound 3.14b	196
Figure A4.6	^{13}C NMR (100 MHz, CDCl_3) of compound 3.14b	196
Figure A4.7	nOe (500 MHz, CDCl_3) of compound 3.14b	197
Figure A4.8	^1H NMR (500 MHz, CDCl_3) of compound 3.14c	198
Figure A4.9	^{13}C NMR (100 MHz, CDCl_3) of compound 3.14c	198
Figure A4.10	^1H NMR (400 MHz, CDCl_3) of compound 3.14d	199
Figure A4.11	^{13}C NMR (100 MHz, CDCl_3) of compound 3.14d	199
Figure A4.12	^1H NMR (400 MHz, CDCl_3) of compound 3.14e	200
Figure A4.13	^{13}C NMR (100 MHz, CDCl_3) of compound 3.14e	200
Figure A4.14	^1H NMR (500 MHz, CDCl_3) of compound 3.14f	201
Figure A4.15	^{13}C NMR (100 MHz, CDCl_3) of compound 3.14f	201
Figure A4.16	^1H NMR (500 MHz, CDCl_3) of compound 3.14g	202
Figure A4.17	^{13}C NMR (100 MHz, CDCl_3) of compound 3.14g	202
Figure A4.18	^1H NMR (500 MHz, CDCl_3) of compound 3.14h	203
Figure A4.19	^{13}C NMR (100 MHz, CDCl_3) of compound 3.14h	203
Figure A4.20	^1H NMR (400 MHz, CDCl_3) of compound 3.14i	204
Figure A4.21	^{13}C NMR (100 MHz, CDCl_3) of compound 3.14i	204
Figure A4.22	^1H NMR (500 MHz, CDCl_3) of compound 3.14j	205
Figure A4.23	^{13}C NMR (100 MHz, CDCl_3) of compound 3.14j	205
Figure A4.24	^1H NMR (500 MHz, CDCl_3) of compound 3.14k	206
Figure A4.25	^{13}C NMR (100 MHz, CDCl_3) of compound 3.14k	206
Figure A4.26	^1H NMR (400 MHz, CDCl_3) of compound 3.14l	207
Figure A4.27	^{13}C NMR (100 MHz, CDCl_3) of compound 3.14l	207
Figure A4.28	^1H NMR (500 MHz, CDCl_3) of compound 3.14m	208
Figure A4.29	^{13}C NMR (100 MHz, CDCl_3) of compound 3.14m	208
Figure A4.30	^1H NMR (400 MHz, CDCl_3) of compound 3.16a	209
Figure A4.31	^{13}C NMR (100 MHz, CDCl_3) of compound 3.16a	209
Figure A4.32	^1H NMR (400 MHz, CDCl_3) of compound 3.16b	210
Figure A4.33	^{13}C NMR (100 MHz, CDCl_3) of compound 3.16b	210
Figure A4.34	^1H NMR (500 MHz, CDCl_3) of compound 3.16c	211

Figure A4.35	^{13}C NMR (100 MHz, CDCl_3) of compound 3.16c	211
Figure A4.36	^1H NMR (400 MHz, CDCl_3) of compound 3.16d	212
Figure A4.37	^{13}C NMR (100 MHz, CDCl_3) of compound 3.16d	212
Figure A4.38	^1H NMR (500 MHz, CDCl_3) of compound 3.16e	213
Figure A4.39	^{13}C NMR (100 MHz, CDCl_3) of compound 3.16e	213
Figure A4.40	^1H NMR (500 MHz, CDCl_3) of compound 3.16f	214
Figure A4.41	^{13}C NMR (125 MHz, CDCl_3) of compound 3.16f	214
Figure A4.42	COSY (500 MHz, CDCl_3) of compound 3.16f	215
Figure A4.43	NOE (125 MHz, CDCl_3) of compound 3.16f	216
Figure A4.44	^1H NMR (500 MHz, CDCl_3) of compound 3.17f	217
Figure A4.45	^{13}C NMR (100 MHz, CDCl_3) of compound 3.17f	217
Figure A4.46	COSY (500 MHz, CDCl_3) of compound 3.17f	218
Figure A4.47	NOE (100 MHz, CDCl_3) of compound 3.17f	219
Figure A4.48	^1H NMR (500 MHz, CDCl_3) of compound 3.16g	220
Figure A4.49	^{13}C NMR (100 MHz, CDCl_3) of compound 3.16g	220
Figure A4.50	COSY (500 MHz, CDCl_3) of compound 3.16g	221
Figure A4.51	^1H NMR (500 MHz, CDCl_3) of compound 3.17g	222
Figure A4.52	^{13}C NMR (100 MHz, CDCl_3) of compound 3.17g	222
Figure A4.53	COSY (500 MHz, CDCl_3) of compound 3.17g	223
Figure A4.54	^1H NMR (500 MHz, CDCl_3) of compound 3.19	224
Figure A4.55	^{13}C NMR (100 MHz, CDCl_3) of compound 3.19	224
Figure A4.56	COSY (500 MHz, CDCl_3) of compound 3.19	225
Figure A4.57	^1H NMR (400 MHz, CDCl_3) of compound 3.20	226
Figure A4.58	^{13}C NMR (100 MHz, CDCl_3) of compound 3.20	226
Figure A4.59	COSY (500 MHz, CDCl_3) of compound 3.20	227

APPENDIX FIVE

Figure A5.1	HPLC Traces of compound 3.16c	229
-------------	--	-----

CHAPTER FOUR

Figure 4.1.1	Strategies for Asymmetric Allylic Functionalization	231
Figure 4.1.2	Comparison of Terminal and Internal Olefins	232
Figure 4.1.3	Stereinduction Models for Asymmetric Kharasch-Sosnovsky	236
Figure 4.1.4	BINAP(O) (4.33) and 4.34	240
Figure 4.1.5	Stereinduction Model for Glyoxylate-Ene Reaction	241
Figure 4.2.1	Strategy for Asymmetric Allylic Functionalization	246
Figure 4.2.2	Proposed Transition States for Thermal Hetero-Ene Reaction.....	248
Figure 4.2.3	Crystal Structure of 4.68	255
Figure 4.2.4	Regioselectivity Trends	257

APPENDIX SIX

Figure A6.1	¹ H NMR (500 MHz, CDCl ₃) of compound S3	316
Figure A6.2	¹³ C NMR (100 MHz, CDCl ₃) of compound S3	316
Figure A6.3	¹ H NMR (500 MHz, CDCl ₃) of compound S4	317
Figure A6.4	¹³ C NMR (100 MHz, CDCl ₃) of compound S4	317
Figure A6.5	¹ H NMR (400 MHz, CDCl ₃) of compound S5	318
Figure A6.6	¹³ C NMR (100 MHz, CDCl ₃) of compound S5	318
Figure A6.7	¹ H NMR (400 MHz, CDCl ₃) of compound S6	319
Figure A6.8	¹³ C NMR (100 MHz, CDCl ₃) of compound S6	319
Figure A6.9	¹ H NMR (500 MHz, CDCl ₃) of compound S7	320
Figure A6.10	¹³ C NMR (100 MHz, CDCl ₃) of compound S7	320
Figure A6.11	¹ H NMR (400 MHz, CDCl ₃) of compound S8	321
Figure A6.12	¹³ C NMR (100 MHz, CDCl ₃) of compound S8	321
Figure A6.13	¹ H NMR (500 MHz, CDCl ₃) of compound S9	322
Figure A6.14	¹³ C NMR (100 MHz, CDCl ₃) of compound S9	322
Figure A6.15	¹ H NMR (400 MHz, CDCl ₃) of compound S10	323
Figure A6.16	¹³ C NMR (100 MHz, CDCl ₃) of compound S10	323

Figure A6.17	^1H NMR (400 MHz, CDCl_3) of compound S11	324
Figure A6.18	^{13}C NMR (100 MHz, CDCl_3) of compound S11	324
Figure A6.19	^1H NMR (400 MHz, CDCl_3) of compound S12	325
Figure A6.20	^{13}C NMR (100 MHz, CDCl_3) of compound S12	325
Figure A6.21	^1H NMR (400 MHz, CDCl_3) of compound S13	326
Figure A6.22	^{13}C NMR (100 MHz, CDCl_3) of compound S13	326
Figure A6.23	^1H NMR (400 MHz, CDCl_3) of compound 4.61	327
Figure A6.24	^{13}C NMR (100 MHz, CDCl_3) of compound 4.61	327
Figure A6.25	^1H NMR (400 MHz, CDCl_3) of crude compound 4.61	328
Figure A6.26	^1H NMR (400 MHz, CDCl_3) of compound S17	329
Figure A6.27	^{13}C NMR (100 MHz, CDCl_3) of compound S17	329
Figure A6.28	^1H NMR (400 MHz, CDCl_3) of compound 4.62	330
Figure A6.29	^{13}C NMR (100 MHz, CDCl_3) of compound 4.62	330
Figure A6.30	^1H NMR (400 MHz, CDCl_3) of compound S18	331
Figure A6.31	^1H NMR (400 MHz, CDCl_3) of compound 4.63	332
Figure A6.32	^{13}C NMR (100 MHz, CDCl_3) of compound 4.63	332
Figure A6.33	^1H NMR (400 MHz, CDCl_3) of compound S19	333
Figure A6.34	^1H NMR (400 MHz, CDCl_3) of compound 4.64	334
Figure A6.35	^{13}C NMR (100 MHz, CDCl_3) of compound 4.64	334
Figure A6.36	^1H NMR (400 MHz, CDCl_3) of compound S20	335
Figure A6.37	^1H NMR (500 MHz, CDCl_3) of compound 4.65	336
Figure A6.38	^{13}C NMR (100 MHz, CDCl_3) of compound 4.65	336
Figure A6.39	^1H NMR (400 MHz, CDCl_3) of compound S20	337
Figure A6.40	^1H NMR (500 MHz, CDCl_3) of compound 4.68	338
Figure A6.41	^{13}C NMR (100 MHz, CDCl_3) of compound 4.68	338
Figure A6.42	^1H NMR (400 MHz, CDCl_3) of compound S21	339
Figure A6.43	^1H NMR (400 MHz, CDCl_3) of compound 4.69	340
Figure A6.44	^{13}C NMR (100 MHz, CDCl_3) of compound 4.69	340
Figure A6.45	^1H NMR (400 MHz, CDCl_3) of compound S22	341
Figure A6.46	^1H NMR (400 MHz, CDCl_3) of compound 4.70	342

Figure A6.47	^{13}C NMR (100 MHz, CDCl_3) of compound 4.70	342
Figure A6.48	^1H NMR (400 MHz, CDCl_3) of compound 4.71	343
Figure A6.49	^{13}C NMR (100 MHz, CDCl_3) of compound 4.71	343
Figure A6.50	^1H NMR (400 MHz, CDCl_3) of compound S23	344
Figure A6.51	^1H NMR (500 MHz, CDCl_3) of compound S24	345
Figure A6.52	^{13}C NMR (100 MHz, CDCl_3) of compound 4.73	346
Figure A6.53	^1H NMR (400 MHz, CDCl_3) of compound 4.73	346
Figure A6.54	^1H NMR (400 MHz, CDCl_3) of compound S25	347
Figure A6.55	^{13}C NMR (100 MHz, CDCl_3) of compound S25	347
Figure A6.56	^1H NMR (400 MHz, CDCl_3) of compound 4.74	348
Figure A6.57	^{13}C NMR (100 MHz, CDCl_3) of compound 4.74	348
Figure A6.58	^1H NMR (400 MHz, CDCl_3) of compound S26	349
Figure A6.59	^1H NMR (500 MHz, CDCl_3) of compound 4.75	350
Figure A6.60	^{13}C NMR (100 MHz, CDCl_3) of compound 4.75	350
Figure A6.61	^1H NMR (500 MHz, CDCl_3) of compound S27	351
Figure A6.62	^1H NMR (500 MHz, CDCl_3) of compound 4.76	352
Figure A6.63	^{13}C NMR (100 MHz, CDCl_3) of compound 4.76	352
Figure A6.64	^1H NMR (400 MHz, CDCl_3) of compound S28	353
Figure A6.65	^1H NMR (500 MHz, CDCl_3) of compound 4.77	354
Figure A6.66	^{13}C NMR (100 MHz, CDCl_3) of compound 4.77	354
Figure A6.67	^1H NMR (400 MHz, CDCl_3) of compound S29	355
Figure A6.68	^1H NMR (400 MHz, CDCl_3) of compound 4.78	356
Figure A6.69	^{13}C NMR (100 MHz, CDCl_3) of compound 4.78	356
Figure A6.70	^1H NMR (400 MHz, CDCl_3) of compound S30	357
Figure A6.71	^{13}C NMR (100 MHz, CDCl_3) of compound S30	357
Figure A6.72	^1H NMR (400 MHz, CDCl_3) of compound 4.79	358
Figure A6.73	^1H NMR (400 MHz, CDCl_3) of compound S31	359
Figure A6.74	^1H NMR (400 MHz, CDCl_3) of compound 4.80	360
Figure A6.75	^{13}C NMR (100 MHz, CDCl_3) of compound 4.80	360
Figure A6.76	^1H NMR (400 MHz, CDCl_3) of compound S32	361

Figure A6.77	¹ H NMR (400 MHz, CDCl ₃) of compound 4.82	362
Figure A6.78	¹³ C NMR (100 MHz, CDCl ₃) of compound 4.82	362
Figure A6.79	¹ H NMR (500 MHz, CDCl ₃) of compound S33	363
Figure A6.80	¹ H NMR (500 MHz, CDCl ₃) of compound 4.83	364
Figure A6.81	¹³ C NMR (100 MHz, CDCl ₃) of compound 4.83	364
Figure A6.82	¹ H NMR (500 MHz, CDCl ₃) of compound S34	365
Figure A6.83	¹ H NMR (400 MHz, CDCl ₃) of compound 4.84	366
Figure A6.84	¹³ C NMR (100 MHz, CDCl ₃) of compound 4.84	366
Figure A6.85	¹ H NMR (400 MHz, CDCl ₃) of compound 4.85	367
Figure A6.86	¹³ C NMR (100 MHz, CDCl ₃) of compound 4.85	367
Figure A6.87	¹ H NMR (400 MHz, CDCl ₃) of compound S35	368
Figure A6.88	¹³ C NMR (100 MHz, CDCl ₃) of compound S35	368
Figure A6.89	¹ H NMR (400 MHz, CDCl ₃) of compound S36	369
Figure A6.90	¹³ C NMR (100 MHz, CDCl ₃) of compound S36	369
Figure A6.91	¹ H NMR (400 MHz, CDCl ₃) of compound 4.86	370
Figure A6.92	¹³ C NMR (100 MHz, CDCl ₃) of compound 4.86	370
Figure A6.93	¹ H NMR (400 MHz, CDCl ₃) of compound 4.37	371
Figure A6.94	¹³ C NMR (100 MHz, CDCl ₃) of compound 4.37	371

APPENDIX SEVEN

Figure A7.1	HPLC Traces of compound 4.60	373
Figure A7.2	HPLC Traces of compound S17	373
Figure A7.3	HPLC Traces of compound S18	374
Figure A7.4	HPLC Traces of compound S19	374
Figure A7.5	HPLC Traces of compound S20	375
Figure A7.6	HPLC Traces of compound S21	376
Figure A7.7	HPLC Traces of compound S22	376
Figure A7.8	HPLC Traces of compound S17	377
Figure A7.9	HPLC Traces of compound S23	377

Figure A7.10	HPLC Traces of compound S24	378
Figure A7.11	HPLC Traces of compound S25	378
Figure A7.12	HPLC Traces of compound S26	379
Figure A7.13	HPLC Traces of compound S27	379
Figure A7.14	HPLC Traces of compound S28	380
Figure A7.15	HPLC Traces of compound S29	380
Figure A7.16	HPLC Traces of compound S30	381
Figure A7.17	HPLC Traces of compound S31	381
Figure A7.18	HPLC Traces of compound S32	382
Figure A7.19	HPLC Traces of compound 4.82	382
Figure A7.20	HPLC Traces of compound S34	383
Figure A7.21	HPLC Traces of compound S36	383
Figure A7.22	HPLC Traces of compound 4.86	384
Figure A7.23	HPLC Traces of compound 4.60 (R/S Mixtures)	384
Figure A7.24	HPLC Traces of compound S17 (Non-Linear Study)	385

APPENDIX EIGHT

Figure A8.1	Crystal Structure of enamine 1.39	373
Figure A8.2	Crystal Structure of sulfinimide 4.68	373

LIST OF SCHEMES

CHAPTER ONE

Scheme 1.2.1	Summary of Scaffold I Analogue Synthesis	5
Scheme 1.2.2	Aniline Derivatives 1.3	6
Scheme 1.2.3	Benzyl Amine Derivatives 1.4	7
Scheme 1.2.4	S- and O-Linkers 1.5 and 1.6	7
Scheme 1.2.5	Synthesis of 1.8	10

Scheme 1.2.6	Synthesis of 1.11	12
Scheme 1.2.7	Synthesis of 1.18-1.19	13
Scheme 1.2.8	Synthesis of 1.23 and 1.24	14
Scheme 1.2.9	Synthesis of 1.25-7	15
Scheme 1.2.10	Synthesis of 1.29 and 1.30	15
Scheme 1.3.1	Strategy for the Asymmetric Synthesis of 1.37	19
Scheme 1.3.2	Proposed Mechanism.....	22
Scheme 1.3.3	Recrystallization of Enantioenriched 1.39	23

CHAPTER TWO

Scheme 2.1.1	Allylic Alkylations of Terminal Olefins	86
Scheme 2.1.2	White and Shi's Allylic Alkylation of Allyl Arenes.....	88
Scheme 2.1.3	White's Allylic Alkylation of Unactivated Terminal Olefins	89
Scheme 2.1.4	Trost's Allylic Alkylation of Unactivated Dienes	90
Scheme 2.1.5	Trost's Asymmetric Allylic Alkylation	91
Scheme 2.1.6	Buchwald's Allylic Trifluoromethylation of Terminal Olefins.....	92
Scheme 2.2.1	Allylic Amination Utilizing Sulfurdiimide Reagent 2.16	94
Scheme 2.2.2	Strategy for the Allylic Alkylation of Terminal Olefins with 2.18 ..	95
Scheme 2.2.3	Synthesis of Dienes 2.24 and 2.26	100
Scheme 2.2.4	Synthesis of Skipped Dienes 2.29	101
Scheme 2.2.5	Grignard Equivalents Study	102
Scheme 2.2.6	TEMPO Study	102
Scheme 2.2.7	Proposed Mechanism of Allylic Alkylation.....	103

CHAPTER THREE

Scheme 3.1.1	Telomerization of Dienes with Nucleophiles.....	158
Scheme 3.1.2	Telomerization of Dienes with Amines	159
Scheme 3.1.3	Heck's Carboamination	160

Scheme 3.1.4	Heteroannulation Reaction Utilizing Dienes	161
Scheme 3.2.1	Strategy for the Aminoarylation of Unactivated Dienes	163
Scheme 3.2.2	Regioselectivity in the Aminoarylation of 3.18	170
Scheme 3.2.3	Strategy for the Asymmetric Aminoarylation of Dienes	170
Scheme 3.2.4	Preliminary Data on the Asymmetric Aminoarylation	171

CHAPTER FOUR

Scheme 4.1.1	The Kharasch-Sosnovsky Reaction.....	233
Scheme 4.1.2	Asymmetric Kharasch-Sosnovsky with Proline-Based Ligands ...	233
Scheme 4.1.3	Asymmetric Kharasch-Sosnovsky with Oxazoline Ligands	234
Scheme 4.1.4	Regioselectivity in the Asymmetric Kharasch-Sosnovsky	235
Scheme 4.1.5	Katsuki's Asymmetric Allylic Amination of Cycloalkenes	237
Scheme 4.1.6	Amination vs Esterification in the Katsuki's Method.....	238
Scheme 4.1.7	Enantioselective Heck Reactions of Unactivated Cycloalkenes ...	239
Scheme 4.1.8	Evan's Asymmetric Glyoxylate-Ene Reaction	241
Scheme 4.1.9	Davie's Asymmetric Allylic Alkylation of Simple Alkenes	243
Scheme 4.1.10	Davie's Asymmetric Allylic Alkylation Using Triazoles.....	244
Scheme 4.2.1	Regioselectivity in the Thermal Ene Reactions of 4.45 and 4.49 ..	247
Scheme 4.2.2	Thermal Reactions of Trans- vs Cis-5-Decene and 4.49	248
Scheme 4.2.3	Study of the Role of Diol in the Enantioselective Ene Reaction ...	258
Scheme 4.2.4	Corey's Asymmetric LBA-Catalyzed Polycyclization.....	259
Scheme 4.2.5	Acid pKa Study	260
Scheme 4.2.6	Study of Cis- vs Trans-5-Decene in the Asymmetric Ene.....	260
Scheme 4.2.7	Non-Linear Effect Study	261
Scheme 4.2.8	Proposed Mechanism of the Enantioselective Ene Reaction.....	262
Scheme 4.2.9	Transition States Dictating Regioselectivity	263
Scheme 4.2.10	Diversification of Ene Adduct 4.53	265

LIST OF TABLES

CHAPTER ONE

Table 1.2.1	AlphaScreen IC ₅₀ Values for Linker-Modified Analogues.....	8
Table 1.2.2	AlphaScreen IC ₅₀ Values for Diarylamine Analogues.....	9
Table 1.2.3	ITC K _D Values for Select Substrates	10
Table 1.3.1	Preliminary Data for the Asymmetric Synthesis of Scaffold II.....	21

CHAPTER TWO

Table 2.2.1	Optimization of the Allylic Alkylation of 2.17a	96
Table 2.2.2	Grignard Scope of the Linear Selective Allylic Alkylation	98
Table 2.2.3	Olefin Scope of the Linear Selective Allylic Alkylation	99

CHAPTER THREE

Table 3.2.1	Optimization of the One-Pot 1,4-Aminoarylation of 3.1	164
Table 3.2.2	Grignard Scope of the One-Pot 1,4-Aminoarylation	167
Table 3.2.3	1,3-Diene Scope of the One-Pot 1,4-Aminoarylation.....	169

CHAPTER FOUR

Table 4.2.1	Development of an Enantioselective Hetero-Ene Reaction.....	249
Table 4.2.2	Optimization of the Diol Co-catalyst	251
Table 4.2.3	Scope of Symmetrical Unfunctionalized Alkenes	252
Table 4.2.4	Functional Group Tolerance Screen.....	253
Table 4.2.5	Scope of Symmetrical Functionalized Alkenes	254
Table 4.2.6	Regioselectivity in the Asymmetric Hetero-Ene Reaction	256

Table 3.2.7	Regioselectivity Imparted by Electronic Bias	257
-------------	--	-----

APPENDIX EIGHT

Table A8.1.1	Crystal data and structure refinement for 1.39	388
Table A8.1.2	Atomic Coord./Equiv. Isotropic Displacement Param. for 1.39	389
Table A8.1.3	Bond Lengths and Angles for 1.39	391
Table A8.1.4	Anisotropic Displacement Parameters for 1.39	395
Table A8.1.5	Hydrogen Coordinates/Isotropic Displacement Param. for 1.39 ...	396
Table A8.1.6	Hydrogen Bonds for 1.39	397
Table A8.2.1	Crystal data and structure refinement for 4.68	399
Table A8.2.2	Atomic Coord./Equiv. Isotropic Displacement Param. for 4.68	401
Table A8.2.3	Bond Lengths and Angles for 4.68	402
Table A8.2.4	Anisotropic Displacement Parameters for 4.68	404
Table A8.2.5	Hydrogen Coordinates/Isotropic Displacement Param. for 4.68 ...	405
Table A8.2.6	Torsion Angles for 4.68	406
Table A8.2.7	Hydrogen Bonds for 4.68	407

LIST OF ABBREVIATIONS

Ac	acetyl
AcOH	acetic acid
app.	apparent
aq.	aqueous
Ar	aryl
ARNT	aryl hydrocarbon receptor nuclear translocator
atm	atmosphere
bHLH	basic helix–loop–helix
BINAP	2,2'-Bis(diphenylphosphino)-1,1'-binaphthalene
BINOL	1,1'-Bi-2-naphthol
Bn	benzyl
<i>n</i> -Bu	butyl
Bz	benzoate
BZA	benzoic acid
<i>t</i> -Bu	<i>tert</i> -butyl
°C	degrees celsius
calc'd	calculated
cat.	catalytic
CCDC	Cambridge Crystallographic Data Centre
<i>m</i> -CPBA	<i>meta</i> -chloroperoxybenzoic acid
d	doublet
dba	dibenzylideneacetone
DBU	1,8-diazabicyclo[5.4.0]undec-7-ene
DCC	1,3-dicyclohexylcarbodiimide
DCE	dichloroethane
DCM	dichloromethane
DMAP	4-dimethylaminopyridine

DMB	1,4-dimethoxybenzene
DMBQ	dimethyl benzoquinone
DME	1,2-dimethoxyethane
DMF	N,N-dimethylformamide
DMSO	dimethyl sulfoxide
dppf	1,1'-bis(diphenylphosphino)ferrocene
dr	diastereomeric ratio
ee	enantiomeric excess
EPO	erythropoietin
equiv	equivalent
EI	electrospray ionization
er	enantiomeric ratio
Et	ethyl
EWG	electron withdrawing group
F	fluoride or fluoro
FAB	fast atom bombardment
g	gram(s)
h	hour(s)
[H]	reduction
HIF	hypoxia inducible factor
HMDS	1,1,1,3,3,3-hexamethyldisilazane
HMPA	hexamethylphosphoramide
HRMS	high resolution mass spectroscopy
Hz	hertz
IC ₅₀	half maximal inhibitory concentration
IR	infrared (spectroscopy)
ITC	isothermal titration calorimetry
<i>J</i>	coupling constant
L	liter
m	multiplet or milli

<i>m</i>	meta
<i>m/z</i>	mass to charge ratio
μ	micro
Me	methyl
MHz	megahertz
min	minute(s)
MMP-2	matrix metalloproteinase-2
mol	mole(s)
mp	melting point
Ms	methanesulfonyl (mesyl)
MS	molecular sieves
ND	not determined
NEt ₃	triethyl amine
NIP-3	nodulin 26-like intrinsic protein-3
NMR	nuclear magnetic resonance
nOe	Nuclear Overhauser Effect
[O]	oxidant
<i>p</i>	para
PAS	period-ARNT-single minded
Ph	phenyl
PhH	benzene
PhMe	toluene
ppm	parts per million
Pr	propyl
<i>i</i> -Pr	<i>iso</i> -propyl
pyr	pyridine
q	quartet
RCC	renal cell carcinoma
RF	retention factor
Rh ₂ (DOSP) ₄	Tetrakis[N-(<i>p</i> -dodecylphenylsulfonyl)prolinato]dirhodium(II)

rt	room temperature
s	singlet
SAR	structure-activity relationship
t	triplet
TBAF	tetrabutylammonium fluoride
TBS	tert-butyldimethylsilyl
TCA	trichloroacetic acid
TEMPO	2,2,6,6-Tetramethyl-1-piperidinyloxy
Tf	trifluoromethanesulfonyl (triflyl)
TFA	trifluoroacetic acid
THF	tetrahydrofuran
TLC	thin layer chromatography
TMS	trimethylsilyl
Ts	<i>p</i> -toluenesulfonyl (tosyl)
UV	ultraviolet
VEGF	vascular endothelial growth factor
VHL	von-Hippel–Lindau-tumour-suppressor
WT	wild type

CHAPTER ONE

The Development of Allosteric Inhibitors of the HIF-2 α Transcription Factor

1.1 Background

1.1.1 Introduction

While numerous advanced therapies have emerged throughout the years for the treatment of various cancer forms, cancer related mortality remains the primary cause of death in nearly half of the United States.¹ These diseases are frequently a consequence of mutations in the host's genetic makeup, leading to the disruption of normal metabolic pathways and the evolution of new pathways through which the deleterious effects attributed to cancer evolve. As a result more and more research has shifted in focus to the development of new therapies targeting the regulation of gene expression.

Specifically, each year, over 60,000 new cases of kidney cancer are diagnosed with less than a 15% likelihood of survival beyond five years.¹ Renal clear cell carcinomas (RCC), the most common form of kidney cancer, are remarkably analogous to one another, exhibiting hypoxia inducible factor (HIF)-dependent pathogenesis.² While numerous experimental and clinical reports exist to support HIF-targeted cancer therapy, the development of new drugs targeting hypoxic cancer cells remains wanting.³

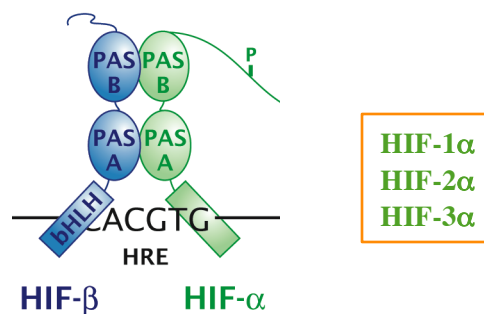
1.1.2 The HIF Family of Transcription Factors

The hypoxic response pathway regulates the cellular response to changing oxygen availability within vertebrate cells, modifying gene expression and allowing for anaerobic

metabolism and increased oxygen delivery.⁴⁻⁶ While human cells necessitate continuous and sufficient O₂ supplies, this pathway is often misused in certain tumor environments, driving the growth and spread of the disease.³ More specifically, the upregulation of HIF is associated with an increase in angiogenesis, tumorigenesis, and therapeutic resistance through the regulation of downstream transcriptional targets including, for example, VEGF (angiogenesis), EPO (metabolic adaption), Nip3 (prevention of apoptosis) and MMP2 (metastasis).⁷⁻¹⁰

The HIF transcription factor itself is a protein heterodimer within the bHLH–PAS (basic helix–loop–helix–period-ARNT-single minded) family of transcriptional proteins consisting of a HIF- α subunit (which exists in 3 separate isoforms HIF-1 α , HIF-2 α or HIF-3 α) and a constitutively expressed HIF- β (ARNT) subunit (Figure 1.1.1)¹¹. When the cellular environment is rich in oxygen, also known as normoxic conditions, the HIF- α subunit is negatively regulated through a series of proline and asparagine hydroxylases to promote von-Hippel–Lindau-tumour-suppressor (pVHL)-dependent proteolysis and prevent the recruitment of co-activators respectively.¹²

Figure 1.1.1

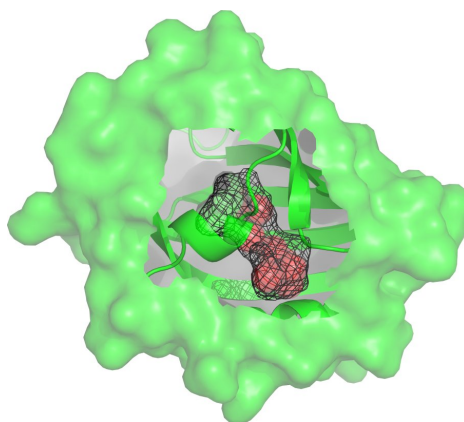


Under low oxygen (or hypoxic) conditions, however, the HIF degradation pathway is attenuated. Instead, the HIF- α subunit translocates from the cytoplasm into the nucleus where it can engage HIF- β through a series of interactions involving bHLH and PAS

domains, and recruit coactivators necessary for transcriptional regulation of over 100 genes.^{10,13-20}

Notably, the PAS-B domain of the HIF-2 α isoform has been extensively studied in recent years revealing an unusually large 290Å³ cavity buried within the domain (Figure 1.1.2).²¹ While the identity of the endogenous ligand remains unclear, the potential for allosteric inhibition via small molecule binding within this cavity serves as a promising strategy for the disruption of the HIF-2 α regulatory pathway and thus a potential therapy for RCC.²¹⁻²⁵

Figure 1.1.2



1.2 Synthesis and Evaluation of Scaffold I Small Molecule Inhibitors

1.2.1 Initial Screening for HIF-2 α Inhibition

In conjunction with several labs, our initial studies began with an extensive data set compiled from a high throughput screen of greater than 200,000 small molecules presenting diverse functionality.²⁶ “Hits” within the screening process were determined based on a compound’s ability to inhibit HIF-2 α – HIF- β dimerization, as determined by

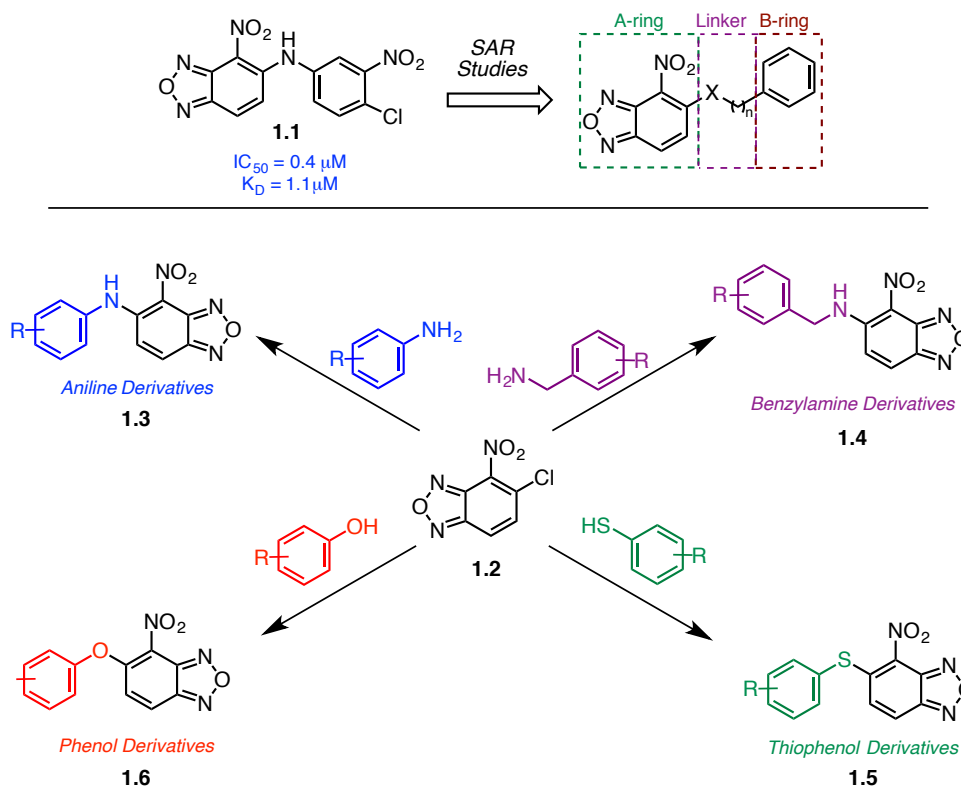
a homogenous, bead-based luminescence proximity assay (AlphaScreen).²⁷

This assay comprises of two tagged proteins (i.e., GST-HIF-2 α PAS-B* and ARNT PAS-B*-FLAG domains, where PAS-B* denotes the HIF-2 α E247R and ARNT PAS-B R362E variants used to crystallize complexes with small molecule ligands) that luminesce when in close proximity with one another. This measurable signal is diminished, however, when antagonistic compounds are bound within the PAS-B cavity inducing conformational changes that prevent the tagged proteins from interacting.

1.2.2 Library Synthesis of Scaffold I Analogues

Compound **1.1**, with an IC₅₀ of 0.4 μ M in the AlphaScreen and a K_D value of 1.1 μ M by isothermal titration calorimetry (ITC) analysis served as a starting point for lead optimization based on its promising activity (Scheme 1.2.1). This structure has been shown to bind within the aforementioned HIF-2 α PAS-B cavity and perturb the heterodimerization process. Diversification of **1.1** to a variety of scaffold I HIF-2 α antagonists focused in on three major regions: (1) modification of the left hand A-ring portion characterized by a nitro-bearing oxadiazole, (2) variation of the central heteroatom-containing linker, and (3) diversification of the right hand aromatic B-ring region.

Scheme 1.2.1

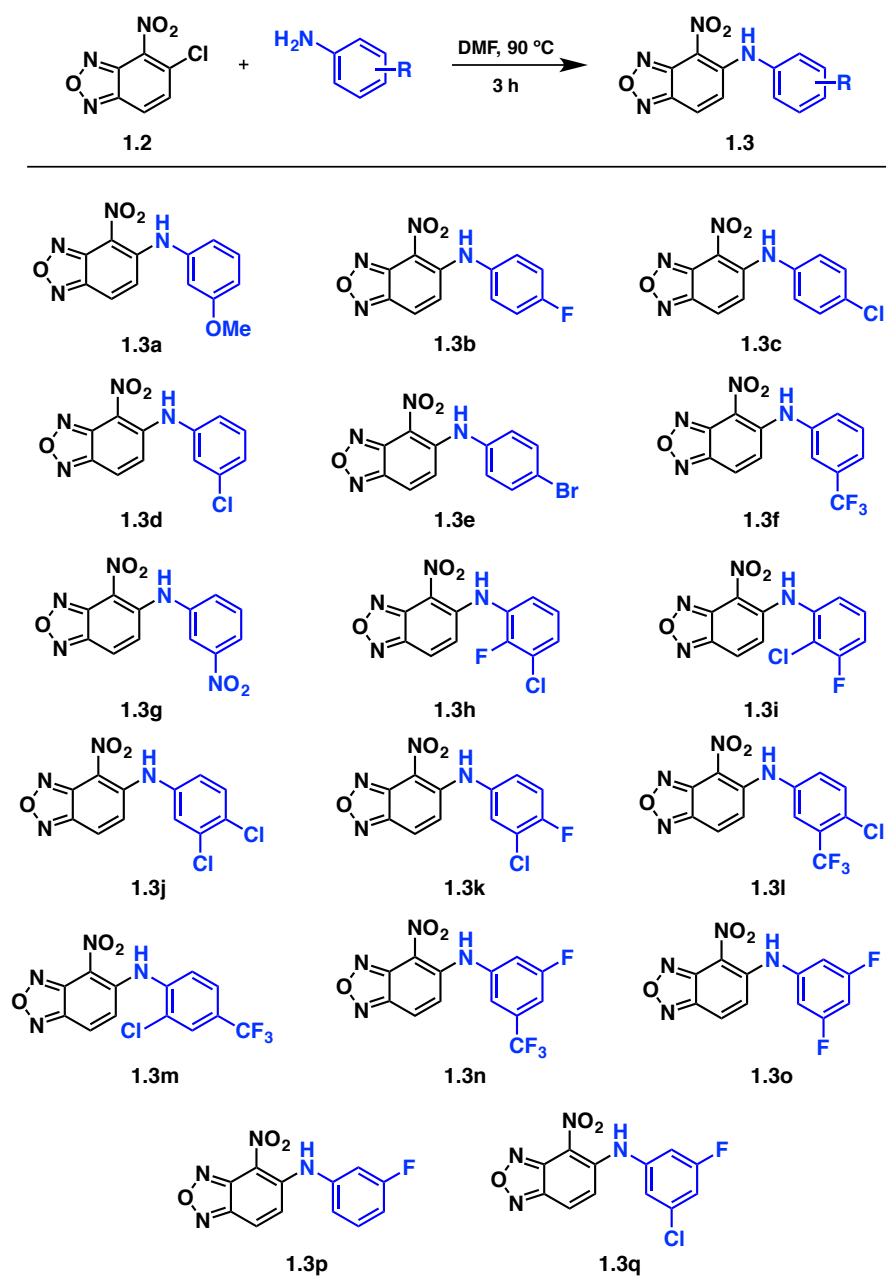


Initial efforts to study scaffold I inhibitors focused on coupling 5-chloro-4-nitrobenzoxadiazole **1.2** with various B-rings. It is important to note, that within this series of analogues, I synthesized derivatives of **1.4** and **1.6**, while **1.3** and **1.5** were supplied by collaborators. A variety of aniline derivatives bearing sterically and electronically differentiated B-rings were accessed through coupling with anilines at elevated temperatures (Scheme 1.2.2, **1.3a-q**). The introduction of both electron donating as well as electron withdrawing functionality was well tolerated, as well as varying substitution patterns in *ortho*, *meta*, and *para* positions of the B-ring.

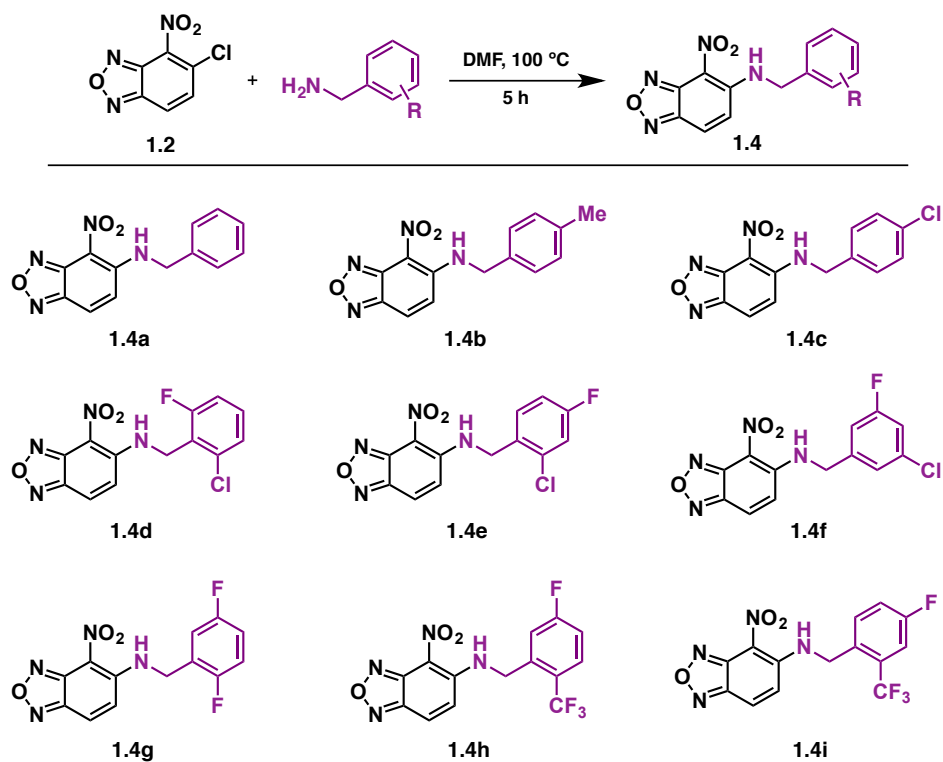
Likewise, synthetic efforts were undertaken to modify the linker of scaffold I. The introduction of a one carbon extended linker was accomplished via coupling to benzylamine compounds (Scheme 1.2.3, **1.4a-i**) at elevated temperatures. Additionally,

variation of the linker to include S- and O-linked analogues was readily achieved through couplings with thiophenol- and phenol-based compounds at room temperature under basic conditions (**1.5a-d** and **1.6** respectively).

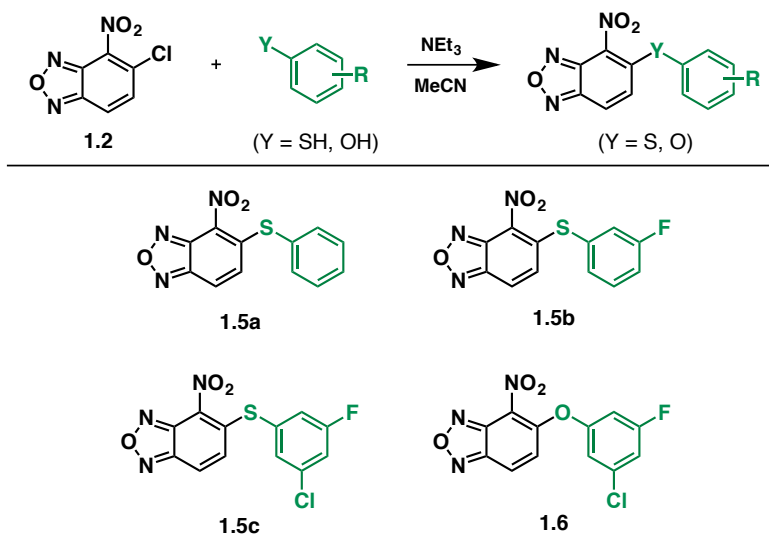
Scheme 1.2.2



Scheme 1.2.3



Scheme 1.2.4



1.2.3 Analysis of Inhibitory Activity of Scaffold I Analogues

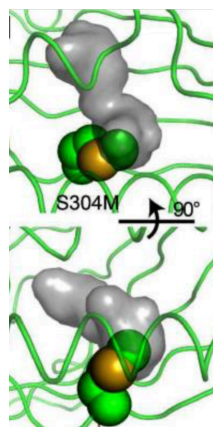
The initial library of benzoxadiazole-based compounds was assayed for inhibitory activity against HIF-2 α PAS-B/HIF- β PAS-B heterodimerization. Preliminary data was gathered through the use of an AlphaScreen assay as described previously. Moreover, a negative control incorporating a S304M mutation within the HIF-2 α PAS-B domain was designed to effectively block ligand binding within the PAS-B cavity while still retaining the ability to form a heterodimer complex with HIF- β .^{22,23}

The IC₅₀ of many compounds was not determined (ND) due to activity against both the wild type and S304M mutant HIF-2 α PAS-B, potentially due to alternative inhibitory pathways. These included predominantly the linker-modified derivatives **1.4c**, **1.5**, and **1.6**. Benzylamine derived **1.4e** and **1.4i**, however, retained some appreciable activity in the assay (Table 1.2.1).

Table 1.2.1- AlphaScreen IC₅₀ Values for Linker-Modified Analogues

Compound	IC ₅₀ (μ M)	Compound	IC ₅₀ (μ M)
1.4a	> 5	1.4h	NA
1.4b	NA	1.4i	0.5
1.4c	ND	1.5a	ND
1.4d	NA	1.5b	ND
1.4e	0.33	1.5c	ND
1.4f	2.0	1.6	ND
1.4g	> 10		

ND: Compound disrupts the control, NA: No activity



Alternatively, the aniline-derived analogues proved to fare better in the assay, revealing trends in inhibitory activity based on B-ring substitution patterns (Table 1.2.2). For example, while *para*-monosubstituted analogues **1.3b**, **1.3c**, and **1.3e** were entirely inactive, some *meta*-monosubstituted analogues retained modest activity (*m*-Cl **1.3d**–

IC₅₀ = 0.18 μ M and *m*-CF₃ **1.3f**– IC₅₀ = 0.46 μ M). Ultimately, disubstituted aniline-based analogues exhibited the strongest inhibitory activity with *para-meta*-disubstituted **1.3i** displaying the most potent disruption.

Table 1.2.2- AlphaScreen IC₅₀ Values for Diarylamine Analogues

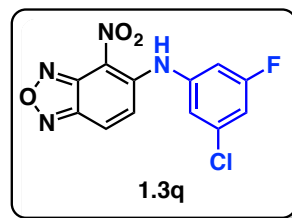
Compound	IC ₅₀ (μ M)	Compound	IC ₅₀ (μ M)
1.3a	NA	1.3j	0.12
1.3b	NA	1.3k	0.17
1.3c	NA	1.3l	0.09
1.3d	0.18	1.3m	NA
1.3e	NA	1.3n	0.43
1.3f	0.46	1.3o	2.0
1.3g	2.8	1.3p	2.1
1.3h	0.76	1.3q	0.1
1.3i	ND		

ND: Compound disrupts the control, NA: No activity

ITC testing was explored for the most active analogues to determine relative binding affinity within the HIF-2 α PAS-B cavity. K_D values not only revealed good correlation with the IC₅₀ values obtained from the AlphaScreen assay, but also confirmed **1.3q** to be the most active inhibitor tested in the scaffold I small molecule library (Table 1.2.3). Interestingly, **1.3d**, which differs from **1.3q** only in the absence of a *meta*-fluoro group on the B-ring, exhibits a two-fold reduced binding affinity in comparison. Similar observations were made when the *meta*-chloro functionality of **1.3q** was substituted for a *meta*-fluoro (**1.3o**) or removed altogether (**1.3p**). These contrasting K_D values suggest that both the *meta*-fluoro and *meta*-chloro substitutions of **1.3q** play a direct role in the observed activity of this molecule.

Table 1.2.3- ITC K_D Values for Select Substrates

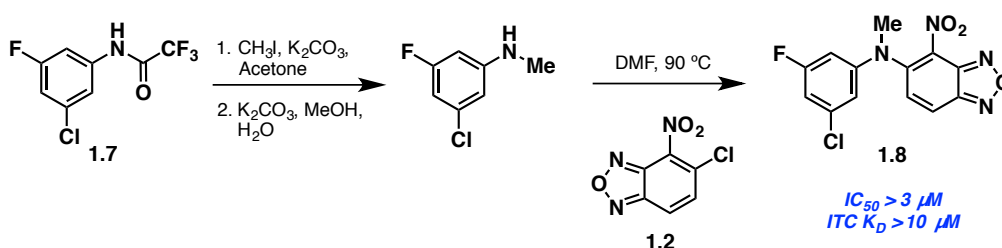
Compound	K_D (μ M)	Compound	K_D (μ M)
1.4e	0.5	1.3j	0.17
1.4f	2.0	1.3k	0.4
1.4i	0.54	1.3l	0.17
1.3d	0.16	1.3n	0.37
1.3f	0.64	1.3o	0.73
1.3g	3.0	1.3p	2.2
1.3h	1.1	1.3q	0.09



ND: Compound disrupts the control, NA: No activity

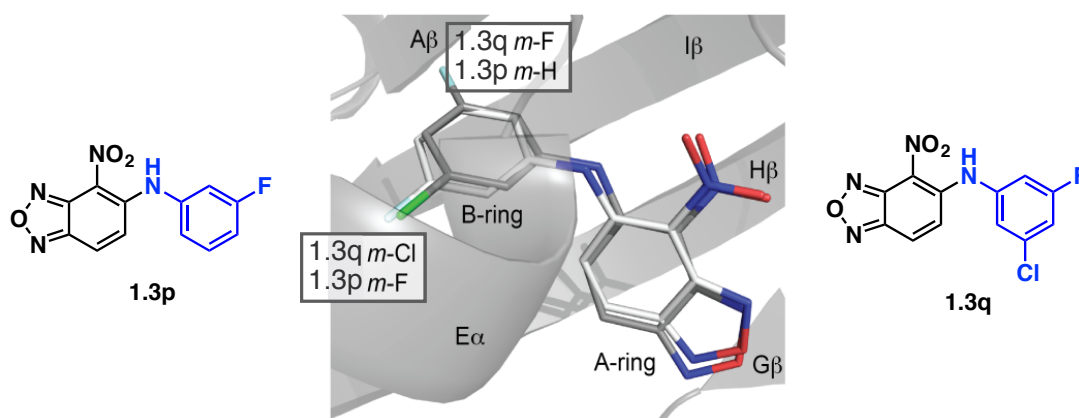
The loss of binding selectivity for S- and O-linked analogues suggests an important role for the hydrogen-bonding ability of N-based linkers. To further test this hypothesis, N-methylated **1.8** was synthesized by a collaborator and tested independently (Scheme 1.2.5). Trifluoromethyl(3-chloro-5-fluorophenyl)carbamate (**1.7**) underwent N-methylation, deprotection and subsequent coupling with **1.2** to furnish **1.8**. Results reveal markedly reduced inhibitory activity ($IC_{50} > 3 \mu$ M) in comparison to the analogous non-methylated **1.3q**, further confirming the important role that hydrogen-bonding ability plays in the linker portion.

Scheme 1.2.5



To better understand the SAR trends seen in both the AlphaScreen and ITC assays, NMR-based structural analysis was paired with X-ray crystallographic studies utilizing co-crystal structures of our compounds bound within an engineered, high affinity HIF2 PAS-B* heterodimer (HIF-2 α E247R and ARNT PAS-B R362E domains, Figure 1.2.1). Co-crystal structures of *meta*-fluorinated **1.3p** and lead compound **1.3q** show both compounds bound within the HIF-2 α PAS-B internal cavity, favoring a weak electrostatic interaction between the nitro functionality of the A-ring and the H248 imidazole side chain. The specificity in positioning required to accommodate this interaction consequently situates the B-rings of these molecules adjacent to the β -sheet directly utilized for HIF dimerization.

Figure 1.2.1

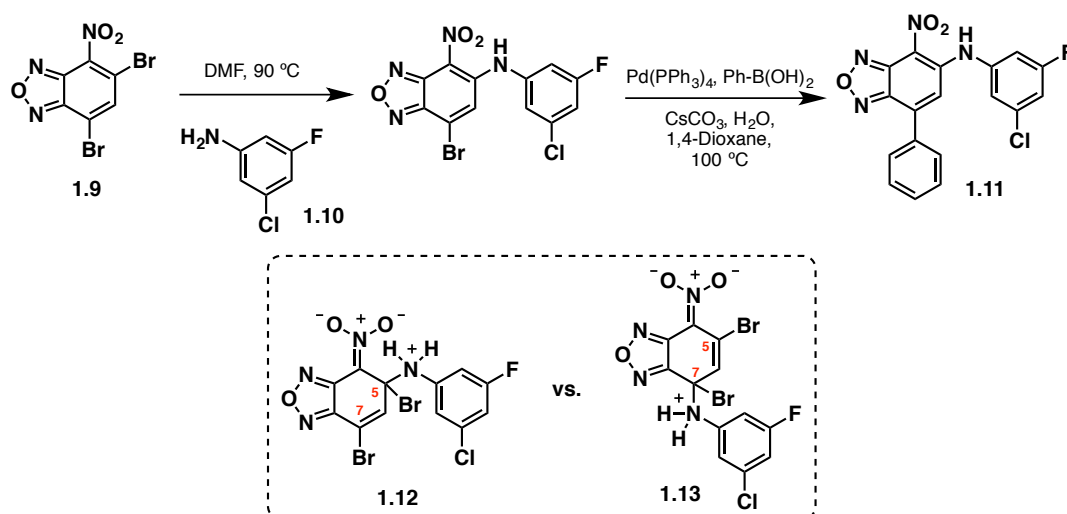


While the B-rings of both **1.3p** and **1.3q** occupy the same binding site within the HIF-2 α PAS-B internal cavity, they take on distinct conformations. These differences are thought to account for the difference in activity seen between mono- and disubstituted analogues of scaffold I. Monosubstituted **1.3p** is situated such that the *meta*-fluoro substituent is placed adjacent to the E helix of the binding site. Conversely, the disubstituted analogue **1.3q** flips its B-ring in order to adopt a lower energy conformation with the *meta*-chloro substituent situated by the E helix and the *meta*-fluoro substituent

forced instead into a suboptimal site against the PAS-B β -sheet. This β -sheet interaction induces a series of notable conformational changes throughout the PAS-B domain as observed by $^{15}\text{N}/^1\text{H}$ HSQC NMR studies of a ^{15}N -enriched HIF-2 α PAS-B-**1.3q** complex.

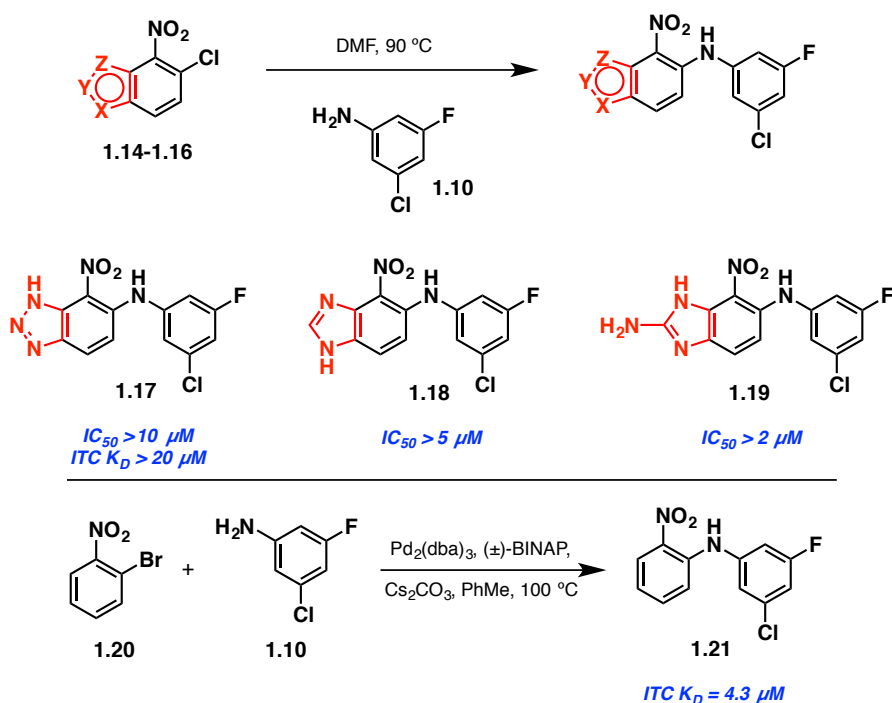
We then shifted our focus to the A-ring portion of scaffold I. The co-crystallization studies revealed an open pocket within the binding space *para* to the nitro substituent of the A-ring of **1.3p** and **1.3q**. Maintaining the optimal linker and B-ring attributes, our efforts fixated on filling the aforementioned pocket with steric bulk. To this end, I coupled dibromo-4-nitrobenzoxadiazole **1.9** with **1.10** utilizing the standard thermal conditions, followed by regioselective displacement of the 5-bromo substituent through a Suzuki-Miyaura cross coupling with phenylboronic acid yielding **1.11** (Scheme 1.2.6). Regioselectivity is thought to stem from both a larger Coulombic term imposed at position 5, as well as superior linear conjugation maintained throughout the system in the reactive intermediate **1.12** over **1.13**.

Scheme 1.2.6



Furthermore, the optimal electronic nature of the A-ring was probed by looking at analogues with different heteroaromatic rings. Collaborators on this project were able to promote nucleophilic aromatic displacements of chloride precursors **1.14**, **1.15** and **1.16** with **1.10** to provide **1.17**, **1.18** and **1.19** respectively (Scheme 1.2.7). The absence of the oxadiazole moiety and its effect on binding affinity was also researched. To this aim, I synthesized analogue **1.21** via Buchwald-Hartwig coupling of nitrochlorobenzene **1.20** and aniline **1.10**.

Scheme 1.2.7

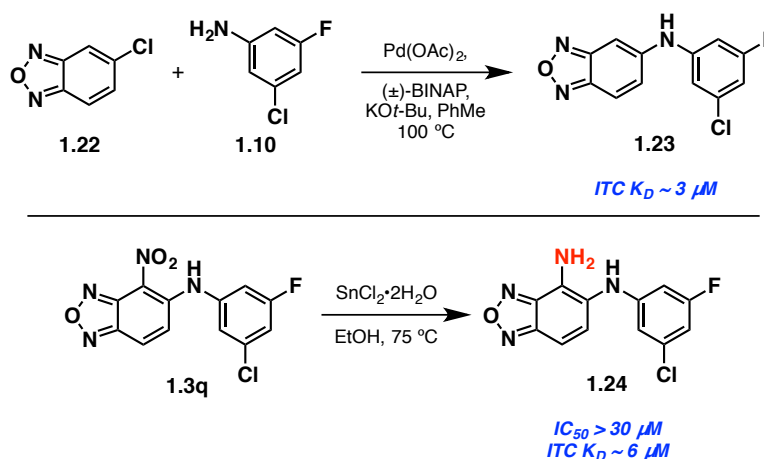


Arylated analogue **1.11** and the 7-bromo intermediate of this compound were analyzed in the AlphaScreen and ITC assays. Surprisingly, in both cases a complete loss in activity was seen. Heteroaromatics **1.17-1.19** and analogue **1.21** likewise displayed substantially reduced activity in the AlphaScreen. Weakened binding was also demonstrated in the diminished K_D values of **1.17** and **1.21** at $>20 \mu\text{M}$ and $4.3 \mu\text{M}$

respectively. These results indicate an important role played by the electronic and steric environment of the A-ring.

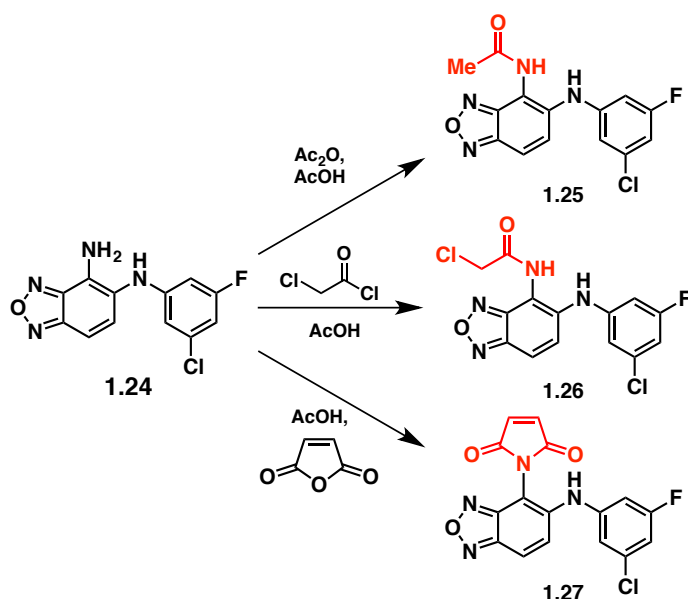
The role of the nitro group of **1.3q** was investigated next in an effort to further understand the significance of the weak electrostatic interaction with H248 in the HIF-2 α PAS-B internal cavity (Scheme 1.2.8). Exclusion of the nitro group entirely (synthesized by collaborators through a modified Buchwald-Hartwig coupling of 5-chlorobenzoxadiazole **1.22** and aniline **1.10**) gave relatively insoluble **1.23**, which exhibited reduced activity in the AlphaScreen as well as additional activity in the S304M control. Reduction of the nitro functionality of **1.3q** to arylamine **1.24** likewise resulted in diminished activity. These results were further validated through ITC and NMR experiments ($K_D = 3 \mu\text{M}$ for **1.23**, $6 \mu\text{M}$ for **1.24**).

Scheme 1.2.8



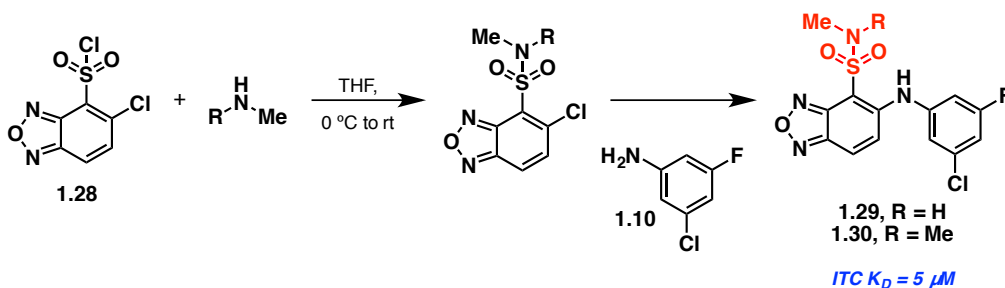
Further modifications were made to primary aniline **1.24** in an attempt to take advantage of potentially irreversible covalent interactions with the C339 side chain proximal to the nitro group of **1.3q** (as seen in the co-crystal structure). Reaction of aniline **1.24** with various electrophiles afforded N-acyl derivatives **1.25**, **1.26**, and **1.27** (Scheme 1.2.9). The resultant amide analogues were all inactive.

Scheme 1.2.9



Finally, 4-sulfonamidobenzoxadiazoles **1.29** and **1.30** were synthesized (Scheme 1.2.10). The metabolic stability of sulfonamides offers an advantage to nitro groups, which generally suffer from adverse pharmacokinetic properties. Moreover, sulfonamides retain the electron deficient character of the A-ring analogous to their nitro counterparts. To this end, I coupled 5-chlorobenzoxadiazole-4-sulfonyl chloride (**1.28**) with methylamine and dimethylamine prior to reaction with aniline **1.10**. While both **1.29** and **1.30** failed to attenuate the dimerization process, they did exhibit modest binding affinity within the HIF-2 α internal cavity ($K_D = 5 \mu\text{M}$).

Scheme 1.2.10



1.2.4 Conclusions

Data collected through AlphaScreen and ITC assays of a diverse assortment of analogues have identified a series of competent small molecule inhibitors of HIF-2 α –HIF- β heterodimerization. This data, in conjunction with NMR-based structural analysis and X-ray crystallographic studies, offers insight into the protein–small molecule interactions required for selective binding within the HIF-2 α PAS-B internal cavity and destabilizing interactions that attenuate heterodimerization. Of the series, analogue **1.3q** exhibited the highest binding affinity ($IC_{50} = 0.1 \mu M$, $K_D = 0.09 \mu M$). Co-crystal structures of this compound within the HIF-2 α PAS-B internal cavity show the presence of a stabilizing electrostatic interaction between the nitro moiety of **1.3q** and the H248 imidazole side chain of the binding pocket. Additionally, conformational changes within the PAS-B domain were noted and accredited to steric clash between the *meta*-fluoro functionality of the B-ring and the PAS-B β -sheet. Attempts to modify the linker and A-ring portions of scaffold I failed to garner any substantial increase in inhibitory activity.

1.3 Progress Toward the Stereoselective Synthesis of Scaffold II Small Molecule Disruptors of HIF-2 α

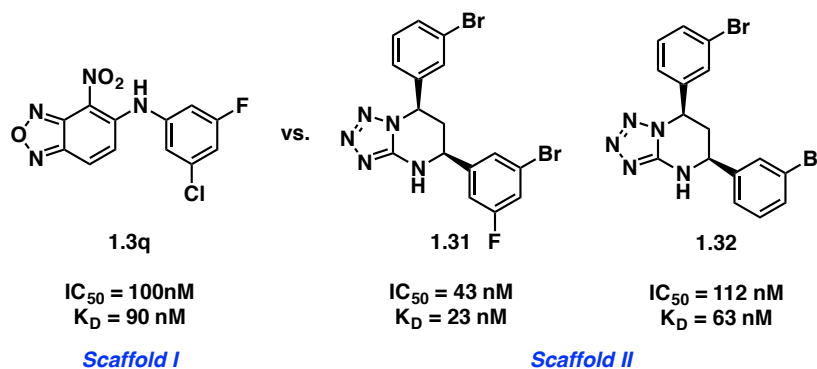
1.3.1 Identification of Scaffold II Allosteric Inhibitors of HIF-2 α

With the completion of our synthetic studies on scaffold I small molecule antagonists of HIF-2 α , we endeavored to identify and optimize a more potent second scaffold (hereafter referred to as scaffold II).²⁴ Upon further review of lead compounds from the original high throughput screen of >200,000 small molecules, tetrazolo-tetrahydropyrimidine-based hits stood out for several reasons (Scaffold II, Figure 1.3.1). First, tetrazolo-tetrahydropyrimidines have been shown to possess biological activity in

other biological settings.^{28,29} Secondly, while the nitro functionality in scaffold I proved to be necessary for activity, it also posed pharmacokinetic disadvantages that are averted in this second scaffold. Additionally, tetrazole moieties increase compound solubility and have been widely studied as pharmacophores for carboxylic acids.^{30,31} Finally, these compounds are unique in that they are chiral molecules and thus may prove to exhibit interesting selectivity.

After an extensive library screen, tetrazolo-tetrahydropyrimidine **1.31** was identified as the most potent inhibitor of HIF-2 α -HIF- β heterodimerization. Furthermore, our studies revealed stereo-preferential binding of this compound, where (S,R)-**1.31** alone presented inhibitory activity (IC_{50} = 43 nM, K_D = 23 nM) and (R,S)-**1.31** was entirely inactive (IC_{50} = >30,000 nM, K_D = >>2,000 nM).

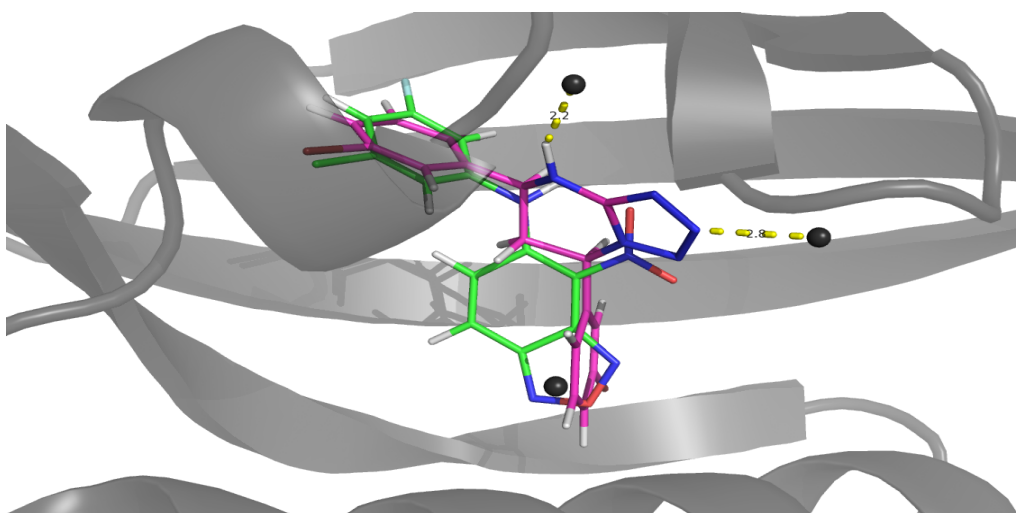
Figure 1.3.1



Co-crystal structures of dibromo-substituted analogue (S,R)-**1.32** bound within the HIF-2 PAS-B* cavity were instrumental in defining the absolute stereochemistry of the active enantiomeric series and providing insight into the structural features that govern binding affinity. Comparison of ternary complex (S,R)-**1.32**-HIF-2 PAS-B* to **1.3q**-HIF-2 Pas-B* revealed that both small molecule scaffolds bind within the same pocket of the PAS-B domain and share many structural similarities as well as some dissimilarities that may account for the enhanced binding witnessed with scaffold II (Figure 1.3.2).

Most notably, the C-ring of (S,R)-**1.32** was shown to occupy the same binding pocket as the A-ring of **1.3q**, but lays perpendicular in comparison. This change in orientation forces the *meta*-bromo substituent of the C-ring within close proximity to the V302 residue of the cavity allowing for a stabilizing halogen bond with the backbone carbonyl. Altogether, these binding interactions observed with (S,R)-**1.32**-HIF-2 PAS-B* lead to a series of conformational changes within the binding domain, allowing for an expanded internal cavity 40-65% larger in volume than that seen with scaffold I inhibitors and increasing the disruption of important intermolecular contacts with the HIF- β PAS-B domain.

Figure 1.3.2

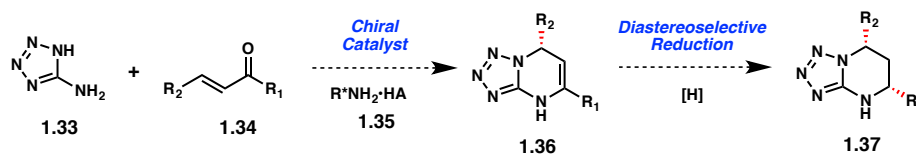


1.3.2 Strategy for the Enantioselective Synthesis of Scaffold II Analogues

Based on our studies of diaryl-tetrazolo-tetrahydropyrimidine antagonists of HIF-2 α , which revealed a stereoselective mode of binding within the HIF-2 α PAS-B internal cavity, we became interested in developing an efficient and cost-effective method of accessing these chiral ligands as a single enantiomer. To this aim, we hypothesized that

the coupling of 5-aminotetrazole (**1.33**) with the requisite chalcones (**1.34**) could be rendered enantioselective through the use of an acid and chiral amine combined catalyst system (**1.35**, Scheme 1.3.1). A subsequent diastereoselective reduction by sodium borohydride would furnish the corresponding diaryl-tetrazolo-tetrahydropyrimidines **1.37**, thus representing the first enantioselective path to these products.

Scheme 1.3.1



In general, chiral aza-heterocycles have become prevalent architectures in bioactive small molecules, however the syntheses of these compounds are often inefficient or not environmentally benign.³²⁻³⁴ The development of organocatalytic strategies to access such scaffolds preclude the use of transition metals and offer relatively mild conditions that accommodate a wide variety of functionality.

More specifically, since the seminal study by Chen et al. in 2007 detailing the application of primary amine cinchona-derived catalysts in the asymmetric Michael-type Friedel-Crafts alkylation of indoles with enones, cinchona-based amines have become privileged catalysts for the activation of ketones and enones.³⁵⁻³⁸ Subsequent to Chen's initial study, several groups have published on the use of cinchona-based amine catalysts in conjunction with an achiral acid to enable enantioselective Michael additions for the construction of aza-heterocycles.³⁹⁻⁴³ The synthesis of such complex molecular scaffolds from simple, achiral precursors showcases both the efficiency and power of this catalyst system.

1.3.3 Progress Toward an Asymmetric Tandem Aza-Michael Addition/Cyclocondensation

We began our studies looking at the tandem aza-Michael addition-cyclocondensation of 5-aminotetrazole (**1.33**) with trans-chalcone (**1.31**) to form dihydropyrimidine **1.32**. Because (\pm)-**1.39** was found to be substantially insoluble in most organic solvents, therefore complicating product analysis, a modified single-flask operation was developed to convert **1.39** to the slightly more soluble tetrahydropyrimidine **1.33** *in situ*. Our preliminary findings are detailed in Table 1.3.1 below.

In the absence of any catalyst we failed to see significant product formation over the course of one day, even at elevated temperatures (entry 1). Quinine-based amine **1.41** (10 mol%) and BINOL-based phosphoric acid (R)-**1.42a** (20 mol%) were chosen as the starting point for the cooperative-catalyst screen based on their precedent as a synergistic catalyst system for enantioselective enone functionalization.⁴⁴⁻⁴⁶ To our delight, product **1.40** was formed in 68% yield and 67:33 enantiomeric ratio (er) (entry 2). Switching the acid from (R)-**1.42a** to (S)-**1.42a** produced **1.40** in elevated yield but slightly diminished er (entry 3). Interestingly, the product was generated as the same major enantiomer regardless of the identity of the phosphoric acid co-catalyst. This observation prompted us to examine achiral phosphoric acid **1.42b** under the reaction conditions. Again, tetrahydropyrimidine **1.40** was accessed in comparable yield and enantiomeric ratio, indicating that enantioface selectivity is predominantly derived from the amine catalyst (entry 4). Furthermore, the absence of a matched/mismatched catalyst pair suggests a mechanism in which the acid's role as a catalyst is dependent on its pK_a rather than sterics.

Table 1.3.1

Entry	Amine 1.41	Acid Co-Catalyst	% Yield ^a	er
1	–	–	< 5	–
2	10 mol%	(R)- 1.42a (20 mol%)	68	67:33
3	10 mol%	(S)- 1.42a (20 mol%)	86	61:39
4	10 mol%	1.42b (20 mol%)	77	64:36
5	–	1.42b (20 mol%)	22 ^b	–
6	10 mol%	–	61	50:50

1.41

(R)-**1.42a**

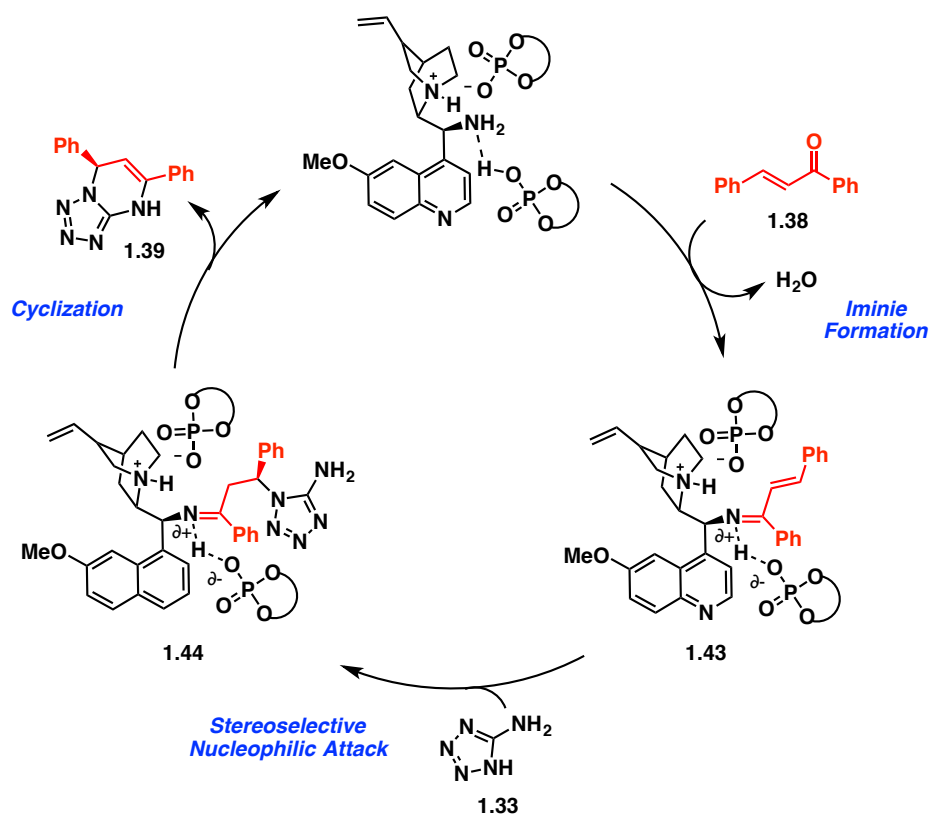
(S)-**1.42a**

1.42b

[a] Two step yield, [b] One step ¹H-NMR yield with DMB as the internal standard

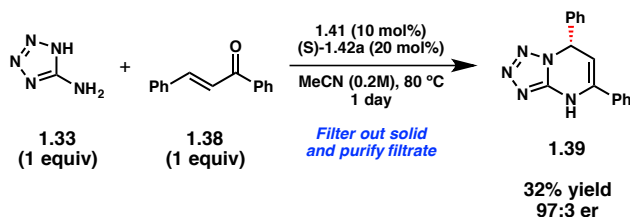
To confirm that this process relies on a dual catalytic system, we ran the reaction with each catalyst independently (entries 5 and 6). In the absence of amine **1.41** product was formed in greatly diminished yield. Interestingly, while yield wasn't dramatically affected in the absence of acid, the product was isolated as a racemate. These findings altogether support the proposed mechanism shown below (Scheme 1.3.2) in which the achiral acid forms a contact ion-pair network with imine intermediate **1.34**.⁴⁷ The resulting ionic-network controls the stereofacial selectivity of nucleophilic attack of the 5-aminotetrazole (**1.33**) into the imine intermediate. Subsequent cycloaddition initiated by a second nucleophilic attack of the primary amine into the imine of **1.35** affords the desired product **1.39**.

Scheme 1.3.2



While the optimization of this reaction remains in progress, our goal to access these dihydropyrimidine products with enantiopurity suited for biological analysis was made possible through recrystallization efforts (Scheme 1.3.3). The aforementioned insolubility of cycloadduct **1.39** arises from the formation of densely packed crystal structures of racemic compound. Conversely, enantiopure **1.39** exhibits markedly higher solubility and remains in solution. This characteristic is similarly exhibited by proline and has been studied extensively.^{48,49} As a result, **1.39** has been obtained in up to 97:3 er (32% overall yield) by simply taking advantage of this solubility difference and filtering out the racemate in CH_2Cl_2 .

Scheme 1.3.3



1.3.4 Conclusions

Inspired by the stereospecific mode of action exhibited by diaryl-tetrazolo-tetrahydropyrimidine-based HIF-2 antagonists, we have identified a potential co-catalyst system for the asymmetric organocatalytic aza-Michael/cyclocondensation cascade between 5-aminotetrazole and trans-chalcone. This reaction involves a synergistic combination of cinchona alkaloid-based primary amine and acid catalysts. While the enantioselectivity of this reaction as it currently stands remains modest, enantioenrichment through recrystallization has afforded the product in up to 97:3 er.

1.4 Experimental

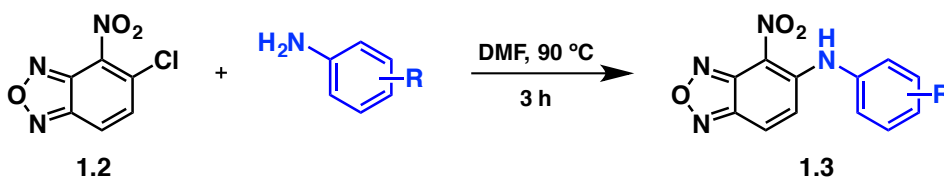
1.4.1 Materials and Methods

All reactions were carried out under an atmosphere of nitrogen in flame-dried glassware with magnetic stirring unless otherwise indicated. Commercially obtained reagents were used as received. Liquids and solutions were transferred via syringe. ^1H and ^{13}C NMR spectra were recorded on a Varian Inova (500 MHz ^1H frequency), or a Varian NMR system (400 MHz or 600 MHz ^1H frequency). Data for ^1H NMR spectra are reported relative to chloroform as an internal standard (7.26 ppm) or acetone (2.05 ppm)

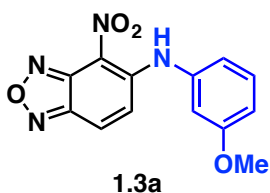
or DMSO (2.54 ppm) and are reported as follows: chemical shift (*d* ppm), multiplicity, coupling constant (Hz), and integration. Data for ^{13}C NMR spectra are reported relative to chloroform as an internal standard (77.2 ppm) or acetone (29.9 ppm) and are reported in terms of chemical shift (*d* ppm). Mass Spectrometry data were obtained on an Agilent 1100 Series LCMS system, which was also used to monitor the progress of reactions. Isothermal calorimetry data was acquired using a Microcal VP calorimeter.

1.4.2 Preparative Procedures

Synthesis of Aniline Derivatives 1.3a-q:



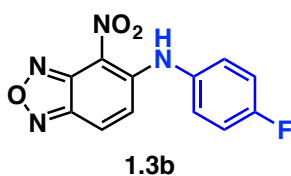
A flame-dried reaction vial was charged with benzoxadiazole **1.2** (50 mg, 0.25 mmol) and anhydrous DMF (1.5 mL). The mixture was treated with an aniline (0.25 mmol) and stirred at 90 °C for 3 h. After cooling to room temperature, the reaction was then diluted with ethyl acetate (5 mL) and washed with water (3 x 5 mL). The combined aqueous layers were extracted with ethyl acetate (2 x 5 mL). The combined organic layers were washed with brine (10 mL), dried over MgSO_4 , and concentrated under reduced pressure. The resulting powder was recrystallized from 30% ethyl acetate in hexanes to provide crystals of the desired aniline derivative.



1.3a: Following the typical procedure for the synthesis of aniline derivatives with *m*-anisidine, recrystallization provided yellow crystals of the desired product **1.3a** (50.1 mg, 70% yield):

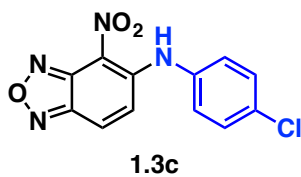
^1H NMR (400 MHz, Acetone- d_6) δ 8.10 (d, $J = 9.9$ Hz, 1H), 7.50 (m, 2H), 7.14 (dd, $J = 2.1$ Hz, 2.1 Hz, 1H), 7.08 (m, 2H), 3.87 (s, 3H) ^{13}C NMR (100 MHz, Acetone- d_6) δ 160.9, 146.9, 145.1, 141.3, 130.6, 130.6, 130.1, 126.1, 123.8, 120.7, 118.5, 93.8, 55.1.

LCMS (ESI) calc'd for $[\text{C}_{13}\text{H}_9\text{N}_4\text{O}_4]^- ([\text{M}-\text{H}]^-)$: m/z 285.1, found 285.0.



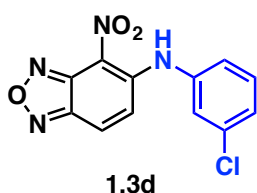
1.3b: Following the typical procedure for the synthesis of aniline derivatives with 4-fluoroaniline, recrystallization provided orange crystals of the desired product **1.3b** (60.9 mg, 88% yield):

^1H NMR (400 MHz, Acetone- d_6) δ 11.73 (bs, 1H), 8.08 (d, $J = 9.9$ Hz, 1H), 7.60 (m, 2H), 7.44 (d, $J = 9.9$ Hz, 1H), 7.38 (m, 2H) ^{13}C NMR (100 MHz, Acetone- d_6) δ 163.0 (d, $J = 252.0$ Hz), 150.3, 147.8, 146.2, 130.0 (d, $J = 8.9$ Hz), 127.2, 127.1, 125.3, 117.6 (d, $J = 23.0$ Hz), 108.8. LCMS (ESI) calc'd for $[\text{C}_{12}\text{H}_6\text{FN}_4\text{O}_3]^- ([\text{M}-\text{H}]^-)$: m/z 273.0, found 273.0.



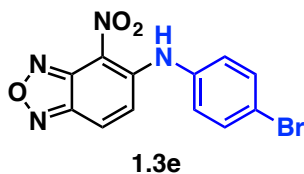
1.3c: Following the typical procedure for the synthesis of aniline derivatives with 4-chloroaniline, recrystallization provided orange crystals of the desired product **1.3c** (36.6 mg, 51% yield):

^1H NMR (400 MHz, Acetone- d_6) δ 11.7 (bs, 1H), 8.10 (d, $J = 9.9$ Hz, 1H), 7.6 (m, 4H), 7.50 (d, $J = 9.9$ Hz, 1H) ^{13}C NMR (100 MHz, Acetone- d_6) δ 147.8, 146.2, 142.3, 134.3, 131.2, 131.2 130.9, 129.4, 127.2, 125.3. LCMS (ESI) calc'd for $[\text{C}_{12}\text{H}_6\text{ClN}_4\text{O}_3]^-$ ([M-H]): m/z 289.0, found 289.0.



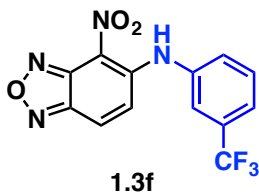
1.3d: Following the typical procedure for the synthesis of aniline derivatives with 3-chloroaniline, recrystallization provided yellow crystals of the desired product **1.3d** (54.4 mg, 75% yield):

^1H NMR (400 MHz, Acetone- d_6) δ 11.7 (bs, 1H), 8.12 (d, $J = 9.9$ Hz, 1H), 7.65 (m, 1H), 7.61 (d, $J = 9.9$ Hz, 1H), 7.65 (m, 1H), 7.61 (d, $J = 7.9$ Hz, 1H), 7.52 (m, 3H) ^{13}C NMR (100 MHz, Acetone- d_6) δ 148.5, 146.9, 145.1, 138.4, 138.3, 134.7, 131.3, 128.1, 126.7, 126.3, 125.3, 124.3. LCMS (ESI) calc'd for $[\text{C}_{12}\text{H}_6\text{ClN}_4\text{O}_3]^-$ ([M-H]): m/z 289.0, found 289.0.



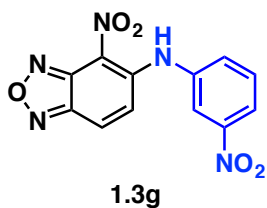
1.3e: Following the typical procedure for the synthesis of aniline derivatives with 4-bromoaniline, recrystallization provided orange crystals of the desired product **1.3e** (55.5 mg, 67% yield):

^1H NMR (400 MHz, Acetone- d_6) δ 11.7 (bs, 1H), 8.10 (d, $J = 9.9$ Hz, 1H), 7.77 (d, $J = 8.8$ Hz, 2H), 7.52 (m, 3H) ^{13}C NMR (100 MHz, Acetone- d_6) δ 147.8, 146.0, 134.0, 133.0, 127.4, 127.4, 127.3, 125.3, 124.8, 122.1 LCMS (ESI) calc'd for $[\text{C}_{12}\text{H}_6\text{BrN}_4\text{O}_3]^-$ ($[\text{M}-\text{H}]^-$): m/z 333.0, found 333.0.



1.3f: Following the typical procedure for the synthesis of aniline derivatives with 3-trifluoromethyl aniline, recrystallization provided yellow crystals of the desired product **1.3f** (43.8 mg, 54% yield):

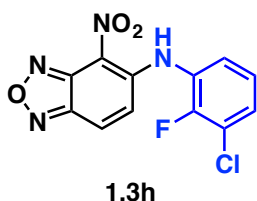
^1H NMR (400 MHz, Acetone- d_6) δ 11.80 (bs, 1H), 8.10 (d, $J = 9.8$ Hz, 1H), 7.95 (s, 1H), 7.87 (m, 1H), 7.84 (m, 2H), 7.53 (d, $J = 9.8$ Hz, 1H). ^{13}C NMR (100 MHz, Acetone- d_6) δ 148.8, 146.8, 145.1, 137.9, 131.6 (q, $J = 32.5$ Hz), 131.0, 130.7, 126.1, 124.7 (q, $J = 3.8$ Hz), 124.4, 123.8 (q, $J = 271$ Hz), 123.7 (q, $J = 3.9$ Hz), 120.0 LCMS (ESI) calc'd for $[\text{C}_{13}\text{H}_6\text{F}_3\text{N}_4\text{O}_3]^-$ ($[\text{M}-\text{H}]^-$): m/z 323.0, found 323.0.



1.3g: Following the typical procedure for the synthesis of aniline derivatives with 3-nitroaniline, recrystallization provided red crystals of the desired product **1.3g** (45.9 mg, 61% yield):

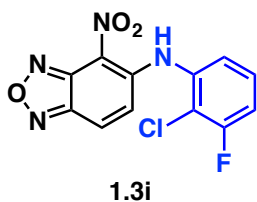
^1H NMR (400 MHz, Acetone- d_6) δ 11.81 (bs, 1H), 8.47 (dd, $J = 2.1$ Hz, 2.1 Hz, 1H), 8.34 (d, $J = 8.2$ Hz, 1H), 8.13 (d, $J = 9.9$ Hz, 1H), 8.04 (d, $J = 9.0$ Hz, 1H), 7.90 (dd, $J = 8.1$

Hz, 8.1 Hz, 1H), 7.60 (d, $J = 9.8$ Hz, 1H). ^{13}C NMR (100 MHz, Acetone- d_6) δ 146.9, 145.7, 138.3, 133.0, 131.1, 128.3, 126.2, 124.8, 124.5, 123.3, 122.6, 121.8. LCMS (ESI) calc'd for $[\text{C}_{12}\text{H}_6\text{N}_5\text{O}_5]^-$ ($[\text{M}-\text{H}]^-$): m/z 300.0, found 300.0.



1.3h: Following the typical procedure for the synthesis of aniline derivatives with 3-chloro-2-fluoroaniline, recrystallization provided yellow crystals of the desired product **1.3h** (51.3 mg, 67% yield):

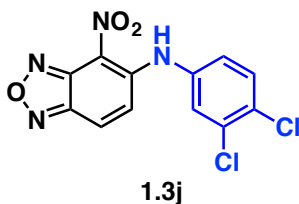
^1H NMR (400 MHz, Acetone- d_6) δ 11.5 (bs, 1H), 8.15 (d, $J = 9.9$ Hz, 1H), 7.67 (m, 2H), 7.46 (m, 2H). ^{13}C NMR (100 MHz, Acetone- d_6) δ 153.5 (d, $J = 249.0$ Hz), 147.9, 146.0, 135.1, 131.5, 129.0, 127.0, 127.0, 126.7 (d, $J = 5.2$ Hz), 125.7, 122.7 (d, $J = 16.3$ Hz), 96.0. LCMS (ESI) calc'd for $[\text{C}_{12}\text{H}_5\text{ClFN}_4\text{O}_3]^-$ ($[\text{M}-\text{H}]^-$): m/z 307.0, found 307.0.



1.3i: Following the typical procedure for the synthesis of aniline derivatives with 2-chloro-3-fluoroaniline, recrystallization provided yellow crystals of the desired product **1.3i** (50.4 mg, 66% yield):

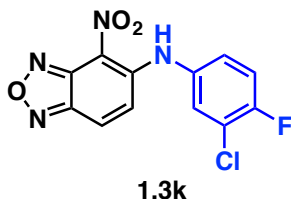
^1H NMR (400 MHz, Acetone- d_6) δ 11.6 (bs, 1H), 8.15 (d, $J = 9.9$ Hz, 1H), 7.60 (m, 2H), 7.50 (ddd, $J = 1.6$ Hz, 8.8 Hz, 8.8 Hz, 1H), 7.39 (dd, $J = 2.7$ Hz, 9.8 Hz, 1H). ^{13}C NMR (100 MHz, Acetone- d_6) δ 158.9 (d, $J = 248.0$ Hz), 148.4, 146.9, 145.0, 136.2, 136.1, 129.0 (d, $J = 9.1$ Hz), 126.8, 126.0, 124.7 (d, $J = 4.2$ Hz), 118.8 (d, $J = 18.5$ Hz), 116.4

(d, $J = 21.1$ Hz) LCMS (ESI) calc'd for $[\text{C}_{12}\text{H}_5\text{ClFN}_4\text{O}_3]^-([\text{M-H}]^-)$: m/z 307.0, found 307.0.



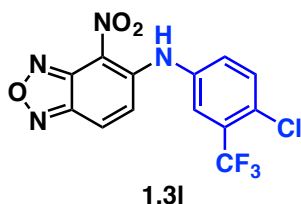
1.3j: Following the typical procedure for the synthesis of aniline derivatives with 3,4-dichloroaniline, recrystallization provided yellow crystals of the desired product **1.3j** (51.2 mg, 63% yield):

^1H NMR (400 MHz, Acetone- d_6) δ 11.7 (bs, 1H), 8.13 (d, $J = 9.9$ Hz, 1H), 7.84 (d, $J = 2.4$ Hz, 1H), 7.79 (d, $J = 8.6$ Hz, 1H), 7.59 (m, 2H). ^{13}C NMR (100 MHz, Acetone- d_6) δ 149.6, 147.9, 146.1, 138.0, 133.8, 132.6, 132.3, 129.8, 127.9, 127.3, 125.3, 107.9. LCMS (ESI) calc'd for $[\text{C}_{12}\text{H}_5\text{Cl}_2\text{N}_4\text{O}_3]^-([\text{M-H}]^-)$: m/z 323.0, found 323.0.



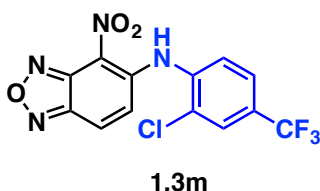
1.3k: Following the typical procedure for the synthesis of aniline derivatives with 3-chloro-4-fluoroaniline, recrystallization provided yellow crystals of the desired product **1.3k** (42.3 mg, 55% yield):

^1H NMR (400 MHz, Acetone- d_6) δ 11.68 (bs, 1H), 8.09 (d, $J = 9.9$ Hz, 1H), 7.96 (s, 1H), 7.80 (dd, $J = 2.3$ Hz, 6.7 Hz, 1H), 7.60 (m, 1H), 7.55 (m, 2H). ^{13}C NMR (100 MHz, Acetone- d_6) δ 162.5, 158.0 (d, $J = 250.0$ Hz), 149.7, 147.4, 145.7, 134.7, 130.0, 128.4 (d, $J = 7.7$ Hz), 126.9, 125.0, 121.9 (d, $J = 19.0$ Hz), 118.4 (d, $J = 18.4$ Hz). LCMS (ESI) calc'd for $[\text{C}_{12}\text{H}_5\text{ClFN}_4\text{O}_3]^-([\text{M-H}]^-)$: m/z 307.0, found 307.0.



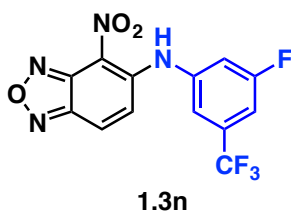
1.3l: Following the typical procedure for the synthesis of aniline derivatives with 4-chloro-3-trifluoromethylaniline, recrystallization provided orange crystals of the desired product **1.3l** (33.6 mg, 38% yield):

^1H NMR (400 MHz, Acetone- d_6) δ 11.73 (bs, 1H), 8.13 (d, $J = 9.9$ Hz, 1H), 8.08 (s, 1H), 7.89 (d, $J = 1.4$ Hz, 1H), 7.62 (d, $J = 9.9$ Hz, 1H), ^{13}C NMR (100 MHz, Acetone- d_6) δ 147.9, 146.0, 138.7, 137.5, 134.0, 133.0, 131.6 (q, $J = 1.9$ Hz), 129.8 (q, $J = 31.6$ Hz), 127.4 (q, $J = 5.2$ Hz), 122.3, 125.3, 123.6 (q, $J = 247.2$ Hz), 120.9. LCMS (ESI) calc'd for $[\text{C}_{13}\text{H}_5\text{ClF}_3\text{N}_4\text{O}_3]^-$ ($[\text{M}-\text{H}]^-$): m/z 357.0, found 357.0.



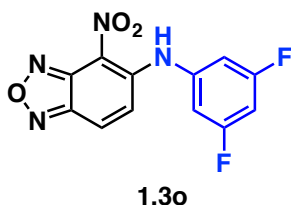
1.3m: Following the typical procedure for the synthesis of aniline derivatives with 2-chloro-4-trifluoromethyl aniline, purification by flash chromatography on silica gel (20% ethyl acetate in hexanes) provided the desired product **1.3m** as an orange powder (67.1 mg, 75% yield)

^1H NMR (400 MHz, Acetone- d_6) δ 9.44 (bs, 1H), 8.68 (d, $J = 8.8$ Hz, 1H), 8.59 (s, 1H), 7.94 (dd, $J = 6.8$ Hz, 8.5 Hz, 1H), 7.84 (s, 1H), 7.71 (d, $J = 8.7$ Hz, 1H). ^{13}C NMR (100 MHz, Acetone- d_6) δ 146.9, 145.0, 138.2, 131.8, 127.7 (q, $J = 3.9$ Hz), 126.3 (q, $J = 3.5$ Hz), 126.2 (q, $J = 278.0$ Hz), 126.0, 125.5 (q, $J = 5.1$ Hz), 124.8 (q, $J = 3.7$ Hz), 124.8, 121.6, 121.5. LCMS (ESI) calc'd for $[\text{C}_{13}\text{H}_5\text{ClF}_3\text{N}_4\text{O}_3]^-$ ($[\text{M}-\text{H}]^-$): m/z 357.0, found 357.0.



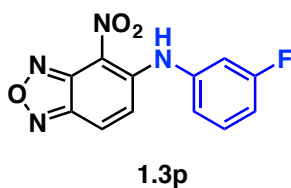
1.3n: Following the typical procedure for the synthesis of aniline derivatives with 3-fluoro-5-trifluoromethylaniline, recrystallization provided orange crystals of the desired product **1.3n** (13.4mg, 26% yield):

^1H NMR (400 MHz, Acetone- d_6) δ 11.67 (bs, 1H), 8.16 (d, $J = 9.9$ Hz, 1H), 7.84 (s, 1H), 7.77 (ddd, $J = 2.2$ Hz, 2.2 Hz, 9.3 Hz, 1H), 7.66 (d, $J = 9.8$ Hz, 1H), 7.66 (d, $J = 8.5$ Hz, 1H). ^{13}C NMR (100 MHz, Acetone- d_6) δ 163.0 (d, $J = 260$ Hz), 148.2, 146.9, 145.0, 140.0 (d, $J = 11.6$ Hz), 138.1 (q, $J = 268.8$ Hz), 133.0, 126.4, 124.5, 121.8 (d $J = 3.2$ Hz), 119.9 (dq, $J = 3.4, 3.7$ Hz), 118.0 (d, $J = 23.8$ Hz), 112.1 (dq, $J = 3.7$ Hz, 30.0 Hz). LCMS (ESI) calc'd for $[\text{C}_{13}\text{H}_5\text{F}_4\text{N}_4\text{O}_3]^-$ ($[\text{M}-\text{H}]^-$): m/z 341.0, found 341.0.



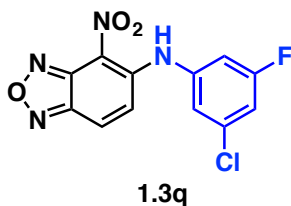
1.3o: Following the typical procedure for the synthesis of aniline derivatives with 3,5-difluoroaniline, recrystallization provided orange crystals of the desired product **1.3o** (52.6 mg, 72% yield):

^1H NMR (400 MHz, Acetone- d_6) δ 11.65 (bs, 1H), 8.15 (d, $J = 9.8$ Hz, 1H), 7.66 (dd, $J = 3.1$ Hz, 9.9 Hz, 1H), 7.32 (d, $J = 5.8$ Hz, 2H), 7.18 (ddd, $J = 2.4$ Hz, 2.4 Hz, 9.9 Hz, 1H), ^{13}C NMR (100 MHz, Acetone- d_6) δ 163.5 (d, $J = 243.9$ Hz), 163.3 (d, $J = 246.7$ Hz), 148.3, 146.9, 145.0, 139.7 (dd, $J = 12.7$ Hz, 13.0 Hz), 126.4, 124.5, 110.3 (d, $J = 27.8$ Hz), 110.3 (d, $J = 11.4$ Hz), 103.3 (dd, $J = 18.0$ Hz, 33.0 Hz), 94.9. LCMS (ESI) calc'd for $[\text{C}_{12}\text{H}_5\text{F}_2\text{N}_4\text{O}_3]^-$ ($[\text{M}-\text{H}]^-$): m/z 291.0, found 291.0.



1.3p: Following the typical procedure for the synthesis of aniline derivatives with 3-fluoroaniline, recrystallization provided yellow crystals of the desired product **1.3p** (25.3 mg, 37% yield):

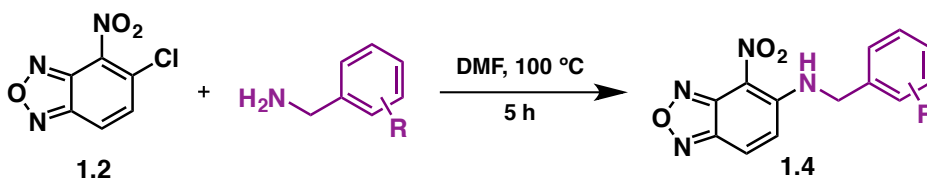
^1H NMR (400 MHz, Acetone- d_6) δ 11.7 (bs, 1H), 8.12 (d, $J = 9.8$ Hz, 1H), 7.65 (dd, $J = 7.2$ Hz, 8.0 Hz, 1H), 7.55 (d, 1H, $J = 9.9$ Hz), 7.41 (d, $J = 7.2$ Hz, 2H), 7.29 (ddd, $J = 2.2$ Hz, 8.7 Hz, 8.7 Hz, 1H), ^{13}C NMR (100 MHz, Acetone- d_6) δ 164.1 (d, $J = 245.0$ Hz), 149.7, 149.7, 147.8, 146.1, 132.5 (d, $J = 9.3$ Hz), 131.6, 127.2, 125.3, 123.6 (d, $J = 3.1$ Hz), 115.9 (d, 21.1 Hz), 114.9 (d, 23.8 Hz). LCMS (ESI) calc'd for $[\text{C}_{12}\text{H}_6\text{FN}_4\text{O}_3]^-$ ([M-H] $^-$): m/z 273.0, found 273.0.



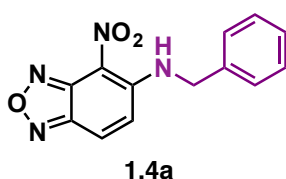
1.3q: Following the typical procedure for the synthesis of aniline derivatives with 3-chloro-5-fluoroaniline, recrystallization provided yellow crystals of the desired product **1.3q** (436.6 mg, 81% yield):

^1H NMR (400 MHz, CDCl_3) δ 11.52 (bs, 1H), 7.97 (d, $J = 9.8$ Hz, 1H), 7.35 (d, $J = 9.8$ Hz, 1H), 7.21 (ddd, $J = 1.9$ Hz, 8.1 Hz, 1H), 7.16 (bs, 1H), 6.99 (ddd, $J = 1.9$ Hz, 8.1, 1H). ^{13}C NMR (100 MHz, CDCl_3) δ 163.2 (d, $J = 253.0$ Hz), 147.6, 146.6, 144.7, 141.1, 138.3, 137.2 (d, $J = 10.7$ Hz), 125.5, 124.5, 122.4 (d, $J = 3.6$ Hz), 116.8 (d, $J = 24.4$ Hz), 112.0 (d, $J = 26.5$ Hz). LCMS (ESI) calc'd for $[\text{C}_{12}\text{H}_5\text{ClFN}_4\text{O}_3]^-$ ([M-H] $^-$): m/z 307.0, found 307.0.

Synthesis of Benzylamine Derivatives 1.4a-i:

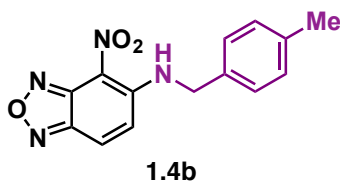


A flame-dried flask was charged with benzoxadiazole **1.2** (50 mg, 0.25 mmol, 1 eq.), and the flask was degassed and purged with nitrogen. Anhydrous dimethylformamide (1.67 mL) and a benzylamine (0.25 mmol, 1 equiv) were added, and the mixture was heated to 100 °C with stirring for 5 h. After cooling to room temperature, the reaction mixture was diluted with water and washed with ethyl acetate (3x). The combined organic layers were washed with water (3x) followed by brine. The organic layers were then dried over MgSO₄ and concentrated under reduced pressure. The resulting solid was recrystallized in hexanes and ethyl acetate to afford the desired benzylamine derivative.



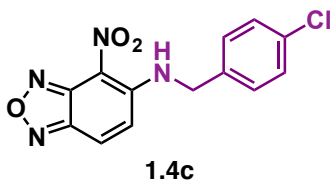
1.4a: Following the typical procedure for the synthesis of benzylamine derivatives with benzylamine, recrystallization provided crystals of the desired product **1.4a** (23 mg, 34% yield):

¹H NMR (400 MHz, Acetone-d₆) δ 8.11 (d, *J* = 9.9 Hz, 1H), 7.72 (d, *J* = 9.9 Hz, 1H), 7.50 (d, *J* = 7.5 Hz, 2H), 7.42 (t, *J* = 7.3 Hz, 2H), 7.34 (t, *J* = 7.4 Hz, 1H), 5.14 (d, *J* = 6.1 Hz, 2H); ¹³C NMR (100 MHz, Acetone-d₆) δ 151.6, 147.2, 146.1, 138.0, 129.9, 128.7, 128.0, 126.0, 125.5, 125.5, 48.1; LCMS (ESI) calc'd for [C₁₃H₉N₄O₃]⁺ ([M-H]⁺): *m/z* 269.1, found 269.1.



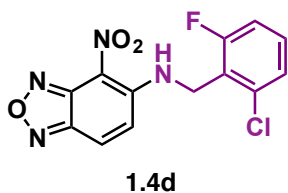
1.4b: Following the typical procedure for the synthesis of benzylamine derivatives with 4-methylbenzylamine, recrystallization provided crystals of the desired product **1.4b** (30 mg, 42% yield):

^1H NMR (400 MHz, Acetone- d_6) δ 8.10 (d, J = 10.0 Hz, 1H), 7.72 (d, J = 10.0 Hz, 1H), 7.38 (d, J = 7.9 Hz, 2H), 7.23 (d, J = 8.3 Hz, 2H), 5.08 (d, J = 6.0 Hz, 2H), 2.32 (s, 3H); ^{13}C NMR (100 MHz, Acetone- d_6) δ 151.6, 147.2, 146.11, 138.4, 135.0, 130.5, 128.1, 126.0, 126.0, 125.5, 48.0, 21.1; LCMS (ESI) calc'd for $[\text{C}_{14}\text{H}_{11}\text{N}_4\text{O}_3]^+([\text{M}-\text{H}]^+)$: m/z 283.1, found 283.1.



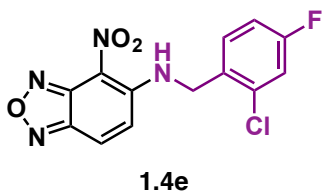
1.4c: Following the typical procedure for the synthesis of benzylamine derivatives with 4-chlorobenzylamine, recrystallization provided crystals of the desired product **1.4c** (32 mg, 41% yield):

^1H NMR (400 MHz, Acetone- d_6) δ 8.10 (d, J = 10.0 Hz, 1H), 7.69 (d, J = 9.9 Hz, 1H), 7.54 (d, J = 11.5 Hz, 2H), 7.43 (d, J = 8.5 Hz, 2H), 5.16 (d, J = 6.7 Hz, 2H); ^{13}C NMR (100 MHz, Acetone- d_6) δ 151.5, 147.2, 146.1, 137.1, 134.0, 129.8, 129.8, 129.8, 125.9, 125.6, 47.4; LCMS (ESI) calc'd for $[\text{C}_{13}\text{H}_8\text{ClN}_4\text{O}_3]^+([\text{M}-\text{H}]^+)$: m/z 303.0, found 303.0.



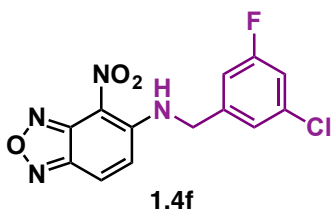
1.4d: Following the typical procedure for the synthesis of benzylamine derivatives with 2-chloro-6-fluorobenzylamine, recrystallization provided crystals of the desired product **1.4d** (31 mg, 38% yield):

^1H NMR (400 MHz, Acetone- d_6) δ 10.84 (bs, 1H), 8.26 (d, $J = 9.9$ Hz, 1H), 7.92 (d, $J = 9.9$ Hz, 1H), 7.52 (m, 1H), 7.43 (d, $J = 8.1$ Hz, 1H), 7.29 (t, $J = 9.7$ Hz, 1H), 5.24 (d, $J = 5.8$ Hz, 2H); ^{13}C NMR (100 MHz, Acetone- d_6) δ 162.3 (d, $J = 247.9$ Hz), 151.0, 147.2, 146.0, 135.9, 132.4 (d, $J = 10.0$ Hz), 129.2, 127.2 (d, $J = 3.4$ Hz), 126.1, 125.2 (d, $J = 2.6$ Hz), 123.1 (d, $J = 17.3$ Hz), 115.9 (d, $J = 22.6$ Hz), 40.2; LCMS (ESI) calc'd for $[\text{C}_{13}\text{H}_7\text{ClFN}_4\text{O}_3]^+([\text{M}-\text{H}]^+)$: m/z 321.0, found 321.0.



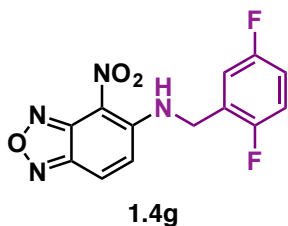
1.4e: Following the typical procedure for the synthesis of benzylamine derivatives with 2-chloro-4-fluorobenzylamine, recrystallization provided crystals of the desired product **1.4e** (25 mg, 31% yield):

^1H NMR (400 MHz, Acetone- d_6) δ 8.15 (d, $J = 9.9$ Hz, 1H), 7.70 (d, $J = 10.0$ Hz, 1H), 7.63 (dd, $J = 6.0$ Hz, 8.7 Hz, 1H), 7.42 (dd, $J = 2.6$ Hz, 8.6 Hz, 1H), 7.18 (dt, $J = 2.7$ Hz, 8.4 Hz, 1H), 5.19 (d, $J = 4.1$ Hz, 2H); ^{13}C NMR (100 MHz, Acetone- d_6) δ 163.0 (d, $J = 247.2$), 151.6, 151.4, 147.3, 146.1, 134.4 (d, $J = 10.6$ Hz), 131.7 (d, $J = 3.5$ Hz), 131.3 (d, $J = 9.0$ Hz), 125.8 (d, $J = 3.4$ Hz), 125.8, 118.0 (d, $J = 25.3$ Hz), 115.5 (d, $J = 21.2$ Hz), 45.7; LCMS (ESI) calc'd for $[\text{C}_{13}\text{H}_7\text{ClFN}_4\text{O}_3]^+([\text{M}-\text{H}]^+)$: m/z 321.0, found 321.0.



1.4f: Following the typical procedure for the synthesis of benzylamine derivatives with 3-chloro-5-fluorobenzylamine, recrystallization provided crystals of the desired product **1.4f** (38 mg, 47% yield):

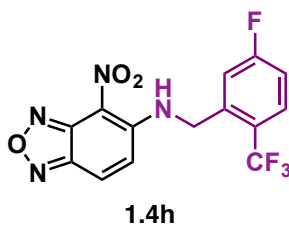
^1H NMR (400 MHz, Acetone- d_6) δ 10.95 (bs, 1H), 8.12 (d, $J = 9.9$ Hz, 1H), 7.68 (d, $J = 10.0$ Hz, 1H), 7.42 (s, 1H), 7.31 (dt, $J = 1.8$ Hz, 9.5 Hz, 1H), 7.22 (dt, $J = 2.1$ Hz, 8.6 Hz, 1H), 5.20 (d, $J = 6.5$ Hz, 2H); ^{13}C NMR (100 MHz, Acetone- d_6) δ 163.8 (d, $J = 247.4$ Hz), 151.5, 147.3, 146.1, 143.0 (d, $J = 8.0$ Hz), 136.0 (d, $J = 10.8$ Hz), 125.8, 125.7, 124.1, 124.1, 116.1 (d, $J = 25.1$ Hz), 113.7 (d, $J = 22.5$ Hz), 47.1; LCMS (ESI) calc'd for $[\text{C}_{13}\text{H}_7\text{ClFN}_4\text{O}_3]^- ([\text{M}-\text{H}]^-)$: m/z 321.0, found 321.0.



1.4g: Following the typical procedure for the synthesis of benzylamine derivatives with 2,5-difluorobenzylamine, recrystallization provided crystals of the desired product **1.4g** (9 mg, 11% yield):

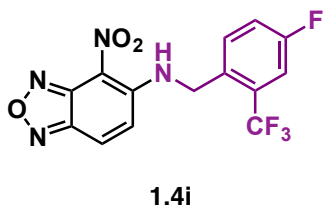
^1H NMR (400 MHz, Acetone- d_6) δ 8.16 (d, $J = 9.9$ Hz, 1H), 7.74 (d, $J = 9.9$ Hz, 1H), 7.35 (m, 1H), 7.28 (m, 1H), 7.17 (m, 1H), 5.21 (d, $J = 5.7$ Hz, 2H); ^{13}C NMR (100 MHz, Acetone- d_6) δ 159.8 (dd, $J = 2.3$ Hz, 245.2 Hz), 157.4 (dd, $J = 1.4$ Hz, 243.6 Hz), 151.5, 151.3, 147.3, 146.1, 127.2 (dd, $J = 7.5$ Hz, 17.1 Hz), 125.8, 125.6, 117.9 (dd, $J = 8.8$ Hz,

24.2 Hz), 116.9 (dd, $J = 8.8$ Hz, 24.3 Hz), 116.4 (dd, $J = 4.3$ Hz, 25.4 Hz), 42.2; LCMS (ESI) calc'd for $[C_{13}H_7F_2N_4O_3]^+([M-H]^+)$: m/z 305.1, found 305.0.



1.4h: Following the typical procedure for the synthesis of benzylamine derivatives with 5-fluoro-2-trifluoromethylbenzylamine, recrystallization provided crystals of the desired product **1.4h** (18.2 mg, 20% yield):

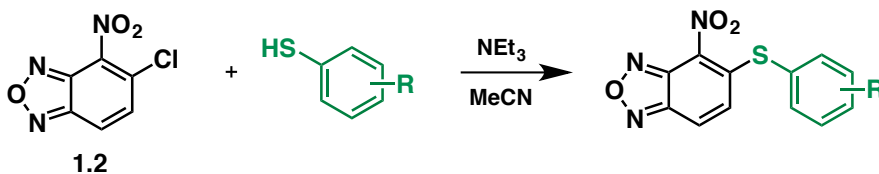
1H NMR (400 MHz, Acetone- d_6) δ 10.92 (bs, 1H), 8.15 (d, $J = 10.0$ Hz, 1H), 7.94 (dd, $J = 5.4$ Hz, 8.7 Hz, 1H), 7.56 (d, $J = 10.0$ Hz, 1H), 7.51 (d, $J = 10.0$ Hz, 1H), 7.34 (t, $J = 8.2$ Hz, 1H), 5.35 (d, $J = 6.3$ Hz, 2H); ^{13}C NMR (100 MHz, Acetone- d_6) δ 166.0 (d, $J = 250.7$ Hz), 151.6, 147.3, 146.2, 140.3 (dq, $J = 8.0, 4.0$ Hz), 130.4 (dq, $J = 9.6$ Hz, 5.9 Hz), 129.2, 125.8 (d, $J = 37$ Hz), 125.0 (q, $J = 246.3$ Hz), 121.5, 116.7 (d, $J = 24$ Hz), 115.8 (d, $J = 22$ Hz), 44.8; LCMS (ESI) calc'd for $[C_{14}H_7F_4N_4O_3]^+([M-H]^+)$: m/z 355.1, found 355.0.



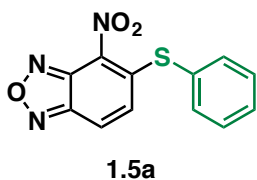
1.4i: Following the typical procedure for the synthesis of benzylamine derivatives with 4-fluoro-2-trifluoromethylbenzylamine, recrystallization provided crystals of the desired product **1.4i** (30 mg, 34% yield):

^1H NMR (400 MHz, Acetone- d_6) δ 10.89 (bs, 1H), 8.15 (d, J = 10 Hz, 1H), 7.79 (dd, J = 5.3 Hz, 8.8 Hz, 1H), 7.65 (dd, J = 2.8 Hz, 9.0 Hz, 1H), 7.60 (d, J = 9.9 Hz, 1H), 7.47 (dt, J = 2.8 Hz, 8.3 Hz, 1H), 5.31 (d, J = 6.1 Hz, 2H); ^{13}C NMR (100 MHz, Acetone- d_6) δ 162.6 (d, J = 246.1 Hz), 151.5, 147.3, 146.1, 142.9, 132.2 (d, J = 8.2 Hz), 131.8, 129.2, 128.6, 125.8 (d, J = 29.8 Hz), 120.6 (d, J = 21.3 Hz), 115.6 (q, J = 277.6 Hz), 115.1 (dq, J = 25.5 Hz, 5.8 Hz), 44.6; LCMS (ESI) calc'd for $[\text{C}_{14}\text{H}_7\text{F}_4\text{N}_4\text{O}_3]^-([\text{M}-\text{H}]^-)$: m/z 355.1, found 355.0.

Synthesis of Thiophenol Derivatives 1.5a-c:

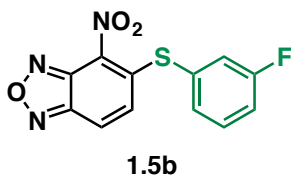


A flame-dried reaction vial was charged with benzoxadiazole **1.2** (50 mg, 0.25 mmol) and anhydrous CH_3CN (1.5 mL). The mixture was treated with a thiophenol (0.25 mmol) and triethylamine (25 mg, 0.25 mmol). The reaction was stirred at ambient temperature and monitored by LCMS. At the completion of the reaction, the solvent was removed under a stream of nitrogen gas. Purification by flash chromatography on silica gel (1:1 hexane:dichloromethane) provided the desired thiophenol derivative.



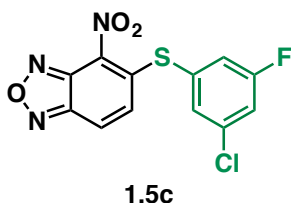
1.5a: Following the typical procedure for the synthesis of thiophenol derivatives with thiobenzene, purification by flash chromatography on silica gel provided the desired product **1.5a** as a yellow solid (42.5 mg, 58% yield):

^1H NMR (400 MHz, Acetone- d_6) δ 8.13 (d, J = 9.6 Hz, 1H), 7.78 (dd, J = 1.4 Hz, 7.8 Hz, 2H), 6.67 (m, 3H), 7.21 (d, J = 9.6 Hz, 1H). ^{13}C NMR (100 MHz, Acetone- d_6) δ 150.3, 149.2, 144.4, 135.5, 131.5, 131.3, 130.7, 129.3, 121.2, 98.8 LCMS (ESI) calc'd for $[\text{C}_{12}\text{H}_6\text{N}_3\text{O}_3\text{S}]^-$ ($[\text{M}-\text{H}]^-$): m/z 272.0, found 272.0.



1.5b: Following the typical procedure for the synthesis of thiophenol derivatives with 3-fluorothiobenzene, purification by flash chromatography on silica gel provided the desired product **1.5b** as a yellow solid (15.8 mg, 20% yield):

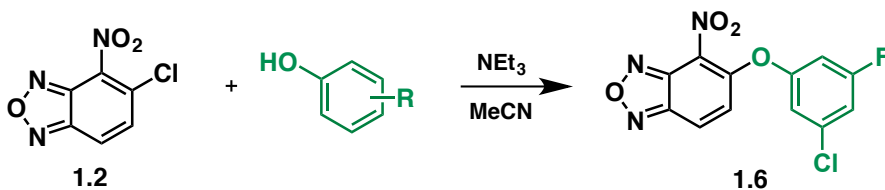
^1H NMR (400 MHz, Acetone- d_6) δ 8.15 (d, J = 9.6 Hz, 1H), 7.71 (m, 1H), 7.62 (m, 2H), 7.48 (m, 1H), 7.29 (d, J = 9.6 Hz, 1H) ^{13}C NMR (100 MHz, Acetone- d_6) δ 168.3 (d, J = 256.0 Hz), 154.6 (d, J = 22.5 Hz), 149.6, 137.6 (d, J = 8.4 Hz), 137.0, 136.8 (d, J = 3.2 Hz), 136.7, 128.2, 127.3 (d, J = 22.6 Hz), 126.6, 126.6, 123.5 (d, J = 21.0 Hz). LCMS (ESI) calc'd for $[\text{C}_{12}\text{H}_5\text{FN}_3\text{O}_3]^-$ ($[\text{M}-\text{H}]^-$): m/z 290.0, found 290.0.



1.5c: Following the typical procedure for the synthesis of thiophenol derivatives with 3-chloro-5-fluorothiobenzene, purification by flash chromatography on silica gel provided the desired product **1.5c** as a yellow solid (123.6 mg, 78% yield):

^1H NMR (400 MHz, Acetone- d_6) δ 7.84 (d, $J = 9.7$ Hz, 1H), 7.21 (d, $J = 9.8$ Hz, 1H), 6.96 (m, 2H), 6.80 (d, $J = 9.4$ Hz, 1H), 3.37 (s, 3H) ^{13}C NMR (100 MHz, Acetone- d_6) δ 163.0 (d, $J = 252$ Hz), 149.3, 148.6, 144.3, 136.4 (d, $J = 10.8$ Hz), 133.3 (d, $J = 8.9$ Hz), 132.1, 131.2 (d, $J = 3.5$ Hz), 122.3, 121.7, 121.0 ($J = 22.7$ Hz), 118.8 ($J = 24.9$ Hz) LCMS (ESI) calc'd for $[\text{C}_{12}\text{H}_6\text{ClFN}_3\text{O}_3\text{S}]^+([\text{M}+\text{H}]^+)$: m/z 326.0, found 326.0.

Synthesis of Phenol Derivative 1.6:

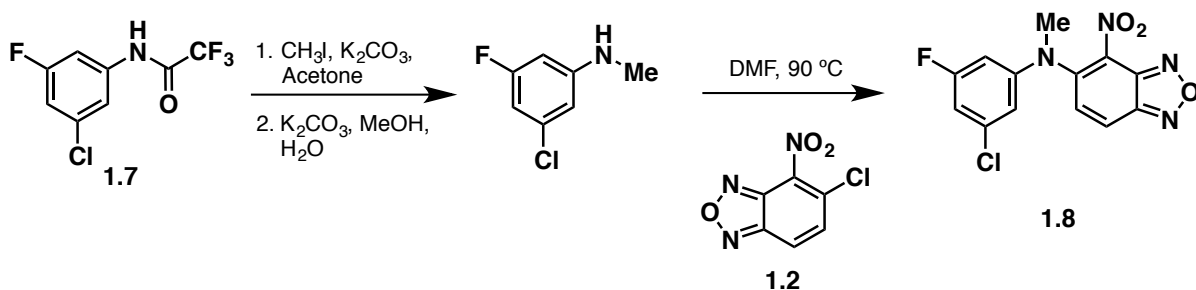


A flame-dried flask was charged with 3-chloro-5-fluorophenol (36.7 mg, 0.25 mmol, 1 equiv) and degassed and purged with nitrogen. The flask was treated with anhydrous CH_3CN (2.75 mL) and triethylamine (31.5 μL , 0.23 mmol, 0.9 equiv). The mixture was stirred for 30 min at room temperature and then treated with benzoxadiazole **1.2** (55.1 mg, 0.28 mmol, 1.1 equiv). The solution was stirred for 24 h and then diluted with ethyl acetate. The mixture was washed with water (3x) and brine. The organic layer was dried over MgSO_4 and concentrated under reduced pressure. The resulting solid was then

recrystallized in hexanes and dichloromethane to afford the product as a yellow solid (48 mg, 62% yield):

^1H NMR (400 MHz, Acetone- d_6) δ 8.44 (d, J = 9.7 Hz, 1H), 7.66 (d, J = 9.6 Hz, 1H), 7.31 (m, 1H), 7.26 (dt, J = 2.2 Hz, 8.5 Hz 1H), 7.23 (dt, J = 2.3 Hz, 9.4 Hz, 1H); ^{13}C NMR (100 MHz, Acetone- d_6) δ 164.2 (d, J = 248.6 Hz), 157.3 (d, J = 12.6 Hz), 153.8, 149.0, 145.4, 136.9 (d, J = 12.8 Hz), 128.9, 124.9, 116.78, 116.8, 114.3 (d, J = 25.1 Hz), 107.1 (d, J = 25.7 Hz); LCMS (ESI) calc'd for $[\text{C}_{12}\text{H}_5\text{ClFN}_3\text{O}_4]^-$ ($[\text{M}-\text{H}]^-$): m/z 309.00, found 309.2.

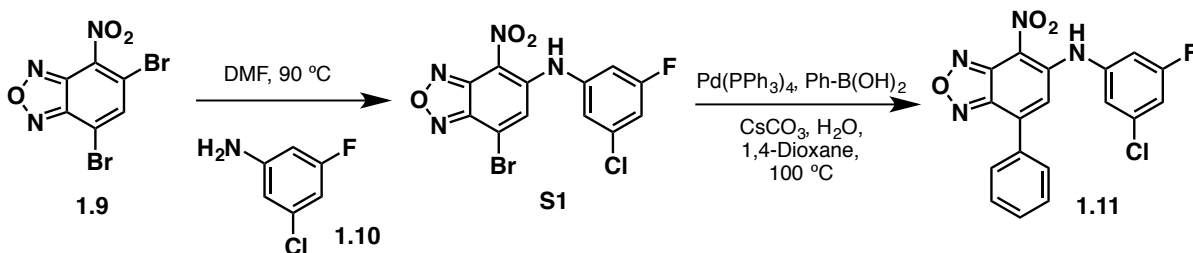
Synthesis of Analogs of Aniline 32



1.8: A solution trifluoroacetamide **1.7** in anhydrous acetone was sequentially treated with K_2CO_3 and methyl iodide. The reaction mixture was heated to reflux for 2 h and then filtered by vacuum filtration. The filtrate was concentrated under reduced pressure and dissolved in CH_2Cl_2 . The solution was washed with H_2O and brine, dried over MgSO_4 and concentrated under reduced pressure to yield a yellow solid (550 mg). The crude material was dissolved in 2:1 MeOH: H_2O (3 mL), and treated with potassium carbonate

(430 mg, 3.1 mmol). The reaction was stirred for 12 h and then diluted with CH_2Cl_2 . The mixture was washed with H_2O and brine, dried over MgSO_4 and concentrated under reduced pressure to provide the methyl aniline intermediate as a clear oil. This oil was dissolved in DMF (1.5 mL) and treated with benzoxadiazole **1.2** (79 mg, 0.39 mmol). After 4 h, the reaction mixture was diluted with ethyl acetate and washed repeatedly with H_2O . The organic layer was dried over MgSO_4 and concentrated under reduced pressure. The crude material was purified by flash chromatography on silica gel (20% ethyl acetate in hexanes) to provide aniline **1.8** as an orange solid (129 mg, 85 % yield):

^1H NMR (400 MHz, CDCl_3) δ 7.84 (d, J = 9.7 Hz, 1H), 7.21 (d, J = 9.8 Hz, 1H), 6.96 (m, 2H), 6.80 (d, J = 9.4 Hz, 1H), 3.37 (s, 3H) ^{13}C NMR (100 MHz, CDCl_3) δ 163.5 (d, J = 250.7 Hz), 147.1 (d, J = 11.3 Hz), 146.9, 145.3, 137.0 (d, J = 12.3 Hz), 131.5, 125.5, 124.5, 121.3 (d, J = 11.3 Hz), 119.1 (d, J = 3.3 Hz), 114.2 (d, J = 22.2 Hz), 108.9 (d, J = 24.3 Hz), 42.6. LCMS (ESI) calc'd for $[\text{C}_{13}\text{H}_9\text{ClFN}_4\text{O}_3]^-$ ($[\text{M}-\text{H}]^-$): m/z 323.0, found 323.0.



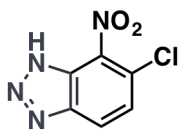
S1: Following the typical procedure for the synthesis of aniline derivatives with dibromo-4-nitrobenzoxadiazole **1.9**,⁵³ recrystallization provided crystals of 7-bromo-4-nitrobenzoxadiazole **S1** (35 mg, 44% yield):

^1H NMR (400 MHz, Acetone- d_6) δ 7.93 (s, 1H), 7.54 (s, 1H), 7.45 (d, J = 9.4 Hz, 1H), 7.40 (d, J = 8.6 Hz, 1H); ^{13}C NMR (100 MHz, Acetone- d_6) δ 164.0 (d, J = 249 Hz), 149.3, 148.2, 145.6, 140.4 (d, J = 11 Hz), 136.6 (d, J = 12 Hz), 129.3, 124.0, 124.0, 119.1, 116.7 (d, J = 25 Hz), 114.0 (d, J = 24 Hz); LCMS (ESI) calc'd for $[\text{C}_{12}\text{H}_4\text{BrClFN}_4\text{O}_3]^-$ ($[\text{M}-\text{H}]^-$): m/z 384.9, found 384.9. The regioselective formation of this

desired was confirmed by examining crystals of benzoxadiazole **S1** that were suitable for X-ray diffraction.

1.11: A flame-dried flask containing benzoxadiazole **S1** (30 mg, 0.077 mmol, 1 equiv) and phenylboronic acid (9.4 mg, 0.077 mmol, 1 equiv) was degassed and purged with nitrogen. Dioxane (4 mL) was added, and the mixture was stirred at room temperature for 20 minutes. Tetrakis(triphenylphosphine)palladium (14.2 mg, 0.012 mmol, 16 mol%) was quickly added to the reaction vessel, followed by cesium carbonate (31.9 mg, 0.231 mmol, 3 equiv) in 1.16 mL water. The reaction mixture was heated to 100°C with a reflux condenser and stirred for 3.5 h. After cooling to room temperature, the reaction was diluted in water and extracted with ethyl acetate (3x). The combined organic layers were washed with brine, dried over Na₂SO₄ and concentrated under reduced pressure. Recrystallization in hexanes and ethyl acetate afforded 7-phenylbenzoxadiazole **1.11** as a solid (6 mg, 19% yield):

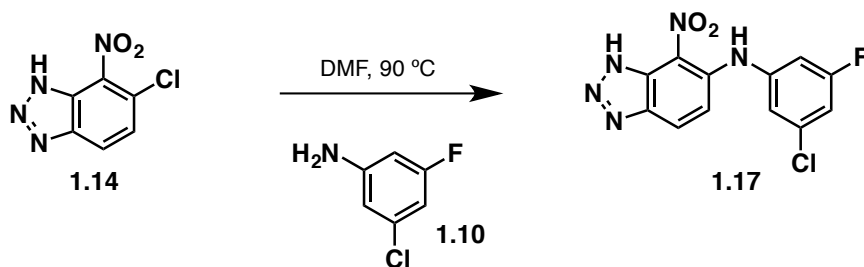
¹H NMR (400 MHz, Acetone-d₆) δ 7.93 (m, 2H), 7.64 (s, 1H), 7.55 (m, 3H), 7.52 (m, 1H), 7.43 (dt, J = 2.2 Hz, 9.8 Hz, 1H), 7.1–31 (dt, J = 2.1 Hz, 8.6 Hz, 1H); ¹³C NMR (100 MHz, Acetone-d₆) δ 162.5 (d, J = 248 Hz), 147.6, 146.7, 140.9, 138.5, 136.6, 136.5, 134.5, 131.8, 129.1, 123.8, 123.7, 123.2, 123.0, 116.3 (d, J = 25 Hz), 113.6 (d, J = 24 Hz); LCMS (ESI) calc'd for [C₁₈H₉ClFN₄O₃]⁺([M-H]⁺): m/z 383.0, found 383.1.



1.14

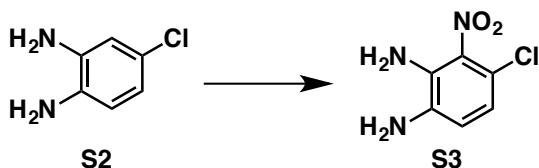
1.14 was prepared following a known literature procedure⁵² and was isolated as a light yellow powder (78% yield):

¹H NMR (400 MHz, Acetone-d₆) δ 8.38 (d, J = 8.7 Hz, 1H), 7.74 (d, J = 8.7 Hz, 1H). LCMS (ESI) calc'd for [C₆H₄ClN₄O₂]⁺([M+H]⁺): m/z 199.0, found 199.0.



1.17: Following the typical procedure for the synthesis of aniline derivatives with chloride **1.14**, purification by flash chromatography on silica gel (10% ethyl acetate in hexanes) provided the desired product **1.17** as a yellow solid (9.4 mg, 16 %):

^1H NMR (400 MHz, Acetone- d_6) δ 7.96 (d, J = 1.2 Hz, 2H), 7.81 (d, J = 5.8 Hz, 1H), 7.62 (d, J = 3.6 Hz, 1H), 7.37 (dd, J = 1.2 Hz, 5.7 Hz, 1H,), 7.30 (d, J = 3.6 Hz, 1H), 6.4 (s, 1H), 6.23 (m, 1H), 5.14 (bs, 1H) ^{13}C NMR (100 MHz, Acetone- d_6) δ 164.8 (d, J = 242.0 Hz), 152.4 (d, J = 12.8 Hz), 145.4, 135.6 (d, J = 13.9 Hz), 135.2, 126.1, 124.0, 123.3, 110.1, 103.9 (d, J = 25.8 Hz), 99.9 (d, J = 24.6 Hz), 95.9. LCMS (ESI) calc'd for $[\text{C}_{12}\text{H}_6\text{ClFN}_5\text{O}_2]^- ([\text{M}-\text{H}]^-)$: m/z 306.0, found 306.0.



S3 was prepared following a known literature procedure⁵⁰: A solution of 3-chloroorthophenylenediamine **S2** (252 mg, 1.77 mmol) in ethanol (2.0 mL) was heated to reflux and treated dropwise with a solution of selenium dioxide (216 mg, 1.94 mmol) in water (1 mL). The reaction was monitored by TLC. After 30 min, the mixture was cooled to ambient temperature and filtered via vacuum filtration to give the desired selenadiazole as a dark brown solid (253 mg, 66%). The crude product was carried forward to the next step without further purification:

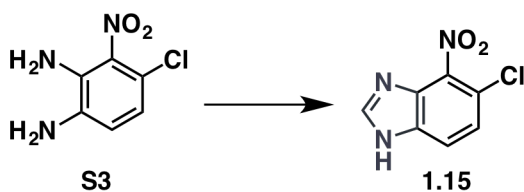
^1H NMR (400 MHz, DMSO- d_6) δ 7.99 (s, 1H), 7.86 (d, J = 6.2 Hz, 1H), 7.55 (d, J = 5.9 Hz, 1H). LCMS (ESI) calc'd for $[\text{C}_6\text{H}_4\text{ClN}_2\text{Se}]^+ ([\text{M}+\text{H}]^+)$: m/z 218.9, found 218.9. The

selenadiazole (157 mg, 0.726 mmol) from the previous step was dissolved in conc. H_2SO_4 (2.4 mL) and cooled in an ice water bath. The dark green solution was treated dropwise with conc. HNO_3 (0.16 mL) and turned dark red in color. After 50 min, the reaction mixture was poured onto ice and filtered via vacuum filtration to yield the nitrated selenadiazole product as a light brown powder (145 mg, 77% yield). The crude product was carried forward to the next step without further purification:

^1H NMR (400 MHz, DMSO-d_6) δ 8.13 (d, $J = 7.6$ Hz, 1H), 7.82 (d, $J = 7.6$ Hz, 1H). LCMS (ESI) calc'd for $[\text{C}_6\text{H}_3\text{ClN}_3\text{O}_2\text{Se}]^+([\text{M}+\text{H}]^+)$: m/z 263.9, found 263.5.

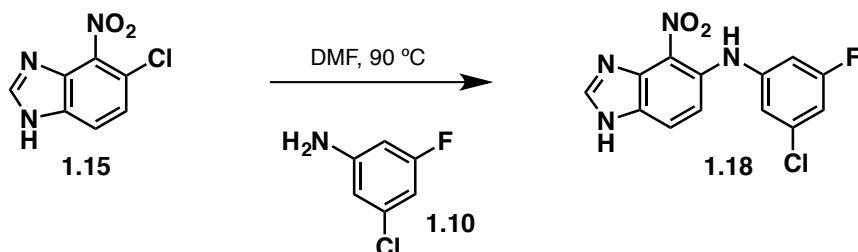
The nitroselenadiazole (83.54 mg, 0.321 mmol) from the previous step was dissolved in conc. HCl (0.78 mL) and cooled in an ice bath. The reaction mixture was treated with a 48% HI solution (0.26 mL) followed by 50% NaOH to get to a pH of 8. The product was extracted with ethyl acetate. The organic layer was washed with brine and concentrated under reduced pressure to provide **S3** as a red powder (45.7 mg, 76%):

^1H NMR (400 MHz, Acetone-d_6) δ 6.78 (d, $J = 8.2$ Hz, 1H), 6.68 (d, $J = 8.2$ Hz, 1H), 5.33 (bs, 2H), 5.18 (bs, 2H). LCMS (ESI) calc'd for $[\text{C}_6\text{H}_7\text{ClN}_3\text{O}_2]^+([\text{M}+\text{H}]^+)$: m/z 188.0, found 188.0.



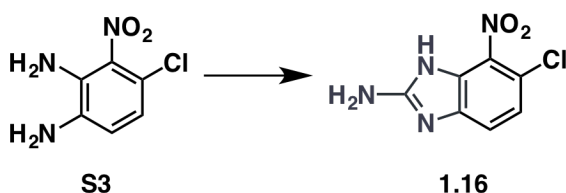
1.15 was prepared following a known literature procedure⁵¹: A solution of **S3** (75 mg, 0.40 mmol) in THF (1.5 mL) was treated sequentially with triethyl orthoformate (178 mg, 1.2 mmol) and *p*-toluenesulfonic acid (7.6 mg, 200 μL , 0.04 mmol). The reaction mixture was stirred at 50 $^\circ\text{C}$, the reaction was monitored by LCMS. After 2 h, the solvent was removed under a stream of nitrogen gas, and the resulting residue was partitioned between ethyl acetate and water. The organic layer was washed with saturated aqueous Na_2CO_3 , dried over MgSO_4 , and concentrated under reduced pressure to provide **1.15** as a light brown solid (57 mg, 72%):

^1H NMR (400 MHz, Acetone- d_6) δ 8.42 (s, 1H), 8.03 (d, J = 8.2 Hz, 1H), 7.87 (d, J = 8.2 Hz, 1H), 7.48 (bs, 1H). LCMS (ESI) calc'd for $[\text{C}_7\text{H}_5\text{ClN}_3\text{O}_2]^+([\text{M}+\text{H}]^+)$: m/z 198.0, found 198.0.



1.18: Following the typical procedure for the synthesis of aniline derivatives with chloride **1.15**, purification by flash chromatography on silica gel (15% ethyl acetate in hexanes) provided the desired product **1.18** as a yellow solid (9.4 mg, 31%):

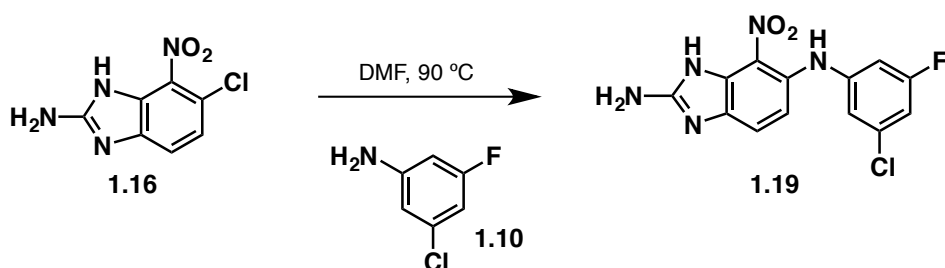
^1H NMR (400 MHz, Acetone- d_6) δ 8.37 (d, J = 8.8 Hz, 1H), 8.01 (s, 1H), 7.72 (d, J = 8.8 Hz, 1H), 6.51 (dd, J = 1.8 Hz, 1.8 Hz, 1H), 6.34 (m, 2H). ^{13}C NMR (100 MHz, Acetone- d_6) δ 164.8 (d, J = 241.6 Hz), 152.3 (d, J = 12.8 Hz), 142.6, 139.5, 135.7, 135.6 (d, J = 14.0 Hz), 129.9, 128.0, 127.1, 125.2, 118.6, 103.9 (d, J = 25.8 Hz), 100.0 (d, J = 24.5 Hz). LCMS (ESI) calc'd for $[\text{C}_{13}\text{H}_7\text{ClF}_2\text{N}_4\text{O}_2]^-([\text{M}-\text{H}]^-)$: m/z 305.0, found 305.0.



1.16 was prepared following a known literature procedure⁵¹: **S3** (75 mg, 0.40 mmol) was dissolved in a 5:1 mixture of CH_3CN and water (1.2 mL) and cooled to 0 °C. The dark red solution was treated with cyanogen bromide (47 mg, 0.44 mmol), and the reaction was monitored by LCMS. At the completion of the reaction, the solvent was removed under a stream of nitrogen gas. Conc. ammonium hydroxide was added, which resulted in a dark red precipitate formation that was filtered via vacuum filtration. The precipitate was washed repeatedly with cold water and dried under vacuum. Purified via flash

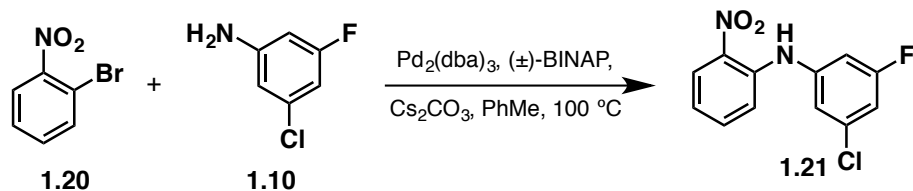
chromatography on silica gel (15% ethyl acetate in hexanes) provided the desired product **1.16** as a red powder (35.0 mg, 41 %):

^1H NMR (CDCl_3 , 400 MHz) δ 6.82 (bs, 2H), 6.78 (d, $J = 8.2$ Hz, 1H), 6.68 (d, $J = 8.2$ Hz, 1H), 5.33 (bs, 1H). LCMS (ESI) calc'd for $[\text{C}_7\text{H}_4\text{ClN}_4\text{O}_2]^-([\text{M}-\text{H}]^-)$: m/z 211.0, found 211.0.



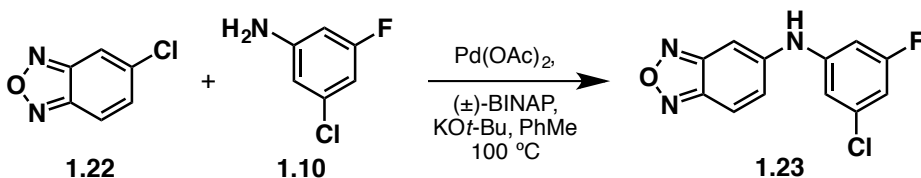
1.19: Following the typical procedure for the synthesis of aniline derivatives with chloride **1.16**, purification by flash chromatography on silica gel (20% ethyl acetate in hexanes) provided the desired product **1.19** as a yellow solid (19.7 mg, 65%):

^1H NMR (400 MHz, Acetone- d_6) δ 7.32 (d, $J = 6.0$ Hz, 1H), 7.28 (bs, 1H), 6.57 (s, 1H), 6.54 (ddd, $J = 1.2$ Hz, 1.3 Hz, 6.7 Hz, 1H), 6.40 (ddd, $J = 1.3$ Hz, 1.3 Hz, 6.7 Hz, 1H), 5.77 (s, 1H). ^{13}C NMR (100 MHz, Acetone- d_6) δ 164.8 (d, $J = 249.3$ Hz), 150.0, 149.8 (d, $J = 12.1$ Hz), 136.1, 136.0, 134.0 (d, $J = 13.6$ Hz), 131.7, 118.8, 118.4 (d, $J = 1.9$ Hz), 110.9, 105.9 (d, $J = 26.0$ Hz), 103.3, 100.3 (d, $J = 25.6$ Hz). LCMS (ESI) calc'd for $[\text{C}_{13}\text{H}_7\text{ClFN}_5\text{O}_2]^-([\text{M}-\text{H}]^-)$: m/z 320.0, found 320.1.



1.21: A flame-dried flask was charged with 2-bromonitrobenzene **1.20** (50 mg, 0.25 mmol, 1 equiv) tris(dibenzylideneacetone)dipalladium (11.3 mg, 0.0012 mmol, 5 mol%), racemic 2,2'-bis(diphenylphosphino)-1,1'-binaphthyl (11.5 mg, 0.0019 mmol, 7.5 mol%), and cesium carbonate (163.1 mg, 0.50 mmol, 2 equiv). The flask was degassed and purged with nitrogen. Toluene (2.88 mL) was added, followed by 2-chloro-4-fluoroaniline **1.10** (35.3 mg, 0.25 mmol, 1 equiv). The reaction was heated to 100 °C with a reflux condenser and stirred for 12 h. The mixture was cooled to room temperature, filtered through a pad of celite, dried over MgSO₄ and concentrated under reduced pressure. Purification by flash chromatography on silica gel (9:1 hexanes:ethyl acetate) afforded the desired aniline **1.21** as an orange solid (58 mg, 88% yield):

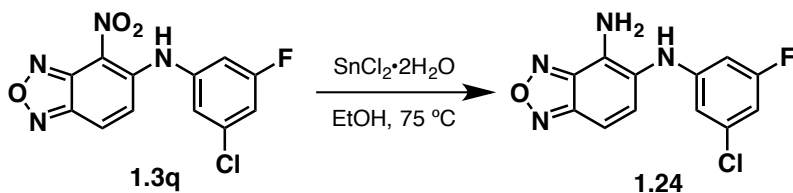
¹H NMR (400 MHz, Acetone-d₆) δ 9.27 (bs, 1H), 8.18 (d, *J* = 8.5 Hz, 1H), 7.63 (d, *J* = 8.6 Hz, 1H), 7.52 (d, *J* = 8.6 Hz, 1H), 7.28 (s, 1H), 7.17 (dt, *J* = 2.2 Hz, 10.4 Hz, 1H), 7.04 (m, 2H); ¹³C NMR (100 MHz, Acetone-d₆) δ 164.2 (d, *J* = 245.7 Hz), 144.0 (d, *J* = 11.8 Hz), 140.9, 136.7, 136.6, 136.2 (d, *J* = 13.0 Hz), 127.2, 120.7, 118.9, 118.9, 112.0 (d, *J* = 25.4 Hz), 108.6 (d, *J* = 24.5 Hz); LCMS (ESI) calc'd for [C₁₂H₇ClFN₂O₂]⁺ ([M-H]): *m/z* 265.0, found 265.1.



1.23: A flame-dried flask was charged 5-chlorobenzofurazan **1.22** (100.0 mg, 0.65 mmol, 1 equiv) and toluene (3mL), and the mixture was stirred at 110 °C for 30 min with a reflux condenser. The solution was cooled to room temperature, and the flask was charged sequentially with palladium (II) acetate (8.8 mg, 0.040 mmol, 6 mol%), racemic 2,2'-bis(diphenylphosphino)-1,1'-binaphthyl (24.9 mg, 0.040 mmol, 6 mol%), 2-chloro-4-fluoroaniline **1.10** (68.4 μL, 0.65 mmol, 1 equiv) and potassium tert-butoxide (80.0 mg, .71 mmol, 1.1 equiv). The mixture was stirred at 90 °C for 12 h, cooled to room

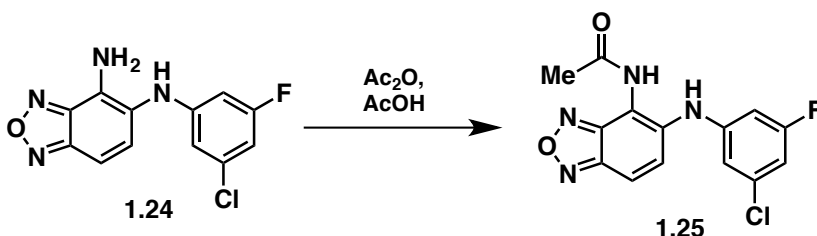
temperature, and diluted with water. The mixture was washed with dichloromethane (3x). The combined organic layers were washed with 1N HCl, 1N NaOH, and brine. The organic layers were then dried over MgSO₄ and concentrated under reduced pressure. The resulting solid was then recrystallized in hexanes to the desired aniline **1.23** as a brown solid (67 mg, 39% yield):

¹H NMR (400 MHz, Acetone-d₆) δ 8.59 (bs, 1H), 7.87 (d, *J* = 9.2 Hz, 1H), 7.40 (dd, *J* = 2.0 Hz, 9.6 Hz, 1H), 7.31 (m, 1H), 7.20 (s, 1H), 7.12 (dt, *J* = 1.3 Hz, 12.0 Hz, 1 Hz), 6.92 (dt, *J* = 2.0 Hz, 8.6 Hz, 1H); ¹³C NMR (100 MHz, Acetone-d₆) δ 164.4 (d, *J* = 245.3 Hz), 151.1, 147.9, 145.4, 144.9 (d, *J* = 11.9 Hz), 136.3 (d, *J* = 13.2 Hz), 131.0, 118.2, 116.3, 110.6 (d, *J* = 25.5 Hz) 105.9 (d, *J* = 25.0 Hz), 91.7; LCMS (ESI) calc'd for [C₁₂H₆ClFN₃O]⁺ ([M-H]⁺): *m/z* 262.0, found 262.0.



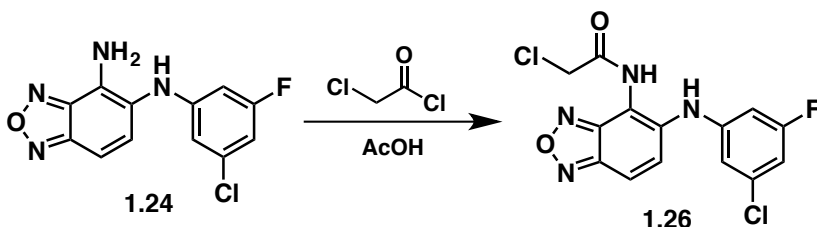
1.24: A solution of aniline **1.3q** (29 mg, 0.094 mmol) in anhydrous EtOH (2 mL) was treated with SnCl₂•2H₂O (63 mg, 0.28 mmol, 3 equiv). The reaction was heated to reflux for 4 h and then quenched with saturated aqueous NaHCO₃. The mixture was diluted with ethyl acetate passed through a pad of celite. The filtrate was washed with brine, dried over MgSO₄ and concentrated under reduced pressure. The crude oil was purified by flash chromatography on silica gel (20% ethyl acetate in hexanes) to provide 4-aminobenzoxadiazole **1.24** as an orange powder (18 mg, 70%):

¹H NMR (600 MHz, CDCl₃) δ 7.17 (dd, *J* = 6.0 Hz, 12.0 Hz, 2H), 6.57 (d, *J* = 6.0 Hz, 1H), 6.44 (m, 2H), 6.25 (m, 1H), 5.26 (bs, 1H), 4.66 (bs, 2H). ¹³C NMR (125 MHz, CDCl₃) δ 164.0 (d, *J* = 246.0 Hz), 149.1, 147.0 (d, *J* = 11.3 Hz), 145.4, 136.2 (*J* = 12.9 Hz), 134.2, 130.3, 118.4, 110.6, 107.6 (d, *J* = 25.2 Hz), 107.5 (d, *J* = 27.9 Hz), 105.0. LCMS (ESI) calc'd for [C₁₂H₇ClFN₄O]⁺ ([M-H]⁺): *m/z* 277.0, found 277.1.



1.25: A solution of 4-aminobenzoxadiazole **1.24** (15.0 mg, 0.054 mmol) in acetic acid (1 mL) was treated with acetic anhydride (5.5 mg, 0.054 mmol). The reaction was stirred at ambient temperature for 19 h and quenched with ice. The desired 4-amidobenzoxadiazole **1.25** was collected by vacuum filtration as a green precipitate (14.0 mg, 81% yield):

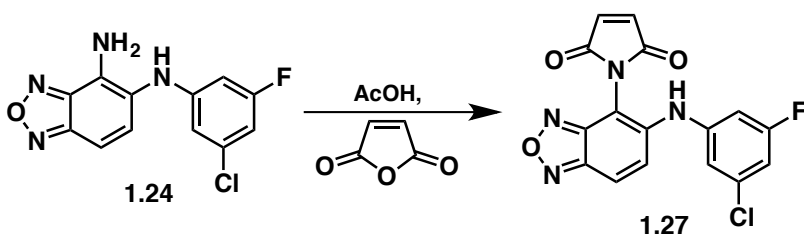
^1H NMR (400 MHz, Acetone- d_6) δ 9.54 (bs, 1H), 8.00 (bs, 1H), 7.83 (d, J = 6.4 Hz, 1H), 7.66 (d, J = 6.4 Hz, 1H), 6.85 (s, 1H), 6.81 (d, J = 5.7 Hz, 1H), 6.74 (d, J = 7.1 Hz, 1H) 2.25 (s, 3H). ^{13}C NMR (100 MHz, Acetone- d_6) δ 169.5, 163.4 (d, J = 240.0 Hz), 147.9, 145.1 (d, J = 11.0 Hz), 135.3, 135.2, 130.2, 113.6, 113.9, 108.4, 108.2, 103.6, 103.3, 22.3. (LCMS (ESI) calc'd for $[\text{C}_{14}\text{H}_9\text{ClFN}_4\text{O}_2]^-$ ($[\text{M}-\text{H}]^-$): m/z 319.0, found 319.0.



1.26: Following the procedure for the synthesis of 4-aminobenzoxadiazole **1.24** with chloroacetylchloride, purification by reverse phase HPLC on a C-18 column (10% acetonitrile in water to 90% acetonitrile in water gradient eluent) provided 4-amidobenzoxadiazole **1.26** as a green powder. (19.6 mg, 51% yield):

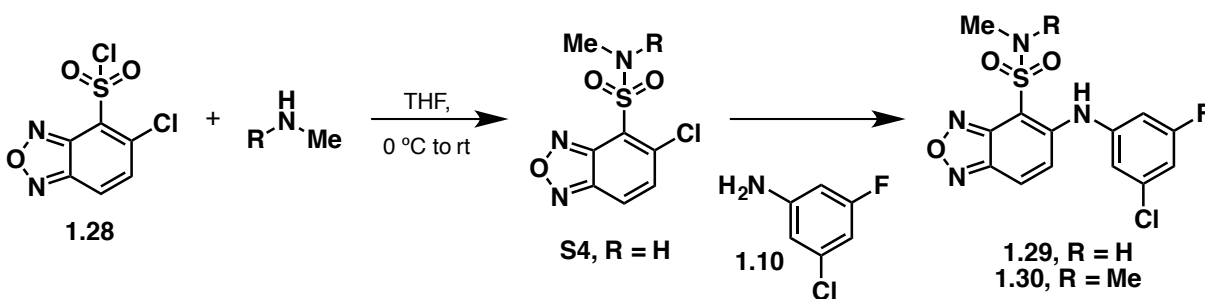
^1H NMR (400 MHz, Acetone- d_6) δ 8.08 (bs, 1H), 7.88 (d, J = 9.6 Hz, 1H), 7.68 (d, J = 9.6 Hz, 1H), 6.90 (s, 1H), 6.86 (d, J = 8.6 Hz, 1H), 6.78 (d, J = 10.6 Hz, 1H), 4.39 (s, 2H). ^{13}C NMR (100 MHz, Acetone- d_6) δ 165.8, 164.4 (d, J = 244.0 Hz), 147.9, 144.7 (d,

$J = 11.9$ Hz), 143.9, 135.2 (d, $J = 10.2$ Hz), 129.9, 115.5, 114.7, 114.5, 108.9 (d, $J = 24.5$ Hz), 104.3 (d, $J = 25.0$ Hz), 95.0, 42.5. LCMS (ESI) calc'd for $[C_{14}H_8Cl_2FN_4O_2]^- ([M-H]^-)$: m/z 353.0, found 353.0.



1.27: Following the procedure for the synthesis of 4-amidobenzoxadiazole **1.24** with maleic anhydride, purification by vacuum filtration provided 4-amidobenzoxadiazole **1.27** as a green precipitate (13.4 mg, 69% yield):

^1H NMR (400 MHz, Acetone- d_6) δ 8.42 (bs, 1H), 7.89 (d, $J = 6.4$ Hz, 1H), 7.72 (d, $J = 6.4$ Hz, 1H), 6.93 (s, 1H), 6.81 (m, 3H), 6.39 (d, $J = 8.4$ Hz, 1H). ^{13}C NMR (100 MHz, Acetone- d_6) δ 166.1, 162.8 (d, $J = 243$ Hz), 149.2, 148.8, 145.5, 145.4, 139.3, 136.2 (d, $J = 13$ Hz), 134.5, 133.3, 116.6, 115.7 (d, $J = 5.8$ Hz), 110.0 (d, $J = 25.6$ Hz), 105.4 (d, $J = 25.3$ Hz). LCMS (ESI) calc'd for $[C_{16}H_7ClFN_4O_3]^- ([M-H]^-)$: m/z 357.0, found 357.0.



S4: A flame-dried flask containing 5-chlorobenzoxadiazole-4-sulfonyl chloride **1.28** (400 mg, 1.58 mmol, 1 equiv) was degassed and purged with nitrogen. The flask was charged with THF (4 mL) and cooled to 0 °C. Methylamine (1.1 mL, 2M in MeOH) was added dropwise, and the mixture was stirred for 5.5 h. The reaction was quenched with 0.125 M

HCl (4 mL) and extracted with ethyl acetate (3x). The combined organic layers were washed with brine, dried over MgSO_4 and concentrated under reduced pressure. The resulting solid was recrystallized in hexanes and dichloromethane to afford secondary sulfonamidobenzoxadiazole **S4** as a yellow solid (220 mg, 56% yield).

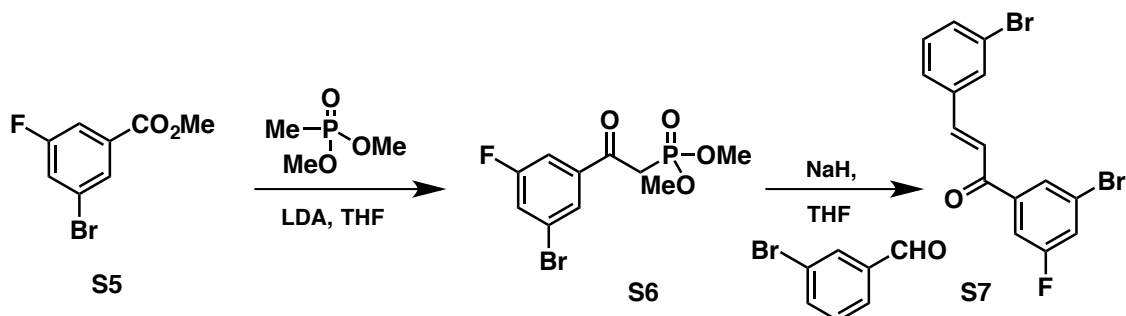
1.29: A flame-dried flask containing secondary sulfonamidobenzoxadiazole **S4** (215.0 mg, 0.868 mmol, 1 equiv) was degassed and purged with nitrogen. Toluene (26.2 mL), 2-chloro-4-fluoroaniline **1.10** (0.436 mL, 4.34 mmol, 5 equiv), and *N,N*-diisopropylethylamine (0.30 mL, 1.74 mmol, 2 equiv) were sequentially added, and the mixture was heated to 110 °C with stirring for 40 h. The reaction was cooled to room temperature and concentrated under reduced pressure. Purification by flash chromatography on silica gel (9:1 hexanes:ethyl acetate with 1% triethylamine) followed by recrystallization in hexanes and dichloromethane provided sulfonamidobenzoxadiazole **1.29** as a yellow solid (9.6 mg, 31% yield):

^1H NMR (400 MHz, Acetone- d_6) δ 8.05 (d, J = 9.8 Hz, 1H), 7.65 (d, J = 9.8 Hz, 1H), 7.34 (m, 1H), 7.26 (dt, J = 2.2 Hz, 10.0 Hz, 1H), 7.20 (dt, J = 2.0 Hz, 8.6 Hz, 1H), 2.71 (s, 3H); ^{13}C NMR (100 MHz, Acetone- d_6) δ 164.1 (d, J = 247.0 Hz), 148.0, 147.5, 147.5, 142.6 (d, J = 11.8 Hz), 136.4 (d, 12.8 Hz), 128.1, 122.3, 121.3, 121.2, 114.1 (d, J = 25.2 Hz), 111.1 (d, J = 24.1 Hz), 101.0; LCMS (ESI) calc'd for $[\text{C}_{13}\text{H}_9\text{ClFN}_4\text{O}_3\text{S}]^+([\text{M}-\text{H}]^-)$: m/z 355.0, found 355.0.

1.30: Following the procedure for the synthesis of sulfonamidobenzoxadiazole **1.29** with dimethylamine, purification by flash chromatography followed by recrystallization provided sulfonamidobenzoxadiazole **1.30** (1.9 mg, 2% yield):

^1H NMR (400 MHz, Acetone- d_6) δ 9.58 (bs, 1H), 8.04 (d, J = 9.8 Hz, 1H), 7.62 (d, J = 9.8 Hz, 1H), 7.35 (m, 1H), 7.25 (dt, J = 2.2 Hz, 7.4 Hz, 1H), 7.19 (dt, J = 2.1 Hz, 8.6 Hz, 1H), 2.94 (s, 3H), 1.29 (s, 3H); LCMS (ESI) calc'd for $[\text{C}_{14}\text{H}_{11}\text{ClFN}_4\text{O}_3\text{S}]^+([\text{M}-\text{H}]^-)$: m/z 369.0, found 369.0.

Synthesis of Chalcones



LDA was generated by the following protocol: A solution of diisopropylamine (1 equiv) in THF (0.8 M) and cooled to 0 °C. A solution of *n*-BuLi in hexanes (1.6 M, 1 equiv) was added dropwise, and the resulting solution was stirred for 30 min at 0 °C. The solution of LDA was then ready for use.

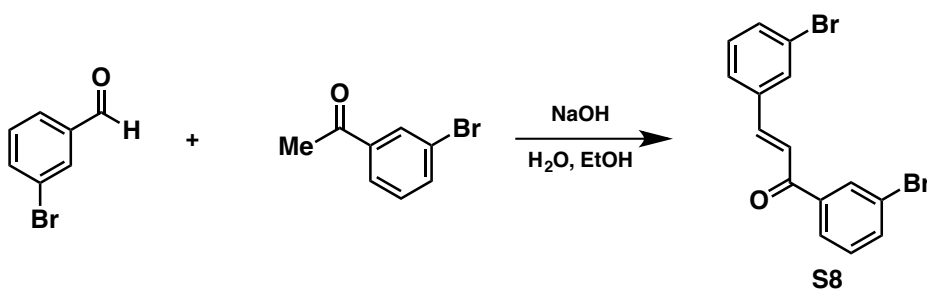
S6: A flame-dried flask was charged with ester **S5** (4.29 mmol, 1 equiv) and dimethyl methylphosphonate (1.5 equiv) in THF (0.6 M). Freshly generated LDA (2 equiv) was added dropwise, and the mixture was stirred at 23 °C for 30 min. The reaction mixture was quenched by the addition of 1M aqueous HCl, and the solution was extracted with ethyl acetate (3x). The combined organic layers were dried over Na₂SO₄ and concentrated under reduced pressure. The resulting residue was purified by column chromatography to yield β -ketophosphonate **S6** (1.04 g, 75% yield):

¹H NMR (400 MHz, Chloroform-*d*) δ 7.93 (t, *J* = 1.6 Hz, 1H), 7.64 (ddd, *J* = 8.8, 2.4, 1.5 Hz, 1H), 7.48 (ddd, *J* = 7.6, 2.3, 1.8 Hz), 3.82 (s, 3H), 3.79 (s, 3H), 3.61 (s, 1H), 3.56 (s, 1H).

S7: A solution of β -ketophosphonate **S6** (1 equiv) in THF (0.6 M) was added to a solution of NaH (1.1 equiv) in THF (0.6 M). The mixture was stirred for 15 min at 23 °C and then treated with 3-bromo-benzaldehyde (1.1 equiv). After stirring at 23 °C for 16 h,

the reaction was quenched by the addition of saturated aqueous NaHCO_3 and extracted with ethyl acetate. The organic layer was washed with brine, dried over Na_2SO_4 , and concentrated under reduced pressure. The resulting residue was purified by column chromatography to provide the desired product (33% yield):

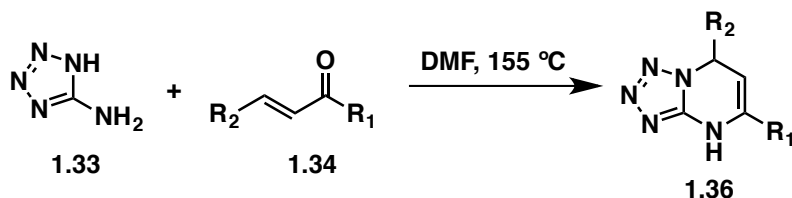
^1H NMR (400 MHz, Chloroform-*d*) δ 7.93 (s, 1H), 7.80 (s, 1H), 7.75 (d, $J = 15.7$ Hz, 1H), 7.66 – 7.61 (m, 1H), 7.58 – 7.53 (m, 2H), 7.49 – 7.45 (m, 1H), 7.39 (d, $J = 15.6$ Hz, 1H), 7.31 (t, $J = 7.8$ Hz, 1H). ^{13}C NMR (100 MHz, CDCl_3) δ 195.3, 144.5, 140.0, 133.8, 131.0, 130.8, 130.5, 130.3, 130.0, 127.4, 126.5, 124.0, 123.5, 122.7, 121.9.



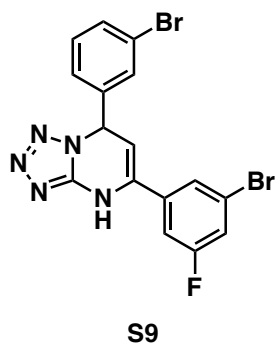
S8: A flask was charged with 3-bromoacetophenone (1 equiv) and 3-bromobenzaldehyde (1 equiv) in EtOH (0.1 M). 1% Aqueous NaOH (0.1 M) was added, and the mixture was stirred at 23 °C for 16 h. The reaction mixture was filtered, and the precipitate was washed with 1:1 EtOH:H₂O (2 x 0.5 M). The precipitate was dried under vacuum provided the desired product (91% yield):

^1H NMR (400 MHz, CDCl_3) δ 8.14 (t, $J = 1.8$ Hz, 1H), 7.94 (dt, $J = 7.8, 1.2$ Hz, 1H), 7.80 (t, $J = 1.8$ Hz, 1H), 7.74 (d, $J = 15.7$ Hz, 1H), 7.74 – 7.71 (m, 1H), 7.56 (d, $J = 7.9, 1.8$ Hz, 2H), 7.45 (d, $J = 15.7$ Hz, 1H), 7.40 (t, $J = 7.9$ Hz, 1H), 7.31 (t, $J = 7.9$ Hz, 1H). ^{13}C NMR (100 MHz, CDCl_3) δ 188.5, 143.8, 136.7, 135.8, 133.5, 131.5, 130.9, 130.5, 130.2, 127.3, 127.0, 123.1, 123.0, 122.6; LCMS (ESI) calc'd for $[\text{C}_{15}\text{H}_{10}\text{Br}_2\text{O}]^+([\text{M}-\text{H}]^+)$: m/z 364.9, found 364.91.

Synthesis of Enamines **S9**, **S10**, and **1.39**



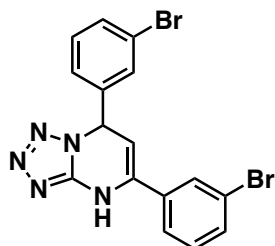
A flame-dried flask outfitted with a condenser was charged with chalcone **1.34** (1 equiv), 5-aminotetrazole **1.33** (1 equiv), and DMF (2.2 M). The reaction mixture was refluxed at 155 °C for 3 h. Then the mixture was cooled to 23 °C and diluted with CH₂Cl₂. After stirring for 45 min, the mixture was filtered, and the precipitate was purified via recrystallization to provide enamine **1.36**.



S9: Following the general method for enamine synthesis provided the desired product:

¹H NMR (400 MHz, CDCl₃) δ 10.62 (s, 1H), 7.67 (s, 1H), 7.5 (s, 2H), 7.43 (d, J = 9.0 Hz, 1H), 7.39 – 7.32 (m, 2H), 7.30 (d, J = 8.0 Hz, 1H), 6.45 (s, 1H), 5.24 (s, 1H). ¹³C NMR (101 MHz, DMSO-d₆) δ 163.7, 150.9, 143.0, 137.5, 133.5, 132.1, 131.7, 130.5,

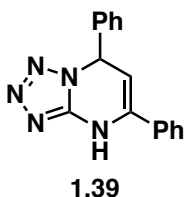
126.9, 125.7, 122.5, 120.0, 119.8, 112.9, 98.9, 58.5. LCMS (ESI) calc'd for $[C_{16}H_{10}Br_2FN_5]+([M-H]^+)$: m/z 449.9, found 450.0, 452.0.



S10

S10: Following the general method for HIF-2 ligand synthesis provided the desired product:

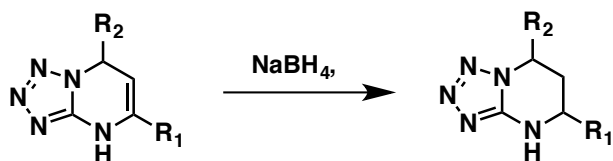
1H NMR (500 MHz, Chloroform-*d*) δ 7.60 (s, 1H), 7.51 (d, J = 7.8 Hz, 2H), 7.38 (s, 1H), 7.36 (s, 1H), 7.29 (t, J = 7.0 Hz, 2H), 7.18 (d, J = 7.7 Hz, 1H), 5.53 (s, 1H), 5.48 (dd, J = 11.2, 4.7 Hz, 1H), 4.75 (d, 11.2 Hz, 1H), 2.60 (d, J = 14.3 Hz, 1H), 2.37 – 2.26 (m, 1H).



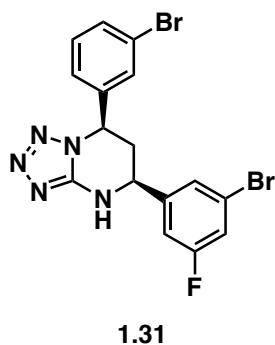
1.39: Following the general method for enamine synthesis provided the desired product:

1H NMR (400 MHz, DMSO-*d*₆) δ 10.53 (s, 1H), 7.69 – 7.59 (m, 2H), 7.48 – 7.29 (m, 8H), 6.59 (d, J = 3.6 Hz, 1H), 5.28 (dd, J = 3.6, 1.7 Hz, 1H). ^{13}C NMR (101 MHz, DMSO-*d*₆) δ 151.12, 141.09, 135.51, 133.99, 129.73, 129.38, 129.07, 127.58, 126.46, 97.52, 59.21, 40.57, 40.36, 40.15, 39.94, 39.73, 39.53, 39.32. LCMS (ES-API) calc'd for $[C_{16}H_{14}N_5]+([M-H]^+)$: m/z 276.1, found 276.1, 375.0.

Synthesis of HIF-2 α Ligands 1.31, 1.32, and 1.40

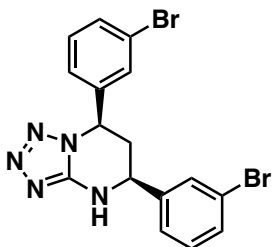


A flame-dried flask was charged with enamine (1 equiv) and MeOH (0.02 M). NaBH₄ (12 equiv) was added slowly over 1 min. After 4 h, the reaction mixture was concentrated to 1/5 the original volume and diluted with H₂O. A precipitate formed, which was filtered and washed using a minimal amount of water. The solid was dried under high vacuum to afford ligand.



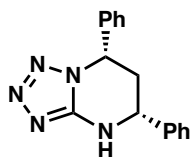
1.31: Following the general method for HIF-2 ligand synthesis provided the desired product:

¹H NMR (400 MHz, CDCl₃) δ 7.50 (d, J = 8.1 Hz, 1H), 7.38 (d, J = 12.1 Hz, 2H), 7.30 – 7.20 (m, 2H), 7.16 (d, J = 8.1 Hz, 1H), 7.13 (d, J = 8.5 Hz, 1H), 6.41 (bs, 1H), 5.49 (dd, J = 10.7, 4.6 Hz, 1H), 4.79 (d, J = 10.7 Hz, 1H), 2.60 (d, J = 14.4 Hz, 1H), 2.37 – 2.24 (m, 1H). ¹³C NMR (101 MHz, DMSO-d₆) δ 163.7, 161.2, 155.4, 146.1, 141.0, 131.7, 131.1, 130.6, 127.2, 126.6, 122.2, 118.4, 113.9, 113.7, 57.5, 53.4. LCMS (ESI) calc'd for [C₁₆H₁₂Br₂FN₅]+([M-H]⁺): m/z 451.9, found 451.2.

**1.32**

1.32: Following the general method for HIF-2 ligand synthesis provided the desired product:

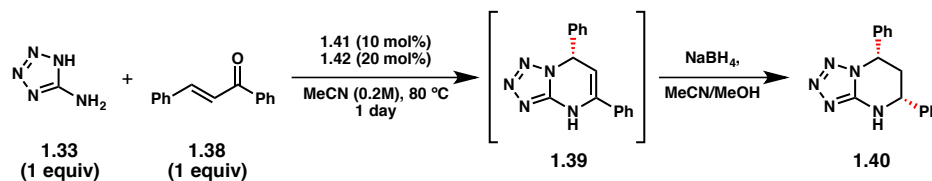
^1H NMR (500 MHz, CDCl_3) δ 7.60 (s, 1H), 7.51 (d, $J = 7.8$ Hz, 2H), 7.38 (s, 1H), 7.36 (s, 1H), 7.29 (t, $J = 7.0$ Hz, 2H), 7.18 (d, $J = 7.7$ Hz, 1H), 5.53 (s, 1H), 5.48 (dd, $J = 11.2$, 4.7 Hz, 1H), 4.75 (d, 11.2 Hz, 1H), 2.60 (d, $J = 14.3$ Hz, 1H), 2.37 – 2.26 (m, 1H). ^{13}C NMR (101 MHz, DMSO-d_6) δ 155.6, 144.1, 141.1, 131.7, 131.1, 131.0, 130.7, 130.1, 127.2, 126.5, 122.2, 57.9, 53.9. LCMS (ESI) calc'd for $[\text{C}_{16}\text{H}_{13}\text{Br}_2\text{N}_2]^+([\text{M-H}]^+)$: m/z 434.0, found 434.0.

**1.40**

1.40: Following the general method for HIF-2 ligand synthesis provided the desired product:

^1H NMR (500 MHz, CDCl_3) δ 7.50 – 7.23 (m, 10H), 5.74 (s, 1H), 5.52 (dd, $J = 11.5$, 4.7 Hz, 1H), 4.79 (dd, $J = 11.5$, 2.3 Hz, 1H), 2.59 (d, $J = 14.2$ Hz, 1H), 2.35 (dt, $J = 14.2$, 11.5 Hz, 1H). ^{13}C NMR (101 MHz, CDCl_3) δ 171.1, 133.2, 133.1, 132.7, 132.7, 128.7, 128.6, 127.8, 125.7, 60.4, 21.0, 14.2, 14.2.

General Procedure for the Asymmetric Synthesis of 1.40:



To a flame-dried vial and stir bar were added cinchona alkaloid catalyst (10 mol%, 0.02 mmol, 6.46 mg), phosphoric acid catalyst (20 mol%, 0.04 mmol, 10.00 mg), chalcone (1 equiv, 0.2 mmol, 41.65 mg) and aminotetrazole (1 equiv, 0.2 mmol, 17.01 mg). The vial was evacuated and purged with nitrogen followed by addition of 1 mL MeCN. The vial was tightly sealed using a non-septa screw cap and the reaction was heated to 80°C and stirred overnight. The mixture was then cooled to room temperature and diluted with methanol (4 mL) followed by addition of sodium borohydride (9.75 equiv, 75 mg) portion-wise. Over the course of 2 hours the reaction became homogenous. The solution was concentrated under reduced pressure and purified by flash chromatography (0-10% MeOH/CH₂Cl₂). The product eluted at 5% MeOH and was isolated as an off-white solid (68% yield, 67:33 er). See the corresponding appendix for HPLC traces.

General Procedure for the Asymmetric Synthesis and Recrystallization of 1.39:

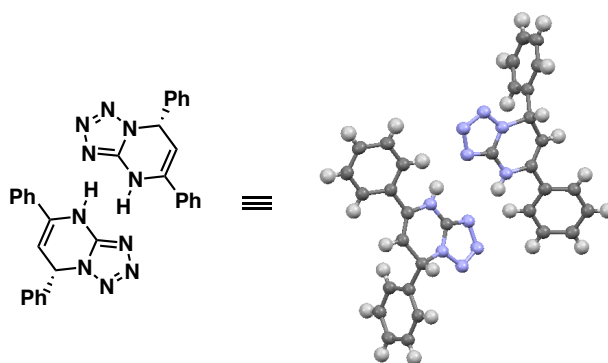
To a flame-dried vial and stir bar were added cinchona alkaloid catalyst (10 mol%, 0.02 mmol, 6.46 mg), phosphoric acid catalyst (20 mol%, 0.04 mmol, 10.00 mg), chalcone (1 equiv, 0.2 mmol, 41.65 mg) and aminotetrazole (1 equiv, 0.2 mmol, 17.01 mg). The vial was evacuated and purged with nitrogen followed by addition of 1 mL MeCN. The vial was tightly sealed using a non-septa screw cap and the reaction was heated to 80°C and stirred overnight. The mixture was then cooled to room temperature and filtered through a fritted funnel. The collected solid was rinsed with a minimal amount of CH₂Cl₂. The filtrate was concentrated under reduced pressure and purified by

flash chromatography (0-10% MeOH/CH₂Cl₂) to afford **1.39** (32% yield, 97:3 er) as a white solid. See the corresponding appendix for HPLC traces.

Determination of Absolute Stereochemistry of Enantioenriched **1.40**

We thank Dr. Jason Hein (Assistant Professor, University of British Columbia) for providing all of the X-ray structural analysis.

A sample of the major product **1.40** was recrystallized and the resulting crystals were suitable for X-ray diffraction. The structure was solved and allowed for the assignment of absolute configuration as shown (see appendix 8 for crystallography data).



1.5 References

- (1) Siegel, R. L.; Miller, K. D.; Jemal, A. *CA: A Cancer Journal for Clinicians* **2016**, 66, 7.
- (2) Patel, S. A.; Simon, M. C. *Cell Death and Differentiation* **2008**, 15, 628.
- (3) Semenza, G. L. *Trends in Pharmacological Sciences*, 33, 207.
- (4) Tian, H.; McKnight, S. L.; Russell, D. W. *Genes & Development* **1997**, 11, 72.
- (5) Greer, S. N.; Metcalf, J. L.; Wang, Y.; Ohh, M. *The EMBO Journal* **2012**, 31, 2448.

- (6) Majmundar, A. J.; Wong, W. J.; Simon, M. C. *Molecular Cell*, **40**, 294.
- (7) Schofield, C. J.; Ratcliffe, P. J. *Nature Reviews Molecular and Cell Biology* **2004**, *5*, 343.
- (8) Zagzag, D.; Zhong, H.; Scalzitti, J. M.; Laughner, E.; Simons, J. W.; Semenza, G. L. *Cancer* **2000**, *88*, 2606.
- (9) Bos, R.; van der Groep, P.; Greijer, A. E.; Shvarts, A.; Meijer, S.; Pinedo, H. M.; Semenza, G. L.; van Diest, P. J.; van der Wall, E. *Cancer* **2003**, *97*, 1573.
- (10) Rankin, E. B.; Giaccia, A. J. *Cell Death and Differentiation* **2008**, *15*, 678.
- (11) I would like to acknowledge the Garder and Bruick labs and Tom Scheuermann for providing this image and the proceeding crystallographic images.
- (12) Bruick, R. K.; McKnight, S. L. *Science* **2001**, *294*, 1337.
- (13) Depping, R.; Steinhoff, A.; Schindler, S. G.; Friedrich, B.; Fagerlund, R.; Metzen, E.; Hartmann, E.; Köhler, M. *Biochimica et Biophysica Acta (BBA) - Molecular Cell Research* **2008**, *1783*, 394.
- (14) Partch, C. L.; Gardner, K. H. *Proceedings of the National Academy of Sciences* **2011**, *108*, 7739.
- (15) Card, P. B.; Erbel, P. J. A.; Gardner, K. H. *Journal of Molecular Biology* **2005**, *353*, 664.
- (16) Guo, Y.; Scheuermann, T. H.; Partch, C. L.; Tomchick, D. R.; Gardner, K. H. *Journal of Biological Chemistry* **2015**, *290*, 7707.
- (17) Scheuermann, T. H.; Yang, J.; Zhang, L.; Gardner, K. H.; Bruick, R. K. In *Methods in Enzymology*; Academic Press: 2007; Vol. Volume 435, p 1.
- (18) Partch, C. L.; Card, P. B.; Amezcua, C. A.; Gardner, K. H. *Journal of Biological Chemistry* **2009**, *284*, 15184.
- (19) Erbel, P. J. A.; Card, P. B.; Karakuzu, O.; Bruick, R. K.; Gardner, K. H. *Proceedings of the National Academy of Sciences* **2003**, *100*, 15504.
- (20) Kewley, R. J.; Whitelaw, M. L.; Chapman-Smith, A. *International Journal of Biochemistry and Cell Biology* **2004**, *36*, 189.
- (21) Scheuermann, T. H.; Tomchick, D. R.; Machius, M.; Guo, Y.; Bruick, R. K.;

- Gardner, K. H. *Proceedings of the National Academy of Sciences* **2009**, *106*, 450.
- (22) Scheuermann, T. H.; Li, Q.; Ma, H.-W.; Key, J.; Zhang, L.; Chen, R.; Garcia, J. A.; Naidoo, J.; Longgood, J.; Frantz, D. E.; Tambar, U. K.; Gardner, K. H.; Bruick, R. K. *Nature Chemical Biology* **2013**, *9*, 271.
- (23) Rogers, J. L.; Bayeh, L.; Scheuermann, T. H.; Longgood, J.; Key, J.; Naidoo, J.; Melito, L.; Shokri, C.; Frantz, D. E.; Bruick, R. K.; Gardner, K. H.; MacMillan, J. B.; Tambar, U. K. *Journal of Medicinal Chemistry* **2013**, *56*, 1739.
- (24) Scheuermann, T. H.; Stroud, D.; Sleet, C. E.; Bayeh, L.; Shokri, C.; Wang, H.; Caldwell, C. G.; Longgood, J.; MacMillan, J. B.; Bruick, R. K.; Gardner, K. H.; Tambar, U. K. *Journal of Medicinal Chemistry* **2015**, *58*, 5930.
- (25) Key, J.; Scheuermann, T. H.; Anderson, P. C.; Daggett, V.; Gardner, K. H. *Journal of the American Chemical Society* **2009**, *131*, 17647.
- (26) This project was done in collaboration with the MacMillan, Bruick, Gardner, Posner, and Williams labs and the UT Southwestern Chemistry Core.
- (27) Ullman, E. F.; Kirakossian H.; Switchenko, A. C.; Ishkanian, J.; Ericson, M.; Wartchow, C. A.; Pirio, M.; Pease, J.; Irvin, B. R.; Singh, S.; Singh, R.; Patel, R.; Dafforn, A.; Davalian, D.; Skold, C.; Kurn, N.; Wagner, D. B. *Clinical Chemistry*, *42*, 1518.
- (28) Cuconati, A., Block, T. M., Xu X. Patent: WO2007131168A2 2007.
- (29) Dougherty, A. M.; Guo, H.; Westby, G.; Liu, Y.; Simsek, E.; Guo, J.-T.; Mehta, A.; Norton, P.; Gu, B.; Block, T.; Cuconati, A. *Antimicrobial Agents and Chemotherapy* **2007**, *51*, 4427.
- (30) Butler, R. N. *Comprehensive Heterocyclic Chemistry*; Pergamon: Oxford, U. K. , 1996; Vol. 4.
- (31) Herr, R. J. *Bioorganic & Medicinal Chemistry* **2002**, *10*, 3379.
- (32) Nekrasov, D. D. *Chemistry of Heterocyclic Compounds* **2001**, *37*, 263.
- (33) Farina, V.; Reeves, J. T.; Senanayake, C. H.; Song, J. J. *Chemical Reviews* **2006**, *106*, 2734.
- (34) Carey, J. S.; Laffan, D.; Thomson, C.; Williams, M. T. *Organic & Biomolecular*

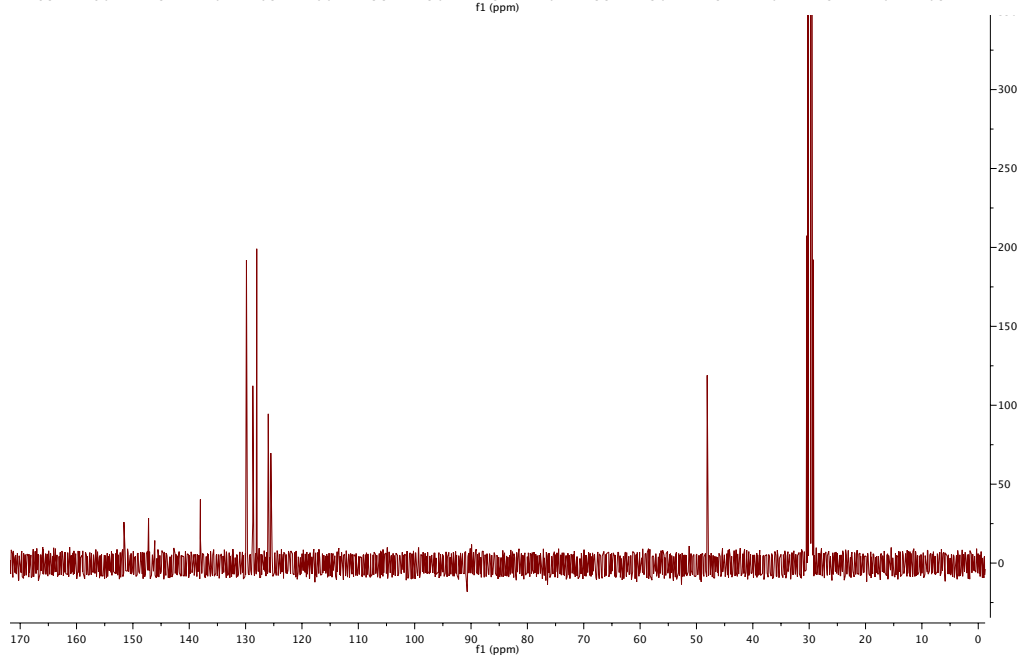
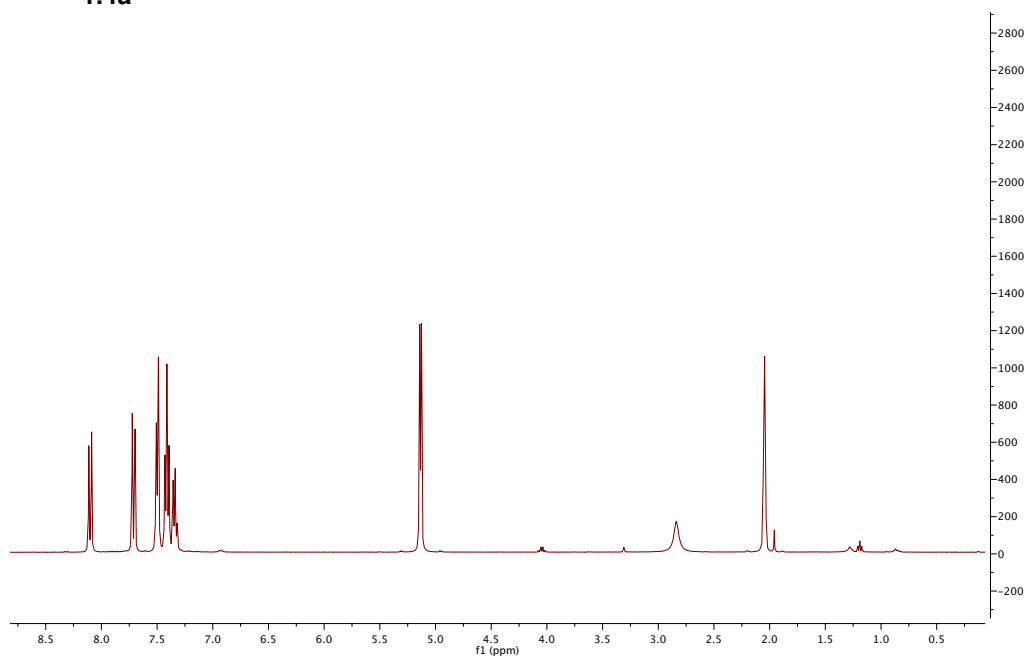
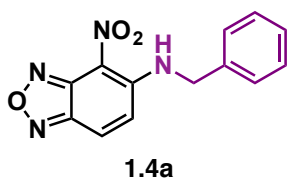
- Chemistry* **2006**, *4*, 2337.
- (35) Melchiorre, P. *Angewandte Chemie International Edition* **2012**, *51*, 9748.
 - (36) Bertelsen, S.; Jorgensen, K. A. *Chemical Society Reviews* **2009**, *38*, 2178.
 - (37) Chen, W.; Du, W.; Yue, L.; Li, R.; Wu, Y.; Ding, L.-S.; Chen, Y.-C. *Organic & Biomolecular Chemistry* **2007**, *5*, 816.
 - (38) Jiang, L.; Chen, Y.-C. *Catalysis Science & Technology* **2011**, *1*, 354.
 - (39) Lan, Y.-B.; Zhao, H.; Liu, Z.-M.; Liu, G.-G.; Tao, J.-C.; Wang, X.-W. *Organic Letters* **2011**, *13*, 4866.
 - (40) Cai, Q.; You, S.-L. *Organic Letters* **2012**, *14*, 3040.
 - (41) Jin, Z.; Wang, X.; Huang, H.; Liang, X.; Ye, J. *Organic Letters* **2011**, *13*, 564.
 - (42) Feng, X.; Zhou, Z.; Zhou, R.; Zhou, Q.-Q.; Dong, L.; Chen, Y.-C. *Journal of the American Chemical Society* **2012**, *134*, 19942.
 - (43) Paradisi, E.; Righi, P.; Mazzanti, A.; Ranieri, S.; Bencivenni, G. *Chemical Communications* **2012**, *48*, 11178.
 - (44) Lifchits, O.; Reisinger, C. M.; List, B. *Journal of the American Chemical Society* **2010**, *132*, 10227.
 - (45) Tian, X.; Cassani, C.; Liu, Y.; Moran, A.; Urakawa, A.; Galzerano, P.; Arceo, E.; Melchiorre, P. *Journal of the American Chemical Society* **2011**, *133*, 17934.
 - (46) Bergonzini, G.; Vera, S.; Melchiorre, P. *Angewandte Chemie International Edition* **2010**, *49*, 9685.
 - (47) Moran, A.; Hamilton, A.; Bo, C.; Melchiorre, P. *Journal of the American Chemical Society* **2013**, *135*, 9091.
 - (48) Klusmann, M.; Iwamura, H.; Mathew, S. P.; Wells, D. H.; Pandya, U.; Armstrong, A.; Blackmond, D. G. *Nature* **2006**, *441*, 621.
 - (49) Kellogg, R. M. *Angewandte Chemie International Edition* **2007**, *46*, 494.
 - (50) Keana, J. F. W.; Kher, S. M.; Cai, S. X.; Dinsmore, C. M.; Glenn, A. G.; Guastella, J.; Huang, J. C.; Ilyin, V.; Lu, Y.; Mouser, D. L.; Woodward, R. M.; Weber, E. *Journal of Medicinal Chemistry* **1995**, *38*, 4367.
 - (51) Valdez, J.; Cedillo, R.; Hernandez-Campos, A.; Yepez, L.; Hernandez-Luis, F.;

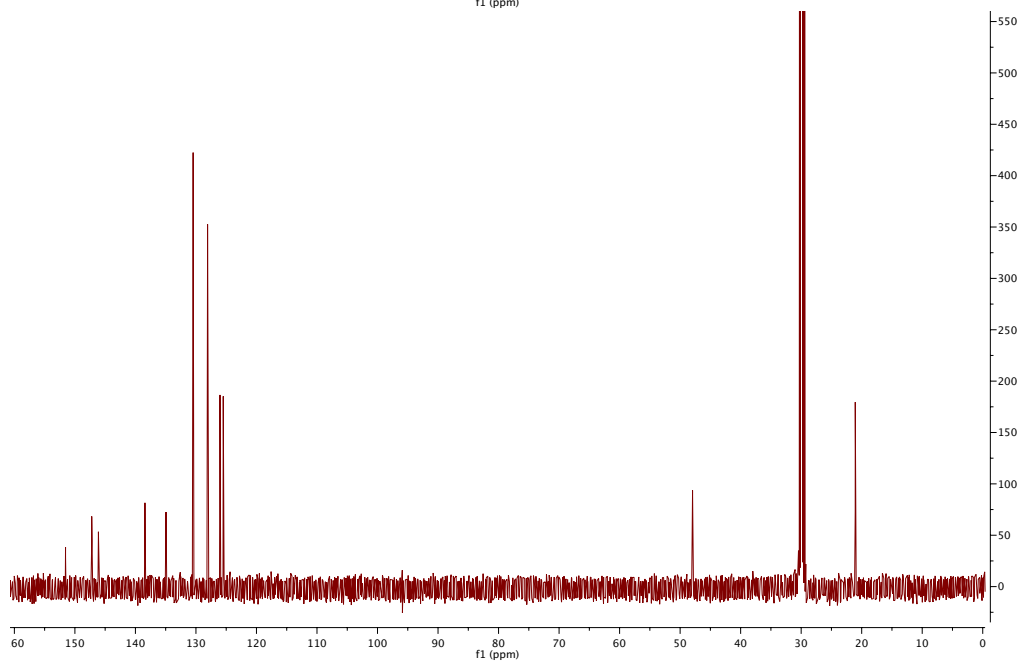
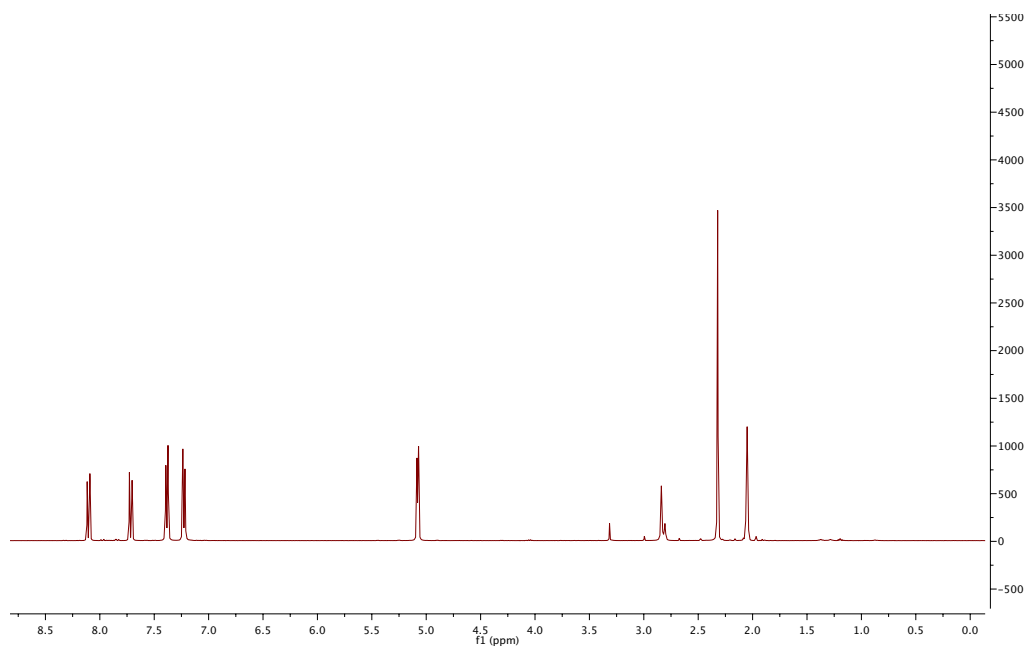
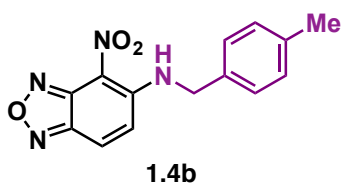
Navarrete-Vazquez, G.; Tapia, A.; Cortes, R.; Hernandez, M.; Castillo, R.
Bioorganic and Medicinal Chemistry Letters **2002**, *12*, 2221.

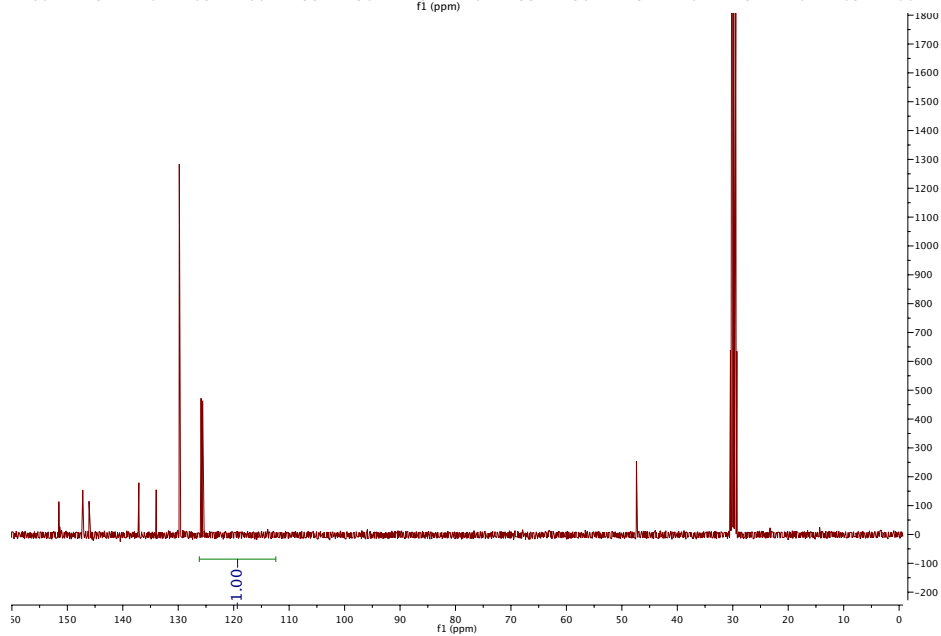
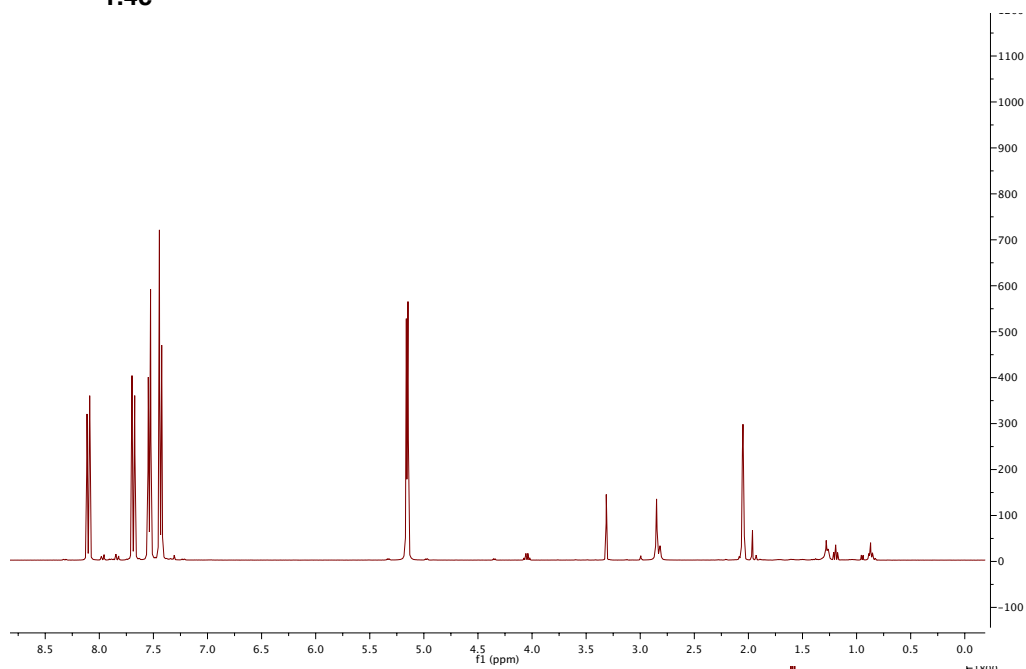
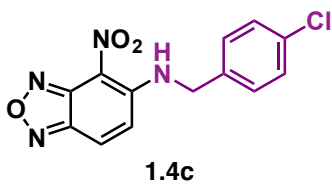
- (52) Reid, A. K.; McHugh, C. J.; Richie, G.; Graham, D. *Tetrahedron Letters* **2006**, *47*, 4201.
- (53) Ghosh, P. B.; Everitt, B. J. *Journal of Medicinal Chemistry* **1974**, *17*, 203.

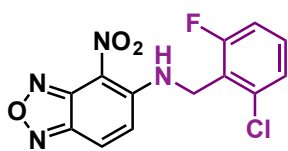
APPENDIX ONE

Spectra Relevant to Chapter One: The Development of Allosteric Inhibitors of the HIF-2 α Transcription Factor

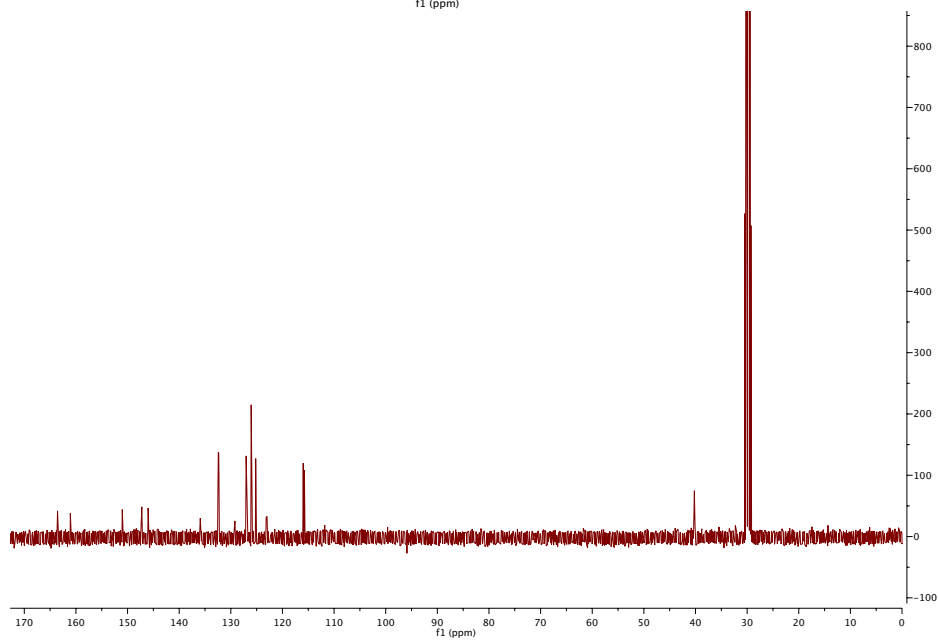
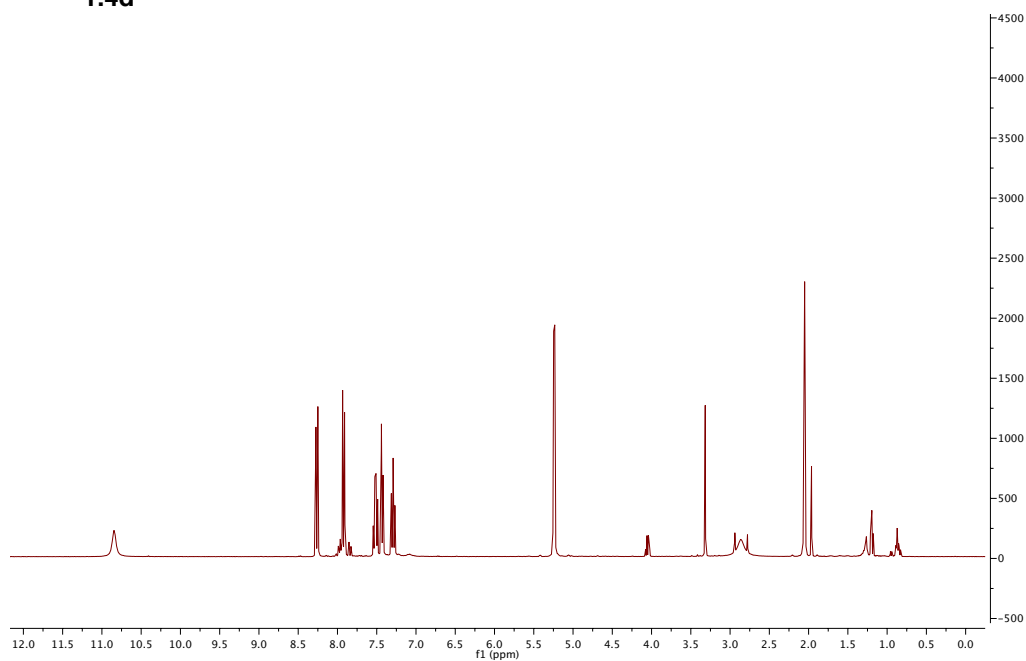


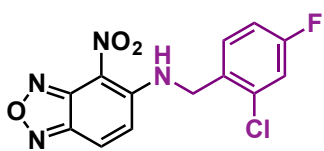




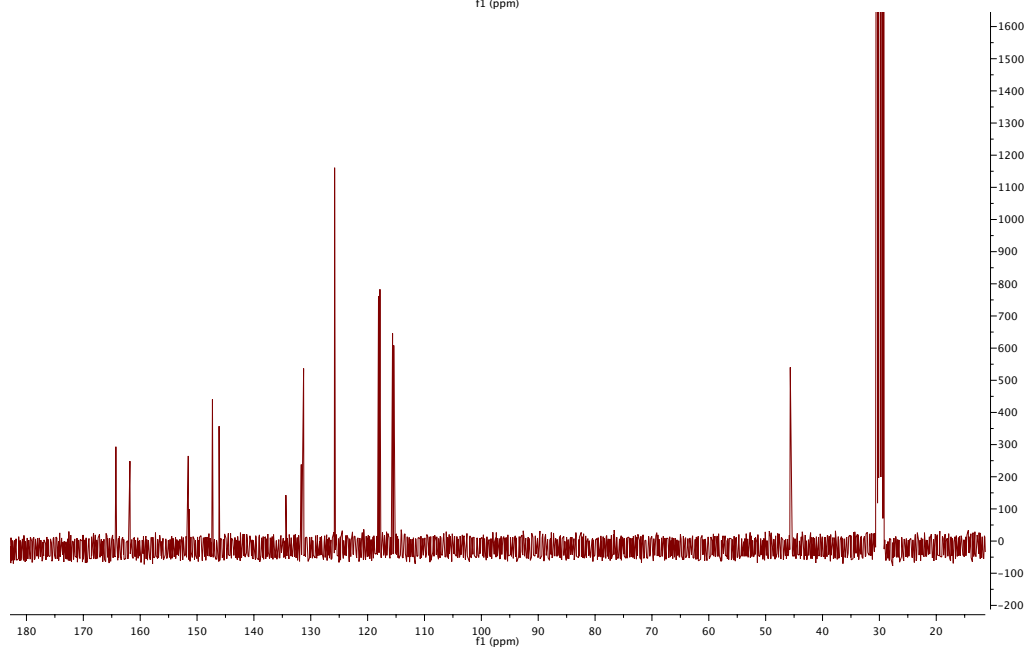
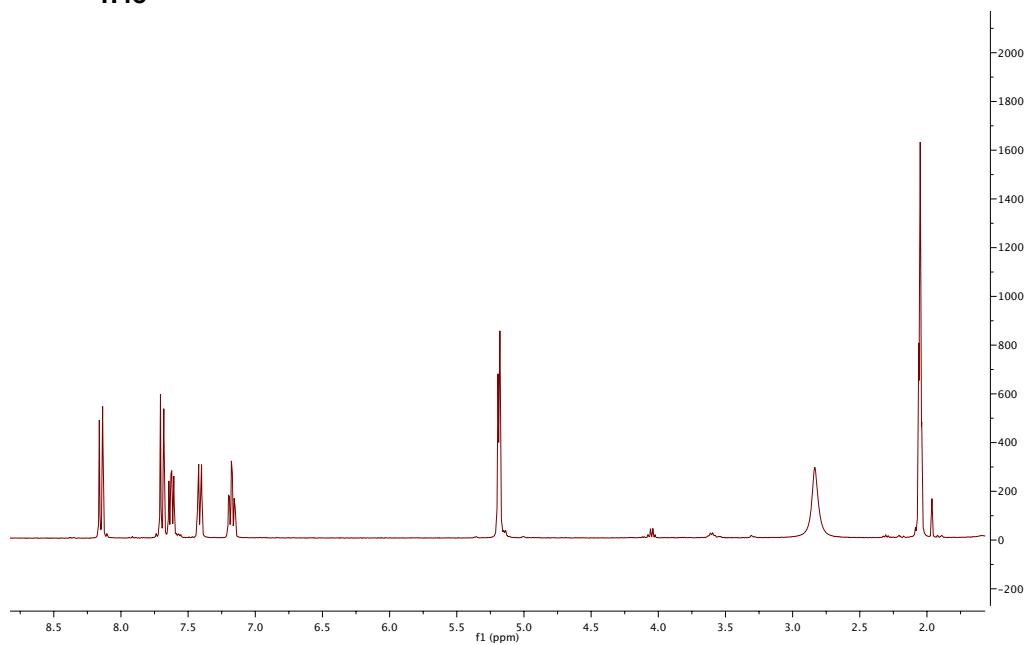


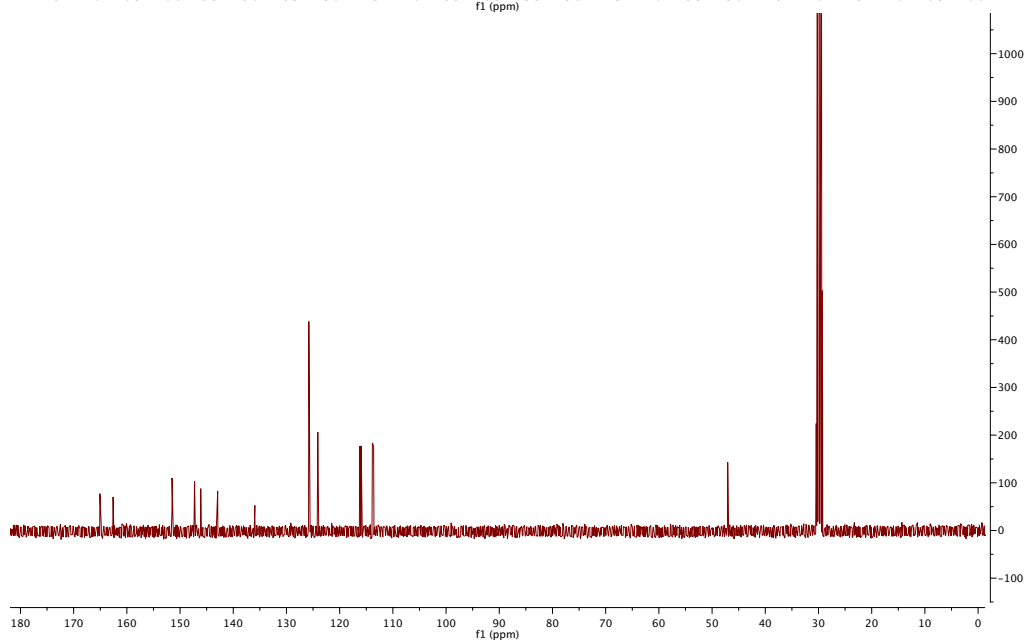
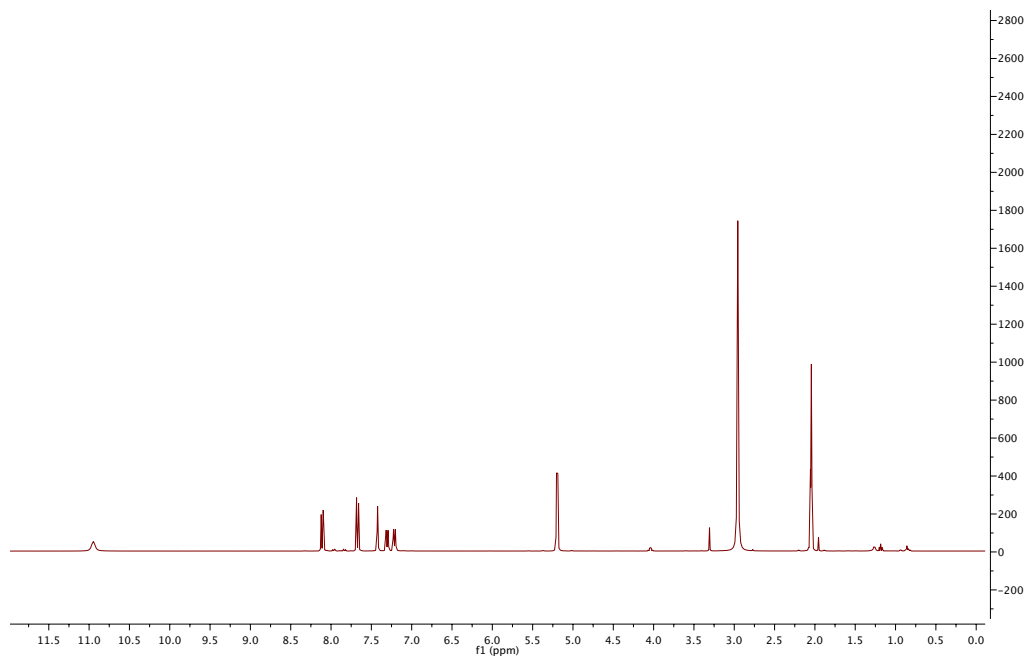
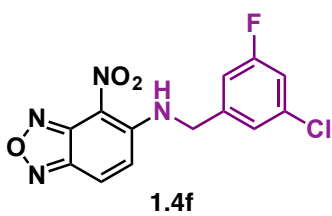
1.4d

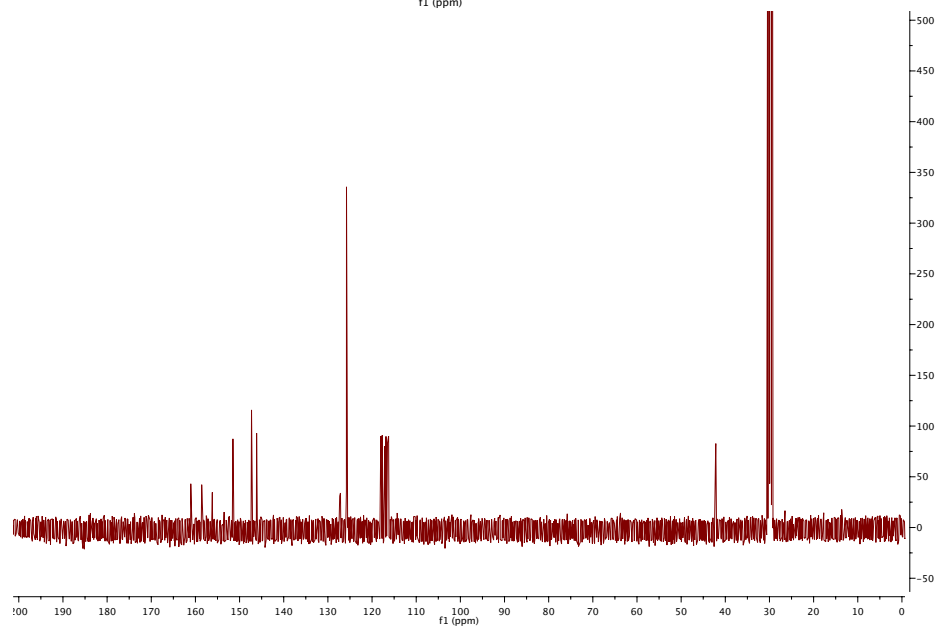
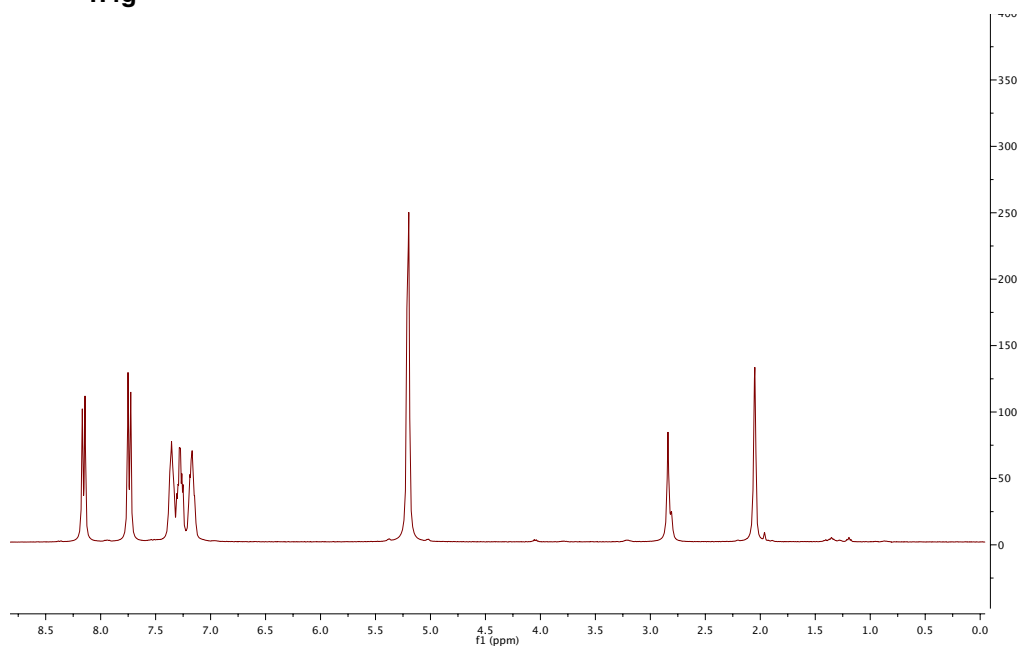
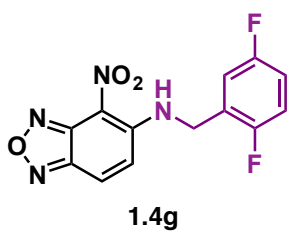


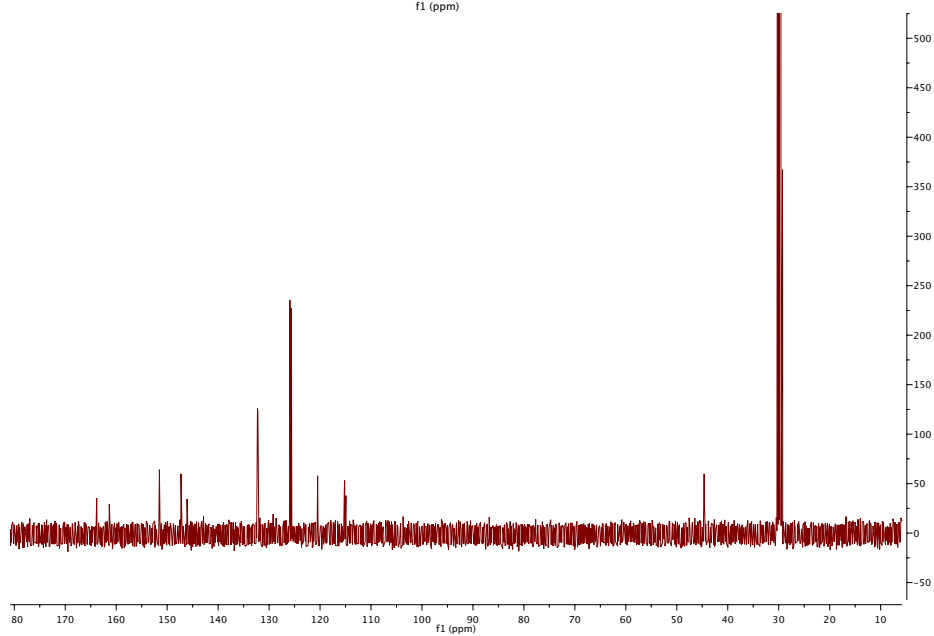
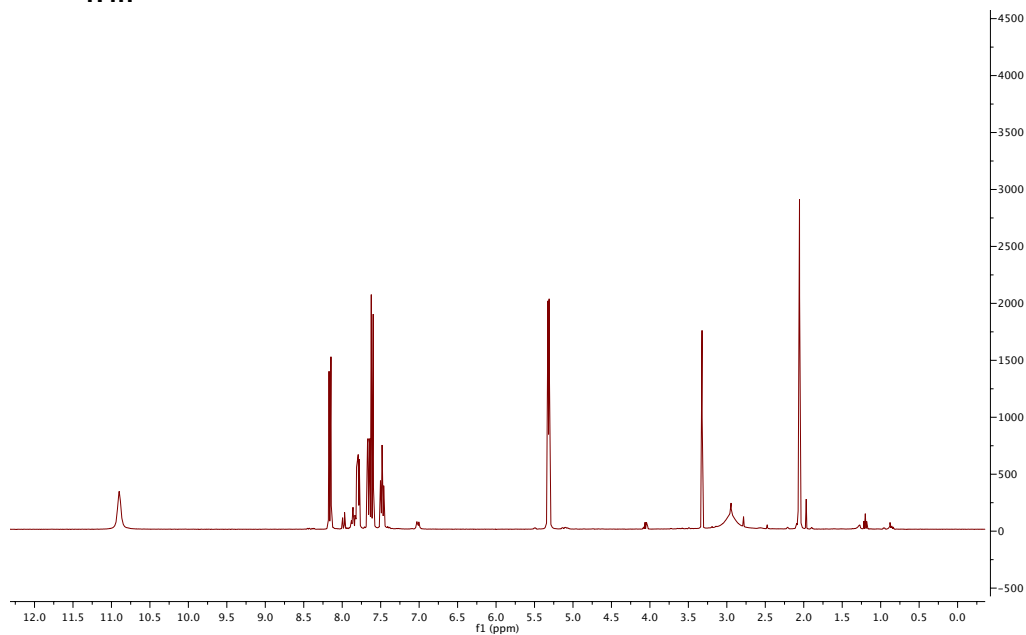
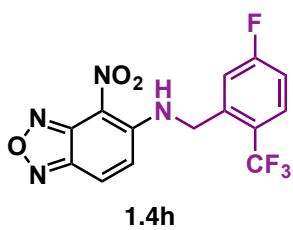


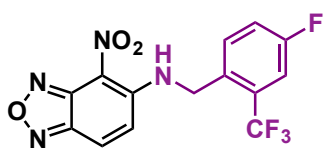
1.4e



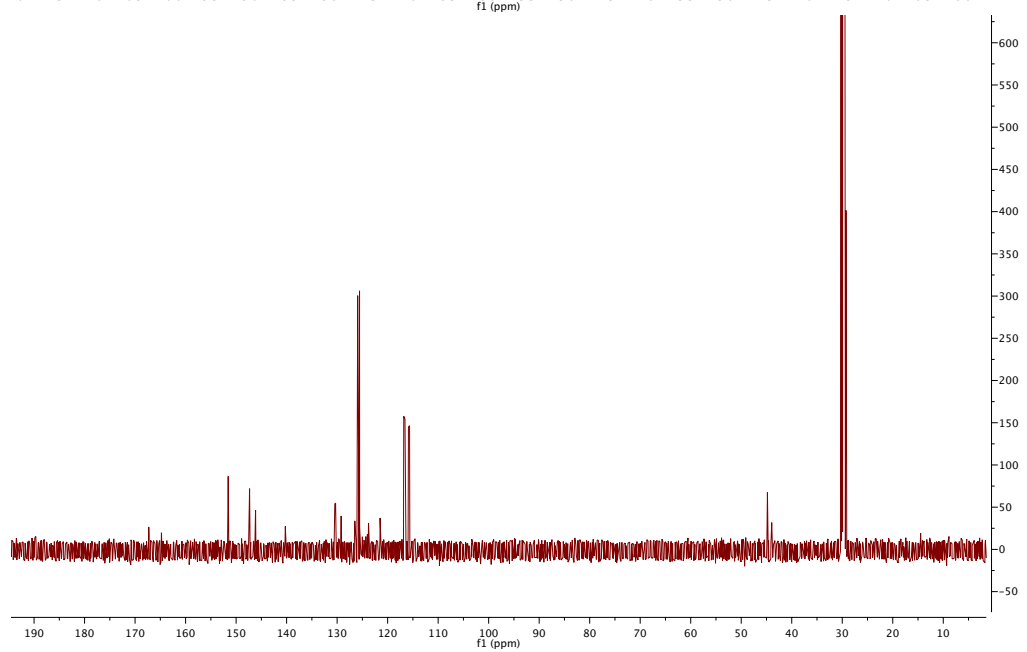
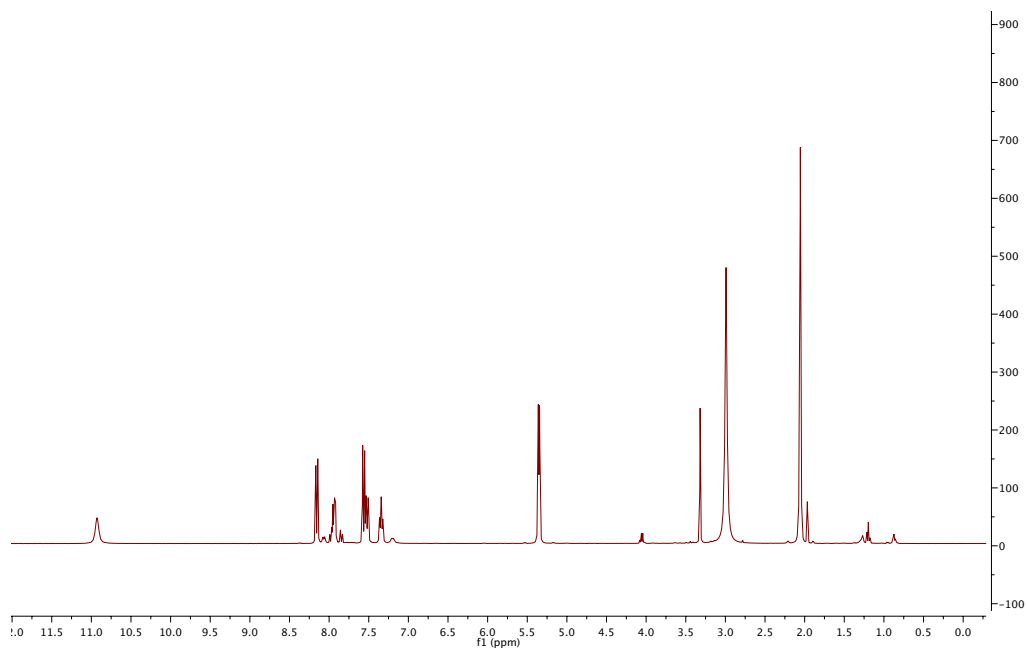


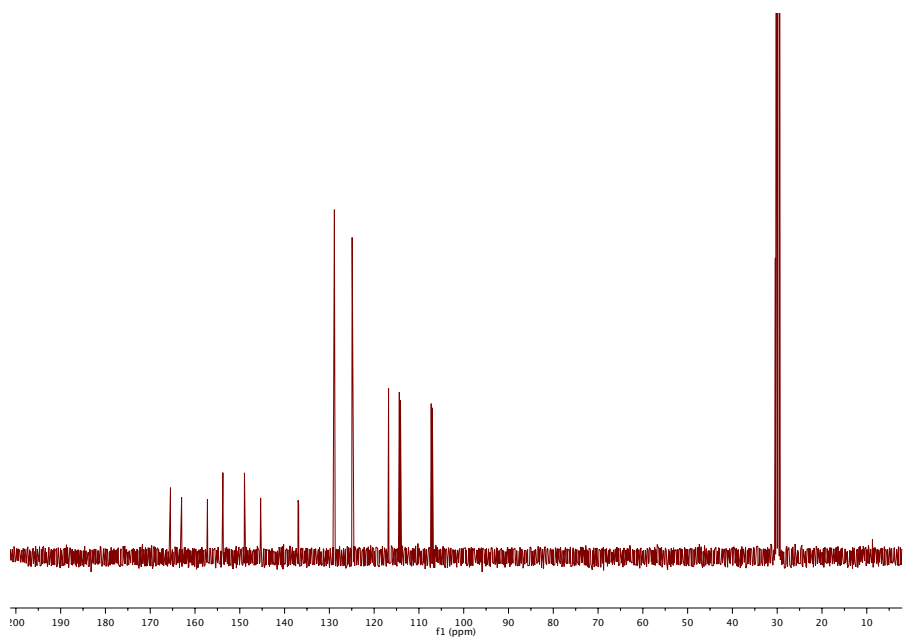
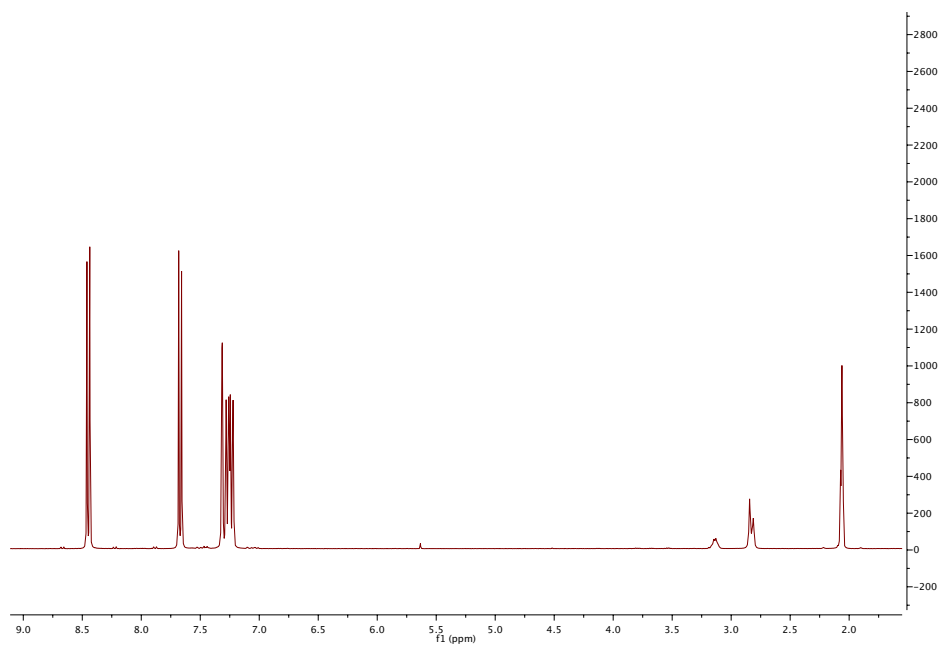
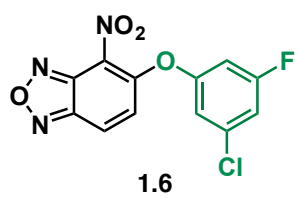


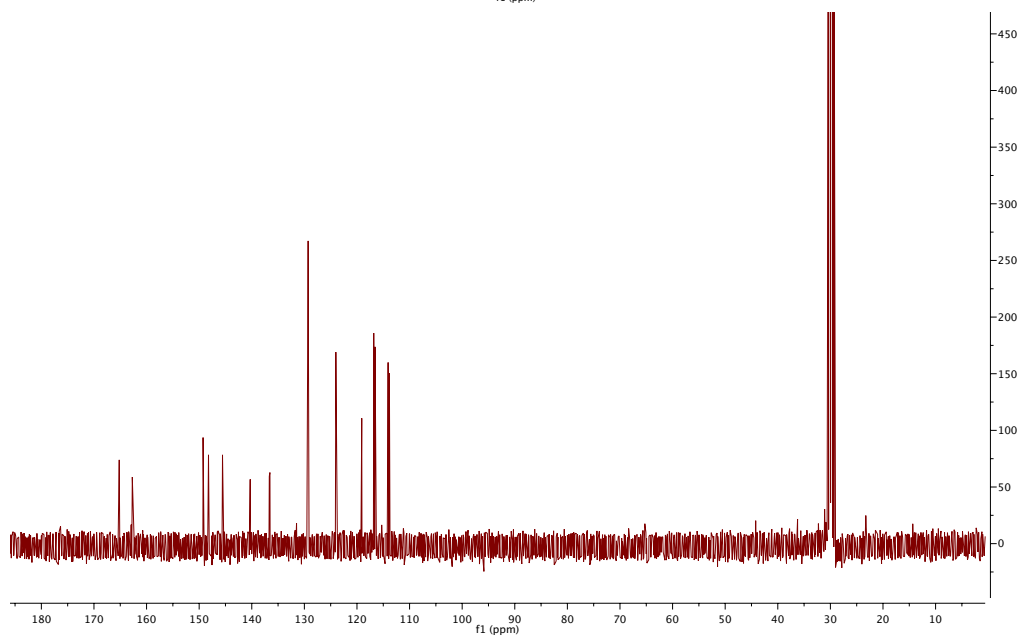
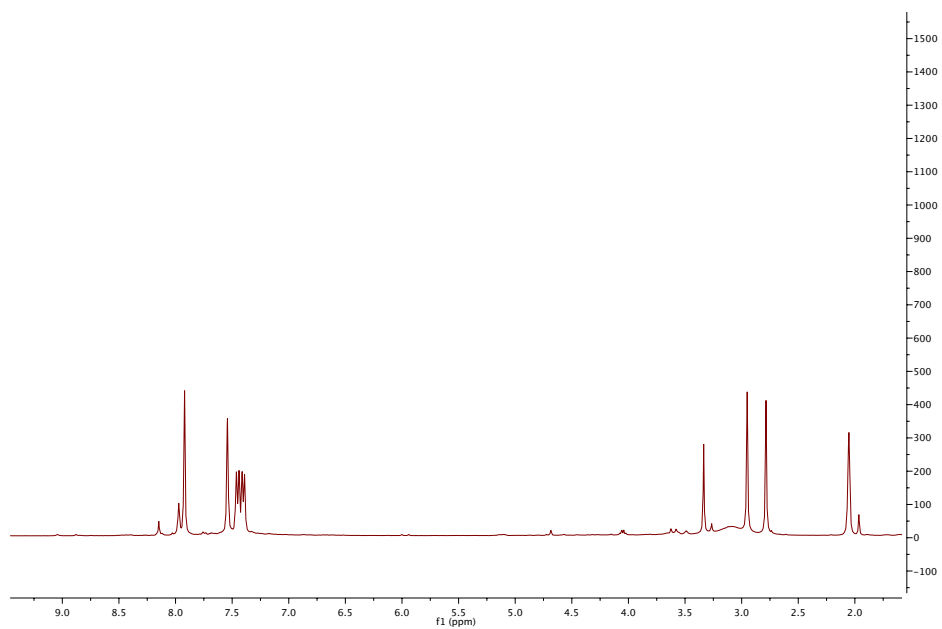
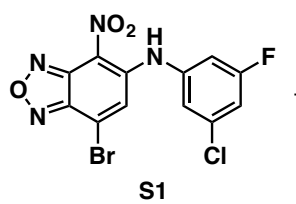


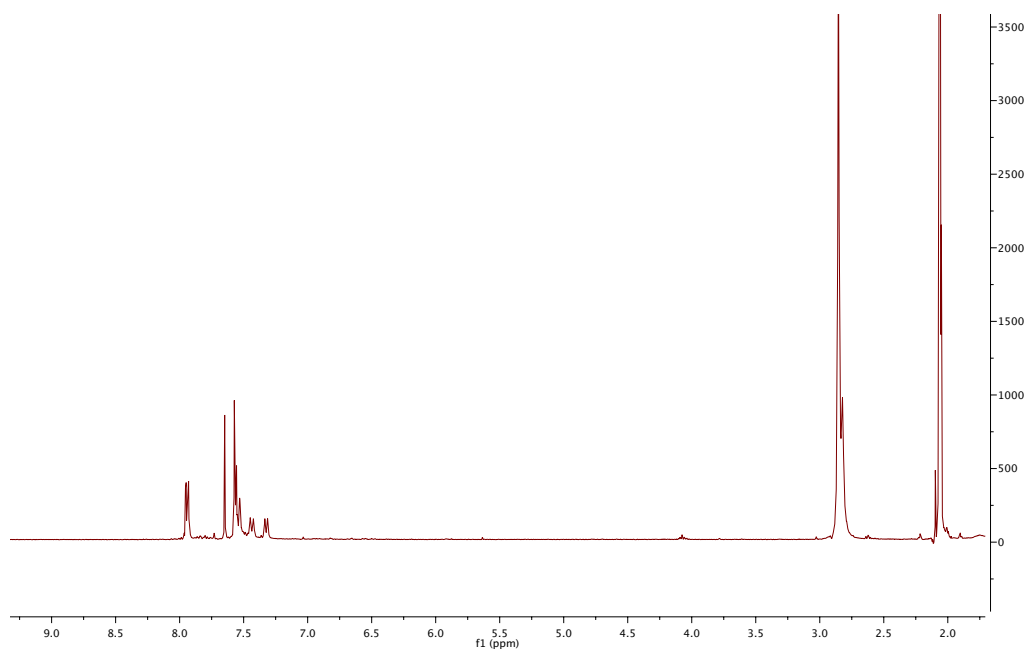
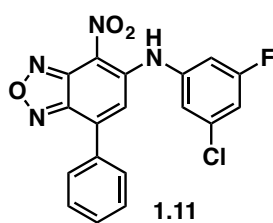


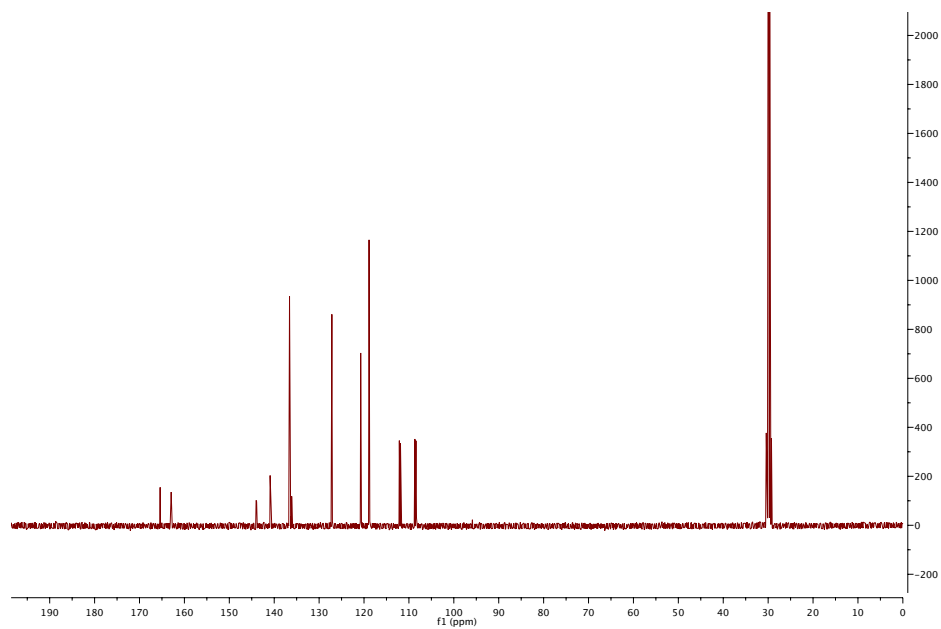
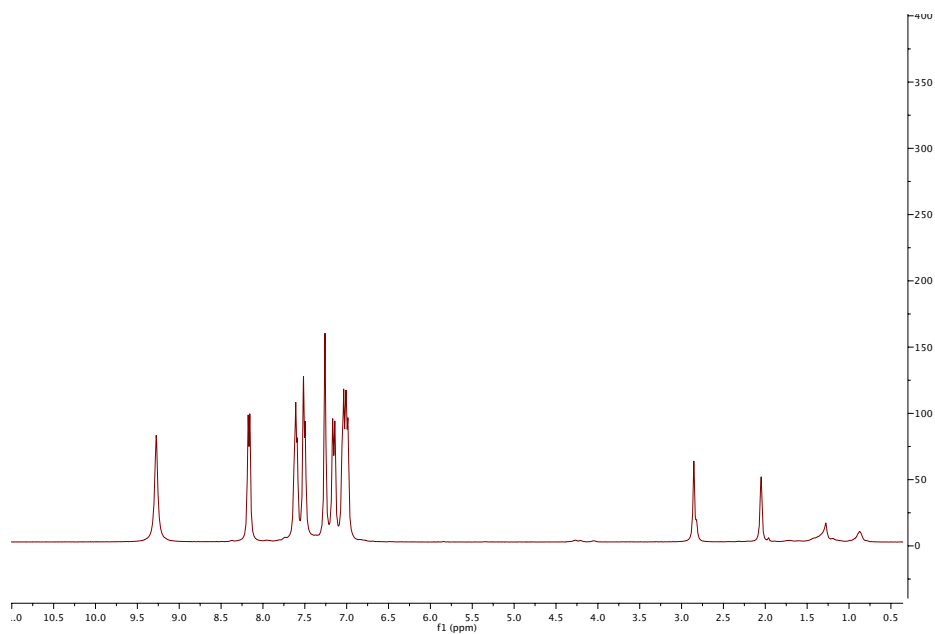
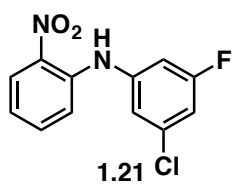
1.4i

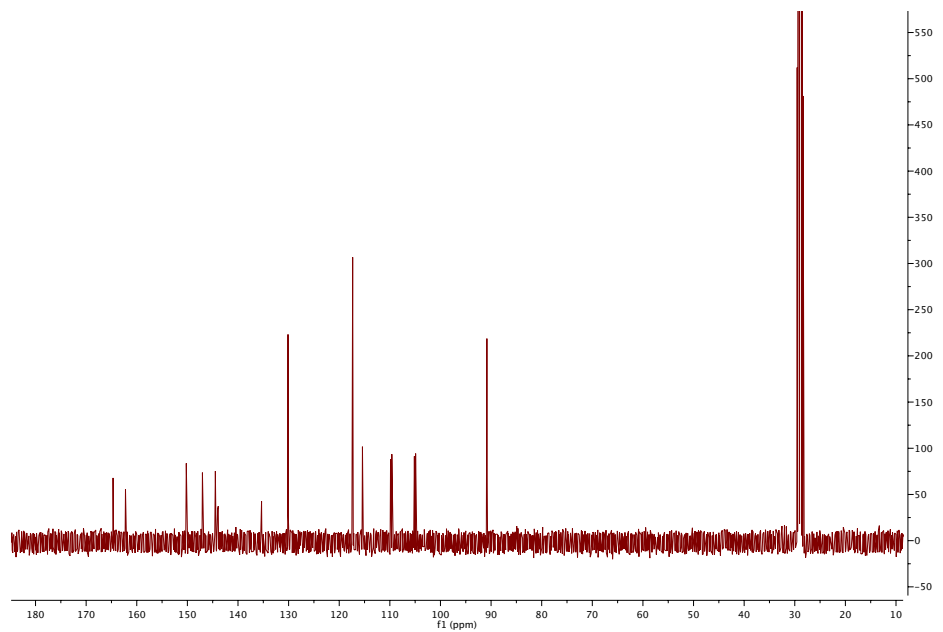
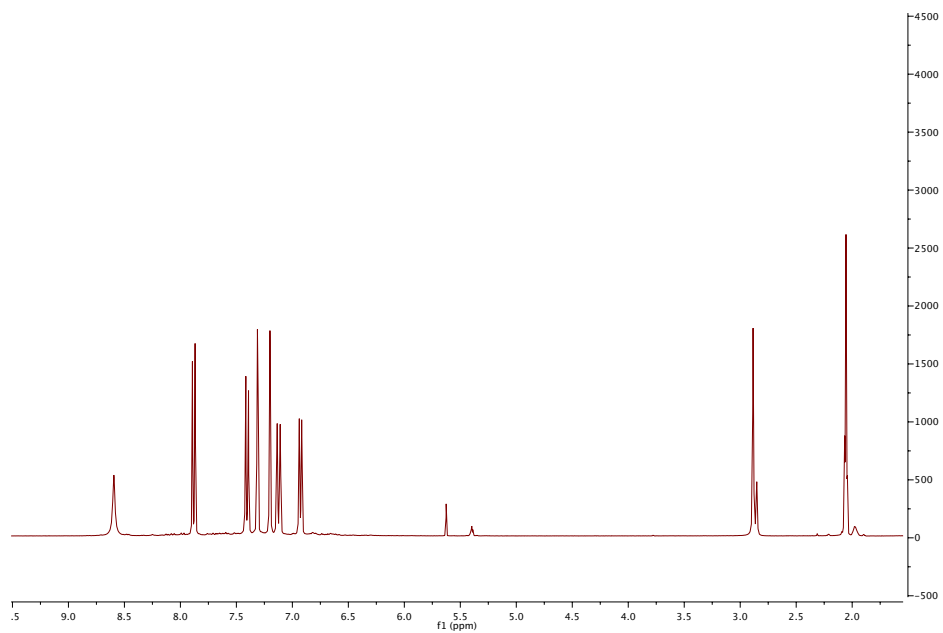
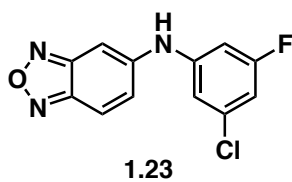


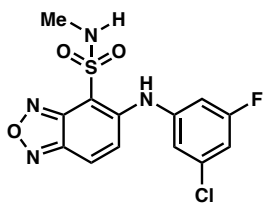




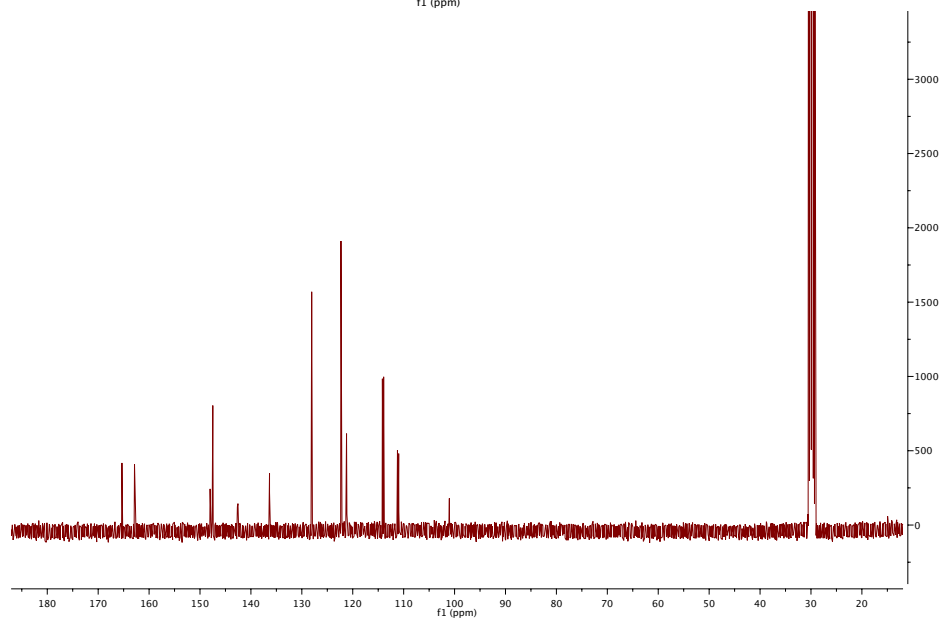
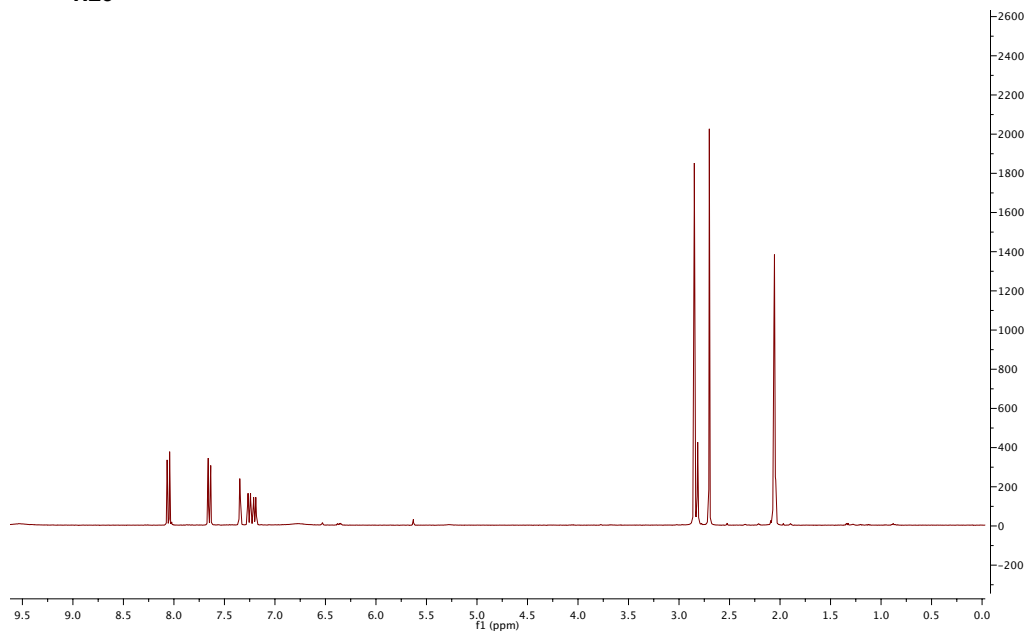


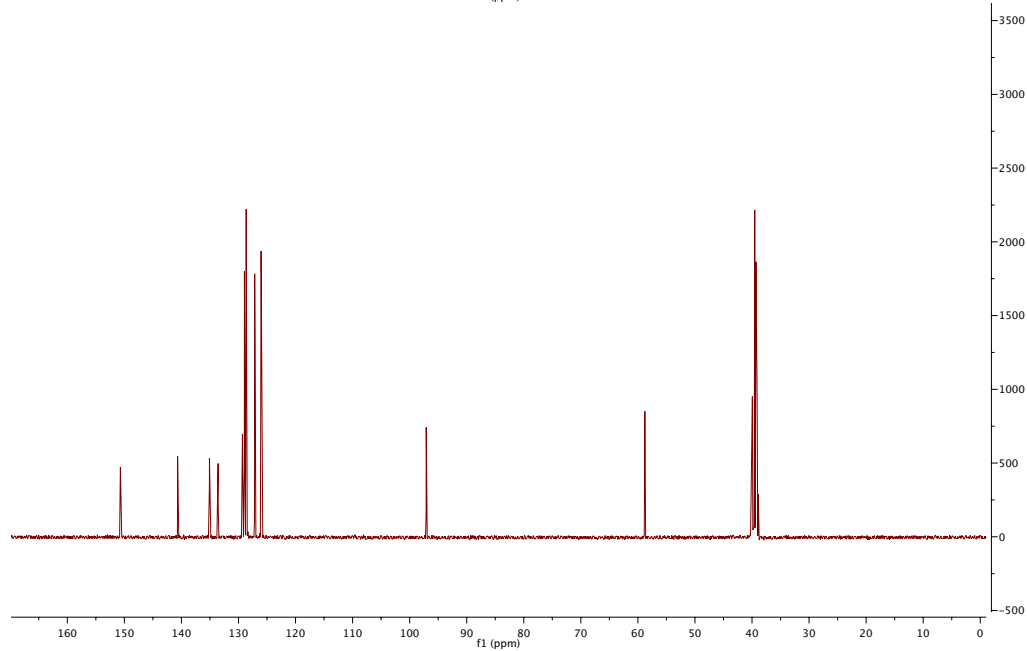
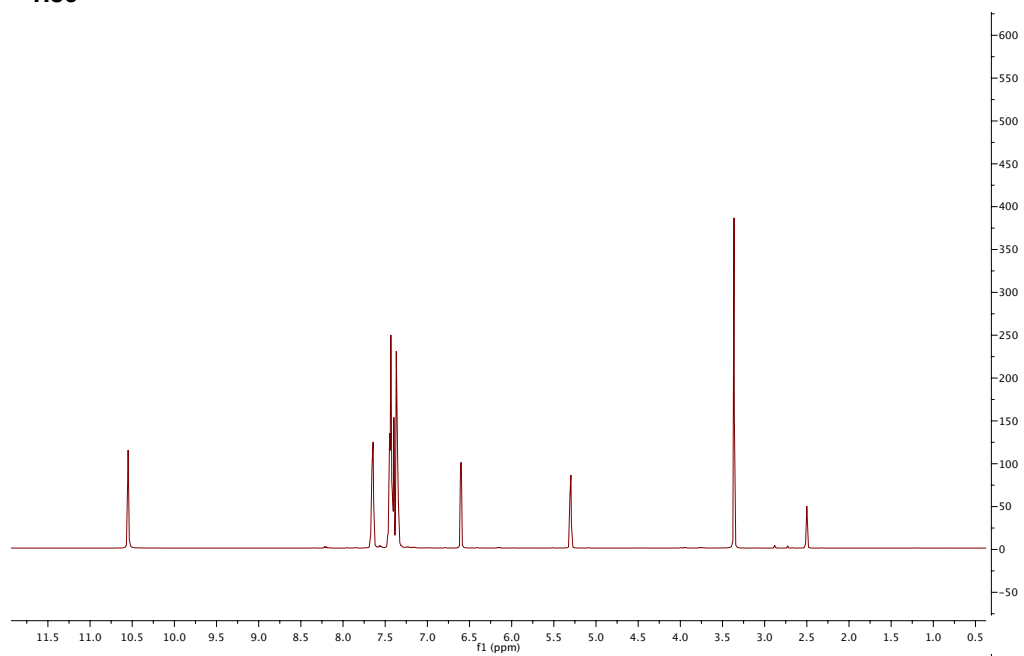
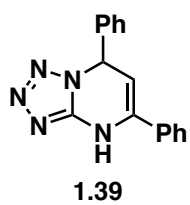


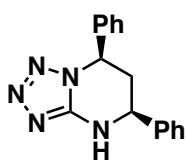




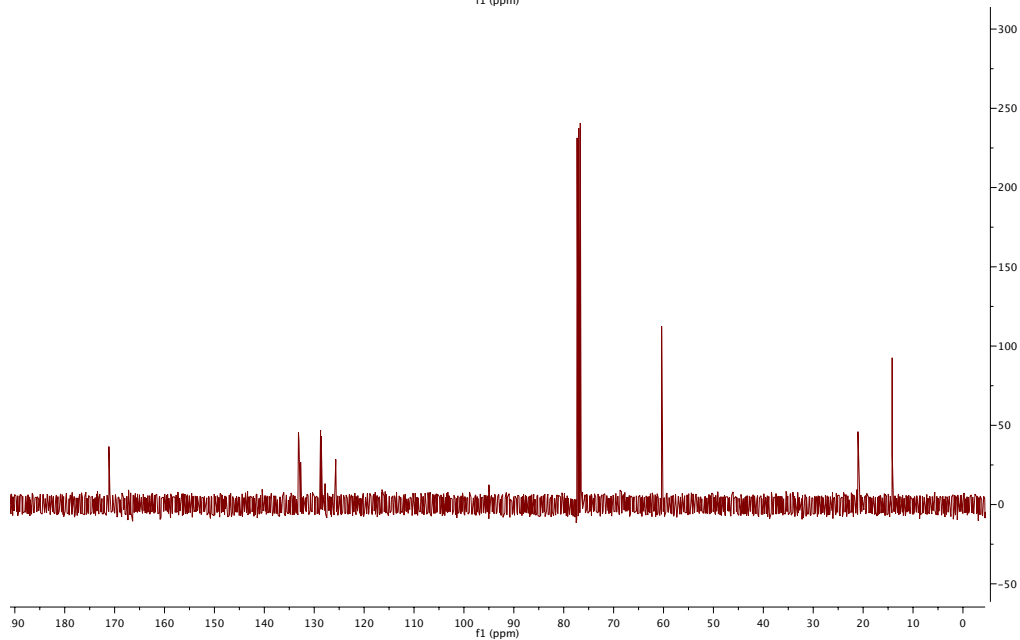
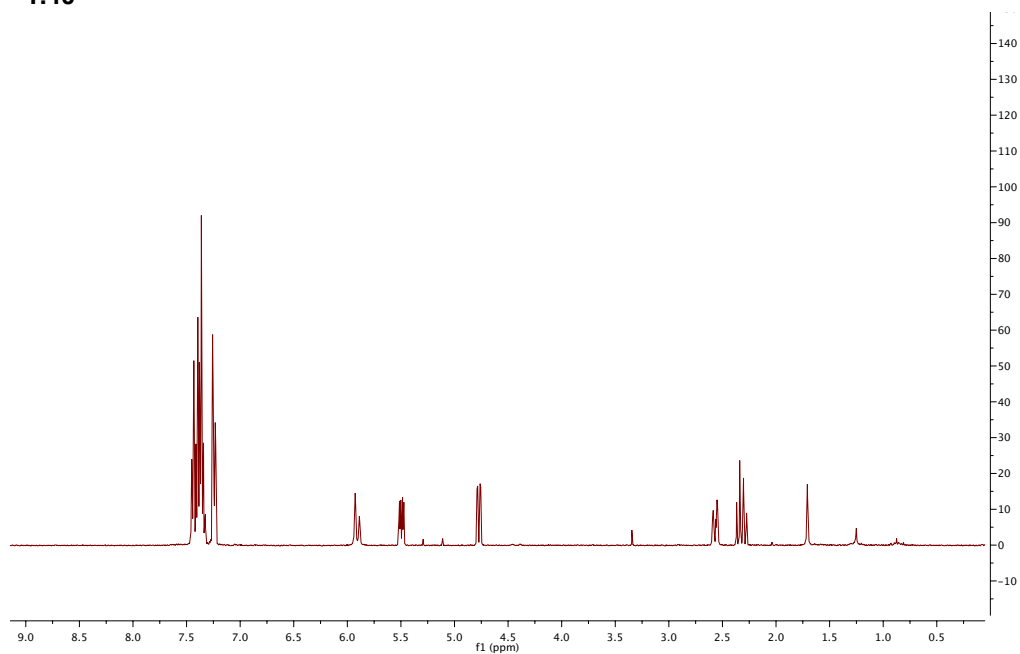
1.29





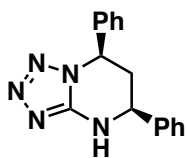


1.40



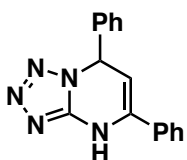
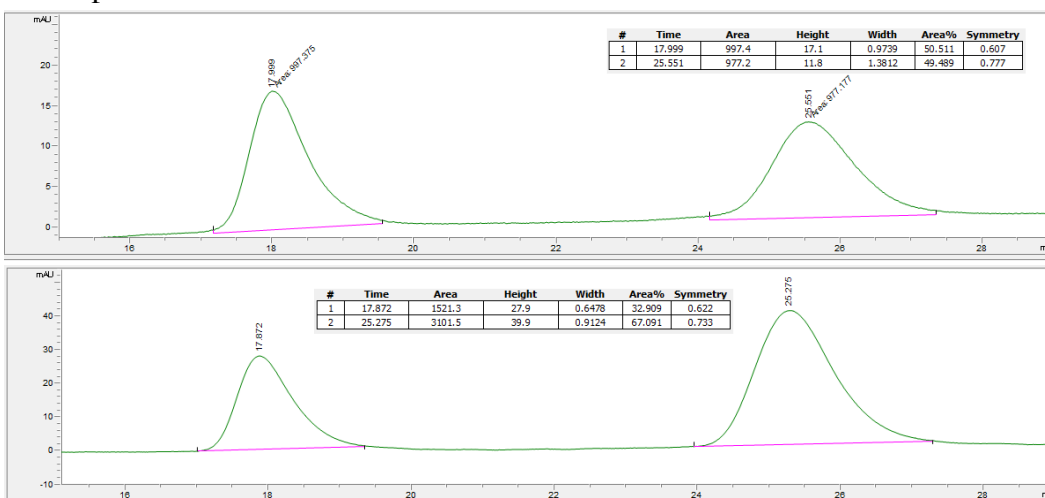
APPENDIX TWO

HPLC Traces Relevant to Chapter One: The Development of Allosteric Inhibitors of the HIF-2 α Transcription Factor



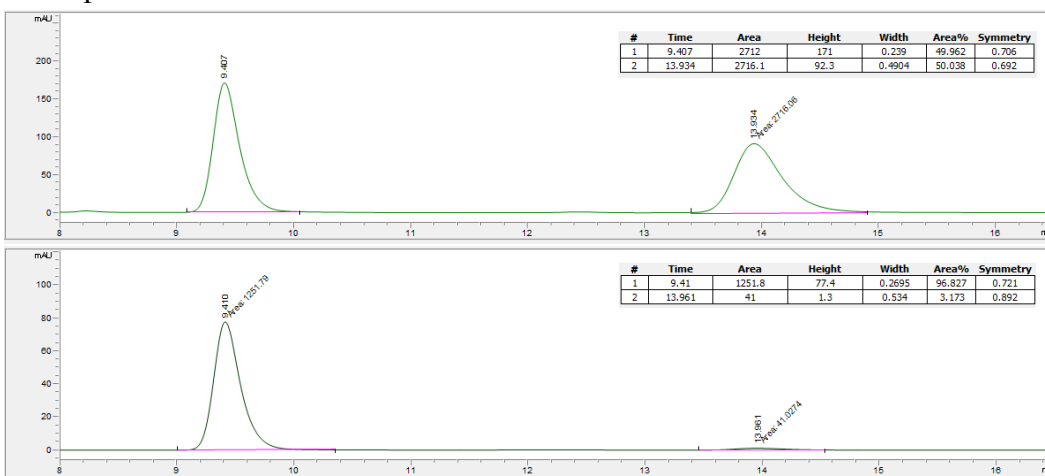
1.40

Chiralpak AD-H 80:20 IPA:Hexane 0.5 ml/min



1.39

Chiralpak AD-H 80:20 IPA:Hexane 0.8 ml/min



CHAPTER TWO

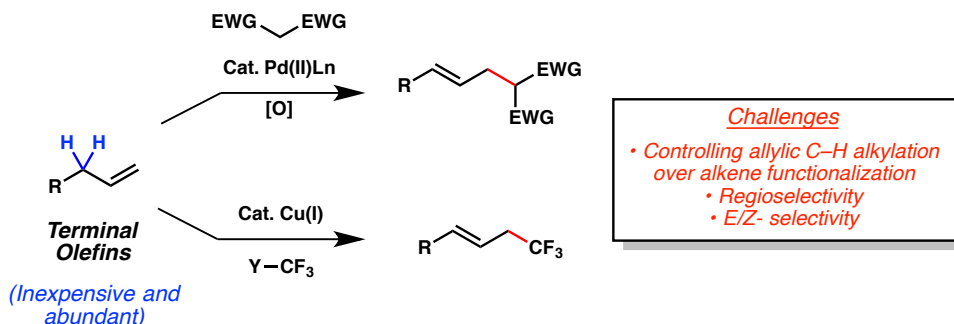
An Allylic Alkylation of Unactivated Terminal Olefins with Grignard Reagents

2.1 Background

2.1.1 Introduction

Unsaturated hydrocarbons represent an inexpensive and readily abundant class of starting materials for chemical synthesis. A large number of terminal olefins, for example, are regularly generated as byproducts of the high temperature ‘cracking’ of natural gas and crude oil hydrocarbons. As a result, both lower order and higher order terminal olefins have found wide-ranging applications in the manufacturing of functional materials, from industrial drilling fluids to sun creams and plastics.¹⁻³ For example, 700,000 tons of 1-butene are used in the industrial manufacturing of linear low density polyethylene *annually*.³

Scheme 2.1.1



Due to the wide availability of hydrocarbons bearing terminal olefins, the functionalization of these compounds with carbon nucleophiles represents an attractive

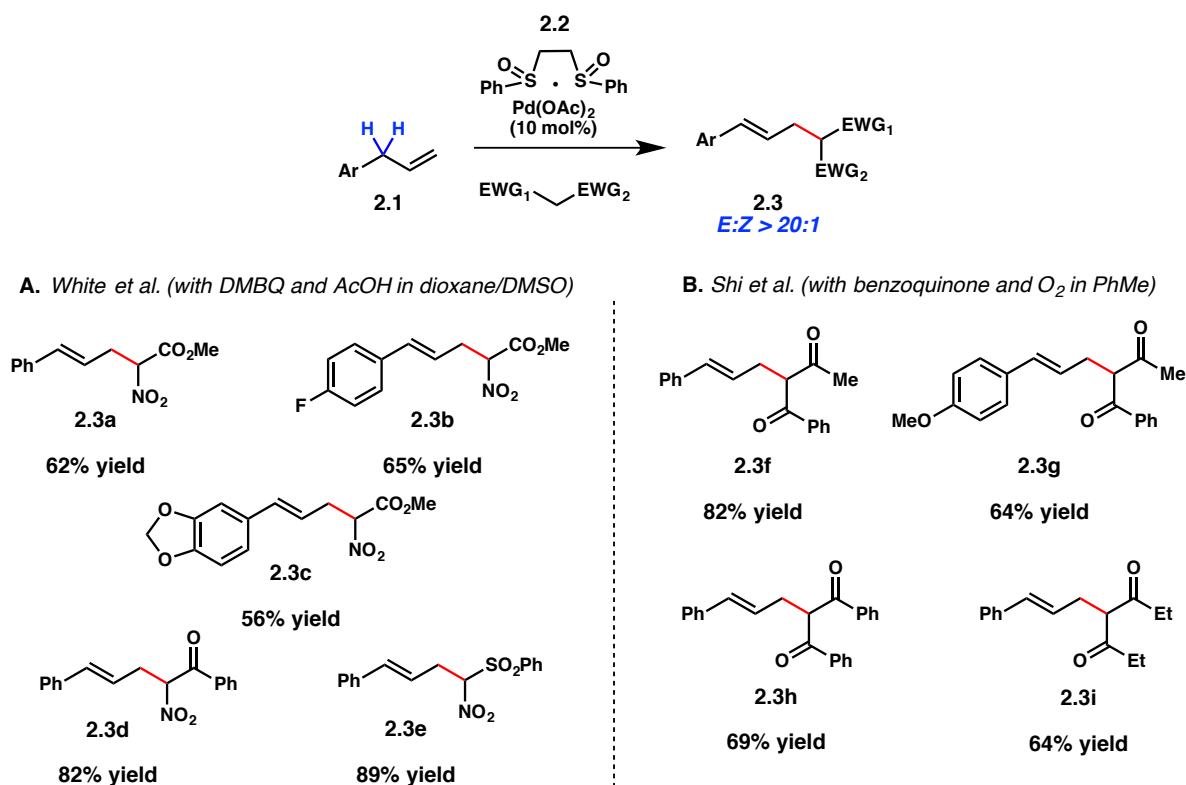
strategy for the construction of value-added materials.^{4,8} More specifically, the direct allylic C(sp³)-H alkylation of terminal alkenes has only recently found success in the context of metal-mediated processes utilizing stabilized carbon nucleophiles and trifluoromethane donors (Scheme 2.1.1).⁹⁻¹¹ Several novel and elegant examples of early reports on intermolecular allylic C(sp³)-C(sp³) bond formation of these types are described herein.

2.1.2 Stabilized Carbon Nucleophiles for the Selective Allylic Alkylation of Terminal Olefins

In 1973 Trost and Fullerton provided the first report of an allylic alkylation utilizing a non-functionalized alkene.¹² While stoichiometric amounts of palladium(II) were necessary, this work provided a better understanding of palladium promoted allylic C-H activation. In the ensuing years, major advances in the field of allylic oxidation by the White group provided the solution to developing a catalytic version of Trost's discovery, revealing that judicious choice of ligand and oxidant was essential.¹³⁻¹⁵

In 2008, independent reports published by the White and Shi groups indicated that allyl arenes (**2.1**) were capable of undergoing linear allylic alkylation with a variety of stabilized 2° carbon nucleophiles (Scheme 2.1.2).^{16,17} In both cases, Pd(OAc)₂ was necessarily ligated with bis(sulfoxide) ligand **2.2**, which has been shown to stabilize the resulting electrophilic palladium π -allyl intermediates toward nucleophilic functionalization. In addition, an external oxidant was required to re-oxidize the resulting Pd(0) species for catalyst turnover. Both of these studies provided a general platform for the construction of styrenyl products (**2.3**) with broad functional group tolerance. In most cases, products were formed with exquisite linear to branch selectivity and synthetically useful yields.

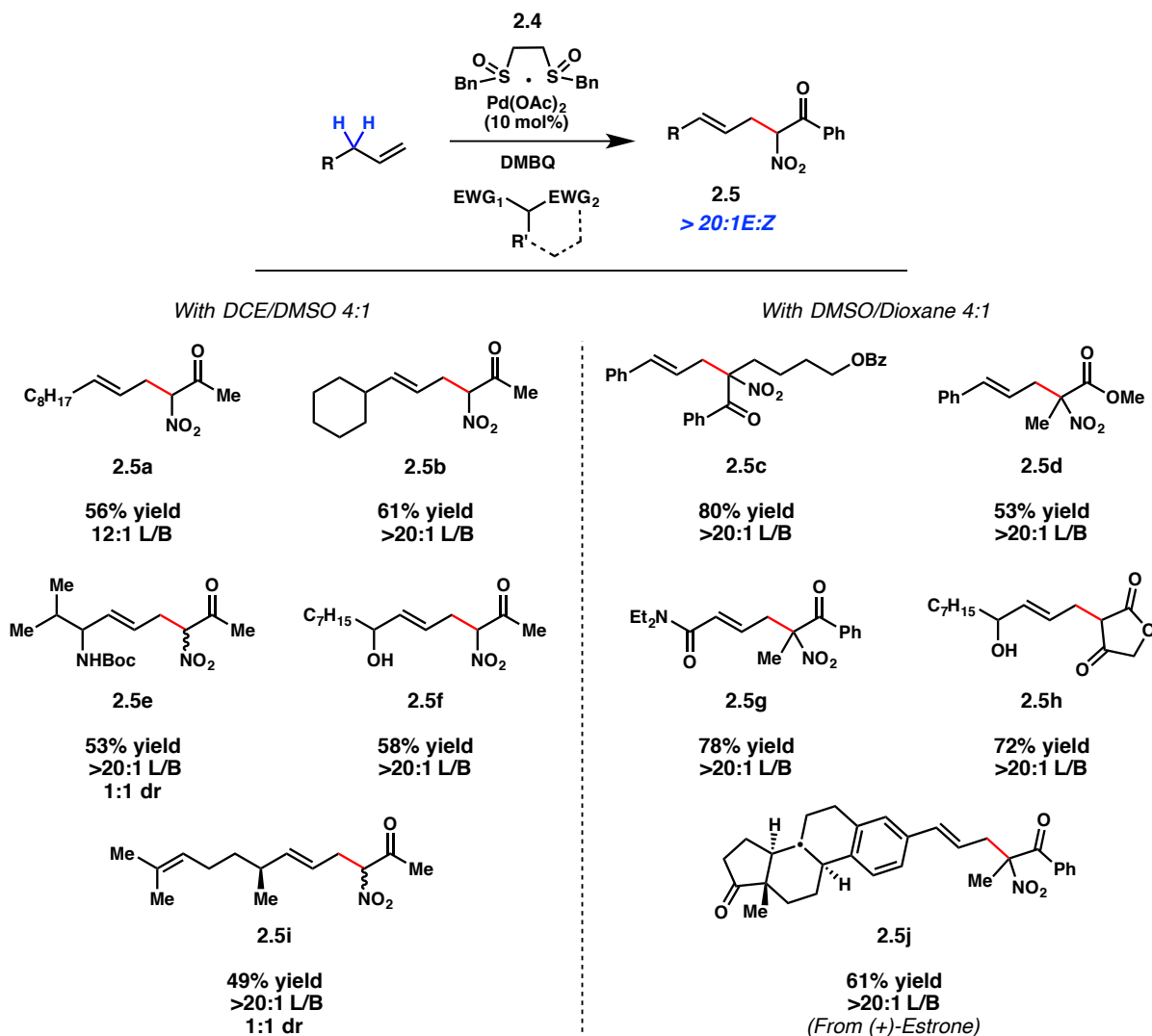
Scheme 2.1.2



An extension of this chemistry was applied to the allylic C–H alkylation of *unactivated* terminal olefins in 2011 by the White group and subsequently to accommodate 3° carbon nucleophiles (Scheme 2.1.3).^{18,19} The key to accommodating this substrate class rested in the identity of the sulfoxide ligand on the palladium catalyst. By modulating the electronic properties of bis(sulfoxide) **2.2**, the benzyl version of this ligand (**2.4**) exhibited better binding affinity to palladium and resulted in a more active catalyst in the presence of competitive ligands like DMSO. As a result, a wide variety of unactivated terminal olefins provided linear, *E*-olefinated products (**2.5**), accommodating a variety of nitrogen- and oxygen-based functionalities, and exhibiting excellent chemoselectivity for terminal olefins over tri-substituted olefins (**2.11i**). These methodologies serve as valuable tools for the construction of complex products, as demonstrated in several examples of late stage functionalization of natural product

derivatives and tandem alkylation–Diels Alder cascades.

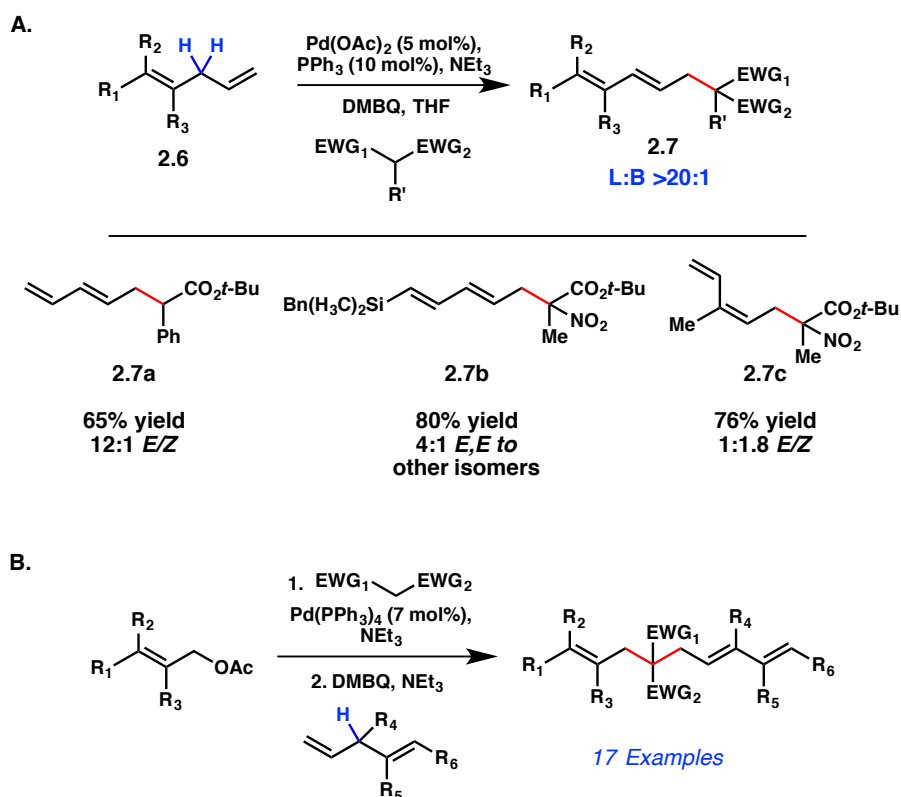
Scheme 2.1.3



The palladium catalyzed allylic C–H alkylation of terminal olefins has been extended to the use of phosphine-based ligands through the efforts of Trost and co-workers.²⁰ In this work stabilized 2° and 3° carbon nucleophiles were used to generate substituted 1,3-dienes from readily accessible 1,4-dienes (**2.6**), affording diene products (**2.7**) in good yields and with high *E*-olefin selectivity (Scheme 2.1.4a).

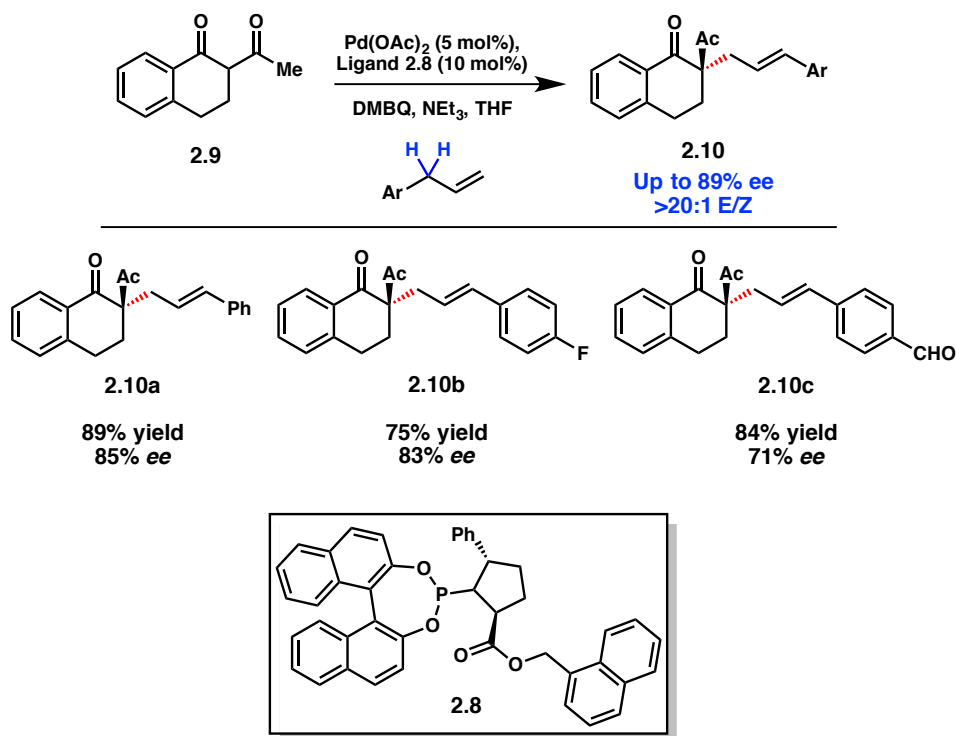
Triphenylphosphine proved to be a suitable ligand for the allylic alkylation, serving as the first example of allylic C–H alkylation in the absence of sulfoxide-containing ligands. They went on to incorporate this methodology into a single-flask tandem allylic alkylation to access three-component couplings (Scheme 2.1.4b).²¹

Scheme 2.1.4



The ability to employ phosphine-based ligands for palladium-catalyzed allylic C–H alkylation was significant as this provided the possibility of expanding the methodology to an enantioselective variant, which was accomplished shortly thereafter.^{22,23} In the presence of chiral phosphoramidite ligand **2.8**, acetyl-tetralone **2.9** was coupled to a variety of allyl arenes in an enantioselective allylic alkylation (Scheme 2.1.5). While the stereoselectivity of this reaction varied substantially with differing aryl substituents on the allyl component, products could be accessed in up to 85% ee (**2.10a**).

Scheme 2.1.5



2.1.3 Allylic C–H Alkylation of Unactivated Olefins with Trifluoromethane

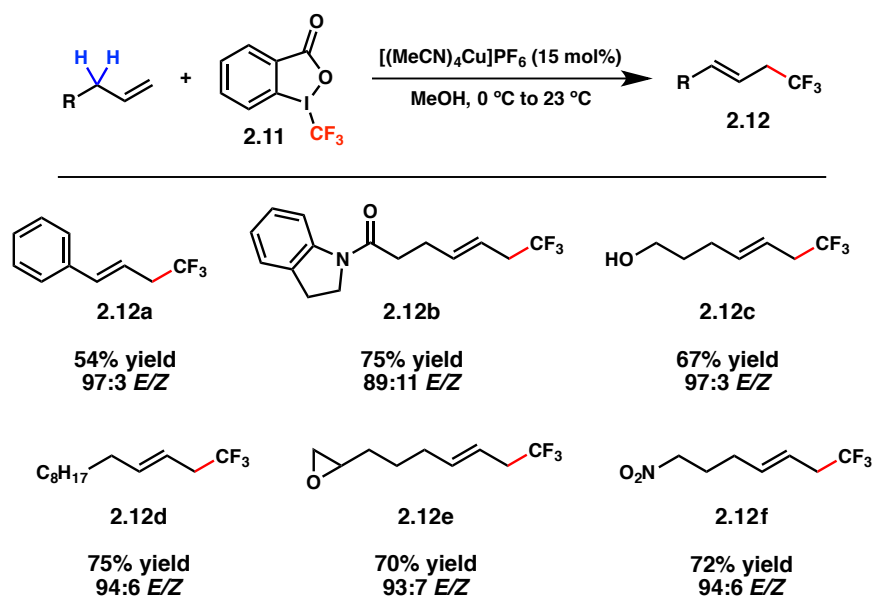
Donors

The addition of trifluoromethyl (CF_3) groups to biologically active molecules often provides increased chemical and metabolic stability and enhances binding affinity by accommodating electrostatic interactions with the protein target.²⁴⁻²⁶ For these reasons, the CF_3 group is widely regarded as a privileged functionality in the area of medicinal chemistry. Recently, several methods have been described for the addition of CF_3 groups to unactivated terminal olefins through the use of various CF_3 sources.²⁷⁻³⁰

The Buchwald lab reported an elegant copper-catalyzed trifluoromethylation of olefins using Togni's electrophilic trifluoromethylating reagent **2.11** to construct new linear allylic C- CF_3 bonds that provided *E*-olefinated products **2.12** (Scheme 2.1.6).^{30,31}

This chemistry obviated the need for pre-functionalized olefins to activate and direct the alkylation, representing a significant advance in the area of allylic C–H functionalization with copper for the assembly of trifluoromethylated molecules. A diverse substrate scope further exemplified the utility of this method, accommodating such functionalities as amide, alcohol, epoxide and nitro groups.

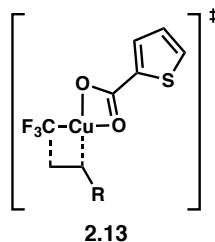
Scheme 2.1.6



These findings were almost simultaneously corroborated by independent publications from the Liu and Wang labs who reported the use of Umemoto's reagent and Togni's reagent respectively for the trifluoromethylation of terminal unactivated olefins with copper catalysts.^{27,28} The exact mechanistic pathway by which this chemistry proceeds is not entirely known, however preliminary studies rule out the possibility of an allyl radical intermediate. Detailed computational analysis by Liu suggests a mechanistic pathway that includes a four-membered Heck-like transition state instead (2.13, Figure 2.1.1).

Figure 2.1.1

Liu's proposed transition state



2.1.4 Conclusions

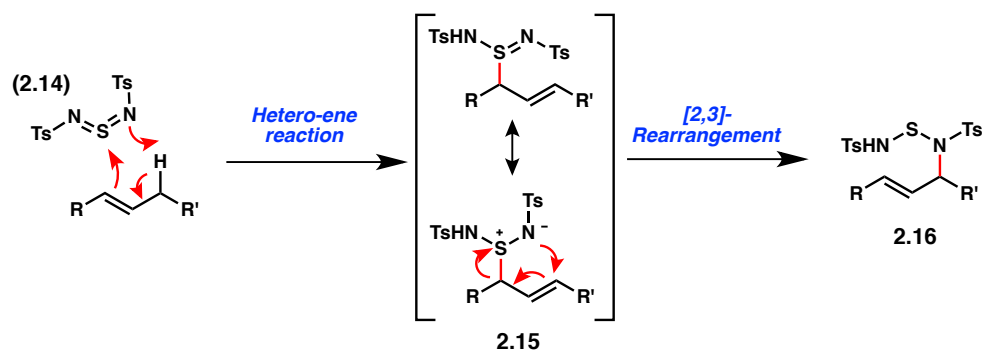
Several reports of direct allylic C–H alkylation strategies have emerged in the last decade, providing new opportunities for intermolecular C(sp³)–C(sp³) bond formation from relatively inert starting materials. Palladium catalyzed alkylation with stabilized carbon nucleophiles and copper catalyzed alkylation with trifluoromethane donors have been described and reveal a general trend in product formation with linear, *E*-olefin selectivity. The advantage of this approach lies in its ability to directly transform petrochemical feedstocks into value-added materials with particularly high levels of regio-, chemo- and *E*-olefin selectivity. New strategies for the allylic C–H alkylation of simple olefins are continually being uncovered to extend the scope of this transformation to other classes of aliphatic and aromatic coupling partners, including very recently to electron deficient arenes.^{32,33}

2.2 Development and Scope of an Allylic Alkylation of Unactivated Olefins with Grignard Reagents

2.2.1 Choice of Oxidant and Optimization

While several methods are known for the allylic alkylation of unactivated terminal olefins, we were interested in developing a complementary approach that utilized a more general class of carbon nucleophiles, Grignard reagents. To this end, we conceptualized an approach that would take advantage of a stoichiometric oxidant to directly activate the olefin component toward a metal-catalyzed coupling, in contrast to previous methods that utilize oxidant to re-oxidize the metal catalyst.

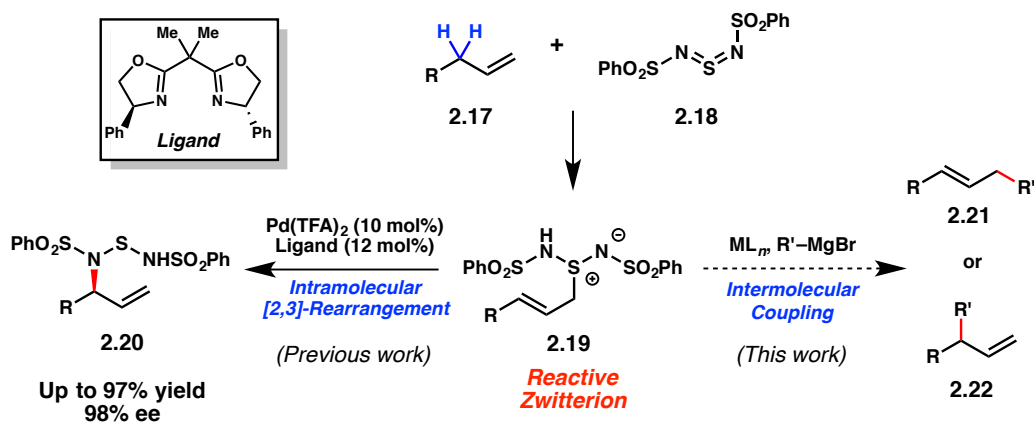
Scheme 2.2.1



Our choice of oxidant was initially inspired from previous reports detailing the use of sulfur diimide **2.14** to affect an allylic amination of unactivated olefins (Scheme 2.2.1).³⁴⁻⁴⁰ The authors postulated that this transformation took place through an initial hetero-ene reaction to generate allylic sulfinamides (**2.15**) followed by a facile [2,3]-rearrangement to amine **2.16**. While our lab has previously exploited this amination process with sulfur diimide **2.18** to develop a palladium-catalyzed asymmetric allylic amination of unactivated terminal olefins (**2.20**),^{40,41} we considered the possibility of

intercepting the same reactive zwitterionic intermediate with a different metal catalyst to instead affect an intermolecular coupling (**2.21** or **2.22**, Scheme 2.2.2).

Scheme 2.2.2

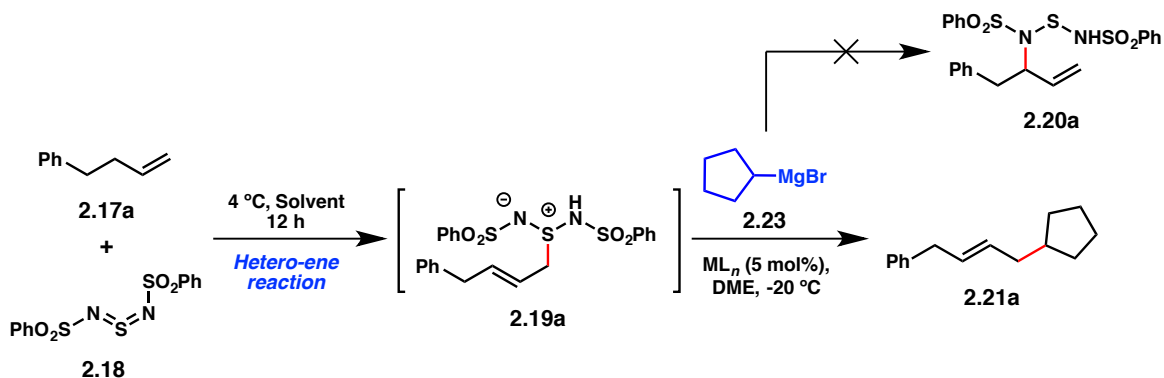


Upon stirring bis(phenylsulfonyl)sulfur diimide (**2.18**) and 4-phenyl-1-butene (**2.17a**) at 4 °C for 12 hours, **2.19a** was generated in near quantitative yield precluding the formation of [2,3]-rearrangement byproduct **2.20a** (Table 2.2.1). While this compound is stable to purification through filtration (and stable to storage at low temperatures for extended periods of time), we were drawn to the synthetic advantage of effecting a single-flask conversion of **2.17** to various coupled products.

Encouraged by numerous reports detailing the use of allylic sulfinamides and sulfoxides for metal-mediated couplings with Grignard reagents,⁴²⁻⁴⁵ we began to investigate the effect of various low-valent metals on the conversion of **2.17a** to alkylation product **2.21a** in the presence of excess cyclopentylmagnesium bromide (**2.23**) at -20 °C. While various metals known to engage allylic electrophiles to generate metal-allyl complexes failed to produce the desired alkylation product (entries 2-7), upon the addition of 10 mol% copper(I) thiophene-2-carboxylate (CuTc) the linear $\text{C}(\text{sp}^3)\text{-C}(\text{sp}^3)$ bond formation product was isolated in 22% yield (entry 8). Upon further screening of

copper(I) sources, copper(I) bromide dimethyl sulfide ($\text{CuBr}\cdot\text{SMe}_2$) was identified as a suitable catalyst for the formation of **2.21a** (entry 10).

Table 2.2.1



Entry	Catalyst	Solvent	% Yield	Entry	Catalyst	Solvent	% Yield
1	–	Et ₂ O	<5	7	$[(\text{C}_7\text{H}_8)\text{Mo}(\text{CO})_3]^a$	Et ₂ O	<5
2	$[\text{Pd}_2(\text{dba})_3]\cdot\text{CHCl}_3$	Et ₂ O	<5	8	CuTc	Et ₂ O	22
3	$[\{\text{Pd}(\text{C}_3\text{H}_5)\text{Cl}\}_2]$	Et ₂ O	<5	9	CuCl	Et ₂ O	6
4	$[\{\text{Ir}(\text{cod})\text{Cl}\}_2]$	Et ₂ O	<5	10	$\text{CuBr}\cdot\text{SMe}_2$	Et ₂ O	25
5	$[\text{Ir}(\text{cod})_2]\text{BF}_4$	Et ₂ O	<5	11	$\text{CuBr}\cdot\text{SMe}_2$	DME	53
6	$[\{\text{Rh}(\text{cod})\text{Cl}\}_2]$	Et ₂ O	<5	12	$\text{CuBr}\cdot\text{SMe}_2$	DME/Et ₂ O (1:1)	72

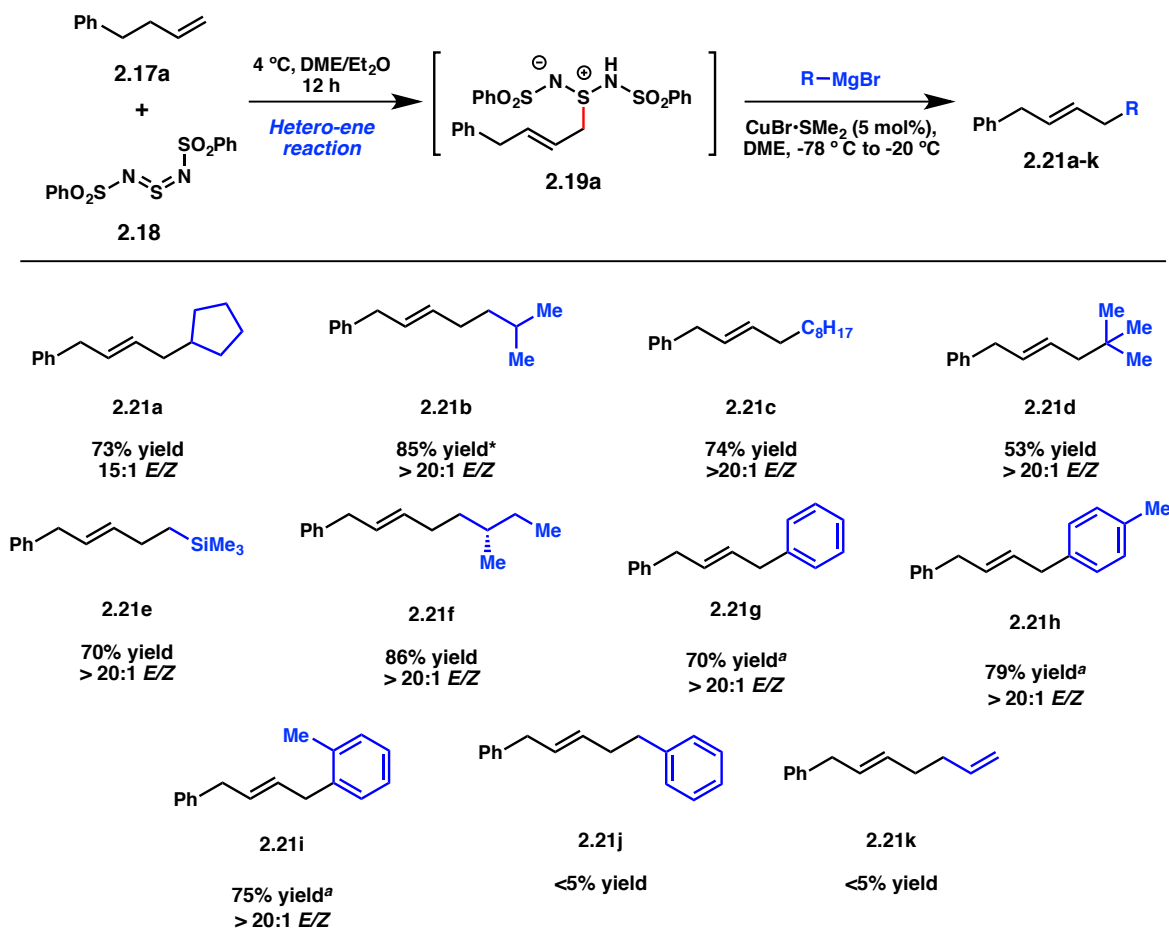
Reaction conditions. Step 1: Olefin (1 equiv), sulfur diimide **2.23** (1.2 equiv), solvent (0.3 M). Step 2: DME (0.2 M), ML_n (5 mol%), Grignard reagent **2.28** (4 equiv). DME = 1,2-dimethoxyethane, cod = cyclo-1,5-octadiene, dba = dibenzylidenacetone. [a] $\text{C}_7\text{H}_8\text{Mo}(\text{CO})_3$ = cycloheptatriene molybdenum tricarbonyl.

Due to the insolubility of intermediate **2.19a** in Et₂O, we examined the effect of a more polar solvent on this reaction. Using 1,2-dimethoxyethane (DME) as solvent improved the overall yield of **2.21a**, albeit with a significant amount of the background [2,3]-rearrangement product **2.20a** (entry 11). Gratifyingly, an ideal solvent combination of 1:1 DME/Et₂O provided the linear alkylation product **2.21a** exclusively with 72% yield and 15:1 *E/Z* selectivity (entry 12).

2.2.2 Grignard and Olefin Scope of the Allylic Alkylation

Next, we explored the generality of this allylic alkylation strategy with a variety of Grignard reagents (Table 2.2.2). 1°, 2°, and 3° Grignard reagents are compatible with this chemistry, providing synthetically useful yields across the series (**2.21a-d**). A Grignard reagent bearing silyl functionality was well tolerated under the reaction conditions (**2.21e**). Aromatic Grignard reagents provided the corresponding products with greatly diminished yields and numerous byproducts. To combat the enhanced reactivity of this Grignard class, a two-pot protocol was implemented. Subsequent to isolation of sulfinamide **2.19a**, the copper-catalyzed coupling in the presence of catalytic amounts of TEMPO took place to afford an array of allyl arenes in good yields regardless of *ortho* or *para* substituents (**2.21g-i**). Of note, benzylic and allylic Grignards were not compatible with this chemistry and failed to provide products **2.21j** and **2.21k**.

Table 2.2.2

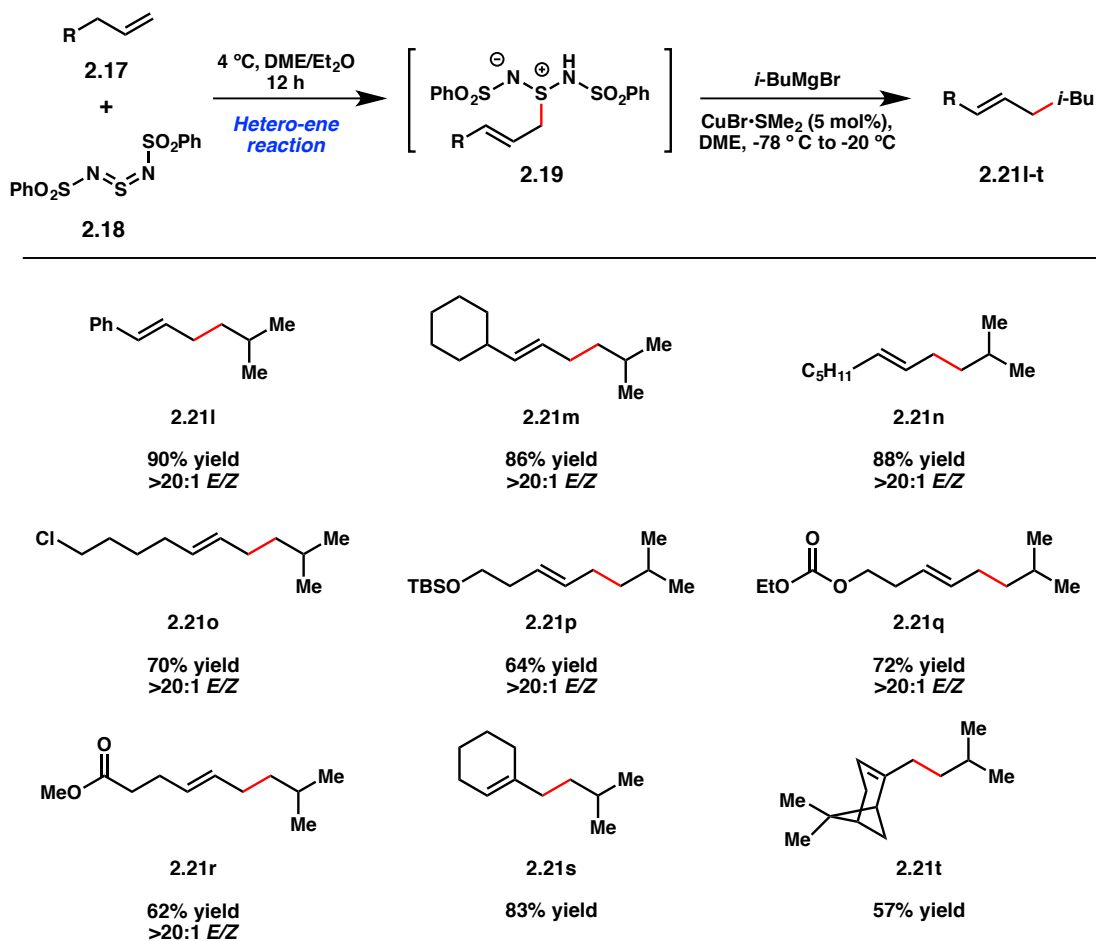


Reaction conditions. Step 1: Olefin (1 equiv), sulfur diimide **2.18** (1.2 equiv), DME/Et₂O 1:1 (0.3 M). Step 2: DME (0.2 M), CuBr·SMe₂ (5 mol%), Grignard reagent (4 equiv). [a] Intermediary adduct was filtered and isolated before treating with copper catalyst and Grignard reagent. In addition, 8 mol % TEMPO was utilized in the second step. TEMPO = 2, 2, 6, 6-tetramethylpiperidine-N-oxyl.

Similarly, we sought to define the substrate scope of this chemistry by assessing the coupling of unactivated terminal olefins with *iso*-butylmagnesium bromide (Table 2.2.3). Various hydrocarbons efficiently provided linear, *E*-olefinated products with exceptional yields and selectivity (**2.21l-n**). Functional group tolerance on the substrate was also explored, revealing wide-ranging compatibility with halogen, silyl ether, ester, and carbonate functional groups (**2.21o-r**). Substrates bearing 1,1-disubstituted olefins furnished the corresponding trisubstituted olefin products **2.21s** and **2.21t** without a

significant loss in reactivity. Although product **2.21a** was formed in a 15:1 ratio of *Z/E*-olefins, products **2.21b-r** were accessed in exclusively the *E*-olefin isomer.

Table 2.2.3



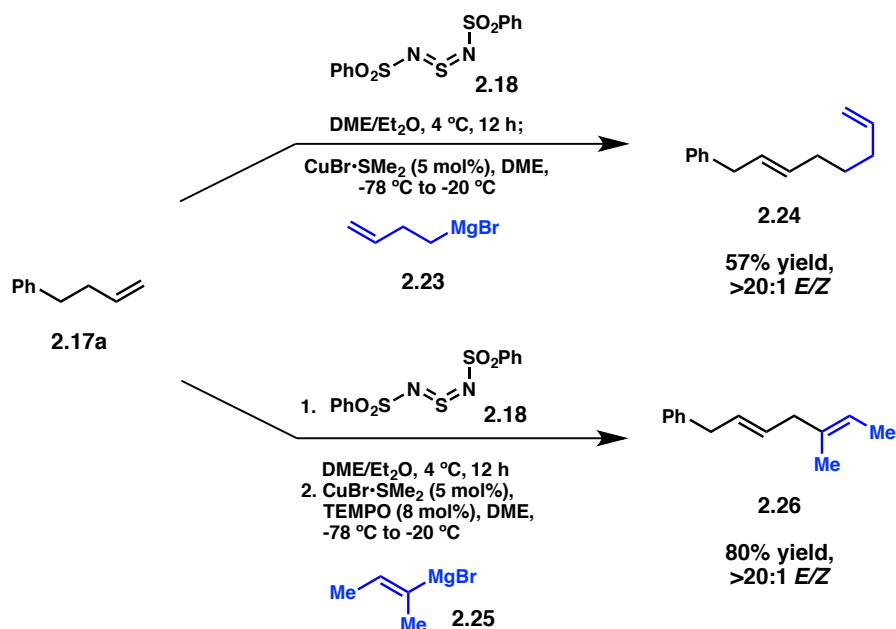
Reaction conditions. Step 1: Olefin (1 equiv), sulfur diimide **2.18** (1.2 equiv), DME/Et₂O 1:1 (0.3 M). Step 2: DME (0.2 M), CuBr·SMe₂ (5 mol%), *i*-BuMgBr (4 equiv).

2.2.3 Application of This Strategy Toward the Synthesis of Polyenes

In the course of our studies, it became apparent to us that this approach to allylic alkylation may be uniquely suited to selectively access a series of skipped dienes. The

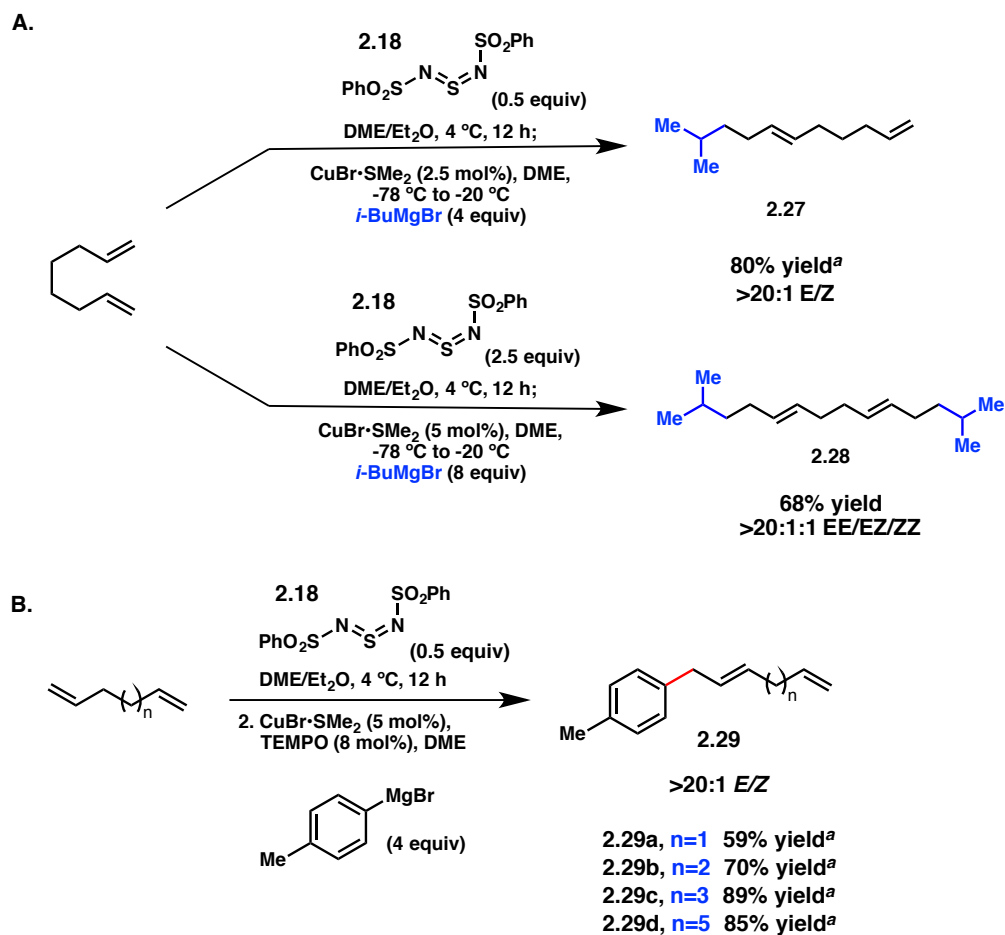
introduction of a second unsaturation to phenyl-butene **2.17a** was achieved by coupling with olefin-containing Grignards **2.23** and **2.25** to deliver the corresponding 1,6- and 2,5-dienes **2.24** and **2.26** (Scheme 2.2.3).

Scheme 2.2.3



An alternative approach to constructing variably substituted dienes was also considered to exploit polyunsaturated starting materials. In this chemistry, the reactivity of an olefin toward alkylation relies on the initial allylic oxidation. Therefore, we postulated that the control of mono- versus bis-alkylation of diene starting materials could be achieved by simply modifying the reaction stoichiometry of the initial hetero-ene reaction (Scheme 2.2.4). To this aim, skipped diene products **2.27** and **2.28** were selectively accessed in the presence of **2.18** by altering the relative equivalents of each substrate and controlling mono- versus bis-oxidation (Scheme 2.2.4a). Under the mono-oxidation conditions, a progressive series of skipped dienes **2.29** were accessed with high selectivity (Scheme 2.2.4b).

Scheme 2.2.4



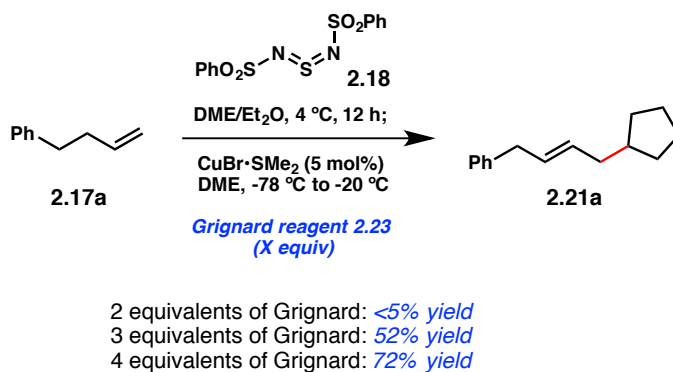
[a] Yield calculated relative to sulfur diimide **2.18** as the limiting reagent

2.2.4 Mechanistic Studies

To better understand the mechanism by which this reaction proceeds, we looked closer at the role of the carbon nucleophile. The amount of Grignard reagent required for this transformation was surveyed by modifying the equivalents of **2.23** (Scheme 2.2.5). Surprisingly, even in the presence of two equivalents of Grignard reagent, the reaction did not yield any substantial amount of product, suggesting that at least two equivalents

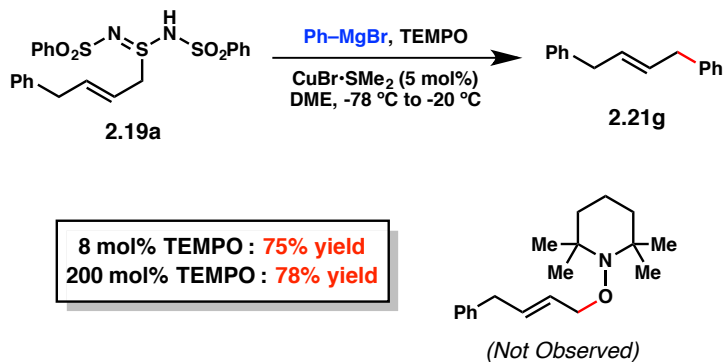
of reagent are consumed in off-cycle side reactions, and therefore **2.23** plays a multifunctional role in this reaction. At three equivalents olefin **2.21a** was generated but at a lower yield than the typical four equivalent loading.

Scheme 2.2.5



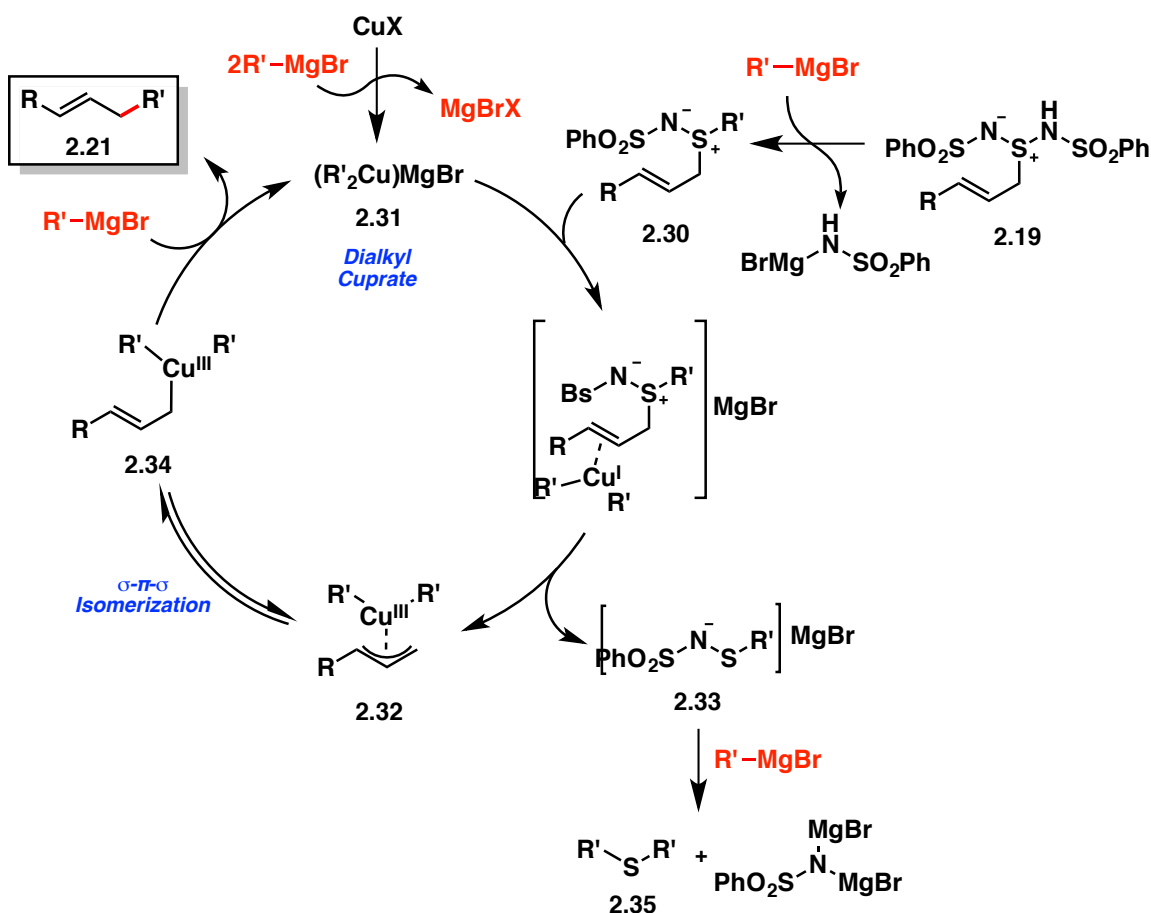
To rule-out the possibility of a radical-based mechanism, allylic sulfinamide **2.19a** was isolated and subjected to the copper-catalyzed alkylation conditions in the presence of TEMPO (Scheme 2.2.6). Even at super-stoichiometric amounts, TEMPO failed to inhibit the formation of **2.21g** or provide any measurable amount of TEMPO adduct, therefore suggesting that this chemistry does not proceed through a free-radical intermediate.

Scheme 2.2.6



Interestingly, although copper-catalyzed S_N2' allylic alkylations utilizing Grignard reagents are well documented, in all cases we isolated products with complete linear S_N2 selectivity. Copper-mediated S_N2' allylic substitutions are thought to arise from the dissymmetric HOMO of heterocuprates, while dialkylcuprates characteristically favor α -alkylation with 1° allylic substrates.⁴⁶⁻⁴⁹ Accordingly, we surmise that the linear selectivity exhibited by this reaction is attributed to reductive elimination from a dialkyl π -allylcuprate intermediate.

Scheme 2.2.7



Based on these observations, we propose a mechanism in which allylic sulfonamide **2.19** undergoes alkylation by one equivalent of Grignard reagent to form sulfimine **2.30**

as the active allylic electrophile in this method (Scheme 2.27). The conversion of **2.19** to **2.30** is analogous to the proposed reactivity of allylic sulfoxides in Grignard-mediated chemistry.⁴²⁻⁴⁴ Oxidative addition by dialkylcuprate **2.31** to sulfimine **2.30** forms π -complex **2.32** and displaces **2.33** as a byproduct. While the exact identity of the resulting copper(III) species is not known, similar copper(III) complexes have been reported and characterized by spectroscopic methods.⁴⁸ Preferential reductive elimination of copper(III) intermediate **2.34** results in S_N2 product **2.21**. Byproduct **2.33** is further consumed by an additional equivalent of Grignard reagent in an unproductive side reaction to generate thioether **2.35**, which accounts for the requisite excess Grignard reagent in this reaction. The presence of **2.40** has been verified by gas chromatography mass spectroscopy analysis of the crude reaction mixture, and in some cases observed as a byproduct in ¹HNMR analysis of semi-purified alkylation products.

2.2.5 Conclusions

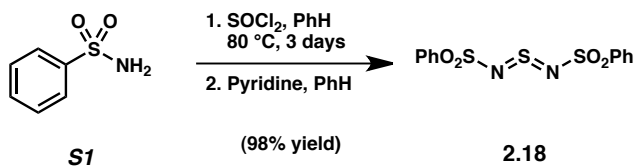
In conclusion, we have developed a novel strategy for the allylic C–H alkylation of unactivated terminal olefins to access differentially substituted *E*-olefinated products. This chemistry takes advantage of hetero-ene chemistry with commercially available bis(phenylsulfonyl)sulfur diimide to generate allylic sulfinamides capable of participating in an intermolecular copper-catalyzed coupling with aliphatic, aromatic and vinyl Grignard reagents. This chemistry furnishes linear alkylation products in >20:1 *E*:*Z* with synthetically useful yields. Diverse functionality both on the olefin starting material as well as the Grignard reagent is well tolerated, and dienes are selectively converted into mono- or dialkylation products by modifying the reaction stoichiometry. The high level of α -selectivity in the alkylation step suggests a mechanism that proceeds through a dialkylcuprate intermediate.

2.3 Experimental Section

2.3.1 Materials and Methods

All reactions were carried out under an atmosphere of nitrogen in flame-dried glassware with magnetic stirring unless otherwise indicated. Commercially obtained reagents were used as received. Solvents were dried by passage through an activated alumina column under argon. Liquids and solutions were transferred via syringe. All reactions were monitored by thin-layer chromatography with E. Merck silica gel 60 F254 pre-coated plates (0.25 mm). Silica gel (particle size 0.032 - 0.063 mm) purchased from SiliCycle was used for flash chromatography. ^1H and ^{13}C NMR spectra were recorded on Varian Inova-400 or 500 spectrometers. Data for ^1H NMR spectra are reported relative to chloroform as an internal standard (7.26 ppm) or benzene as an internal standard (7.16 ppm) and are reported as follows: chemical shift (δ ppm), multiplicity, coupling constant (Hz), and integration. Data for ^{13}C NMR spectra are reported relative to chloroform as an internal standard (77.23 ppm) and are reported in terms of chemical shift (δ ppm). Infrared spectra were recorded on a Perkin-Elmer 1000 series FTIR. HRMS data were obtained at The Scripps Center for Mass Spectrometry.

2.3.2 Preparative Procedures



Benzenesulfonyl Sulfurdiimide 2.18: Our procedure was modified from a method reported in the literature for the synthesis of similar arylsulfonyl sulfurdiimides⁵⁰: A solution of benzenesulfonamide **S1** (50 g, 0.318 mol) and SOCl_2 (80 mL, 1.1 mol) in benzene (30 mL) was refluxed at 80 °C for 3 days (over the course of the reaction, the

mixture became a clear solution). When the starting material was consumed by ^1H NMR analysis of an aliquot, the mixture was concentrated under vacuum to remove benzene and excess SOCl_2 . Trace amounts of SOCl_2 were removed by redissolving the residue in toluene (50 mL), concentrating under reduced pressure, and storing under vacuum at 50 °C for 6 h. The residue was then treated with benzene (70 mL) and heated slightly to ensure all material dissolved in the solvent. Once the solution was cooled to 23 °C, pyridine (0.5 mL) was added, and the mixture was stirred. After 12 h, stirring was ceased, and a yellow precipitate crystallized slowly from the solution. The precipitate was separated by vacuum filtration and stored under vacuum at 50 °C for 8 h. Benzenesulfonyl sulfurdiiimide **2.18** was obtained as a yellow solid (53.5 g, 98% yield). *Since benzenesulfonyl sulfurdiiimide 2.18 is sensitive to water, we store it in a dessicator inside a sealed flask that has been purged with N_2 . Optimal results for the enantioselective allylic amination were obtained when benzenesulfonyl sulfurdiiimide 2.18 was broken into a fine powder immediately before use.*

^1H NMR (400 MHz, CDCl_3) δ 7.95 (d, J = 8.0 Hz, 2H), 7.67 (t, J = 8.0 Hz, 1H), 7.53 (t, J = 8.0 Hz, 2H). ^{13}C NMR (100 MHz, CDCl_3) δ 137.9, 135.0, 129.6, 128.3. IR (thin film): 3348, 3255, 1557, 1332, 1159 cm^{-1} .

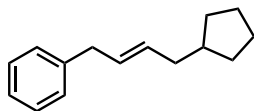
General Procedures for the Functionalization of Unactivated Olefins

General procedure for the catalytic functionalization of unactivated olefins with Grignard reagents (Method A): A solution of benzenesulfonyl sulfurdiiimide **2.18** (206 mg, 0.6 mmol, 1.2 equiv) in Et_2O (1 M) and DME (1 M) was cooled to 0 °C and treated with the terminal olefin (0.5 mmol). After stirring for 6-12 h at 4 °C, the reaction was diluted with DME (0.2 M) and treated with $\text{CuBr}\cdot\text{SMe}_2$ (5 mg, 0.025 mmol, 0.05 equiv). The reaction was cooled to -78 °C, and the Grignard reagent (2 mmol, 4 equiv) was added quickly. After stirring at -20 °C for 30 min to 3 h, the reaction mixture was diluted with wet pentane/ CH_2Cl_2 (30:20 mL) or wet pentane/ Et_2O (30:20 mL). This mixture was passed through a silica gel plug (about 5 cm long), which was flushed with CH_2Cl_2 or

Et₂O. The resulting solution was concentrated under reduced pressure and purified by flash chromatography using hexanes or pentanes.

General two-pot procedure for the catalytic functionalization of unactivated olefins with aryl and vinyl Grignard reagents (Method B): A solution of benzensulfonyl sulfurdiiimide **2.18** (684 mg, 2 mmol) in Et₂O (0.5 M) was cooled to 0 °C and treated with the terminal olefin (4 mmol, 2 equiv). The reaction was gently stirred at 4 °C for 12 h. The hetero-ene adduct, which formed a white precipitate, was purified at room temperature by vacuum filtration, washed with anhydrous Et₂O (20–40 mL), and dried under vacuum. The hetero-ene adduct (0.5 mmol), CuBr•SMe₂ (0.05 equiv), and TEMPO (0.08 equiv) were dissolved in DME (0.2 M). The reaction was cooled to –78 °C, and the Grignard reagent (2 mmol, 4 equiv) was added quickly. After stirring for at –20 °C for 3 h, the reaction mixture was diluted with wet pentane/CH₂Cl₂ (30:20 mL) or wet pentane/Et₂O (30:20 mL). This mixture was passed through a silica gel plug (about 5 cm long), which was flushed with CH₂Cl₂ or Et₂O. The resulting solution was concentrated under reduced pressure and purified by flash chromatography using hexanes or pentanes.

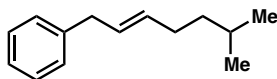
Note: We were able to achieve 4 °C in a Thermo Scientific Neslab Low-Temperature Cryobath with Magnetic Stirring (Fisher Scientific Catalog# 13-265-83) and a Temperature Controller Cryotrol (Fisher Scientific Catalog# 13-265-85). Alternatively, we were able to achieve 4 °C in a cold room in our department.



2.21a: Following the general procedure for the catalytic functionalization of unactivated olefins (Method A), 4-phenyl-1-butene⁵² (0.5 mmol) and cyclopentylmagnesium bromide⁵¹ (2M in Et₂O) were converted to the desired product. The hetero-ene reaction

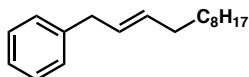
was stirred for 10 h, and the copper-catalyzed step was stirred for 3 h. Purification by flash chromatography (pentane only) afforded **2.21a** (72% yield, 15:1 E:Z) as a clear oil:

^1H NMR (500 MHz, CDCl_3) δ 7.31 (q, $J = 5.6$ Hz, 2H), 7.21 – 7.19 (m, 3H), 5.64 – 5.49 (m, 2H), 3.34 (d, $J = 5.7$ Hz, 2H), 2.04 (t, $J = 5.9$ Hz, 2H), 1.86 (s, $J = 7.6$ Hz, 1H), 1.77 – 1.71 (m, 2H), 1.64 – 1.56 (m, 2H), 1.53 – 1.47 (m, 2H), 1.18 – 1.10 (m, 2H); ^1H NMR (500 MHz, benzene- d_6) δ 7.16-7.03 (m, 5H), 5.51 (dt, $J = 15.0$ Hz, $J = 7.0$ Hz, 1H), 5.42 (dt, $J = 15.0$ Hz, $J = 6.5$ Hz, 1H), 3.21 (d, $J = 6.5$ Hz, 2H), 1.95 (dd, $J = 7.0$ Hz, $J = 6.5$ Hz, 2H), 1.76-1.64 (m, 3H), 1.54-1.37 (m, 4H), 1.09-1.02 (m, 2H). ^{13}C NMR (100 MHz, CDCl_3) δ 141.3, 131.7, 129.3, 128.7, 128.5, 126.0, 40.2, 39.3, 39.2, 32.5, 25.4; IR (thin film): 3027, 2949, 2360, 1452, 968, 744 cm^{-1} . HRMS (ESI) calcd for $[\text{C}_{15}\text{H}_{21}]^+$ ($[\text{M}+\text{H}]^+$): 201.1638, found 201.1630.



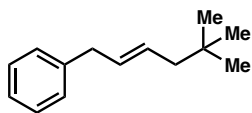
2.21b: Following the general procedure for the catalytic functionalization of unactivated olefins (Method A), 4-phenyl-1-butene⁵¹ (0.5 mmol) and isobutylmagnesium bromide solution⁵¹ (2 M in Et_2O) were converted to the desired product. The hetero-ene reaction was stirred for 10 h, and the copper-catalyzed step was stirred for 3 h. Purification by flash chromatography (pentane only) afforded **2.21b** (85% yield, >20:1 E:Z) as a clear oil:

^1H NMR (400 MHz, CDCl_3) δ 7.28 (q, $J = 7.6$ Hz, 2H), 7.21 – 7.17 (m, 3H), 5.61 – 5.47 (m, 2H), 3.33 (d, $J = 6.1$ Hz, 2H), 2.03 (q, $J = 5.8$ Hz, 2H), 1.57 (s, $J = 6.7$ Hz, 1H), 1.26 (q, $J = 6.7$ Hz, 2H), 0.88 (d, $J = 6.6$ Hz, 6H); ^{13}C NMR (100 MHz, CDCl_3) δ 141.3, 132.4, 128.7, 128.7, 128.5, 126.0, 39.3, 38.9, 30.6, 27.8, 22.7; IR (thin film): 3027, 2956, 1494, 1453, 970, 698 cm^{-1} . HRMS (ESI) calcd for $[\text{C}_{14}\text{H}_{21}]^+$ ($[\text{M}+\text{H}]^+$): 189.1638, found 189.1625.



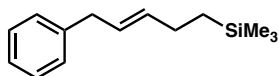
2.21c: Following the general procedure for the catalytic functionalization of unactivated olefins (Method A), 4-phenyl-1-butene.⁵¹ (0.5 mmol) and octylmagnesium chloride solution⁵¹ (2 M in THF) were converted to the desired product. The hetero-ene reaction was stirred for 10 h, and the copper-catalyzed step was stirred for 3 h. Purification by flash chromatography (pentane only) afforded **2.21c** (74% yield, >20:1 E:Z) as a clear oil:

¹H NMR (400 MHz, CDCl₃) δ 7.28 (q, *J* = 7.4 Hz, 2H), 7.21 – 7.17 (m, 3H), 5.62– 5.47 (m, 2H), 3.33 (d, *J* = 5.8 Hz, 2H), 2.02 (q, *J* = 6.5 Hz, 2H), 1.41 – 1.32 (m, 2H), 1.31 – 1.24 (m, 12H), 0.89 (t, *J* = 6.6 Hz, 3H); ¹³C NMR (100 MHz, CDCl₃) δ 141.4, 132.4, 128.9, 128.7, 128.5, 126.0, 39.3, 32.7, 32.1, 29.8, 29.7, 29.7, 29.6, 29.4, 22.9, 14.3; IR (thin film): 3028, 2924, 1494, 1454, 968, 697 cm⁻¹. HRMS (ESI) calcd for [C₁₈H₂₇]⁺ ([M-H]): 243.2118 found 243.2117.



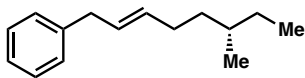
2.21d: Following the general procedure for the catalytic functionalization of unactivated olefins (Method A), 4-phenyl-1-butene⁵¹ (0.5 mmol) and *tert*-butylmagnesium chloride solution⁵¹ (2 M in Et₂O) were converted to the desired product. The hetero-ene reaction was stirred for 10 h, and the copper-catalyzed step was stirred for 3 h. Purification by flash chromatography (pentane only) afforded **2.21d** (53% yield, >20:1 E:Z) as a clear oil:

^1H NMR (400 MHz, CDCl_3) δ 7.30 (q, $J = 78.3$ Hz, 2H), 7.23 – 7.19 (m, 3H), 5.62– 5.53 (m, 2H), 3.38 (d, $J = 5.2$ Hz, 2H), 1.93 (d, $J = 4.4$ Hz, 2H), 0.91 (s, 9H); ^{13}C NMR (100 MHz, CDCl_3) δ 131.1, 129.3, 128.7, 128.5, 126.0, 47.3, 39.4, 31.2, 29.5; IR (thin film): 3029, 2956, 1494, 1364, 971, 698 cm^{-1} HRMS (ESI) calcd for $[\text{C}_{14}\text{H}_{19}]^+$ ($[\text{M}-\text{H}]^+$): 187.1492, found 187.1479.



2.21e: Following the general procedure for the catalytic functionalization of unactivated olefins (Method A), 4-phenyl-1-butene⁵¹ (0.5 mmol) and (trimethylsilyl)methylmagnesium chloride solution⁵¹ (1 M in Et_2O) were converted to the desired product. The hetero-ene reaction was stirred for 10 h, and the copper-catalyzed step was stirred for 3 h. Purification by flash chromatography (pentane only) afforded **2.21e** (70% yield, >20:1 E:Z) as a clear oil:

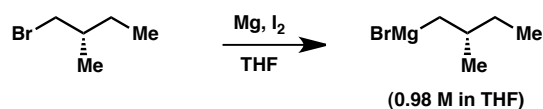
^1H NMR (400 MHz, CDCl_3) δ 7.28 (q, $J = 7.4$ Hz, 2H), 7.20 – 7.17 (m, 3H), 5.61 – 5.51 (m, 2H), 2.04 (m, 2H), 0.60 (m, 2H), -0.02 (s, 9H); ^{13}C NMR (100 MHz, CDCl_3) δ 141.4, 135.0, 128.7, 128.5, 127.5, 126.1, 39.2, 27.0, 16.7, -1.4; IR (thin film): 2953, 1495, 1248, 968, 835, 698 cm^{-1} . HRMS (ESI) calcd for $[\text{C}_{13}\text{H}_{20}\text{SiNa}]^+$ ($[\text{M}+\text{Na}]^+$): 227.1226, found 227.1066.



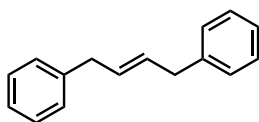
2.21f: Following the general procedure for the catalytic functionalization of unactivated olefins (Method A), 4-phenyl-1-butene⁵¹ (0.5 mmol) and (2*S*)-methylbutyl-1-magnesium bromide (0.98 M in THF) were converted to the desired product. The hetero-ene reaction

was stirred for 10 h, and the copper-catalyzed step was stirred for 3 h. Purification by flash chromatography (pentane only) afforded **2.21f** (86% yield, >20:1 E:Z) as a clear oil:

^1H NMR (400 MHz, CDCl_3) δ 7.28 (q, $J = 8.3$ Hz, 2H), 7.21 – 7.19 (m, 3H), 5.62 – 5.48 (m, 2H), 3.34 (d, $J = 5.9$ Hz, 2H), 2.11 – 1.96 (m, 2H), 1.45 – 1.32 (m, 3H), 1.24 – 1.11 (m, 2H), 0.89 – 0.86 (m, 6H); ^{13}C NMR (100 MHz, CDCl_3) δ 141.4, 132.6, 128.7, 128.7, 128.5, 126.1, 39.3, 36.6, 34.2, 30.3, 29.6, 19.3, 11.6; IR (thin film): 3028, 2961, 1494, 1453, 969, 698 cm^{-1} . HRMS (ESI) calcd for $[\text{C}_{14}\text{H}_{21}]^+$ ($[\text{M}+\text{H}]^+$): 189.1638, found 189.1640.



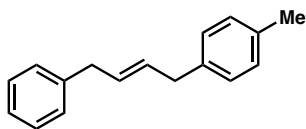
Synthesis of (2*S*)-methylbutyl-1-magnesium bromide: A flame-dried 3-neck round-bottom flask was fitted with an additional funnel and charged with magnesium chips (1g, 1.25 equiv) and catalytic amounts of iodine. (*S*)-(+)-1-Bromo-2-methylbutane⁵¹ (5g, 33 mmol) in THF (10 mL) was transferred to the additional funnel, and 0.5 mL of this solution was added slowly to the flask with no stirring. The reaction mixture became colorless within 2 minutes. The remaining solution of (*S*)-(+)-1-bromo-2-methylbutane was added dropwise to the reaction flask with stirring. When addition of the solution was complete, the reaction mixture was stirred at 23 °C for 1 h and diluted with THF (10 mL). Titration of the resulting Grignard reagent (2*S*)-methylbutyl-1-magnesium bromide indicated a concentration was 0.98 M.



2.21g: Following the general two-pot procedure for the catalytic functionalization of unactivated olefins with aryl and vinyl Grignard reagents (Method B), benzenesulfonyl

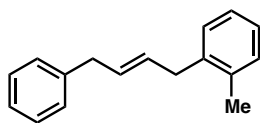
sulfurdiimide **2.18** (0.5 mmol), 4-phenyl-1-butene⁵¹ (2 equiv), and phenylmagnesium bromide solution⁵¹ (3 M in Et₂O) were converted to the desired product. The hetero-ene reaction was stirred for 10 h, and the copper-catalyzed step was stirred for 3 h. Purification by flash chromatography (pentane only) afforded **2.21g** (70% yield for two steps, >20:1 E:Z) as a clear oil:

¹H NMR (500 MHz, CDCl₃), δ 7.33 (t, *J* = 9.0 Hz, 2H), 7.24 (m, 3H), 5.75-6.68 (m, 2H), 3.42 (d, *J* = 5.0 Hz, 3H). ¹³C NMR (125 MHz, CDCl₃), δ 140.7, 130.4, 128.0, 128.4, 125.9, 39.0. IR (thin film): 3027, 1602, 1494, 1453, 969, 745 cm⁻¹.



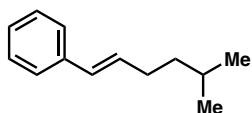
2.21h: Following the general two-pot procedure for the catalytic functionalization of unactivated olefins with aryl and vinyl Grignard reagents (Method B), benzenesulfonyl sulfurdiimide **2.18** (0.5 mmol), 4-phenyl-1-butene⁵¹ (2 equiv), and 4-methylphenylmagnesium bromide solution⁵¹ (1 M in THF) were converted to the desired product. The hetero-ene reaction was stirred for 10 h, and the copper-catalyzed step was stirred for 3 h. Purification by flash chromatography (pentane only) afforded **2.21h** (79% yield for two steps, >20:1 E:Z) as a clear oil:

¹H NMR (500 MHz, CDCl₃), δ 7.42-7.39 (m, 2H), 7.34-7.30 (m, 3H), 7.23-7.18 (m, 4H), 5.82-5.74 (m, 2H), 3.48 (d, *J* = 5.0 Hz), 3.45 (d, *J* = 5.0 Hz), 2.44 (s, 3H). ¹³C NMR (125 MHz, CDCl₃), δ 140.7, 137.6, 135.4, 130.7, 130.1, 129.0, 128.5, 128.4, 128.3, 125.9. IR (thin film): 3026, 2919, 1603, 1514, 1493, 1453, 969 cm⁻¹. HRMS (ESI) calcd for [C₁₇H₁₉]⁺ ([M+H]⁺): 223.1481, found 223.1478.



2.21i: Following the general two-pot procedure for the catalytic functionalization of unactivated olefins with aryl and vinyl Grignard reagents (Method B), benzenesulfonyl sulfurdiiimide **2.18** (0.5 mmol), 4-phenyl-1-butene⁵¹ (2 equiv), and 2-methylphenylmagnesium bromide solution⁵¹ (1 M in THF) were converted to the desired product. The hetero-ene reaction was stirred for 10 h, and the copper-catalyzed step was stirred for 3 h. Purification by flash chromatography (pentane only) afforded **2.21i** (75% yield for two steps, >20:1 E:Z) as a clear oil:

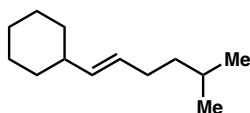
¹H NMR (500 MHz, CDCl₃), δ 7.37 (t, *J* = 7.5 Hz, 2H), 7.29-7.26 (m, 3H), 7.24-7.21 (m, 4H), 5.77-5.65 (m, 2H), 3.45-3.43 (m, 4H), 2.37 (s, 3H). ¹³C NMR (125 MHz, CDCl₃), δ 140.7, 138.7, 136.2, 130.1, 130.0, 129.6, 128.9, 128.4, 128.3, 126.1, 126.0, 125.9, 38.9, 36.5, 19.4. IR (thin film): 3026, 2910, 1603, 1493, 1453, 970 cm⁻¹. HRMS (ESI) calcd for [C₁₇H₁₉]⁺ ([M+H]⁺): 223.1481, found 223.1481.



2.21l: Following the general procedure for the catalytic functionalization of unactivated olefins (Method A), allylbenzene⁵¹ (0.5 mmol) and isobutylmagnesium bromide solution⁵¹ (2 M in Et₂O) were converted to the desired product. The hetero-ene reaction was stirred for 6 h, and the copper-catalyzed step was stirred for 3 h. Purification by flash chromatography (pentane only) afforded **2.21l** (90% yield, >20:1 E:Z) as a clear oil:

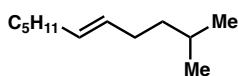
¹H NMR (500 MHz, CDCl₃), δ 7.36-7.34 (m, 2H), 7.31-7.28 (m, 2H), 7.21-7.18 (m, 1H), 6.37 (d, *J* = 16 Hz, 1H), 6.23 (dt, *J* = 16 Hz, *J* = 6.5 Hz, 1H), 2.22 (ddt, *J* = 8Hz, *J* = 6.5Hz, *J* = 1Hz, 2H), 1.64-1.56 (m, 1H), 1.36 (dt, *J* = 8.5 Hz, *J* = 7.0 Hz, 2H), 0.92 (d, *J*

= 7.0 Hz, 6H). ^{13}C NMR (125 MHz, $=\text{CDCl}_3$), δ 137.9, 131.4, 129.5, 128.4, 126.7, 125.9, 38.5, 30.9, 27.5, 22.5. IR (thin film): 2955, 2926, 1467, 963, 691 cm^{-1} . HRMS (ESI) calcd for $[\text{C}_{13}\text{H}_{17}]^+$ ($[\text{M}+\text{H}]^+$): 173.1336., found 173.1319.



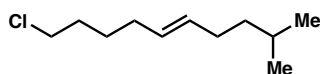
2.21m: Following the general procedure for the catalytic functionalization of unactivated olefins (Method A), allylcyclohexane⁵¹ (0.5 mmol) and isobutylmagnesium bromide solution⁵¹ (2 M in Et_2O) were converted to the desired product. The hetero-ene reaction was stirred for 6 h, and the copper-catalyzed step was stirred for 3 h. Purification by flash chromatography (pentane only) afforded **2.21m** (86% yield, >20:1 E:Z) as a clear oil:

^1H NMR (500 MHz, CDCl_3), δ 5.36-5.35 (m, 2H), 2.00-1.96 (m, 2H), 1.89-1.86 (m, 1H), 1.75-1.60 (m, 5H), 1.60-1.51 (m, 1H), 1.26-1.09 (m, 5 H), 1.08-0.98 (m, 1H), 0.88 (d, J = 7.0 Hz, 6H). ^{13}C NMR (100 MHz, CDCl_3), δ 136.2, 127.8, 40.7, 38.9, 33.3, 30.54, 27.4, 26.2, 26.1, 22.5. IR (thin film): 2955, 2925, 2851, 1448, 967 1088 cm^{-1} . HRMS (ESI) calcd for $[\text{C}_{13}\text{H}_{25}]^+$ ($[\text{M}+\text{H}]^+$): 181.1951, found 181.1947.



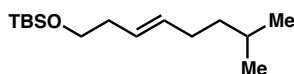
2.21n: Following the general procedure for the catalytic functionalization of unactivated olefins (Method A), 1-octene⁵¹ (0.5 mmol) and isobutylmagnesium bromide solution⁵¹ (2 M in Et_2O) were converted to the desired product. The hetero-ene reaction was stirred for 6 h, and the copper-catalyzed step was stirred for 3 h. Purification by flash chromatography (pentane only) afforded **2.21n** (88% yield, >20:1 E:Z) as a clear oil:

^1H NMR (500 MHz, CDCl_3), δ 5.41-5.36 (m, 2H), 2.01-1.96 (m, 4H), 1.57-1.53 (m, 1H), 1.31-1.16 (m, 8H), 0.91-0.87 (m, 9H). ^{13}C NMR (125 MHz, CDCl_3), δ 130.4, 130.2, 38.9, 32.6, 31.4, 30.5, 29.4, 27.5, 22.6, 22.5, 14.1. IR (thin film): 2957, 2926, 2872, 1467, 968 cm^{-1} . HRMS (ESI) calcd for $[\text{C}_{12}\text{H}_{23}]^+$ ($[\text{M}-\text{H}]^+$): 167.1805, found 167.1782.



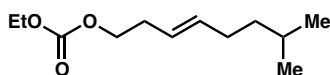
2.21o: Following the general procedure for the catalytic functionalization of unactivated olefins (Method A), 7-chloro-1-heptene⁵⁰ (0.5 mmol) and isobutylmagnesium bromide solution⁵¹ (2 M in Et_2O) were converted to the desired product. The hetero-ene reaction was stirred for 6 h, and the copper-catalyzed step was stirred for 3 h. Purification by flash chromatography (pentane only) afforded **2.21o** (70% yield, >20:1 E:Z) as a clear oil:

^1H NMR (500 MHz, CDCl_3), δ 5.45-5.35 (m, 2H), 3.54 (t, $J = 7.0$ Hz, 2H), 2.04-1.97 (m, 4H), 1.81-1.75 (m, 2H), 1.55-1.47 (m, 13H), 1.25-1.21 (m, 2H), 0.88 (d, $J = 7.0$ Hz, 6H). ^{13}C NMR (125 MHz, CDCl_3), δ 131.3, 129.1, 45.0, 38.9, 32.0, 31.7, 30.4, 27.4, 26.7, 22.5, 21.7. IR (thin film): 2955, 2869, 1466, 1310, 968 cm^{-1} . HRMS (ESI) calcd for $[\text{C}_{11}\text{H}_{22}\text{Cl}]^+$ ($[\text{M}+\text{H}]^+$): 189.1404, found 189.1241.



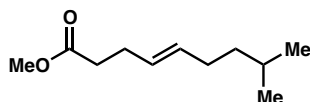
2.21p: Following the general procedure for the catalytic functionalization of unactivated olefins (Method A), (1,1-dimethylethyl)(dimethyl)(4-pentenyl)oxy silane⁵¹ (0.5 mmol) and isobutylmagnesium bromide solution⁵¹ (2 M in Et_2O) were converted to the desired product. The hetero-ene reaction was stirred for 6 h, and the copper-catalyzed step was stirred for 1 h. Purification by flash chromatography (hexanes and ethyl acetate) afforded **2.21p** (64% yield, >20:1 E:Z) as a clear oil:

^1H NMR (500 MHz, CDCl_3), δ 5.50-5.37 (m, 2H), 3.61 (t, $J = 7.0$ Hz, 2H), 2.21 (dt, $J = 7.0$ Hz, $J = 6.5$ Hz, 2H), 2.01 (dt, $J = 7.5$ Hz, $J = 7.0$ Hz, 2H), 1.56-1.52 (m, 1H), 1.23 (dt, $J = 7.5$ Hz, $J = 7.0$ Hz, 2H), 0.90 (s, 9H), 0.88 (d, $J = 6.5$ Hz, 6H), -0.06 (s, 6H). ^{13}C NMR (125 MHz, CDCl_3), δ 132.8, 126.1, 63.4, 38.7, 36.3, 30.5, 27.4, 25.9, 22.5, 18.4, -5.2. IR (thin film): 2955, 2858, 1464, 1255, 1102, 937, 836 cm^{-1} . HRMS (ESI) calcd for $[\text{C}_{15}\text{H}_{33}\text{OSi}]^+$ ($[\text{M}+\text{H}]^+$): 257.2295, found 257.2299.



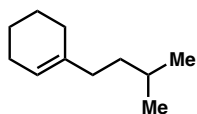
2.21q: Following the general procedure for the catalytic functionalization of unactivated olefins (Method A), ethyl pent-4-en-1-yl carbonate⁵⁴ (0.5 mmol) and isobutylmagnesium bromide solution⁵¹ (2 M in Et_2O) were converted to the desired product. The hetero-ene reaction was stirred for 6 h, and the copper-catalyzed step was stirred for 40 min. Purification by flash chromatography (hexanes and ethyl acetate) afforded **2.21q** (72% yield, >20:1 E:Z) as a clear oil:

^1H NMR (500 MHz, CDCl_3), δ 5.50 (dt, $J = 19.0$ Hz, $J = 8.0$ Hz, 1H), 5.36 (dt, $J = 19.0$ Hz, $J = 8.0$ Hz, 1H), 4.18 (q, $J = 7.0$ Hz, 2H), 4.10 (t, $J = 7.0$ Hz), 2.35 (dt, $J = 7.0$ Hz, $J = 6.5$ Hz, 2H), 1.99 (dt, $J = 8.0$ Hz, 6.5 Hz, 2H), 1.55-1.50 (m, 1H), 1.30 (t, 7.0 Hz, 3H), 0.86 (d, $J = 7.0$ Hz). ^{13}C NMR (125 MHz, CDCl_3), δ 155.1, 134.0, 124.3, 67.4, 63.7, 38.5, 31.9, 30.4, 27.4, 22.4, 14.2. IR (thin film): 2957, 2871, 1747, 1468, 1384, 1257 cm^{-1} . HRMS (ESI) calcd for $[\text{C}_{12}\text{H}_{23}\text{O}_3]^+$ ($[\text{M}+\text{H}]^+$): 215.1642, found 215.1641.



2.21r: Following the general procedure for the catalytic functionalization of unactivated olefins (Method A), methyl 5-hexenoate⁵¹ (0.5 mmol) and isobutylmagnesium bromide solution⁵¹ (2 M in Et₂O) were converted to the desired product. The hetero-ene reaction was stirred for 6 h, and the copper-catalyzed step was stirred for 30 min. Purification by flash chromatography (pentane only) afforded **2.21r** (62% yield, >20:1 E:Z) as a clear oil:

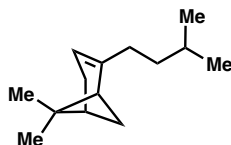
¹H NMR (500 MHz, CDCl₃), δ 5.48-5.36 (m, 2H), 3.66 (s, 3H), 2.38-2.35 (m, 2H), 2.30 (t, *J* = 7.0 Hz, 2H), 1.97 (dt, *J* = 8.5 z, 7.0 Hz, 2H), 1.55 (m, 1H), 1.32-1.18 (m, 2H), 0.86 (d, *J* = 7.0 Hz, 6H). ¹³C NMR (125 MHz, CDCl₃), δ 173.7, 131.9, 127.6, 51.5, 38.6, 34.1, 27.9, 27.4, 22.6. IR (thin film): 2955, 2927, 1743, 1436, 1197, 1167 cm⁻¹. HRMS (ESI) calcd for [C₁₂H₂₂O₂]⁺ ([M+H]⁺): 199.1692, found 199.1760.



2.21s: Following the general procedure for the catalytic functionalization of unactivated olefins (Method A), methylenecyclohexane⁵¹ (0.5 mmol) and isobutylmagnesium bromide solution⁵¹ (2 M in Et₂O) were converted to the desired product. The hetero-ene reaction was stirred for 6 h, and the copper-catalyzed step was stirred for 1 h. Purification by flash chromatography (pentane only) afforded **2.21s** (83% yield, >20:1 E:Z) as a clear oil:

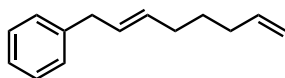
¹H NMR (500 MHz, CDCl₃), δ 5.42-5.39 (m, 1H), 2.01-1.97 (m, 2H), 1.94-1.91(m, 4H), 1.64-1.60 (m, 2H), 1.58-1.48 (m, 3H), 1.30-1.25 (m, 2H), 0.89 (d, *J* = 7.0 Hz, 6H). ¹³C NMR (125 MHz, CDCl₃), δ 138.3, 120.3, 37.0, 35.9, 28.4, 27.8, 25.3, 23.0, 22.6, 22.5. IR

(thin film): 2954, 2927, 2837, 1467, 1366 cm^{-1} . HRMS (ESI) calcd for $[\text{C}_{11}\text{H}_{21}]^+$ ($[\text{M}+\text{H}]^+$) 153.1638, found 153.1166.



2.21t: Following the general procedure for the catalytic functionalization of unactivated olefins (Method A), (-)- β -Pinene⁵¹ (0.5 mmol) and isobutylmagnesium bromide solution⁵¹ (2 M in Et_2O) were converted to the desired product. The hetero-ene reaction was stirred for 6 h, and the copper-catalyzed step was stirred for 40 min. Purification by flash chromatography (pentane only) afforded **2.21t** (57% yield, >20:1 E:Z) as a clear oil:

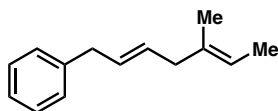
^1H NMR (500 MHz, CDCl_3), δ 5.18-5.15(m, 1H), 2.37-2.33 (m, 1H), 2.27-2.16 (m, 2H), 2.09-2.06 (m, 1H), 2.01-1.99 (m, 1H), 1.95-1.91 (m, 2H), 1.55-1.50 (m, 1H), 1.27 (s, 3H), 1.26-1.18 (m, 2H), 1.43 (d, $J = 8.5$ Hz, 1H), 0.88 (d, $J = 7.0$ Hz, 3H), 0.88 (d, $J = 7.0$ Hz, 3H), 0.83 (s, 3H). ^{13}C NMR (100 MHz, CDCl_3), δ 148.8, 115.3, 45.8, 40.9, 37.9, 36.4, 34.8, 31.7, 31.3, 27.8, 26.4, 22.6, 22.5, 21.2. IR (thin film): 3378, 2985, 1467, 1382, 1365 cm^{-1} . LRMS (ESI) calcd for $[\text{C}_{14}\text{H}_{25}]^+$ ($[\text{M}+\text{H}]^+$): 193.2, found 193.2.



2.24: Following the general procedure for the catalytic functionalization of unactivated olefins (Method A), 4-phenyl-1-butene⁵¹ (0.5 mmol) and 3-butenylmagnesium bromide solution **2.23**⁵¹ (0.5 M in Et_2O) were converted to the desired product. The hetero-ene reaction was stirred for 10 h, and the copper-catalyzed step was stirred for 3 h.

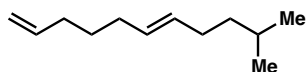
Purification by flash chromatography (pentane only) afforded **2.24** (57% yield, >20:1 E:Z) as a clear oil:

^1H NMR (400 MHz, CDCl_3) δ 7.28 (q, $J = 7.6$ Hz, 2H), 7.22 – 7.18 (m, 3H), 5.82 (ddt, $J = 6.7$ Hz, 10.2 Hz, 17.0 Hz, 1H), 5.63 – 5.48 (m, 2H), 5.04 – 4.94 (m, 2H), 3.34 (d, $J = 6.4$ Hz, 2H), 2.06 (p, $J = 6.9$ Hz, 4H), 1.49 (p, $J = 7.7$ Hz, 2H); ^{13}C NMR (100 MHz, CDCl_3) δ 141.3, 139.0, 131.8, 129.4, 128.7, 128.5, 126.1, 114.7, 39.3, 33.5, 32.2, 28.9; IR (thin film): 3028, 2926, 1640, 968, 910, 698 cm^{-1} HRMS (ESI) calcd for $[\text{C}_{14}\text{H}_{18}]^+$ ($[\text{M}+\text{H}]^+$): 187.1481, found 187.1472.



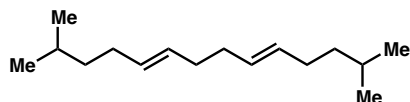
2.26: Following the general two-pot procedure for the catalytic functionalization of unactivated olefins with aryl and vinyl Grignard reagents (Method B), 4-phenyl-1-butene⁵¹ (2 mmol) and 1-methyl-1-propenylmagnesium bromide solution **2.25**⁵¹ (0.5 M in THF) were converted to the desired product. The hetero-ene reaction was stirred for 10 h, and the copper-catalyzed step was stirred for 3 h. Purification by flash chromatography (pentane only) afforded **2.26** (80% yield for two steps, >20:1 E:Z) as a clear oil:

^1H NMR (400 MHz, CDCl_3) δ 7.28 (q, $J = 7.6$ Hz, 2H), 7.21 – 7.18 (m, 3H), 5.65 – 5.58 (m, 1H), 5.50 – 5.45 (m, 1H), 5.27 (q, $J = 6.7$ Hz, 1H), 3.36 (d, $J = 6.8$ Hz, 2H), 2.76 (d, $J = 6.5$ Hz, 2H), 1.69 (s, 3H), 1.59 (d, $J = 6.8$ Hz, 3H); ^{13}C NMR (100 MHz, CDCl_3) δ 141.2, 134.6, 129.8, 129.2, 128.7, 128.5, 126.1, 119.7, 39.2, 35.0, 23.6, 13.5; IR (thin film): 2915, 1494, 1453, 969, 746, 698 cm^{-1} HRMS (ESI) calcd for $[\text{C}_{18}\text{H}_{22}\text{N}_2\text{O}_4\text{S}_3\text{Na}]^+$ ($[\text{M}+\text{Na}]^+$): 187.1481, found 187.1242.



2.27 Following the general procedure for the catalytic functionalization of unactivated olefins (Method A), benzenesulfonyl sulfurdiiimide **2.18** (0.5 mmol), 1,7-octadiene⁵¹ (2 equiv), and isobutylmagnesium bromide solution⁵¹ (2 M in Et₂O) were converted to the desired product. The hetero-ene reaction was stirred for 10 h in Et₂O (1.0 mL) and DME (0.5 mL), and the copper-catalyzed step was stirred for 3 h. Purification by flash chromatography (pentane only) afforded **2.27** (80% yield, >20:1 E:Z) as a clear oil:

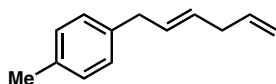
¹H NMR (500 MHz, CDCl₃), δ 5.85-5.78 (m, 1H), 5.41-5.39 (m, 2H), 5.03-4.94(m, 2H), 2.08-1.97 (m, 6H), 1.58-1.51 (m, 1H), 1.48-1.41 (m, 2H), 1.26-1.21 (m, 2H), 0.88 (d, *J* = 7.0 Hz, 6H). ¹³C NMR (125 MHz, CDCl₃), δ 138.9, 130.9, 129.7, 114.4, 38.9, 33.2, 32.0, 30.5, 28.8, 27.5, 22.5. IR (thin film): 3078, 2956, 1641, 1467, 1366 cm⁻¹. HRMS (ESI) calcd for [C₁₂H₂₃]⁺ ([M+H]⁺): 167.1794, found 167.1780.



2.28: Following the general procedure for the catalytic functionalization of unactivated olefins (Method A), 1,7-octadiene⁵¹ (0.5 mmol), benzenesulfonyl sulfurdiiimide **2.18** (2.5 equiv), and isobutylmagnesium bromide solution **15**⁵¹ (2 M in Et₂O) were converted to the desired product. The hetero-ene reaction was stirred for 10 h in Et₂O (0.5 mL) and DME (0.5 mL), and the copper-catalyzed step was stirred for 3 h. Purification by flash chromatography (pentane only) afforded **2.28** (68% yield, >20:1 E:Z) as a clear oil:

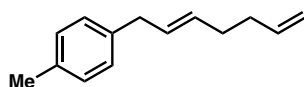
¹H NMR (500 MHz, CDCl₃), δ 5.41-5.39 (m, 2H), 2.04, 2.00 (m, 4H), 1.57-1.53 (m, 1H), 1.25-1.22 (m, 2H), 0.88 (d, *J* = 7.0 Hz, 6H). ¹³C NMR (125 MHz, CDCl₃),

δ 130.8, 129.6, 38.8, 32.8, 30.5, 27.4, 22.5. IR (thin film): 3078, 2921, 2847, 1467, 1366 cm^{-1} . HRMS (ESI) calcd for $[\text{C}_{16}\text{H}_{31}]^+$ ($[\text{M}+\text{H}]^+$): 223.2426, found 223.2414.



2.29a: Following the general two-pot procedure for the catalytic functionalization of unactivated olefins with aryl and vinyl Grignard reagents (Method B), benzensulfonyl sulfurdiiimide **2.18** (1 mmol), 1,5-hexadiene⁵¹ (2 equiv), and 4-methylphenylmagnesium bromide solution⁵¹ (1 M in THF) were converted to the desired product. The hetero-ene reaction was stirred for 10 h, and the copper-catalyzed step was stirred for 3 h. Purification by flash chromatography (pentane only) afforded **2.29a** (62% yield for two steps, >20:1 E:Z) as a clear oil:

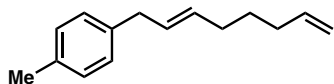
^1H NMR (500 MHz, CDCl_3), δ 7.14 (d, J = 8.0 Hz, 2H), 7.11 (d, J = 8.0 Hz, 2H), 5.92-5.82 (m, 1H), 5.63-5.51 (m, 2H), 5.10-5.01 (m, 2H), 3.35 (d, J = 7.0 Hz, 2H), 2.81 (dd, J = 6.0 Hz, 5.5 Hz, 2H), 2.36 (s, 3H). ^{13}C NMR (125 MHz, CDCl_3), δ 137.8, 137.2, 135.5, 130.6, 129.2, 129.0, 128.5, 115.2, 38.8, 36.8, 21.2. IR (thin film): 3004, 2978, 1638, 1514, 1431, 993, 912 cm^{-1} . LRMS (ESI) calcd for $[\text{C}_{13}\text{H}_{17}]^+$ ($[\text{M}+\text{H}]^+$): 173.1, found 173.1.



2.29b: Following the general two-pot procedure for the catalytic functionalization of unactivated olefins with aryl and vinyl Grignard reagents (Method B), benzensulfonyl sulfurdiiimide **2.18** (1 mmol), 1,6-heptadiene⁵¹ (2 equiv), and 4-methylphenylmagnesium bromide solution⁵¹ (1 M in THF) were converted to the desired product. The hetero-ene reaction was stirred for 10 h, and the copper-catalyzed step was stirred for 3 h.

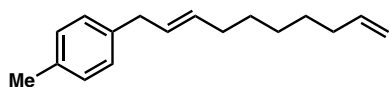
Purification by flash chromatography (pentane only) afforded **2.29b** (65% yield for two steps, >20:1 E:Z) as a clear oil:

^1H NMR (500 MHz, CDCl_3), δ 7.16 (d, $J = 8.0$ Hz, 2H), 7.13 (d, $J = 8.0$ Hz, 2H), 5.90-5.84 (m, 1H), 5.67-5.54 (m, 2H), 5.10-5.01 (m, 2H), 3.35 (d, $J = 6.5$ Hz, 2H), 2.36 (s, 3H), 2.20-2.17 (m, 4H). ^{13}C NMR (125 MHz, CDCl_3), δ 138.6, 138.0, 135.5, 131.0, 129.8, 129.2, 128.5, 114.8, 38.8, 33.9, 32.1, 21.2. IR (thin film): 3077, 2922, 1640, 1514, 1435, 969 cm^{-1} . HRMS (ESI) calcd for $[\text{C}_{14}\text{H}_{19}]^+$ ($[\text{M}+\text{H}]^+$): 187.1481, found 187.1379.



2.29c: Following the general two-pot procedure for the catalytic functionalization of unactivated olefins with aryl and vinyl Grignard reagents (Method B), benzensulfonyl sulfurdiiimide **2.18** (1 mmol), 1,7-octadiene⁵¹ (2 equiv), and 4-methylphenylmagnesium bromide solution⁵¹ (1 M in THF) were converted to the desired product. The hetero-ene reaction was stirred for 10 h, and the copper-catalyzed step was stirred for 3 h. Purification by flash chromatography (pentane only) afforded **2.29c** (79% yield for two steps, >20:1 E:Z) as a clear oil:

^1H NMR (500 MHz, CDCl_3), δ 7.14 (d, $J = 8.0$ Hz, 2H), 7.10 (d, $J = 8.0$ Hz, 2H), 5.87-5.81 (m, 1H), 5.59-5.50 (m, 2H), 5.05-4.97 (m, 2H), 3.32 (d, $J = 6.5$ Hz, 2H), 2.35 (s, 3H), 2.10-2.05 (m, 4H), 1.57-1.47 (m, 2H). ^{13}C NMR (125 MHz, CDCl_3), δ 139.0, 138.2, 135.5, 131.5, 129.6, 129.2, 128.5, 114.6, 38.8, 33.5, 32.1, 28.8, 21.2. IR (thin film): 3076, 2925, 1640, 1514, 1436, 969, 910 cm^{-1} . HRMS (ESI) calcd for $[\text{C}_{15}\text{H}_{21}]^+$ ($[\text{M}+\text{H}]^+$): 201.1683, found 201.1491.



2.29d: Following the general two-pot procedure for the catalytic functionalization of unactivated olefins with aryl and vinyl Grignard reagents (Method B), benzenesulfonyl sulfurdiiimide **2.18** (1 mmol), 1,9-decadiene⁵¹ (2 equiv), and 4-methylphenylmagnesium bromide solution⁵¹ (1 M in THF) were converted to the desired product. The hetero-ene reaction was stirred for 10 h, and the copper-catalyzed step was stirred for 3 h. Purification by flash chromatography (pentane only) afforded **2.29d** (80% yield for two steps, >20:1 E:Z) as a clear oil:

¹H NMR (500 MHz, CDCl₃), δ 7.22 (d, J = 8.0 Hz, 2H), 7.20 (d, J = 8.0 Hz, 2H), 5.97-5.91 (m, 1H), 5.70-5.60 (m, 2H), 5.15-5.06 (m, 2H), 3.40 (d, J = 6.5 Hz, 2H), 2.44 (s, 3H), 2.18-2.13 (m, 4H), 1.57-1.44 (m, 6H). ¹³C NMR (125 MHz, CDCl₃), δ 139.3, 138.2, 135.4, 131.9, 129.3, 129.2, 128.5, 114.4, 38.9, 33.9, 32.7, 29.5, 28.9, 28.8, 21.2. IR (thin film): 3076, 2926, 1640, 1514, 1436, 968, 909 cm⁻¹. HRMS (ESI) calcd for [C₁₇H₂₅]⁺ ([M+H]⁺): 229.1951, found 229.1941.

Determination of E-Olefin Geometry of Products: The large coupling constants for the vinyl protons of products **2.21a** (J = 15 Hz), **2.21l** (J = 16 Hz), and **2.21q** (J = 19 Hz) allowed the assignment of the E-olefin geometry for these three internal olefins. The E-olefin geometry for all other products was assumed by analogy.

2.4 References

- (1) Rose, J. *Applied Organometallic Chemistry* **1999**, *13*, 857.
- (2) Geilen, F. M. A.; Stochniol, G.; Peitz, S.; Schulte-Koerne, E. In *Ullmann's Encyclopedia of Industrial Chemistry*; Wiley-VCH Verlag GmbH & Co. KGaA: 2000.
- (3) Geilen, F. M. A.; Stochniol, G.; Peitz, S.; Schulte-Koerne, E. In *Ullmann's Encyclopedia of Industrial Chemistry*; Wiley-VCH Verlag GmbH & Co. KGaA: Weinheim, 2000.
- (4) Newhouse, T.; Baran, P. S. *Angewandte Chemie International Edition* **2011**, *50*, 3362.
- (5) White, M. C. *Science* **2012**, *335*, 807.
- (6) Yamaguchi, J.; Yamaguchi, A. D.; Itami, K. *Angewandte Chemie International Edition* **2012**, *51*, 8960.
- (7) Engle, K. M.; Mei, T.-S.; Wasa, M.; Yu, J.-Q. *Accounts of Chemical Research* **2012**, *45*, 788.
- (8) White, M. C. *Synlett* **2012**, *23*, 2746.
- (9) Jensen, T.; Fristrup, P. *Chemistry – A European Journal* **2009**, *15*, 9632.
- (10) Engelin, C. J.; Fristrup, P. *Molecules* **2011**, *16*.
- (11) Barata-Vallejo, S.; Lantaño, B.; Postigo, A. *Chemistry – A European Journal* **2014**, *20*, 16806.
- (12) Trost, B. M.; Fullerton, T. J. *Journal of the American Chemical Society* **1973**, *95*, 292.
- (13) Chen, M. S.; White, M. C. *Journal of the American Chemical Society* **2004**, *126*, 1346.
- (14) Chen, M. S.; Prabakaran, N.; Labenz, N. A.; White, M. C. *Journal of the American Chemical Society* **2005**, *127*, 6970.
- (15) Reed, S. A.; White, M. C. *Journal of the American Chemical Society* **2008**, *130*, 3316.

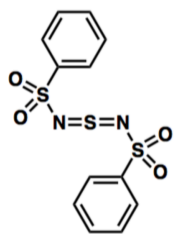
- (16) Lin, S.; Song, C.-X.; Cai, G.-X.; Wang, W.-H.; Shi, Z.-J. *Journal of the American Chemical Society* **2008**, *130*, 12901.
- (17) Young, A. J.; White, M. C. *Journal of the American Chemical Society* **2008**, *130*, 14090.
- (18) Young, A. J.; White, M. C. *Angewandte Chemie International Edition* **2011**, *50*, 6824.
- (19) Howell, J. M.; Liu, W.; Young, A. J.; White, M. C. *Journal of the American Chemical Society* **2014**, *136*, 5750.
- (20) Trost, B. M.; Hansmann, M. M.; Thaisrivongs, D. A. *Angewandte Chemie International Edition* **2012**, *51*, 4950.
- (21) Trost, B. M.; Thaisrivongs, D. A.; Hansmann, M. M. *Angewandte Chemie International Edition* **2012**, *51*, 11522.
- (22) Trost, B. M.; Thaisrivongs, D. A.; Donckele, E. J. *Angewandte Chemie International Edition* **2013**, *52*, 1523.
- (23) Trost, B. M.; Donckele, E. J.; Thaisrivongs, D. A.; Osipov, M.; Masters, J. T. *Journal of the American Chemical Society* **2015**, *137*, 2776.
- (24) Müller, K.; Faeh, C.; Diederich, F. *Science* **2007**, *317*, 1881.
- (25) Hagmann, W. K. *Journal of Medicinal Chemistry* **2008**, *51*, 4359.
- (26) Purser, S.; Moore, P. R.; Swallow, S.; Gouverneur, V. *Chemical Society Reviews* **2008**, *37*, 320.
- (27) Xu, J.; Fu, Y.; Luo, D.-F.; Jiang, Y.-Y.; Xiao, B.; Liu, Z.-J.; Gong, T.-J.; Liu, L. *Journal of the American Chemical Society* **2011**, *133*, 15300.
- (28) Wang, X.; Ye, Y.; Zhang, S.; Feng, J.; Xu, Y.; Zhang, Y.; Wang, J. *Journal of the American Chemical Society* **2011**, *133*, 16410.
- (29) Chu, L.; Qing, F.-L. *Organic Letters* **2012**, *14*, 2106.
- (30) Parsons, A. T.; Buchwald, S. L. *Angewandte Chemie International Edition* **2011**, *50*, 9120.
- (31) Kieltsch, I.; Eisenberger, P.; Togni, A. *Angewandte Chemie International Edition* **2007**, *46*, 754.

- (32) Cuthbertson, J. D.; MacMillan, D. W. C. *Nature* **2015**, 519, 74.
- (33) Sekine, M.; Ilies, L.; Nakamura, E. *Organic Letters* **2013**, 15, 714.
- (34) Sharpless, K. B.; Hori, T. *The Journal of Organic Chemistry* **1976**, 41, 176.
- (35) Sharpless, K. B.; Hori, T.; Truesdale, L. K.; Dietrich, C. O. *Journal of the American Chemical Society* **1976**, 98, 269.
- (36) Bussas, R.; Muenster, H.; Kresze, G. *The Journal of Organic Chemistry* **1983**, 48, 2828.
- (37) Muensterer, H.; Kresze, G.; Lamm, V.; Gieren, A. *The Journal of Organic Chemistry* **1983**, 48, 2833.
- (38) Deleris, G.; Dunogues, J.; Gadras, A. *Tetrahedron* **1988**, 44, 4243.
- (39) Katz, T. J.; Shi, S. *The Journal of Organic Chemistry* **1994**, 59, 8297.
- (40) Bayeh, L.; Tambar, U. K. In *Encyclopedia of Reagents for Organic Synthesis*; John Wiley & Sons, Ltd: 2001.
- (41) Bao, H.; Tambar, U. K. *Journal of the American Chemical Society* **2012**, 134, 18495.
- (42) Gendreau, Y.; Normant, J. F.; Villieras, J. *Journal of Organometallic Chemistry* **1977**, 142, 1.
- (43) Julia, M.; Righini, A.; Verpeaux, J.-N. *Tetrahedron Letters* **1979**, 20, 2393.
- (44) Masaki, Y.; Sakuma, K.; Kaji, K. *Journal of the Chemical Society, Chemical Communications* **1980**, 434.
- (45) Deleris, G.; Dunogues, J.; Gadras, A. *Tetrahedron Letters* **1984**, 25, 2135.
- (46) Bäckvall, J.-E. *Acta Chemica Scandinavica* **1995**, 49, 899.
- (47) Baeckvall, J. E.; Sellen, M.; Grant, B. *Journal of the American Chemical Society* **1990**, 112, 6615.
- (48) Yoshikai, N.; Nakamura, E. *Chemical Reviews* **2012**, 112, 2339.
- (49) Kar, A.; Argade, N. P. *Synthesis* **2005**, 2005, 2995.
- (50) Smyth, T. P.; O'Donnell, M. E.; O'Connor, M. J.; St. Ledger, J. O. *Journal of Organic Chemistry* **1998**, 63, 7600
- (51) Purchased from Sigma-Aldrich.

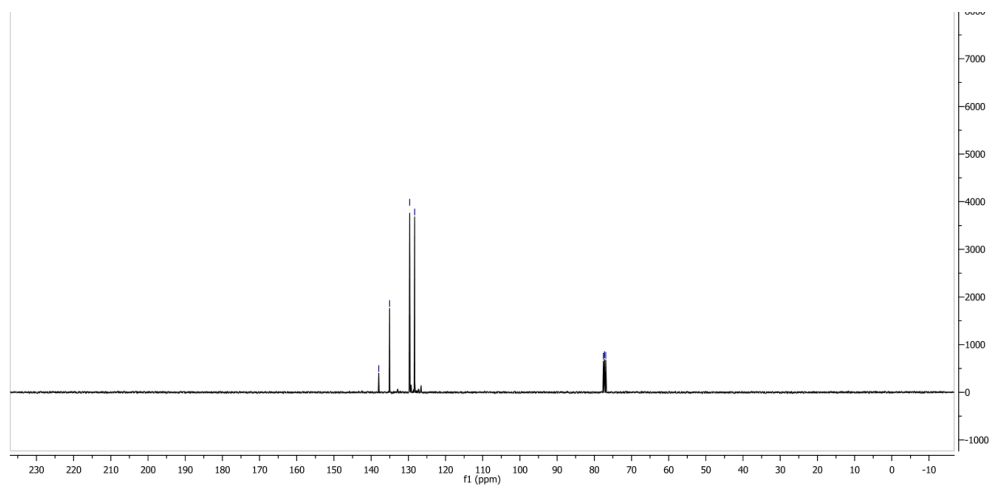
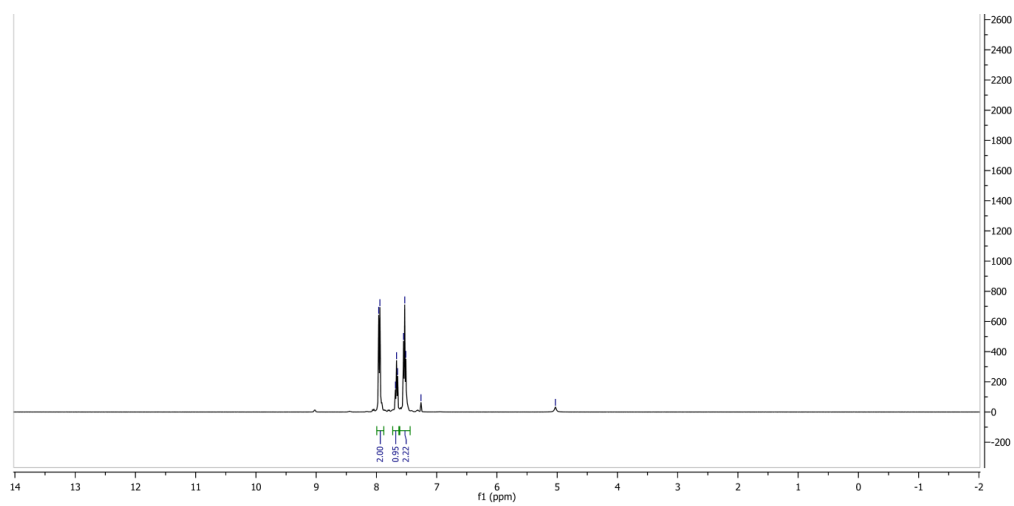
- (52) Purchased from GFS Chemicals.
- (53) Essig, S.; Bretzke, S.; Müller, R.; Menche, D. *Journal of the American Chemical Society* **2012**, *134*, 19362
- (54) Ethyl pent-4-en-1-yl carbonate has been reported in the literature (Nakamura, S.; Uchiyama, M. *Journal of the American Chemical Society* **2007**, *129*, 28-29). We synthesized this substrate by reacting 4-penten-1-ol (1 equiv), with pyridine (1 equiv) and ethyl chloroformate (1 equiv) in CH₂Cl₂ (1 M).

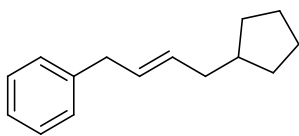
APPENDIX THREE

Spectra Relevant to Chapter Two: An Allylic Alkylation of Unactivated Terminal Olefins With Grignard Reagents

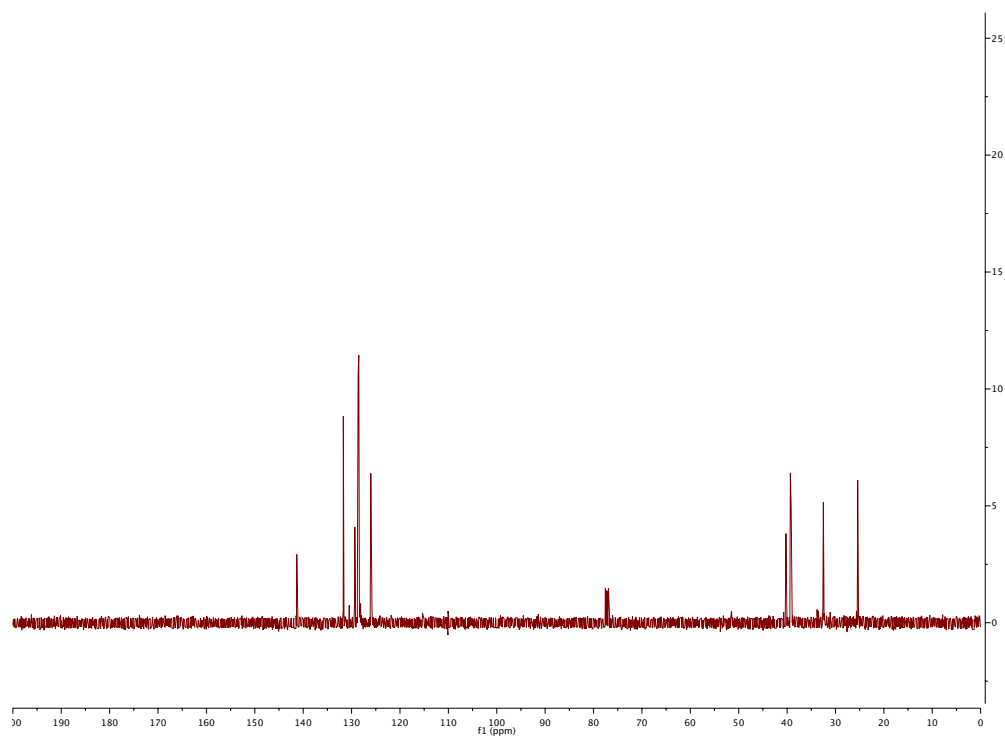
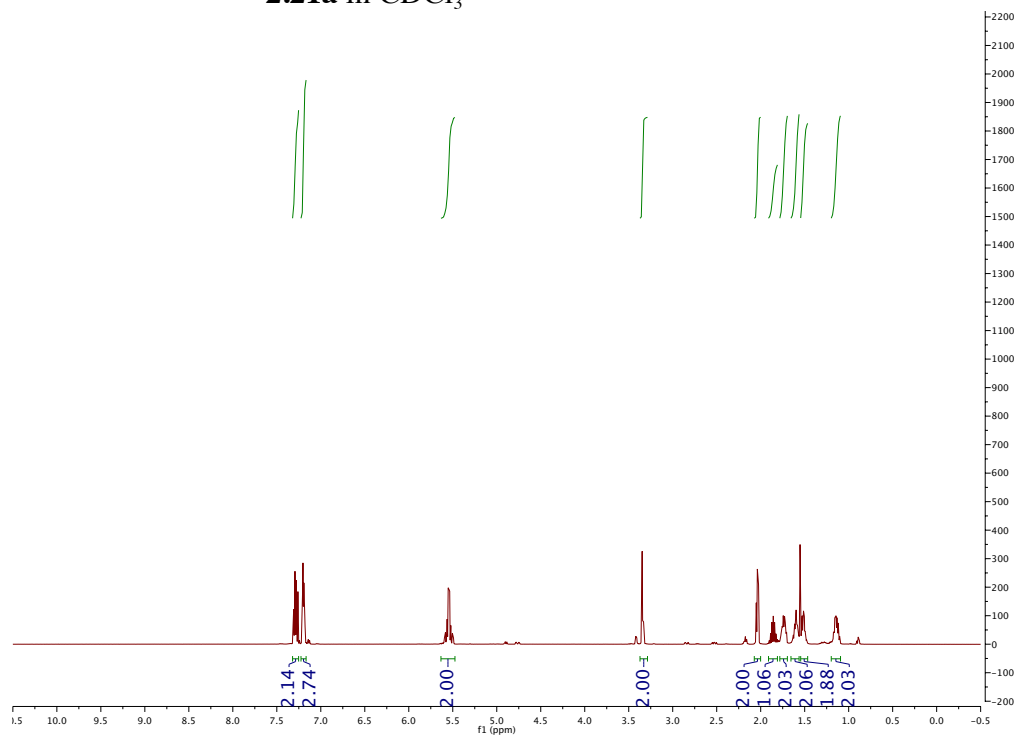


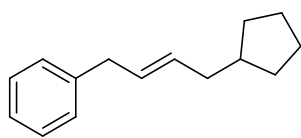
2.18 in CDCl_3



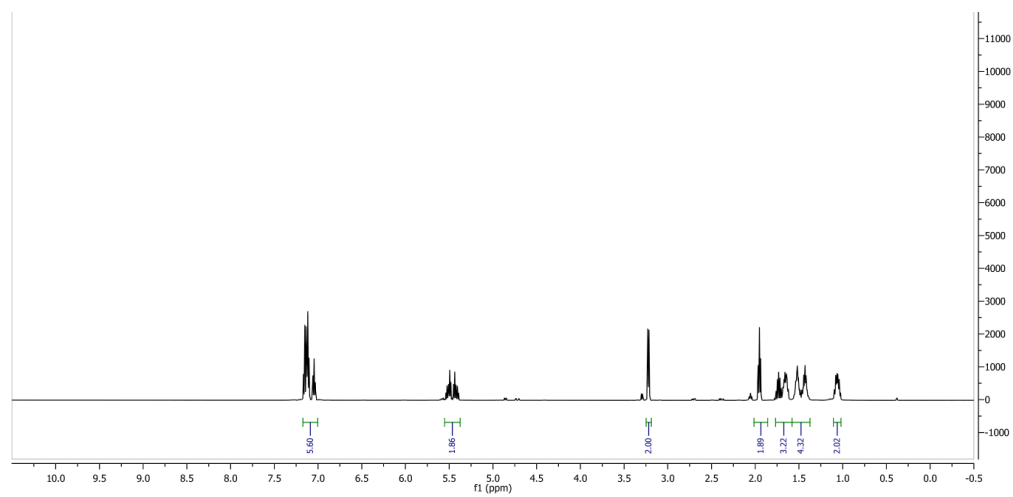


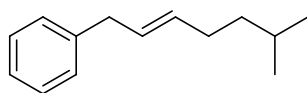
2.21a in CDCl₃



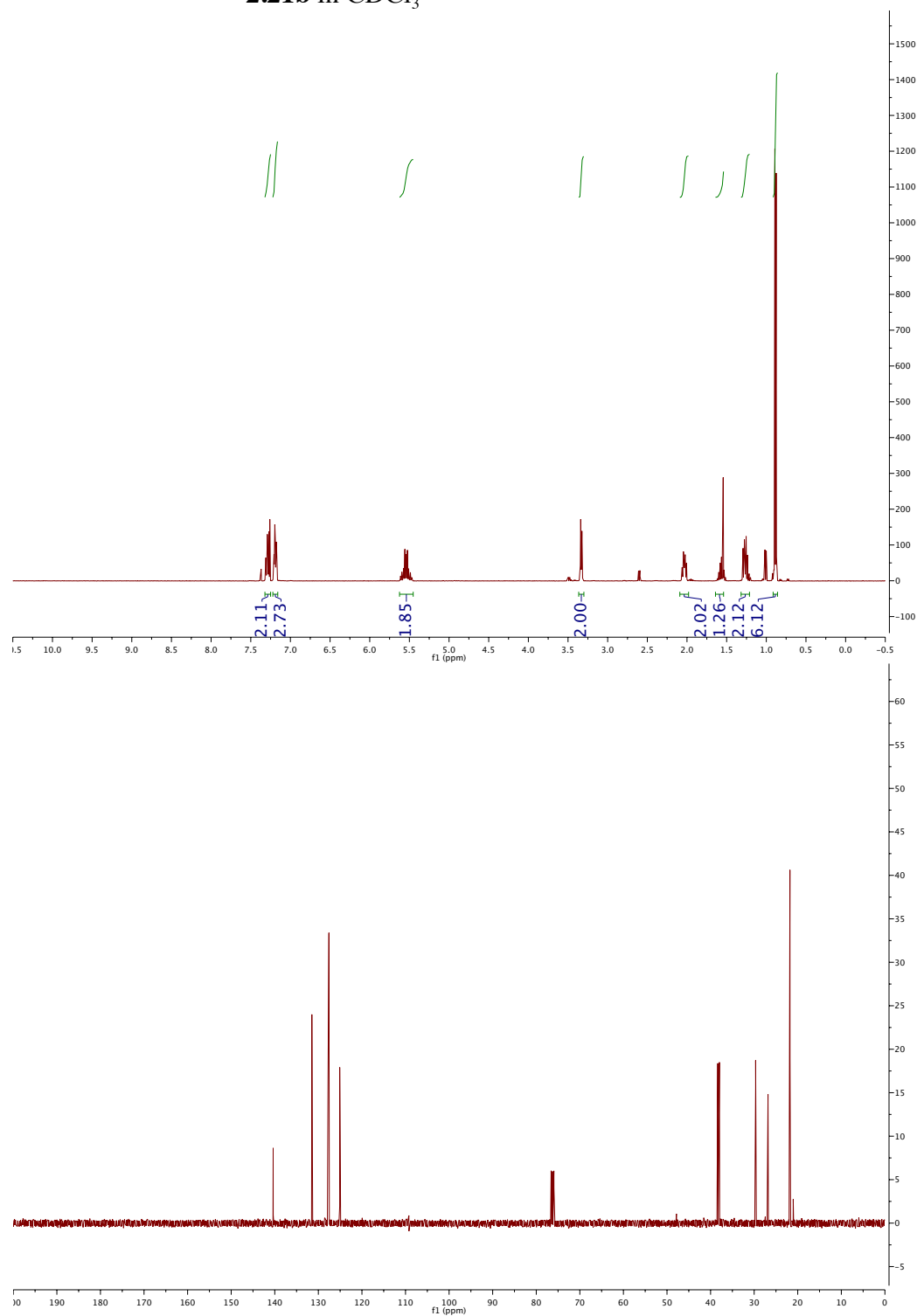


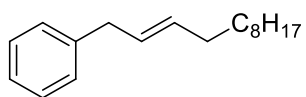
2.21a in C₆D₆



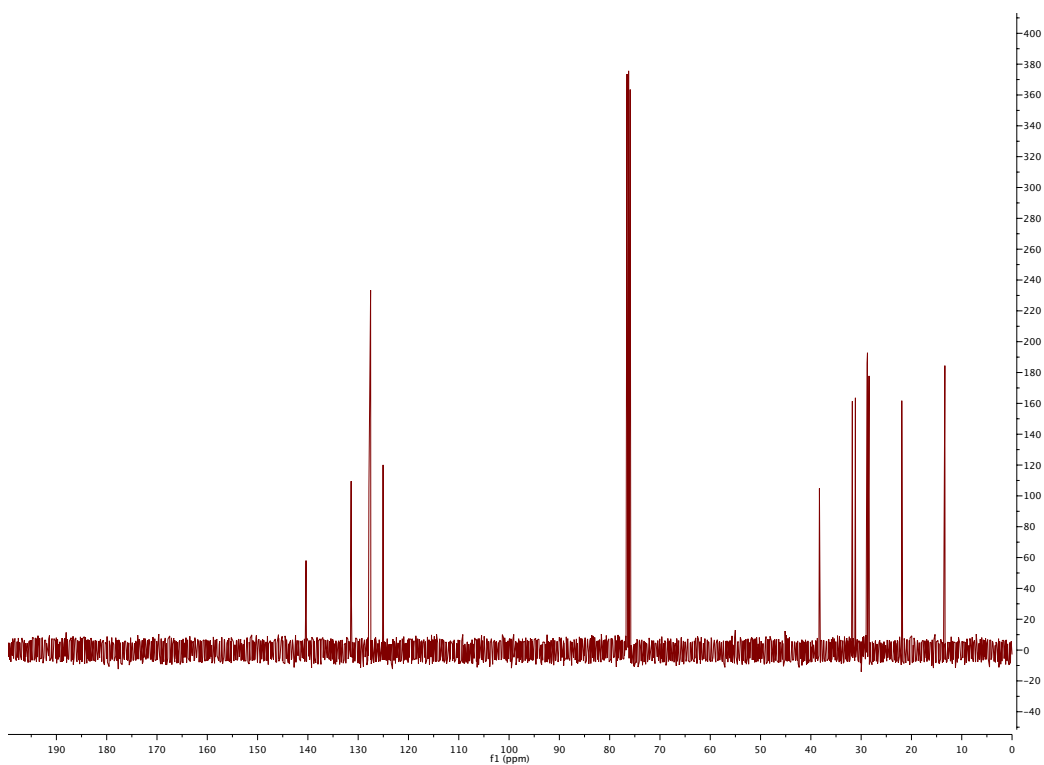
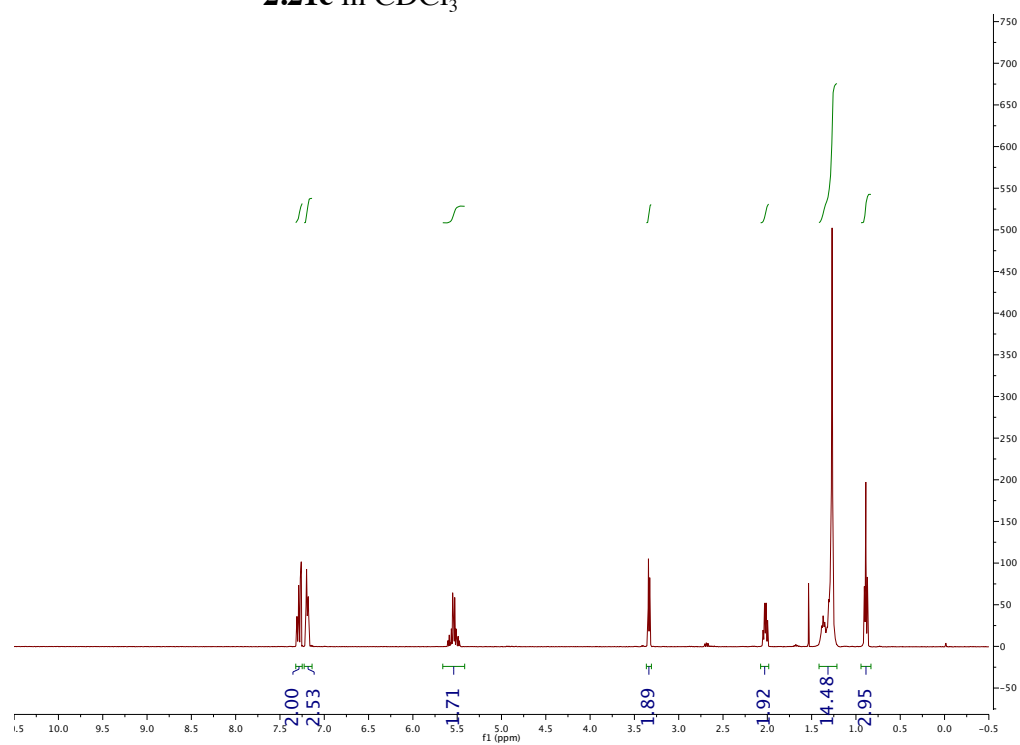


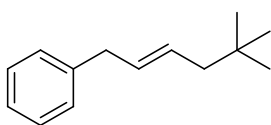
2.21b in CDCl₃



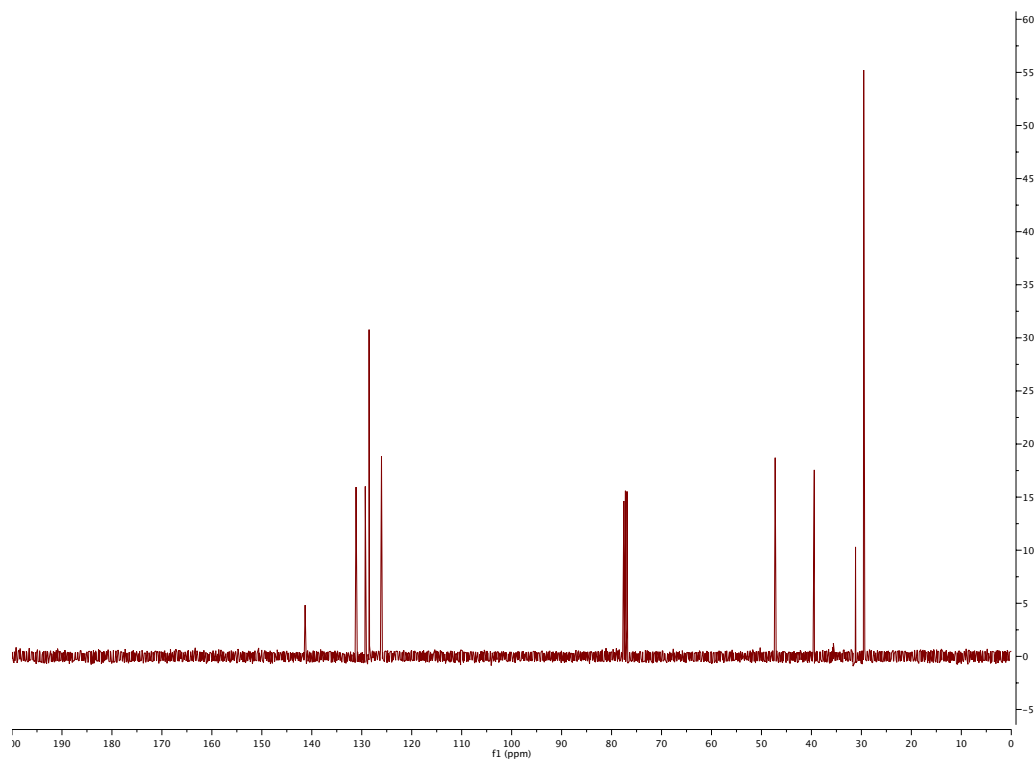
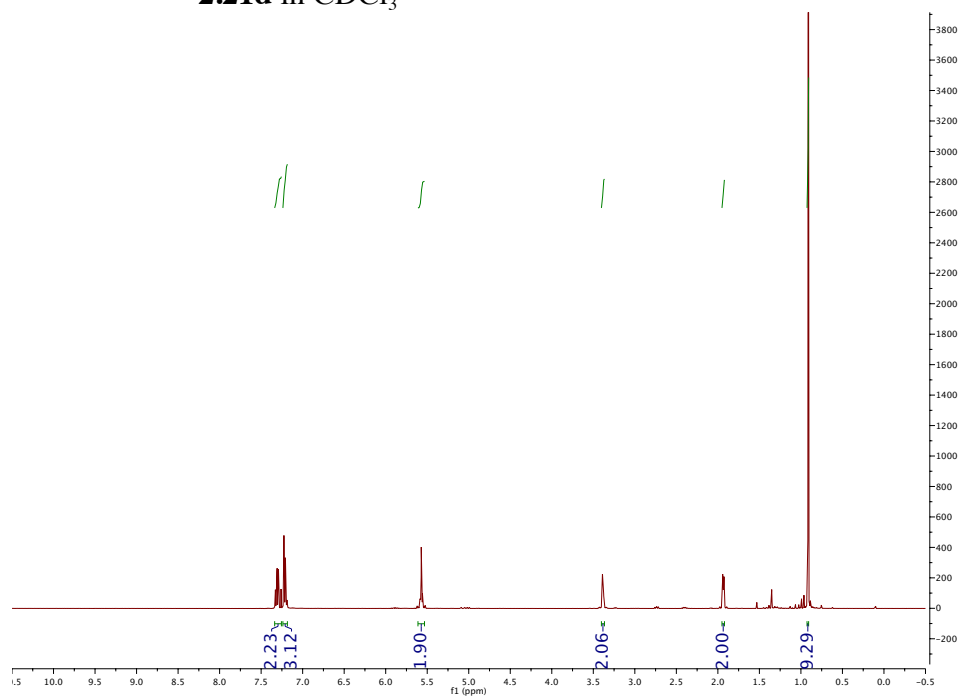


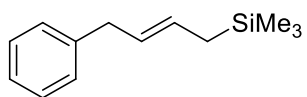
2.21c in CDCl₃



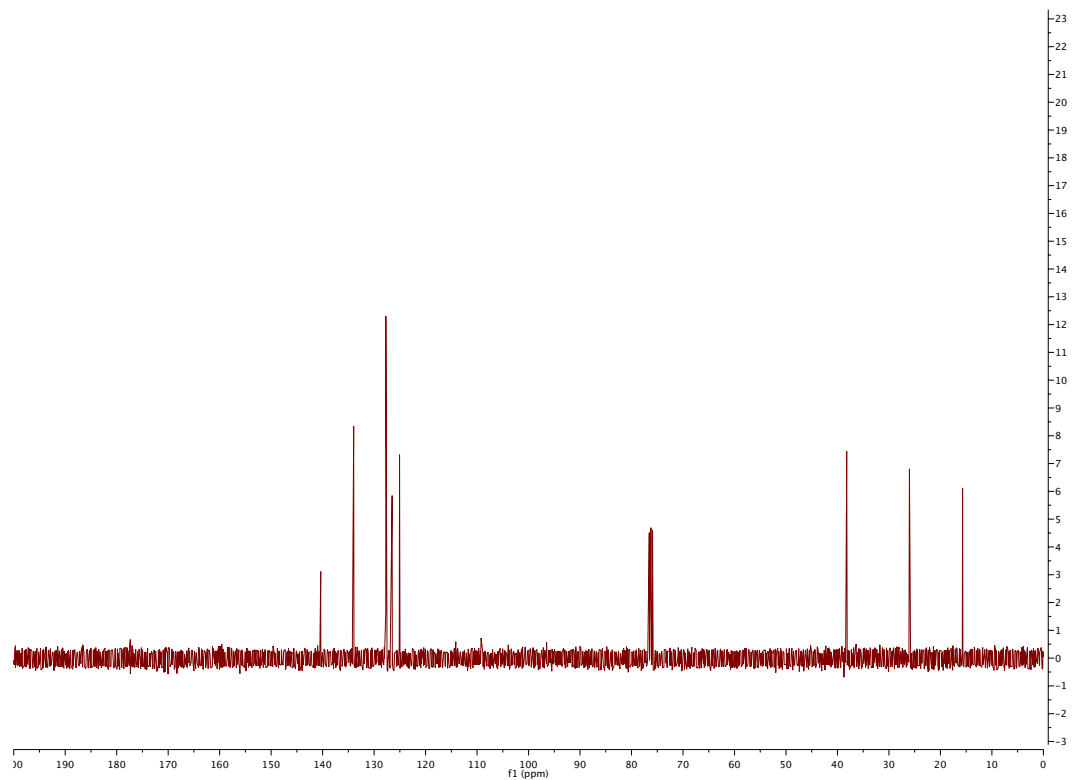
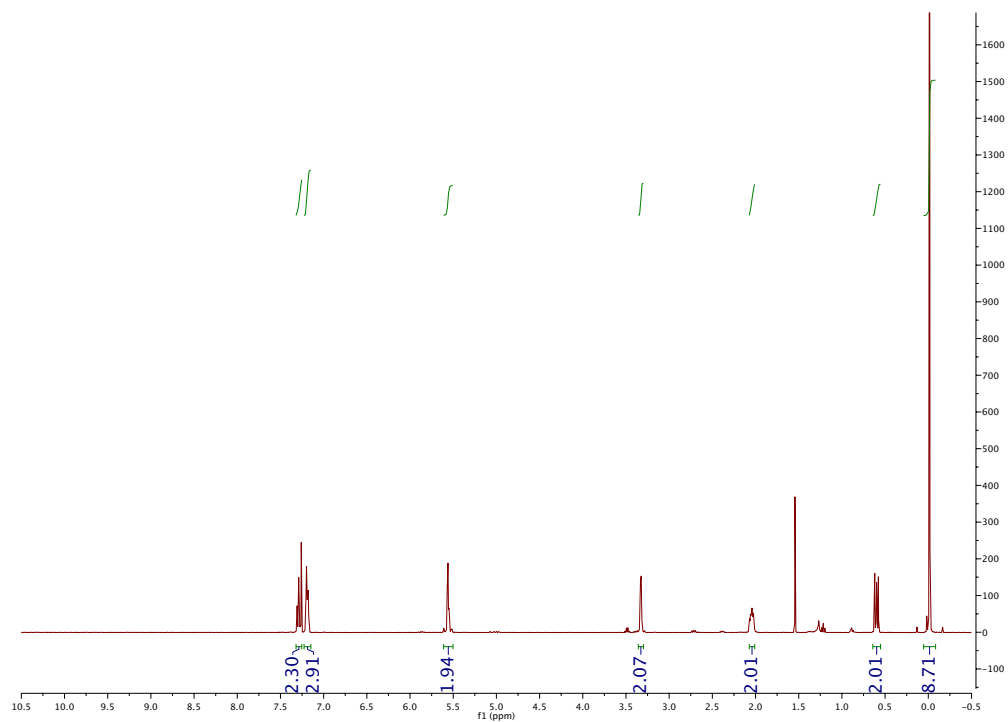


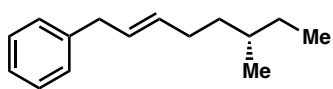
2.21d in CDCl₃



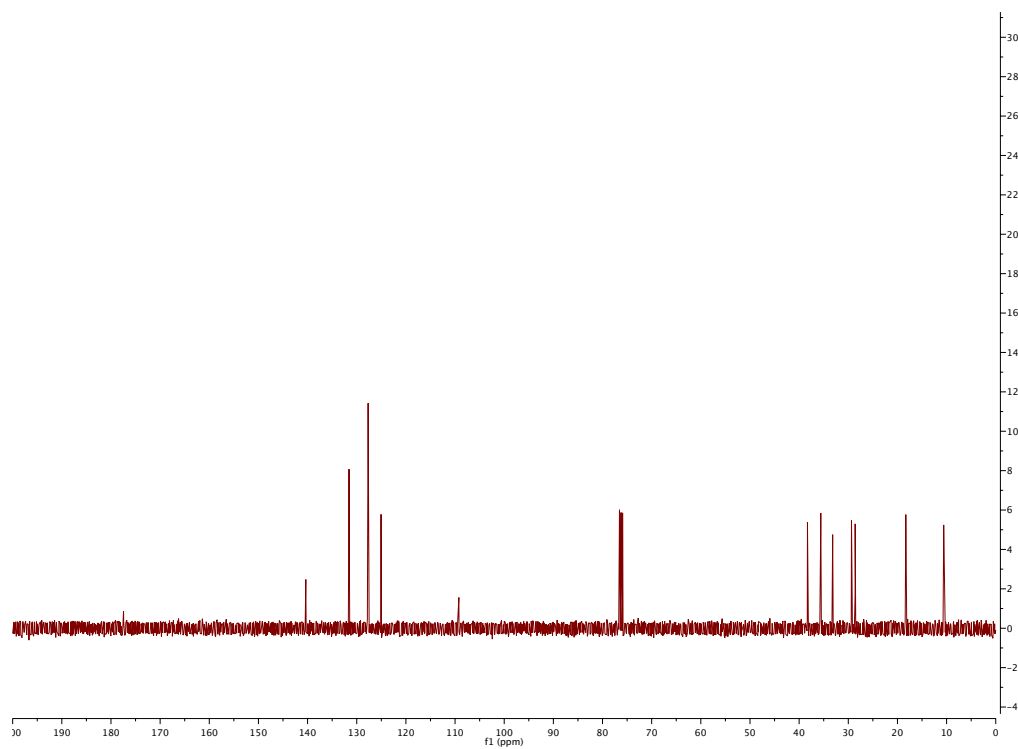
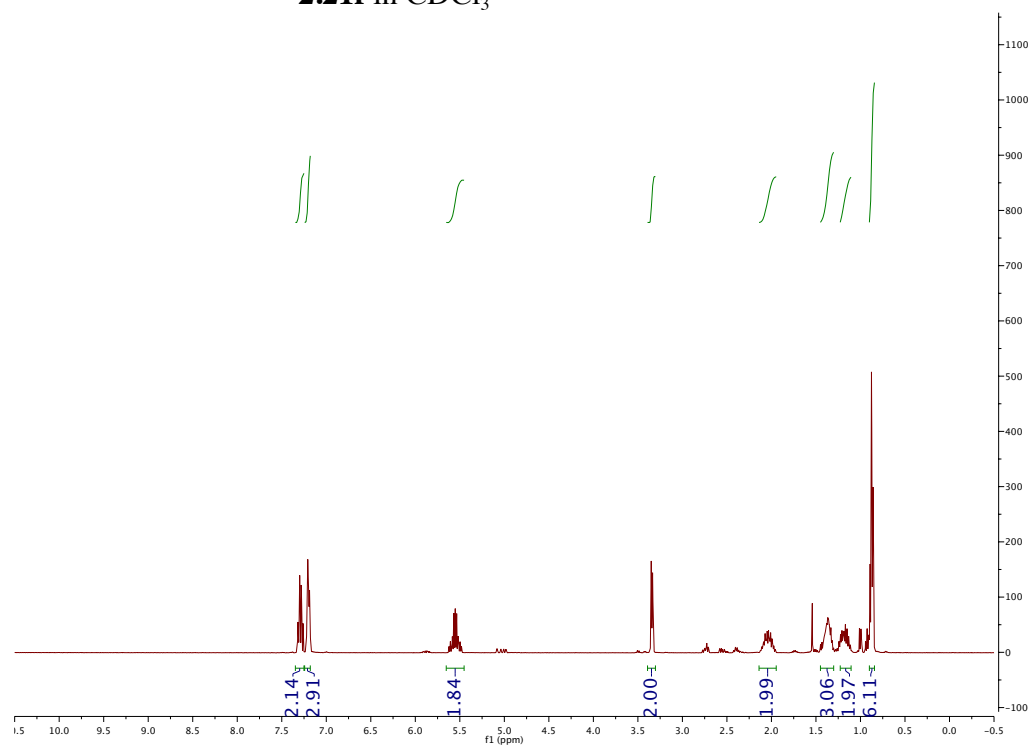


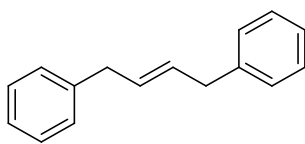
2.21e in CDCl₃



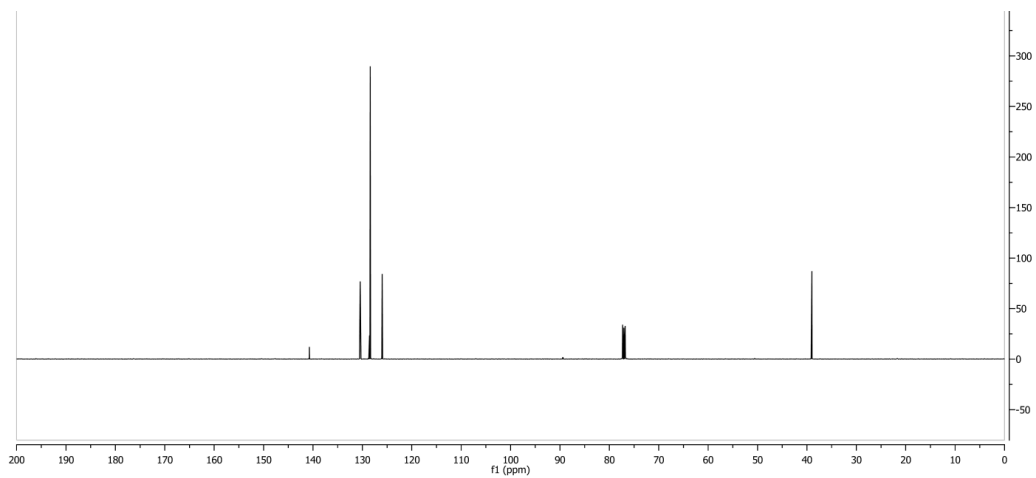
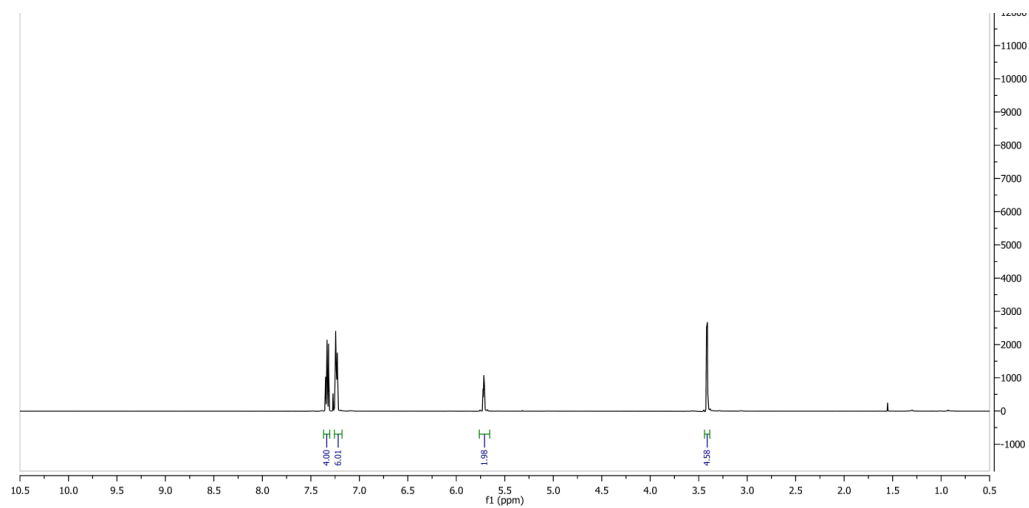


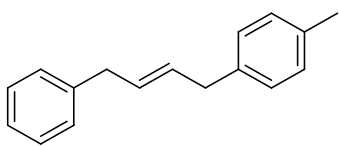
2.21f in CDCl₃



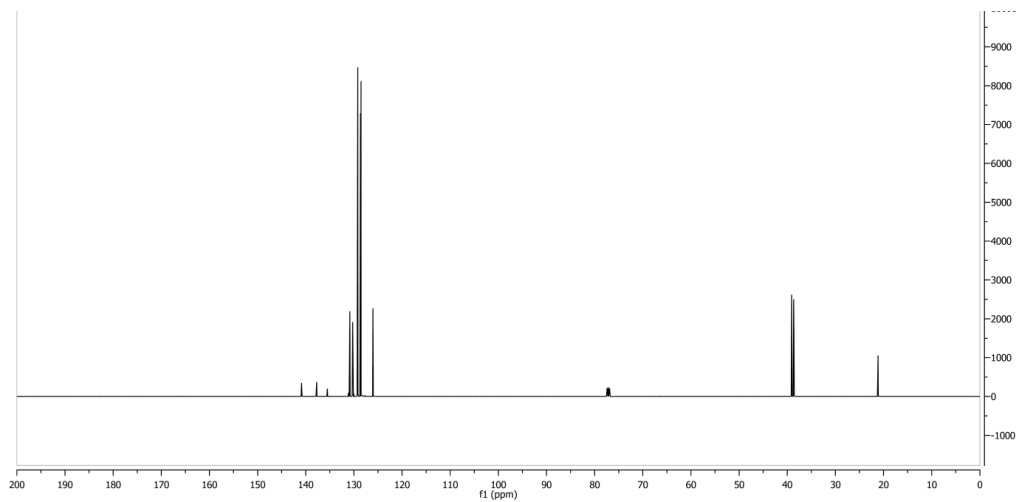
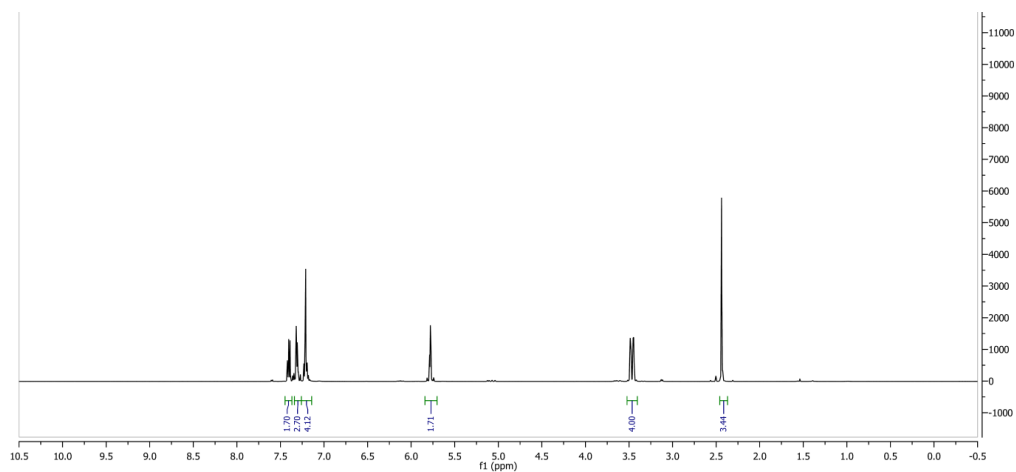


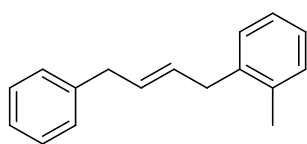
2.21g in CDCl₃



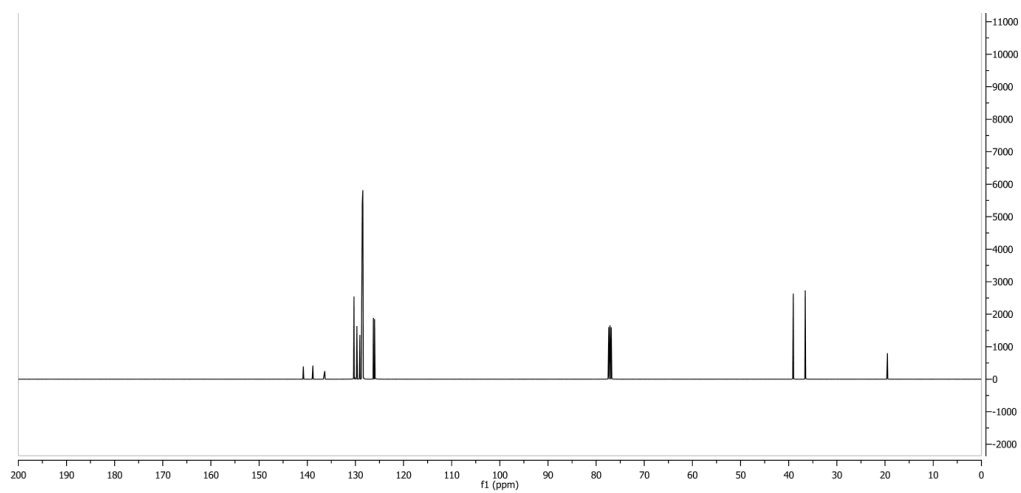
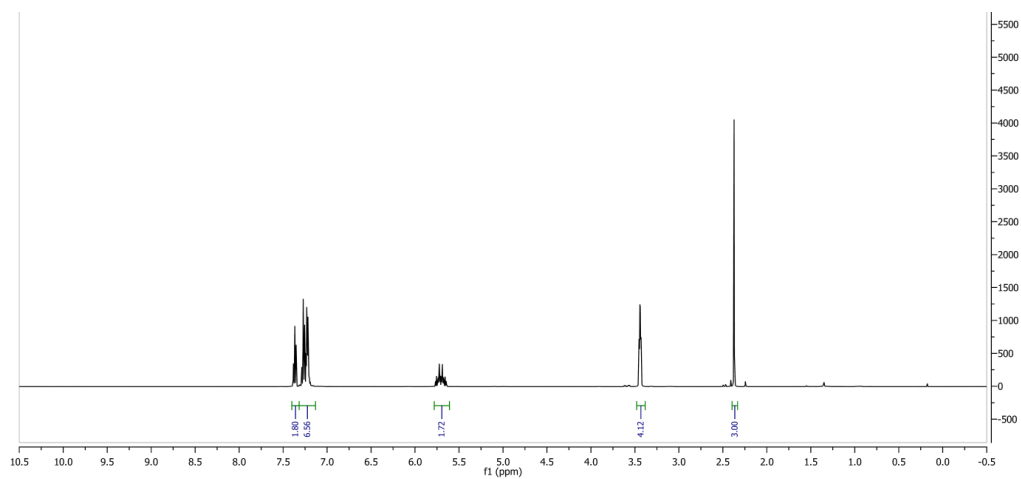


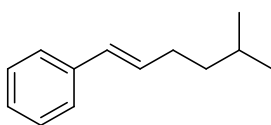
2.21h in CDCl₃



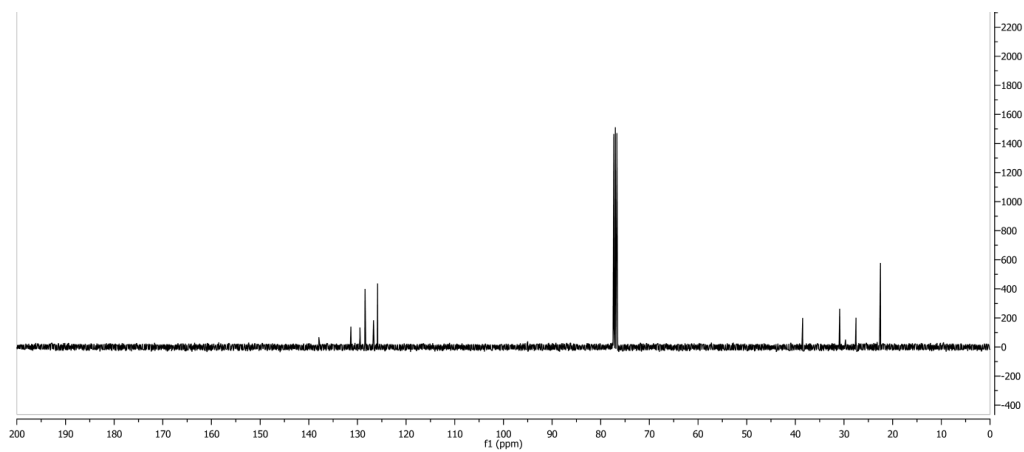
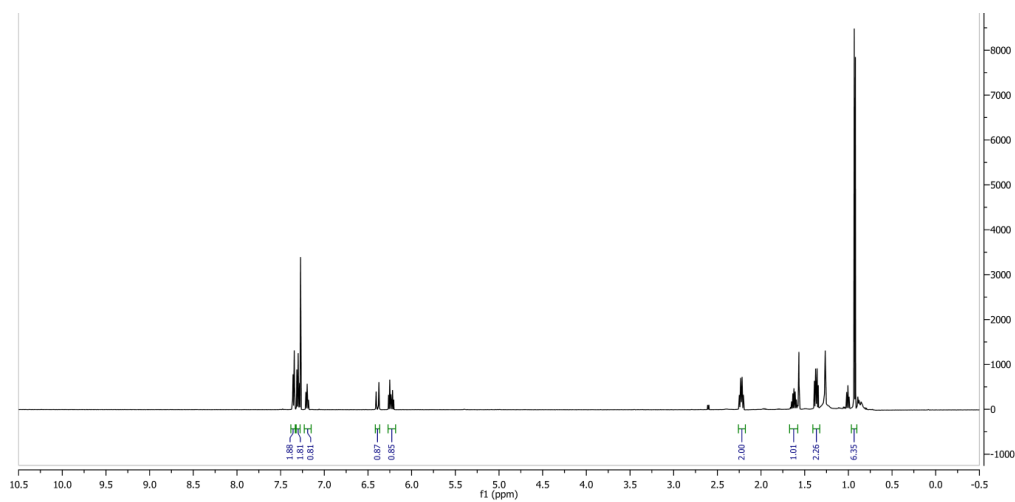


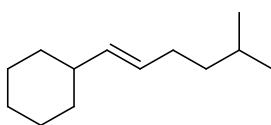
2.21i in CDCl₃



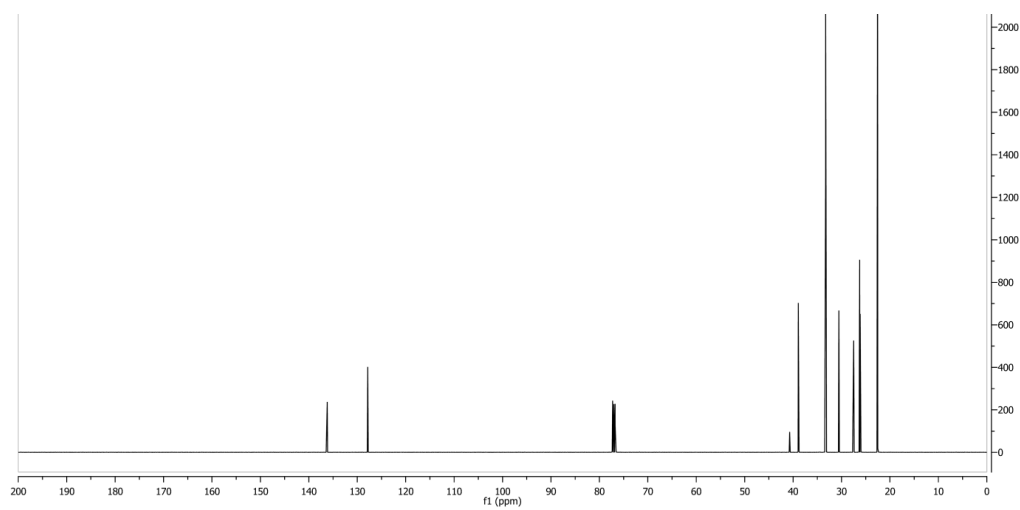
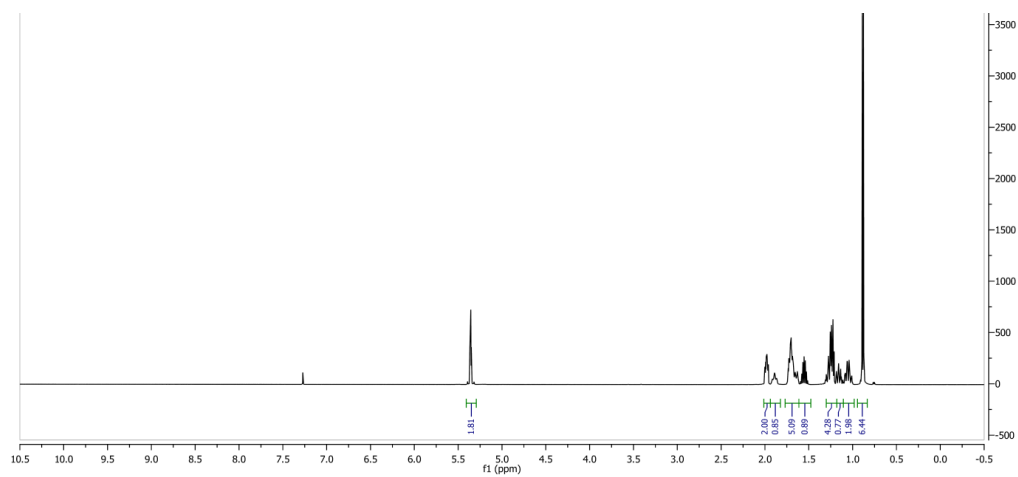


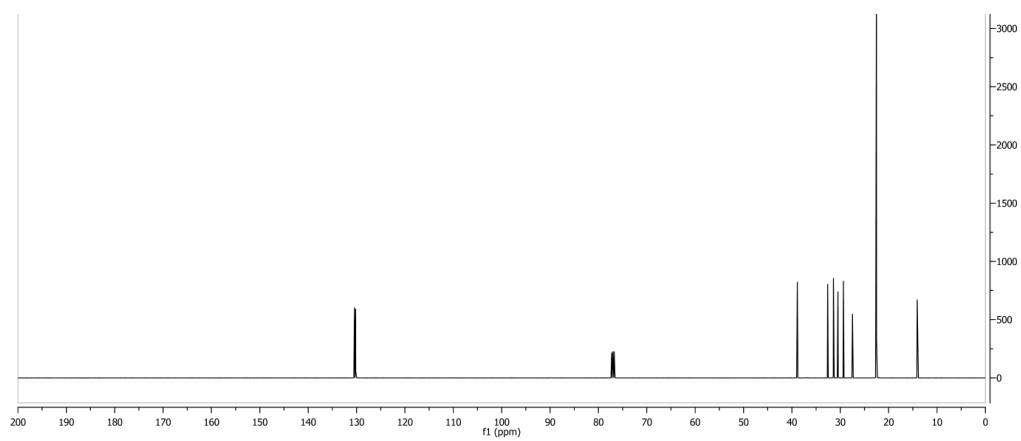
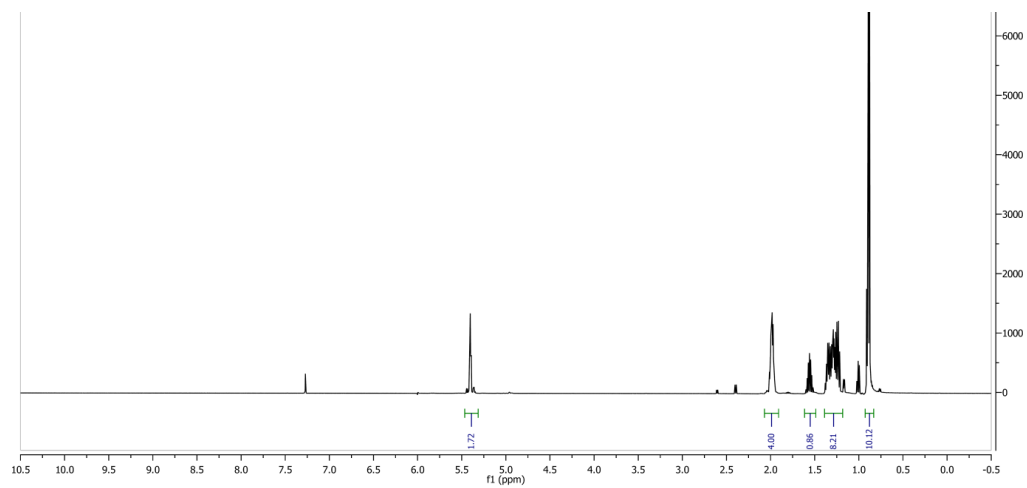
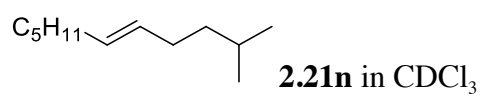
2.211 in CDCl₃

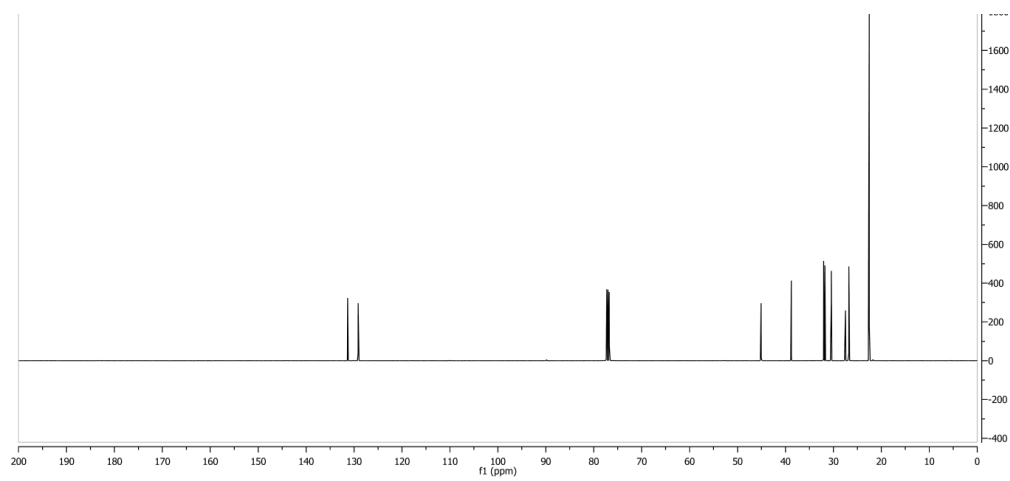
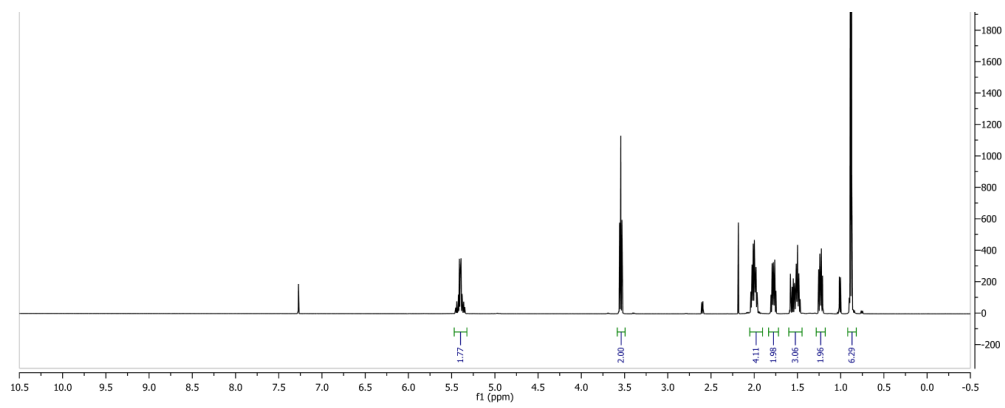
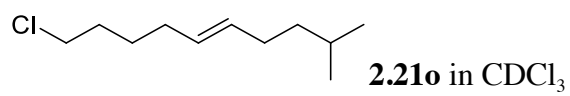


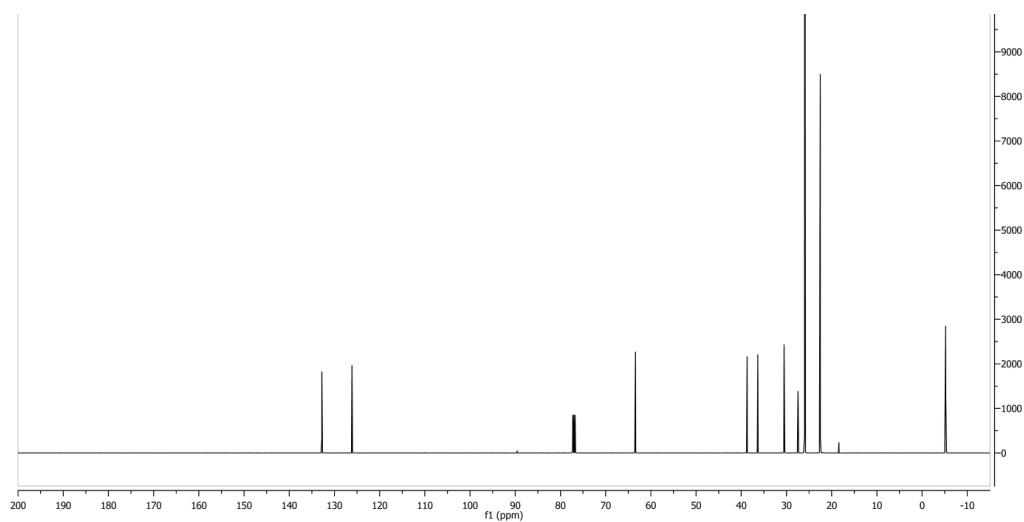
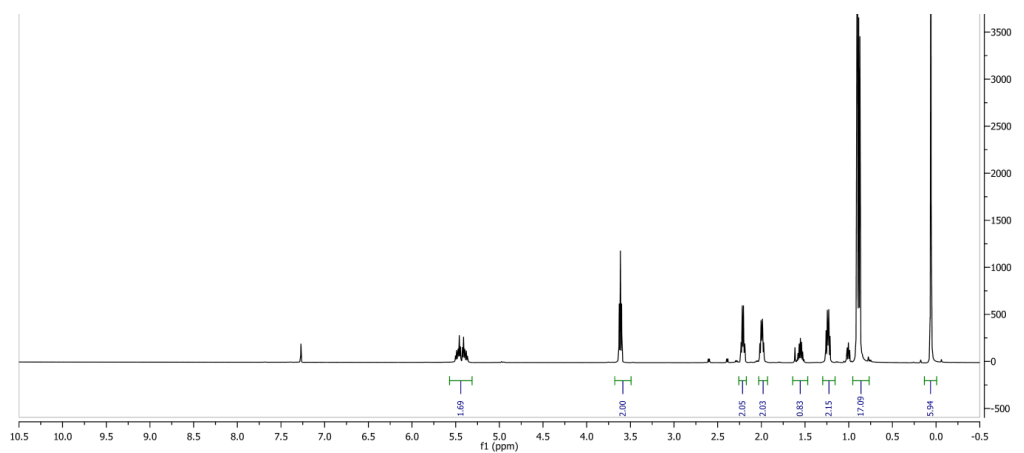
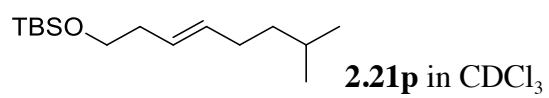


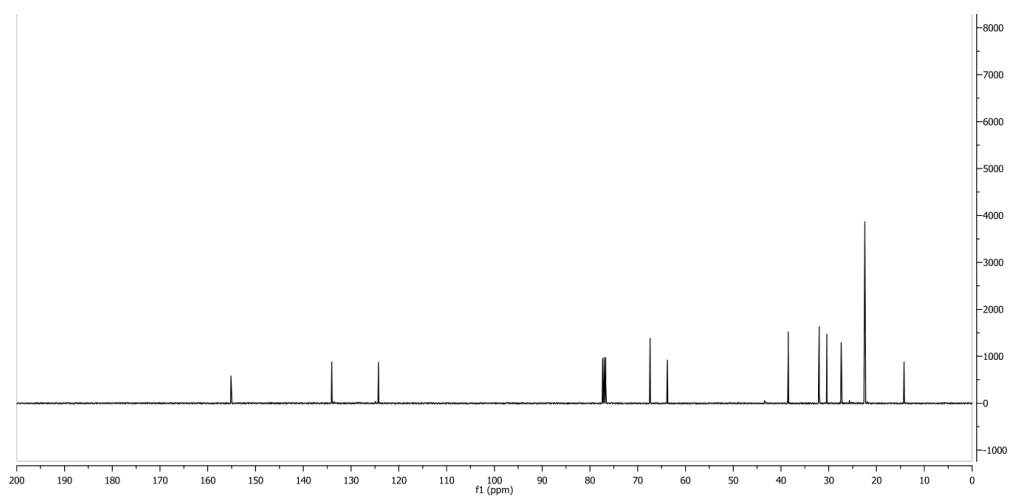
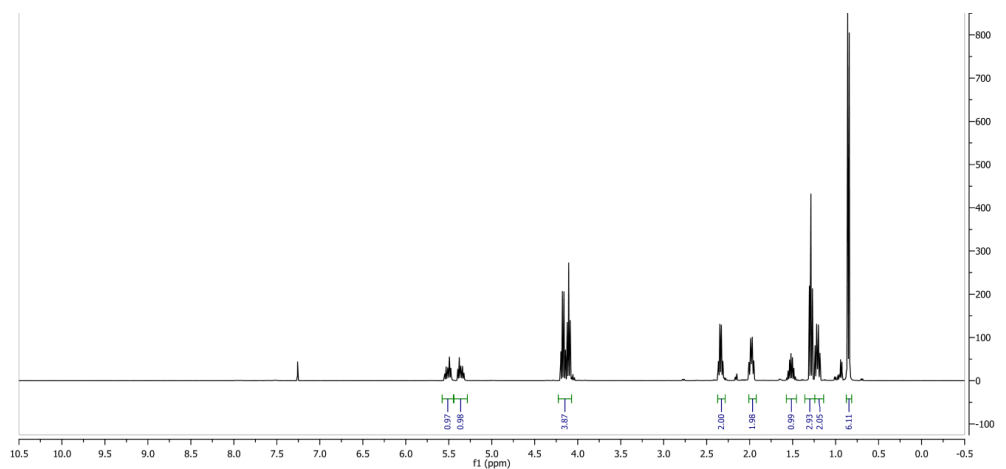
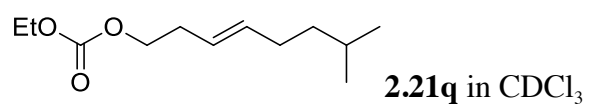
2.21m in CDCl₃

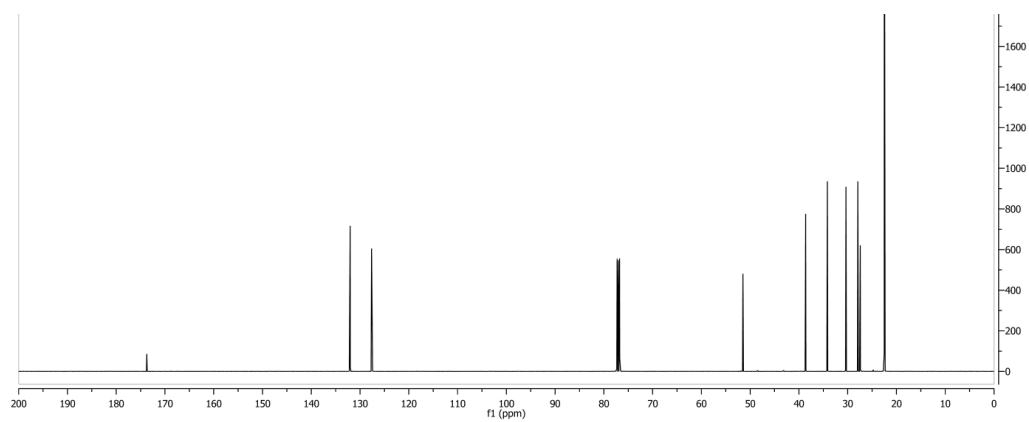
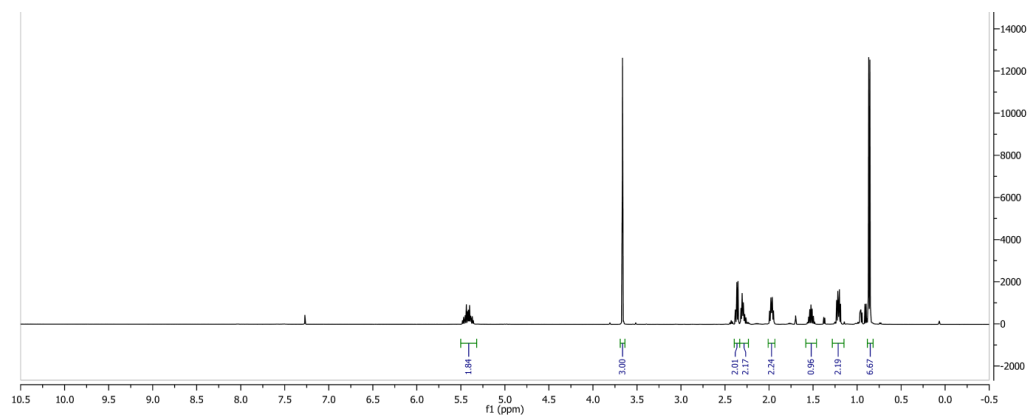
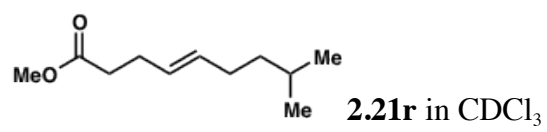


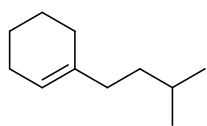




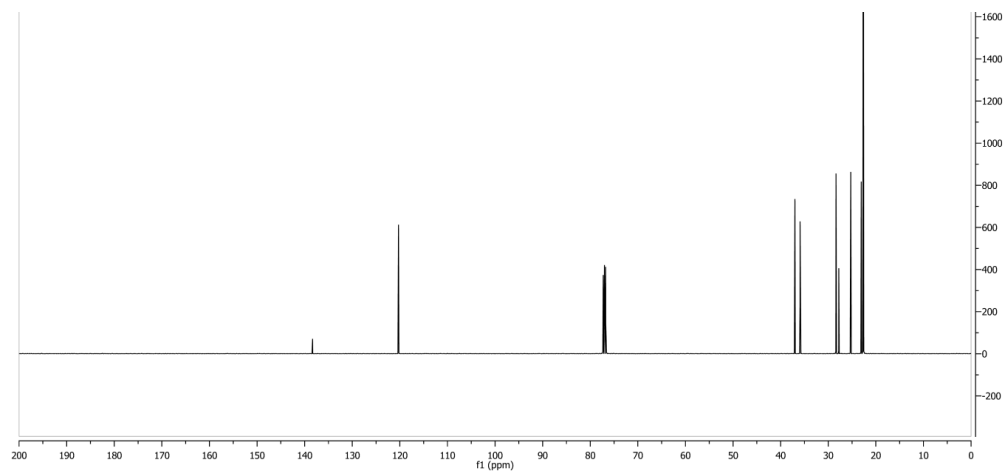
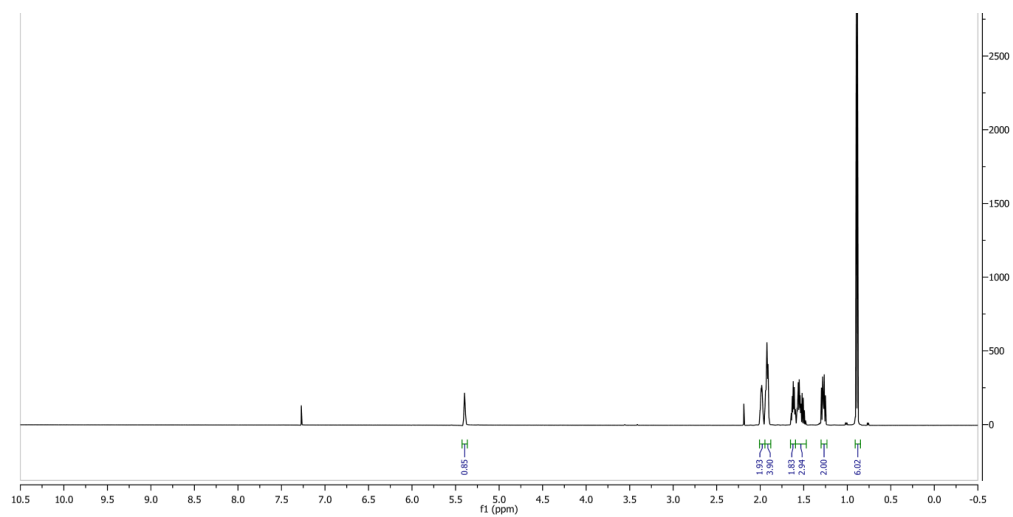


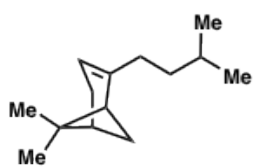




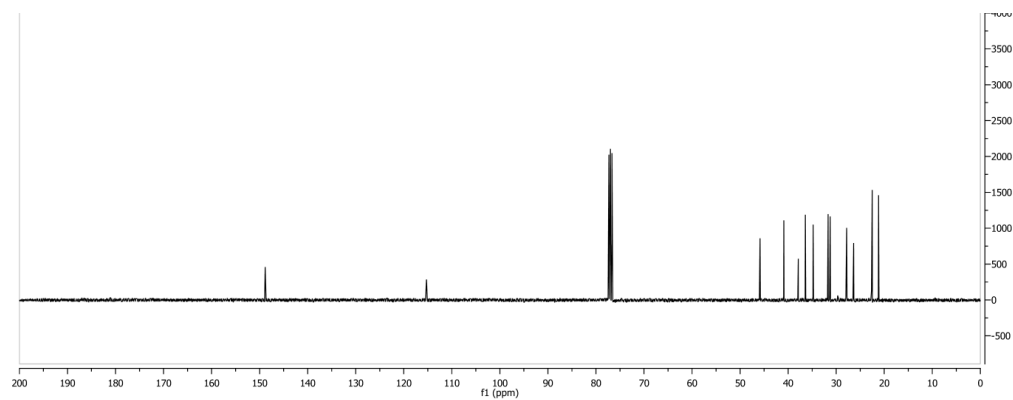
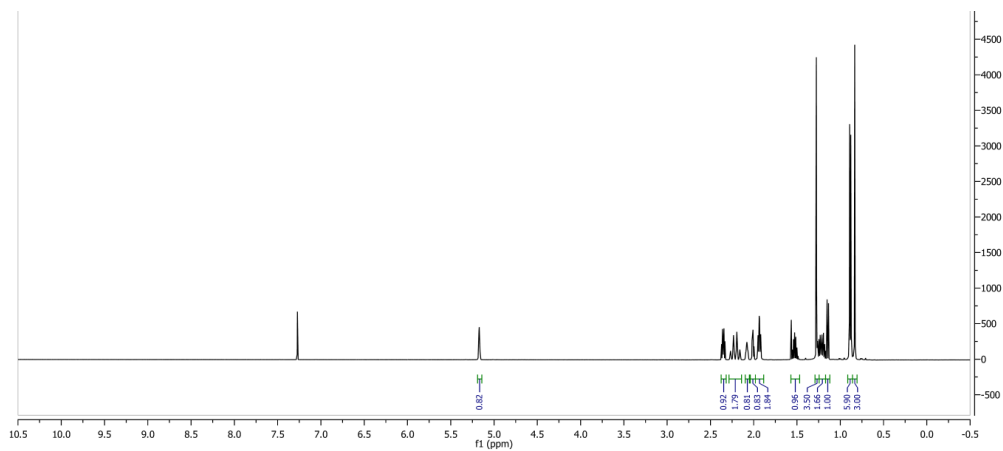


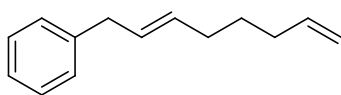
2.21s in CDCl₃



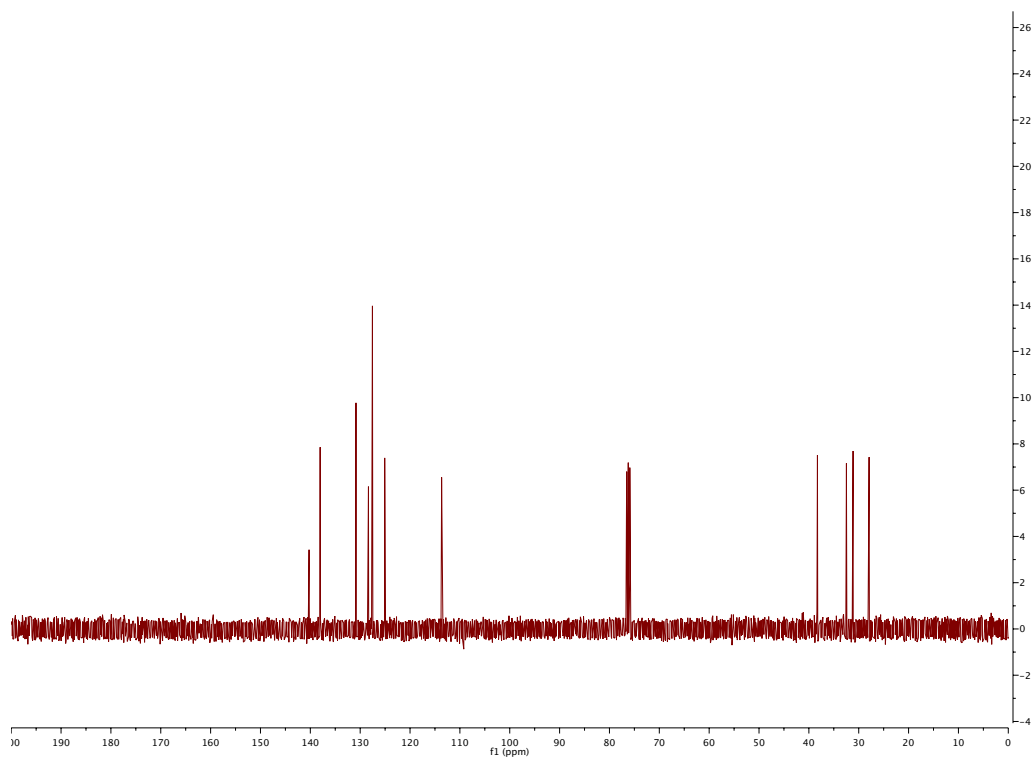
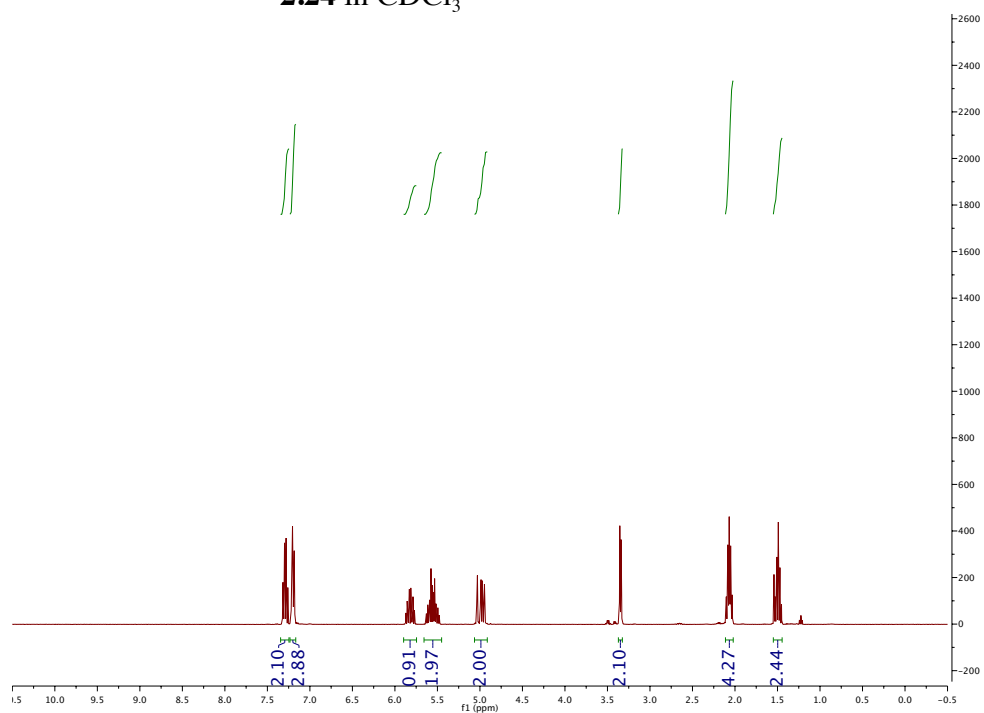


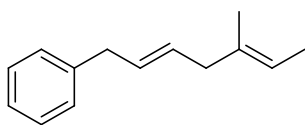
2.21t in CDCl₃



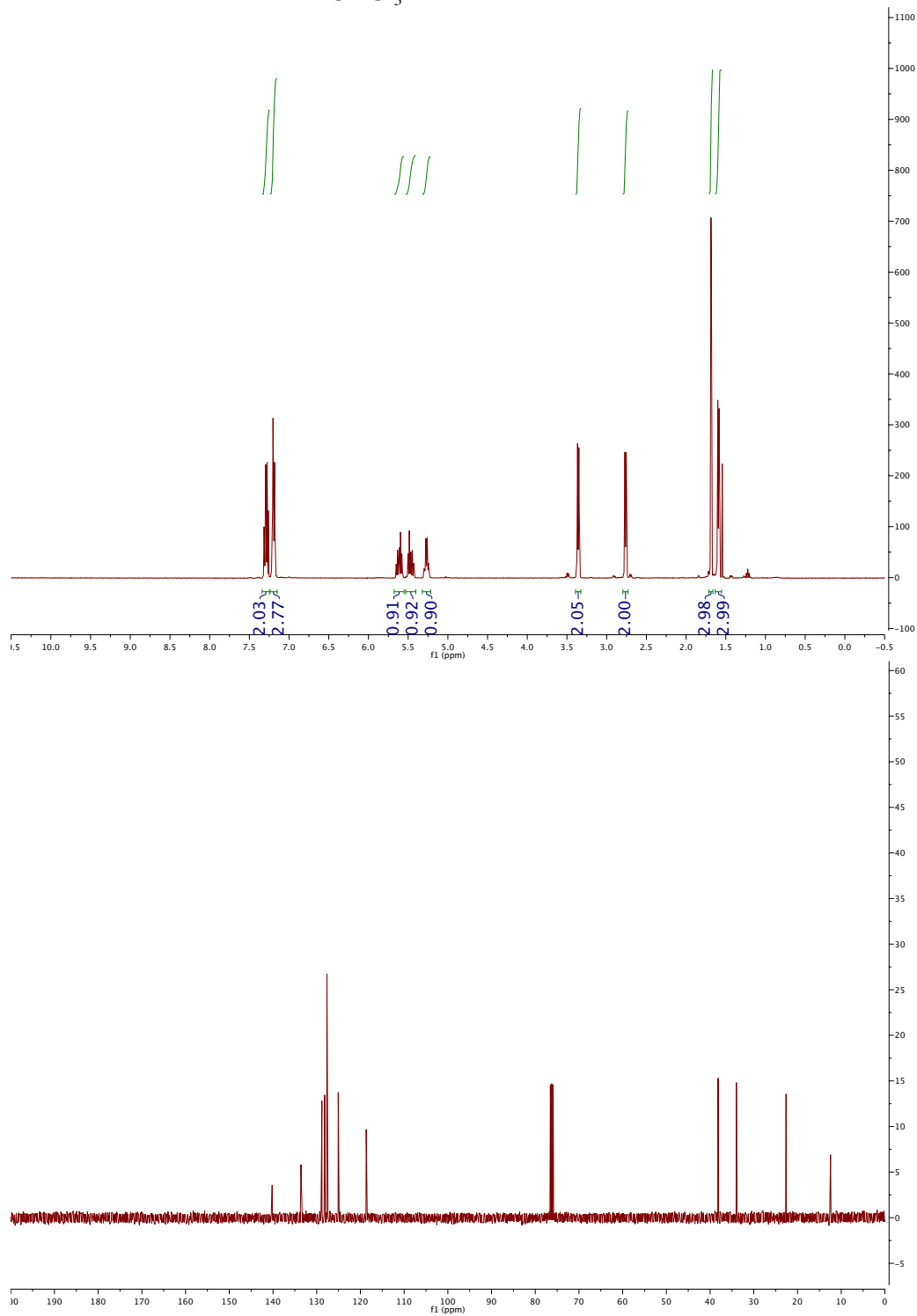


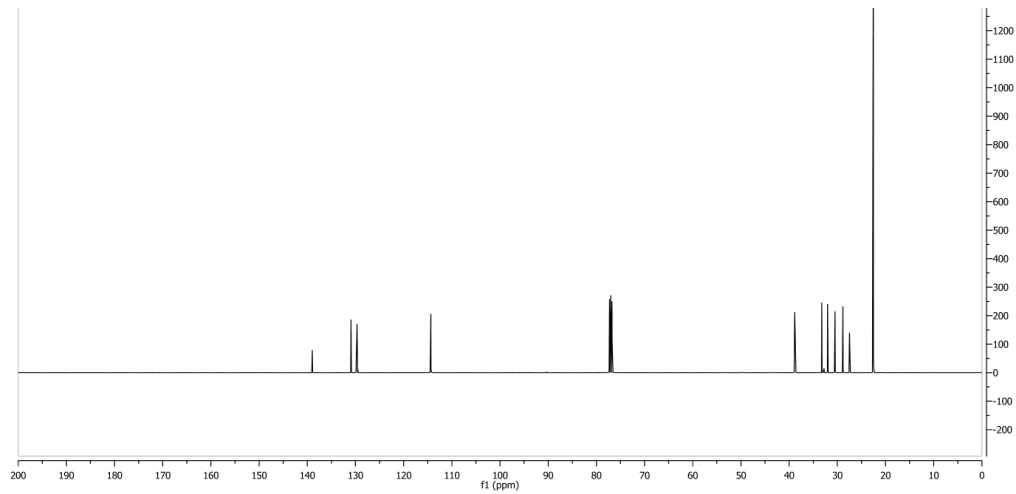
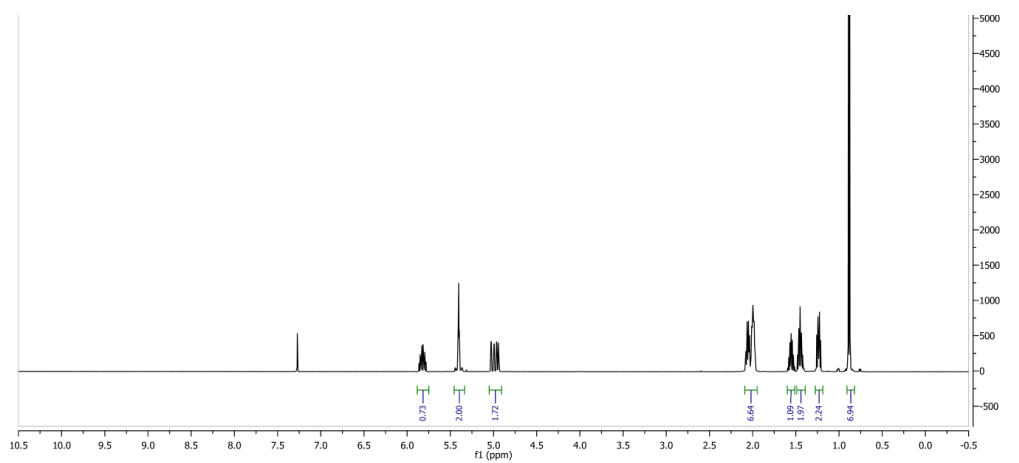
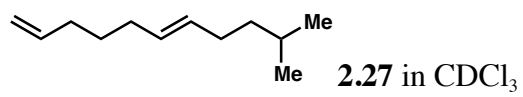
2.24 in CDCl_3

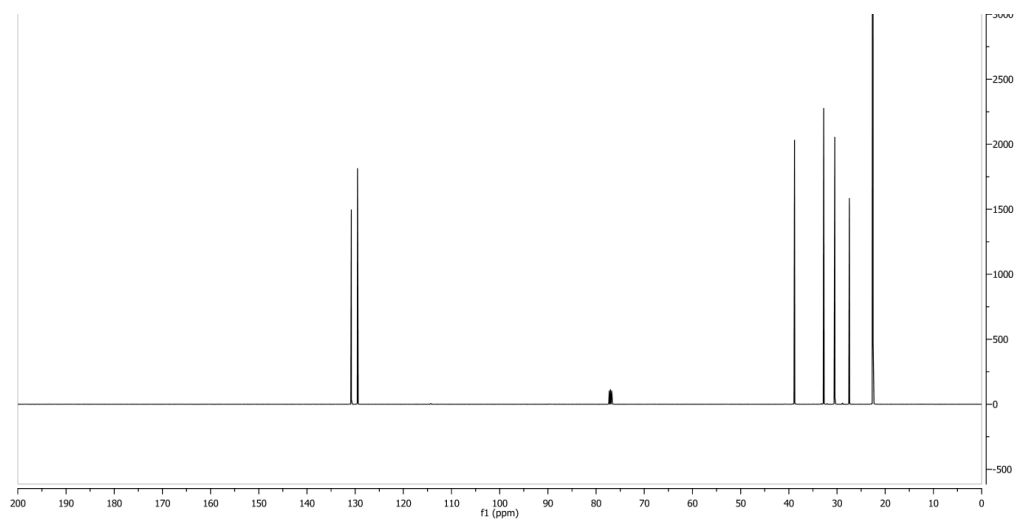
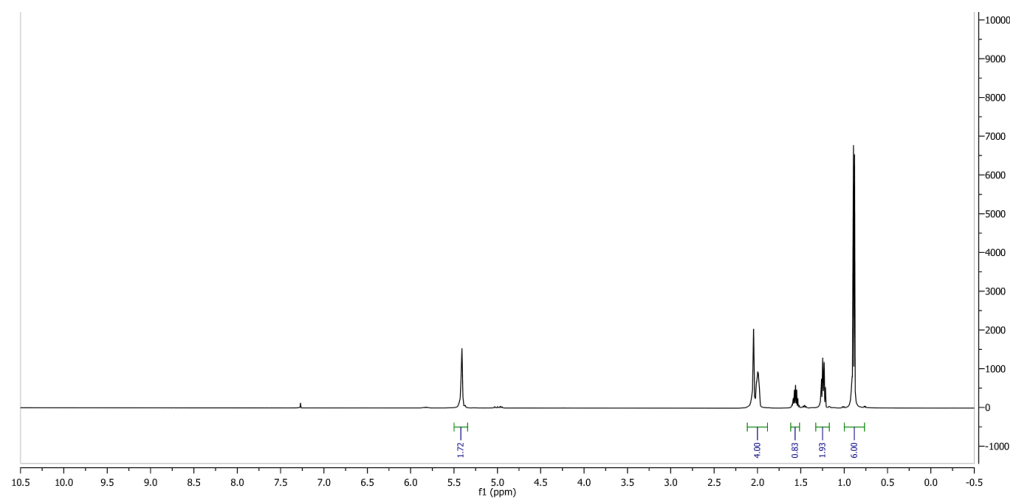
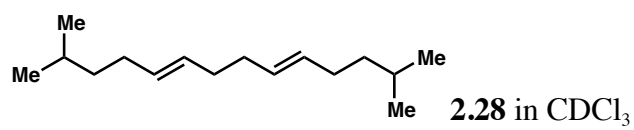


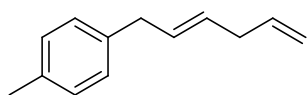


2.25 in CDCl₃

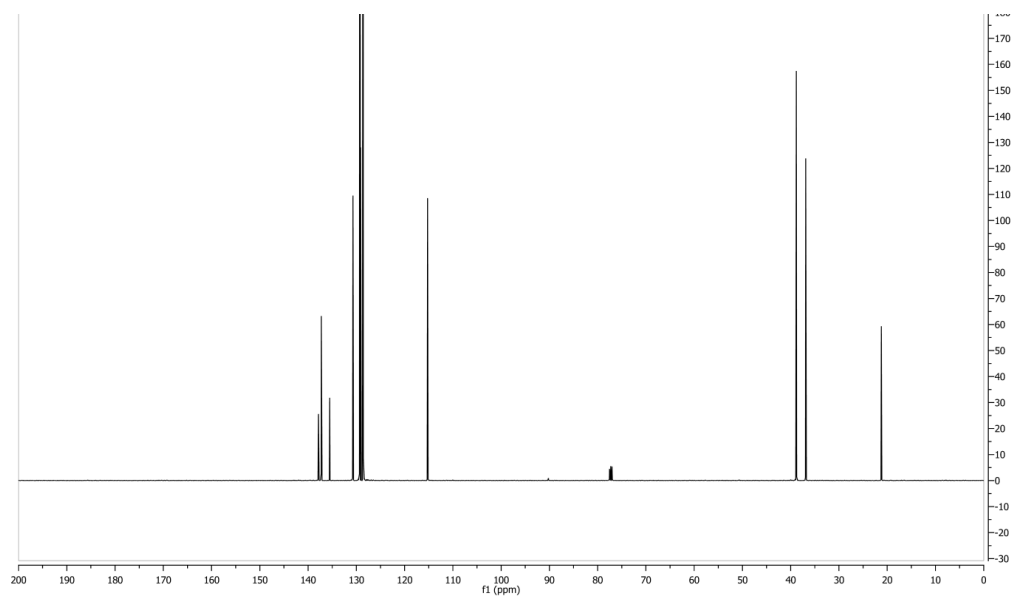
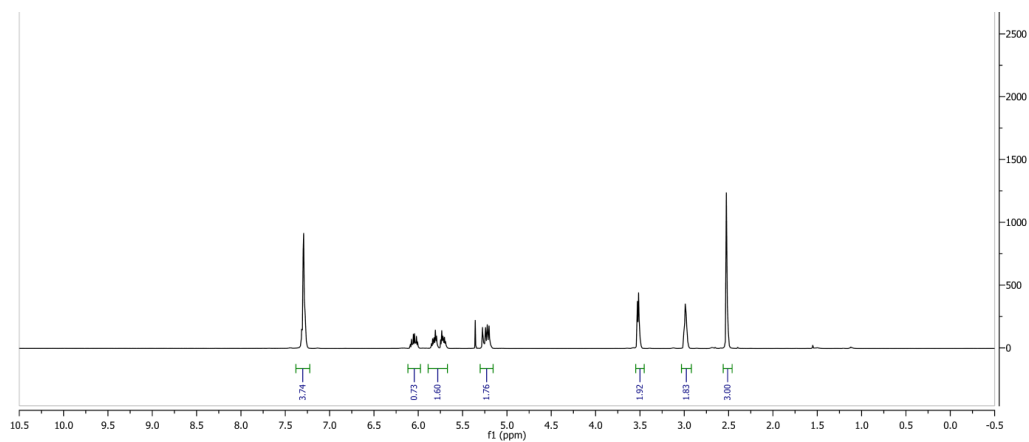


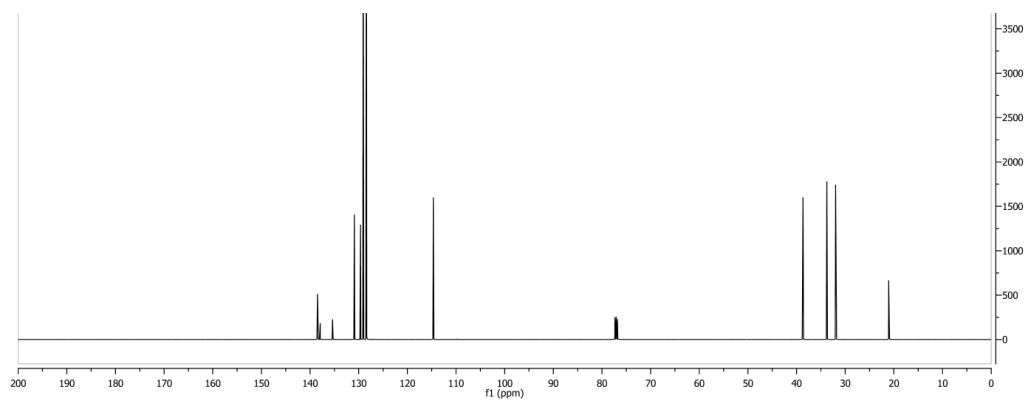
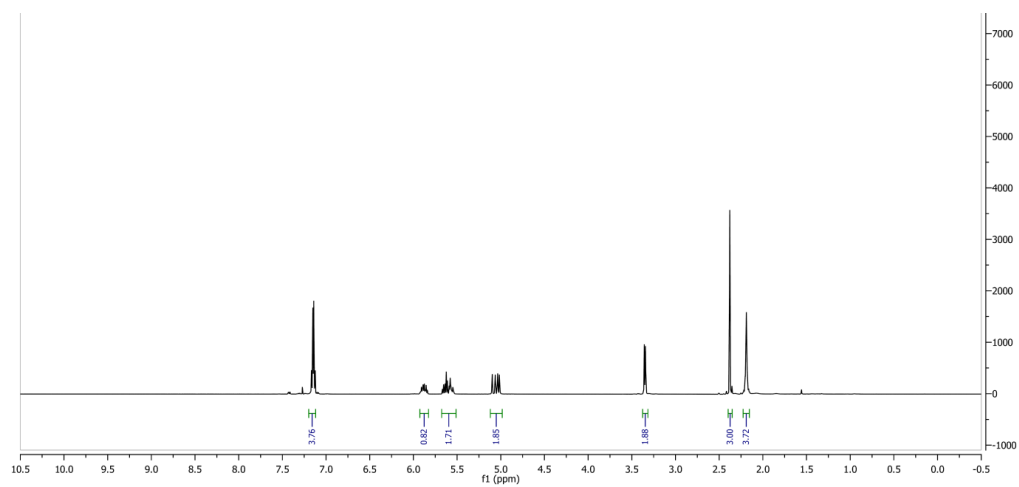
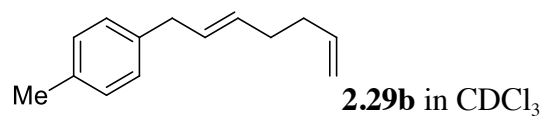


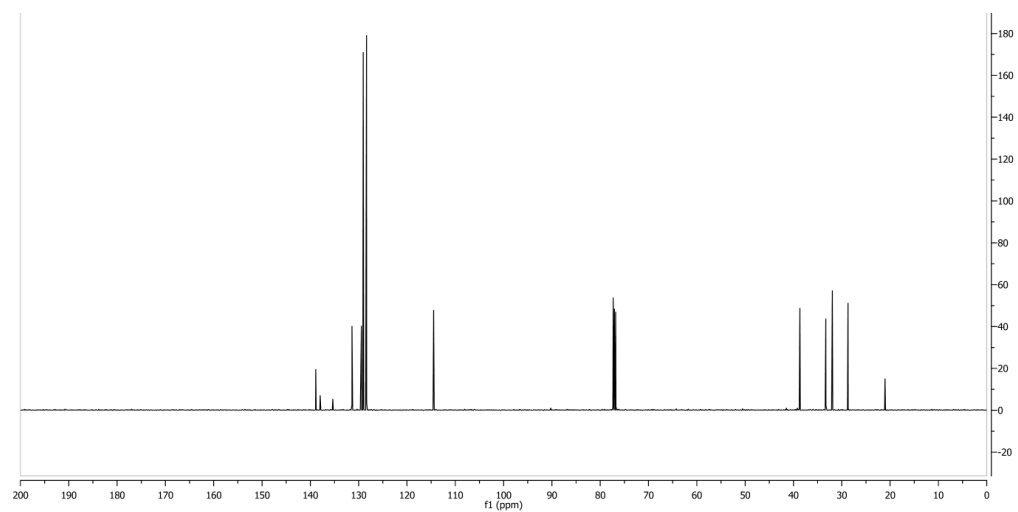
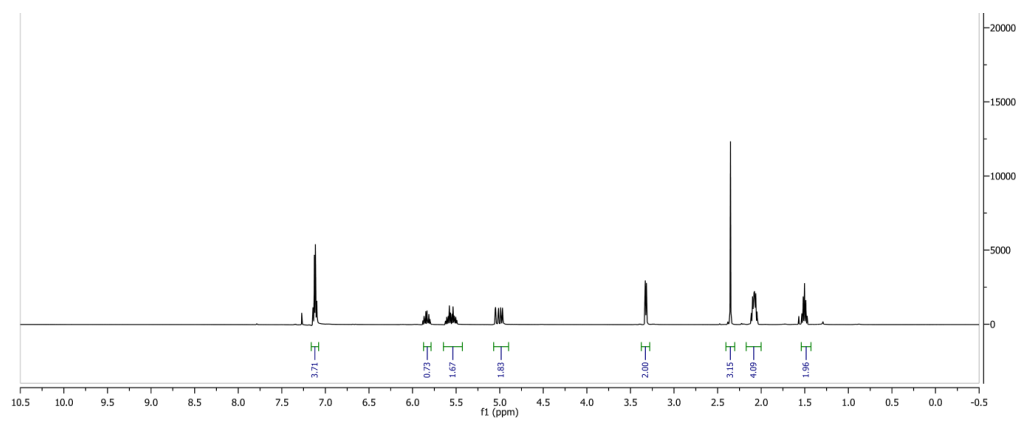
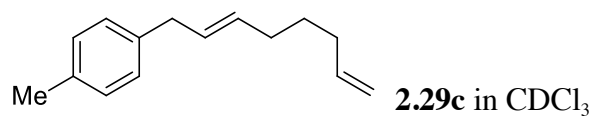


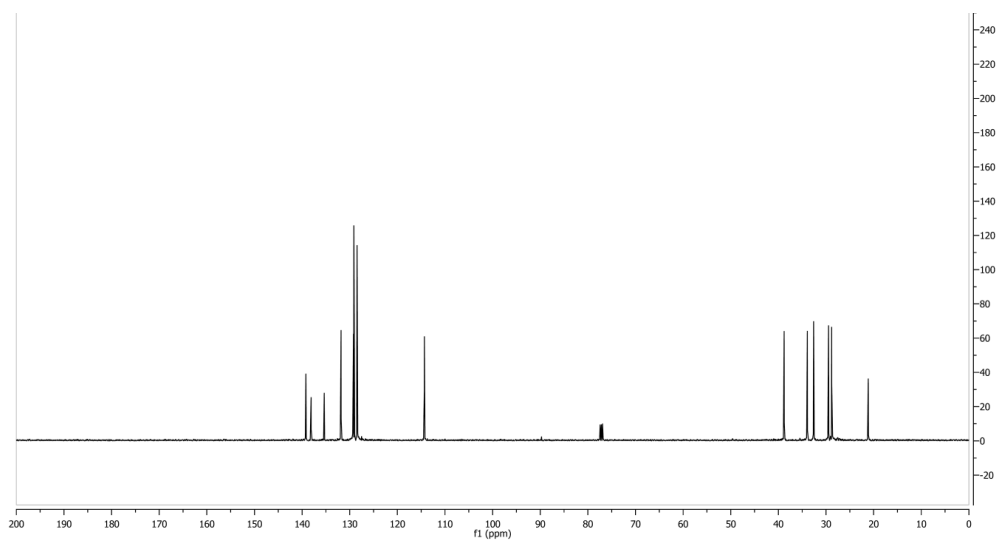
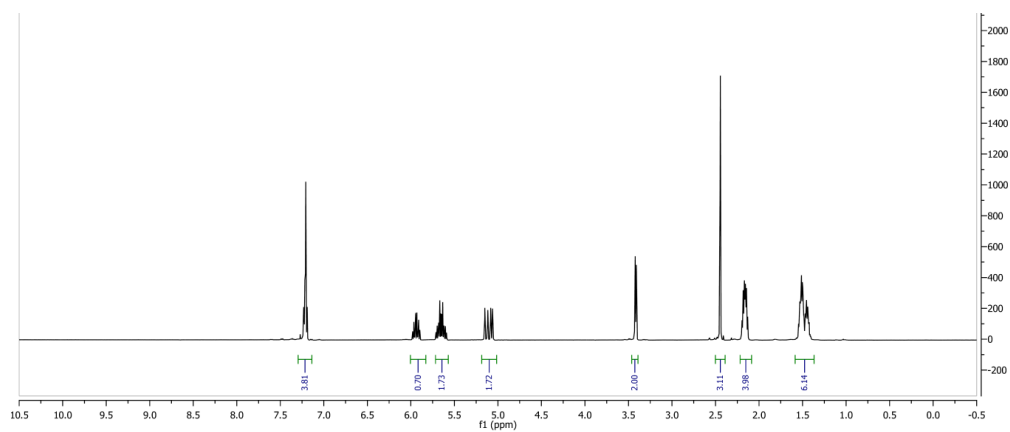
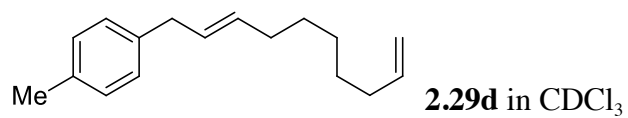


2.29a in CDCl₃









CHAPTER THREE

The Development of a Regio- and Diastereoselective Aminoarylation of Simple Dienes

3.1 Background

3.1.1 Introduction

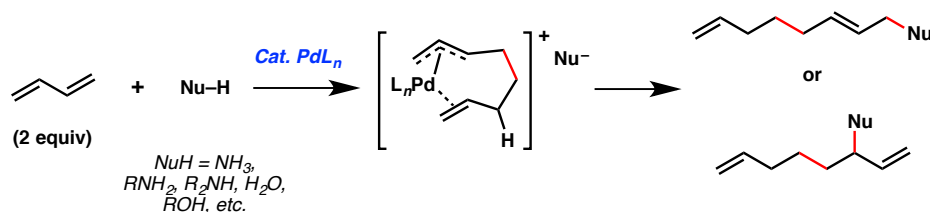
Nitrogen-containing compounds are represented in a sizeable portion of bioactive small molecules, making up more than 80 percent of FDA approved pharmaceutical drugs.¹⁻³ The selective introduction of C–N bonds into unsaturated hydrocarbons has evolved into a powerful synthetic strategy for the construction of these functional materials, enabling the use of inexpensive chemical feedstocks.^{2,4-6} In particular, allylic amines represent an important class of nitrogenated compounds, because they serve as fundamental intermediates in chemical synthesis in addition to functional materials themselves.⁷⁻¹⁰

The carboamination of diene starting materials represents an underutilized chemical strategy for the construction of allylic amines, presumably due to the challenge of controlling the carboamination pathway over competing bisalkylation or bisamination pathways. In addition, matters of both regioselectivity and diastereoselectivity become increasingly more difficult when introducing multiple new bonds into conjugated systems lacking directing or activating functionality. To date, only a handful of strategies have been developed for the catalytic intermolecular carboamination of unactivated dienes.¹¹⁻¹³

3.1.2 Catalytic Telomerization of Dienes with Amines

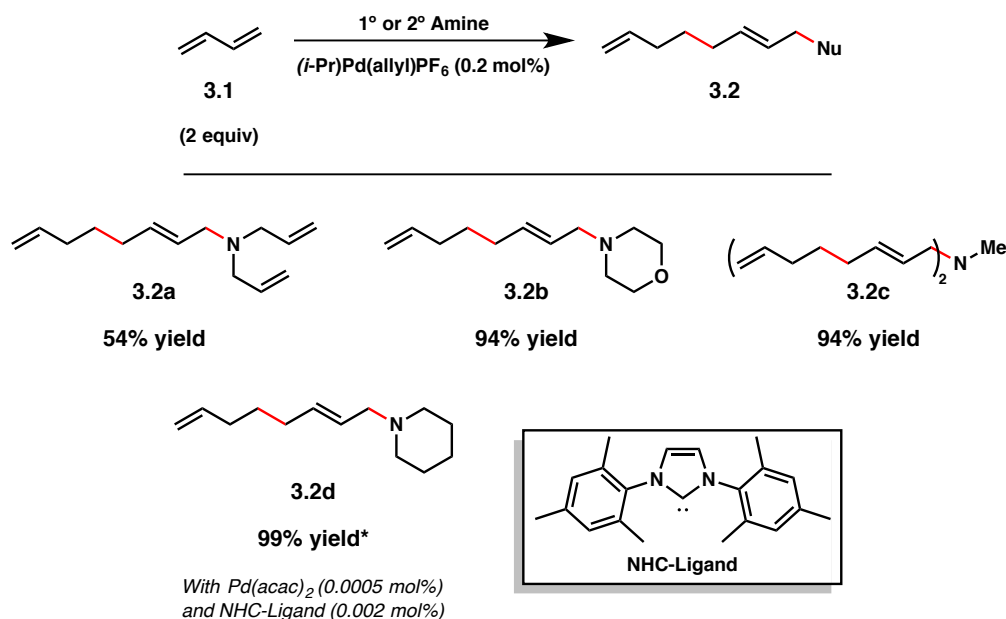
Telomerization, or the metal catalyzed linear dimerization of 1,3-dienes in the presence of a nucleophile, has been widely explored as a method for the selective incorporation of new C–N and C–C bonds within a single operation (Scheme 3.1.1).^{11,14-26} Since the establishment of this strategy by Takahashi and Smutny independently in 1967 as an atom economic and environmentally benign process,^{17,19} the palladium-catalyzed telomerization of simple dienes in the presence of ammonia, 1° or 2° amines has found its niche in chemical synthesis and industrial processes and represents one of the earliest examples of the selective carboamination of simple dienes.

Scheme 3.1.1



In recent years, several labs have expanded on the palladium-catalyzed telomerization of 1,3-butadiene (**3.1**) with amines to selectively access a wide variety of amino-2,7-dienes (**3.2**, Scheme 3.1.2). There are several advantages to this strategy, including low catalyst loadings, and excellent *E*-olefin selectivity. *N*-heterocyclic carbenes represent particularly exceptional ligands for this process and have been shown to provide catalyst turnover numbers as high as 400,000.^{16,26} While this chemistry is predominantly utilized for the functionalization of 1,3-butadiene, and therefore circumvents additional regioselectivity concerns, recently the regioselective telomerization of isoprene has found some success.^{14,20,24,25}

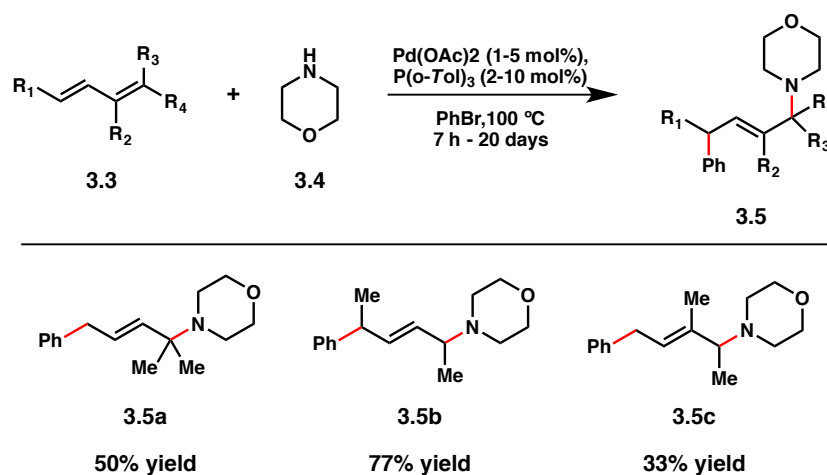
Scheme 3.1.2



3.1.3 Heck's Palladium-Catalyzed Aminoarylation of 1,3-Dienes

Subsequent to the discovery and study of telomerization with amines, Heck and coworkers reported an elegant study on the palladium-catalyzed aminoarylation of 1,3-dienes that accommodates a wider variety of acyclic and cyclic diene substrates (Scheme 3.1.3).¹² This reaction takes place through the palladium-catalyzed coupling of aryl bromides and secondary amines to a series of unactivated diene starting materials. For example, variably substituted dienes **3.3** were coupled with morpholine **3.4** and bromobenzene to furnish selectively the corresponding 1,4-aminoarylation products **3.5**. The *E*-allylic amine products were generally accessed in moderate yield with high linear to branched selectivity. Higher catalyst loadings and temperatures were required to evade polymerization of the diene, however a competing β -hydride elimination pathway led to substantial formation of diene byproducts in most cases.

Scheme 3.1.3



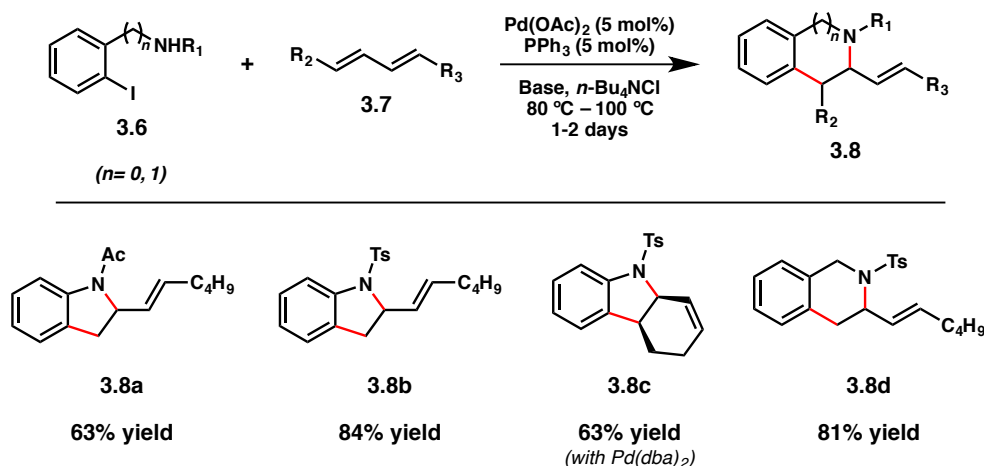
Mechanistic studies indicate that regioselectivity in the arylation event stems from preferential carbopalladation to the sterically least hindered olefin. Accordingly, trends in reactivity were observed based on olefin substitution, with monosubstituted olefins reacting favorably to 1,1-disubstituted olefins or 1,2-disubstituted olefins. The resulting palladium π -allyl complex is susceptible to either regioselective nucleophilic attack by the 2° amine or β -hydride elimination. Thus, not only is olefin geometry dictated by the palladium catalyst, but regioselectivity as well.

3.1.4 Palladium-Catalyzed Heteroannulation to Vinyl Heterocycles

The heteroannulation of 1,3-dienes with anilines and benzyl amines represents a noteworthy advance in the area of combined C–C and C–N bond formation (Scheme 3.1.4). While original examples of this methodology employed the stoichiometric use of toxic mercury and thallium-based reagents,²⁷⁻²⁹ modified procedures were developed independently by the Dieck and Larock labs to accommodate the palladium-mediated coupling of *ortho*-iodo arenes bearing various oxygen and nitrogen functionalities with

unfunctionalized dienes.^{13,30} This chemistry provides an efficient one-pot strategy to vinyl indoline and tetrahydroisoquinoline products in addition to analogous oxygen heterocycles.

Scheme 3.1.4



The reaction proceeds through oxidative addition of the active $\text{Pd}(0)$ species to iodoarene **3.6** followed by coupling to diene **3.7** and concomitant heteroannulation. The initial palladium coupling of the aryl iodide takes place with good regio-discrimination when differentially substituted 1,3-dienes are used and follow the same guiding principles as the above-mentioned Heck chemistry. Moreover, the 1,2-carboamination products are generated with a strong preference for the *E*-olefin isomer.

3.1.5 Conclusions

To date, only a handful of examples have been reported for the intermolecular carboamination of simple dienes lacking activating or directing functionality. These instances illustrate the utility of this chemistry for the highly selective construction of value-added *E*-allylic amine products. Despite the long-standing precedence for this type of transformation, new strategies for the carboamination of unactivated dienes to

accommodate an expanded scope of 1,3-dienes or to access Z-allylic amine products have not been developed and require further consideration.

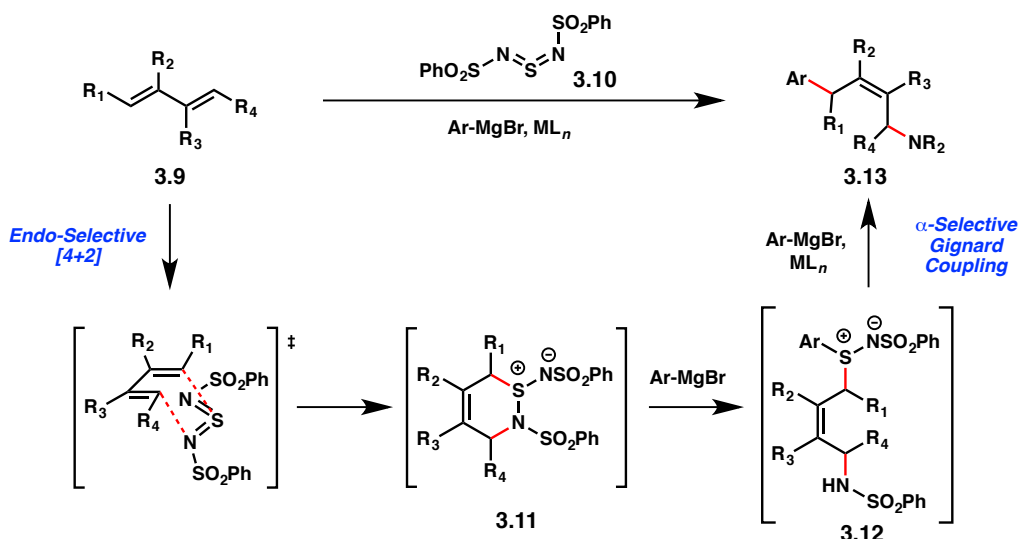
3.2 The Development of a Regio- and Diastereoselective Aminoarylation of Unactivated 1,3-Dienes

3.2.1 An Alternative Strategy for Carboamination

We conceptualized a novel approach to the difunctionalization of 1,3-dienes to install both carbon- and nitrogen-based functionality within a single-flask operation. Following our previous work on the allylic alkylation of unactivated olefins with sulfurdiimide **3.10**,^{31,32} we became interested in understanding the reactivity of this oxidant in the context of other π -systems, such as 1,3-dienes. Based on numerous reports detailing the superior reactivity of sulfurdiimide reagents as dienophiles, we wondered if this reagent could serve not only for the *in situ* generation of an allylic electrophile for a copper-mediated alkylation, but additionally as an aminating reagent.³³⁻³⁷

To this end, we envisioned a strategy that could take advantage of the propensity of sulfurdiimide **3.10** to undergo spontaneous hetero Diels-Alder reactions with diene **3.9** to afford [4+2] adducts **3.11** exhibiting new C-S and C-N bond linkages (Scheme 3.2.1). We hypothesized that the resulting adduct **3.11** could directly convert to ring-opened intermediate **3.12** and subsequently undergo a copper-catalyzed allylic alkylation to afford carboamination product **3.13**. Similar cycloadducts of sulfurdiimide and sulfurimide reagents have been reported to undergo this type of ring-opening in the presence of Grignard reagent.³⁸

Scheme 3.2.1



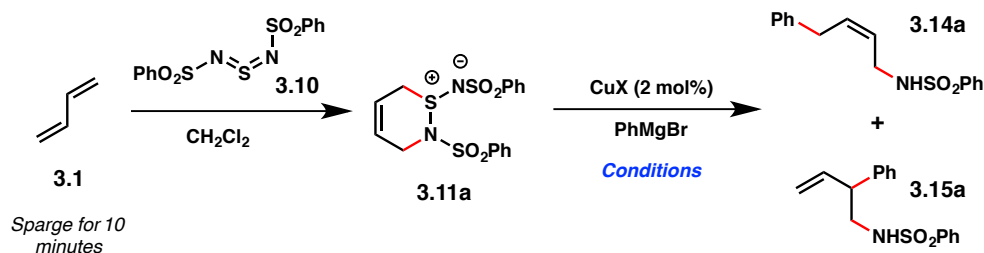
We anticipated that the initial generation of [4+2] adduct **3.11** would benefit from the robust trends in regio- and diastereoselectivity exhibited by Diels-Alder processes. Additionally, with respect to α -alkylation product **3.13**, we wondered if this chemistry would proceed to selectively preserve the *Z*-olefin stereochemistry of intermediate **3.12**, as witnessed previously with some copper-mediated allylic alkylations.³⁹⁻⁴² Taken altogether, this chemistry would serve as a unique strategy toward a highly selective bisfunctionalization of dienes to access allylic amines with exceptional selectivity.

3.2.2 Optimization of the Aminoarylation of 1,3-Butadiene

We began our studies with the difunctionalization of 1,3-butadiene (**3.1**) with phenylmagnesium bromide in the presence of bis(phenylsulfonyl)sulfur diimide (**3.10**). The formation of cycloadduct **3.11a** proved to be a robust reaction, providing the desired product after sparging a solution of sulfur diimide **3.10** with butadiene **3.1** for only ten minutes. The [4+2] adduct **3.11a**, which was stable to purification, was isolated and

subjected to a variety of conditions monitoring for the formation of either the 1,4-aminoarylation product **3.14a** or the 1,2-aminoarylation product **3.15a** (Table 3.2.1).

Table 3.2.1



Entry	CuX	PhMgBr (equiv)	Solvent	Time (h)	NMR Yield ^a (%)	3.14 : 3.15
1	–	3	DME	2	< 5	–
2	CuTc	3	DME	0.5	75	14:1
3	CuTc	3	CH_2Cl_2	2	< 5	–
4	CuTc	3	PhMe	2	< 5	–
5	CuCl	3	DME	0.5	60	15:1
6	CuBF_4	3	DME	0.5	67	9:1
7	$\text{Cu}(\text{OTf})_2$	3	DME	0.5	70	10:1
8	CuI	3	DME	0.5	78	10:1
9	$\text{CuBr}\cdot\text{SMe}_2$	3	DME	0.5	95 (82) ^b	20:1
10	$\text{CuBr}\cdot\text{SMe}_2$	1	DME	0.5	21	20:1
11	$\text{CuBr}\cdot\text{SMe}_2$	2	DME	0.5	45	20:1
12	$\text{CuBr}\cdot\text{SMe}_2$	3	DME	0.5	88 ^{b,c}	9:1

Reaction conditions. Step 1: sulfurdiiimide **3.10** (1 equiv.), solvent (0.2 M), 1,3-butadiene **3.1** (sparge for 10 min and then stir for 10 min at 23 °C). Step 2: CuX (2 mol%), Ph-MgBr (3 equiv), solvent (0.2 M). [a] Two-step ^1H NMR yield, with 1,4-dimethoxybenzene as an internal standard. [b] Isolated yield. [c] Two steps performed in one flask, –78 °C to 23 °C, without isolation of cycloadduct **3.11a**

In the absence of a metal catalyst, neither product was formed when cycloadduct **3.11a** was treated with three equivalents of phenyl Grignard over the course of two hours

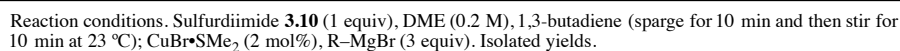
(entry 1). Based on our previous success in the alkylation of analogous acyclic allylic sulfinamides with Grignard reagents, we explored the use of copper catalysts in this reaction. In the presence of 2 mol% CuTc we were gratified to see the formation of product in less than an hour, furnishing primarily the linear aminoarylation product **3.14a** in good yield (entry 2). Solvent proved to have a drastic effect on the productivity of the copper-catalyzed process, revealing the superiority of ethereal solvent DME for this reaction (entries 2-4).

After a brief survey of copper sources, CuBr•SMe₂ was selected as the optimal catalyst for this system, providing an isolated yield of 82% and exhibiting pronounced α -selectivity in the allylic alkylation and complete Z-olefin selectivity (entries 5-9). In accordance with our previous studies on allylic alkylation, a minimum of three equivalents of Grignard reagent were necessary for good conversion in this reaction (entries 10-11). Finally, the conversion of butadiene **3.1** to aminoarylation product **3.14a** was improved to a single-flask operation by modifying the initial reaction temperature (entry 12). This adjustment was necessary to minimize disadvantageous side reactions of the Grignard reagent with any remaining sulfurdiiimide **3.10** or byproducts thereof.

3.2.3 Scope of Grignard Reagents and 1,3-Dienes

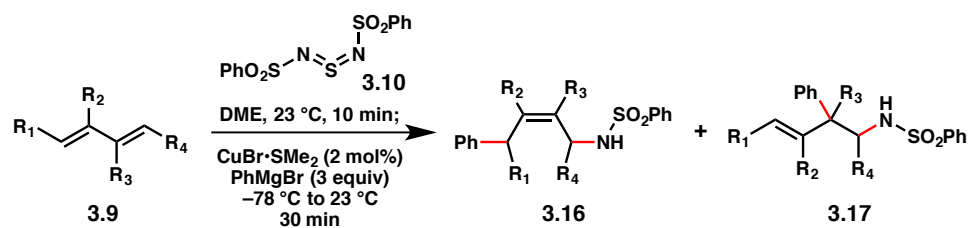
Next we examined the electronic and structural requirements of the Grignard reagent in the Z-olefin selective 1,4-difunctionalization of butadiene **3.1** (Table 3.2.2). A series of *para*-substituted aromatic Grignard reagents were all well tolerated in this reaction regardless of the identity of the substituent (**3.14a-d**). While *meta*- and *ortho*-substitution led to diminished yield, an enhancement in selectivity between regioisomers **3.14** and **3.15** was observed with *ortho*-substituents (**3.14e-g**). Interestingly, *ortho*-methoxy phenylmagnesium bromide afforded aminoarylation product **3.14h** with excellent yield and selectivity. Fused aromatic systems were smoothly incorporated into the product (**3.14i** and **3.14j**) as was a heteroaromatic Grignard, which afforded

thiophenylated product **3.14k**. Most notably, aliphatic Grignards failed to produce the expected aminoalkylation products and instead supplied the thioamination products **3.14l** and **3.14m** instead. Although the exact mechanism by which this occurs is not yet fully understood, we believe the mechanistic dichotomy between aromatic and aliphatic Grignards stems from the generation of electronically distinct sulfur intermediates prior to ring opening.



The scope of the diene component proved to be diverse and accommodated a number of substitution patterns along the diene backbone (Table 3.2.3). 2,3-Disubstitution did not hinder product formation in the presence of phenylmagnesium bromide (entry 1). As anticipated, unsymmetrical diene substrates demonstrated remarkable regioselectivity in the aminoarylation providing exclusively 1,4-aminoarylation products **3.16a-d** each as one of four possible regioisomeric products (entries 2-5). Of note, in the presence of a flanking trisubstituted olefin the hetero Diels-Alder reaction predominated over the potential hetero-ene reaction to cleanly afford **3.16d**. While cyclic olefins provided a mixture of α - and γ -alkylation products, the phenyl ring and sulfonamide were incorporated *anti* to one another in all cases, suggesting that cuprate oxidative addition occurs by an invertive mechanism with a subsequent retentive reductive elimination (entries 6 and 7).

Table 3.2.3



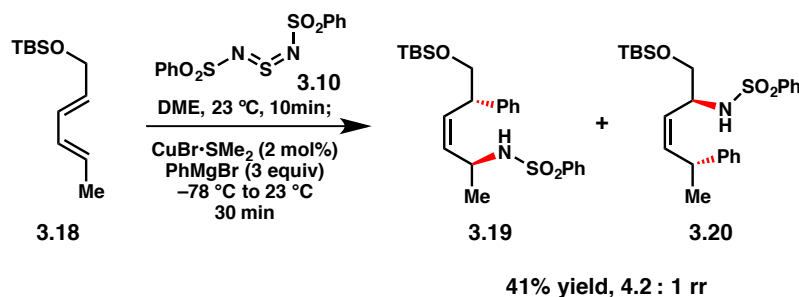
Entry	Diene	Major Product	Yield ^a (%)	3.16 : 3.17	Compound #
1			61	>20 : 1	3.16a
2			77	>20 : 1	3.16b
3			80	>20 : 1	3.16c
4			56	>20 : 1	3.16d
5			79	>20 : 1	3.16e
6			90	4 : 1	3.16f
7			85	5 : 1	3.16g

Reaction conditions. Sulfur diimide **3.10** (1 equiv), DME (0.2 M), diene **3.9** (1.5 equiv.), stir for 10 min at 23 °C; $\text{CuBr}\cdot\text{SMe}_2$ (2 mol%), R-MgBr (3 equiv.). [a] Isolated yield.

We chose to further investigate the regioselective control exhibited by this one-pot aminoarylation reaction by evaluating 1,4-disubstituted diene **3.18** under the optimized reaction parameters (Scheme 3.2.2). Product formation favored predominantly regioisomer **3.19** in a 4.2:1 ratio with **3.20**. This regioselectivity is thought to arise from

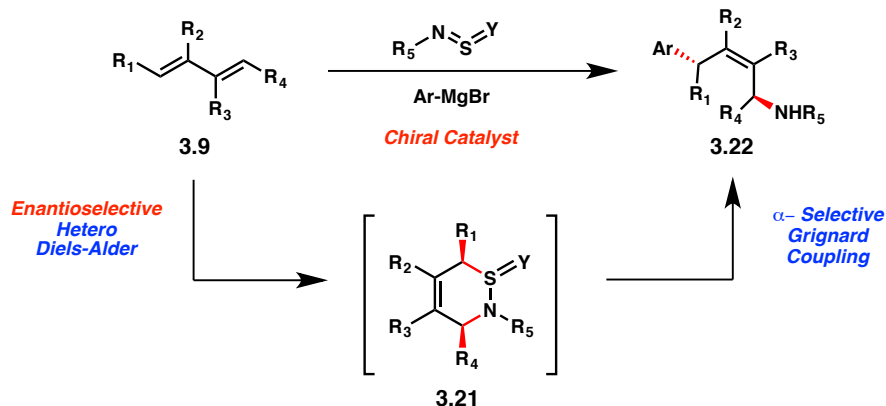
slight inductive differences between the silyl ether and the methyl functionalities. In addition, both **3.19** and **3.20** were accessed as single diastereomers of the *Z*-olefin isomers, further illustrating the remarkable selectivity achieved in these transformations.

Scheme 3.2.2



3.2.4 Initial Studies Toward an Enantioselective Aminoarylation of Dienes

Scheme 3.2.3

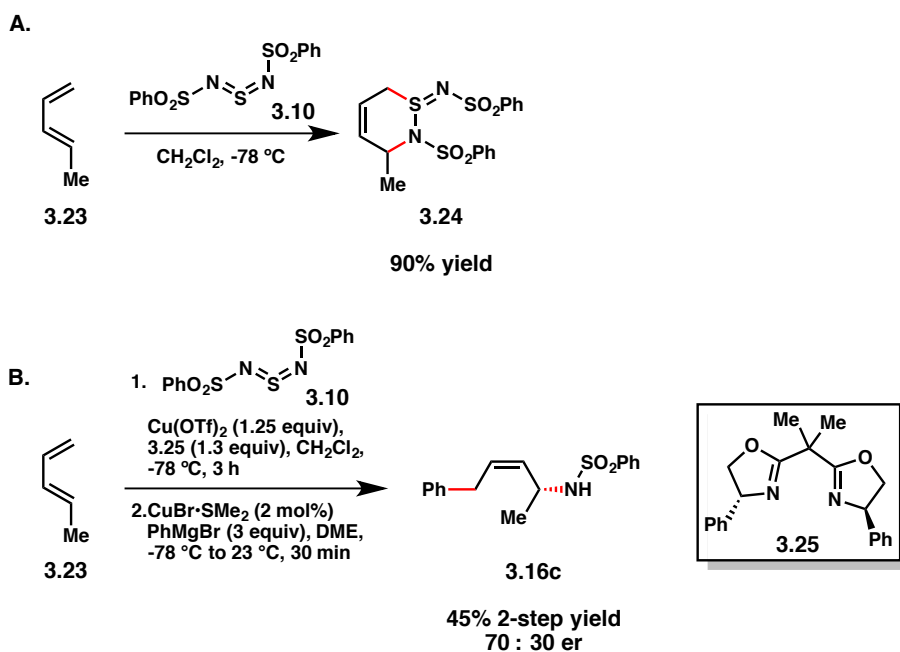


Subsequent to the optimization and evaluation of a highly regio- and diastereoselective aminoarylation of 1,3-dienes, we considered whether this process could be rendered enantioselective as well (Scheme 3.2.3). Based on promising precedence in analogous systems, we postulated that through an asymmetric hetero Diels-Alder reaction with diene **3.9** the resulting cycloadduct **3.21** could be generated with

enantioselectivity in addition to the inherent regio- and diastereoselectivity.⁴³⁻⁴⁶ We anticipated that the subsequent aminoarylation reaction would afford allylic amine **3.22** with high enantiospecificity due to the high α -selectivity and diastereospecificity exhibited in the copper-catalyzed alkylation.

We chose to begin optimization with 1,3-pentadiene **3.23** in the presence of sulfurdiimide **3.10** (Scheme 3.2.4). While this reagent gave a strong background reaction even at $-78\text{ }^{\circ}\text{C}$ (Scheme 3.2.4a), we found that some enantioenrichment could be achieved in the formation of allylic amine **3.16c** when stoichiometric amounts of copper-bis(oxazoline) complexes were employed (Scheme 3.2.4b). In order for the copper-bis(oxazoline) complex to affect better enantio-control in the cycloaddition, a less reactive oxidant will need to be identified.⁴³⁻⁴⁶

Scheme 3.2.4



These initial findings indicate that the asymmetric aminoarylation of 1,3-dienes is a feasible strategy to afford enantioenriched Z-allylic amines from simple diene precursors.

Continued efforts to optimize this chemistry into a single-flask operation for the catalytic asymmetric aminoarylation of dienes are currently underway. We hope that this strategy will enable efficient access to a variety of allylic amine products with exceptionally high enantio-, regio- and diastereoselectivity.

3.2.5 Conclusions

We have developed a novel strategy for the 1,4-aminoarylation of unfunctionalized 1,3-dienes. This reaction proceeds through an initial [4+2]-cycloaddition of the diene component with bis(phenylsulfonyl)sulfur diimide to produce cycloadducts that are uniquely suited for a copper-catalyzed allylic substitution with aromatic Grignards. This one-flask operation rapidly generates the 1,4-aminoarylation products in good yield with complete *Z*-olefin selectivity as well as high regio- and diastereoselectivity. This methodology accommodates a wide variety of functionalized Grignard reagents, and the dienes utilized in this reaction undergo oxidation and Grignard coupling smoothly, irrespective of substitution along the diene backbone.

We are now exploring an asymmetric variant of this reaction via chiral Lewis acid catalysis. Preliminary data suggests that copper-bis(oxazoline) complexes are capable of facilitating an enantioselective [4+2]-coupling to access cycloadducts capable of undergoing the α -selective Grignard coupling with high stereospecificity. Current efforts to optimize the enantioselectivity of this reaction are focused on screening oxidants to identify a dienophile suitable for this chemistry.

3.3 Experimental Section

3.3.1 Materials and Methods

All reactions were carried out under an atmosphere of nitrogen in flame-dried glassware

with magnetic stirring unless otherwise indicated. Commercially obtained reagents were used as received. Solvents were dried by passage through an activated alumina column under argon. Liquids and solutions were transferred via syringe. All reactions were monitored by thin-layer chromatography with E. Merck silica gel 60 F254 pre-coated plates (0.25 mm). All flash chromatography purifications were performed on a Teledyne Isco CombiFlash® Rf unless otherwise indicated. ^1H and ^{13}C NMR spectra were recorded on Varian Inova-400 or 500 spectrometers. Data for ^1H NMR spectra are reported relative to chloroform as an internal standard (7.26 ppm) and are reported as follows: chemical shift (d ppm), multiplicity, coupling constant (Hz), and integration. Data for ^{13}C NMR spectra are reported relative to chloroform as an internal standard (77.23 ppm) and are reported in terms of chemical shift (d ppm). Infrared spectra were recorded on a Perkin-Elmer 1000 series FTIR. HRMS data were obtained at The Scripps Center for Mass Spectrometry.

3.3.2 Preparative Procedures

Grignard Reagents and 1,3-Dienes

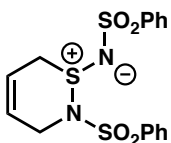
All Grignard Reagents and 1,3-dienes in Tables 2 and 3 were purchased from Sigma-Aldrich. Diene **3.18** was synthesized according to a previously reported literature procedure.⁴⁷ Spectroscopic data for diene **3.18** was identical to the reported data in the literature.

Synthesis of Benzenesulfonyl Sulfurdiimide

Benzenesulfonyl sulfurdiimide **3.10** was synthesized as per the procedure in chapter 2.

General Procedures for the Aminoarylation of Dienes

Table 3.2.1 – Two-pot procedure for the aminoarylation of 1,3-butadiene:



3.11a: A solution of benzenesulfonyl sulfurdiimide **3.10** (360 mg, 1.0 mmol, 1.0 equiv) in CH_2Cl_2 (5 mL, 0.2 M) was sparged with 1,3-butadiene for 10 min at 23 °C. The resulting solution was stirred at 23 °C in the absence of sparging for an additional 10 min. The mixture was concentrated under reduced pressure and purified by flash chromatography to yield [4+2] cycloadduct **3.11a** (gradient eluent hexanes:ethyl acetate) as a white solid:

^1H NMR (400 MHz, CDCl_3), δ 7.96 (d, J = 8.0 Hz, 2H), 7.77 (d, J = 8.0 Hz, 2H), 7.68 (t, J = 8.0 Hz, 1H), 7.58 (t, J = 7.6 Hz, 2H), 7.48 (t, J = 7.8 Hz, 1H), 7.40 (d, J = 7.6 Hz, 2H), 5.95-5.89 (m, 1H), 5.81-5.76 (m, 1H), 4.14-4.08 (m, 1H), 4.00-3.94 (m, 1H), 3.76-3.69 (m, 1H), 3.35-3.28 (m, 1H). ^{13}C NMR (100 MHz, CDCl_3) δ 143.46, 136.86, 134.65, 131.94, 129.79, 128.88, 128.28, 126.32, 124.25, 115.31, 47.72, 39.08. LRMS (ESI) calcd for $[\text{C}_{16}\text{H}_{17}\text{N}_2\text{O}_4\text{S}_3]^+([\text{M}+\text{H}]^+)$: 396.03, found 397.0.

The [4+2] cycloadduct **3.11a** was dissolved in solvent (5 mL, 0.2 M) and treated with copper catalyst (2 mol%, 0.02 mmol). The solution was treated with Grignard reagent (3 mmol, 3 equiv) and stirred at 23 °C for 30–120 min. The reaction was quenched by the addition of saturated aqueous NH_4Cl (10 mL) and extracted with ethyl acetate (10 mL). The organic layer was dried over MgSO_4 , concentrated under reduced pressure, and purified by flash chromatography (gradient eluent hexanes:ethyl acetate).

Table 3.2.2 – Procedure for the aminoarylation of 1,3-butadiene:

A solution of benzenesulfonyl sulfurdiimide **3.10** (360 mg, 1.0 mmol, 1.0 equiv) in DME (5 mL, 0.2 M) was sparged with 1,3-butadiene for 10 min at 23 °C. The resulting solution was stirred at 23 °C in the absence of 1,3-butadiene for an additional 10 min. The mixture was treated with $\text{CuBr}\cdot\text{SMe}_2$ (2 mol%, 0.02 mmol) and cooled to –78 °C. The Grignard reagent (3 mmol, 3 equiv) was added at –78 °C, and the solution was stirred at 23 °C for

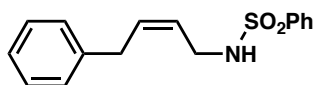
30 min. The reaction was quenched by the addition of saturated aqueous NH_4Cl (10 mL), and the mixture was extracted with ethyl acetate (10 mL). The organic layer was dried over MgSO_4 , concentrated under reduced pressure, and purified by flash chromatography (gradient eluent hexanes:ethyl acetate).

Table 3.2.3 – Procedure for the aminoarylation of substituted 1,3-dienes:

A solution of benzenesulfonyl sulfurdiiimide **3.10** (360 mg, 1.0 mmol, 1.0 equiv) in DME (5 mL, 0.2 M) was treated with the 1,3-diene (1.5 mmol, 1.5 equiv) and stirred at 23 °C for 10 min. The mixture was treated with $\text{CuBr}\cdot\text{SMe}_2$ (2 mol%, 0.02 mmol) and cooled to –78 °C. The Grignard reagent (3 mmol, 3 equiv) was added at –78 °C, and the solution was stirred at 23 °C for 30 min. The reaction was quenched by the addition of saturated aqueous NH_4Cl (10 mL), and the mixture was extracted with ethyl acetate (10 mL). The organic layer was dried over MgSO_4 , concentrated under reduced pressure, and purified by flash chromatography (gradient eluent hexanes:ethyl acetate).

Characterization Data for Products

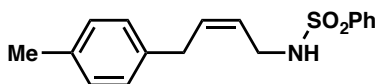
NB: Linear to branched regioselectivity was determined by HNMR. Flash chromatography afforded an inseparable mixture of linear and branched products.



3.14a: Following the general procedure for the aminoarylation of 1,3-butadiene (Table 3.2.2 procedure), purification by flash chromatography afforded the desired 1,4-aminoarylation product along with the 1,2-aminoarylation product as an inseparable mixture (252 mg, 88% yield for two steps, 9:1) as a clear oil:

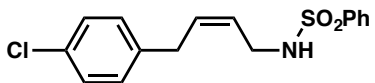
^1H NMR (500 MHz, CDCl_3), δ 7.92 (d, J = 8.0 Hz, 2H), 7.61-7.58 (m, 1H), 7.52 (t, J = 8.0 Hz, 2H), 7.28 (t, J = 7.5 Hz, 2H), 7.20 (t, J = 7.5 Hz, 1H), 7.10 (d, J = 7.5 Hz, 2H), 5.72-5.67 (m, 1H), 5.47-5.42 (m, 1H), 5.05 (t, J = 5.8 Hz, 1H for NH), 3.74 (d, J = 6.8 Hz, J = 5.8 Hz, 2H), 3.32 (d, J = 7.6 Hz, 2H). ^{13}C NMR (100 MHz, CDCl_3) δ 138.95, 139.79, 132.84, 132.70, 129.26, 128.67, 128.35, 127.25, 126.31, 124.97, 40.24, 33.50. IR

(thin film): 3282, 3062, 3026, 1585, 1601, 1480, 1495, 1447, 1325, 1161, 1094, 1071, 753, 689 cm^{-1} . HRMS (ESI) calcd for $[\text{C}_{16}\text{H}_{18}\text{NO}_2\text{S}]^+([\text{M}+\text{H}]^+)$: 288.1053, found 288.1055.



3.14b: Following the general procedure for the aminoarylation of 1,3-butadiene (Table 3.2.2 procedure), purification by flash chromatography afforded the desired 1,4-aminoarylation product along with the 1,2-aminoarylation product as an inseparable mixture (261 mg, 87 % yield for two steps, 7:1) as a clear oil:

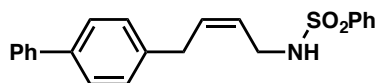
^1H NMR (500 MHz, CDCl_3), δ 7.88 (d, $J = 8.0$ Hz, 2H), 7.61-7.58 (m, 1H), 7.53 (t, $J = 8.0$ Hz, 2H), 7.09 (d, $J = 8.0$ Hz, 2H), 6.97 (d, $J = 8.0$ Hz, 2H), 5.73-5.68 (m, 1H), 5.44-5.40 (m, 1H), 4.42 (br, 1H for NH), 3.73 (t, $J = 6.5$ Hz, 2H), 3.27 (d, $J = 7.5$ Hz, 2H). ^{13}C NMR (100 MHz, CDCl_3) δ 139.82, 136.50, 135.79, 133.17, 132.73, 129.26, 129.13, 128.04, 127.11, 124.48, 40.12, 32.93, 20.97. IR (thin film): 3278, 3021, 1585, 1447, 1326, 1162, 1092, 863, 589, 1509, 1088 cm^{-1} . HRMS (ESI) calcd for $[\text{C}_{17}\text{H}_{20}\text{NO}_2\text{S}]^+([\text{M}+\text{H}]^+)$: 302.1209, found 302.1207.



3.14c: Following the general procedure for the aminoarylation of 1,3-butadiene (Table 3.2.2 procedure), purification by flash chromatography afforded the desired 1,4-aminoarylation product along with the 1,2-aminoarylation product as an inseparable mixture (263 mg, 82 % yield for two steps, 9:1) as a clear oil:

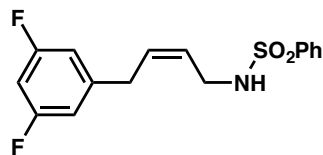
^1H NMR (500 MHz, CDCl_3), δ 7.89 (d, $J = 8.0$ Hz, 2H), 7.61-7.58 (m, 1H), 7.52 (t, $J = 8.0$ Hz, 2H), 7.23 (d, $J = 8.0$ Hz, 2H), 7.01 (d, $J = 8.0$ Hz, 2H), 5.68-5.63 (m, 1H), 5.47-5.42 (m, 1H), 4.61 (br, 1H for NH), 3.72 (t, $J = 6.4$ Hz, 2H), 3.28 (d, $J = 7.5$ Hz, 2H). ^{13}C NMR (100 MHz, CDCl_3) δ 139.78, 138.02, 132.78, 132.18, 132.00, 129.53, 129.15, 128.64, 127.09, 125.22, 40.06, 32.70. IR (thin film): 3279, 3026, 1586, 1476, 1324, 1160,

1092, 587 cm^{-1} . HRMS (ESI) calcd for $[\text{C}_{16}\text{H}_{17}\text{ClNO}_2\text{S}]^+$ ($[\text{M}+\text{H}]^+$): 322.0663, found 322.0661.



3.14d: Following the general procedure for the aminoarylation of 1,3-butadiene (Table 3.2.2 procedure), purification by flash chromatography afforded the desired 1,4-aminoarylation product along with the 1,2-aminoarylation product as an inseparable mixture (323 mg, 89 % yield for two steps, 5:1) as a clear oil:

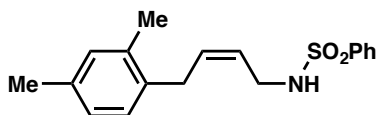
^1H NMR (400 MHz, CDCl_3) δ 7.94 – 7.87 (m, 2H), 7.55 (m, 7H), 7.44 (t, $J = 7.6\text{Hz}$, 2H), 7.34 (t, $J = 7.0\text{Hz}$, 1H), 7.16 (d, $J = 7.9\text{Hz}$, 2H), 5.77–5.71 (m, 1H), 5.52 – 5.41 (m, 1H), 4.61 (br, 1H), 3.76 (t, $J = 6.1\text{Hz}$, 2H), 3.35 (d, $J = 7.6\text{Hz}$, 2H). ^{13}C NMR (100 MHz, CDCl_3) δ 140.81, 139.83, 139.26, 138.68, 132.77, 132.67, 129.16, 128.76, 128.62, 127.32, 127.18, 127.13, 126.99, 124.92, 40.16, 33.02. IR (thin film): 3282, 3027, 1600, 1487, 1447, 1325, 1161, 1094, 759, 584 cm^{-1} . HRMS (ESI) calcd for $[\text{C}_{22}\text{H}_{22}\text{NO}_2\text{S}]^+$ ($[\text{M}+\text{H}]^+$): 364.1366, found 364.1367.



3.14e: Following the general procedure for the aminoarylation of 1,3-butadiene (Table 3.2.2 procedure), purification by flash chromatography afforded the desired 1,4-aminoarylation product along with the 1,2-aminoarylation product as an inseparable mixture (213 mg, 66 % yield for two steps, 5:1) as a clear oil:

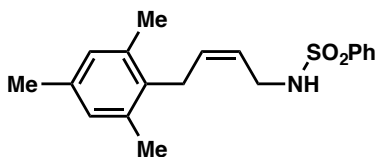
^1H NMR (400 MHz, CDCl_3) δ 7.99 – 7.83 (m, 2H), 7.65 – 7.38 (m, 3H), 6.68 – 6.50 (m, 3H), 5.69 – 5.52 (m, 1H), 5.52 – 5.36 (m, 1H), 5.15 (s, 1H), 3.67 (t, $J = 6.0\text{ Hz}$, 2H), 3.26 (d, $J = 7.4\text{ Hz}$, 2H). ^{13}C NMR (100 MHz, CDCl_3) δ 163.15 (dd, $J_1 = 249.4\text{ Hz}$, $J_3 = 12.9\text{ Hz}$), 143.71 (t, $J_3 = 9.0\text{ Hz}$), 139.91, 132.96, 130.87, 129.32, 127.23, 126.34, 111.20 (dd, $J_2 = 25.0\text{ Hz}$, $J_4 = 6.6\text{ Hz}$), 101.81 (t, $J_2 = 25.4\text{ Hz}$), 40.12, 33.09 (t, $J_4 = 1.9\text{ Hz}$). IR (thin

film): 3281, 3089, 3067, , 2924, 1625, 1594, 1460, 1447, 1322, 1161, 1117, 991, 848, 586 cm^{-1} . HRMS (ESI) calcd for $[\text{C}_{16}\text{H}_{16}\text{F}_2\text{NO}_2\text{S}]^+$ ($[\text{M}+\text{H}]^+$): 324.0864, found 324.0864.



3.14f: Following the general procedure for the aminoarylation of 1,3-butadiene (Table 3.2.2 procedure), purification by flash chromatography afforded the desired 1,4-aminoarylation product along with the 1,2-aminoarylation product as an inseparable mixture (176 mg, 56 % yield for two steps, 10:1) as a clear oil:

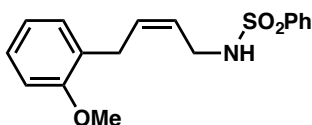
^1H NMR (500 MHz, CDCl_3) δ 7.89 (d, $J = 7.9\text{ Hz}$, 2H), 7.67 – 7.49 (m, 3H), 7.03 – 6.85 (m, 3H), 5.67-5.62(m, 1H), 5.44-5.40 (m, 1H), 4.46 (s, 1H), 3.73 (t, $J = 6.4\text{ Hz}$, 2H), 3.22 (d, $J = 7.4\text{ Hz}$, 2H), 2.29 (s, 3H), 2.18 (s, 3H). ^{13}C NMR (100 MHz, CDCl_3) δ 140.01, 136.19, 136.00, 134.99, 132.94, 132.82, 131.29, 129.34, 128.50, 127.33, 126.99, 124.76, 40.41, 30.99, 21.08, 19.58. IR (thin film): 3283, 3018, 2920, 1615, 1501, 1447, 1325, 1161, 1094, 1057, 792, 755 cm^{-1} . HRMS (ESI) calcd for $[\text{C}_{18}\text{H}_{22}\text{NO}_2\text{S}]^+$ ($[\text{M}+\text{H}]^+$): 316.1366, found 316.1367.



3.14g: Following the general procedure for the aminoarylation of 1,3-butadiene (Table 3.2.2 procedure), purification by flash chromatography afforded the desired 1,4-aminoarylation product along with the 1,2-aminoarylation product as an inseparable mixture (105 mg, 32 % yield for two steps, >20:1) as a clear oil:

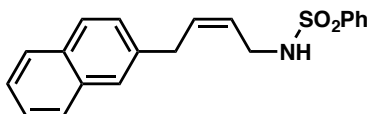
^1H NMR (500 MHz, CDCl_3), d 7.95 (δ , $J = 8.0\text{ Hz}$, 2H), 7.63-7.60 (m, 1H), 7.56 (t, $J = 8.0\text{ Hz}$, 2H), 6.83 (s, 2H), 5.39-5.31 (m, 2H), 4.82 (br, 1H for NH), 3.78 (t, $J = 8.0\text{ Hz}$, 2H), 3.25 (d, $J = 8.0\text{ Hz}$, 2H), 2.25 (s, 3H), 2.18 (s, 6H). ^{13}C NMR (100 MHz, CDCl_3) δ 139.80, 136.06, 135.65, 133.37, 132.76, 132.05, 129.16, 128.99, 128.96, 128.94, 127.16, 123.93, 40.38, 27.66, 20.80, 19.91. IR (thin film): 3284, 3064, 2919, 1613, 1581, 1446,

1326, 1162, 1094, 1060, 851, 586, cm^{-1} . HRMS (ESI) calcd for $[\text{C}_{19}\text{H}_{24}\text{NO}_2\text{S}]^+$ ($[\text{M}+\text{H}]^+$): 330.1522, found 330.1528.



3.14h: Following the general procedure for the aminoarylation of 1,3-butadiene (Table 3.2.2 procedure), purification by flash chromatography afforded the desired 1,4-aminoarylation product along with the 1,2-aminoarylation product as an inseparable mixture (300 mg, 95 % yield for two steps, >20:1) as a clear oil:

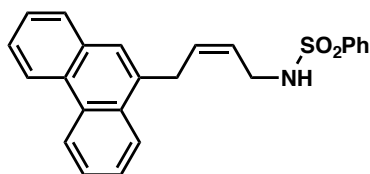
^1H NMR (500 MHz, CDCl_3), d 7.89-7.86 (m, 2H), 7.58-7.54 (m, 1H), 7.51-7.46 (m, 2H), 7.20-7.16 (m, 1H), 7.03-7.01 (m, 1H), 6.88-6.82 (m, 2H), 5.64-5.57 (m, 1H), 5.37-5.33 (m, 1H), 4.89 (br, 1H for NH), 3.80 (s, 3H), 3.71 (t, $J = 6.5\text{Hz}$, 2H), 3.23 (d, $J = 7.5\text{ Hz}$, 2H). ^{13}C NMR (100 MHz, CDCl_3) δ 157.20, 140.04, 133.04, 132.78, 129.79, 129.24, 127.94, 127.78, 127.25, 124.12, 120.87, 110.58, 55.45, 40.08, 28.52. IR (thin film): 3284, 3023, 1656, 1587, 1493, 1325, 1159, 722, cm^{-1} . HRMS (ESI) calcd for $[\text{C}_{17}\text{H}_{20}\text{NO}_3\text{S}]^+$ ($[\text{M}+\text{H}]^+$): 318.1158, found 318.1157.



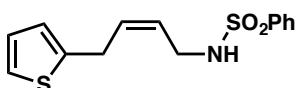
3.14i: Following the general procedure for the aminoarylation of 1,3-butadiene (Table 3.2.2 procedure), purification by flash chromatography afforded the desired 1,4-aminoarylation product along with the 1,2-aminoarylation product as an inseparable mixture (286 mg, 85 % yield for two steps, 7:1) as a clear oil:

^1H NMR (400 MHz, CDCl_3) δ 7.92 – 7.86 (m, 2H), 7.83 – 7.78 (m, 1H), 7.76 (d, $J = 8.0\text{ Hz}$, 2H), 7.59 – 7.41 (m, 6H), 7.24 – 7.19 (m, 1H), 5.80-5.76 (m, 1H), 5.54 – 5.42 (m, 1H), 4.78 (s, 1H), 3.78 (t, $J = 6.5\text{ Hz}$, 2H), 3.47 (d, $J = 7.6\text{ Hz}$, 2H). ^{13}C NMR (100 MHz, CDCl_3) δ 139.98, 137.28, 133.72, 132.90, 132.68, 132.24, 129.31, 128.38, 127.79,

127.62, 127.28, 127.08, 126.45, 126.29, 125.62, 125.28, 40.36, 33.70. IR (thin film): 3282, 3056, 1631, 1599, 1508, 1447, 1324, 1161, 1093, 817 cm^{-1} . HRMS (ESI) calcd for $[\text{C}_{20}\text{H}_{20}\text{NO}_2\text{S}]^+$ ($[\text{M}+\text{H}]^+$): 338.1209, found 338.1209.



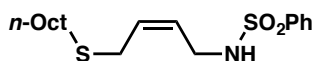
3.14j: Following the general procedure for the aminoarylation of 1,3-butadiene (Table 3.2.2 procedure), purification by flash chromatography afforded the desired 1,4-aminoarylation product along with the 1,2-aminoarylation product as an inseparable mixture (313 mg, 81 % yield for two steps, >20:1) as a clear oil: ^1H NMR (500 MHz, CDCl_3) δ 8.74 (d, $J = 8.2$ Hz, 1H), 8.66 (d, $J = 8.1$ Hz, 1H), 7.94 (d, $J = 8.1$ Hz, 1H), 7.87 (d, $J = 7.7$ Hz, 2H), 7.81 (d, $J = 8.0$ Hz, 1H), 7.72 – 7.57 (m, 5H), 7.53 (t, $J = 7.1$ Hz, 1H), 7.45 (t, $J = 7.7$ Hz, 2H), 5.91–5.86 (m, 1H), 5.59–5.54 (m, 1H), 4.65 (s, 1H), 3.82 (t, $J = 5.6$ Hz, 3H), 3.77 (d, $J = 7.2$, 2H). ^{13}C NMR (100 MHz, CDCl_3) δ 139.86, 134.03, 132.79, 132.00, 131.80, 131.07, 130.76, 129.82, 129.21, 128.31, 127.18, 126.85, 126.79, 126.52, 126.40, 126.13, 125.83, 124.30, 123.33, 122.55, 40.39, 31.11. IR (thin film): 3280, 3063, 2922, 1602, 1495, 1447, 1325, 1161, 1093, 1069, 887, 750 cm^{-1} . HRMS (ESI) calcd for $[\text{C}_{24}\text{H}_{22}\text{NO}_2\text{S}]^+$ ($[\text{M}+\text{H}]^+$): 388.1366, found 388.1368.



3.14k: Following the general procedure for the aminoarylation of 1,3-butadiene (Table 3.2.2 procedure), purification by flash chromatography afforded the desired 1,4-aminoarylation product along with the 1,2-aminoarylation product as an inseparable mixture (219 mg, 75 % yield for two steps, 12:1) as a clear oil:

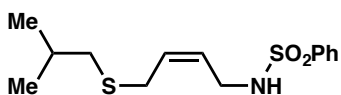
^1H NMR (500 MHz, CDCl_3) δ 7.87–7.85 (m, 2H), 7.87–7.85 (m, 2H), 7.58–7.54 (m, 1H), 7.51–7.47 (m, 2H), 7.10–7.08 (m, 1H), 6.70–6.69 (m, 1H), 5.72–5.67 (m, 1H), 5.44–5.39 (m, 1H), 4.78 (br, 1H for NH), 3.68 (t, $J = 6.5$ Hz, 2H), 3.46 (d, $J = 7.5$ Hz, 2H). ^{13}C

NMR (100 MHz, CDCl_3) δ 142.47, 139.94, 132.92, 131.86, 129.32, 127.27, 127.12, 125.60, 124.65, 123.86, 40.17, 27.76. IR (thin film): 3281, 3026, 1585, 1447, 1324, 1160, 1093, 849 cm^{-1} . HRMS (ESI) calcd for $[\text{C}_{14}\text{H}_{16}\text{NO}_2\text{S}_2]^+$ ($[\text{M}+\text{H}]^+$): 294.0617, found 294.0617.



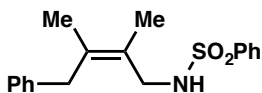
3.14l: Following the general procedure for the aminoarylation of 1,3-butadiene (Table 3.2.2 procedure), purification by flash chromatography afforded the observed product (195 mg, 55 % yield for two steps) as a clear oil:

^1H NMR (400 MHz, CDCl_3) δ 7.94 – 7.80 (m, 2H), 7.66 – 7.55 (m, 1H), 7.51 (dd, J = 8.2, 6.8 Hz, 2H), 5.58 (m, 1H), 5.42 (m, 1H), 4.89 (s, 1H), 3.62 (t, J = 6.6 Hz, 2H), 3.02 (d, J = 7.9 Hz, 2H), 2.50 – 2.22 (m, 2H), 1.53 – 1.44 (m, 2H), 1.37 – 1.20 (m, 10H), 0.87 (t, J = 6.9, 3H). ^{13}C NMR (100 MHz, CDCl_3) δ 139.96, 132.92, 130.48, 129.31, 127.27, 126.57, 39.97, 31.96, 31.75, 29.55, 29.35, 29.05, 28.20, 25.90, 22.81, 14.27. IR (thin film): 3281, 3066, 3027, 2925, 1586, 1447, 1327, 1161, 1094, 754, 689 cm^{-1} . HRMS (ESI) calcd for $[\text{C}_{18}\text{H}_{30}\text{NO}_2\text{S}_2]^+$ ($[\text{M}+\text{H}]^+$): 356.1712, found 356.1714.



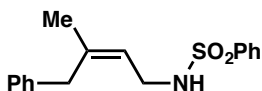
3.14m: Following the general procedure for the aminoarylation of 1,3-butadiene (Table 3.2.2 procedure), purification by flash chromatography afforded the observed product (134 mg, 45 % yield for two steps) as a clear oil:

^1H NMR (500 MHz, CDCl_3) δ 7.93 – 7.84 (m, 2H), 7.61 (dd, J = 8.4, 6.5 Hz, 1H), 7.54 (t, J = 7.6 Hz, 2H), 5.67 – 5.58 (m, 1H), 5.45 (m, 1H), 4.63 (s, 1H), 3.64 (t, J = 6.3 Hz, 2H), 3.03 (d, J = 8.0 Hz, 2H), 2.31 (d, J = 6.9 Hz, 2H), 1.73 (dp, J = 13.4, 6.7 Hz, 1H), 0.96 (d, J = 6.7 Hz, 6H). ^{13}C NMR (100 MHz, CDCl_3) δ 140.01, 133.01, 130.76, 129.38, 127.33, 126.59, 41.00, 40.05, 28.72, 28.63, 22.25. IR (thin film): 3280, 3065, 3027, 2957, 1586, 1447, 1425, 1326, 1161, 1094, 900, 755, 720, 588 cm^{-1} . HRMS (ESI) calcd for $[\text{C}_{14}\text{H}_{22}\text{NO}_2\text{S}_2]^+$ ($[\text{M}+\text{H}]^+$): 300.1086, found 300.1089.



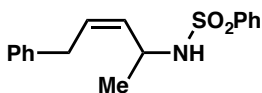
3.16a: Following the general procedure for the aminoarylation of substituted 1,3-dienes (Table 3.2.3 procedure), purification by flash chromatography afforded the desired 1,4-aminoarylation product along with the 1,2-aminoarylation product as an inseparable mixture (192 mg, 61 % yield for two steps, >20:1) as a clear oil:

^1H NMR (400 MHz, CDCl_3) δ 7.84 (d, $J = 7.8$, 2H), 7.54 (t, $J = 7.4$, 1H), 7.47 (t, $J = 7.7$, 2H), 7.30 – 7.08 (m, 3H), 6.99 (d, $J = 7.4$, 2H), 4.82–4.78(m, 1H), 3.65 (d, $J = 5.9$, 2H), 3.28 (s, 2H), 1.64 (s, 3H), 1.55 (s, 3H). ^{13}C NMR (100 MHz, CDCl_3) δ 139.96, 133.30, 132.69, 129.13, 128.58, 128.35, 127.18, 126.17, 125.03, 46.11, 39.73, 19.28, 17.20. IR (thin film): 3282, 3061, 3026, 2861, 1601, 1493, 1447, 1323, 1161, 1093, 1048, 830, 754, 727, 588 cm^{-1} . HRMS (ESI) calcd for $[\text{C}_{18}\text{H}_{22}\text{NO}_2\text{S}]^+$, ($[\text{M}+\text{H}]^+$): 316.1366, found 316.1363.



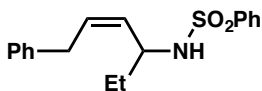
3.16b: Following the general procedure for the aminoarylation of substituted 1,3-dienes (Table 3.2.3 procedure), purification by flash chromatography afforded the desired 1,4-aminoarylation product along with the 1,2-aminoarylation product as an inseparable mixture (231 mg, 77 % yield for two steps, >20:1) as a clear oil:

^1H NMR (400 MHz, CDCl_3) δ 7.89–7.85 (m, 2H), 7.59–7.55 (m, 1H), 7.54 – 7.46 (m, 2H), 7.29 – 7.22 (m, 2H), 7.22 – 7.14 (m, 1H), 7.08 – 6.98 (m, 2H), 5.24 (t, $J = 7.2$ Hz, 1H), 4.52 (s, 1H), 3.70 (t, $J = 6.2$ Hz, 2H), 3.27 (d, $J = 8.1$ Hz, 2H), 1.60 (s, 3H). ^{13}C NMR (100 MHz, CDCl_3) δ 140.05, 139.03, 132.83, 129.27, 128.69, 128.53, 127.29, 126.41, 120.82, 77.55, 77.23, 76.91, 41.26, 37.95, 23.68. IR (thin film): 3282, 3061, 3026, 2970, 2916, 1668, 1600, 1494, 1447, 1326, 1161, 1094, 1045, 840, 755, 585 cm^{-1} . HRMS (ESI) calcd for $[\text{C}_{17}\text{H}_{20}\text{NO}_2\text{S}]^+$ ($[\text{M}+\text{H}]^+$): 302.1209, found 302.1208.



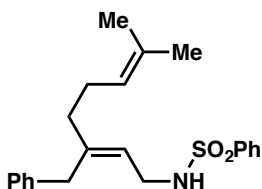
3.16c: Following the general procedure for the aminoarylation of substituted 1,3-dienes (Table 3.2.3 procedure), purification by flash chromatography afforded the desired 1,4-aminoarylation product along with the 1,2-aminoarylation product as an inseparable mixture (242 mg, 80 % yield for two steps, >20:1) as a clear oil:

^1H NMR (500 MHz, CDCl_3) δ 7.93 – 7.88 (m, 2H), 7.55 (t, J = 7.4 Hz, 1H), 7.47 (t, J = 7.7 Hz, 2H), 7.28 (t, J = 7.4 Hz, 2H), 7.21 (t, J = 7.4 Hz, 1H), 7.07 (d, J = 7.5 Hz, 2H), 5.47-5.42 (m, 1H), 5.28-5.23 (m, 1H), 5.15 (br, 1H), 4.36-4.32 (m, 1H), 3.25-3.21 (m, 2H), 1.24 (d, J = 6.7 Hz, 3H). ^{13}C NMR (100 MHz, CDCl_3) δ 141.06, 139.98, 132.66, 131.49, 129.73, 129.09, 128.65, 128.41, 127.30, 126.27, 47.28, 33.59, 22.80. IR (thin film): 3274, 3062, 3026, 2976, 1658, 1601, 1495, 1447, 1326, 1162, 1092, 1070, 879, 744, 721, 593 cm^{-1} . HRMS (ESI) calcd for $[\text{C}_{17}\text{H}_{19}\text{NO}_2\text{SNa}]^+$ ($[\text{M}+\text{Na}]^+$): 324.1029, found 324.1024.



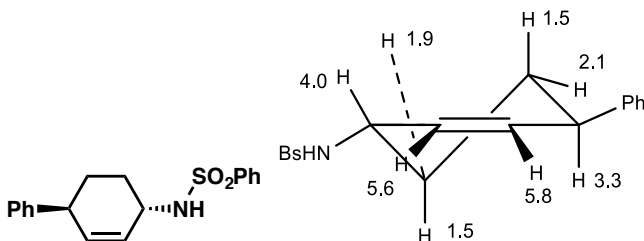
3.16d: Following the general procedure for the aminoarylation of substituted 1,3-dienes (Table 3.2.3 procedure), purification by flash chromatography afforded the desired 1,4-aminoarylation product along with the 1,2-aminoarylation product as an inseparable mixture (176 mg, 56 % yield for two steps, >20:1) as a clear oil:

^1H NMR (400 MHz, CDCl_3) δ 7.94 – 7.73 (m, 2H), 7.51 (t, J = 7.4 Hz, 1H), 7.41 (t, J = 7.6 Hz, 2H), 7.25 (t, J = 7.3 Hz, 2H), 7.17 (t, J = 7.3 Hz, 1H), 7.04 (d, J = 7.3, 2H), 5.52 – 5.41 (m, 1H), 5.25 – 5.05 (m, 2H), 4.15 – 4.02 (m, 1H), 3.20-3.16 (m, 2H), 1.74 – 1.55 (m, 1H), 1.55 – 1.40 (m, 1H), 0.85 (t, J = 7.4, 3H). ^{13}C NMR (100 MHz, CDCl_3) δ 141.23, 140.07, 132.55, 130.73, 130.02, 129.00, 128.59, 128.43, 127.25, 126.21, 52.75, 33.77, 29.52, 10.08. IR (thin film): 3276, 3062, 1601, 1447, 1326, 1161, 1093, 729, 563, 1509 cm^{-1} . HRMS (ESI) calcd for $[\text{C}_{18}\text{H}_{22}\text{NO}_2\text{S}]^+$ ($[\text{M}+\text{H}]^+$): 316.1366, found 316.1368.



3.16e: Following the general procedure for the aminoarylation of substituted 1,3-dienes (Table 3.2.3 procedure), purification by flash chromatography afforded the desired 1,4-aminoarylation product along with the 1,2-aminoarylation product as an inseparable mixture (292 mg, 79 % yield for two steps, >20:1) as a clear oil:

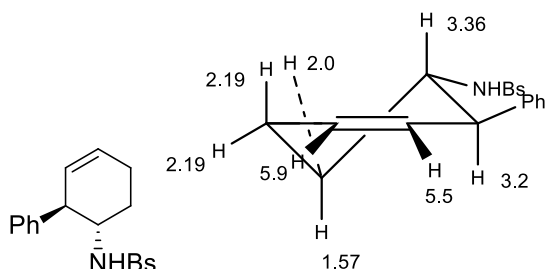
^1H NMR (500 MHz, CDCl_3) δ 7.86 (d, $J = 8.0$ Hz, 2H), 7.59 (t, $J = 7.4$ Hz, 1H), 7.52 (t, $J = 7.7$ Hz, 2H), 7.30 – 7.23 (m, 3H), 7.19 (t, $J = 7.2$ Hz, 1H), 7.03 (d, $J = 7.5$ Hz, 2H), 5.27 (t, $J = 7.2$ Hz, 1H), 4.98 (t, $J = 6.3$, 1H), 4.30 (t, $J = 5.5$ Hz, 1H), 3.71 (t, $J = 6.5$ Hz, 2H), 3.30 (s, 2H), 2.03 – 1.87 (m, 4H), 1.67 (d, $J = 15.5$, 3H), 1.55 (d, $J = 10.7$, 3H). ^{13}C NMR (100 MHz, CDCl_3) δ 143.80, 140.14, 139.26, 132.88, 132.19, 129.36, 129.31, 128.99, 128.74, 128.52, 127.31, 126.44, 123.74, 120.51, 41.35, 36.84, 36.46, 26.45, 25.86, 17.89. IR (thin film): 3281, 3061, 3026, 2923, 1665, 1601, 1494, 1447, 1326, 1161, 1094, 1046, 754, 730 cm^{-1} . HRMS (ESI) calcd for $[\text{C}_{22}\text{H}_{28}\text{NO}_2\text{S}]^+$ ($[\text{M}+\text{H}]^+$): 370.1835, found 370.1833.



3.16f: Following the general procedure for the aminoarylation of substituted 1,3-dienes (Table 3.2.3 procedure), purification by flash chromatography afforded the desired 1,4-aminoarylation product along with the 1,2-aminoarylation product as an inseparable mixture (226 mg, 72 % yield for two steps) as a clear oil:

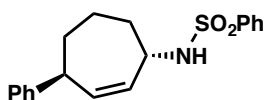
^1H NMR (500 MHz, CDCl_3) δ 8.09 – 7.96 (m, 2H), 7.70 – 7.49 (m, 3H), 7.41 – 7.26 (m, 2H), 7.21 (t, $J = 7.3$, 1H), 7.17 – 6.96 (m, 2H), 5.80–5.76 (m, 1H), 5.61–5.58 (m, 1H),

5.14 (d, $J = 8.7$, 1H), 4.07 – 3.94 (m, 1H), 3.41 – 3.22 (m, 1H), 2.13 – 1.92 (m, 2H), 1.65 – 1.41 (m, 2H). ^{13}C NMR (125 MHz, CDCl_3) δ 144.93, 134.16, 132.77, 129.32, 128.75, 128.62, 127.63, 127.11, 126.55, 49.97, 41.48, 30.86, 30.07. IR (thin film): 3276, 3061, 3026, 1601, 1491, 1447, 1326, 1160, 1088, 897, 757 cm^{-1} . HRMS (ESI) calcd for $[\text{C}_{18}\text{H}_{19}\text{NO}_2\text{SNa}]^+$ ($[\text{M}+\text{Na}]^+$): 336.1029, found 336.1026.



Purification by flash chromatography also afforded the 1,2-aminoarylation product (56 mg, 18 % yield for two steps) as a clear oil:

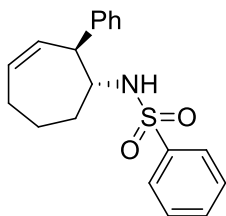
^1H NMR (500 MHz, CDCl_3) δ 7.62 (t, $J = 11.0$ Hz, 2H), 7.50 (t, $J = 7.5$, 1H), 7.37 (t, $J = 7.8$ Hz, 2H), 7.21 – 7.14 (m, 3H), 6.97 (dd, $J = 6.1$, 3.3 Hz, 2H), 5.95 – 5.83 (m, 1H), 5.56-5.50 (m, 1H), 4.86 (d, $J = 7.2$, 1H), 3.34 (td, $J = 9.6$, 2.9 Hz, 1H), 3.22 (d, $J = 2.9$, 1H), 2.19 (s, 2H), 2.10 – 1.98 (m, 1H), 1.60 (dt, $J = 21.5$, 6.6, 1H). ^{13}C NMR (100 MHz, CDCl_3) δ 141.84, 140.36, 132.42, 129.12, 128.73, 128.49, 128.43, 127.42, 127.11, 127.04, 55.91, 48.28, 26.86, 23.08. IR (thin film): 3281, 3061, 3026, 1650, 1601, 1479, 1447, 1325, 1161, 1071, 906, 720, 688, 578 cm^{-1} . HRMS (ESI) calcd for $[\text{C}_{18}\text{H}_{20}\text{NO}_2\text{S}]^+$ ($[\text{M}+\text{H}]^+$): 314.1209, found 314.1207.



3.16g: Following the general procedure for the aminoarylation of substituted 1,3-dienes (Table 3.2.3 procedure), purification by flash chromatography afforded the desired 1,4-aminoarylation product (229 mg, 70% yield for two steps) as a clear oil:

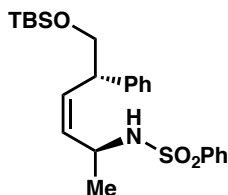
^1H NMR (500 MHz, CDCl_3) δ 8.02 – 7.87 (m, 2H), 7.60-7.55 (m, 3H), 7.29 (t, $J = 7.5$ Hz, 2H), 7.20 (t, $J = 7.3$ Hz, 1H), 7.12 (d, $J = 7.3$ Hz, 2H), 5.76 – 5.62 (m, 1H), 5.41-5.48

(m, 1H), 5.12 (d, $J = 8.1$, 1H), 4.13-4.10 (m, 1H), 3.52 (s, 1H), 1.87-1.60 (m, 6H). ^{13}C NMR (100 MHz, CDCl_3) δ 145.92, 141.12, 137.11, 132.79, 132.08, 129.30, 128.71, 127.39, 127.21, 126.35, 53.14, 45.83, 35.35, 34.22, 23.19. IR (thin film): 3279, 3061, 3025, 2929, 1650, 1600, 1447, 1327, 1160, 1093, 911, 755, 594 cm^{-1} . HRMS (ESI) calcd for $[\text{C}_{19}\text{H}_{22}\text{NO}_2\text{S}]^+$ ($[\text{M}+\text{H}]^+$): 328.1366, found 328.1366.



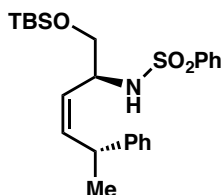
Purification by flash chromatography also afforded the 1,2-aminoarylation product (49 mg, 15 % yield for two steps) as a clear oil:

^1H NMR (500 MHz, CDCl_3) δ 7.77 – 7.68 (m, 2H), 7.56 (t, $J = 7.4\text{Hz}$, 1H), 7.46 (t, $J = 7.7\text{ Hz}$, 2H), 7.23 – 7.14 (m, 3H), 7.03 – 6.91 (m, 2H), 6.01 (dt, $J = 11.7$, 6.0Hz, 1H), 5.54 (dd, $J = 11.6$, 6.0Hz, 1H), 4.69 (d, $J = 7.5\text{Hz}$, 1H), 3.66 – 3.54 (m, 1H), 3.50 (t, $J = 6.6\text{Hz}$, 1H), 2.27-2.13 (m, 2H), 2.03 – 1.89 (m, 1H), 1.79 – 1.59 (m, 2H), 1.55-1.47 (m, 1H). ^{13}C NMR (100 MHz, CDCl_3) δ 140.73, 140.64, 134.59, 132.55, 130.31, 129.17, 128.93, 128.24, 127.15, 126.95, 56.90, 51.61, 34.40, 28.88, 22.30. IR (thin film): 3286, 3061, 3025, 1650, 1600, 1493, 1447, 1326, 1161, 1094, 754, 689 cm^{-1} . HRMS (ESI) calcd for $[\text{C}_{19}\text{H}_{22}\text{NO}_2\text{S}]^+$ ($[\text{M}+\text{H}]^+$): 328.1366, found 328.1364.



3.19: Following the general procedure for the aminoarylation of substituted 1,3-dienes (Table 3.2.3 procedure), purification by flash chromatography afforded the desired 1,4-aminoarylation product (148 mg, 33 % yield for two steps) as a clear oil:

^1H NMR (500 MHz, CDCl_3) δ 7.98 (d, $J = 7.3$ Hz, 2H), 7.63 (t, $J = 7.4$ Hz, 1H), 7.57 (t, $J = 7.6$ Hz, 3H), 7.28-7.22 (m, 3H), 7.18 (t, $J = 7.3$ Hz, 1H), 6.97 (d, $J = 7.1$ Hz, 2H), 5.68-5.62 (m, 1H), 5.46 – 5.31 (m, 2H), 4.04-3.97 (m, 1H), 3.65-3.58 (m, 2H), 3.31-3.25 (m, 1H), 1.12 (d, $J = 6.5$ Hz, 3H), 0.90 (s, 9H), 0.04 (d, $J = 8.0$ Hz, 6H). ^{13}C NMR (100 MHz, CDCl_3) δ 141.43, 140.71, 132.74, 132.67, 129.08, 128.48, 127.87, 127.54, 126.72, 67.62, 47.26, 46.26, 26.15, 21.97, 18.64, -5.26, -5.34. IR (thin film): 3270, 2928, 1447, 1327, 1163, 1094, 836 cm^{-1} . HRMS (ESI) calcd for $[\text{C}_{24}\text{H}_{36}\text{NO}_3\text{SSi}]^+$ ($[\text{M}+\text{H}]^+$): 446.2180, found 446.2184.

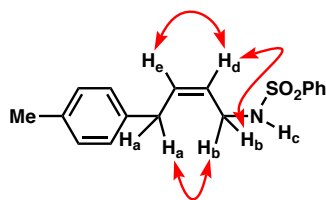


3.20: Purification by flash chromatography afforded the regioisomeric 1,4-aminoarylation product (36 mg, 8 % yield for two steps) as a clear oil:

^1H NMR (400 MHz, CDCl_3) δ 7.90 (d, $J = 8.2$ Hz, 2H), 7.59 (d, $J = 7.0$ Hz, 1H), 7.53 – 7.45 (m, 2H), 7.29 – 7.21 (m, 3H), 7.16 (d, $J = 6.5$ Hz, 1H), 7.10 (d, $J = 7.8$ Hz, 2H), 5.60 (t, $J = 10.3$ Hz, 1H), 5.21 (t, $J = 10.0$ Hz, 1H), 5.07 (d, $J = 4.4$ Hz, 1H), 4.10 (s, 1H), 3.55 (s, 1H), 3.36 – 3.28 (m, 1H), 3.28 – 3.17 (m, 1H), 1.26 (s, 3H), 0.83 – 0.77 (m, 9H), -0.11 (d, $J = 6.1$ Hz, 6H). ^{13}C NMR (100 MHz, CDCl_3) δ 146.28, 140.78, 138.25, 132.82, 129.15, 128.78, 127.50, 126.91, 126.36, 125.87, 77.55, 77.23, 76.91, 64.86, 53.15, 38.14, 29.91, 25.99, 22.87, 18.39, -5.33, -5.43. IR (thin film): 3274, 3026, 1147, 1160, 1094 cm^{-1} . HRMS (ESI) calcd for $[\text{C}_{24}\text{H}_{36}\text{NO}_3\text{SSi}]^+$ ($[\text{M}+\text{H}]^+$): 446.2180, found 446.2180.

Determination of Z-Olefin Geometry of Products

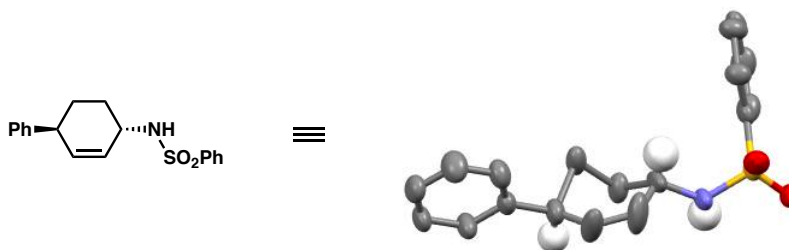
NOE studies of the product **3.14b** allowed the assignment of the Z-olefin geometry for the aminoarylation product. The Z-olefin geometry for all other products was assumed by analogy.



Determination of Relative Stereochemistry of Aminoarylation Products

We thank Dr. Vincent Lynch (Manager of the X-ray Diffraction Lab at UT Austin) for all the X-ray structural analysis.

A sample of the major product **3.16f** was recrystallized from methylene chloride and hexanes (slow diffusion). The resulting crystals were suitable for X-ray diffraction and the structure was solved. This structure allowed the assignment of relative configuration as shown (see additional crystallographic data in appendix 8).



General Procedure for the Asymmetric Hetero Diels-Alder with Sulfurdiimide **3.10**

3.24: To a solution of copper(II) triflate (0.34 mmol, 1.25 equiv) in CH_2Cl_2 (16 mL, 0.02 M) was added bis(oxazoline) ligand **3.25** (0.36 mmol, 1.32 equiv) in CH_2Cl_2 (4 mL, 0.09 M) and the mixture was allowed to stir at 23 °C for 3 hours. Subsequently, the reaction was cooled to -78 °C and treated with sulfurdiimide reagent **3.10** (0.34 mmol, 1.25 equiv) in CH_2Cl_2 (4 mL, 0.09 M). After stirring for ten minutes the solution a solution of the 1,3-diene (0.274 mmol, 1.0 equiv) in CH_2Cl_2 (28 mL, 0.01 M) was added by gradual addition over ten minutes. The resulting mixture was stirred at -78 °C for 3 hours. The reaction was quenched by addition of water (6 mL) at -78 °C, and slowly

warmed to room temperature with stirring. The crude mixture was extracted with CH_2Cl_2 and the combined organics were dried over sodium sulfate. The product was purified by flash chromatography to yield the [4+2] cycloadduct **3.24** (0 to 10% methanol / CH_2Cl_2) as a 3:1 diastereomeric mixture in 71% yield. This material was taken directly on to the aminoarylation.

3.16c: Following the general two-pot procedure for the aminoarylation of 1,3-dienes, cycloadduct **3.24** was transferred to the 1,4-aminoarylation product **3.16c** (37 mg, 63 % yield, 70:30 er). See the corresponding appendix for HPLC traces. Absolute configuration of the product was assigned by analogy to literature reports of similar asymmetric [4+2] reactions .⁴⁶

3.4 References

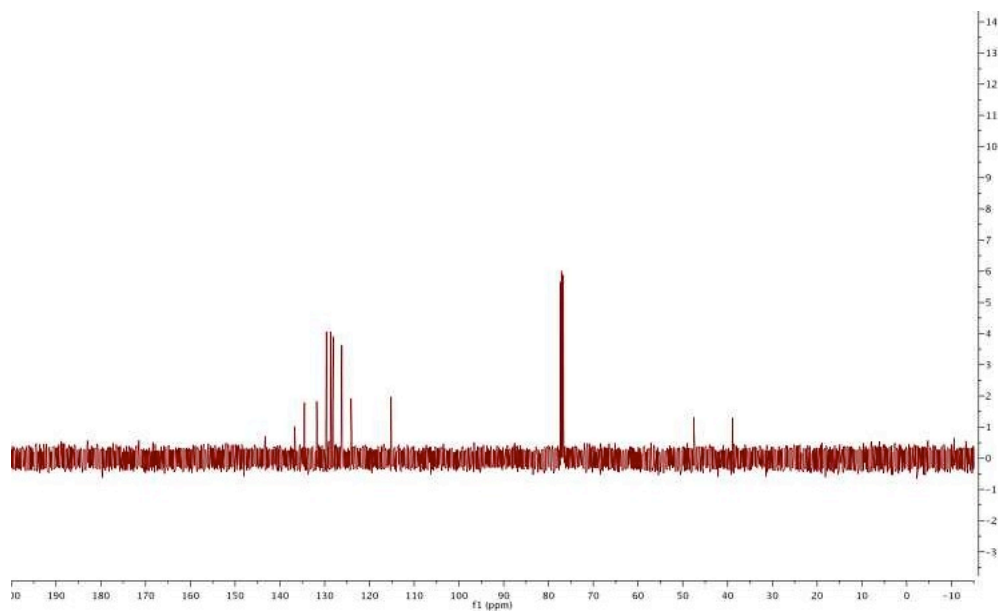
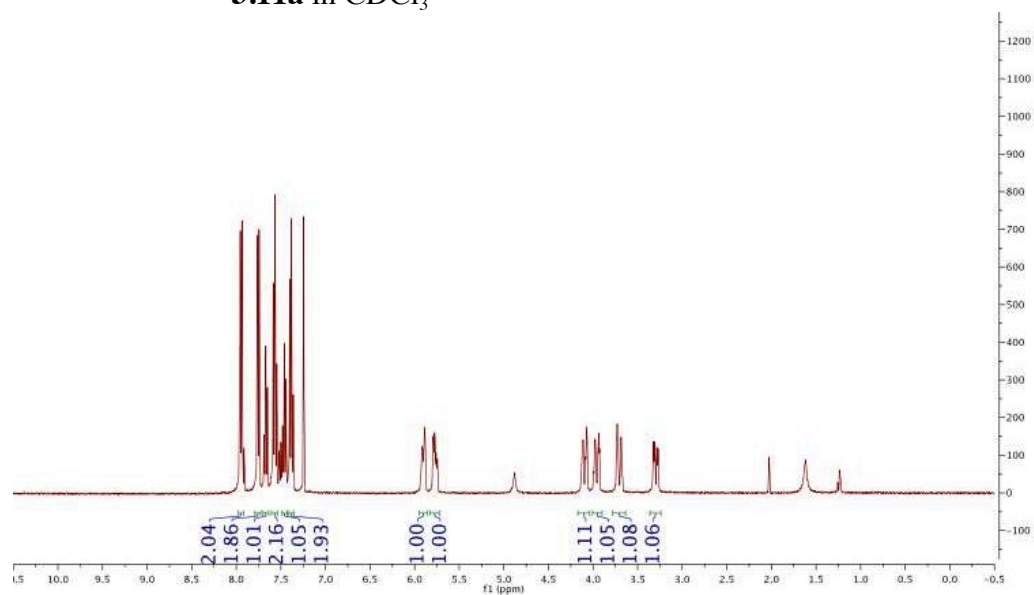
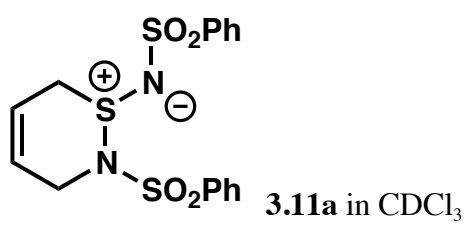
- (1) Bao, H.; Bayeh, L.; Tambar, U. K. *Synlett* **2013**, 24, 2459.
- (2) Hili, R.; Yudin, A. K. *Nat Chem Biol* **2006**, 2, 284.
- (3) Roughley, S. D.; Jordan, A. M. *Journal of Medicinal Chemistry* **2011**, 54, 3451.
- (4) McDonald, R. I.; Liu, G.; Stahl, S. S. *Chemical Reviews* **2011**, 111, 2981.
- (5) Pirnot, M. T.; Wang, Y.-M.; Buchwald, S. L. *Angewandte Chemie International Edition* **2016**, 55, 48.
- (6) Wolfe, J. P. In *Synthesis of Heterocycles via Metal-Catalyzed Reactions That Generate One or More Carbon-Heteroatom Bonds*; Wolfe, J. P., Ed.; Springer-Verlag: Berlin Heidelberg, 2013; Vol. 32, p 1.
- (7) Liu, G.; Wu, Y. In *C-H Activation*; Yu, J.-Q., Shi, Z., Eds.; Springer Berlin Heidelberg: Berlin, Heidelberg, 2010, p 195.
- (8) Trost, B. M.; Zhang, T.; Sieber, J. D. *Chemical Science* **2010**, 1, 427.
- (9) Hartwig, J. F.; Stanley, L. M. *Accounts of Chemical Research* **2010**, 43, 1461.
- (10) Johannsen, M.; Jørgensen, K. A. *Chemical Reviews* **1998**, 98, 1689.
- (11) Behr, A.; Becker, M.; Beckmann, T.; Johnen, L.; Leschinski, J.; Reyer, S. *Angewandte Chemie International Edition* **2009**, 48, 3598.
- (12) Stakem, F. G.; Heck, R. F. *The Journal of Organic Chemistry* **1980**, 45, 3584.
- (13) Larock, R. C.; Berrios-Pena, N.; Narayanan, K. *The Journal of Organic Chemistry* **1990**, 55, 3447.
- (14) Behr, A.; Johnen, L.; Vorholt, A. J. *ChemCatChem* **2010**, 2, 1271.
- (15) Prinz, T.; Driessen-Hölscher, B. *Chemistry – A European Journal* **1999**, 5, 2069.
- (16) Viciu, M. S.; Zinn, F. K.; Stevens, E. D.; Nolan, S. P. *Organometallics* **2003**, 22, 3175.
- (17) Takahashi, S.; Shibano, T.; Hagihara, N. *Tetrahedron Letters* **1967**, 8, 2451.
- (18) Suslov, D. S.; Bykov, M. V.; Belova, M. V.; Abramov, P. A.; Tkach, V. S. *Journal of Organometallic Chemistry* **2014**, 752, 37.
- (19) Smutny, E. J. *Journal of the American Chemical Society* **1967**, 89, 6793.
- (20) Keim, W.; Kurtz, K.-R.; Röper, M. *Journal of Molecular Catalysis* **1983**, 20, 129.

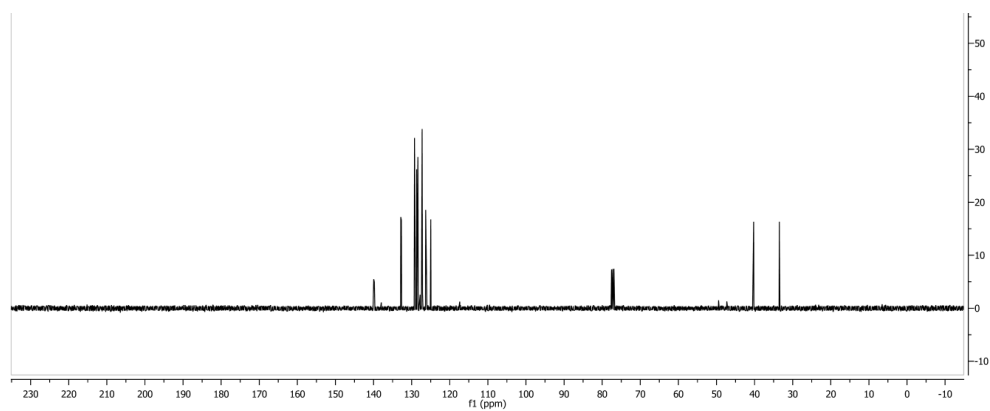
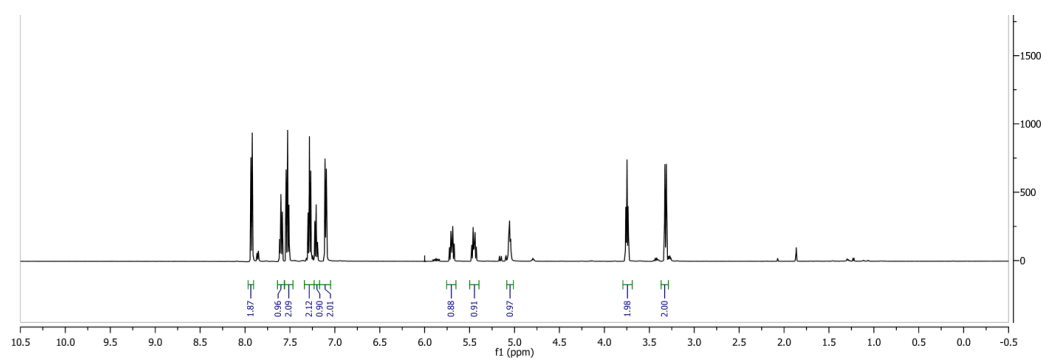
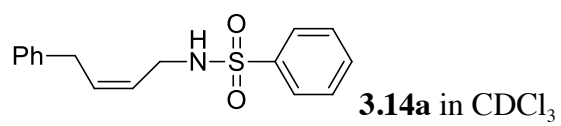
- (21) Safuanova, R. M.; Fakhretdinov, R. N.; Dzhemilev, U. M. *Bulletin of the Academy of Sciences of the USSR, Division of chemical science* **1988**, 37, 703.
- (22) Groult, A.; Guy, A. *Tetrahedron* **1983**, 39, 1543.
- (23) Dzhemilev, U. M.; Kunakova, R. V.; Sidorova, V. V. *Bulletin of the Academy of Sciences of the USSR, Division of chemical science* **1987**, 36, 362.
- (24) Petrushkina, E. A.; Mysova, N. E.; Orlinkov, A. V. *Zeitschrift für anorganische und allgemeine Chemie* **2005**, 631, 2232.
- (25) Maddock, S. M.; Finn, M. G. *Organometallics* **2000**, 19, 2684.
- (26) Grotevendt, A.; Bartolome, M.; Nielsen, D. J.; Spannenberg, A.; Jackstell, R.; Cavell, K. J.; Oro, L. A.; Beller, M. *Tetrahedron Letters* **2007**, 48, 9203.
- (27) Larock, R. C.; Harrison, L. W.; Hsu, M. H. *The Journal of Organic Chemistry* **1984**, 49, 3662.
- (28) Larock, R. C.; Varaprath, S.; Lau, H. H.; Fellows, C. A. *Journal of the American Chemical Society* **1984**, 106, 5274.
- (29) Larock, R. C.; Liu, C. L.; Lau, H. H.; Varaprath, S. *Tetrahedron Letters* **1984**, 25, 4459.
- (30) O'Connor, J. M.; Stallman, B. J.; Clark, W. G.; Shu, A. Y. L.; Spada, R. E.; Stevenson, T. M.; Dieck, H. A. *The Journal of Organic Chemistry* **1983**, 48, 807.
- (31) Bao, H.; Bayeh, L.; Tambar, U. K. *ChemInform* **2014**, 45, no.
- (32) Bao, H.; Bayeh, L.; Tambar, U. K. *Angewandte Chemie International Edition* **2014**, 53, 1664.
- (33) Kresze, G.; Wucherpfennig, W. *Angewandte Chemie International Edition in English* **1967**, 6, 149.
- (34) Kresze, G.; Maschke, A.; Albrecht, R.; Bederke, K.; Patzschke, H. P.; Smalla, H.; Trede, A. *Angewandte Chemie International Edition in English* **1962**, 1, 89.
- (35) Zibarev, A.; Yakobson, G. *Russian Chemical Reviews* **1985**, 54, 1006.
- (36) Weinreb, S. M.; Boger, D. In *Hetero Diels-Alder Methodology in Organic Synthesis*; Academic Press: San Diego, 1987, p 1.

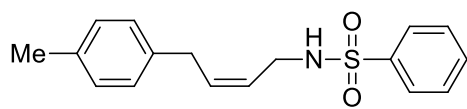
- (37) Kresze, G. In *1,4-Cycloaddition Reactions: The Diels-Alder Reaction in Heterocyclic Syntheses* Hamer, J., Ed.; Academic Press: New York, 1967.
- (38) Weinreb, S. M. *Accounts of Chemical Research* **1988**, *21*, 313.
- (39) Levisalles, J.; Rudler-Chauvin, M.; Rudler, H. *Journal of Organometallic Chemistry* **1977**, *136*, 103.
- (40) Trost, B. M.; Verhoeven, T. R. *Journal of the American Chemical Society* **1980**, *102*, 4730.
- (41) Tanigawa, Y.; Kanamaru, H.; Sonoda, A.; Murahashi, S. *Journal of the American Chemical Society* **1977**, *99*, 2361.
- (42) Goering, H. L.; Kantner, S. S. *The Journal of Organic Chemistry* **1981**, *46*, 2144.
- (43) Endeshaw, M. M.; Bayer, A.; Hansen, L. K.; Gautun, O. R. *European Journal of Organic Chemistry* **2006**, *2006*, 5249.
- (44) Bayer, A.; Hansen, L. K.; Gautun, O. R. *Tetrahedron: Asymmetry* **2002**, *13*, 2407.
- (45) Bayer, A.; Gautun, O. R. *Tetrahedron: Asymmetry* **2001**, *12*, 2937.
- (46) Bayer, A.; Endeshaw, M. M.; Gautun, O. R. *The Journal of Organic Chemistry* **2004**, *69*, 7198.
- (47) Frohn, M.; Dalkiewicz, M.; Tu, Y.; Wang, Z.-X.; Shi, Y. *Journal of Organic Chemistry* **1998**, *63*, 2948

APPENDIX FOUR

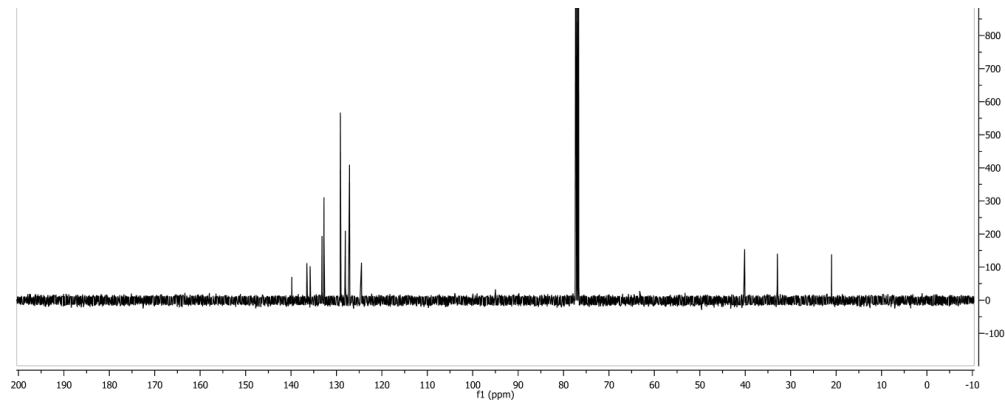
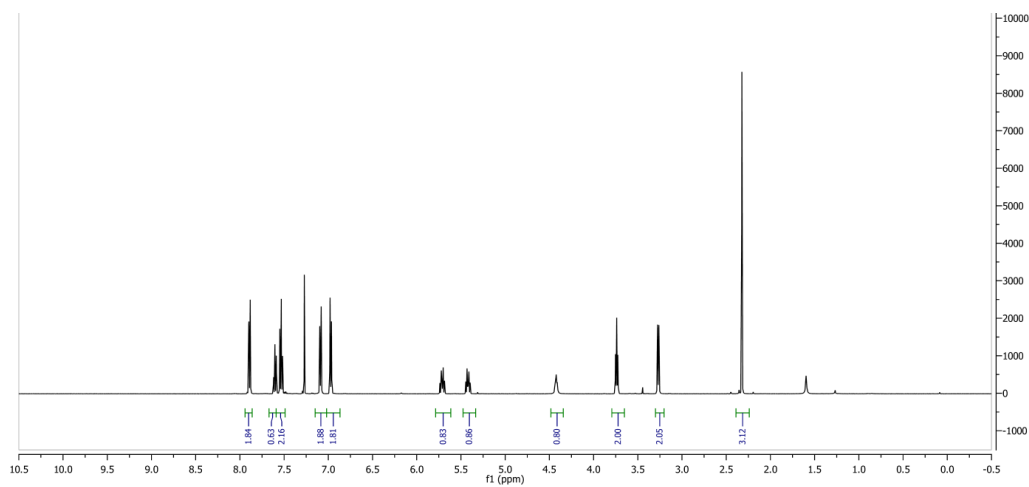
Spectra Relevant to Chapter Three: The Development of a Regio- and Diastereoselective Aminoarylation of Simple Dienes

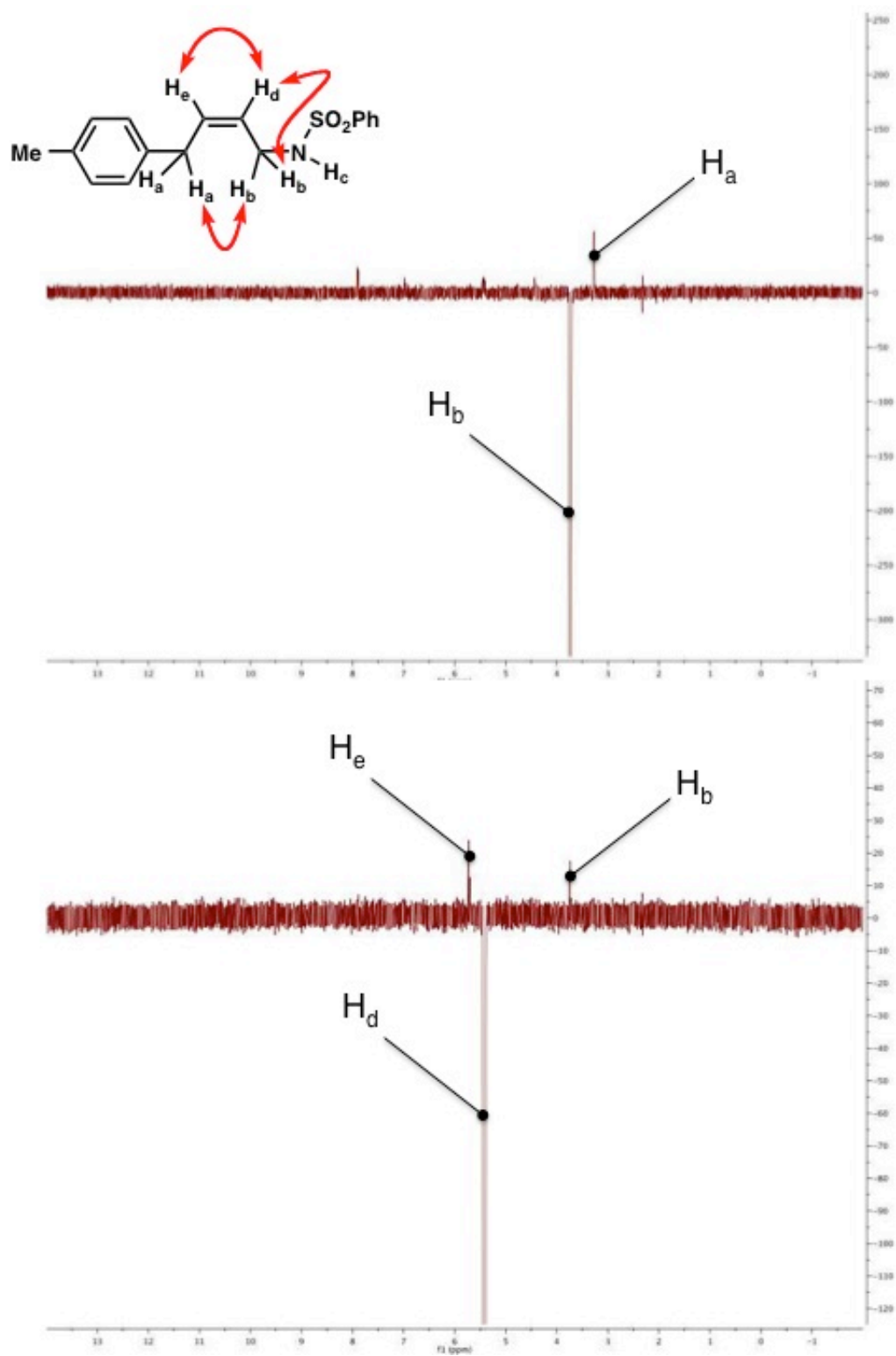


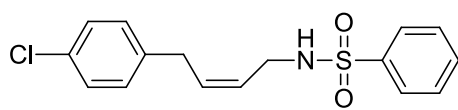




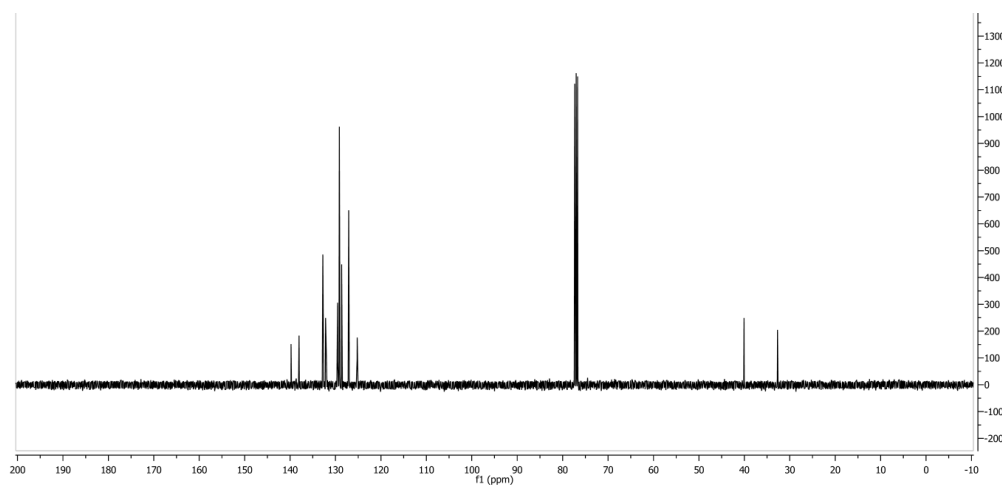
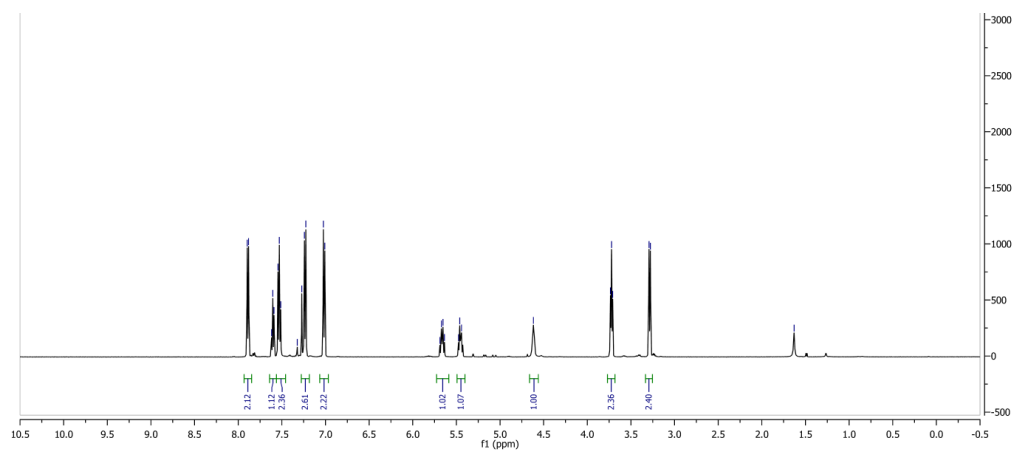
3.14b in CDCl₃

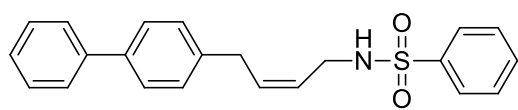




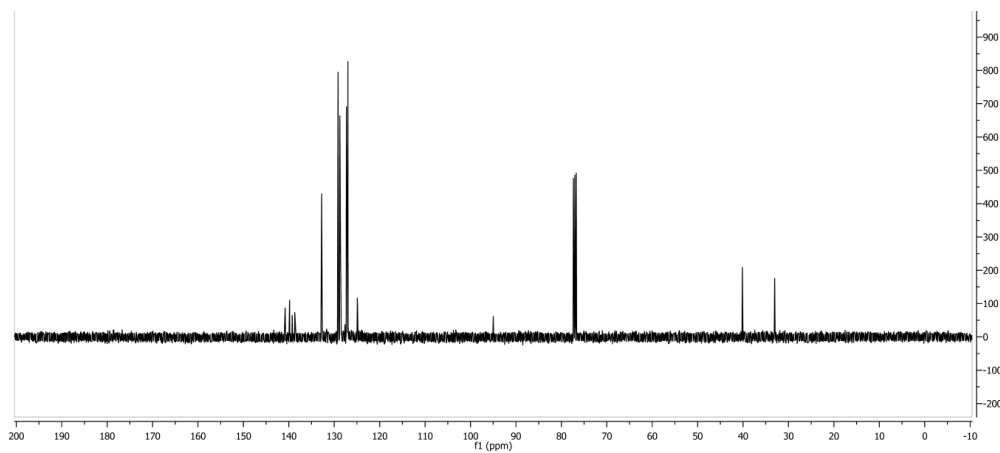
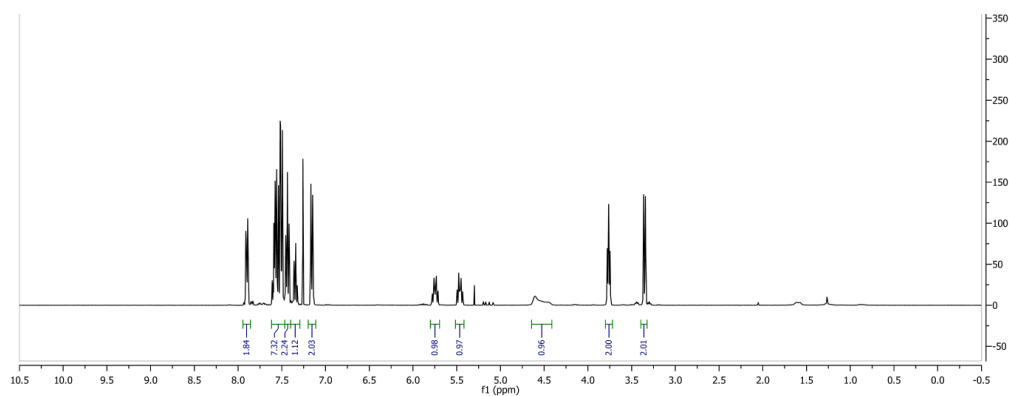


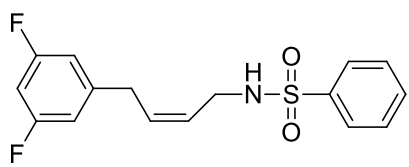
3.14c in CDCl₃



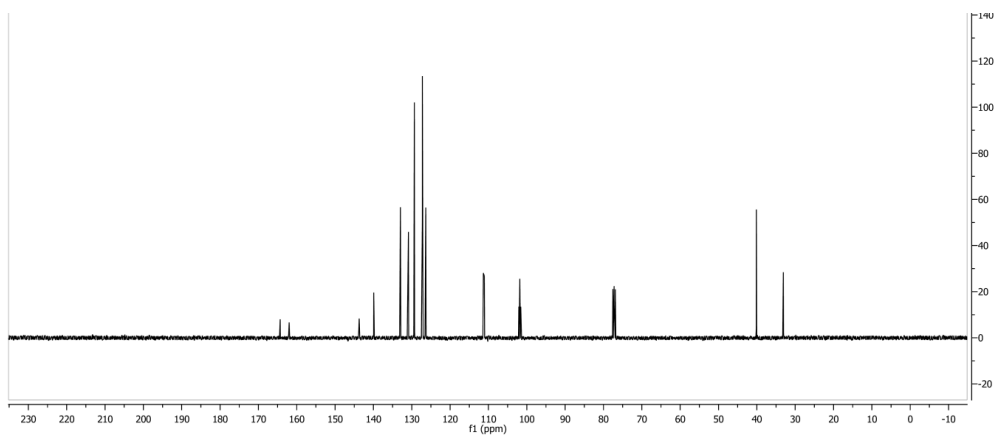
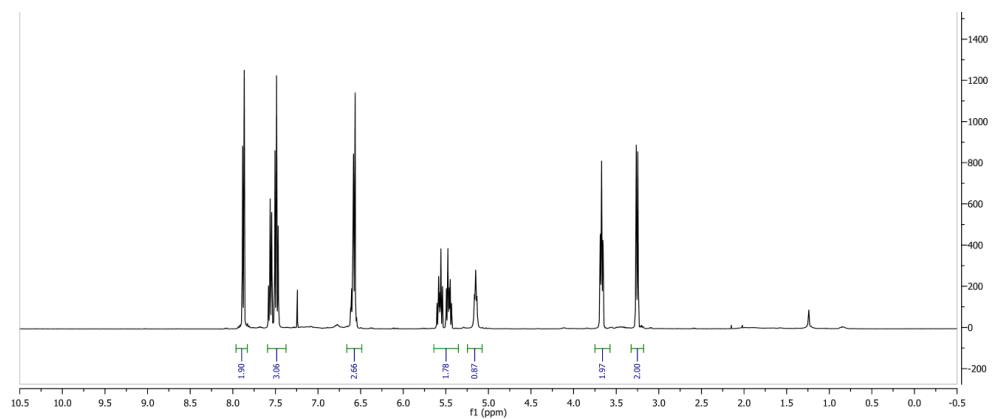


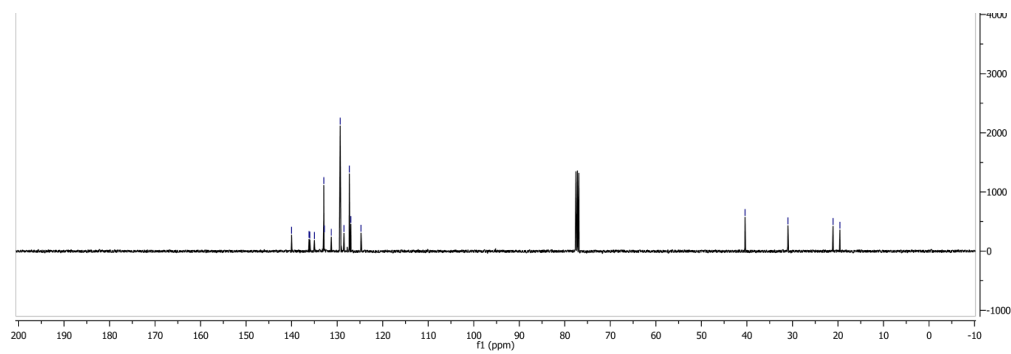
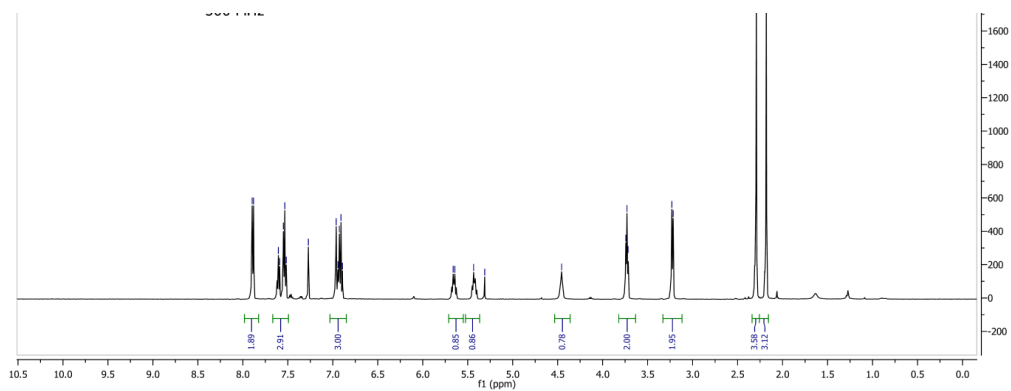
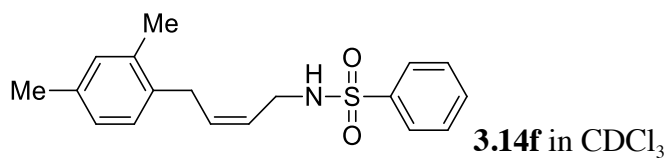
3.14d in CDCl₃

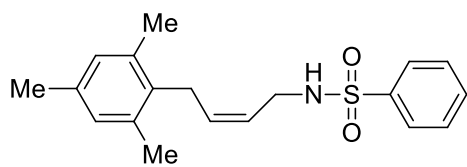




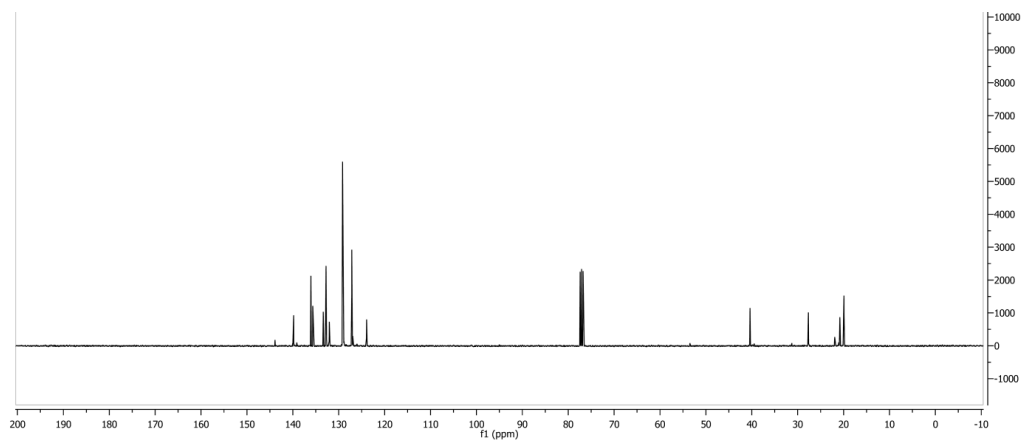
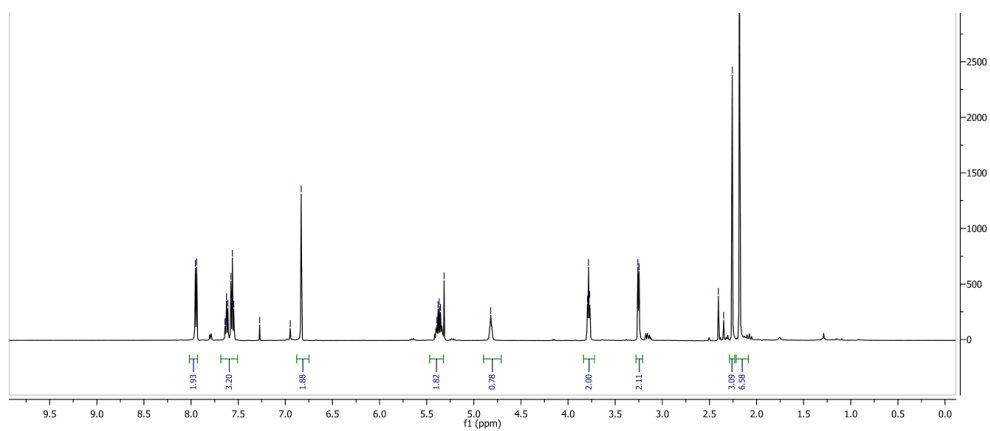
3.14e in CDCl₃

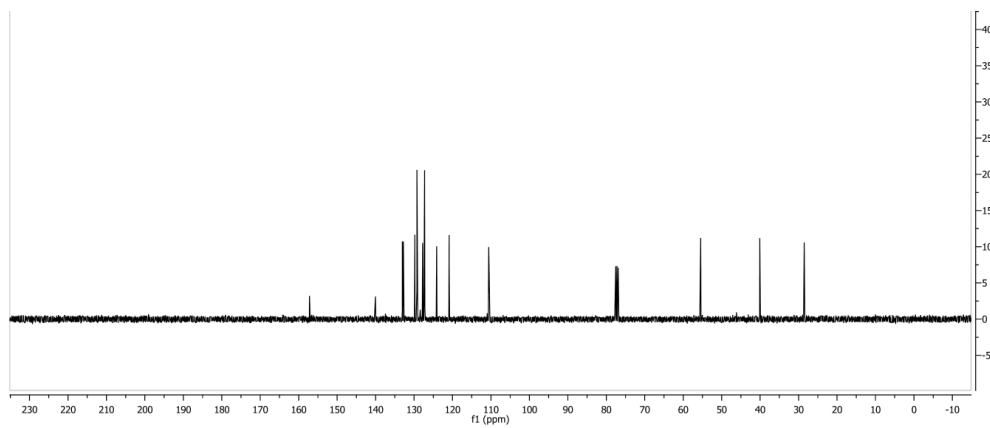
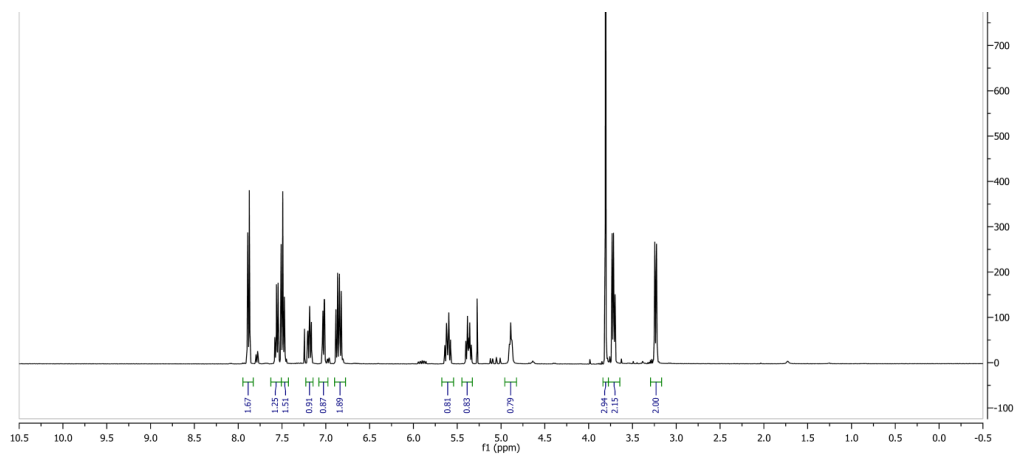
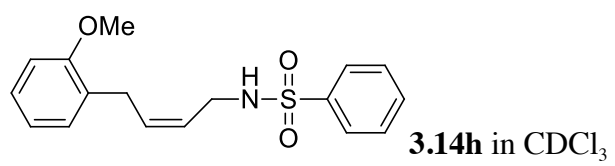


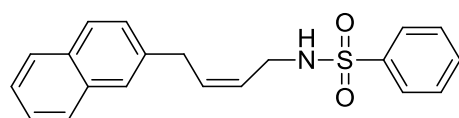




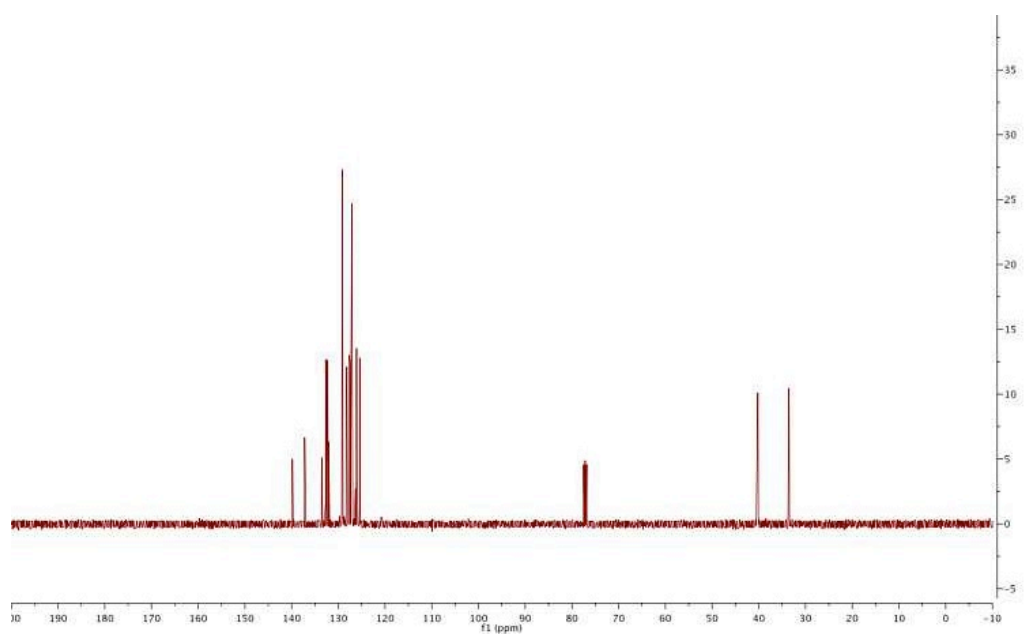
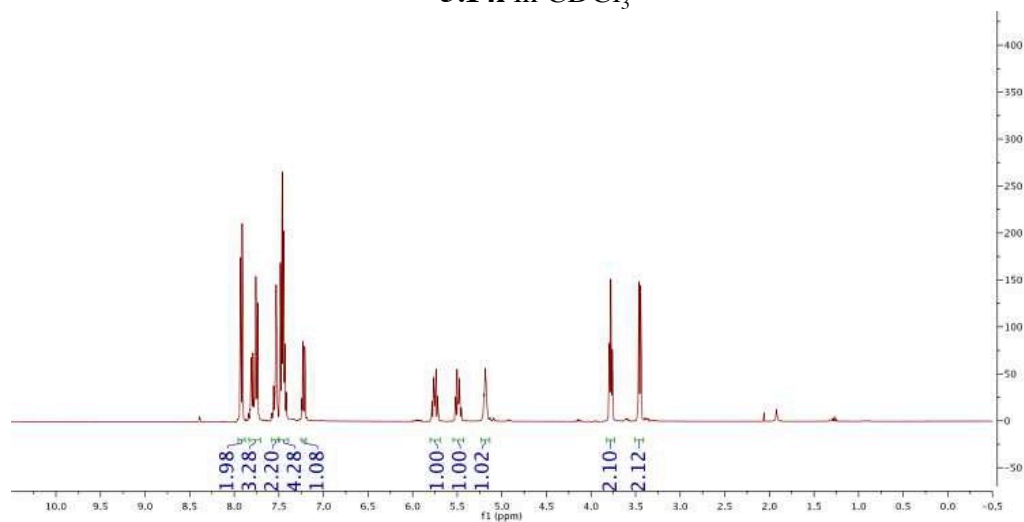
3.14g in CDCl_3

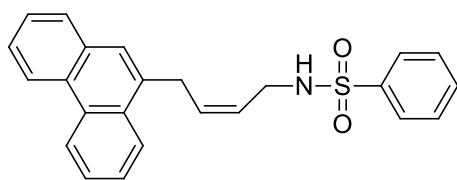




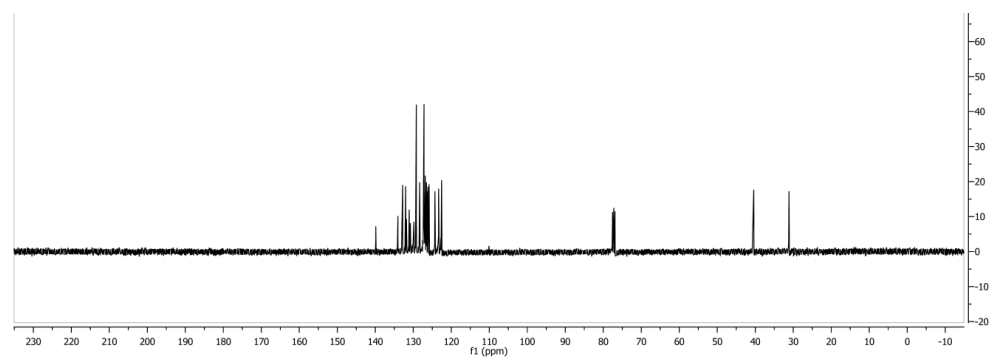
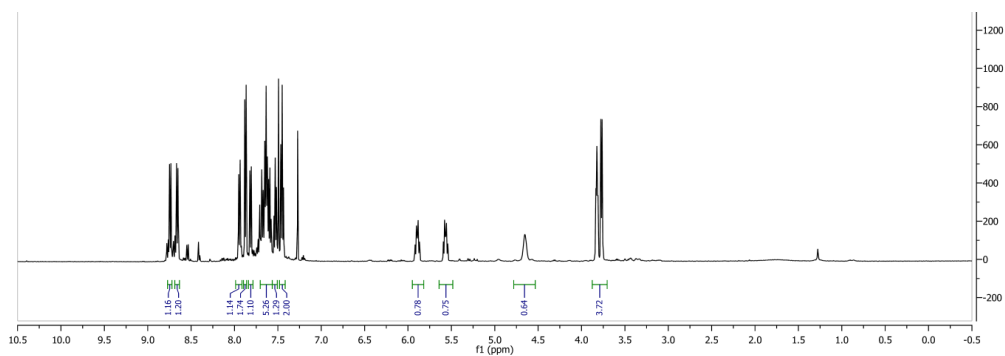


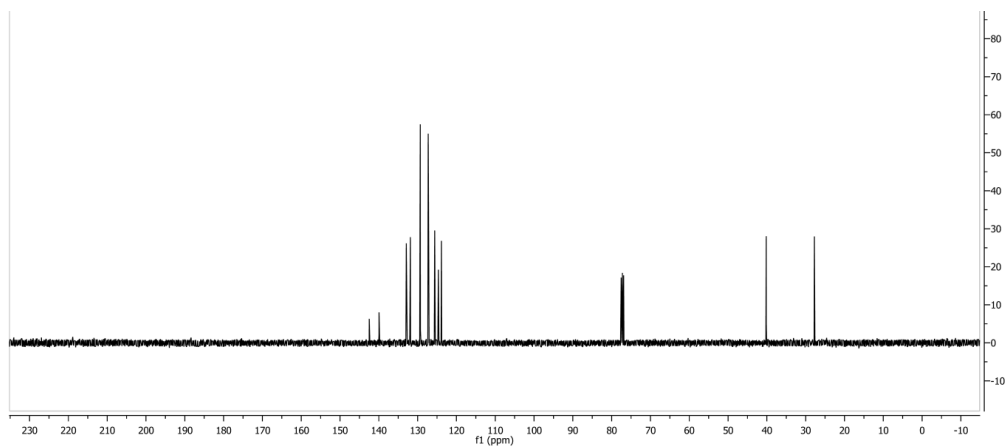
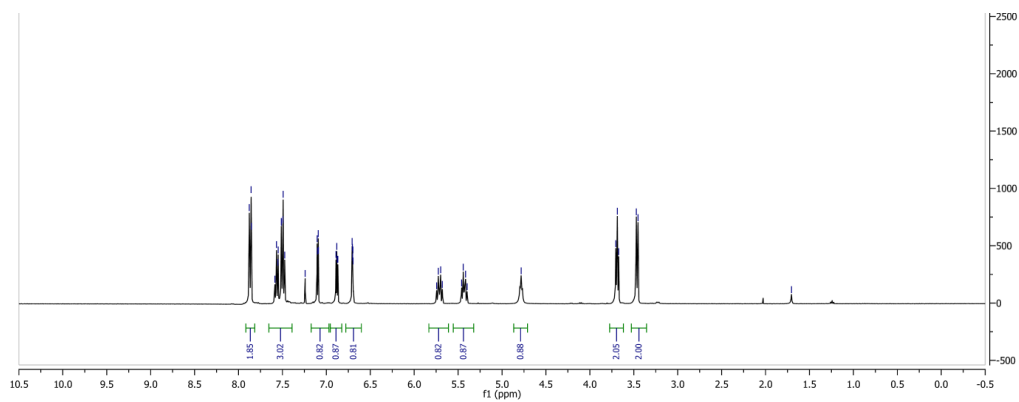
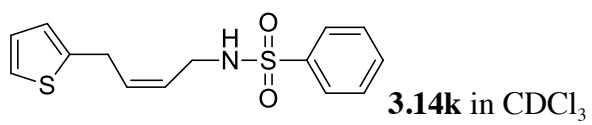
3.14i in CDCl₃

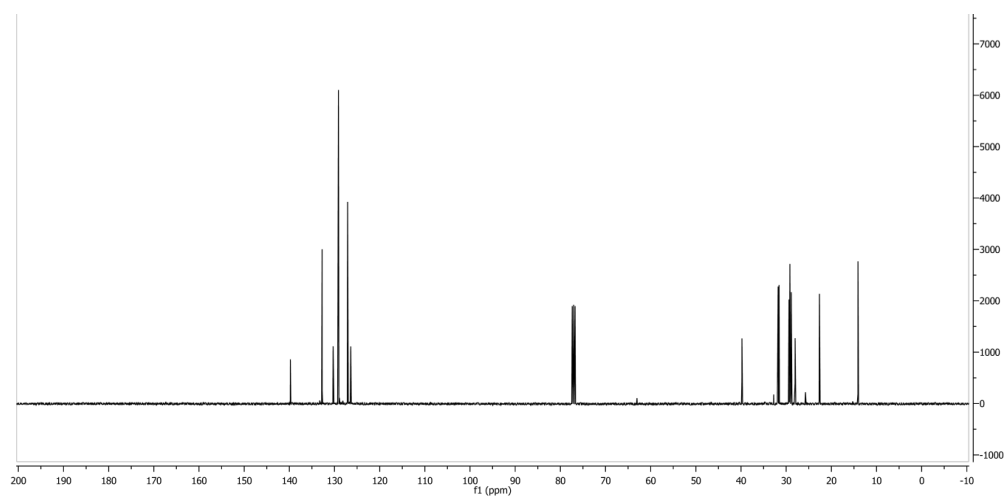
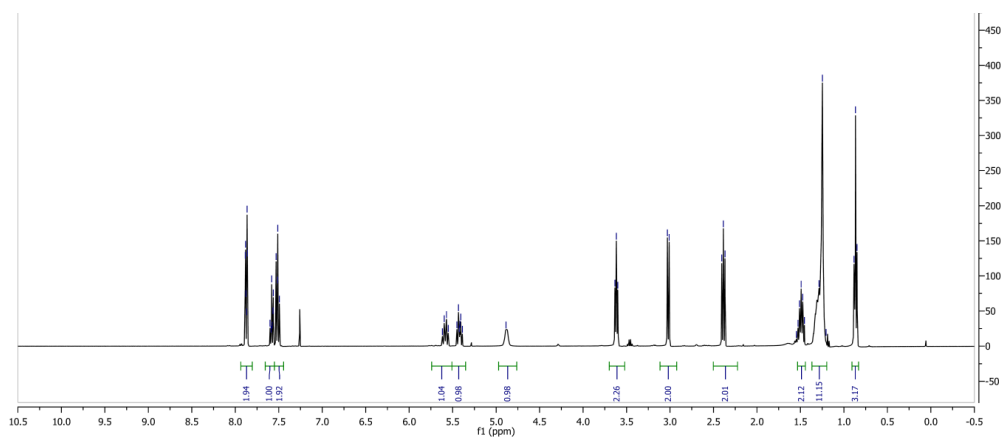
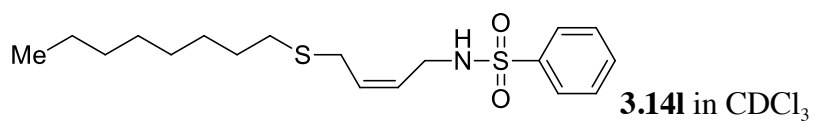


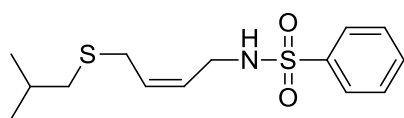


3.14j in CDCl₃

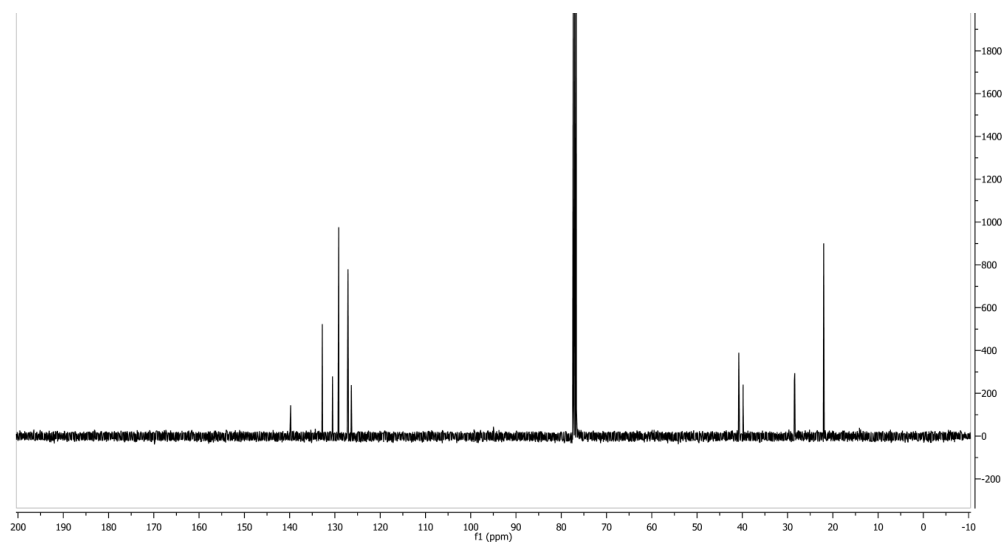
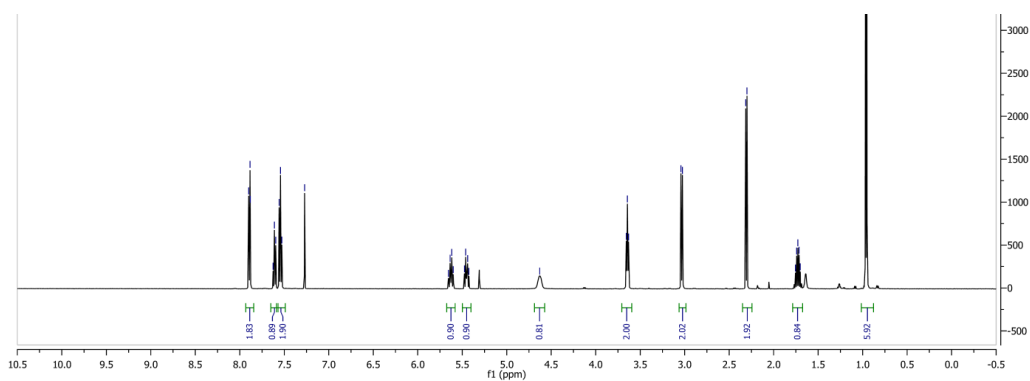


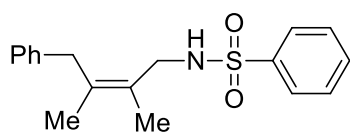




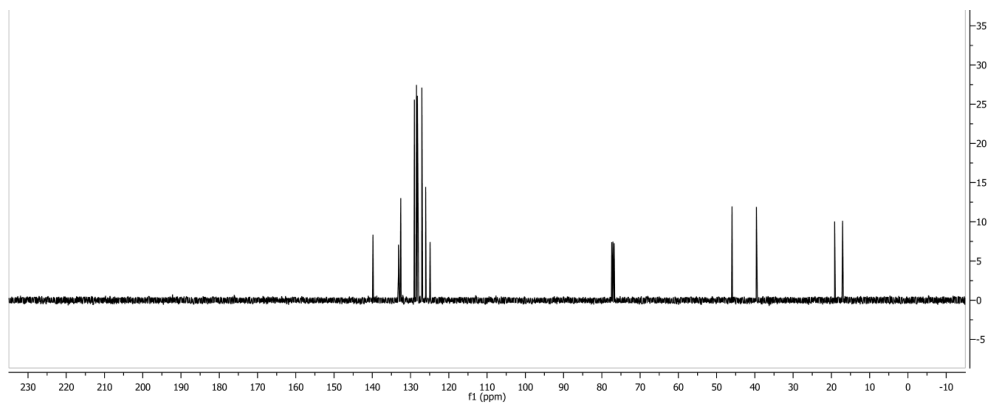
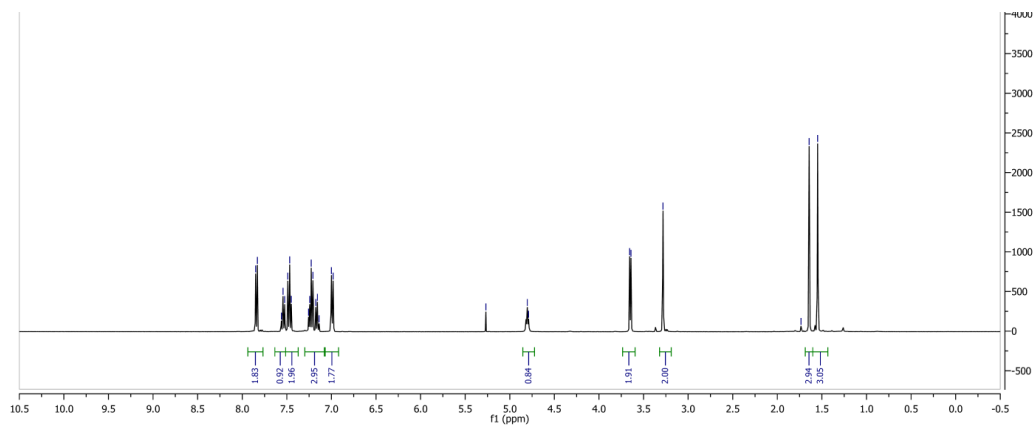


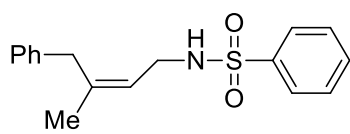
3.14m in CDCl₃



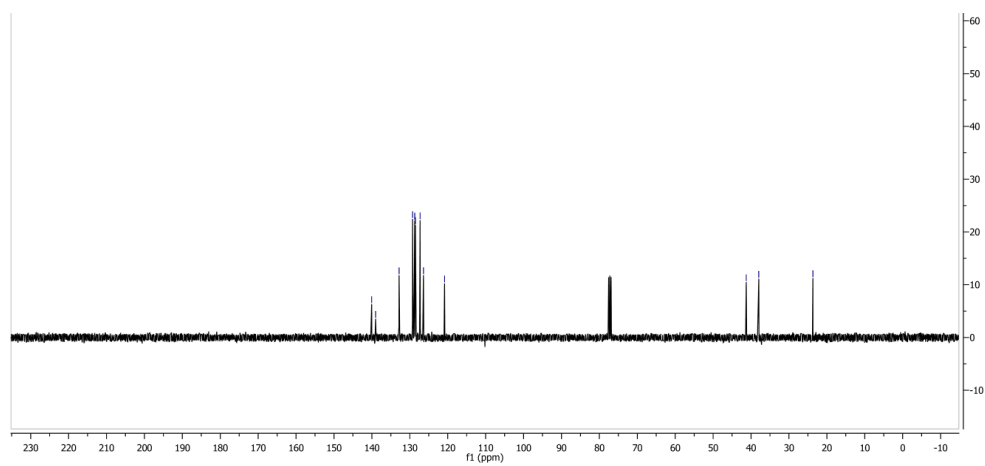
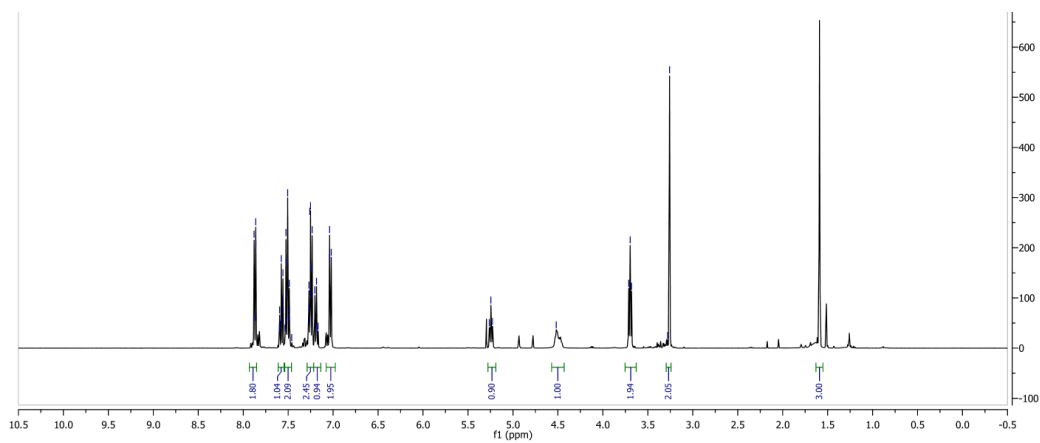


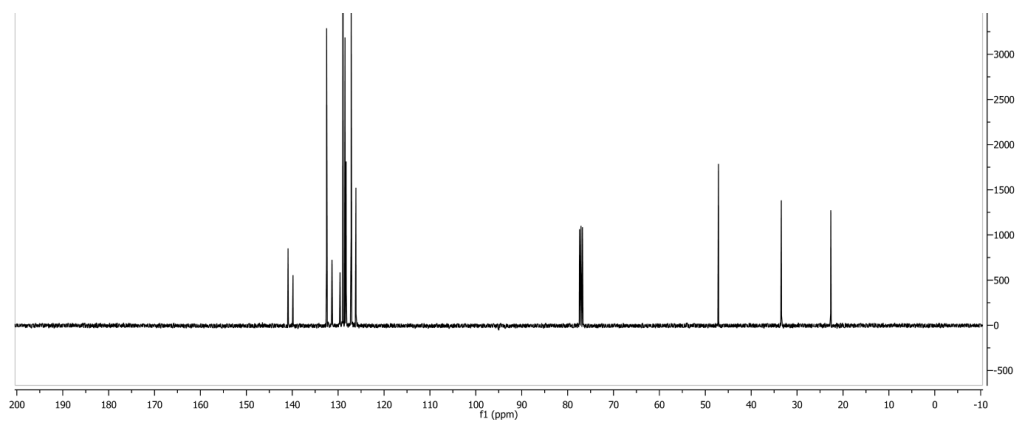
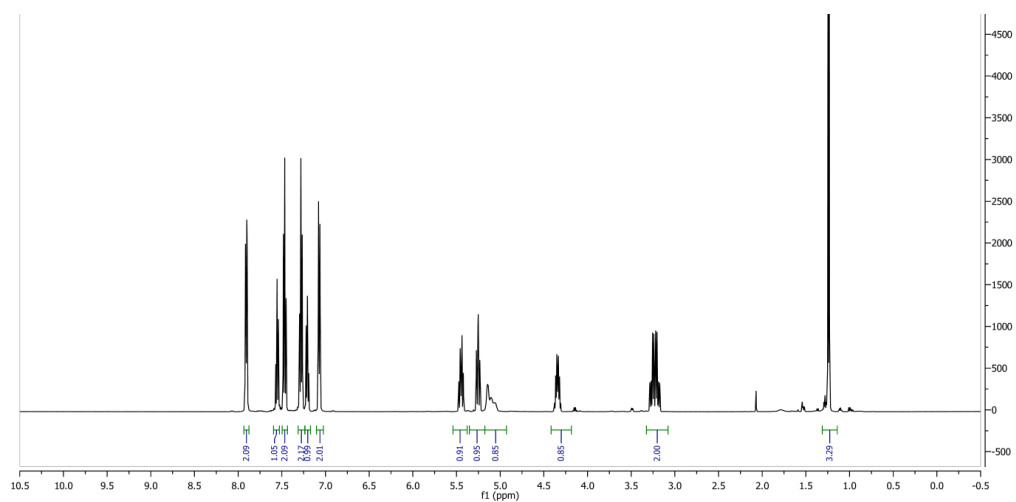
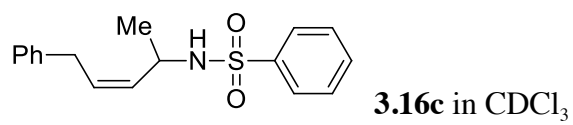
3.16a in CDCl₃

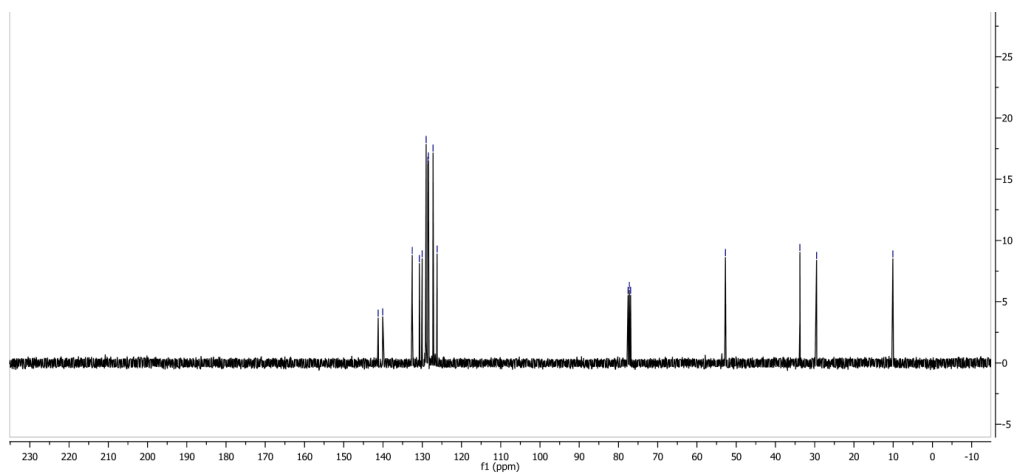
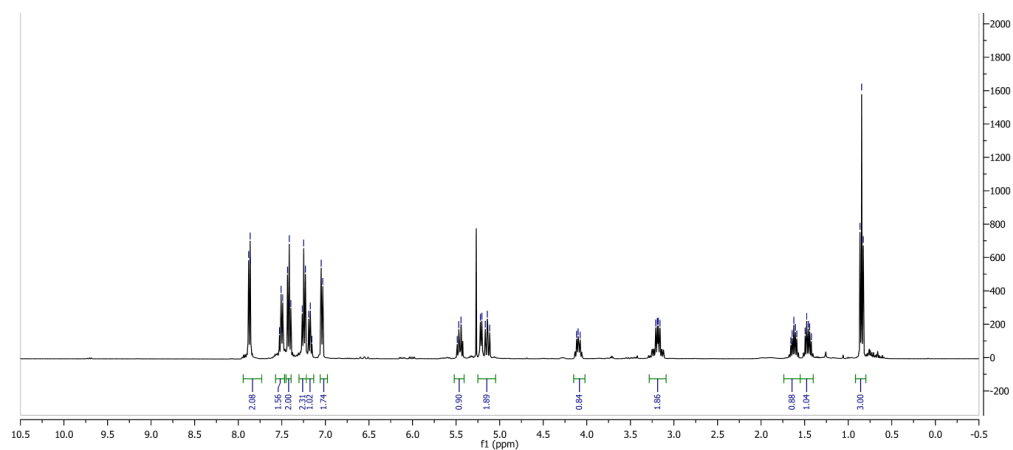
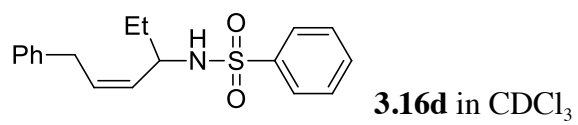


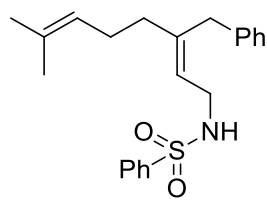


3.16b in CDCl₃

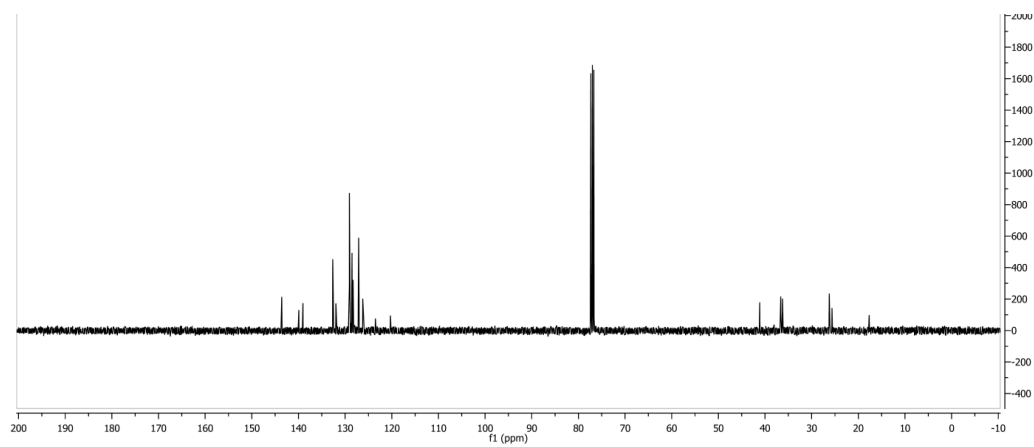
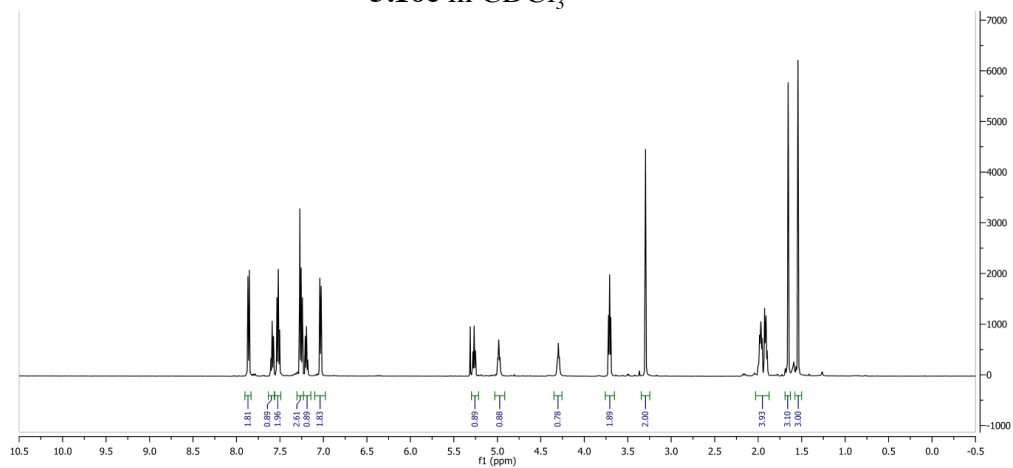


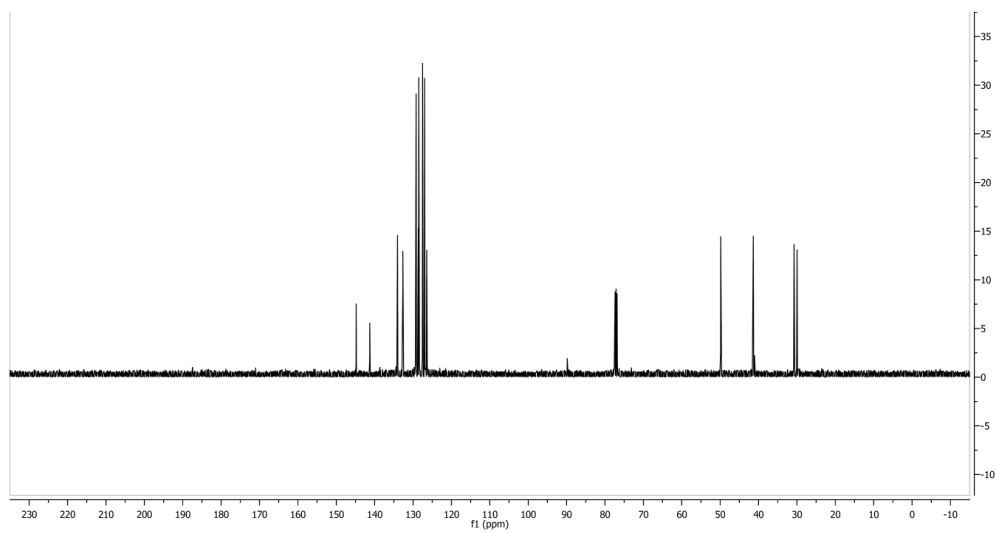
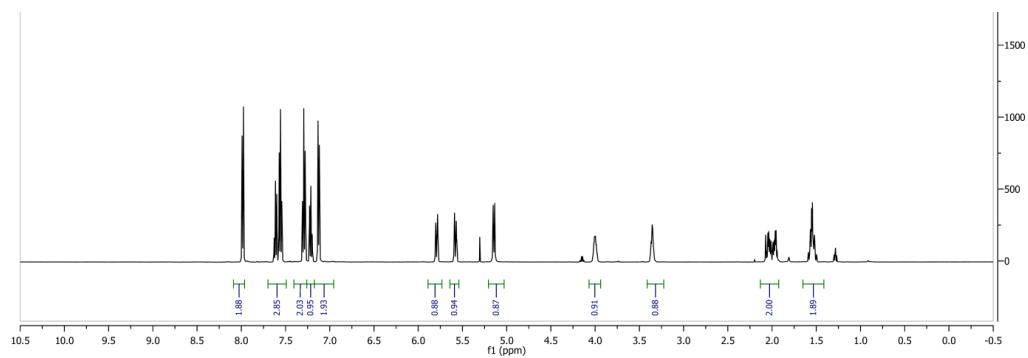
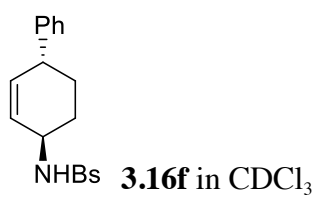


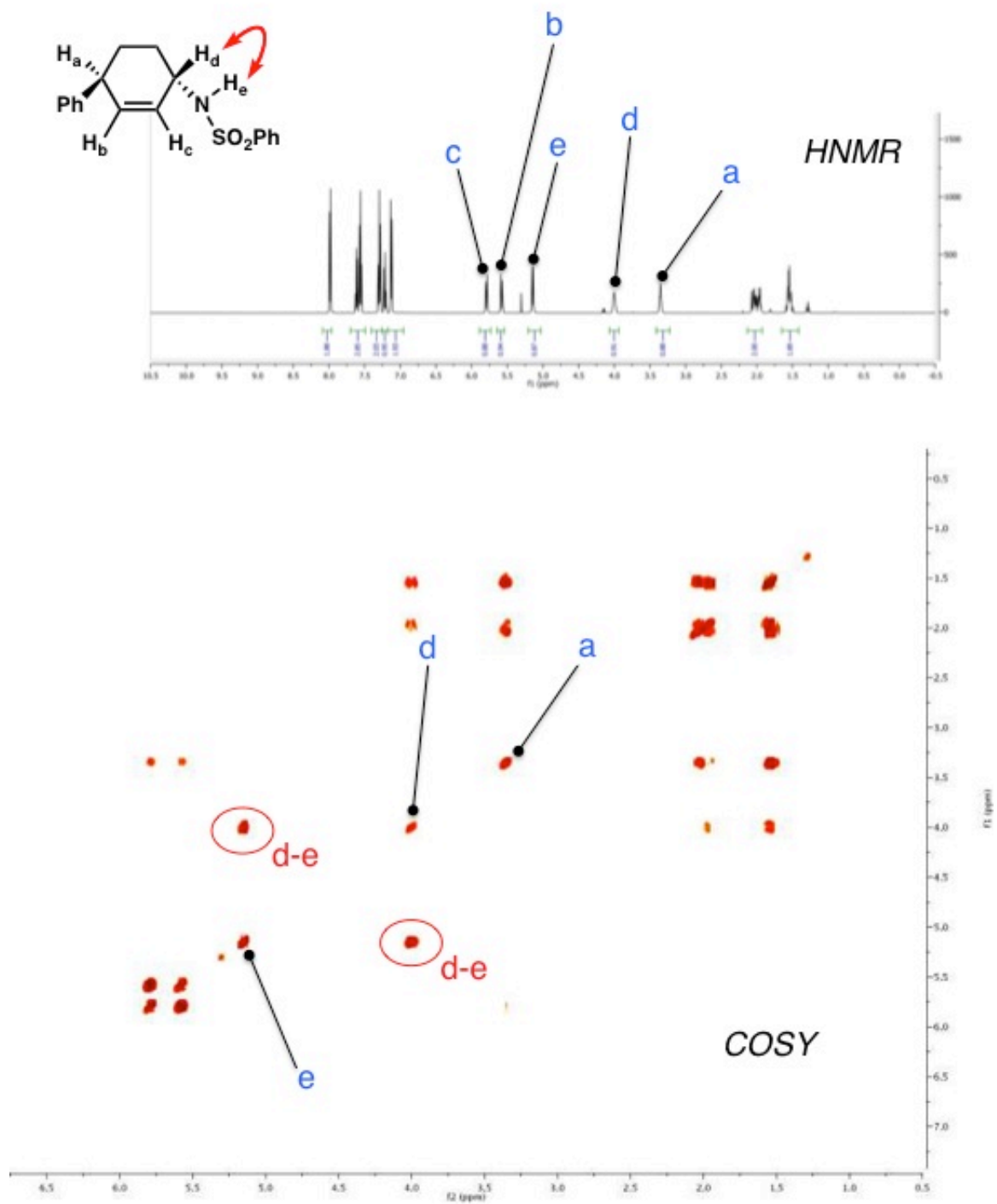


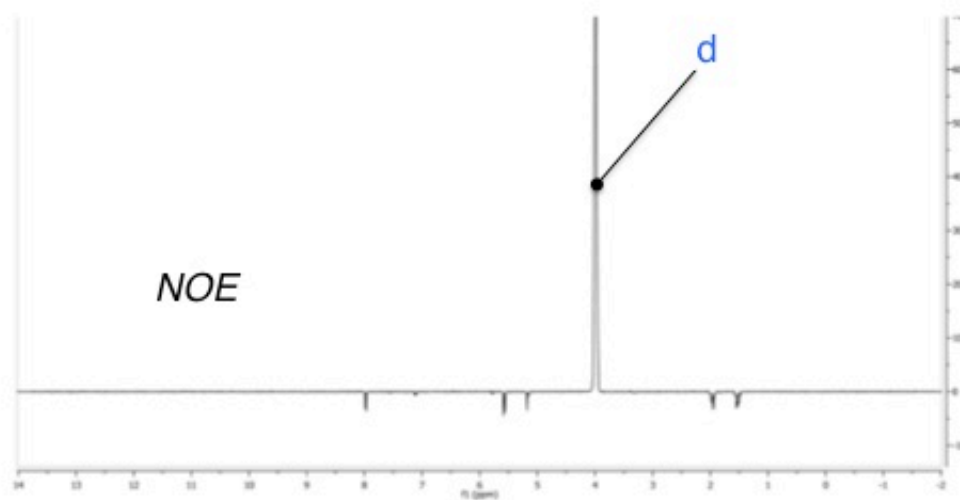
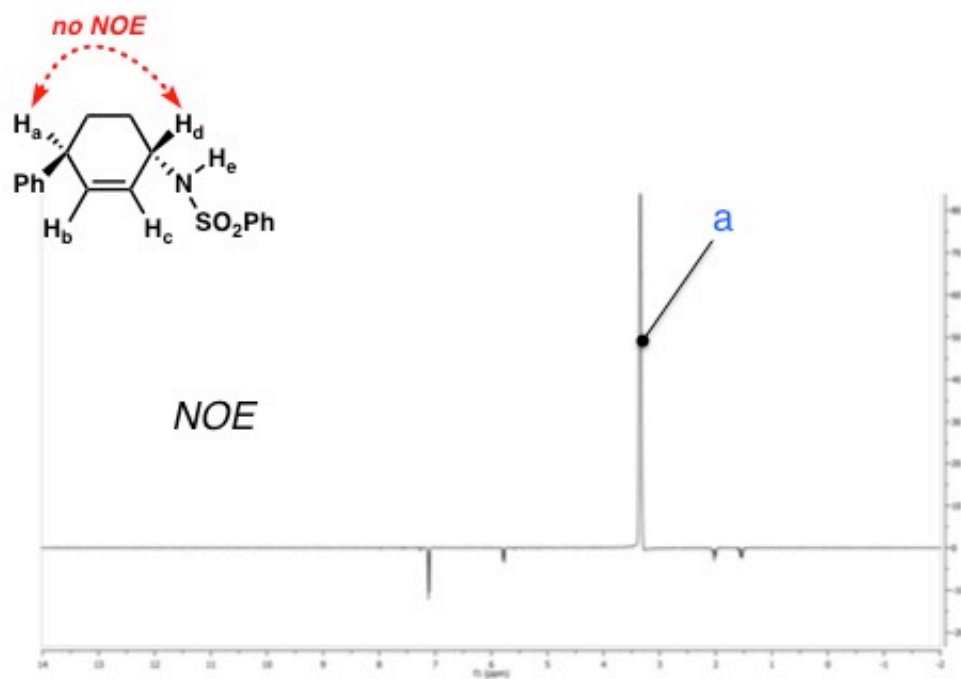


3.16e in CDCl_3

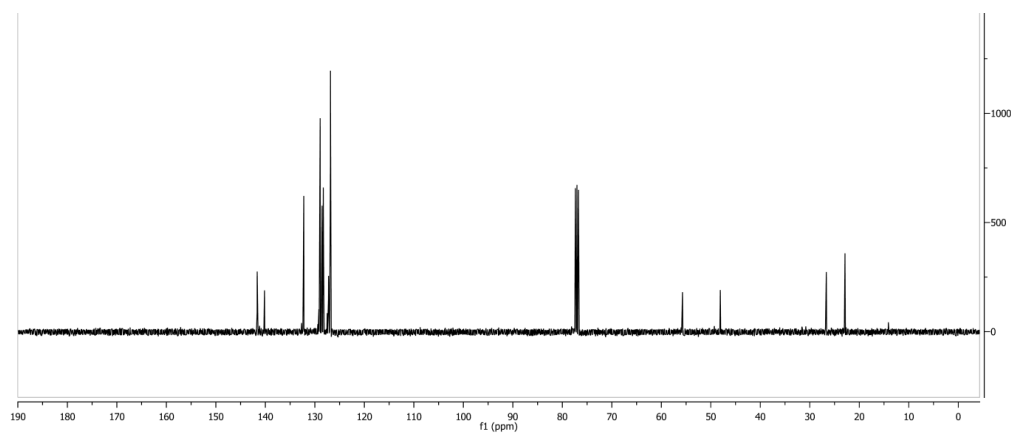
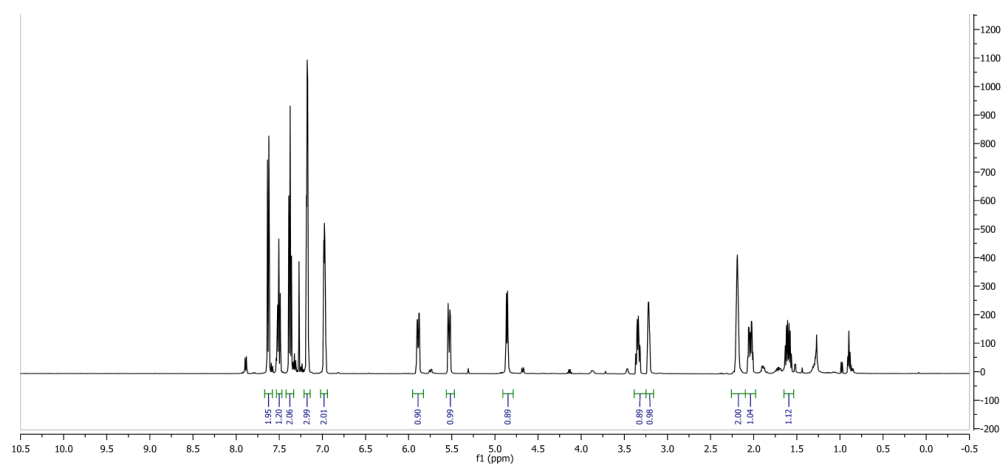


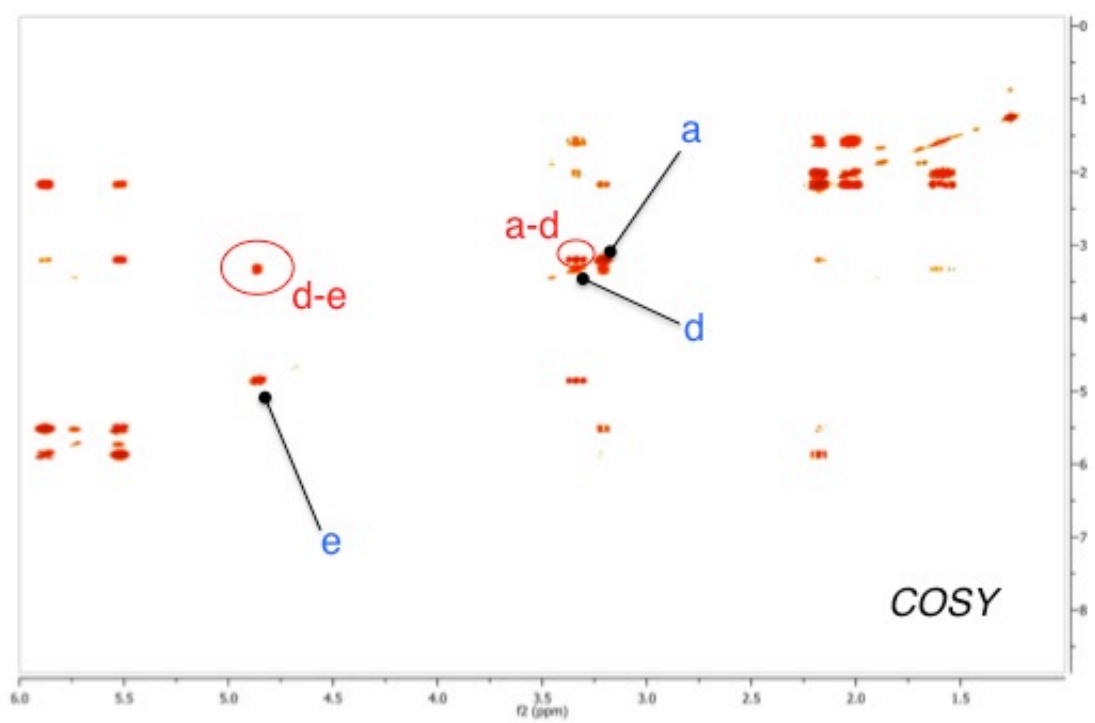
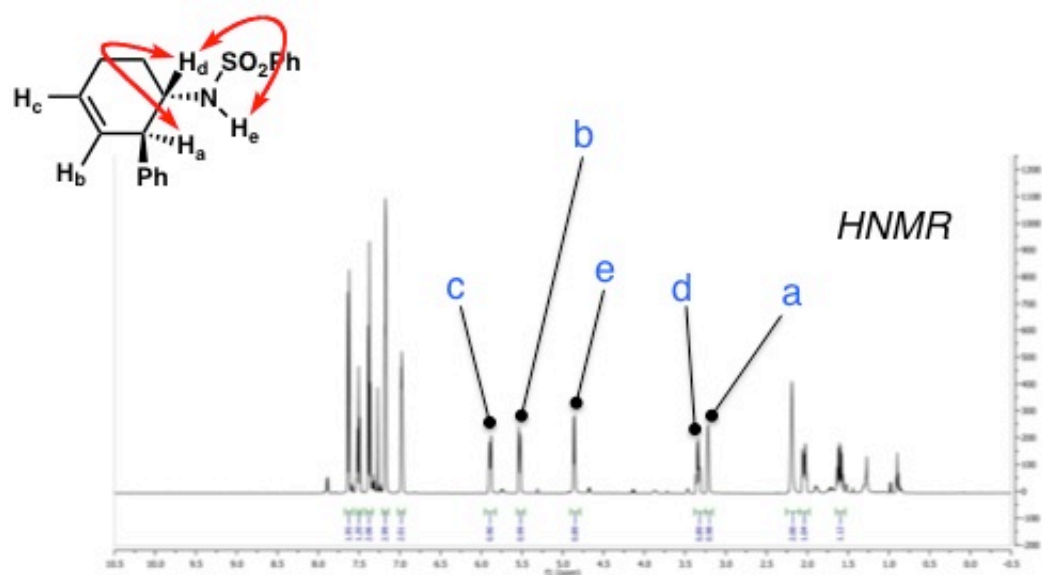


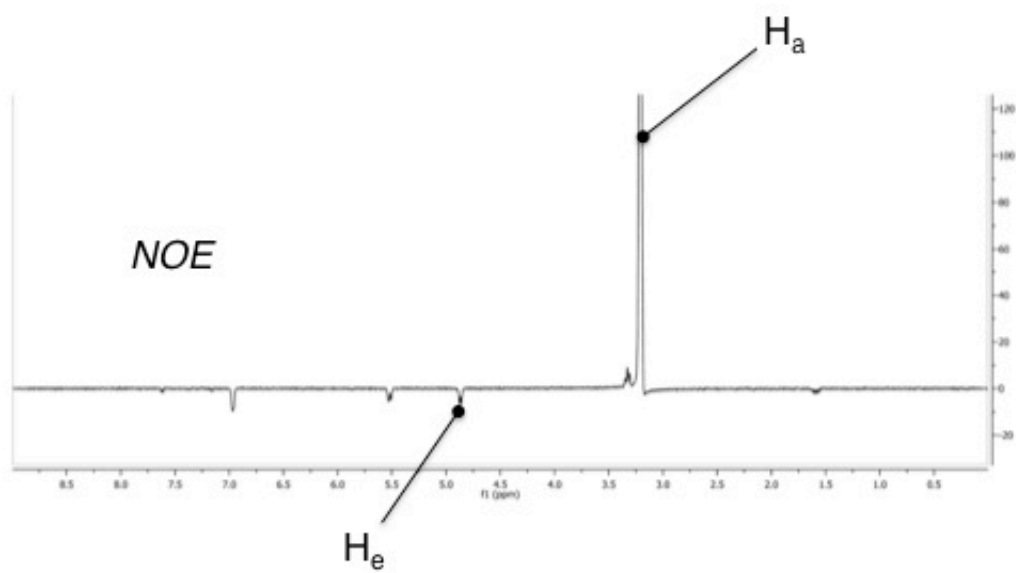
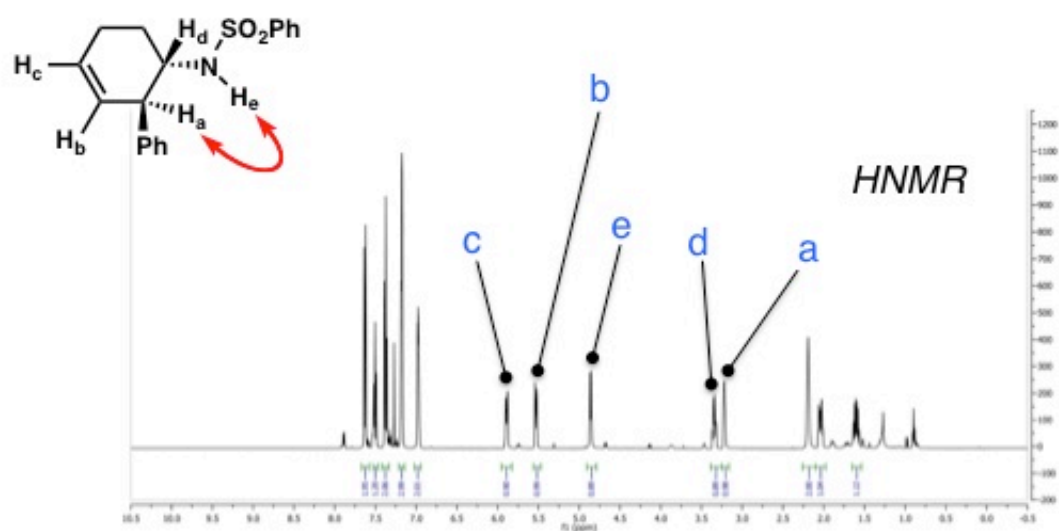


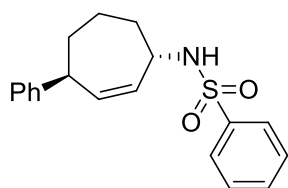


NOE was not detected between H_a and H_d \longrightarrow anti relationship

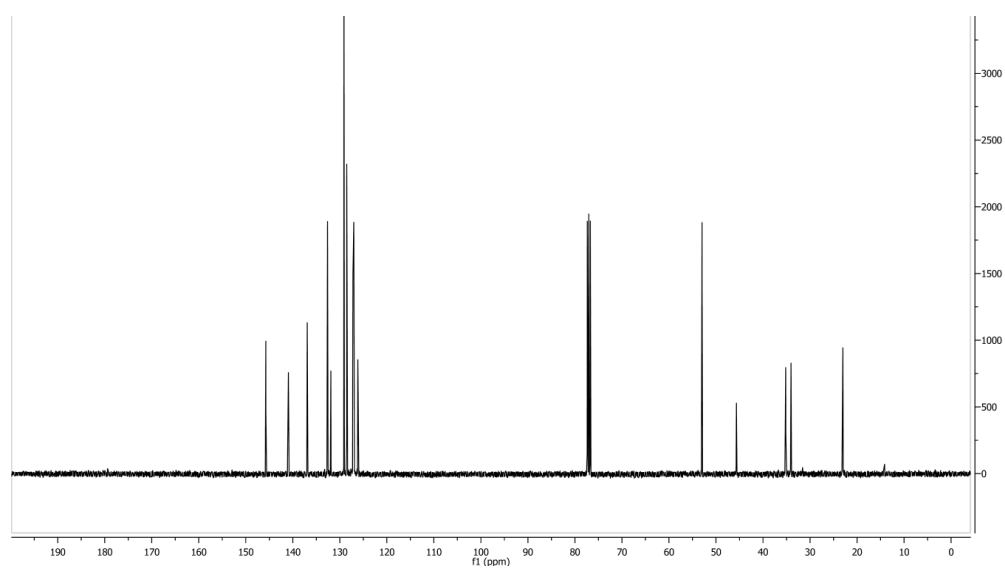
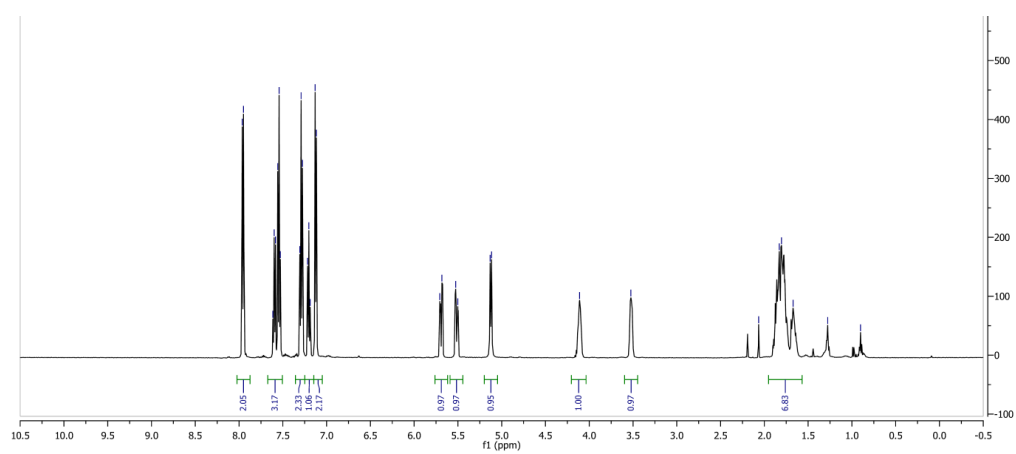


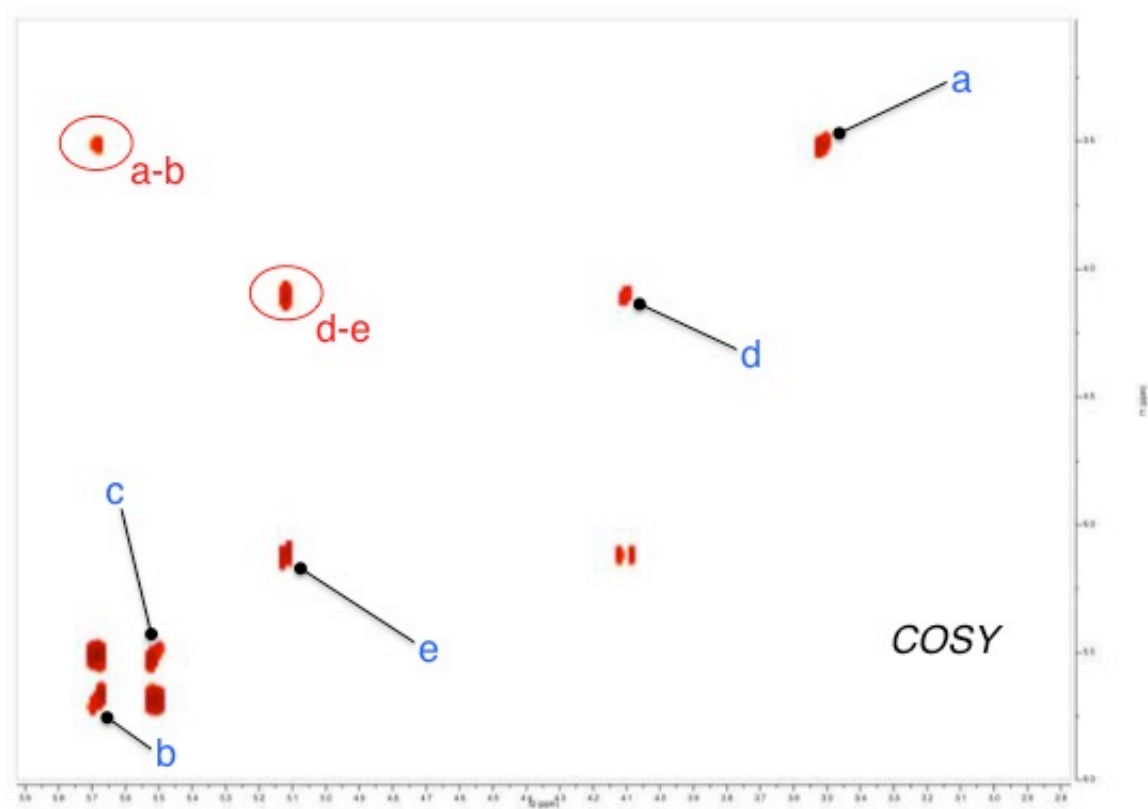
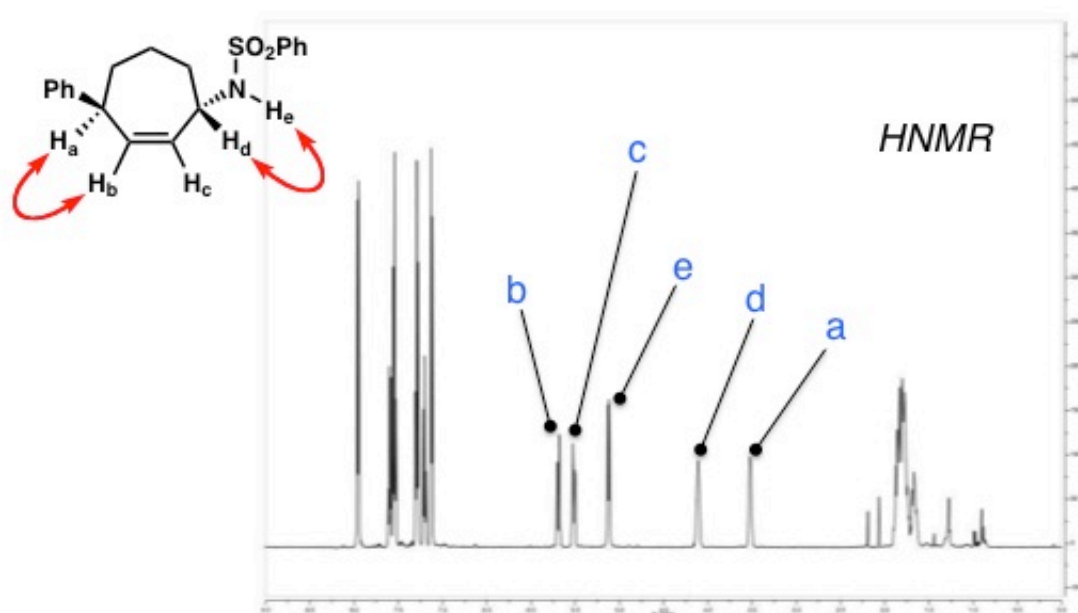


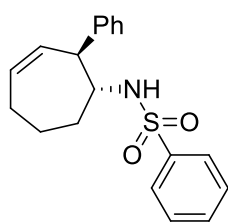




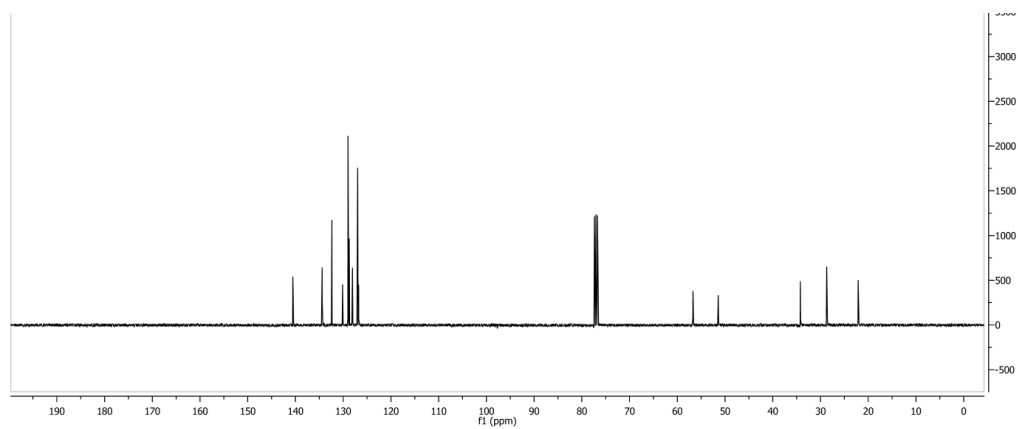
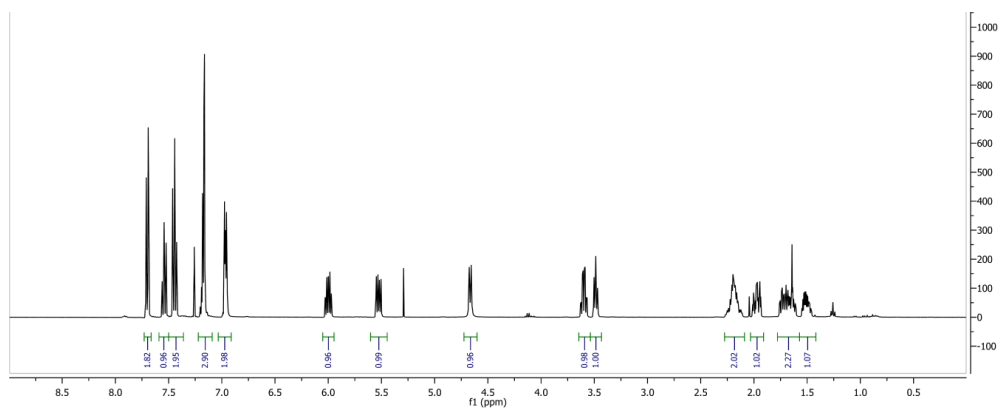
3.16g in CDCl₃

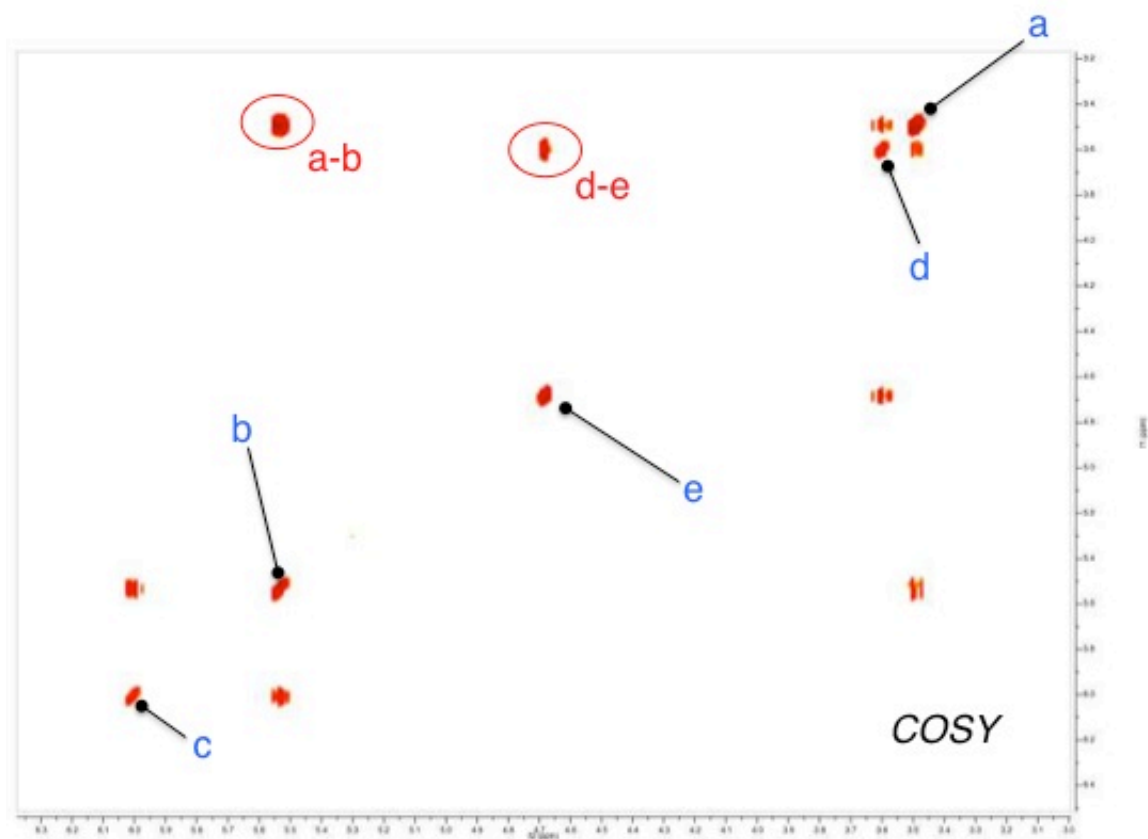
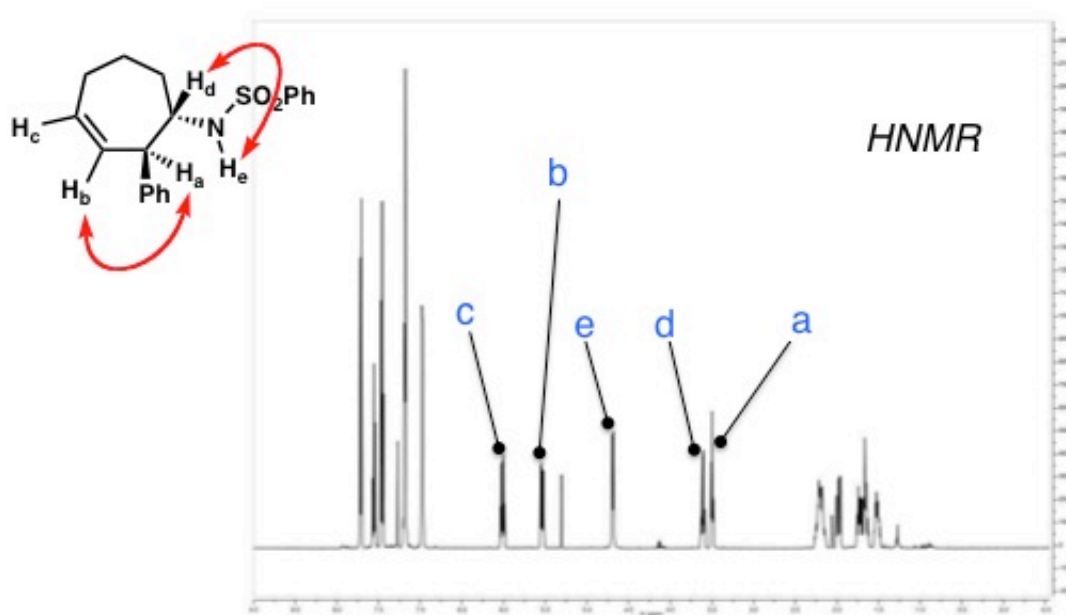


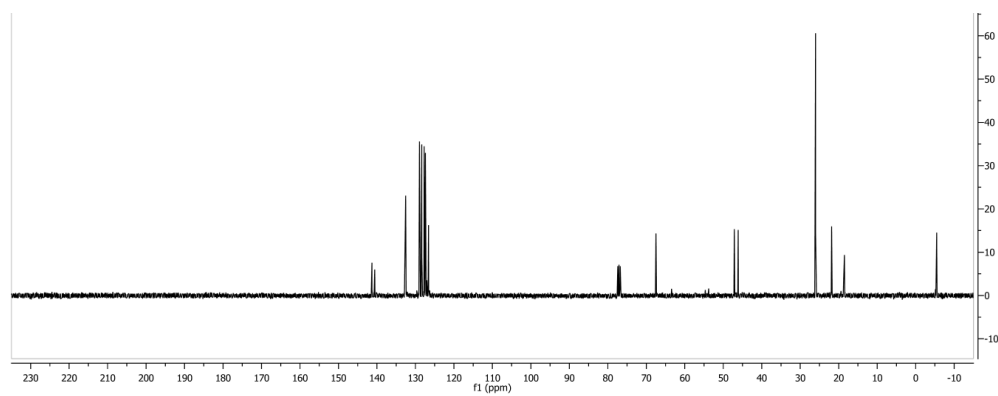
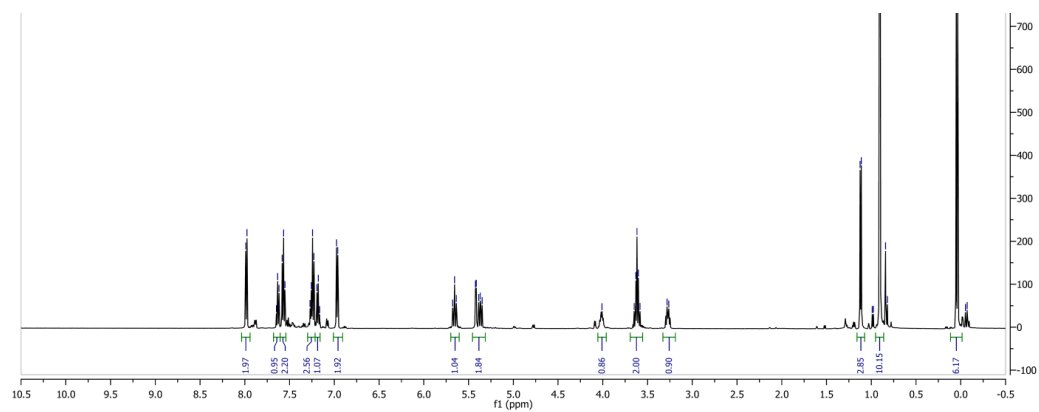
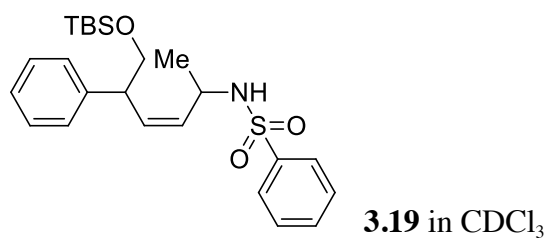


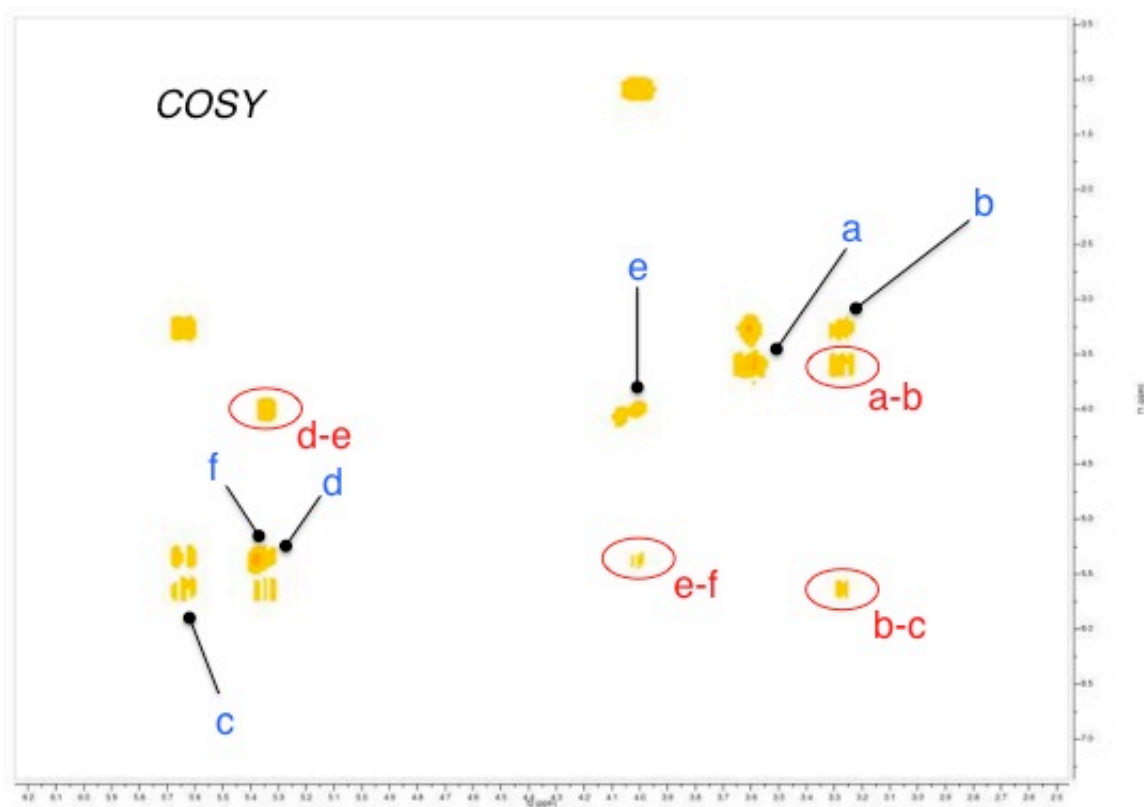
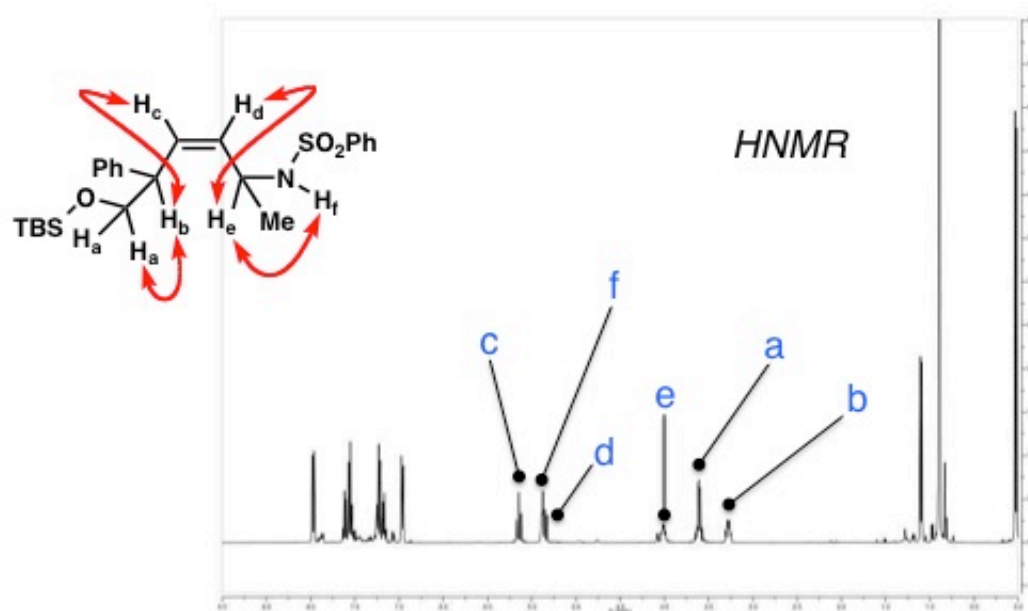


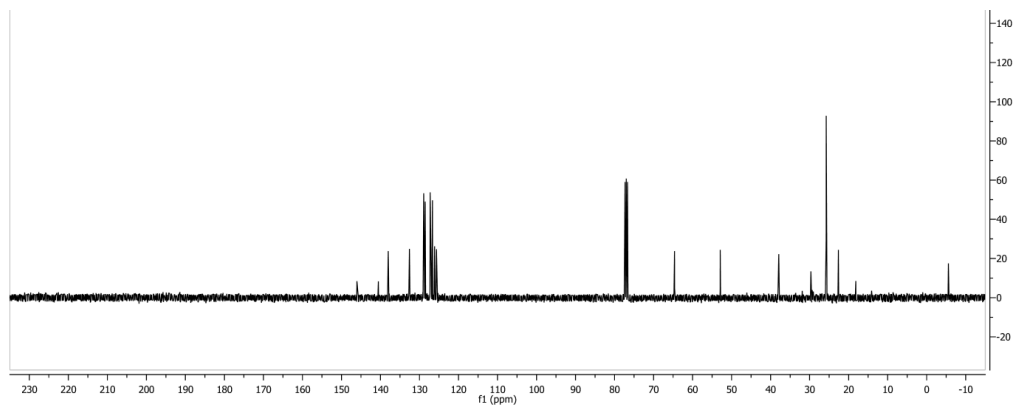
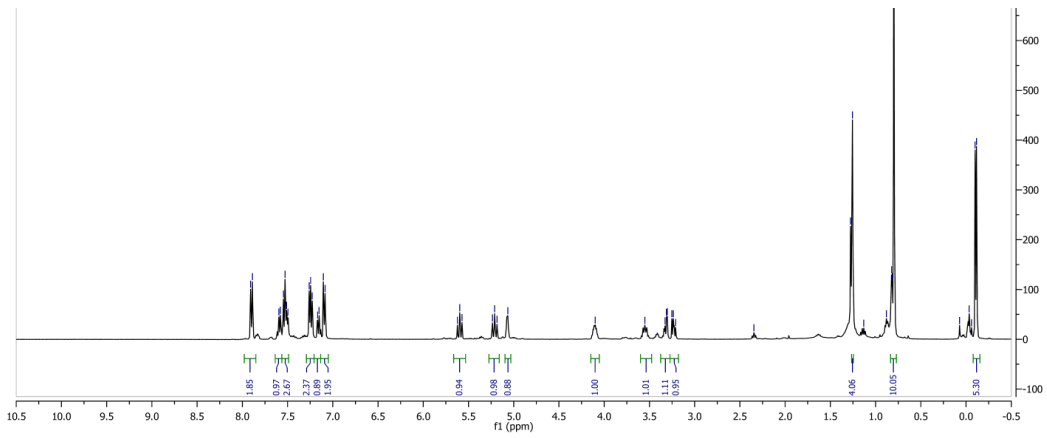
3.16g in CDCl₃ (Continued)

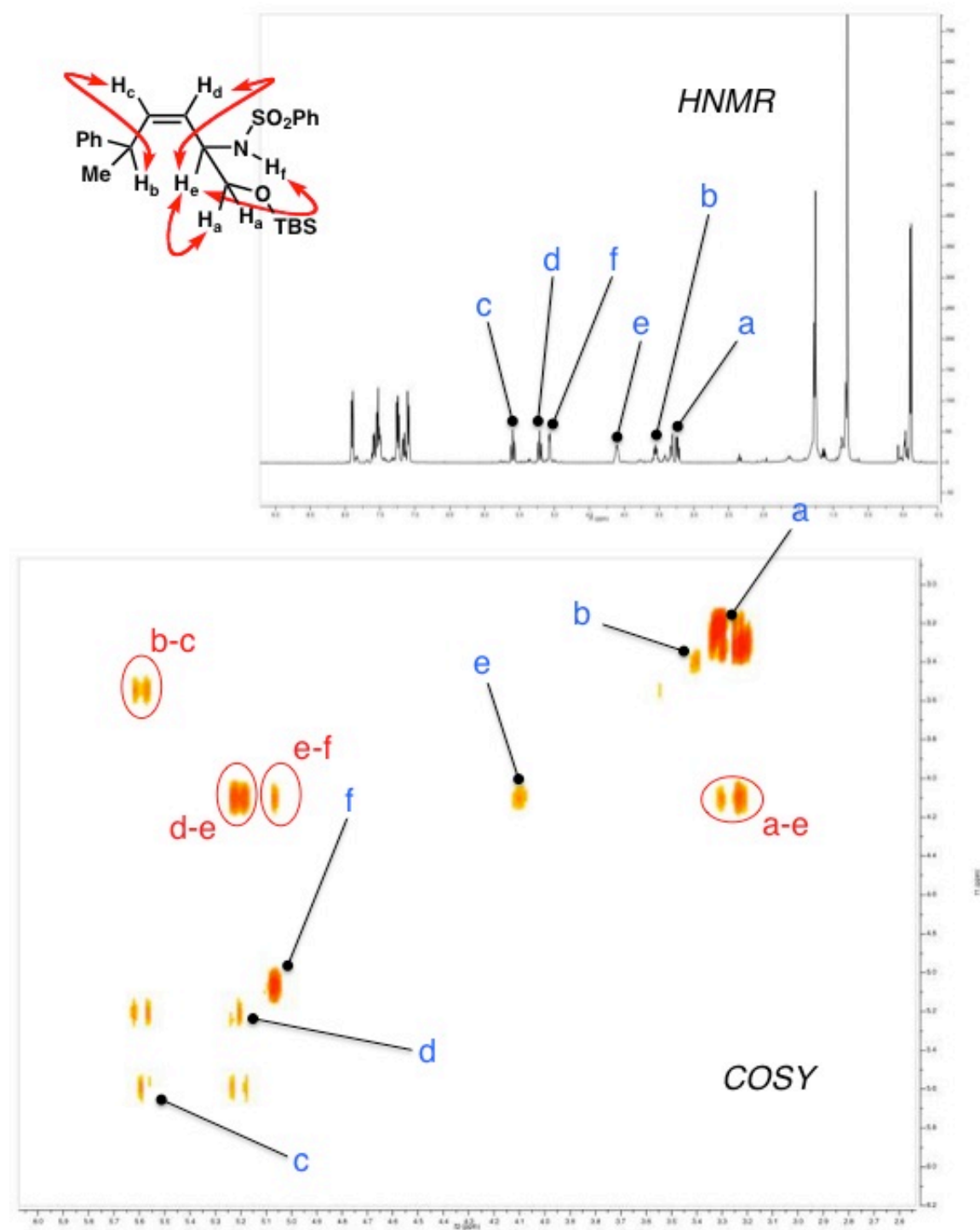






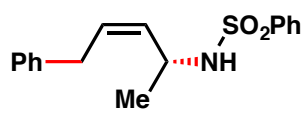






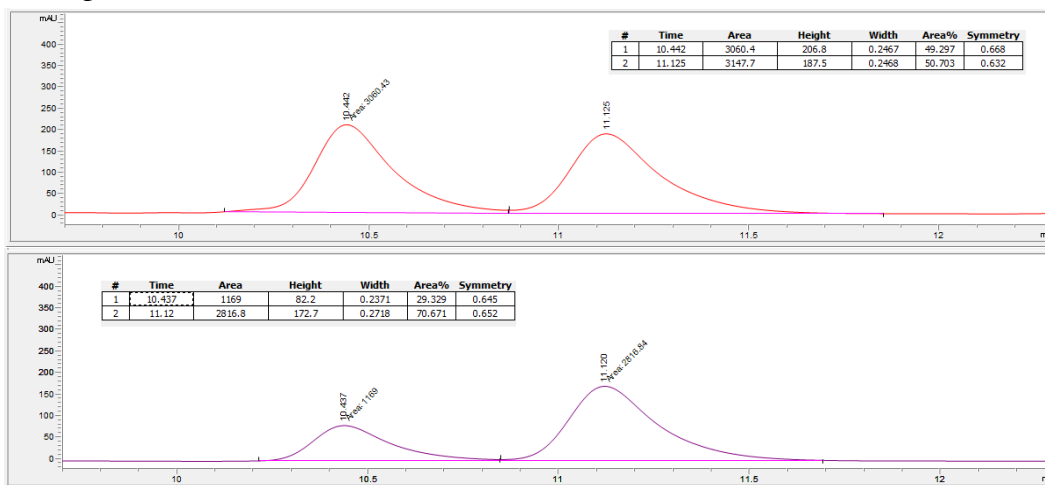
APPENDIX FIVE

HPLC Traces Relevant to Chapter Three: The Development of a Regio- and Diastereoselective Aminoarylation of Simple Dienes



3.16c

Chiralpak AD-H 70:30 IPA:Hexane 0.6 ml/min



CHAPTER FOUR

The Development of a General, Highly Selective Method for the Allylic Functionalization of Unactivated Internal Olefins

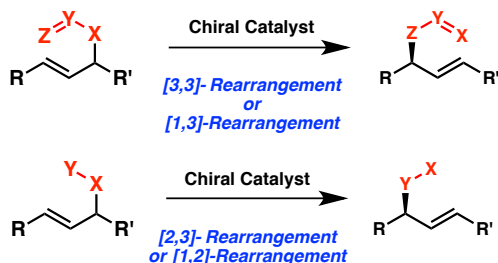
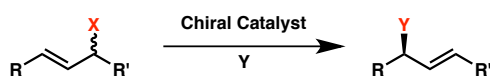
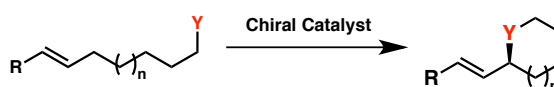
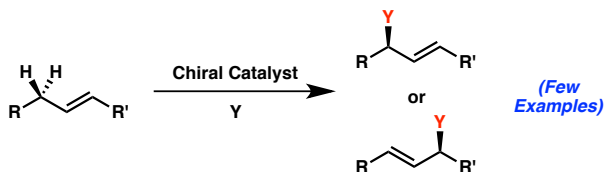
4.1. Background

4.1.1. Introduction

The stereo- and site-selective transformation of simple unsaturated hydrocarbons through allylic functionalization provides a direct path toward the construction of chiral synthons while preserving the olefin functionality as a handle for further elaboration. The advantage of this method lies in its ability to harness petrochemical feedstocks for the rapid construction of enantioenriched building blocks. As a result, catalytic enantioselective allylic functionalization has emerged as a useful synthetic tool, streamlining the production of pharmaceuticals, natural products, fine chemicals and other functional materials.¹⁻⁵

The most widely used and developed approaches for catalytic asymmetric allylic functionalization fall within four distinct categories: 1) intramolecular allylic rearrangement, 2) transition metal-mediated allylic substitution/coupling, 3) intramolecular allylic C–H functionalization, and 4) intermolecular allylic C–H functionalization (Figure 4.1.1).⁶⁻¹⁶ The first three categories rely on the presence of activating or directing groups embedded within the starting material. In these cases, chemists often find themselves in a chemical two-step of sorts, inserting and/or deleting these additional functionalities in order to obtain the final desired product.

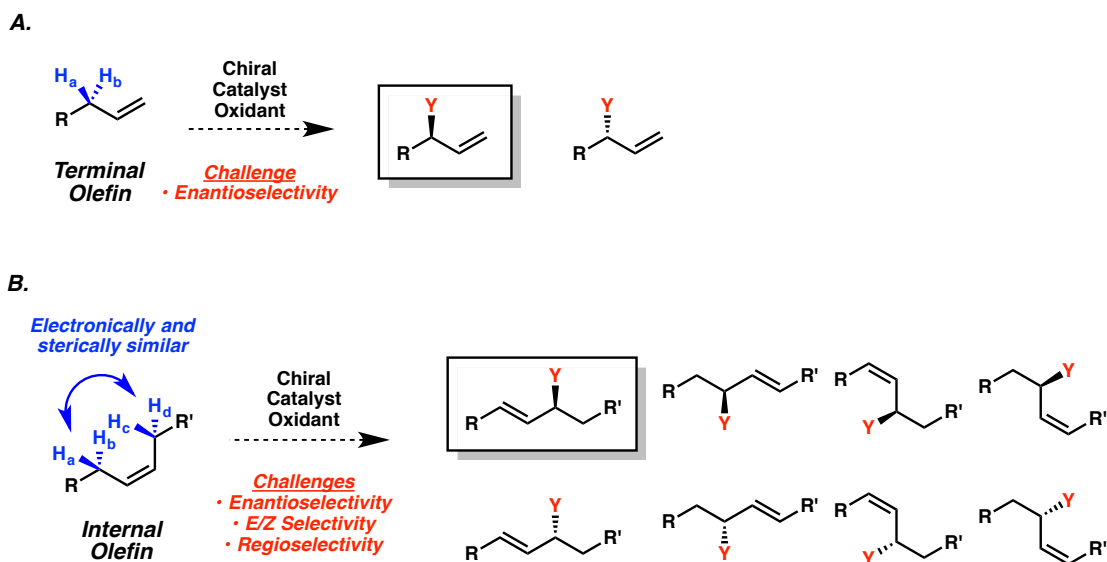
Figure 4.1.1

A. Asymmetric Intramolecular Rearrangements:**B. Asymmetric Allylic Substitutions/Couplings:****C. Asymmetric Intramolecular Allylic C-H Functionalization:****D. Asymmetric Intermolecular Allylic C-H Functionalization:**

The fourth method of allylic functionalization relies solely on the presence of an olefin moiety. Unfortunately, the vast majority of these reactions are limited in scope, requiring the use of terminal olefin starting materials.¹⁷⁻¹⁹ A general catalytic enantioselective allylic C–H functionalization of unactivated internal olefins remains a longstanding challenge in the field of synthetic chemistry.

The utility of allylic C–H functionalization for the synthesis of valuable commodities and materials relies heavily on the ability to access products with significant chemo-, regio- and stereocontrol. Unlike terminal olefins, which only contain a single set of enantiotopic allylic protons (Figure 4.1.2a), internal olefins possess two sets of protons on either side of the olefin moiety thereby posing the additional challenge of regioselectivity. Furthermore, when the resulting product is an internal olefin, the further issue of E/Z selectivity subsists (Figure 4.1.2b). The inability to control indiscriminate C–H functionalization of electronically and sterically similar allylic protons, therefore, has the potential to produce a mixture of regio-, diastereo-, and enantiomeric isomers that are difficult to separate via preparative methods.

Figure 4.1.2



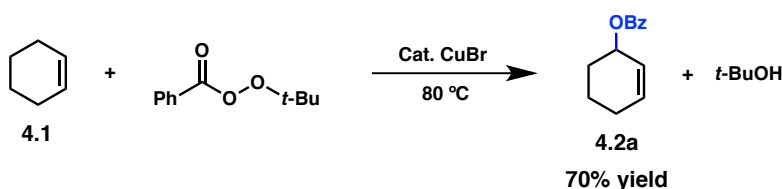
The first examples of asymmetric allylic C–H functionalization utilizing unfunctionalized internal olefins began to appear nearly three decades ago, however these chemical transformations have been largely limited to symmetrical cycloalkenes. Nonetheless, these studies provided the first insights into the difficulty of tackling stereoselective allylic C–H activation while precluding the challenges of *E/Z*- and regioselectivity.

4.1.2. Asymmetric Kharasch-Sosnovsky Reaction with Unactivated Cycloalkenes

Most notable of these advances is the copper-catalyzed enantioselective Kharasch-Sosnovsky allylic oxidation. Kharasch and Sosnovsky's initial discovery that copper(I) species catalyze the oxidation of olefins with *tert*-butyl peroxybenzoate to yield allylic benzoates (for example **4.1** to **42a**, Scheme 4.1.1) laid the groundwork for one of the most common catalytic asymmetric allylic oxidations of unactivated olefins.^{20,21} More specifically, following two seminal modest attempts at rendering this radical process

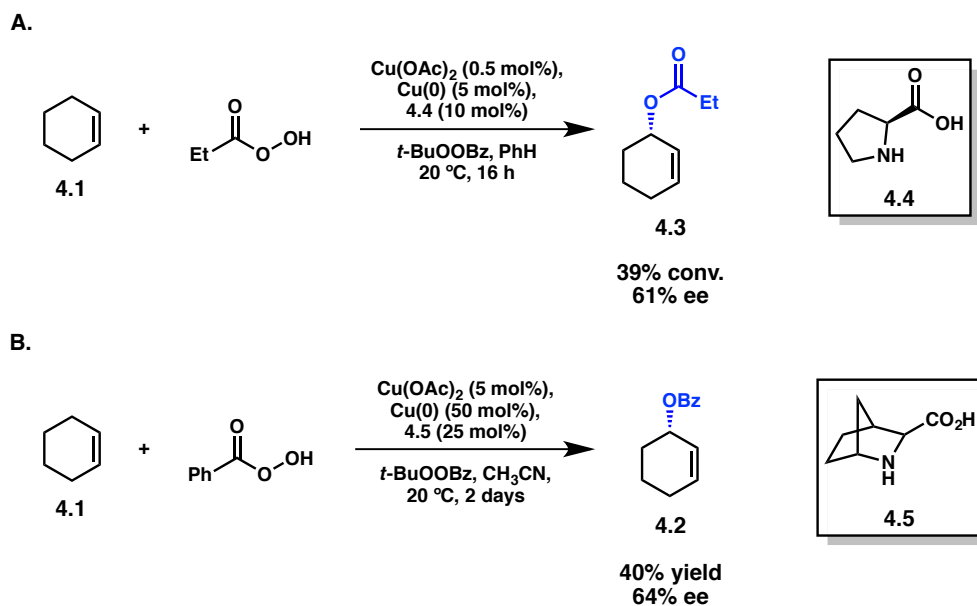
enantioselective (up to 16% ee),^{22,23} several groups reported enantioselective variants of this oxidation with unfunctionalized cycloalkenes in the 1990's.²⁴⁻³⁷ Enantioselectivity, yield and reaction time varied substantially throughout these reports and appeared to be largely dependent on ligand identity.

Scheme 4.1.1

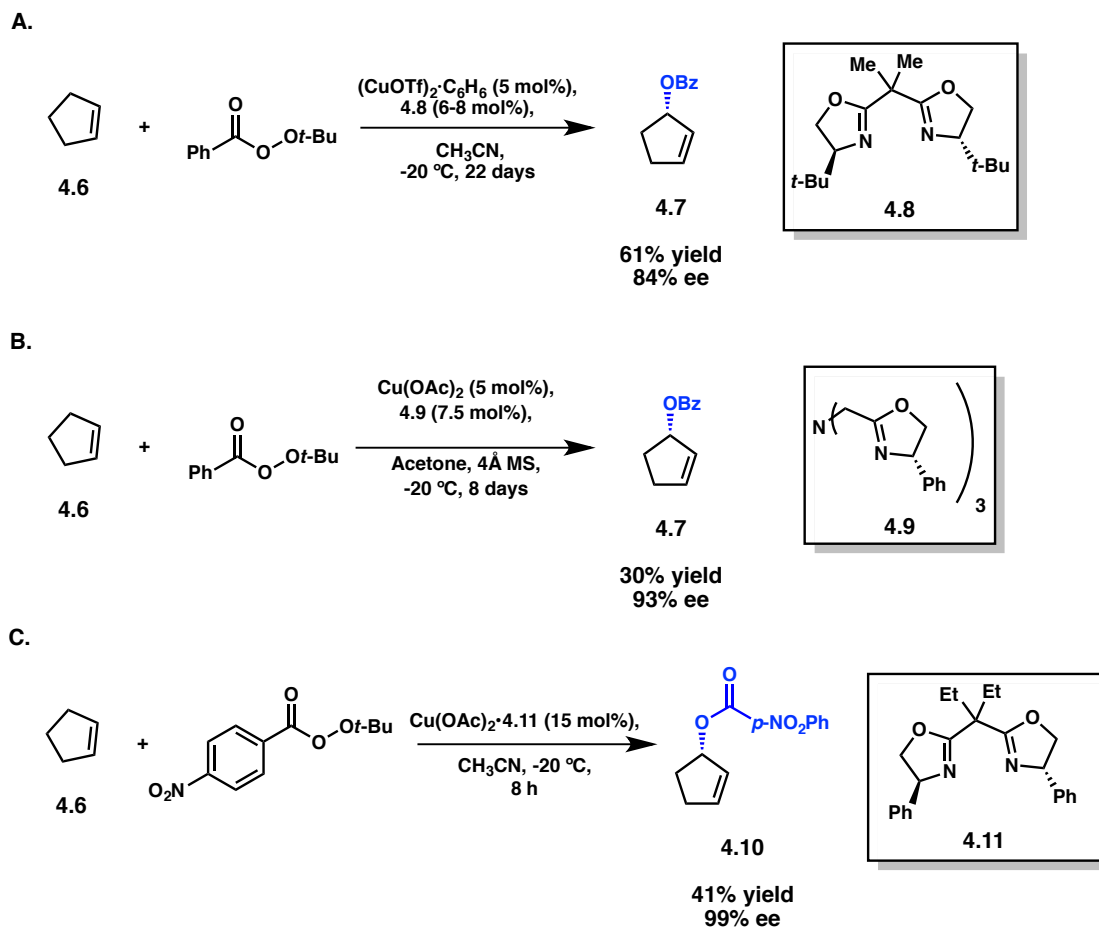


The Muzart, Andersson and Feringa labs independently explored the use of proline-based ligands for the stereoselective oxidation of cyclohexene (**4.1**) with catalytic Cu(OAc)_2 (Scheme 4.1.2).^{26,28,33,35} Andersson's bicyclic amino acid **4.5** appeared to be superior to the conventional L-proline **4.4**, exhibiting the best selectivity of the series (40% yield, 64% ee). Feringa and co workers further studied the effect of modifying **4.4** but these efforts failed to increase the enantioselectivity of this process.³⁷

Scheme 4.1.2



Scheme 4.1.3

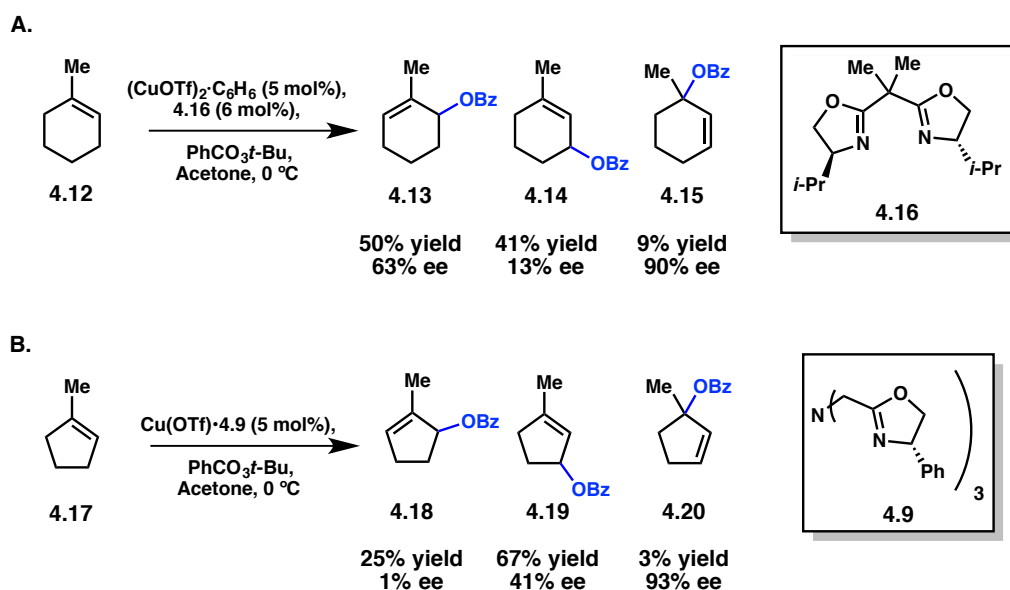


Several examples of the asymmetric Kharasch-Sosnovsky reaction have also been reported utilizing bis(oxazoline)-based ligands.^{25,29,30,32,34,38-42} One of the earliest examples originated from Pfaltz and coworkers who were able to utilize catalytic Cu(OTf) and bis(oxazoline) ligand **4.8** in the presence of *tert*-butyl perbenzoate to access benzoate **4.7** from cyclopentene (**4.6**) in 61% yield and 84% ee (Scheme 4.1.3a).²⁵ Low temperatures were necessary to obtain higher selectivity, but resulted in a slow reaction requiring 22 days to complete. Similar enantioselectivities were observed with a variety of C2-symmetric bis(oxazoline) ligands in studies conducted by numerous research groups with wide ranging reaction times and yields. Katsuki later discovered that **4.6** could be

converted to the allylic ester in 93% ee using a modified C3-symmetric tris(oxazoline) ligand **4.9** (Scheme 4.1.3b).³⁰ While various other ligand classes have been examined in the asymmetric Kharasch-Sosnovsky reaction, including bipyridines, β -pinene, and diazabis(oxazoline)-based scaffolds, bis(oxazoline) ligands have shown the highest enantioselectivity to date with ligand **4.11** leading to the formation of allylic ester **4.10** in 99% ee (Scheme 4.1.3c).^{31,43-48}

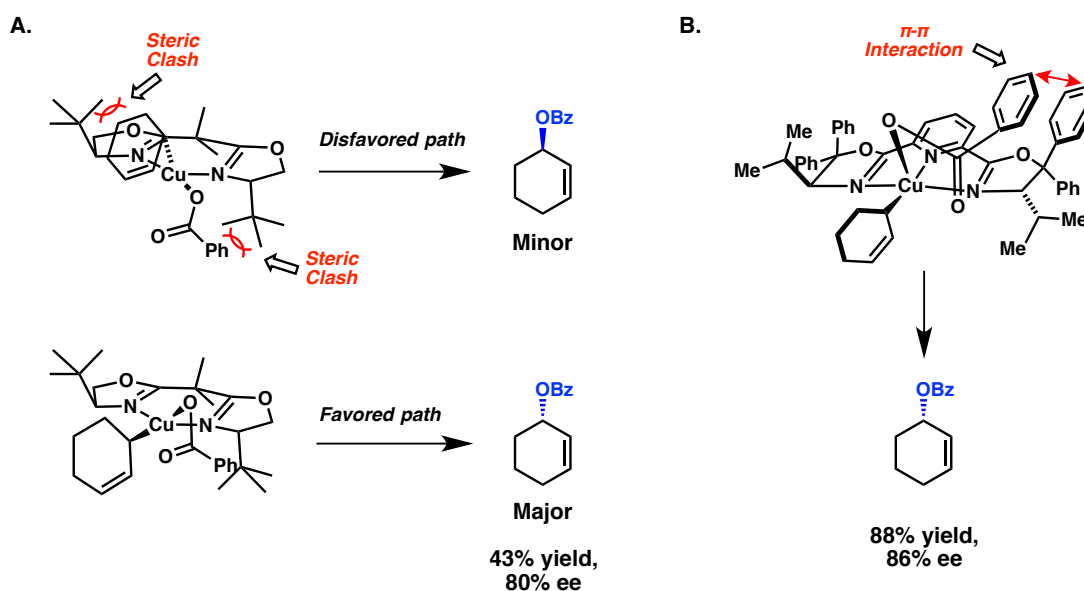
Trisubstituted olefins **4.12** and **4.17** were also investigated under various reaction conditions (Scheme 4.1.4). In all cases the secondary radical intermediate was preferentially formed over the tertiary, precluding any significant formation of **4.15** or **4.20**. Still, regioselectivity between products **4.13** and **4.14** or **4.18** and **4.19** was poor, and the enantiomeric excess varied substantially between all of the regioisomers. With regard to acyclic olefins, those surveyed in this chemistry were limited to terminal alkenes that displayed diminished enantioselectivities.^{25,30}

Scheme 4.1.4



Andrus and Singh have both offered stereoinduction models in an attempt to explain the manner by which enantioselectivity is derived (Figure 4.1.3).^{29,32} In the model proposed by Andrus, the minimization of steric interactions between the substrate, benzoate functionality, and chiral ligand dictate the substrate's approach (Figure 4.1.3a). Singh's model employing a tridentate pyridyl bis(oxazoline) ligand invokes an additional stabilizing π - π interaction between one of the phenyl groups of the chiral ligand and the aromatic functionality of the benzoate (Figure 4.1.3b). In both cases, stereochemical models account for the lowered selectivity exhibited by acyclic olefins lacking in conformational rigidity.

Figure 4.1.3

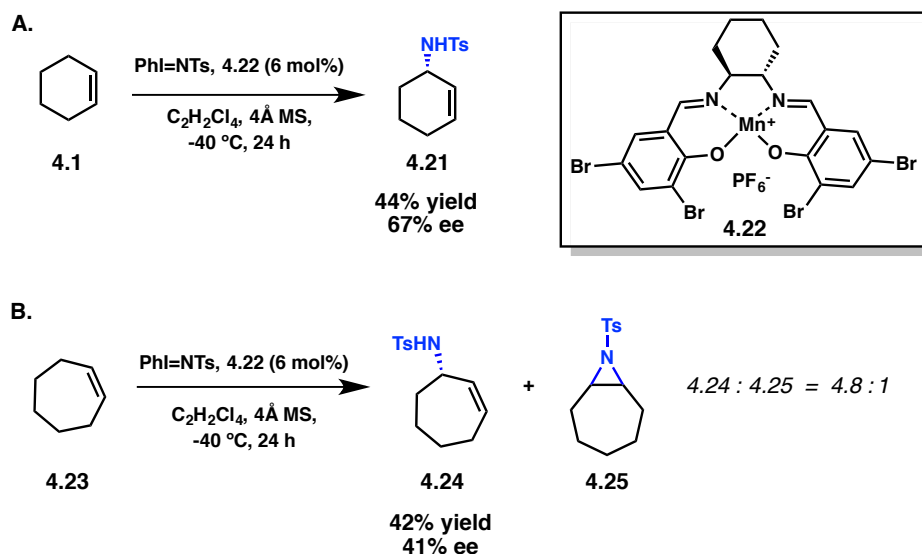


4.1.3. Asymmetric Allylic Amination of Unactivated Cycloalkenes

Despite the plethora of reports that began emerging in the 1990's for catalytic asymmetric allylic C-H esterification, the first C-H amination utilizing unactivated cycloalkenes did not appear until 2001. In the course of examining the aziridination chemistry between [N-(*p*-toluenesulfonyl)imino]phenyliodinane and cyclohexene, Katsuki discovered that various electron deficient salen-manganese(III) complexes

catalyzed the formation of C–H amination product **4.21** instead (Scheme 4.1.5).⁴⁹ While it is not uncommon for this reaction pathway to compete with aziridination, the electron deficient cationic catalyst **4.22** was particularly suited for asymmetric allylic amination, exclusively affording **4.21** in 44% yield and 67% ee (Scheme 4.1.5a). Additionally cycloheptene (**4.23**) was assayed under the reactions conditions yielding **4.24** with lower enantioselectivity and as a mixture with the corresponding aziridine byproduct **4.25** (Scheme 4.1.5b).

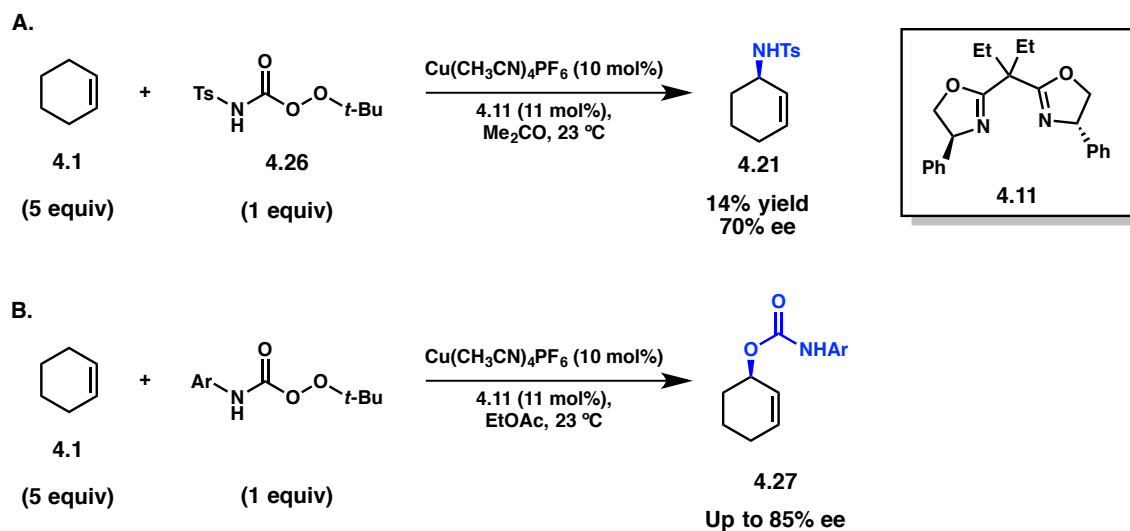
Scheme 4.1.5



Four years later the Clark lab reported a copper catalyzed allylic C–H amination that proceeded with comparable levels of enantioselectivity.⁵⁰ Inspired by a racemic report on allylic C–H amination by Katsuki and their own work in the field of asymmetric allylic oxidation, they were able to develop an enantioselective amination variant of the Kharasch-Sosnovsky reaction. With acetone as the optimal solvent, catalytic amounts of $[\text{Cu}(\text{CH}_3\text{CN})_4]\text{PF}_6$ and bis(oxazoline) **4.11** facilitated the amination of cyclohexene (**4.1**) with peroxycarbamate **4.26** to furnish allylic amination product **4.21** in up to 70% ee (Scheme 4.1.6a).

Interestingly, the identity of the peroxy-carbamate was critical for the formation of the amination product over that of the alternative oxidation product **4.27**, which was in some cases isolated exclusively. They do note, however, that the aryl carbamates of allylic alcohols undergo stereospecific rearrangement to yield the desired allylic amines. Likewise, the introduction of ligand was shown to bias reactivity toward esterification rather than the amination in some cases, suggesting that the ligand plays a crucial role in moderating the reactivity of the copper–carbamate complex prior to olefin addition.

Scheme 4.1.6

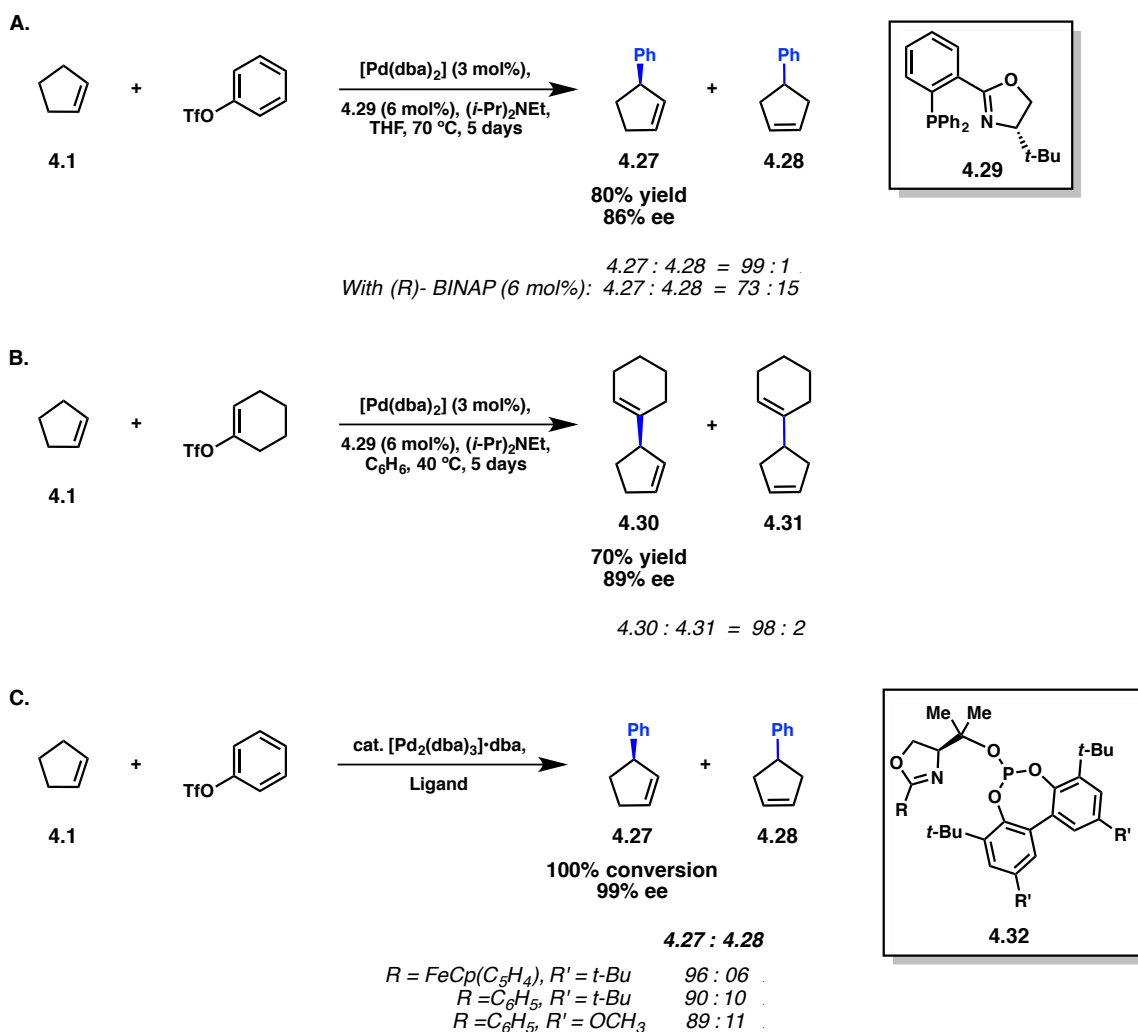


4.1.4. Enantioselective Heck Reactions with Unactivated Cycloalkenes

The asymmetric Heck reaction has garnered a lot of attention in recent years, due to the immense popularity of the robust and widely functional group tolerant racemic version of this reaction.^{51,52} This chemistry, however, is inherently more challenging for unactivated alkenes, as these substrates often suffer extensive double bond migration resulting in isomeric product mixtures. Fortunately, several research groups have been able to mitigate this problem through judicious choice of metal catalyst and ligand.

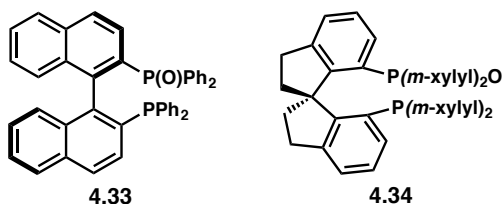
With the goal of enhancing the scope and selectivity of the asymmetric Heck reaction, Pfaltz et al. identified phosphonyldihydrooxazole **4.29** as a suitable ligand for the palladium-catalyzed coupling of cycloalkenes with aryl and vinyl triflates (Scheme 4.1.7a).²⁷ Among these substrates, cyclopentene afforded enantioenriched products **4.27** and **4.30** when coupled with phenyl triflate and 1-cyclohexenyl triflate respectively. The Heck products were formed preferentially to isomerization byproducts **4.28** and **4.31** when ligand **4.29** was used in contrast to (R)-BINAP. Subsequent to Pfaltz's findings, additional studies with P-N ligands identified biaryl phosphite-oxazoline **4.32** as the optimal ligand scaffold for the formation of **4.27** (Scheme 4.1.7c).⁵³⁻⁵⁵

Scheme 4.1.7



Whereas BINAP failed to suppress disadvantageous double bond migration in Heck reactions with unactivated cycloalkenes, (R)-BINAP-monooxide (**4.33**), a common contaminant produced when palladium(II) acetate is reduced with BINAP, was revealed to be a competent ligand for this process (Figure 4.1.4). In Oestreich's studies **4.33** outcompeted (R)-BINAP for the formation of **4.27**, suppressing alkene migration and providing enhanced enantioselectivities up to 86% ee.⁵⁶ Later, the Zhou group improved upon the yield and selectivity when spirocycle **4.34** was used as a ligand.⁵⁷ The effectiveness of this chemistry was highlighted through the Heck coupling of a variety of aromatic systems to **4.1** with excellent yields and levels of stereinduction (73% yield, 98% ee for **4.27**).

Figure 4.1.4

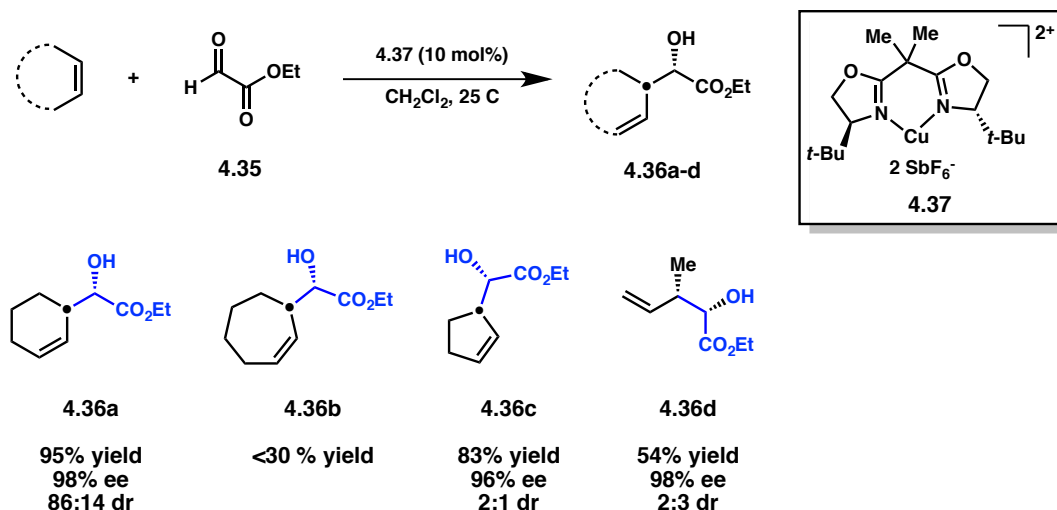


4.1.5. Enantioselective Ene Reactions of Glyoxylates

The Lewis acid catalyzed enantioselective hetero-ene reaction between glyoxylate esters and unfunctionalized olefins, first examined by the Evans group, represents one of the earliest advances in the asymmetric functionalization of internal unactivated olefins.⁵⁸⁻

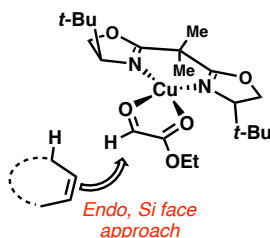
⁶¹ Various cationic copper(II)-bis(oxazoline) catalysts were investigated for their ability to catalyze the formation of α -hydroxy esters with both 1,1- and 1,2-disubstituted olefins. Copper complex **4.37** reacted smoothly with ethyl glyoxylate **4.35** and cyclohexene (**4.1**), for example, to provide α -hydroxy ester **4.36a** in great yield and with exquisite enantioselectivity (Scheme 4.1.8).

Scheme 4.1.8



X-ray crystallography and calculation studies of $[\text{Cu}((\text{S,S})\text{-}t\text{-Bu-BOX})(\text{glyoxylate})]^{2+}$ indicate that the catalyst takes on a distorted square planar geometry with glyoxylate **4.35** (Figure 4.1.5). This conformation provides insight into the controlling factors that govern stereoselectivity, as the flanking *t*-butyl groups of the ligand both block the *Re* face approach of the enophile and sterically disfavor the *exo* transition state.

Figure 4.1.5



In non-coordinating solvents various unfunctionalized internal olefins furnished products in up to 98% ee and modest diastereoselectivity (**4.36a-d**). Even acyclic *cis*-2-

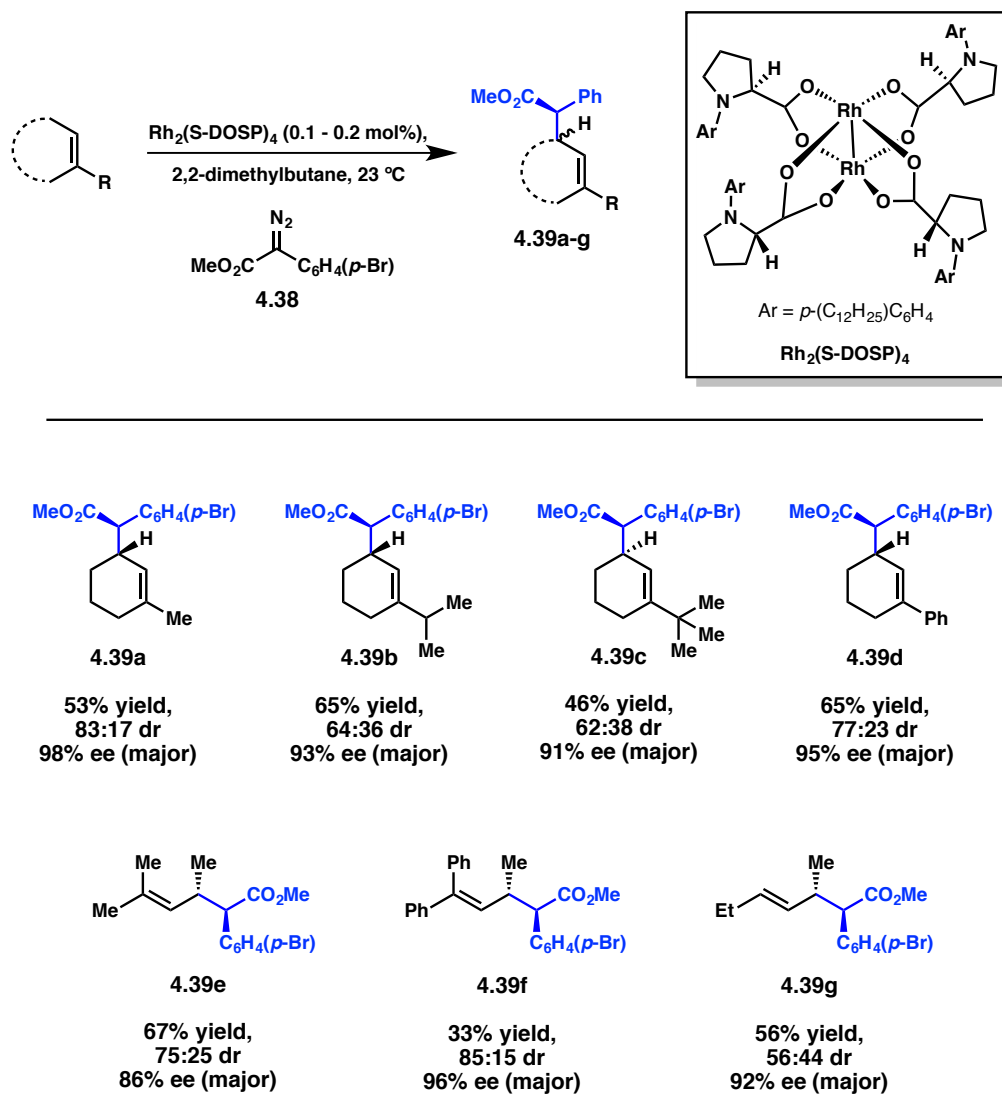
butene produced α -hydroxy ester **4.36d** with comparable enantioselectivity to the structurally rigid cycloalkenes. Interestingly, this trend did not extend to cycloheptene, which failed to afford synthetically useful yield under any of the conditions screened. Since this initial discovery by Evans, a palladium(II) catalyzed version of this reaction has also been developed.⁶²

4.1.6. Enantioselective Allylic Alkylation of Unactivated Olefins with Donor/Acceptor Stabilized Carbenoids

Site selective carbenoid C–H functionalization has emerged as one of the most effective ways of accessing new C–C bonds in unactivated substrates with impressive regio- and stereoselectivity.^{63,64,6} Around the same time as Müller's initial report of an acceptor/acceptor substituted carbenoid for moderately enantioselective allylic C–H alkylations, Davies began to explore this mode of C–H functionalization with donor/acceptor stabilized carbenoids.⁶⁵⁻⁷⁰ To his success, the $\text{Rh}_2(\text{DOSP})_4$ catalyzed decomposition of aryldiazoacetates has become one of the most selective methods for $\text{C}(\text{sp}^3)\text{--H}$ functionalization.

In 2001 Davies reported a catalytic asymmetric allylic C–H activation to access γ,δ -unsaturated esters, providing an alternative route to Claisen rearrangement products (Scheme 4.1.9).⁶⁹ The donor/acceptor stabilized carbenoids resulted in enhanced stability and chemoselectivity toward the C–H functionalization product over the alternative cyclopropanation pathway. A variety of substituted cyclohexenes were smoothly alkylated in the presence of catalytic D_2 -symmetric $\text{Rh}_2(\text{S-DOSP})_4$ and **4.38** (**4.39a-d**) revealing high levels of regioselectivity as a result of steric and electronic bias. Enantioselectivity was generally high, even when acyclic internal olefins were used (**4.39e-g**), however the diastereomeric ratios varied substantially with some dropping as low as 1.3:1 in response to changing steric environments.

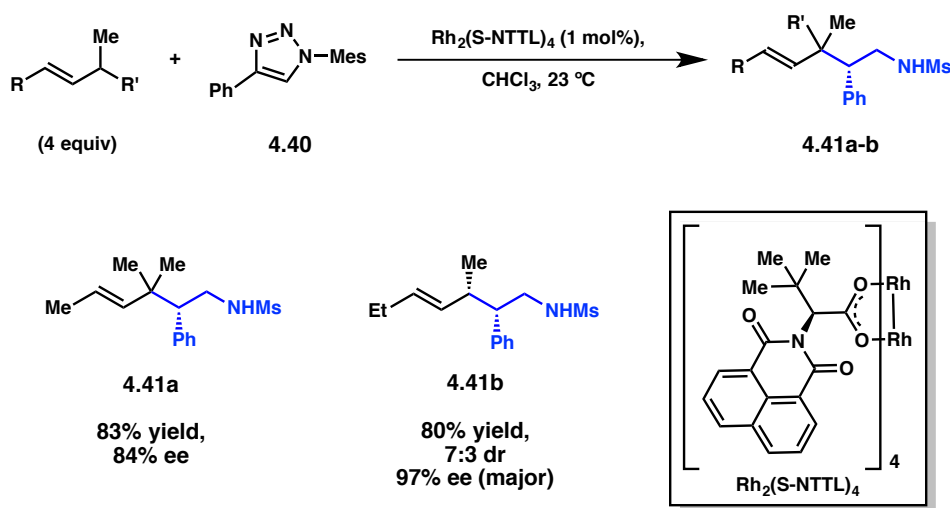
Scheme 4.1.9



Recently, Davies reported a new method for accessing C–H functionalized products similar to **4.39e-g** with increased selectivity (Scheme 4.1.10).⁷⁰ N-Sulfonyl-1,2,3-triazole **4.40** generates a donor/acceptor carbene with chiral rhodium(II) catalyst $\text{Rh}_2(\text{S-NTTL})_4$ that exhibits increased regio-, diastereo- and enantioselectivity for allylic alkylation. Though only four examples are described, the conversion of acyclic olefins to **4.41a-b**

represents two of the most selective direct allylic alkylations of unactivated acyclic internal alkenes to date.

Scheme 4.1.10



4.1.7. Conclusions

Recent advances in catalytic enantioselective allylic C–H oxidation, amination and alkylation of unactivated internal olefins have begun to address the long list of selectivity issues encountered when utilizing unsaturated hydrocarbons. These powerful strategies have provided chemists with the ability to directly access value-added products from relatively inexpensive and abundant starting materials. Despite these innovations, few examples of selective allylic C–H functionalization utilizing acyclic systems have been demonstrated, and are largely limited to allylic alkylation chemistry. More significantly, enantioselective intermolecular allylic C–S bond formation of unactivated internal olefins remains limited to the use of non-catalytic systems employing chiral auxiliaries.

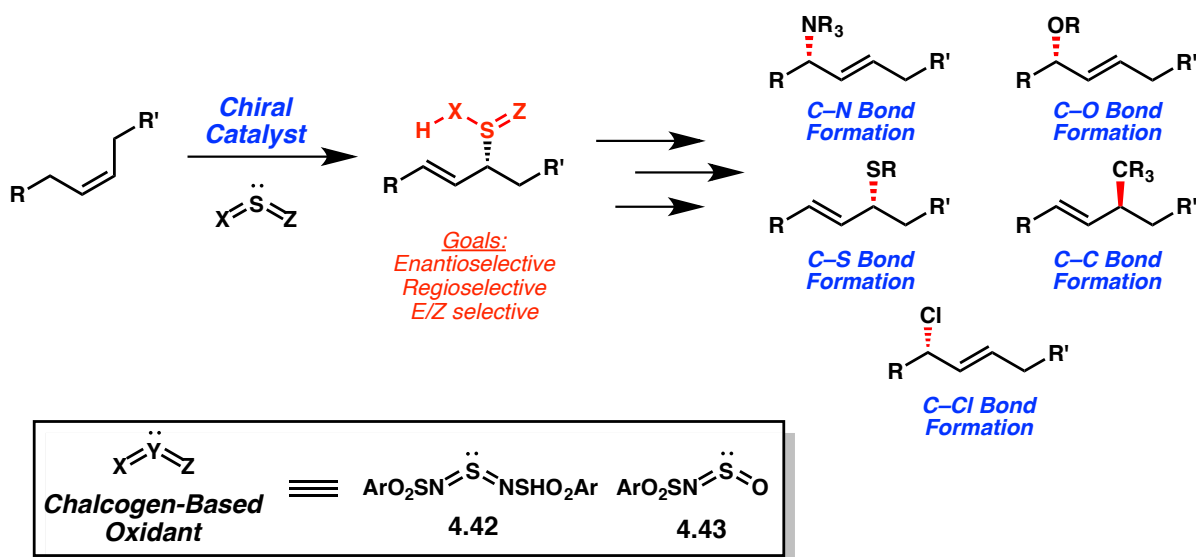
4.2. The Development of a Catalytic Highly Selective Allylic Oxidation of Unactivated Internal Olefins

4.2.1. Strategy and Choice of Oxidant

Our studies initiated with the ultimate goal of developing a general platform for the construction of chiral olefinic building blocks from inexpensive commodity olefins. To this aim, we set out to develop a catalytic enantioselective hetero-ene reaction that would provide access to a multifunctional intermediate capable of stereospecific differentiation toward a variety of products (Figure 4.2.1). This strategy would provide chemists with the ability to selectively introduce allylic C-N, C-O, C-S, C-C, and C-Cl bonds, enabling rapid library synthesis of analogous enantioenriched products.

While most examples of asymmetric allylic oxidation necessitate the use of terminal olefins or functionalized internal olefins to direct regioselectivity, our approach would instead exploit the inherent regioselective bias of the oxidant. Initial reports of chalcogen-based oxidants for the racemic allylic oxidation of unfunctionalized internal olefins indicated that this class of enophile might serve as suitable starting point for this strategy.⁷¹⁻⁸¹ More specifically, we were drawn to sulfurimide and sulfurdiimide reagents **4.42** and **4.43** due to the robust trends in regioselectivity exhibited by these oxidants with unfunctionalized internal olefins.

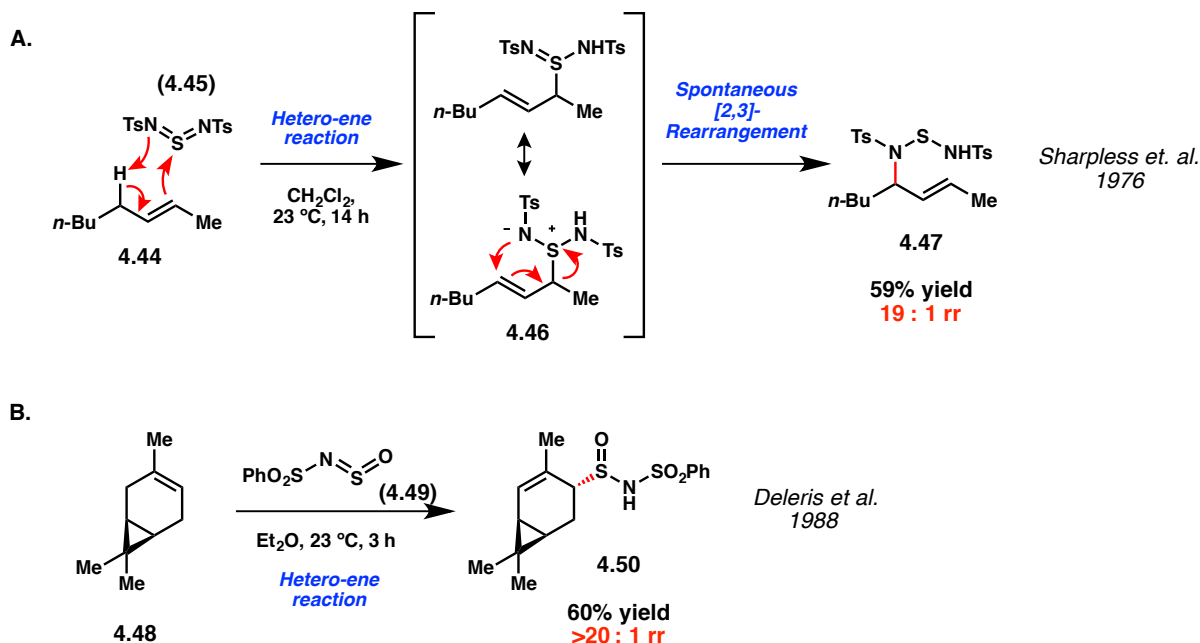
Figure 4.2.1



Determining the exact identity of the chalcogen-based oxidant was a critical step in the development of this novel approach to the stereoselective allylic oxidation of internal olefins. While our previous studies in allylic alkylation utilized enophiles akin to **4.42**, Sharpless has shown that the ene adduct generated between internal olefin **4.44** and sulfur diimide **4.45** spontaneously undergoes [2,3]-rearrangement to afford **4.47** (Scheme 4.2.1a).⁷¹ While this reagent is robust and highly regioselective, the facile [2,3]-rearrangement precludes the capability to diversify the resulting ene adducts.

In contrast, sulfurimide reagent **4.49** is reported to be less reactive than the analogous diimide reagent and ene adducts generated from this oxidant are stable to thermal [2,3]-rearrangement, as exemplified by the isolation of allylic sulfinimides like **4.50** (Scheme 4.2.1b).⁷⁸ Moreover, sulfurimide-based reagents **4.43** contain both nitrogen and oxygen moieties on the central sulfur atom providing the opportunity for C-N or C-O bond formation through divergent [2,3]-rearrangements.

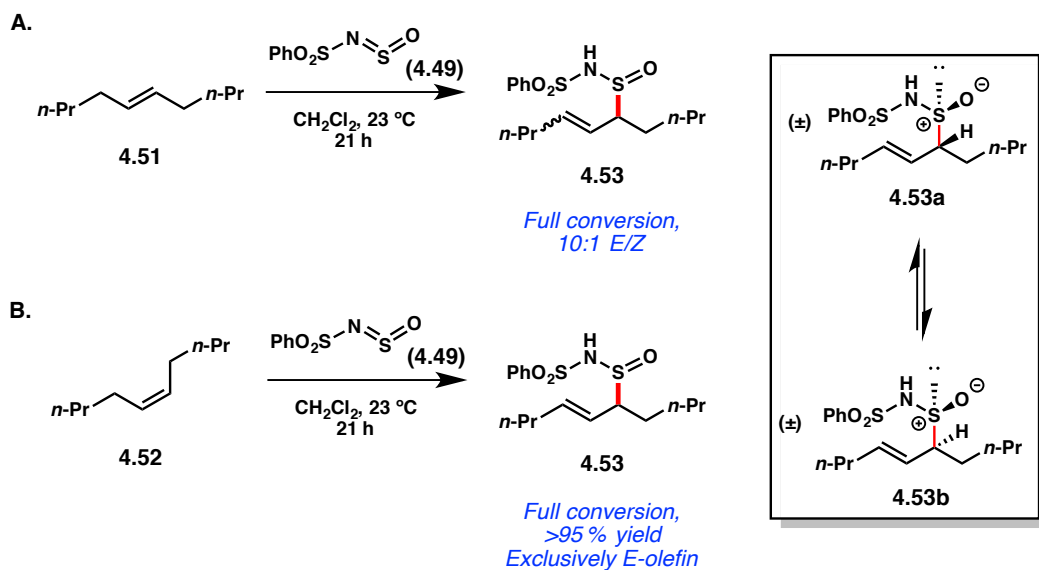
Scheme 4.2.1



4.2.2. Optimization of a Catalytic Enantioselective Hetero-Ene Reaction with *Cis*-5-Decene

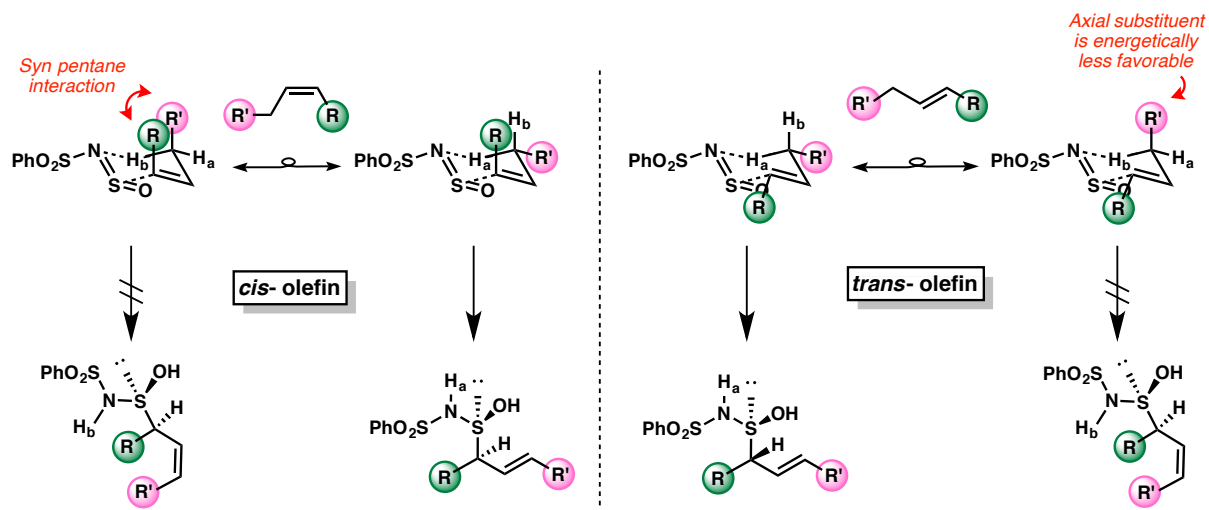
The reactivity of sulfurimide **4.49** was assessed thermally with both *trans*- and *cis*-5-decene (**4.51** and **4.52** respectively) to provide allylic sulfinimide **4.53** (Scheme 4.2.2). With *trans*-5-decene **4.51** the product was isolated as a 10:1 mixture of *E/Z*-isomers (Scheme 4.2.2a), however *cis*-5-decene **4.52** cleanly provided ene adduct **4.53** as a single olefin isomer in quantitative yield (Scheme 4.2.2b). Although the ene adduct of **4.52** was isolated initially in a 5:1 mixture of epimers at sulfur (majorly **4.53a**) 5 hours into the reaction, this mixture equilibrated over several hours to a 1.2:1 mixture of **4.53a**/**4.53b**.

Scheme 4.2.2



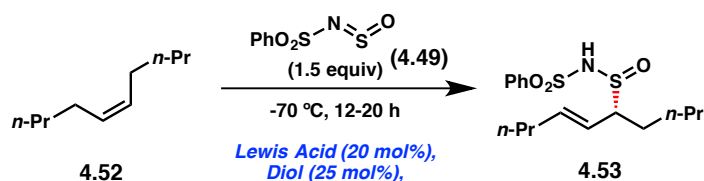
Under thermal conditions *trans*-5-decene **4.51** and *cis*-5-decene **4.52** provided opposite major diastereomers. Additionally, in both cases the product was formed predominantly as the *E*-olefin isomer. These observations can be rationalized on the basis of disfavored steric interactions in an *endo* closed transition state (Figure 4.2.2).

Figure 4.2.2



With a better understanding of the inherent reactivity and selectivity of **4.49** established, we sought to identify reaction conditions that would shut down the background hetero-ene reaction with **4.52** and instead allow for a chiral Lewis acid complex to mediate the formation of allylic oxidation product **4.53** (Table 4.2.1). At -70 °C in CH₂Cl₂ product failed to form in any significant amount (entry 1). When strong Lewis acids such as TiCl₄, and SnCl₄ were added to the reaction, allylic sulfinimide **4.53** was produced with some catalyst turnover. In comparison, at 20 mol% loading SbCl₅ afforded the product in only 17% yield (entries 2-4).

Table 4.2.1



Entry	Lewis Acid	Diol	Solvent	% Yield	Enantiomeric Ratio
1	–	–	CH ₂ Cl ₂	<5	–
2	TiCl ₄	–	CH ₂ Cl ₂	33	–
3	SnCl ₄	–	CH ₂ Cl ₂	35	–
4	SbCl ₅	–	CH ₂ Cl ₂	17	–
5	TiCl ₅	(R)-BINOL	CH ₂ Cl ₂	24	56.5 : 43.5
6	SnCl ₄	(R)-BINOL	CH ₂ Cl ₂	29	57 : 43
7	SbCl ₅	(R)-BINOL	CH ₂ Cl ₂	75	84 : 16
8 ^a	SbCl ₅	(R)-BINOL	CH ₂ Cl ₂	88	86.5 : 13.5
9 ^a	SbCl ₅	(R)-BINOL	PhMe	17	88.5 : 11.5
10 ^a	SbCl ₅	(R)-BINOL	PhMe/CH ₂ Cl ₂ (2:1)	84	90 : 10
11 ^{a,b}	SbCl ₅	(R)-BINOL	PhMe/CH ₂ Cl ₂ (2:1)	55	90 : 10
12 ^{a,c}	SbCl ₅	(R)-BINOL	PhMe/CH ₂ Cl ₂ (2:1)	82	90 : 10

Reaction conditions. Cis-5-decene (1 equiv), sulfinimide reagent **4.49** (1.5 equiv), solvent (0.13M), Lewis acid (20 mol%), (R)-BINOL (25 mol%). Yields were determined by ¹HNMR using DMB as an internal standard. [a] 0.5 equiv trifluoroacetic acid added to reaction. [b] 10 mol% SbCl₅ and 25 mol% (R)-BINOL was used instead. [c] 40 mol% SbCl₅ and 25 mol% (R)-BINOL was used instead.

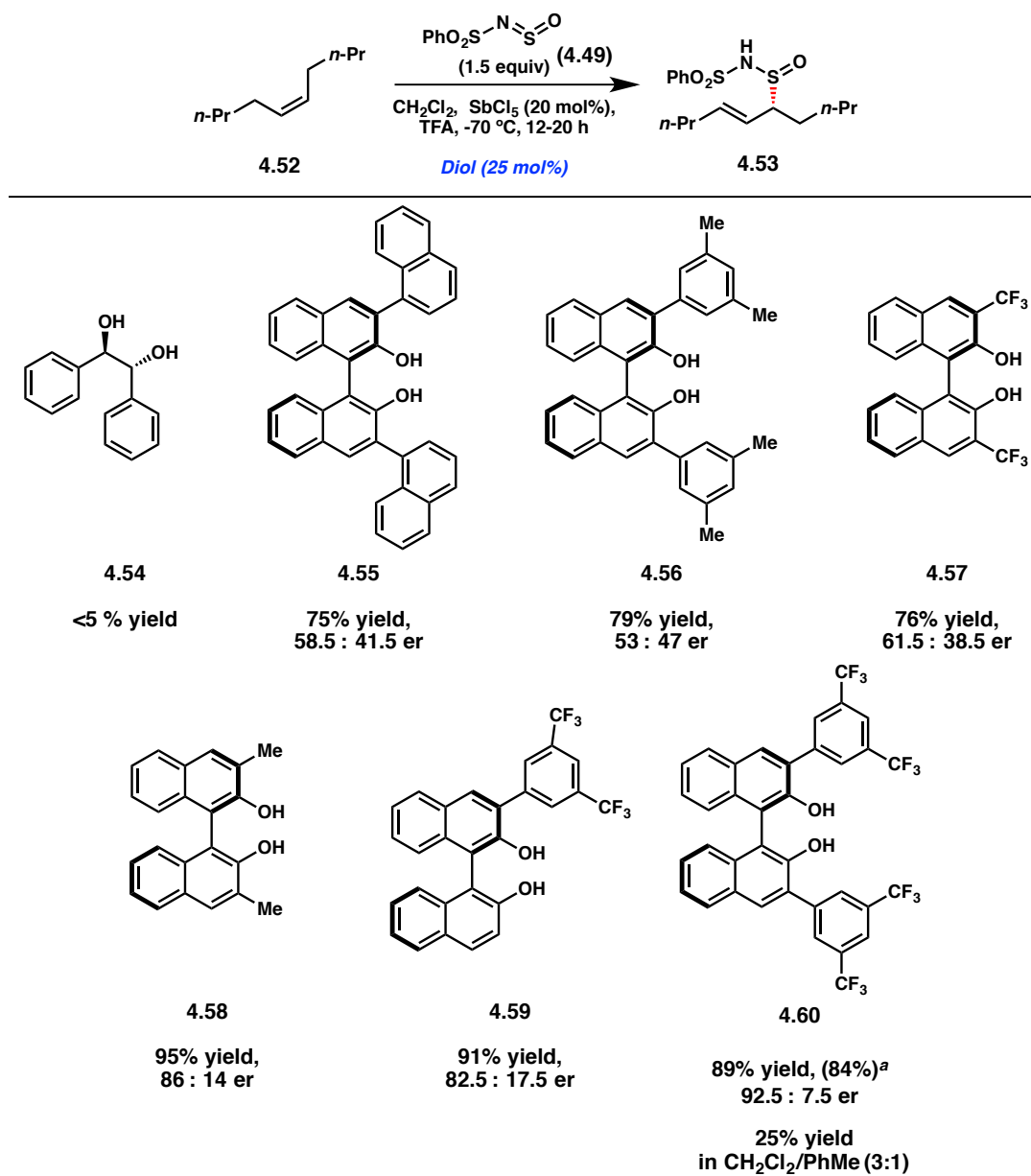
The addition of a coordinating diol, (R)-BINOL, diminished the yield of allylic oxidation product **4.53** when tin or titanium catalysts were used (entries 5 and 6). To our surprise, in the presence of (R)-BINOL the antimony-catalyzed process was not only amplified, but **4.53** was formed with moderate enantiomeric enrichment (entry 7). When 50 mol% of trifluoroacetic acid (TFA) was dosed into the reaction the overall yield was enhanced (entry 8).

Next, we surveyed the effect of solvent identity on the catalytic hetero-ene reaction. While the conversion of *cis*-5-decene **4.52** to sulfinimide **4.53** was highest yielding in CH₂Cl₂, we noticed a slight boost in enantioselectivity when PhMe was used as solvent, albeit at greatly diminished yield (entry 9). In this case, sulfurimide **4.49** was largely insoluble in PhMe, resulting in a sluggish reaction with *cis*-5-decene **4.52**. Fortunately, a 2:1 ratio of PhMe and CH₂Cl₂ provided a favorable environment for both solubility and selectivity, affording ene adduct **4.53** in 84% yield and 90:10 enantiomeric ratio (er) using (R)-BINOL (entry 10). When the amount of Lewis acid was decreased in the 2:1 PhMe/CH₂Cl₂ solvent mixture a corresponding decrease in yield was observed (entry 11). In contrast, increasing SbCl₅ catalyst loading to 40 mol% did not result in any significant change in yield or er (entry 12).

An extensive study of the diol-based co-catalyst followed, providing substantial yield and er disparities throughout the entire series (Table 4.2.2). Most notably, in the absence of the 1,1'-binaphthyl backbone the reaction failed to proceed (**4.54**). Several coordinating diols bearing sterically and electronically varied 3,3'-substituents gave similar yield and enantiomeric enrichment despite these differences (**4.55-4.57**). Of the series, derivatives **4.58-4.60** provided allylic sulfinimide **4.53** in high yield and increased enantiomeric ratios, with diol **4.60** providing the best selectivity at 92.5:7.5 er. Under these optimized conditions the product was isolated in 84% yield with complete *E*-olefin selectivity and a >20:1 initial ratio of epimers at sulfur. It is important to note that even a minimal amount of PhMe in the solvent composition resulted in a significantly diminished yield and was therefore excluded from the reaction when **4.60** was used as the

coordinating diol (25% NMR yield in 3:1 CH₂Cl₂/PhMe). This observation suggests that the 3,3'-aryl substituents assist in enantiodiscrimination by partaking in some form of electrostatic π -interaction that is precluded when aromatic solvent is added.^{82,83}

Table 4.2.2

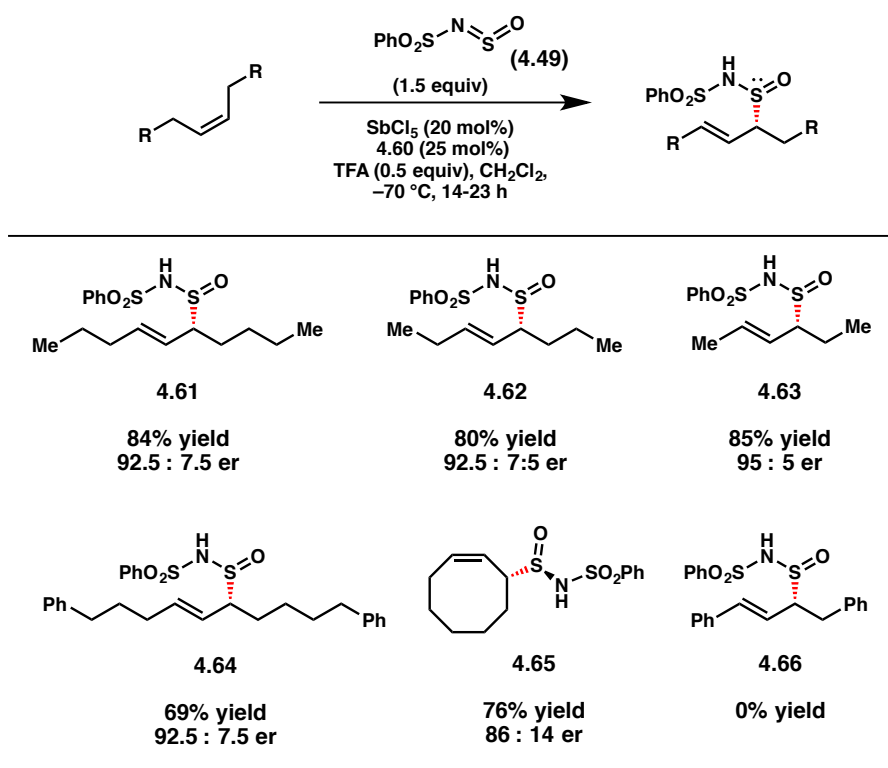


Reaction conditions. *Cis*-5-decene (1 equiv), sulfurimide reagent **4.49** (1.5 equiv), CH₂Cl₂ (0.13M), SbCl₅ (20 mol%), diol (25 mol%), trifluoroacetic acid (0.5 equiv). Yields were determined by ¹HNMR using DMB as an internal standard. [a] Isolated yield.

4.2.3. Substrate Scope and Trends in Regioselectivity

With an optimized system for the enantioselective, *E/Z*-selective and diastereoselective construction of allylic sulfinimides in hand, we explored the potential of this strategy with a series of symmetrical unsaturated hydrocarbons (Table 4.2.3). Acyclic *cis*-internal olefins with varying chain length and functionality all afforded the oxidized product **4.53** with comparably good yield and stereoinduction (**4.61–4.64**) representing the most general strategy for this class of substrate to date. Cycloalkene **4.65** was generated with lower enantiomeric excess than its acyclic counterparts, presumably due to unfavorable steric interactions encountered with more rigid cyclic olefins. Interestingly, the sulfur stereocenter was stable and did not epimerize in this product. Unfortunately, ene adduct **4.66** was not produced under these reaction conditions, suggesting that allyl arenes in general may not be suitable substrates for this chemistry.

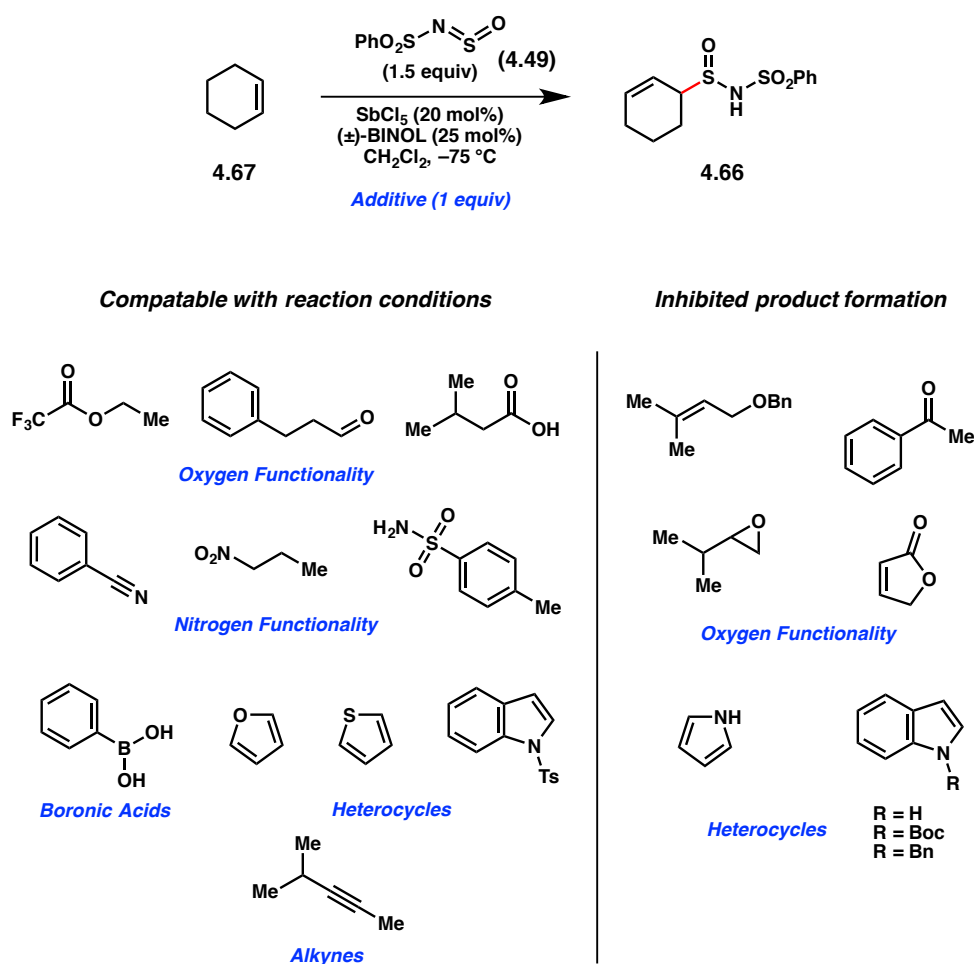
Table 4.2.3



Reaction conditions. *Cis*-5-decene (1 equiv), sulfinamide reagent **4.49** (1.5 equiv), CH₂Cl₂ (0.13M), SbCl₅ (20 mol%), diol **4.60** (25 mol%), trifluoroacetic acid (0.5 equiv). Reported as isolated yields.

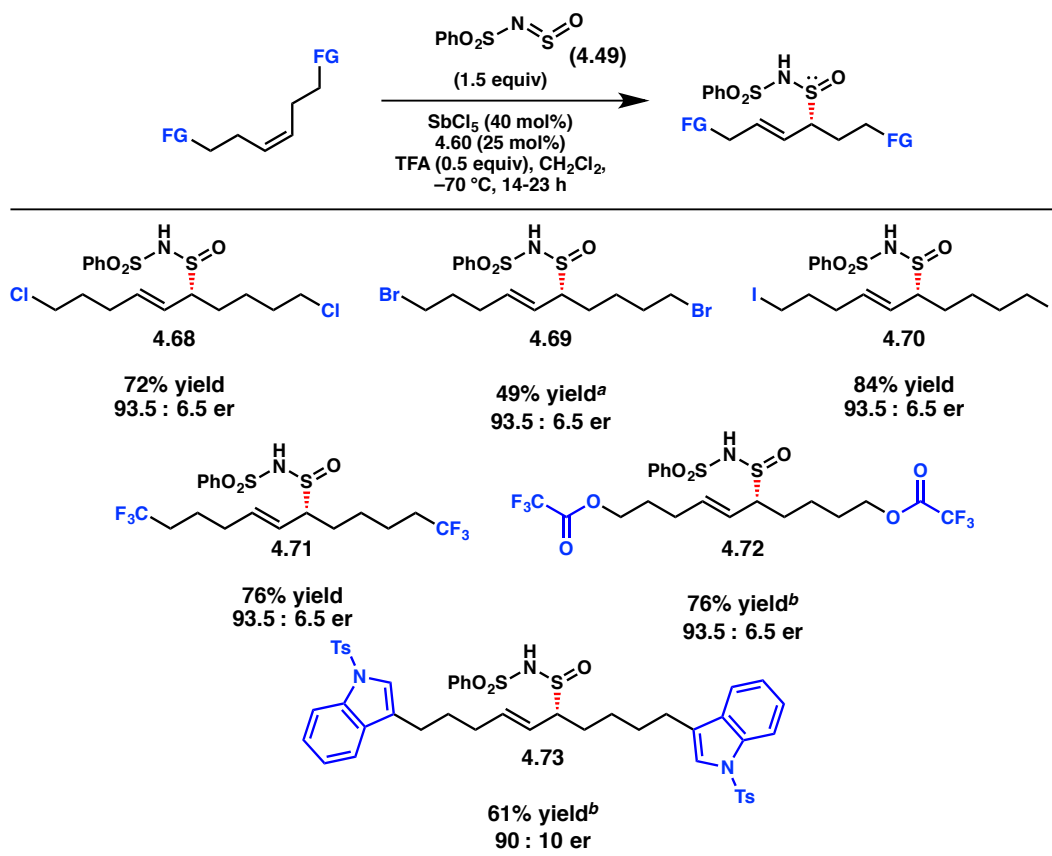
In addition, we were interested in determining the functional group tolerance of this chemistry in order to expand its synthetic utility to more complex settings. A qualitative functional group compatibility screen was initiated monitoring for the formation of ene adduct **4.66** from cyclohexene **4.67** under simplified racemic conditions (Table 4.2.4).⁸⁴ Gratifyingly, a wide variety of functionalities were tolerated under the reaction conditions, including compounds that are not traditionally compatible with strong Lewis acid conditions. In addition to oxygen, nitrogen, heterocycle and boron functionality, interestingly an alkyne was tolerated in this reaction and did not compete with cyclohexene **4.67** for reaction with sulfurimide **4.49**.

Table 4.2.4



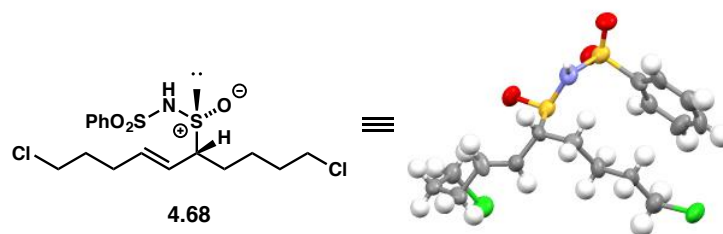
We decided to test functional group tolerance within the optimized reaction conditions by synthesizing a variety of symmetrical substrates bearing heteroatom functionality (Table 4.2.5). Increased loadings of SbCl_5 to 40 mol% was necessary to maintain synthetically useful yields, with the exception of **4.69** which appeared to provide relatively similar yields regardless of Lewis acid loading. Halogen functionality was tolerated across the board (**4.68–4.71**) providing exceptional enantioselectivity. The absolute configuration of products generated from *cis*-olefins was confirmed through X-ray crystallographic analysis of the major diastereomer formed initially for allylic oxidation product **4.68** (Figure 4.2.3). Likewise, trifluoroacetate- and indole-containing substrates provided enantioenriched allylic sulfinimides **4.72** and **4.73** respectively, further confirming the utility of this chemistry within more complex chemical settings.

Table 4.2.5



Reaction conditions. *Cis*-5-decene (1 equiv), sulfurimide reagent **4.49** (1.5 equiv), CH_2Cl_2 (0.13M), SbCl_5 (20 mol%), diol **4.60** (25 mol%), trifluoroacetic acid (0.5 equiv). Reported as isolated yields. [a] 20 mol% SbCl_5 was used. [b] Yields were determined by ^1H NMR using DMB as an internal standard.

Figure 4.2.3



We chose sulfurimide reagent **4.49** because we thought it was uniquely suited to address the long-standing issue of regioselectivity with unfunctionalized internal olefins. As a proof of concept, we assessed the inherent regioselectivity of the asymmetric allylic oxidation with a series of unsymmetrical olefins (Table 4.2.6). While altogether the yields of **4.74-4.8** were lower in comparison to symmetrical substrates, these reactions proceeded with complete regioselectivity in addition to *E/Z*-, diastereo- and enantioselectivity. For instance, when a substrate presents the choice between a proton belonging to a methylene and methine, the oxidant preferentially abstracts the less hindered proton (entry 1, **4.74**). Conversely, when the choice lies between methylene and methyl protons the internal olefin product is predominant (entries 2-4, **4.75-4.77**). Consequently, as a result of the oxidant's predilection for abstracting methylene protons over that of methyl and methine protons, terminal olefin **4.78** was isolated in low yield (again as a single regioisomer) (entry 5). In these instances (R)-BINOL provided superior stereoselectivity in comparison to diol **4.60**.

Table 4.2.6

$ \begin{array}{c} \text{R}-\text{CH}_2-\text{CH}=\text{CH}-\text{R}' \\ \xrightarrow[\text{SbCl}_5 \text{ (20 mol\%)}]{\text{PhO}_2\text{S}-\text{N}=\text{S}=\text{O} \text{ (4.49) (1.5 equiv)}} \\ \text{4.60 or (R)-BINOL (25 mol\%)} \\ \text{TFA (0.5 equiv)} \\ \text{Solvent, } -70^\circ\text{C, 14-23 h} \\ \text{R}-\text{CH}=\text{CH}-\text{CH}_2-\text{CH}(\text{R}')-\text{S}(\text{O})_2\text{Ph} \end{array} $					
Entry	Internal Olefin	Allylic Oxidation Product	Yield (%)	Enantiomeric Ratio Regioisomeric Ratio	Compound #
1 ^a			68	96 : 4 > 20 : 1	4.74
2 ^b			54	90 : 10 > 20 : 1	4.75
3 ^b			61	89.5 : 10.5 > 20 : 1	4.76
4 ^b			63	88.5 : 11.5 > 20 : 1	4.77
5 ^a			21	87.5 : 12.5 > 20 : 1	4.78

Reaction conditions. *Cis*-5-decene (1 equiv), sulfurimide reagent **4.49** (1.5 equiv), solvent (0.13M). Yields were determined by isolated yield. [a] Reaction run with **4.60** as the diol in CH₂Cl₂ [b] Reaction run with (R)-BINOL as the diol in PhMe/CH₂Cl₂ (2:1).

In the course of our studies we realized that olefins disfavored the catalytic hetero-ene reaction when flanked by electronic perturbing substituents such as a chloride (Table 4.2.7, entry 1). This raised the question as to whether or not regioselective bias between two methylene protons existed when subtle electronic differences were present. To our satisfaction, allylic sulfonimide **4.79** was accessed as a single regioisomer favoring the hetero-ene reaction with the distal allylic protons. However, this inductive effect is markedly less effective when employing bis-homoallylic chlorides, as exhibited by the

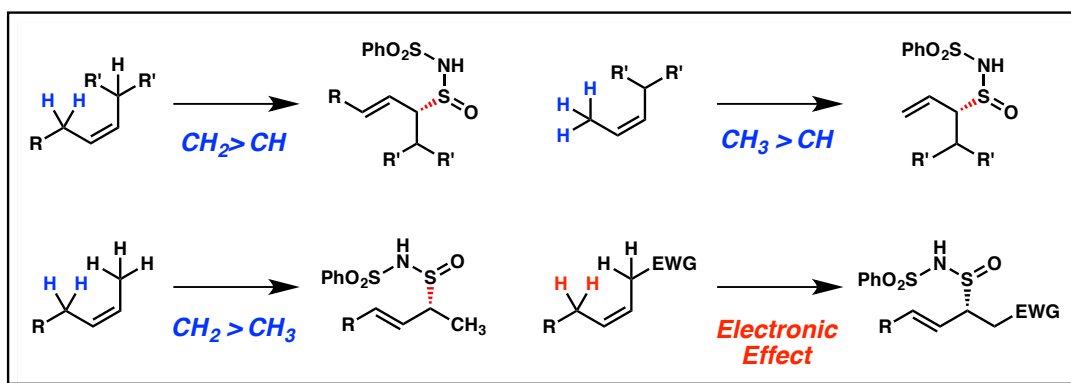
poor regioselectivity for **4.80** (entry 3). Nevertheless, these reactions still provided the allylic sulfenimides with excellent enantiomeric enrichment. Taken altogether, our synthetic studies have revealed a robust set of rules that predict regioselectivity with this catalytic system (Figure 4.2.4).

Table 4.2.7

Entry	Internal Olefin	Allylic Oxidation Product	Yield (%)	Enantiomeric Ratio Regioisomeric Ratio	Compound #
1			0	—	—
2			59 ^a	93 : 7 > 20 : 1	4.79
3			62	96 : 4 1.2 : 1	4.80

Reaction conditions. *Cis*-5-decene (1 equiv), sulfurimide reagent **4.49** (1.5 equiv), CH₂Cl₂ (0.13M), SbCl₅ (40 mol%), diol **4.60** (25 mol%). Reported as isolated yields. [a] Yield was determined by ¹HNMR using DMB as an internal standard.

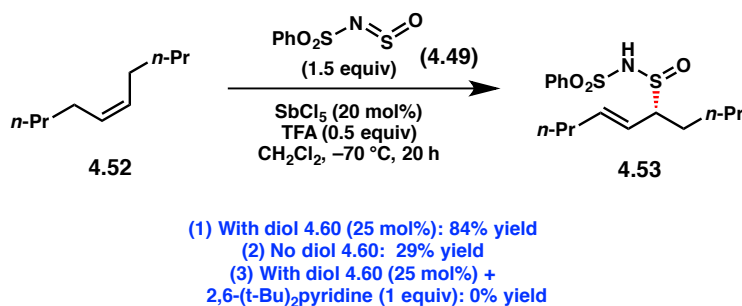
Figure 4.2.4



4.2.4. Mechanistic Insight Into the Catalytic Asymmetric Allylic Oxidation of Unfunctionalized Olefins

Our findings that a catalytic antimony-BINOL system effects remarkably pronounced enantio-, regio-, diastereo- and *E*-olefin selectivity in the hetero-ene reaction between sulfurimide **4.49** and simple acyclic internal olefins prompted us to better understand the mechanism by which this selectivity is derived. The observation that the yield of decene-derived sulfinimide **4.53** is markedly diminished in the absence of diol **4.60** suggests that the diol plays a greater role in promoting the catalytic reaction rather than serving as merely a chiral ligand to antimony (Scheme 4.2.3). We attribute this enhanced reactivity to the Lewis acid-assisted Brønsted acidity (LBA) of BINOL, a concept pioneered by the Yamamoto group.⁸⁵⁻⁹¹ The addition of sterically hindered base, 2,6-di-*tert*-butylpyridine (which does not exhibit any interaction with SbCl₅ via low temperature ¹H NMR analysis at -30 °C) shut down the allylic oxidation entirely, further endorsing the LBA-based mechanism.

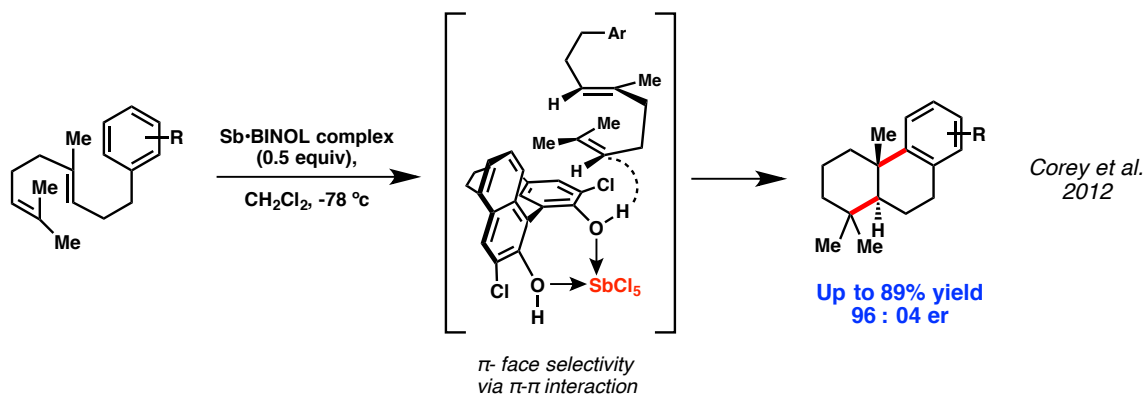
Scheme 4.2.3



One other report utilizing this form of catalysis was disclosed by the Corey group for an enantioselective polycyclization of polyenes (Scheme 4.2.4).⁹² Coordination of the Lewis acid to the BINOL co-catalyst restricts the orientation of the diol and further acidifies these protons therefore creating a chiral source of proton. In this chemistry they attribute π -face selectivity to a π - π interaction between the developing cation of the olefin

and the BINOL backbone.

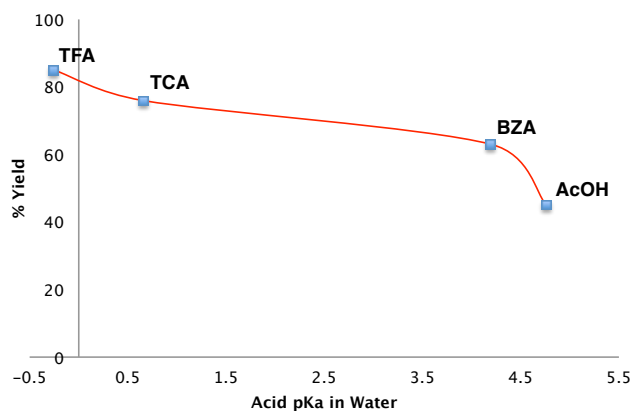
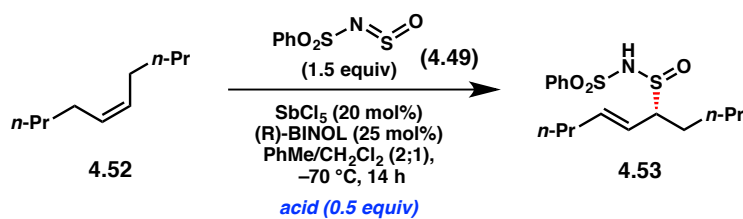
Scheme 4.2.4



The role of the acid additive was further investigated (Scheme 4.2.5). When TFA was substituted with an acid of lower pK_a value a corresponding decrease in yield was observed. The difference between the acidity of TFA and acetic acid (AcOH) provided a 40% difference in yield of sulfinimide **5.53** with (R)-BINOL as the diol co-catalyst. Interestingly, the enantiomeric ratio of the product was not affected. Based on this, we believe that the function of the acid additive is to stabilize the protonated form of the LBA complex and prevent its decomposition.

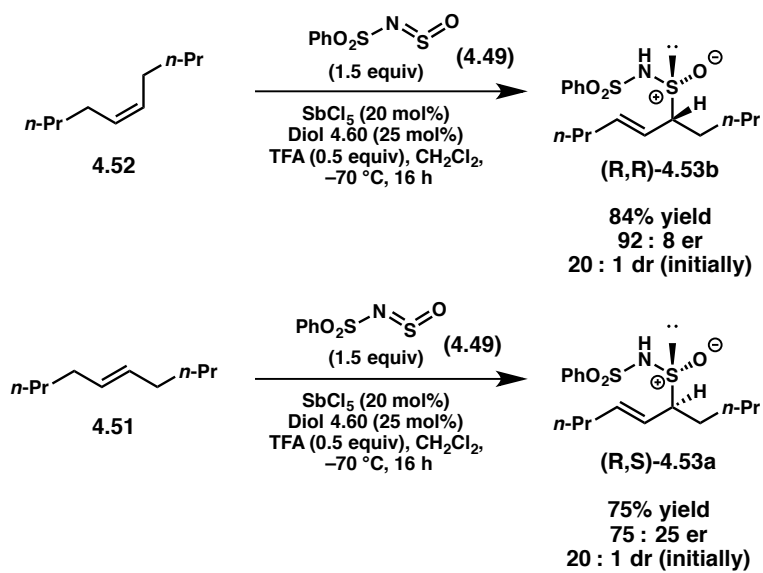
In addition to the difference in reactivity and enantioselectivity exhibited between *cis*- and *trans*-5-decene (**4.52** and **4.51** respectively), each substrate yielded different diastereomeric forms of **4.53** (Scheme 4.2.6). Moreover, the major diastereomer in each case was opposite to that of the corresponding thermal products. Finally, unreacted **4.52** under the optimized reaction conditions did not appear to have isomerized to the more stable *trans*- isomer. This data altogether suggests that this reaction proceeds through a closed transition state with sulfinimide **4.49**.

Scheme 4.2.5



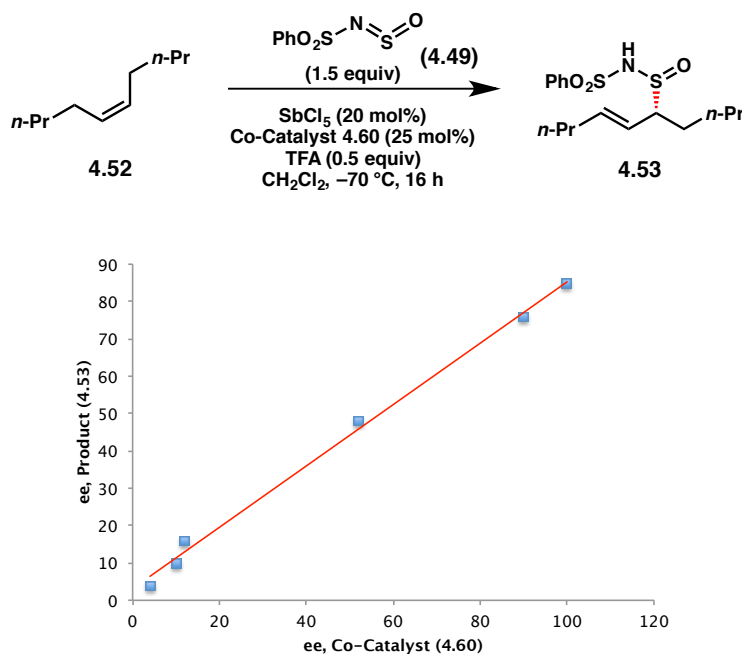
Reaction conditions. *Cis*-5-decene (1 equiv), sulfur ylide reagent (1.5 equiv), solvent (0.13M), SbCl_5 (20 mol%), (R)-BINOL (25 mol%), acid (0.5 equiv). Yields were determined by ^1H NMR using DMB as an internal standard.

Scheme 4.2.6



In an effort to better understand the identity of the active catalyst complex facilitating this oxidation, we conducted a non-linear effect study of the enantiomeric composition of co-catalyst **4.60** and the resulting product **4.53** (Scheme 4.2.7). The outcome of this study indicated a linear relationship, which suggests a 1:1 stoichiometry between **4.60** and the olefin substrate in the transition state.

Scheme 4.2.7

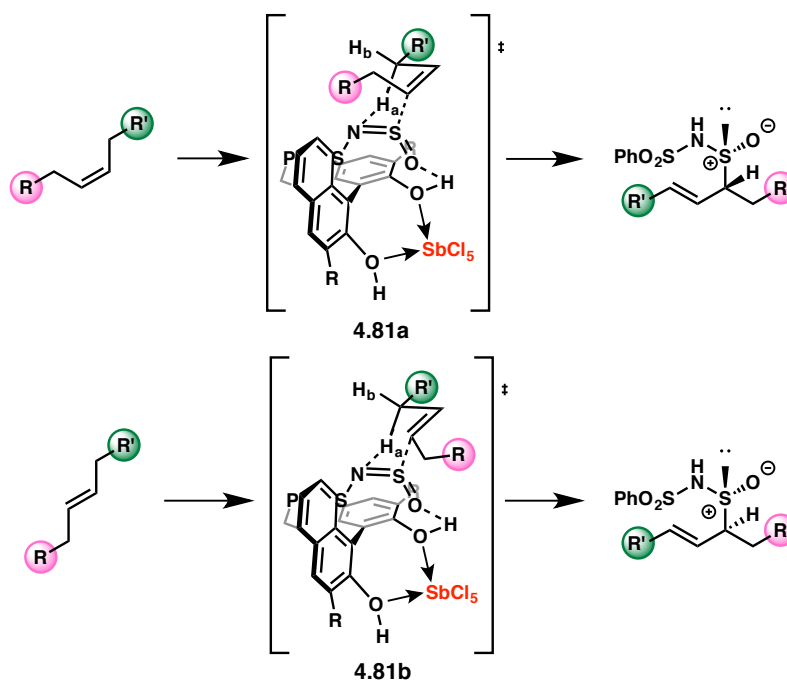


Reaction conditions. *Cis*-5-decene (1 equiv), sulfurimide reagent **4.49** (1.5 equiv), CH_2Cl_2 (0.13M), SbCl_5 (20 mol%), co-catalyst **4.60** (25 mol%), trifluoroacetic acid (0.5 equiv).

Based on the above-mentioned mechanistic analysis, a proposed transition state is detailed below (Scheme 4.2.8). We believe that the hetero-ene reaction taking place between sulfurimide reagent **4.49** and *cis*-olefins proceeds through a closed transition state in which the LBA catalyst is activating the sulfurimide reagent through a LUMO lowering effect (Scheme 4.2.8). Transition states **4.81a** and **4.81b** benefit from stabilizing π -interactions between the coordinated oxidant **4.49** and the naphthyl backbone. π -Face selectivity may be ascribed to steric shielding by the adjacent naphthyl

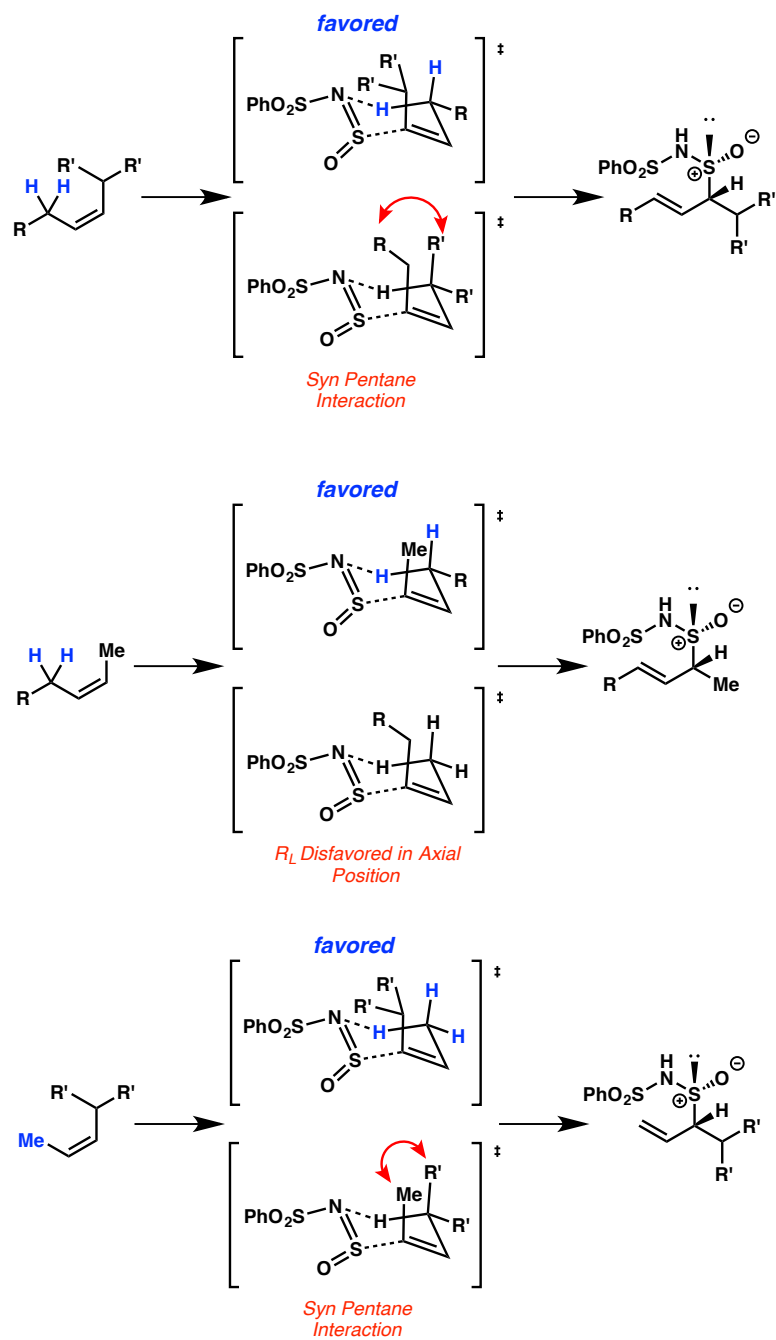
group. Additionally, the switch in diastereoselectivity between the thermal endo-selective hetero-ene reaction and the catalyzed reaction suggests that the catalyzed reaction is taking place through an *exo* transition state.

Scheme 4.2.8



Perhaps even more suggestive of a closed 6-membered transition state is the strong sense of regiopreference. The established trends in regioselectivity can be rationalized on the basis of steric strain in the developing transition state where the lowest energy chair conformation is favored (Scheme 4.2.9).

Scheme 4.2.9



4.2.5. Stereospecific Diversification of Allylic Sulfinimides

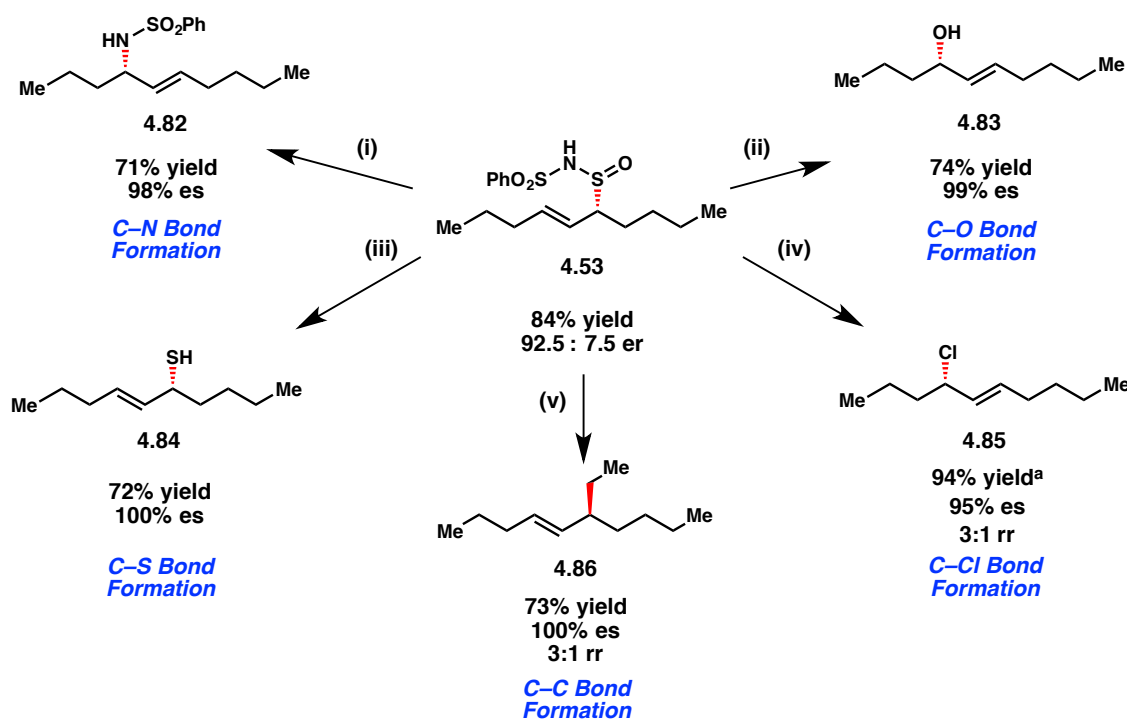
We sought to diversify allylic sulfinimide **4.53** in order to better understand the utility of these products in chemical synthesis (Scheme 4.2.10). We initially selected sulfurimide reagent **4.49** because it contains both nitrogen and oxygen functionality and could therefore yield an oxidized product capable of undergoing chemodivergent rearrangements. While allylic sulfinimides have been shown to preferentially undergo exclusively the nitrogen centered [2,3]-rearrangement under thermal conditions, this required the use of high temperatures.^{71,78,80} In the case of oxidized product **4.53**, the presence of catalytic $\text{TiCl}(\text{O}i\text{-Pr})_3$ was sufficient to promote the rearrangement at 60 °C with the sole formation of amine product **4.82**. Gratifyingly, this product was generated exclusively as the *E*-olefin isomer with 98% enantiospecificity (es). Because the oxygen centered [2,3]-rearrangement is thermally disfavored, conversion of **4.53** to the corresponding allylic aryl sulfoxide and subsequent Mislow-Evans rearrangement was necessary to provide the free allylic alcohol **4.83**, again with high enantiospecificity (99% es).

Additional chiral heteroatom-containing products were similarly accessed from allylic oxidation product **4.53**. Through reduction with lithium aluminum hydride the corresponding thiol (**4.84**) was isolated with good yield.⁷⁶ Notably, the stereoselective introduction of a C-Cl bond was achieved when the allylic sulfinimide was stirred at low temperatures in the presence of sulfuryl chloride. 4-Chloro-5-decene **4.85** was cleanly isolated with 95% es, presumably through a retro-ene process. While a previous report of this retro-ene chemistry utilized N-chlorosuccinimide at elevated temperatures, we found that the switch in halogenating reagent and lower temperatures increased the regioselectivity of this chemistry from 1:1 to 3:1.⁹³

Finally, based on our previous allylic alkylation research we wondered if allylic sulfinimide **4.53** would be compatible with these substitution conditions to afford chiral hydrocarbon **4.86** with regioselectivity and enantiospecificity.⁹⁴ Under the copper-catalyzed conditions with ethylmagnesium chloride, hydrocarbon **4.86** was formed with

perfect enantiospecificity, complete *E*-olefin selectivity and a 3:1 regioisomeric ratio. The stereochemistry of **4.86** was assigned based on analogy to our previous studies in the aminoarylation of dienes where we were able to confirm that oxidative addition of the cuprate and consequent reductive elimination results in a net inversion of stereochemistry.⁹⁵ The allylic alkylation of these sulfinimides represents a significant advance in the regioselective allylic substitution of an unbiased internal allylic electrophile.

Scheme 4.2.10



(i) TiCl(O*i*-Pr)₃ (20 mol%), PhMe, 60 °C; P(OMe)₃, MeOH, 23 °C (ii) 1. Me₂SO₄, Et₃N, CH₂Cl₂, 23 °C. 2. PhMgBr, THF, 0 °C; P(OMe)₃, MeOH, 23 °C (iii) LiAlH₄, Et₂O, 0 °C to 23 °C (iv) SO₂Cl₂ (1.1 equiv), Et₂O, -70 °C to 0 °C. [a] Product was isolated crude after filtration through Celite. (v) CuBr₂·SMe₂ (5 mol%), EtMgCl, DME, -70 °C to 0 °C

4.2.6. Conclusions

In conclusion, we have explored the use of benzenesulfonyl sulfurimide (**4.49**) with catalytic amounts of SbCl₅•BINOL complexes to enable a regio- and stereoselective

hetero-ene reaction via Lewis acid-assisted Brønsted acidity. This methodology produces stable allylic sulfinimide products with exclusive *E*-olefin selectivity and high regio- and enantioselectivity precluding the use of directing or activating groups. To date, we have been able to achieve up to 84% yield, >20:1 regiomer ratio and 96:4 enantiomeric ratio with a general and diverse scope of cis-olefins. The products of this oxidation are amenable to stereospecific diversification thus representing a general platform for the formal enantioselective, regioselective and *E*-olefin selective allylic C-X bond formations of internal olefins, where X can be carbon, nitrogen, oxygen, sulfur, or chloride based functionality.

4.3. Experimental Section

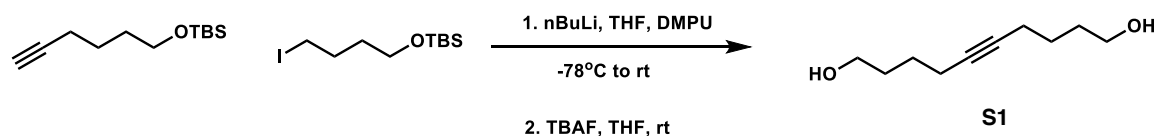
4.3.1. Methods and Materials

All reactions were carried out under an atmosphere of argon in flame-dried glassware with magnetic stirring unless otherwise indicated. Commercially obtained reagents were used as received. Solvents were dried by passage through an activated alumina column under argon. Liquids and solutions were transferred via syringe. All reactions were monitored by thin-layer chromatography with E. Merck silica gel 60 F254 pre-coated plates (0.25 mm). Silica gel (particle size 0.032 - 0.063 mm) purchased from SiliCycle was used for flash chromatography. ¹H and ¹³C NMR spectra were recorded on Varian Inova-400 or 500 spectrometers. Data for ¹H NMR spectra are reported relative to chloroform as an internal standard (7.26 ppm) and are reported as follows: chemical shift (δ ppm), multiplicity, coupling constant (Hz), and integration. Data for ¹³C NMR spectra are reported relative to chloroform as an internal standard (77.16 ppm) and are reported in terms of chemical shift (δ ppm). Optical rotations were measured on a JAS DIP-360 digital polarimeter. Infrared spectra were recorded on a Perkin-Elmer 1000 series FTIR.

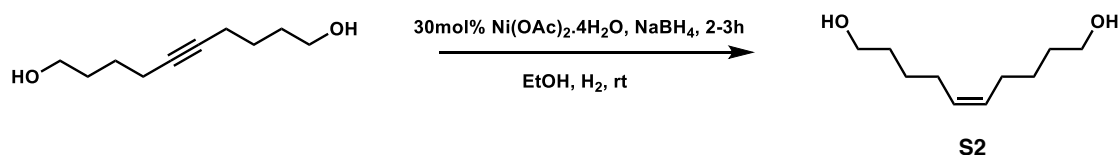
Chiral HPLC analyses were performed on an Agilent 1200 Series system. GC analyses were performed on an Agilent 7820A system. HRMS data were obtained at The Scripps Center for Mass Spectrometry and The UT Austin Center for Mass Spectrometry.

4.3.2. Preparative Procedures

Synthesis of olefin starting materials

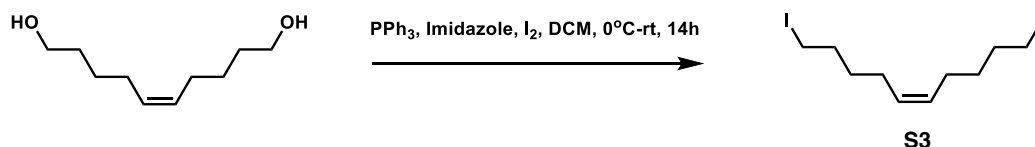


S1: Dec-5-yne-1,10-diol was synthesized by the following procedure and the corresponding spectroscopic data was identical to the reported data in the literature.⁹⁶



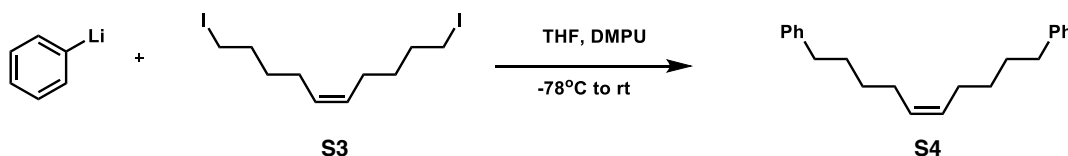
S2: A flame-dried round-bottom flask was charged with nickel (II) acetate tetra hydrate (0.746 g, 3 mmol, 3 equiv). The flask was then put under high vacuum and was back-filled with hydrogen gas from a balloon. Ethanol anhydrous (20 mL) was then added. To a stirred suspension of nickel (II) acetate tetra hydrate in ethanol was added 3.1 mL of a 1 M solution of NaBH_4 (3.1 equiv) in ethanol at room temperature. The new formed solution of black solid was stirred for 30 minutes after which an ethanol solution (5 mL) of 1,10-decyne-diol **S1** (1.71g, 10 mmol, 1eq) was added. The reaction mixture was then kept stirring for 2 h. After completion, the reaction was filtered through a celite plug,

concentrated to yield crude product. The crude product was purified by column chromatography (gradient 40-80% EtOAc/hexanes). The product **S2** was obtained as a light yellow oil (1.6 g, 93% yield). The spectra were identical with those reported in literature.⁹⁶



S3: Imidazole (0.51 g, 7.5 mmol, 3 equiv) and triphenylphosphine (1.84 g, 7.0 mmol, 2.8 equiv) was added to a stirred solution of (Z)-dec-5-ene-1,10-diol **S2** (0.43 g, 2.5 mmol, 1 equiv) in CH_2Cl_2 (10 mL, 0.25 M) at 0 °C. Iodine was then added in portions to the reaction mixture. The resulting solution was stirred for 30 min at 0 °C and 14 hours at room temperature. After completion, the reaction mixture was poured into hexanes (100 mL) and filtered through a silica plug. The solid residue was washed with hexanes (5 x 50 mL) and the combined solvent was removed under reduced pressure to give the title compound. The product **S3** was obtained as a clear oil (0.924 g, 94% yield).

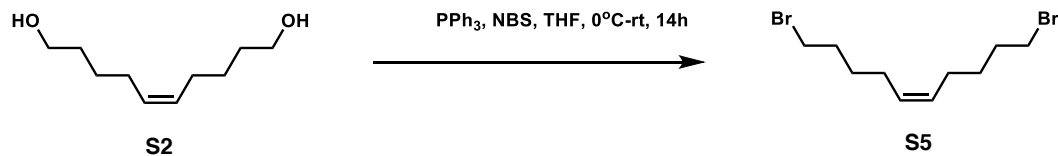
^1H NMR (500 MHz, CDCl_3) δ 5.40 (ddd, J = 5.6, 4.3, 1.1 Hz, 2H), 3.22 (t, J = 7.0 Hz, 4H), 2.17 – 2.00 (m, 4H), 1.94 – 1.77 (m, 4H), 1.55 – 1.43 (m, 4H). ^{13}C NMR (101 MHz, CDCl_3) δ 129.62, 33.03, 30.45, 26.09, 6.98. IR (thin film): 2929, 2341, 1425, 1207, 720 cm^{-1} . HRMS (CI^+) calcd for $[\text{C}_{10}\text{H}_{18}\text{I}_2]$: 391.9498, found 391.9508



S4: A flame-dried round-bottom flask was charged with anhydrous THF (0.5 M), and the flask was cooled to -78 °C in a dry ice/acetone bath. (Z)-1,10-diiododec-5-ene **S3** (0.784 g, 2.0 mmol, 1 equiv) was then added under an argon atmosphere. Phenyllithium (4.4 mL, 8 mmol, 4 equiv, 1.8 M) was added dropwise to the flask while maintaining the

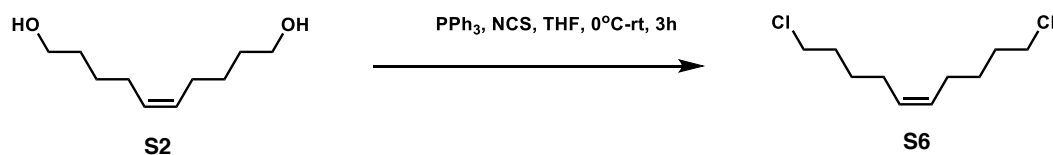
reaction temperature at $-78\text{ }^{\circ}\text{C}$. After 30 minutes at $-78\text{ }^{\circ}\text{C}$, the reaction mixture was allowed to warm to room temperature and stirred overnight. After completion, saturated NH_4Cl solution was added. The reaction mixture was extracted with Et_2O (3x), and the organic phases were combined and washed with sodium thiosulfate and brine, dried over anhydrous magnesium sulfate, filtered, and concentrated to yield crude product. The crude product was purified by column chromatography on silica gel using 100% hexanes as an eluent. Olefin **S4** was obtained as a colorless oil (0.429 g, 73% yield)

^1H NMR (500 MHz, CDCl_3) δ 7.31 (d, $J = 7.7\text{ Hz}$, 4H), 7.24 – 7.17 (m, 6H), 5.41 – 5.29 (m, 2H), 2.71 – 2.55 (m, 4H), 2.08 (td, $J = 7.5, 5.2\text{ Hz}$, 4H), 1.65 (ddt, $J = 9.6, 7.8, 3.6\text{ Hz}$, 4H), 1.42 (t, $J = 7.6\text{ Hz}$, 4H). ^{13}C NMR (101 MHz, CDCl_3) δ 142.72, 129.78, 128.38, 128.22, 125.58, 35.84, 31.08, 29.35, 27.05. IR (thin film): 2930, 2855, 1495, 1453, 746 cm^{-1} . HRMS $[\text{M}+\text{Cl}]$ calcd for $[\text{C}_{22}\text{H}_{28}]$: 292.2191, found 292.2191



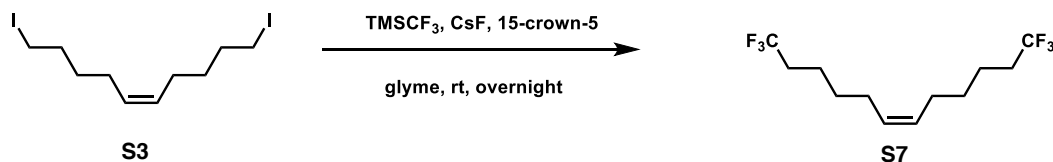
S5: N-Bromosuccinimide (0.62 g, 3.48 mmol, 3 equiv) was added in portions to a stirred solution of (Z)-dec-5-ene-1,10-diol **S2** (0.2 g, 1.16 mmol, 1 equiv) and triphenylphosphine (0.852 g, 3.25 mmol, 2.8 equiv) in THF (5 mL) at $0\text{ }^{\circ}\text{C}$, and the resulting solution was stirred for 30 min at $0\text{ }^{\circ}\text{C}$ and 14 hours at room temperature. After completion, the reaction mixture was poured into hexanes (20 mL) and filtered through a silica plug. The solid residue was washed with hexanes (5 x 20 mL) and the combined solvent was removed under reduced pressure to give the title compound. Olefin **S5** was obtained as a clear oil (0.346 g, 99% yield).

^1H NMR (400 MHz, CDCl_3) δ 5.37 (t, $J = 4.9\text{ Hz}$, 2H), 3.41 (t, $J = 6.8\text{ Hz}$, 4H), 2.06 (td, $J = 7.3, 5.0\text{ Hz}$, 4H), 1.86 (q, $J = 7.2\text{ Hz}$, 4H), 1.51 (h, $J = 7.0\text{ Hz}$, 4H). ^{13}C NMR (101 MHz, CDCl_3) δ 129.64, 33.78, 32.29, 28.12, 26.29. IR (thin film): 2935, 1437, 1248, 740, 645 cm^{-1} . HR-MS (CI+) calcd for $[\text{C}_{10}\text{H}_{1779}\text{Br}_81\text{Br}]$: 296.9677, found 296.9679



S6: N-Chlorosuccinimide (0.6 g, 4.5 mmol, 3 equiv) was added in portions to a stirred solution of (Z)-dec-5-ene-1,10-diol **S2** (0.258 g, 1.5 mmol, 1 equiv) and triphenylphosphine (1.1 g, 4.2 mmol, 2.8 equiv) in THF (6 mL) at 0 °C, and the resulting solution was stirred for 30min at 0 °C and 3 hours at room temperature. After completion, the reaction mixture was poured into hexanes (20 mL) and filtered through a silica plug. The solid residue was washed hexanes (5 x 20 mL) and the combined solvent was removed under reduced pressure to give the title compound. Olefin **S6** was obtained as a clear oil (0.289 g, 97% yield).

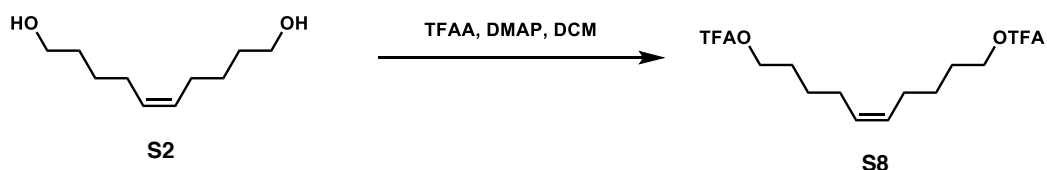
^1H NMR (400 MHz, CDCl_3) δ 5.38 (t, $J = 4.9$ Hz, 2H), 3.54 (t, $J = 6.7$ Hz, 4H), 2.06 (q, $J = 6.9$ Hz, 4H), 1.78 (q, $J = 7.1$ Hz, 4H), 1.61 – 1.39 (m, 4H). ^{13}C NMR (101 MHz, CDCl_3) δ 129.66, 44.98, 32.12, 26.84, 26.41. IR (thin film): 2861, 2360, 1445, 1309, 720 cm^{-1} . HR-MS (CI^+) calcd for $[\text{C}_{10}\text{H}_{17}\text{Cl}_2]$: 207.0707, found 207.0710



S7: To a solution of (Z)-1,10-diiododec-5-ene **S3** (0.392 g, 1.0 mmol, 1 equiv) in monoglyme (5 mL) in a flame-dried round-bottom flask, TMSCF_3 (2 mL, 4.0 mmol, 4.0 equiv, 2M in THF) was added. The resulting mixture was then cooled to -10 °C in an ethylene glycol/dry ice bath. CsF (0.607 g, 4 mmol, 4 equiv) and 15-crown-5 (1.5 mL, 8 mmol, 8 equiv) were successively added and the mixture was allowed to warm up to room temperature and stirred for 14 h. After completion, the reaction mixture was filtered through a celite plug and concentrated. The liquid residue was then washed with pentane (5 x 5 mL) to give a solution of desired product and 15-crown-5. This solution was

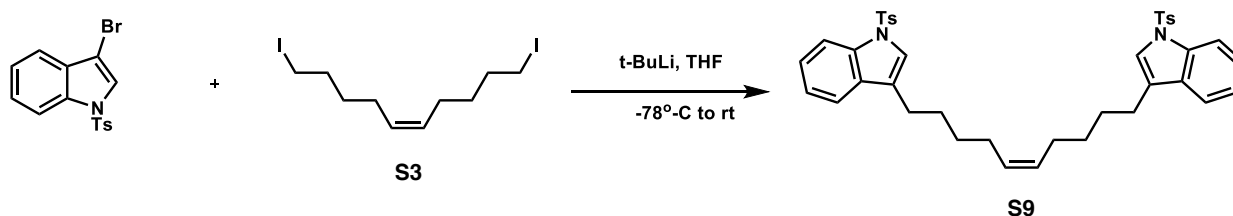
washed with brine (3x) and water (2x), dried over Magnesium sulfate, and concentrated under reduced pressure to give olefin **S7** as a clear oil (0.268 g, 97% yield).

^1H NMR (500 MHz, CDCl_3) δ 5.40 (dd, $J = 5.5, 4.2$ Hz, 2H), 2.09 (ddd, $J = 13.1, 9.1, 5.2$ Hz, 8H), 1.63 – 1.50 (m, 4H), 1.46 (q, $J = 7.6$ Hz, 4H). ^{13}C NMR (101 MHz, CDCl_3) δ 129.54, 33.77, 33.49, 28.64, 26.74, 21.47, 21.44. ^{19}F NMR (470 MHz, CDCl_3) δ -66.39. IR (thin film): 2947, 1389, 1136, 1027, 653 cm^{-1} . HR-MS (CI+) calcd for $[\text{C}_{12}\text{H}_{18}\text{F}_6]$: 276.1313, found 276.1311



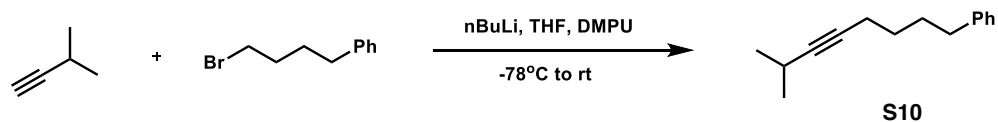
S8: A flame-dried round-bottom flask was charged with anhydrous CH_2Cl_2 (10 mL), (Z)-dec-5-ene-1,10-diol **S2** (0.43 g, 2.5 mmol, 1 equiv) and the flask was cooled to 0 °C in an ice bath. 4-Dimethylaminopyridine (0.062 g, 0.5 mmol, 0.2 equiv) was then added under an argon atmosphere. Trifluoroacetic anhydride (1.4 mL, 10 mmol, 4 equiv) was added dropwise to the flask while maintaining the reaction temperature at 0 °C. The reaction mixture was then allowed to warm to room temperature and stirred overnight. After completion, the reaction mixture was poured into hexanes (100 mL) and filtered through a silica gel plug. The reaction residue on silica gel was washed with hexanes (5 x 30 mL) and the combined solvent was removed under reduced pressure to give the title compound. Olefin **S8** was obtained as a clear oil (0.476 g, 52% yield). CH_2Cl_2

^1H NMR (400 MHz, CDCl_3) δ 5.38 (td, $J = 4.5, 2.2$ Hz, 2H), 4.36 (t, $J = 6.6$ Hz, 4H), 2.08 (td, $J = 7.3, 5.3$ Hz, 4H), 1.84 – 1.67 (m, 4H), 1.52 – 1.36 (m, 4H). ^{13}C NMR (101 MHz, CDCl_3) δ 129.60, 68.05, 27.66, 26.53, 25.49. ^{19}F NMR (470 MHz, CDCl_3) δ -75.15. IR (thin film): 2943, 1789, 1352, 1222, 777 cm^{-1} . HR-MS (CI+) calcd for $[\text{C}_{14}\text{H}_{19}\text{O}_4\text{F}_6]$: 365.1188, found 365.1202



S9: A flame-dried round-bottom flask was charged with anhydrous THF (6 mL), 3-bromo-1-tosyl-1H-indole (1.314 g, 3.75 mmol, 2.5 equiv),⁹⁷ and the flask was cooled to -78 °C in a dry ice/acetone bath. *t*-BuLi (2.2 mL, 3.75 mmol, 2.5 equiv, 1.7 M) was added dropwise to the flask while maintaining the reaction temperature at -78 °C. After the reaction was stirred for additional 1 hour, a solution of (Z)-1,10-diiododec-5-ene **S3** (0.588 g, 1.5 mmol, 1 equiv) in THF (3 mL) was added. The reaction mixture was allowed to warm to room temperature and stirred for 21 hours. After completion, saturated NH₄Cl solution was added. The reaction mixture was extracted with Et₂O (3x), and the organic phases were combined and washed with sodium thiosulfate, and brine, dried over anhydrous Magnesium sulfate, filtered, and concentrated to yield crude product. The crude product was purified by column chromatography (gradient 0-10% EtOAc/hexanes). Olefin **S9** was obtained as a white solid (0.3 g, 29% yield).

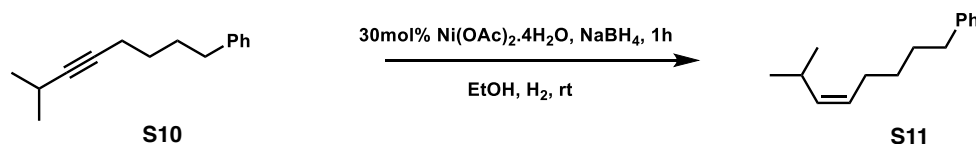
¹H NMR (500 MHz, CDCl₃) δ 8.23 – 8.18 (m, 2H), 7.65 – 7.58 (m, 4H), 7.43 (ddd, *J* = 7.4, 1.6, 0.8 Hz, 2H), 7.37 – 7.29 (m, 6H), 7.19 (d, *J* = 8.1 Hz, 4H), 5.42 – 5.36 (m, 2H), 3.15 – 3.06 (m, 4H), 2.35 (s, 6H), 2.17 – 2.04 (m, 4H), 1.82 – 1.69 (m, 4H), 1.53 – 1.44 (m, 4H). ¹³C NMR (101 MHz, CDCl₃) δ 144.96, 138.78, 135.95, 135.63, 129.86, 129.71, 129.22, 126.30, 125.14, 124.10, 119.22, 115.09, 101.92, 29.47, 29.46, 27.42, 26.99, 21.56. IR (thin film): 2924, 2341, 1448, 1175, 668 cm⁻¹. HRMS (ESI-TOF) calcd for [C₄₀H₄₂N₂O₄S₂]: 679.2659, found 679.2654



S10: A flame-dried round-bottom flask was charged with anhydrous THF (10 mL), 3-methylbut-1-yne (0.66 g, 6.5 mmol, 1.3 equiv) and the flask was cooled to -78 °C in a dry ice/acetone bath. *n*-BuLi (2.5 mL, 6.25 mmol, 1.25 equiv, 2.5 M) was added dropwise to

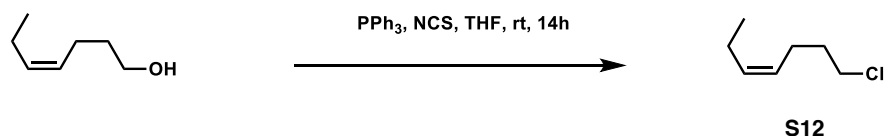
the flask while maintaining the reaction temperature at $-78\text{ }^{\circ}\text{C}$. After the reaction was stirred for additional 1 hour, (4-bromobutyl)benzene (0.84 mL, 5 mmol, 1 equiv) and 1,3-Dimethyl-3,4,5,6-tetrahydro-2(1H)-pyrimidinone (5 mL) were successively added. The reaction mixture was then allowed to warm to room temperature and stirred for 17 hours. After completion, saturated NH_4Cl solution was added. The reaction mixture was extracted with Et_2O (3x), and the organic phases were combined and washed with brine, dried over anhydrous magnesium sulfate, filtered, and concentrated to yield crude product. The crude product was purified by column chromatography (100% hexanes). Alkyne **S10** was obtained as a clear oil (0.826 g, 88% yield).

^1H NMR (400 MHz, CDCl_3) δ 7.30 – 7.27 (m, 2H), 7.18 (d, $J = 7.3\text{ Hz}$, 3H), 2.62 (t, $J = 7.7\text{ Hz}$, 2H), 2.51 (ddt, $J = 9.1, 6.8, 3.4\text{ Hz}$, 1H), 2.23 – 2.10 (m, 2H), 1.72 (tt, $J = 9.0, 6.8\text{ Hz}$, 2H), 1.55 – 1.47 (m, 2H), 1.13 (d, $J = 6.8\text{ Hz}$, 6H). ^{13}C NMR (101 MHz, CDCl_3) δ 142.49, 128.38, 128.24, 125.63, 86.26, 78.99, 35.39, 30.47, 28.65, 23.45, 20.51, 18.55. IR (thin film): 2935, 2860, 1496, 746, 698 cm^{-1} . HR-MS (CI+) calcd for $[\text{C}_{15}\text{H}_{20}]$: 200.1565, found 200.1566



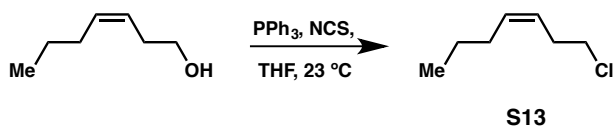
S11: To a flame-dried round-bottom flask was charged with nickel (II) acetate tetra hydrate (0.134 g, 0.54 mmol, 0.27 equiv). The flask was then put under high vacuum and was back-filled with hydrogen gas from a balloon. Ethanol anhydrous (4 mL) was then added. To a stirred suspension of nickel (II) acetate tetra hydrate in ethanol was added 0.5 mL of a 1 M solution of NaBH_4 (0.25 equiv) in ethanol at room temperature. The new formed solution of black solid was stirred for 30 minutes after which an ethanol solution (2 mL) of alkyne **S10** (0.4 g, 2 mmol, 1eq) was added. The reaction mixture was stirred for 1 hour. After completion, the reaction was filtered through a celite plug, concentrated to yield crude product. The crude product was purified by column chromatography (100% hexanes). Olefin **S11** was obtained as a clear oil (0.368 g, 91% yield).

^1H NMR (400 MHz, CDCl_3) δ 7.32 – 7.23 (m, 2H), 7.21 – 7.11 (m, 3H), 5.26 – 5.14 (m, 2H), 2.60 (dt, J = 13.7, 7.2 Hz, 3H), 2.07 (td, J = 7.5, 6.2 Hz, 2H), 1.71 – 1.58 (m, 2H), 1.45 – 1.33 (m, 2H), 0.94 (d, J = 6.7 Hz, 6H). ^{13}C NMR (101 MHz, CDCl_3) δ 142.72, 137.67, 128.38, 128.21, 127.16, 125.57, 35.83, 31.06, 29.53, 27.11, 26.45, 23.23. IR (thin film): 2955, 2857, 1496, 1454, 745 cm^{-1} . HR-MS (CI+) calcd for $[\text{C}_{15}\text{H}_{22}]$: 202.1722, found 202.1721



S12: N-Chlorosuccinimide (2.0 g, 15 mmol, 1.5 equiv) was added in portions to a stirred solution of (Z)-hept-4-en-1-ol (1.4 g, 10 mmol, 1 equiv) and triphenylphosphine (2.27 g, 14 mmol, 1.4 equiv) in THF (20 mL) at 0 °C. The resulting solution was stirred for 30 min at 0 °C and 14 hours at room temperature. After completion, the reaction mixture was poured into hexanes (100 mL) and filtered through a silica plug. The solid residue was washed hexanes (5 x 30 mL) and the combined solvent was removed under reduced pressure to give the title compound. The product was obtained as a clear oil (0.976 g, 74% yield).

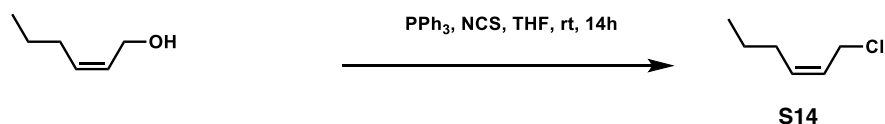
^1H NMR (400 MHz, CDCl_3) δ 5.50 – 5.37 (m, 1H), 5.36 – 5.20 (m, 1H), 3.54 (t, J = 6.6 Hz, 2H), 2.26 – 2.12 (m, 2H), 2.12 – 2.00 (m, 2H), 1.83 (dt, J = 7.6, 6.6 Hz, 2H), 0.97 (t, J = 7.5 Hz, 3H). ^{13}C NMR (101 MHz, CDCl_3) δ 133.29, 126.93, 44.51, 32.45, 24.24, 20.53, 14.31. IR (thin film): 2934, 1458, 1308, 726, 654 cm^{-1} . HR-MS (CI+) calcd for $[\text{C}_7\text{H}_{13}\text{Cl}]$: 132.0706, found 132.0708



S13: Triphenylphosphine (5.6 mmol, 1.4 equiv) was diluted in THF (8 mL, 0.5 M) within a flame-dried flask set under argon atmosphere. Cis-3-hexen-1-ol (4.0 mmol) was added to the solution followed by N-chlorosuccinimide (6.0 mmol, 1.5 equiv) carefully. The reaction was stirred at room temperature until complete as determined by TLC analysis (2 h). After diluting with pentane (roughly 30 mL), the suspension was filtered through a

celite plug and purified by flash chromatography (100% pentane) afforded **S13** (92% yield) as a colorless oil:

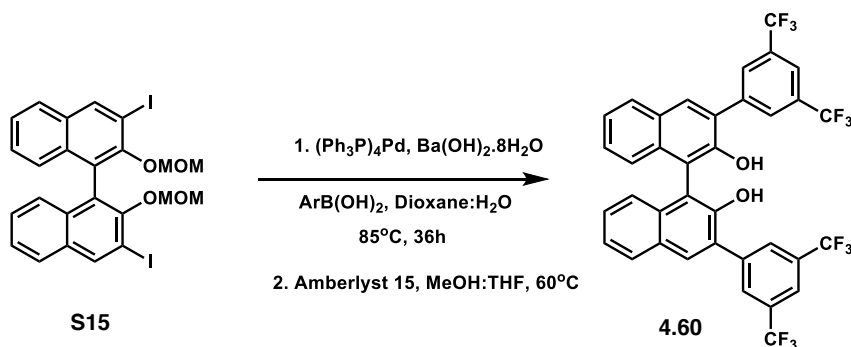
^1H NMR (400 MHz, CDCl_3) δ 5.60 – 5.48 (m, 1H), 5.45 – 5.33 (m, 1H), 3.51 (t, J = 7.1 Hz, 2H), 2.52 (q, J = 7.4 Hz, 2H), 2.03 (q, J = 7.1 Hz, 2H), 1.39 (h, J = 7.4 Hz, 2H), 0.91 (t, J = 7.3 Hz, 3H); ^{13}C NMR (101 MHz, CDCl_3) δ 133.2, 125.1, 44.4, 30.9, 29.6, 22.8, 13.9.



S14: N-Chlorosuccinimide (1.0 g, 7.5 mmol, 1.5 equiv) was added in portions to a stirred solution of (Z)-hex-2-en-1-ol (0.59 g, 5 mmol, 1 equiv) and triphenylphosphine (1.84 g, 7 mmol, 1.4 equiv) in THF (10 mL) at 0 °C, and the resulting solution was stirred for 30 min at 0 °C and 2 hours at room temperature. After completion, the reaction mixture was poured into pentane (100 mL) and filtered through a silica plug. The solid residue was washed pentane (5x30 mL) and the combined solvent was removed under reduced pressure to give the title compound. The product was obtained as a clear oil (0.358 g, 60% yield). The collected spectra were consistent with those reported in literature.⁹⁸

Synthesis of BINOL Derivatives

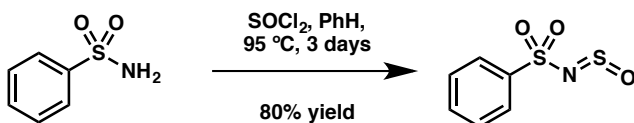
Binol co-catalysts **4.54** and **4.56** were purchased from Sigma Aldrich. BINOL co-catalysts **4.55**, **4.57** and **4.58** were synthesized according to the corresponding literature procedures.⁹⁹⁻¹⁰¹



S15: (R)-3,3'-diiodo-2,2'-bis(methoxymethoxy)-1,1'-binaphthalene was prepared according to literature procedure.¹⁰²

4.60: A flame-dried round-bottom flask was charged with **S15** (4.38 g, 7 mmol, 1 equiv) 3,5-bis(trifluoromethyl)-phenylboronic acid (5.42 g, 21 mmol, 3 equiv), and barium hydroxide octahydrate (6.63 g, 21 mmol, 3 equiv). The flask was put under vacuum and back-filled with argon (3 times). Tetrakis(triphenylphosphine)palladium(0) (0.81 g, 0.7 mmol, 0.1 equiv) was added and the flask was again put under vacuum and back-filled with argon (3 times). Degassed dioxane and H₂O (60 mL, 3:1) was finally added and the reaction mixture was heated to 85°C with stirring for 36h. After completion, CH₂Cl₂ was added and the reaction mixture was extracted with CH₂Cl₂ (3x). The combined organic extracts were washed with brine, dried over anhydrous magnesium sulfate, filtered, and concentrated to yield crude mixture. Purification by column chromatography (gradient 0-5% EtOAc/ hexanes) afforded the MOM protected intermediate. This material was transferred to a round bottom flask and THF and methanol (20 mL, 1:1) were added, followed by amberlyst 15 (8 g). The reaction mixture was heated to 60 °C and stirred overnight. After completion, the reaction was filtered through a celite plug and concentrated to yield the crude product, which was purified by column chromatography (gradient 0-5% EtOAc/ hexanes) as an eluent. The product was obtained as a white solid (4.15 g, 83% yield). Chiral HPLC show the product was obtained with enantiomeric ratio 99:1. ¹HNMR and ¹³CNMR spectra were consistent with those reported in literature.⁹⁹

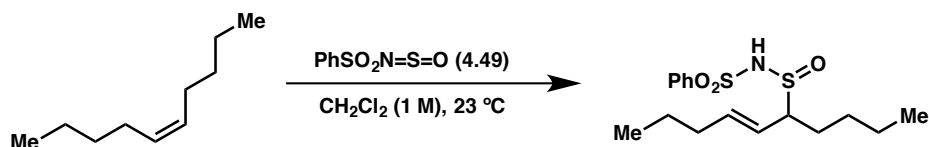
Synthesis of Benzenesulfonyl Sulfurimide 4.49



4.49: Our procedure was modified from a method reported in the literature for the synthesis of similar arylsulfonyl sulfurdiimides:¹⁰³ A solution of benzenesulfonamide

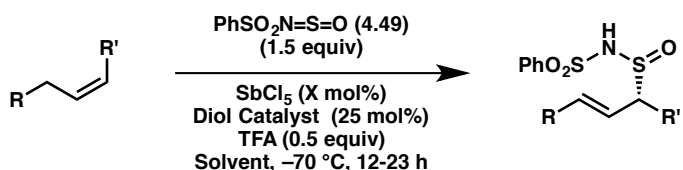
(14.55 g, 92.5 mmol) and SOCl_2 (20 mL, 0.275 mol) in benzene (20 mL) was refluxed at 95 °C for 3 days (over the course of the reaction, the mixture became a clear solution). When the starting material was consumed by ^1H NMR analysis of an aliquot, the mixture was concentrated under vacuum to remove benzene and excess SOCl_2 . Trace amounts of SOCl_2 were removed by redissolving the residue in toluene (20 mL) and concentrating under reduced pressure. The residue was redissolved in toluene (8 mL) and stored at 0 °C until a yellow precipitate crystallized slowly from the solution. The precipitate was obtained by vacuum filtration under an argon atmosphere, washed with cold toluene (3 x 5 mL) and stored under vacuum until dry. Benzenesulfonyl sulfurimide **4.49** was obtained as a pale yellow solid (15 g, 80% yield). ^1H NMR and ^{13}C NMR spectra were consistent with those reported in literature. *Since benzenesulfonyl sulfurimide 3 is sensitive to water, we store it in a vacuum desiccator within a sealed flask that has been purged with argon.*

Representative Procedure for Thermal Hetero-Ene Reactions



4.53: A flame-dried flask was charged with benzenesulfonyl sulfurimide **4.49** (3.5 mmol, 1.25 equiv) and diluted with CH_2Cl_2 (2.8 mL, 1M) under argon atmosphere. *Cis*-5-decene (2.8 mmol, 1 equiv) was added in and the reaction was stirred 4 h or until TLC indicated the complete disappearance of olefin starting material. The solution was concentrated under reduced pressure and diluted in a minimal amount of CHCl_3 . Benzenesulfonamide was precipitated out by trituration with hexanes and removed under vacuum filtration. The filtrate was concentrated under reduced pressure to afford ene adduct **4.53** (>95% yield) as a pale yellow oil. (See **4.61** for characterization data).

General Procedures for the Catalytic Enantioselective Allylic Oxidation



General Procedure for the Enantioselective Hetero-Ene Reaction (Method A):

Benzenesulfonyl sulfurimide **4.49** (122mg, 1.5 equiv), and (*R*)-(+)-3,3'-Bis(3,5-bis(trifluoromethyl)phenyl)-1,1'-bi-2-naphthol (**4.60**) (71mg, 25 mol%) were set under vacuum in a flame dried flask for approximately 10 minutes before purging with argon. The solids were dissolved in PhMe (1 mL) and cooled to -70 °C. The resulting yellow solution was then treated with SbCl₅ (80 mL, 1M in CH₂Cl₂, 20 mol%) dropwise while stirring vigorously. After 20 minutes, olefin (0.4 mmol) was added followed immediately by the addition of 1 mL PhMe and 1 mL CH₂Cl₂ to wash the sides of the reaction vessel (solvents were added slowly to ensure that the internal reaction temperature did not significantly rise). The resulting black solution was treated with TFA (200 mL, 1M CH₂Cl₂, 0.5 equiv) and the vessel septum was sealed with wax to prevent contamination by moisture. The solution was stirred at -70 °C for 14-23 h. The reaction was quenched by addition of water (3 mL) at -70 °C, and allowed to warm to room temperature over the span of 1 h while stirring vigorously (~ 1,300 rpm). The resulting organics were collected and the aqueous layer was washed with EtOAc (3 x 6 mL, or until the aqueous layer went colorless). The combined organics were dried over Na₂SO₄ and concentrated under reduced pressure.

The resultant crude material was dissolved in a minimal amount of CHCl₃. Benzenesulfonamide was precipitated out by trituration with hexanes and removed under vacuum filtration. The filtrate was concentrated under reduced pressure and suspended in Et₂O (20 mL) and NEt₃ (123 mL, 2.2 equiv). The cloudy solution was washed with water (2 x 7 mL), and the combined aqueous extracts were washed with 20 mL Et₂O. The organic layer was back extracted with 5 mL water. All combined aqueous washes were

acidified with 1N HCl until cloudy (approximately pH = 2), and washed with EtOAc (3 x 20 mL). The combined organics were dried over Na₂SO₄ and concentrated under reduced pressure to afford pure ene adduct.

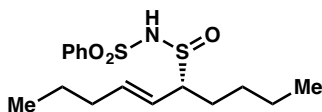
Modified Procedure for the Enantioselective Hetero-Ene Reaction (Method B)

Benzenesulfonyl sulfurimide **4.49** (122mg, 1.5 equiv), and (*R*)-(+)-3,3'-Bis(3,5-bis(trifluoromethyl)phenyl)-1,1'-bi-2-naphthol (**4.60**) (71mg, 25 mol%) were set under vacuum in a flame dried flask for approximately 10 minutes before purging with argon. The solids were dissolved in PhMe (1 mL) and cooled to -70 °C. The resulting yellow solution was then treated with SbCl₅ (160 mL, 1M in CH₂Cl₂, 40 mol%) dropwise while stirring vigorously. After 20 minutes, olefin (0.4 mmol) was added followed immediately by the addition of 1 mL PhMe and 1 mL CH₂Cl₂ to wash the sides of the reaction vessel (solvents were added slowly to ensure that the internal reaction temperature did not significantly rise). The resulting black solution was treated with TFA (200 mL, 1M CH₂Cl₂, 0.5 equiv) and the vessel septum was sealed with wax to prevent contamination by moisture. The solution was stirred at -70 °C for 14-23 h. The reaction was quenched by addition of water (3 mL) at -70 °C, and allowed to warm to room temperature over the span of 1 h while stirring vigorously (~ 1,300 rpm). The resulting organics were collected and the aqueous layer was washed with EtOAc (3 x 6 mL, or until the aqueous layer went colorless). The combined organics were dried over Na₂SO₄ and concentrated under reduced pressure. The product was purified according to Method A.

General Procedure for the Enantioselective Hetero-Ene Reaction (Method C)

Benzenesulfonyl sulfurimide **4.49** (122mg, 1.5 equiv), and (*R*)-1,1'-Bi-2-naphthol (29 mg, 25 mol%) were set under vacuum in a flame dried flask for approximately 10 minutes before purging with argon. The solids were dissolved in PhMe (1 mL) and cooled to -70 °C. The resulting yellow solution was then treated with SbCl₅ (160 mL, 1M

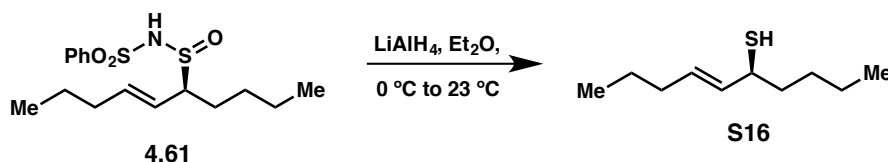
in CH_2Cl_2 , 40 mol%) dropwise while stirring vigorously. After 20 minutes, olefin (0.4 mmol) was added followed immediately by the addition of 1 mL PhMe and 1 mL CH_2Cl_2 to wash the sides of the reaction vessel (solvents were added slowly to ensure that the internal reaction temperature did not significantly rise). The resulting black solution was treated with TFA (200 mL, 1M CH_2Cl_2 , 0.5 equiv) and the vessel septum was sealed with wax to prevent contamination by moisture. The solution was stirred at $-70\text{ }^\circ\text{C}$ for 14-23 h. The reaction was quenched by addition of water (3 mL) at $-70\text{ }^\circ\text{C}$, and allowed to warm to room temperature over the span of 1 h while stirring vigorously ($\sim 1,300$ rpm). The resulting organics were collected and the aqueous layer was washed with EtOAc (3 x 6 mL, or until the aqueous layer went colorless). The combined organics were dried over Na_2SO_4 and concentrated under reduced pressure. The product was purified according to Method A.



4.61: Following the general procedure for the asymmetric catalytic oxidation of unactivated olefins (Method A), *cis*-5-decene (0.4 mmol) was converted to the desired product. The hetero-ene reaction was stirred for 16 h. The product was purified according to the general procedure to afford **4.61** (84% yield, 4:1 dr) as a viscous colorless oil. The enantiomeric ratio of the product was determined to be 92.5:7.5 after conversion to thiocarbamate **S17** (see experimental procedure for **S17**):

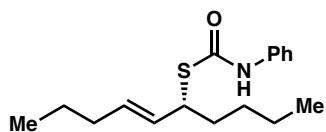
$[\alpha]_{\text{D}}^{23} = -39.4^\circ$ ($c = 1.34$, CH_2Cl_2). ^1H NMR (400 MHz, CDCl_3) δ 7.99 – 7.89 (m, 2H), 7.62 (td, $J = 7.3, 1.6$ Hz, 1H), 7.59 – 7.49 (m, 2H), 5.83 (dt, $J = 15.6, 7.0$ Hz, 1H), 5.40 – 5.23 (m, 1H), 3.43 (td, $J = 8.8, 5.1$ Hz, 0.2H), 3.11 (td, $J = 9.7, 5.5$ Hz, 0.8H), 2.20 – 1.99 (m, 2H), 1.96 – 1.82 (m, 0.8H), 1.79 – 1.62 (m, 1H), 1.61 – 1.49 (m, 0.2H), 1.48 – 1.22 (m, 6H), 0.89 (dt, $J = 7.0, 2.5$ Hz, 6H); ^{13}C NMR (101 MHz, CDCl_3) δ 142.3, 141.6, 140.4, 140.4, 133.8, 133.8, 129.5, 129.5, 127.3, 127.3, 120.4, 119.7, 69.1, 69.0, 35.0, 34.8, 29.1, 28.9, 28.9, 27.5, 22.5, 22.4, 22.3, 22.2, 13.9, 13.7, 13.7; IR (thin film): 2958,

2360, 1375, 1149, 1071, 856 cm^{-1} . HRMS (ESI-TOF) calcd for $[\text{C}_{16}\text{H}_{25}\text{NO}_3\text{S}_2]^+$ ($[\text{M}+\text{H}]^+$): 344.1349, found 344.1351



S16: Ene adduct **4.61** (0.1mmol) was converted to thiol **S16** according to the literature procedure.⁷⁶ Following quenching, the crude suspension was stirred vigorously for 1 h. Extraction by Et_2O and concentration gave a grey residue, which was purified by flash chromatography (100% pentane) to afford **S16** (72% yield) as a colorless oil.

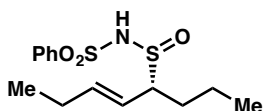
$[\alpha]_D^{23} = -23.2^{\circ}$ ($c = 0.19$, CH_2Cl_2). ^1H NMR (400 MHz, CDCl_3) δ 5.49 (dt, $J = 15.1$, 6.4 Hz, 1H), 5.39 (dd, $J = 15.1$, 8.5 Hz, 1H), 3.41 (qd, $J = 7.4$, 4.7 Hz, 1H), 1.98 (q, $J = 6.8$, 6.4 Hz, 2H), 1.64 – 1.53 (m, 2H), 1.44 – 1.24 (m, 6H), 0.89 (t, $J = 7.3$ Hz, 6H); ^{13}C NMR (101 MHz, CDCl_3) δ 134.1, 130.4, 42.6, 38.3, 34.3, 29.8, 22.5, 22.5, 14.1, 13.8; IR (thin film): 2958, 2928, 1464, 1378, 964, 730 cm^{-1} . HRMS (CI) calcd for $[\text{C}_{10}\text{H}_{19}\text{S}]^-$ ($[\text{M}-\text{H}]^-$): 171.1207, found 171.1212.



S17: Thiol **S16** (0.13 mmol) was suspended in pyridine (200 mL, 0.65 M) and phenyl isothiocyanate (21 mL, 1.4 equiv) was added. The reaction was stirred for 35 minutes. Pyridine was azeotroped off with heptane and the resulting residue was purified by flash chromatography (gradient from 100% hexanes to 10% hexanes/ethyl acetate) to afford **S17** as a white solid (81% yield):

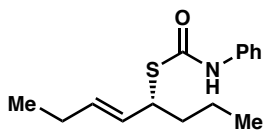
$[\alpha]_D^{23} = +69.6^{\circ}$ ($c = 0.81$, CH_2Cl_2). ^1H NMR (400 MHz, CDCl_3) δ 7.40 (d, $J = 7.5$ Hz, 2H), 7.30 (t, $J = 7.9$ Hz, 2H), 7.16 – 7.02 (m, 2H), 5.70 (dt, $J = 14.3$, 6.8 Hz, 1H), 5.42

(dd, $J = 15.2, 8.7$ Hz, 1H), 4.05 (q, $J = 8.0$ Hz, 1H), 2.01 (q, $J = 7.1$ Hz, 2H), 1.81 – 1.62 (m, 2H), 1.47 – 1.28 (m, 6H), 0.89 (q, $J = 7.0$ Hz, 6H); ^{13}C NMR (101 MHz, CDCl_3) δ 137.9, 132.9, 130.2, 129.2, 124.4, 119.8, 48.0, 35.0, 34.5, 29.5, 25.5, 22.5, 22.4, 14.1, 13.7; IR (thin film): 2920, 2342, 1440, 1146, 751, 668 cm^{-1} . HRMS (CI) calcd for $\text{C}_{17}\text{H}_{25}\text{NOS}$: 291.1657, found 291.1650.



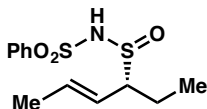
4.62: Following the general procedure for the asymmetric catalytic oxidation of unactivated olefins (Method A), *cis*-4-octene (0.4 mmol) was converted to the desired product. The hetero-ene reaction was stirred for 16 h. The product was purified according to the general procedure to afford **4.62** (80% yield, 4:1 dr) as a viscous colorless oil. The enantiomeric ratio of the product was determined to be 92.5:7.5 after conversion to thiocarbamate **S18** (see experimental procedure for **S18**):

$[\alpha]_{\text{D}}^{23} = -79.3^\circ$ ($c = 0.30$, CH_2Cl_2). ^1H NMR (400 MHz, CDCl_3) δ 7.99 – 7.89 (m, 2H), 7.68 – 7.58 (m, 1H), 7.59 – 7.49 (m, 2H), 5.89 (dt, $J = 15.6, 6.3$ Hz, 1H), 5.32 (ddt, $J = 15.5, 9.8, 1.7$ Hz, 1H), 3.45 (td, $J = 8.9, 5.2$ Hz, 0.2H), 3.14 (td, $J = 9.6, 5.4$ Hz, 0.8H), 2.22 – 2.02 (m, 2H), 1.93 – 1.79 (m, 0.8H), 1.76 – 1.30 (m, 3.2H), 1.07 – 0.87 (m, 6H); ^{13}C NMR (101 MHz, CDCl_3) δ 144.0, 143.3, 140.4, 140.3, 133.9, 133.8, 129.5, 129.5, 127.3, 127.3, 119.1, 118.5, 68.8, 68.7, 31.3, 29.9, 26.0, 26.0, 20.1, 20.0, 13.9, 13.8, 13.6, 13.4; IR (thin film): 2962, 2360, 1374, 1169, 1071, 840 cm^{-1} . HRMS (CI) calcd for $[\text{C}_{14}\text{H}_{22}\text{NO}_3\text{S}_2]^+$ ($[\text{M}+\text{H}]^+$): 316.1041, found 316.1050.



S18: 4.62 (0.2 mmol) was converted to **S18** under the previously described conditions for the synthesis of carbamothioate **S17**. Purification by preparative TLC yielded **S18** as a white solid (13% yield for 2 steps; $R_f = 0.43$ in 15% EtOAc/Hexanes):

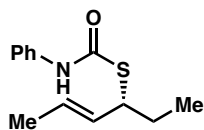
$[\alpha]_D^{23} = +40.0^\circ$ ($c = 0.18$, CH_2Cl_2). ^1H NMR (400 MHz, CDCl_3) δ 7.40 (d, $J = 8.0$ Hz, 2H), 7.31 (t, $J = 7.9$ Hz, 2H), 7.10 (t, $J = 7.4$ Hz, 1H), 6.98 (s, 1H), 5.76 (dt, $J = 13.6, 6.4$ Hz, 1H), 5.42 (dd, $J = 15.2, 8.8$ Hz, 1H), 4.06 (q, $J = 8.4, 7.9$ Hz, 1H), 2.05 (p, $J = 7.1$ Hz, 2H), 1.80 – 1.59 (m, 2H), 1.42 (h, $J = 7.3$ Hz, 2H), 0.96 (dt, $J = 22.1, 7.4$ Hz, 6H); IR (thin film): 2959, 1656, 1534, 1309, 1146, 751 cm^{-1} . HRMS (CI) calcd for $\text{C}_{15}\text{H}_{21}\text{NOS}$: 263.1344, found 263.1347.



4.63: Following the general procedure for the asymmetric catalytic oxidation of unactivated olefins (Method A), *cis*-3-hexene (0.4 mmol) was converted to the desired product. The hetero-ene reaction was stirred for 17 h. The product was purified according to the general procedure to afford **4.63** (80% yield, 4:1 dr) as a viscous colorless oil. The enantiomeric ratio of the product was determined to be 95:5 after conversion to thiocarbamate **S19** (see experimental procedure for **S19**):

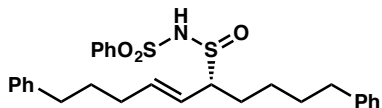
$[\alpha]_D^{23} = -14.0^\circ$ ($c = 1.30$, CH_2Cl_2). ^1H NMR (400 MHz, CDCl_3) δ 7.98 – 7.86 (m, 2H), 7.65 – 7.58 (m, 1H), 7.57 – 7.48 (m, 2H), 5.91 – 5.70 (m, 1H), 5.33 (ddq, $J = 15.1, 9.7, 1.7$ Hz, 0.8H), 5.20 (ddq, $J = 15.4, 8.5, 1.7$ Hz, 0.2H), 3.36 (td, $J = 9.3, 4.8$ Hz, 0.2H), 3.06 (td, $J = 9.6, 5.4$ Hz, 0.8H), 1.98 – 1.78 (m, 3.4H), 1.73 – 1.52 (m, 1.6H), 0.98 (dt, $J = 13.4, 7.4$ Hz, 3H); ^{13}C NMR (101 MHz, CDCl_3) δ 140.4, 140.4, 136.9, 136.2, 133.7, 133.5, 129.5, 129.4, 127.2, 127.2, 121.3, 121.0, 70.5, 70.5, 22.6, 21.5, 18.5, 18.5, 11.4,

11.3; IR (thin film): 2970, 1448, 1373, 1168, 1072, 860 cm^{-1} . HRMS (CI) calcd for $[\text{C}_{12}\text{H}_{18}\text{NO}_3\text{S}_2]^+$ ($[\text{M}+\text{H}]^+$): 288.0728, found 288.0741.



S19: 4.63 (0.2 mmol) was converted to **S19** under the previously described conditions for the synthesis of carbamothioate **S17**. Purification by preparative TLC yielded **S19** as a white solid (10% yield for 2 steps; $R_f = 0.43$ in 15% EtOAc/Hexanes):

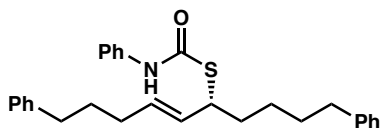
$[\alpha]_{\text{D}}^{23} = +32.3^\circ$ ($c = 0.16$, CH_2Cl_2). ^1H NMR (400 MHz, CDCl_3) δ 7.40 (d, $J = 7.2$ Hz, 2H), 7.31 (t, $J = 7.9$ Hz, 2H), 7.10 (t, $J = 7.3$ Hz, 1H), 6.99 (s, 1H), 5.79 – 5.68 (m, 1H), 5.45 (ddd, $J = 15.2, 8.7, 1.7$ Hz, 1H), 3.98 (q, $J = 7.4$ Hz, 1H), 1.84 – 1.66 (m, 5H), 0.99 (t, $J = 7.3$ Hz, 3H); IR (thin film): 2958, 1656, 1440, 1149, 882, 750 cm^{-1} . HRMS (CI) calcd for $\text{C}_{13}\text{H}_{17}\text{NOS}$: 235.1031, found 235.1035.



4.64: Following the general procedure for the asymmetric catalytic oxidation of unactivated olefins (Method A), *cis*-1,10-diphenyl-5-decene (0.4 mmol) was converted to the desired product. The hetero-ene reaction was stirred for 16 h. The product was purified according to the general procedure to afford **4.64** (80% yield, 4:1 dr) as a viscous colorless oil. The enantiomeric ratio of the product was determined to be 92.5:7.5 after conversion to thiocarbamate **S20** (see experimental procedure for **S20**):

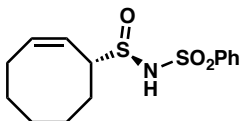
$[\alpha]_{\text{D}}^{23} = -101.7^\circ$ ($c = 0.59$, CH_2Cl_2). ^1H NMR (400 MHz, CDCl_3) δ 8.01 – 7.87 (m, 4H), 7.66 – 7.44 (m, 6H), 7.35 – 7.10 (m, 20H), 5.89 – 5.73 (m, 2H), 5.29 (ddd, $J = 30.5, 15.6, 9.0$ Hz, 2H), 3.41 (dt, $J = 8.9, 4.9$ Hz, 1H), 3.11 (dt, $J = 9.6, 5.3$ Hz, 1H), 2.59 (q, $J = 7.3$ Hz, 8H), 2.22 – 2.00 (m, 4H), 2.00 – 1.83 (m, 1H), 1.84 – 1.28 (m, 15H); ^{13}C NMR (101 MHz, CDCl_3) δ 142.1, 142.0, 142.1, 141.9, 141.9, 141.2, 140.4, 140.4, 133.8, 133.7, 129.5, 129.5, 129.0, 128.7, 128.6, 128.5, 128.5, 128.5, 127.3, 127.2, 126.3, 126.2, 126.1,

126.0, 126.0, 125.9, 120.7, 120.0, 69.0, 68.8, 35.6, 35.5, 35.5, 35.5, 32.5, 32.4, 31.1, 31.0, 30.9, 30.7, 29.1, 27.7, 26.4, 26.3; IR (thin film): 2931, 1448, 1375, 1152, 1072, 700 cm^{-1} . HRMS (ESI) calcd for $[\text{C}_{28}\text{H}_{33}\text{NO}_3\text{S}_2]^+$ ($[\text{M}+\text{Na}]^+$): 518.1794, found 518.1796.



S20: 4.64 (0.1 mmol) was converted to **S20** under the previously described conditions for the synthesis of carbamothioate **S17**. Purification by preparative TLC yielded **S20** as a white solid (16% yield for 2 steps; R_f = 0.48 in 15% EtOAc/Hexanes):

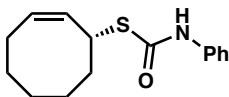
$[\alpha]^{23}_{\text{D}} = +45.7^\circ$ ($c = 0.53$, CH_2Cl_2). ^1H NMR (400 MHz, CDCl_3) δ 7.40 (d, $J = 7.9$ Hz, 2H), 7.34 – 7.22 (m, 5H), 7.22 – 7.05 (m, 6H), 6.99 (s, 1H), 5.72 (dt, $J = 14.2$, 6.8 Hz, 1H), 5.43 (dd, $J = 15.3$, 8.8 Hz, 1H), 4.06 (q, $J = 7.8$ Hz, 1H), 2.61 (q, $J = 7.7$ Hz, 4H), 2.07 (q, $J = 7.2$ Hz, 2H), 1.85 – 1.58 (m, 6H), 1.52 – 1.43 (m, 2H); IR (thin film): 2920, 1645, 1439, 1308, 1143, 752 cm^{-1} . HRMS (CI) calcd for $\text{C}_{29}\text{H}_{33}\text{NOS}$: 443.2283, found 443.2270.



4.65: Following the general procedure for the asymmetric catalytic oxidation of unactivated olefins (Method A), cyclooctene (0.4 mmol) was converted to the desired product. The hetero-ene reaction was stirred for 15 h. The product was purified according to the general procedure to afford **4.65** (76% yield, >20:1 dr) as a white solid. The enantiomeric ratio of the product was determined to be 86:14 after conversion to thiocarbamate **S20** (see experimental procedure for **S20**):

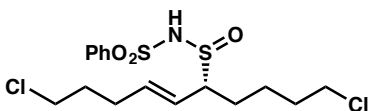
$[\alpha]^{23}_{\text{D}} = -172.8^\circ$ ($c = 1.6$, CH_2Cl_2). ^1H NMR (500 MHz, CDCl_3) δ 7.96 (d, $J = 7.7$ Hz, 2H), 7.62 (t, $J = 7.4$ Hz, 1H), 7.54 (t, $J = 7.8$ Hz, 2H), 6.12 (dt, $J = 9.6$, 7.9 Hz, 1H), 5.68 (ddd, $J = 10.2$, 8.9, 1.3 Hz, 1H), 3.77 (ddd, $J = 12.5$, 8.9, 4.1 Hz, 1H), 2.24 – 2.13 (m, 1H), 2.15 – 2.03 (m, 1H), 2.02 – 1.92 (m, 1H), 1.77 – 1.52 (m, 5H), 1.46 – 1.30 (m, 2H);

^{13}C NMR (101 MHz, CDCl_3) δ 140.4, 137.9, 133.8, 129.5, 127.3, 119.1, 62.7, 30.0, 29.0, 27.0, 26.3, 25.2; IR (thin film): 2930, 1448, 1374, 1152, 1073, 840 cm^{-1} . HRMS (CI) calcd for $[\text{C}_{14}\text{H}_{20}\text{NO}_3\text{S}_2]^+$ ($[\text{M}+\text{H}]^+$): 314.0885, found 314.0885.



S20: 4.65 (0.2 mmol) was converted to **S20** under the previously described conditions for the synthesis of carbamothioate **S17**. Purification by preparative TLC yielded **S20** as a white solid (33% yield for 2 steps; R_f = 0.36 in 10% EtOAc/Hexanes):

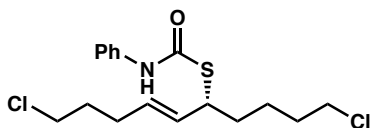
$[\alpha]^{23}_{\text{D}} = -80.0^\circ$ ($c = 0.22$, CH_2Cl_2). ^1H NMR (400 MHz, CDCl_3) δ 7.40 (d, $J = 7.2$ Hz, 2H), 7.30 (t, $J = 7.9$ Hz, 2H), 7.09 (t, $J = 7.4$ Hz, 1H), 7.02 (s, 1H), 5.77 (q, $J = 8.8$ Hz, 1H), 5.49 (t, $J = 10.3$ Hz, 1H), 4.56 – 4.45 (m, 1H), 2.40 (q, $J = 12.0, 11.4$ Hz, 1H), 2.22 – 2.09 (m, 1H), 2.04 – 1.91 (m, 1H), 1.80 – 1.62 (m, 4H), 1.56 – 1.42 (m, 2H), 1.40 – 1.28 (m, 1H); IR (thin film): 2926, 1599, 1441, 1152, 883, 750 cm^{-1} . HRMS (CI) calcd for $\text{C}_{15}\text{H}_{19}\text{NOS}$: 261.1187, found 261.1192.



4.68: Following the general procedure for the asymmetric catalytic oxidation of unactivated olefins (Method B), *cis*-1,10-dichlorodec-5-ene (0.4 mmol, 40 mol% SbCl_5) was converted to the desired product. The hetero-ene reaction was stirred for 18.5 h. The product was purified according to the general procedure to afford **4.68** (72% yield, 4:1 dr) as a white solid. The enantiomeric ratio of the product was determined to be 93.5:6.5 after conversion to thiocarbamate **S21** (see experimental procedure for **S21**):

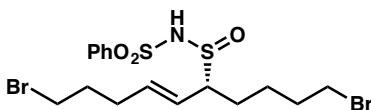
$[\alpha]^{23}_{\text{D}} = -20.4^\circ$ ($c = 2.11$, CH_2Cl_2). ^1H NMR (500 MHz, CDCl_3) δ 8.00 – 7.88 (m, 2H), 7.69 – 7.48 (m, 3H), 5.89 – 5.71 (m, 1H), 5.39 (dd, $J = 15.4, 9.6$ Hz, 0.8H), 5.28 (dd, $J = 15.5, 8.8$ Hz, 0.2H), 3.64 – 3.39 (m, 4.2H), 3.22 (dt, $J = 9.7, 5.0$ Hz, 0.8H), 2.30 (q, $J = 7.1$ Hz, 1.6H), 2.21 (q, $J = 7.4$ Hz, 0.4H), 1.95 – 1.41 (m, 8H); ^{13}C NMR (101 MHz, CDCl_3) δ 140.2, 140.2, 139.6, 139.6, 133.8, 133.7, 129.4, 129.4, 127.2, 127.1, 121.3,

121.0, 68.7, 68.5, 44.5, 44.4, 44.2, 44.2, 32.0, 31.9, 31.1, 30.7, 29.8, 29.7, 28.0, 27.3, 24.1, 24.0; IR (thin film): 2956, 1448, 1373, 1072, 855, 688 cm^{-1} . HRMS (CI) calcd for $[\text{C}_{16}\text{H}_{24}\text{NO}_3\text{S}_2\text{Cl}_2]^+$ ($[\text{M}+\text{H}]^+$): 412.0575, found 412.0571.



S21: 4.68 (0.1 mmol) was converted to **S21** under the previously described conditions for the synthesis of carbamothioate **S17**. Purification by preparative TLC yielded **S21** as a white solid (15% yield for 2 steps; $R_f = 0.38$ in 20% EtOAc/Hexanes):

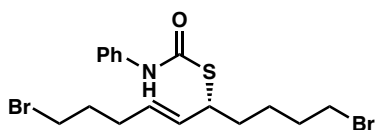
$[\alpha]_D^{23} = +75.6^\circ$ ($c = 0.59$, CH_2Cl_2). ^1H NMR (400 MHz, CDCl_3) δ 7.43 – 7.36 (m, 2H), 7.36 – 7.27 (m, 1H), 7.11 (t, $J = 7.3$ Hz, 1H), 7.00 (s, 1H), 5.74 – 5.62 (m, 1H), 5.49 (dd, $J = 15.2, 8.7$ Hz, 1H), 4.05 (q, $J = 8.2$ Hz, 1H), 3.53 (dt, $J = 8.2, 6.5$ Hz, 4H), 2.20 (q, $J = 7.1, 6.5$ Hz, 2H), 1.93 – 1.66 (m, 6H), 1.56 (q, $J = 7.3$ Hz, 2H); IR (thin film): 2919, 1652, 1438, 1308, 1144, 751 cm^{-1} . HRMS (CI) calcd for $[\text{C}_{17}\text{H}_{24}\text{NOSCl}_2]^+$ ($[\text{M}+\text{H}]^+$): 360.0956, found 360.0944.



4.69: Following the general procedure for the asymmetric catalytic oxidation of unactivated olefins (Method A), *cis*-1,10-dibromodec-5-ene (0.4 mmol) was converted to the desired product. The hetero-ene reaction was stirred for 16.5 h. The product was purified according to the general procedure to afford **4.69** (49% yield, 12:1 dr) as a white solid. The enantiomeric ratio of the product was determined to be 93.5:6.5 after conversion to thiocarbamate **S22** (see experimental procedure for **S22**):

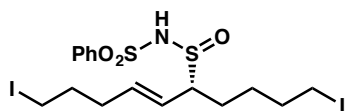
$[\alpha]_D^{23} = -70.7^\circ$ ($c = 1.8$, CH_2Cl_2). ^1H NMR (400 MHz, CDCl_3) δ 8.00 – 7.90 (m, 2H), 7.64 (t, $J = 7.4$ Hz, 1H), 7.55 (t, $J = 7.6$ Hz, 2H), 5.82 (dt, $J = 15.5, 6.8$ Hz, 1H), 5.43 (ddt, $J = 15.6, 9.7, 1.5$ Hz, 0.92H), 5.32 (dd, $J = 15.5, 8.6$ Hz, 0.08H), 3.40 (qd, $J = 6.6, 2.1$ Hz, 4.07H), 3.20 (td, $J = 9.6, 5.1$ Hz, 0.93H), 2.38 – 2.20 (m, 2H), 2.02 – 1.81 (m, 5H), 1.76 –

1.47 (m, 3H); ^{13}C NMR (101 MHz, CDCl_3) δ 140.3, 140.1, 133.9, 129.5, 127.3, 121.6, 68.6, 33.2, 33.2, 32.2, 31.2, 31.1, 28.1, 25.4; IR (thin film): 2937, 1448, 1371, 1168, 1073, 849 cm^{-1} . HRMS (ESI) calcd for $[\text{C}_{16}\text{H}_{23}\text{Br}_2\text{NO}_3\text{S}_2]^+$ ($[\text{M}+\text{Na}]^+$): 521.9378, found 521.9375.



S22: 4.69 (0.1 mmol) was converted to **S22** under the previously described conditions for the synthesis of carbamothioate **S17**. Purification by preparative TLC yielded **S22** as a white solid (16% yield for 2 steps; R_f = 0.36 in 20% EtOAc/Hexanes):

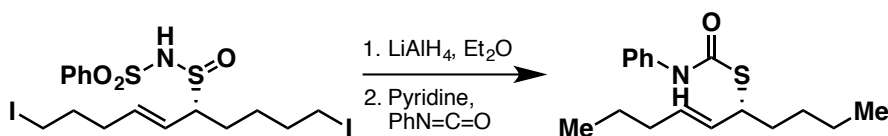
$[\alpha]_D^{23} = +40.0^\circ$ (c = 0.19, CH_2Cl_2). ^1H NMR (400 MHz, CDCl_3) δ 7.39 (d, J = 7.4 Hz, 2H), 7.32 (t, J = 7.9 Hz, 2H), 7.11 (t, J = 7.3 Hz, 1H), 6.97 (s, 1H), 5.67 (dt, J = 14.0, 6.8 Hz, 1H), 5.50 (dd, J = 15.2, 8.7 Hz, 1H), 4.05 (q, J = 8.1 Hz, 1H), 3.40 (dt, J = 8.5, 6.6 Hz, 4H), 2.21 (q, J = 6.7 Hz, 2H), 1.99 – 1.83 (m, 4H), 1.82 – 1.66 (m, 2H), 1.57 (q, J = 7.4 Hz, 2H); IR (thin film): 2920, 1652, 1438, 1308, 1142, 751 cm^{-1} . HRMS (CI) calcd for $[\text{C}_{17}\text{H}_{24}\text{NOSBr}_2]^+$ ($[\text{M}+\text{H}]^+$): 447.9945, found 447.9926.



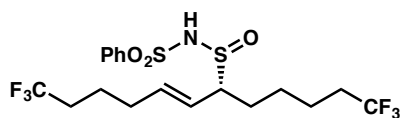
4.70: Following the general procedure for the asymmetric catalytic oxidation of unactivated olefins (Method B), *cis*-1,10-diiododec-5-ene (0.4 mmol, 40 mol% SbCl_5) was converted to the desired product. The hetero-ene reaction was stirred for 16 h. The product was purified according to the general procedure to afford **4.70** (84% yield, 9:1 dr) as a white solid. The enantiomeric ratio of the product was determined to be 93.5:6.5 after conversion to thiocarbamate **S17** (see experimental procedure for **S17**):

$[\alpha]_D^{23} = -53.6^\circ$ (c = 5.29, CH_2Cl_2). ^1H NMR (400 MHz, CDCl_3) δ 7.99 – 7.87 (m, 2H), 7.64 (t, J = 7.4 Hz, 1H), 7.61 – 7.49 (m, 2H), 5.79 (dt, J = 15.5, 6.8 Hz, 1H), 5.69 (dt, J =

14.6, 7.0 Hz, 0.1H), 5.43 (dd, $J = 15.5, 9.6$ Hz, 0.9H), 5.32 (dd, $J = 15.4, 8.5$ Hz, 0.1H), 3.39 (td, $J = 9.2, 5.0$ Hz, 0.1H), 3.25 – 3.10 (m, 4.9H), 2.35 – 2.14 (m, 2H), 1.96 – 1.77 (m, 5H), 1.75 – 1.60 (m, 1H), 1.60 – 1.42 (m, 2H); ^{13}C NMR (101 MHz, CDCl_3) δ 140.2, 139.9, 139.5, 139.5, 133.9, 133.8, 129.5, 129.5, 127.2, 127.2, 121.6, 121.2, 68.8, 68.6, 33.4, 33.3, 32.9, 32.7, 31.8, 31.2, 27.7, 27.6, 27.4, 27.1, 7.5, 6.4, 6.4, 6.3; IR (thin film): 2933, 1448, 1372, 1152, 1073, 854 cm^{-1} . LRMS (CI) calcd for $[\text{C}_{16}\text{H}_{24}\text{I}_2\text{NO}_3\text{S}_2]^+$ ($[\text{M}+\text{H}]^+$): 594.92, found 595.85.



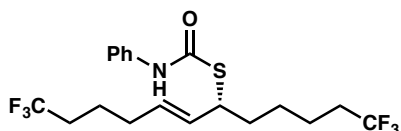
4.70 (0.15 mmol) was converted to **S17** under the previously described conditions for the synthesis of carbamothioate **S17**. Purification by preparative TLC yielded **S17** as a white solid (19% yield for 2 steps): $[\alpha]_{\text{D}}^{23} = +74.2^\circ$ ($c = 0.655$, CH_2Cl_2).



4.71: Following the general procedure for the asymmetric catalytic oxidation of unactivated olefins (Method B), *cis*-1,1,1,12,12,12-hexafluorododec-6-ene (0.34 mmol, 40 mol% SbCl_5) was converted to the desired product. The hetero-ene reaction was stirred for 14 h. The product was purified according to the general procedure to afford **4.71** (76% yield, 1:1 dr) as a pale yellow solid. The enantiomeric ratio of the product was determined to be 93.5:6.5 after conversion to thiocarbamate **S23** (see experimental procedure for **S23**):

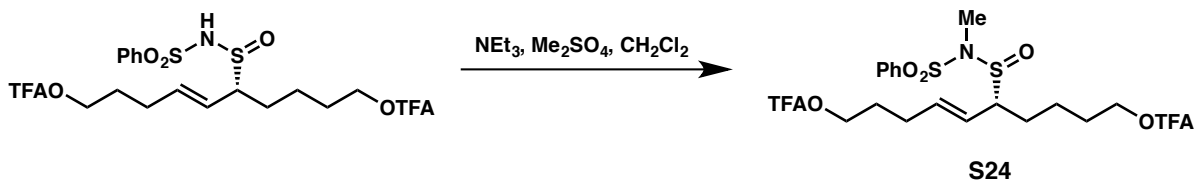
$[\alpha]_{\text{D}}^{23} = -34.0^\circ$ ($c = 2.07$, CH_2Cl_2). ^1H NMR (400 MHz, CDCl_3) δ 7.97 – 7.86 (m, 2H), 7.68 – 7.58 (m, 1H), 7.58 – 7.49 (m, 2H), 5.78 (ddt, $J = 22.1, 15.3, 6.7$ Hz, 1H), 5.34 (dd, $J = 15.5, 9.6$ Hz, 0.5H), 5.23 (dd, $J = 15.5, 8.8$ Hz, 0.5H), 3.47 (dt, $J = 9.5, 4.7$ Hz, 0.5H),

3.22 (dt, $J = 9.7, 4.9$ Hz, 0.5H), 2.28 – 1.95 (m, 6H), 1.94 – 1.76 (m, 1H), 1.71 – 1.34 (m, 7H); ^{13}C NMR (101 MHz, CDCl_3) δ 140.5, 140.4, 140.3, 139.8, 133.8, 133.6, 129.5, 129.4, 127.2, 127.2 (q, $J = 275$ Hz), 127.1 (q $J = 275$ Hz, 2C), 127.1 (q, $J = 275$ Hz), 127.1, 121.9, 121.4, 68.7, 68.5, 33.4 (q, $J = 28.5$ Hz, 2C), 33.1 (q, $J = 28.4$ Hz), 33.1 (q, $J = 28.4$ Hz), 31.6, 31.6, 28.0, 27.9, 25.9, 25.9, 21.8 (dq, $J = 8.2, 3.1$ Hz; 2C), 21.3 (q, $J = 2.9$ Hz), 21.2 (q, $J = 2.9$ Hz); IR (thin film): 2950, 1449, 1256, 1134, 1031, 838 cm^{-1} . HRMS (CI) calcd for $[\text{C}_{18}\text{H}_{24}\text{NO}_3\text{F}_6\text{S}_2]^+$ ($[\text{M}+\text{H}]^+$): 480.1102, found 480.1097.



S23: 4.71 (0.15 mmol) was converted to **S23** under the previously described conditions for the synthesis of carbamothioate **S17**. Purification by preparative TLC yielded **S23** as a white solid (14% yield for 2 steps; $R_f = 0.63$ in 20% EtOAc/Hexanes):

$[\alpha]_D^{23} = +67.4^\circ$ ($c = 0.78$, CH_2Cl_2). ^1H NMR (400 MHz, CDCl_3) δ 7.43 – 7.27 (m, 4H), 7.11 (t, $J = 7.2$ Hz, 1H), 7.00 (s, 1H), 5.67 (dt, $J = 15.1, 6.8$ Hz, 1H), 5.46 (dd, $J = 15.1, 8.8$ Hz, 1H), 4.04 (q, $J = 8.2$ Hz, 1H), 2.18 – 1.98 (m, 6H), 1.83 – 1.42 (m, 8H); IR (thin film): 2945, 1655, 1599, 1254, 1029, 752 cm^{-1} . HRMS (ESI) calcd for $[\text{C}_{19}\text{H}_{23}\text{F}_6\text{NOS}]^+$ ($[\text{M}+\text{Na}]^+$): 450.1297, found 450.1305.

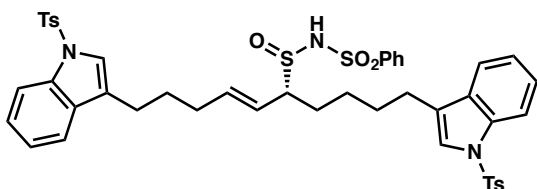


4.72: Following the general procedure for the asymmetric catalytic oxidation of unactivated olefins (Method B), *cis*-1,10-bis(2,2,2-trifluoroacetate)-5-decene (0.4 mmol, 40 mol% SbCl_5) was converted to the desired product **4.72**. The hetero-ene reaction was stirred for 14.5 h. The product was not stable to the purification procedure for method A,

so the crude product mixture was taken directly on to **S24** for analysis (75% yield by ^1H NMR analysis with 1,4-DMB as internal standard).

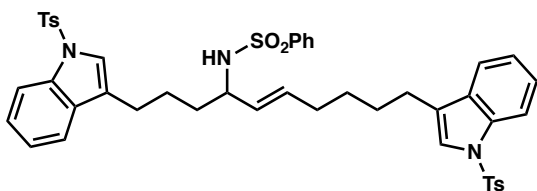
S24: Crude **4.72** was diluted in CH_2Cl_2 (2 mL, 0.2 M). Dimethylsulfate (2 mmol, 5 equiv) and trimethylamine (1.2 mmol, 3 equiv) were added sequentially and the reaction mixture was stirred at room temperature overnight. Upon completion, the reaction was concentrated under reduced pressure and purified by preparative TLC ($R_f = 0.46$ in 45% EtOAc/Hexanes) to yield **S24** as a mixture of diastereomers. The enantiomeric ratio of the product was averaged to be 93.5:6.5 by comparison to a sample of the racemate.

^1H NMR (500 MHz, CDCl_3) 7.91 (tdd, $J = 7.1, 3.1, 1.6$ Hz, 6H), 7.70 – 7.64 (m, 2H), 7.59 (dddd, $J = 13.5, 11.7, 8.9, 7.2$ Hz, 7H), 5.92 – 5.77 (m, 2H), 5.50 – 5.41 (m, 1H), 5.41 – 5.32 (m, 1H), 4.67 – 4.18 (m, 7H), 3.78 – 3.57 (m, 2H), 3.37 (dt, $J = 7.0, 4.8$ Hz, 2H), 2.83 – 2.77 (m, 6H), 2.70 (d, $J = 5.3$ Hz, 2H), 2.35 – 2.23 (m, 5H), 2.05 – 1.88 (m, 6H), 1.83 (ddt, $J = 16.2, 8.1, 6.3$ Hz, 3H), 1.73 (dddd, $J = 15.0, 8.8, 6.2, 3.6$ Hz, 3H), 1.68 – 1.54 (m, 6H), 1.54 – 1.42 (m, 2H). HRMS (ESI-TOF) calcd for $[\text{C}_{21}\text{H}_{25}\text{F}_6\text{NO}_7\text{S}_2]$: 582.1049, found 582.1048.



4.73: Following the general procedure for the asymmetric catalytic oxidation of unactivated olefins (Method B), *cis*-1,10-bis(1-tosyl-1*H*-indol-3-yl)-5-decene (0.2 mmol, 40 mol% SbCl_5) was converted to the desired product. The hetero-ene reaction was stirred for 19 h to afford **4.73** as a crude mixture (61% yield by ^1H NMR analysis with 1,4-DMB as internal standard, 1:1 dr). The enantiomeric ratio of the product was determined to be 90:10 after conversion to amine **S25** (see experimental procedure for **S25**):

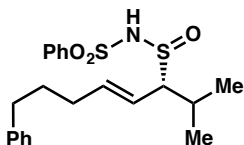
^1H NMR (400 MHz, CDCl_3) δ 8.18 (dd, $J = 8.2, 3.3$ Hz, 2H), 7.97 – 7.86 (m, 2H), 7.62 – 7.07 (m, 19H), 5.91 (ddt, $J = 16.6, 10.0, 6.7$ Hz, 1H), 5.43 (dt, $J = 15.8, 9.0$ Hz, 1H), 3.50 (td, $J = 8.6, 4.6$ Hz, 0.5H), 3.28 – 2.95 (m, 4.5H), 2.35 – 2.14 (m, 7H), 2.06 – 1.41 (m, 9H); ^{13}C NMR (101 MHz, CDCl_3) δ 150.0, 145.2, 145.2, 141.1, 140.4, 140.4, 139.6, 138.4, 138.2, 138.2, 138.2, 136.0, 136.0, 135.6, 135.5, 135.4, 135.3, 133.6, 133.5, 133.4, 132.4, 131.8, 131.5, 130.1, 129.9, 129.9, 129.5, 129.5, 129.4, 129.4, 129.3, 129.2, 129.0, 128.7, 127.8, 127.3, 127.3, 127.2, 126.4, 126.4, 126.4, 126.4, 125.5, 125.5, 125.5, 125.4, 125.3, 124.7, 124.4, 124.4, 124.3, 124.1, 123.4, 121.0, 120.3, 120.3, 119.5, 119.4, 119.4, 115.3, 115.2, 115.2, 114.9, 113.6, 111.9, 109.1, 102.5, 102.4, 102.3, 102.2, 68.7, 68.7, 32.4, 32.3, 31.7, 29.8, 29.2, 29.1, 28.9, 27.2, 27.2, 27.2, 27.1, 26.3, 26.3, 21.7, 14.3; HRMS (ESI-TOF) calcd for $[\text{C}_{46}\text{H}_{46}\text{N}_3\text{O}_7\text{S}_4]^-$ ($[\text{M}-\text{H}]^-$): 880.2224, found 880.9169.



S25: 4.73 (0.06 mmol) was converted to **S25** under the allylic amination conditions reported for **4.82**. Purification by flash chromatography (gradient from 100% hexanes to 50% hexanes/ethyl acetate) afforded the product (52% yield) as a pale yellow solid:

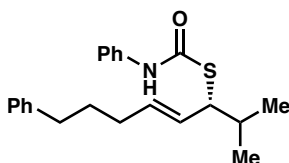
$[\alpha]_{\text{D}}^{23} = +8.0^\circ$ ($c = 0.95$, CH_2Cl_2). ^1H NMR (400 MHz, CDCl_3) δ 8.18 (d, $J = 7.7$ Hz, 2H), 7.80 (ddd, $J = 5.4, 2.9, 1.5$ Hz, 2H), 7.58 (dd, $J = 8.4, 1.6$ Hz, 4H), 7.44 – 7.25 (m, 11H), 7.17 (dd, $J = 8.2, 3.3$ Hz, 4H), 5.33 (dt, $J = 15.5, 6.5$ Hz, 1H), 5.05 (dd, $J = 15.6, 7.3$ Hz, 1H), 4.46 (d, $J = 8.0$ Hz, 1H), 3.78 (p, $J = 7.1$ Hz, 1H), 3.03 (dq, $J = 7.9, 4.1$ Hz, 4H), 2.33 (s, 6H), 1.84 (q, $J = 7.7$ Hz, 2H), 1.71 – 1.50 (m, 8H); ^{13}C NMR (101 MHz, CDCl_3) δ 145.3, 145.2, 141.2, 138.8, 138.1, 136.1, 136.0, 135.6, 135.6, 132.9, 132.4, 130.1, 130.0, 129.3, 129.3, 129.2, 128.9, 127.3, 126.4, 126.4, 125.5, 125.4, 124.4, 124.3, 119.5, 119.4, 115.2, 115.2, 102.3, 102.2, 56.1, 35.5, 31.6, 29.8, 29.3, 28.3, 27.4, 27.1, 25.8,

21.7; IR (thin film): 2926, 1448, 1372, 1175, 1091, 754 cm^{-1} . HRMS (ESI-TOF) calcd for $[\text{C}_{46}\text{H}_{48}\text{N}_3\text{O}_6\text{S}_3]^+$ ($[\text{M}+\text{H}]^+$): 834.2700, found 834.0742.



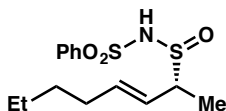
4.74: Following the general procedure for the asymmetric catalytic oxidation of unactivated olefins (Method A), *cis*-(7-methyl-5-octenyl)benzene (0.4 mmol) was converted to the desired product. The hetero-ene reaction was stirred for 16 h. The product was purified according to the general procedure to afford **4.74** (68% yield, >20:1 rr, 1.5:1 dr) as a viscous colorless oil. The enantiomeric ratio of the product was determined to be 96:4 after conversion to **S26** (see experimental procedure for **S26**):

$[\alpha]_{\text{D}}^{23} = -5.4^\circ$ ($c = 0.56$, CH_2Cl_2). ^1H NMR (400 MHz, CDCl_3) δ 7.98 – 7.85 (m, 2H), 7.67 – 7.41 (m, 3H), 7.29 (t, $J = 7.4$ Hz, 2H), 7.24 – 7.12 (m, 3H), 5.80 (ddt, $J = 30.4, 15.4, 6.8$ Hz, 1H), 5.46 (dd, $J = 15.6, 10.2$ Hz, 0.4H), 5.14 (dd, $J = 15.3, 9.9$ Hz, 0.6H), 3.31 (dd, $J = 9.9, 5.9$ Hz, 0.6H), 2.82 – 2.76 (t, $J = 9.7$ Hz, 0.4H), 2.69 – 2.51 (m, 2H), 2.30 – 2.06 (m, 2H), 2.03 – 1.92 (m, 1H), 1.75 (p, $J = 7.6$ Hz, 1H), 1.69 – 1.56 (m, 1H), 1.18 (d, $J = 6.6$ Hz, 1H), 0.99 (td, $J = 6.9, 4.2$ Hz, 5H); ^{13}C NMR (101 MHz, CDCl_3) δ 142.5, 142.3, 142.1, 141.8, 140.4, 140.4, 133.8, 133.6, 129.5, 129.4, 128.6, 128.5, 128.5, 128.4, 127.2, 127.2, 126.0, 125.9, 119.7, 117.9, 76.7, 76.3, 35.5, 35.4, 32.5, 32.4, 31.1, 30.7, 28.8, 27.7, 20.8, 20.6, 20.4, 18.4; IR (thin film): 2930, 1449, 1371, 1169, 1090, 865 cm^{-1} . HRMS (CI) calcd for $[\text{C}_{21}\text{H}_{28}\text{NO}_3\text{S}_2]^+$ ($[\text{M}+\text{H}]^+$): 406.1511, found 406.1503.



S26: **4.74** (0.07 mmol) was converted to **S26** under the previously described conditions for the synthesis of carbamothioate **S17**. Purification by preparative TLC yielded **S26** as a white solid (6% yield for 2 steps; R_f = 0.78 in 20% EtOAc/Hexanes):

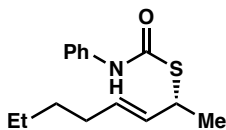
$[\alpha]_D^{23} = +57.5^\circ$ ($c = 0.08$, CH_2Cl_2). ^1H NMR (400 MHz, CDCl_3) δ 7.43 – 7.35 (m, 2H), 7.38 – 7.24 (m, 3H), 7.28 – 7.20 (m, 1H), 7.16 (td, $J = 7.8, 1.3$ Hz, 3H), 7.14 – 7.04 (m, 1H), 5.73 (dt, $J = 14.7, 6.7$ Hz, 1H), 5.47 (ddt, $J = 15.2, 9.3, 1.4$ Hz, 1H), 4.01 (dd, $J = 9.3, 5.5$ Hz, 1H), 2.64 – 2.55 (m, 2H), 2.08 (q, $J = 8.2, 7.6$ Hz, 2H), 1.99 (dq, $J = 13.3, 6.7$ Hz, 1H), 1.70 (p, $J = 7.5$ Hz, 2H), 1.00 (dd, $J = 6.7, 1.2$ Hz, 6H); IR (thin film): 2926, 1598, 1437, 1308, 1144, 750 cm^{-1} . HRMS (CI) calcd for $\text{C}_{22}\text{H}_{27}\text{NOS}$: 353.1813, found 353.1802.



4.75: Following the general procedure for the asymmetric catalytic oxidation of unactivated olefins (Method C), *cis*-2-octene (0.4 mmol) was converted to the desired product. The hetero-ene reaction was stirred for 16 h. The product was purified according to the general procedure to afford **4.75** (54% yield, >20:1 rr, 12:1 dr) as a viscous colorless oil. The enantiomeric ratio of the product was determined to be 90:10 after conversion to thiocarbamate **S27** (see experimental procedure for **S27**):

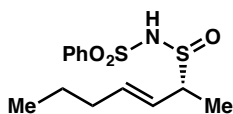
$[\alpha]_D^{23} = -68.3^\circ$ ($c = 0.80$, CH_2Cl_2). ^1H NMR (500 MHz, CDCl_3) δ 7.98 – 7.90 (m, 2H), 7.67 – 7.59 (m, 1H), 7.58 – 7.51 (m, 2H), 5.88 – 5.76 (m, 1H), 5.48 – 5.30 (m, 1H), 3.61 (p, $J = 7.1$ Hz, 0.08H), 3.33 (dp, $J = 7.1, 3.4$ Hz, 2H), 2.14 – 2.03 (m, 2H), 1.43 (dd, $J = 7.0, 2.3$ Hz, 3H), 1.40 – 1.25 (m, 5H), 0.88 (dt, $J = 7.2, 2.5$ Hz, 3H); ^{13}C NMR (101 MHz, CDCl_3) δ 141.1, 140.4, 133.8, 129.5, 127.3, 121.5, 63.6, 32.5, 31.2, 22.3, 14.4, 14.0; IR

(thin film): 2930, 1448, 1376, 1169, 1073, 854 cm^{-1} . HRMS (CI) calcd for $[\text{C}_{14}\text{H}_{22}\text{NO}_3\text{S}_2]^+$ ($[\text{M}+\text{H}]^+$): 316.1041, found 316.1044.



S27: **4.75** (0.13 mmol) was converted to **S27** under the previously described conditions for the synthesis of carbamothioate **S17**. Purification by preparative TLC yielded **S27** as a white solid (26% yield for 2 steps; $R_f = 0.5$ in 15% EtOAc/Hexanes):

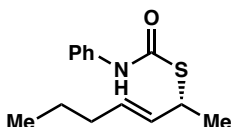
$[\alpha]_D^{23} = +83.2^\circ$ ($c = 0.375$, CH_2Cl_2). ^1H NMR (500 MHz, CDCl_3) δ 7.40 (d, $J = 8.0$ Hz, 2H), 7.31 (t, $J = 7.7$ Hz, 2H), 7.10 (t, $J = 7.4$ Hz, 1H), 6.99 (s, 1H), 5.69 (dt, $J = 14.0, 6.6$ Hz, 1H), 5.53 (dd, $J = 15.3, 7.4$ Hz, 1H), 4.19 (p, $J = 6.9$ Hz, 1H), 2.02 (q, $J = 7.0$ Hz, 2H), 1.47 (d, $J = 7.0$ Hz, 3H), 1.36 – 1.27 (m, 4H), 0.88 (t, $J = 7.0$ Hz, 3H); IR (thin film): 2926, 1655, 1440, 1309, 1149, 751 cm^{-1} . HRMS (CI) calcd for $[\text{C}_{15}\text{H}_{21}\text{NOS}]$: 263.1344, found 263.1339.



4.76: Following the general procedure for the asymmetric catalytic oxidation of unactivated olefins (Method C), cis-2-heptene (0.4 mmol) was converted to the desired product. The hetero-ene reaction was stirred for 16 h. The product was purified according to the general procedure to afford **4.76** (61% yield, >20:1 rr, 11:1 dr) as a viscous colorless oil. The enantiomeric ratio of the product was determined to be 89.5:10.5 after conversion to thiocarbamate **S28** (see experimental procedure for **S28**):

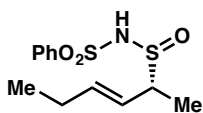
$[\alpha]_D^{23} = -69.6^\circ$ ($c = 0.75$, CH_2Cl_2). ^1H NMR (500 MHz, CDCl_3) δ 7.99 – 7.89 (m, 2H), 7.62 (t, $J = 7.4$ Hz, 1H), 7.54 (t, $J = 8.0$ Hz, 2H), 5.87 – 5.74 (m, 1H), 5.45 – 5.30 (m, 1H), 3.62 (p, $J = 6.9$ Hz, 0.08H), 3.35 (dq, $J = 9.4, 7.1$ Hz, 0.92H), 2.12 – 1.98 (m, 2H),

1.47 – 1.36 (m, 5H), 0.91 – 0.84 (m, 3H); ^{13}C NMR (101 MHz, CDCl_3) δ 140.9, 140.4, 133.8, 129.5, 127.3, 121.7, 63.6, 34.8, 22.2, 14.4, 13.7; IR (thin film): 2960, 1448, 1373, 1168, 1073, 852 cm^{-1} . HRMS (CI) calcd for $[\text{C}_{13}\text{H}_{20}\text{NO}_3\text{S}_2]^+$ ($[\text{M}+\text{H}]^+$): 302.0885, found 302.0876.



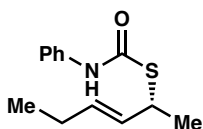
S28: 4.76 (0.17 mmol) was converted to **S28** under the previously described conditions for the synthesis of carbamothioate **S17**. Purification by preparative TLC yielded **S28** as a white solid (7% yield for 2 steps; R_f = 0.30 in 15% EtOAc/Hexanes):

$[\alpha]_D^{23} = +57.6^\circ$ (c = 0.30, CH_2Cl_2). ^1H NMR (400 MHz, CDCl_3) δ 7.40 (dd, J = 8.6, 1.3 Hz, 2H), 7.31 (t, J = 7.9 Hz, 2H), 7.10 (t, J = 7.3 Hz, 0H), 6.96 (s, 1H), 5.69 (dt, J = 15.4, 6.8 Hz, 1H), 5.54 (ddt, J = 15.3, 7.3, 1.3 Hz, 1H), 4.20 (p, J = 6.9 Hz, 1H), 2.00 (q, J = 7.4 Hz, 2H), 1.47 (d, J = 7.0 Hz, 3H), 1.39 (h, J = 7.3 Hz, 2H), 0.88 (t, J = 7.4 Hz, 4H); IR (thin film): 2920, 1652, 1599, 1440, 1142, 750 cm^{-1} . HRMS (ESI-TOF) calcd for $[\text{C}_{14}\text{H}_{19}\text{NOS}]^-$ ($[\text{M}-\text{H}]^-$): 248.1115, found 248.0656.



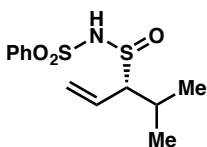
4.77: Following the general procedure for the asymmetric catalytic oxidation of unactivated olefins (Method C), *cis*-2-hexene (0.4 mmol) was converted to the desired product. The hetero-ene reaction was stirred for 16.5 h. The product was purified according to the general procedure to afford **4.77** (63% yield, >20:1 rr, 7:1 dr) as a viscous colorless oil. The enantiomeric ratio of the product was determined to be 88.5:11.5 after conversion to thiocarbamate **S29** (see experimental procedure for **S29**):

$[\alpha]_D^{23} = -78.0^\circ$ ($c = 1.02$, CH_2Cl_2). ^1H NMR (500 MHz, CDCl_3) δ 8.02 – 7.93 (m, 2H), 7.66 (t, $J = 7.4$ Hz, 1H), 7.57 (t, $J = 7.8$ Hz, 2H), 5.91 (dt, $J = 15.5$, 6.3 Hz, 1H), 5.49 – 5.33 (m, 1H), 3.64 (p, $J = 7.0$ Hz, 0.12H), 3.37 (dq, $J = 9.2$, 7.1 Hz, 0.88H), 2.20 – 2.08 (m, 2H), 1.46 (d, $J = 7.0$ Hz, 2.64H), 1.35 (d, $J = 7.0$ Hz, 0.36H), 1.09 – 0.97 (m, 3H); ^{13}C NMR (101 MHz, CDCl_3) δ 42.6, 140.4, 133.8, 129.5, 127.3, 120.5, 63.6, 25.9, 14.5, 13.5; IR (thin film): 2967, 1449, 1372, 1168, 1073, 857 cm^{-1} . HRMS (CI) calcd for $[\text{C}_{12}\text{H}_{18}\text{NO}_3\text{S}_2]^+$ ($[\text{M}+\text{H}]^+$): 288.0728, found 288.0730.



S29: 4.77 (0.24 mmol) was converted to **S29** under the previously described conditions for the synthesis of carbamothioate **S17**. Purification by preparative TLC yielded **S29** as a white solid (5% yield for 2 steps; $R_f = 0.39$ in 15% EtOAc/Hexanes):

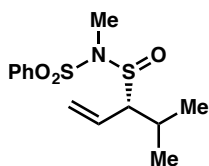
$[\alpha]_D^{23} = +51.3^\circ$ ($c = 0.16$, CH_2Cl_2). ^1H NMR (500 MHz, CDCl_3) δ 7.40 (dd, $J = 8.5$, 1.2 Hz, 2H), 7.31 (dd, $J = 8.6$, 7.3 Hz, 2H), 7.10 (tt, $J = 7.3$, 1.2 Hz, 1H), 7.02 (s, 1H), 5.74 (dtd, $J = 15.4$, 6.3, 1.2 Hz, 1H), 5.54 (ddt, $J = 15.3$, 7.3, 1.6 Hz, 1H), 4.20 (p, $J = 7.0$ Hz, 1H), 2.10 – 2.00 (m, 2H), 1.47 (d, $J = 7.0$ Hz, 3H), 0.98 (t, $J = 7.5$ Hz, 3H); IR (thin film): 2925, 1599, 1442, 1311, 1238, 751 cm^{-1} . HRMS (CI) calcd for $[\text{C}_{13}\text{H}_{17}\text{NOS}]$: 235.1031, found 235.1032.



4.78: Following the general procedure for the asymmetric catalytic oxidation of unactivated olefins (Method A), *cis*-4-methyl-2-pentene (0.4 mmol) was converted to the desired product. The hetero-ene reaction was stirred for 15 h. The product was purified according to the general procedure to afford **4.78** (21% yield, >20:1 rr, 9:1 dr) as a

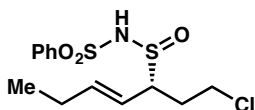
viscous colorless oil. The enantiomeric ratio of the product was determined to be 87.5:12.5 after conversion to **S30** (see experimental procedure for **S30**):

$[\alpha]_D^{23} = -70.7^\circ$ ($c = 0.22$, CH_2Cl_2). ^1H NMR (400 MHz, CDCl_3) δ 8.00 – 7.86 (m, 2H), 7.67 – 7.47 (m, 3H), 5.80 (dt, $J = 17.1, 10.2$ Hz, 0.9H), 5.65 (dd, $J = 10.2, 1.7$ Hz, 0.9H), 5.61 – 5.46 (m, 0.1H), 5.43 – 5.25 (m, 1.1H), 3.26 (dt, $J = 9.5, 6.2$ Hz, 0.1H), 2.80 (t, $J = 9.7$ Hz, 0.9H), 2.29 – 2.06 (m, 1H), 1.19 (d, $J = 6.6$ Hz, 3H), 1.05 – 0.95 (m, 3H); ^{13}C NMR (101 MHz, CDCl_3) δ 140.3, 133.9, 129.5, 128.2, 127.3, 125.7, 77.0, 28.6, 20.6, 20.3; IR (thin film): 3251, 1448, 1370, 1161, 1090, 756 cm^{-1} . HRMS (CI) calcd for $[\text{C}_{12}\text{H}_{18}\text{NO}_3\text{S}_2]^+$ ($[\text{M}+\text{H}]^+$): 288.0728, found 288.0734.



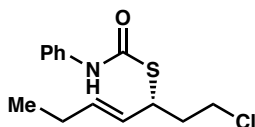
S30: 4.78 (0.06 mmol) was converted to **S30** by dissolving the ene adduct in CH_3Cl_2 (0.1 M) and adding NEt_3 (1.2 equiv) and dimethylsulfate (2 equiv) sequentially. After stirring at 23 $^\circ\text{C}$ for 2 hours, the reaction was concentrated. Purification by preparative TLC yielded **S30** as a colorless oil (49% yield, 9:1 dr; $R_f = 0.2$ in 15% EtOAc/Hexanes):

$[\alpha]_D^{23} = -43.9^\circ$ ($c = 0.41$, CH_2Cl_2). ^1H NMR (400 MHz, CDCl_3) δ 7.97 – 7.83 (m, 2H), 7.60 (dt, $J = 33.7, 7.2$ Hz, 3H), 5.97 – 5.83 (m, 0.9H), 5.79 – 5.64 (m, 0.1H), 5.56 – 5.34 (m, 2H), 3.22 (dd, $J = 10.1, 5.9$ Hz, 1H), 2.78 (bs, 3H), 2.41 – 2.18 (m, 1H), 1.12 (d, $J = 6.8$ Hz, 3H), 1.06 (d, $J = 6.7$ Hz, 3H); ^{13}C NMR (101 MHz, CDCl_3) δ 137.6, 133.8, 129.6, 127.9, 127.7, 124.8, 78.1, 28.4, 26.3, 21.0, 18.9; IR (thin film): 2967, 1447, 1354, 1168, 1087, 804 cm^{-1} . HRMS (CI) calcd for $[\text{C}_{13}\text{H}_{20}\text{NO}_3\text{S}_2]^+$ ($[\text{M}+\text{H}]^+$): 302.0885, found 302.0874.



4.79: Following the general procedure for the asymmetric catalytic oxidation of unactivated olefins (Method B), *cis*-1-chloro-3-heptene (0.4 mmol, 40 mol% SbCl_5) was converted to the desired product. The hetero-ene reaction was stirred for 23 h to afford **4.79** as a crude mixture (59% ^1H NMR yield, >20:1 rr, dr). This product was not stable to the purification procedure for method A, so the crude product mixture was taken directly on to **S31** (see experimental procedure for **S31**). The enantiomeric ratio of the product was determined to be 93:7 after conversion to **S31**.

HRMS (CI) calcd for $[\text{C}_{13}\text{H}_{19}\text{NO}_3\text{S}_2\text{Cl}]^+$ ($[\text{M}+\text{H}]^+$): 336.0495, found 336.0493.

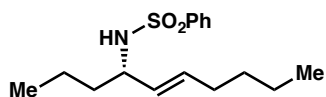


S31: Crude **4.79** was converted to **S31** under the previously described conditions for the synthesis of carbamothioate **S17**. Purification by preparative TLC yielded **S31** as a white solid ($R_f = 0.79$ in 20% EtOAc/Hexanes):

$[\alpha]_D^{23} = +40.0^\circ$ ($c = 0.10$, CH_2Cl_2). ^1H NMR (400 MHz, CDCl_3) δ 7.40 (d, $J = 7.8$ Hz, 2H), 7.31 (t, $J = 7.8$ Hz, 2H), 7.11 (t, $J = 7.3$ Hz, 1H), 7.03 (s, 1H), 5.82 (dt, $J = 15.3, 6.3$ Hz, 1H), 5.44 (dd, $J = 15.4, 8.8$ Hz, 1H), 4.22 (q, $J = 7.9$ Hz, 1H), 3.60 (qt, $J = 10.9, 7.1$ Hz, 2H), 2.31 – 1.98 (m, 4H), 0.99 (t, $J = 7.4$ Hz, 3H); IR (thin film): 2924, 1600, 1441, 1309, 1146, 751 cm^{-1} . HRMS (CI) calcd for $[\text{C}_{14}\text{H}_{19}\text{NOSCl}]^+$ ($[\text{M}+\text{H}]^+$): 284.0876, found 284.0869.

$[\alpha]_D^{23} = +11.6^\circ$ ($c = 0.43$, CH_2Cl_2). ^1H NMR (400 MHz, CDCl_3) δ 7.40 (d, $J = 7.3$ Hz, 1H), 7.31 (dd, $J = 8.6, 7.2$ Hz, 2H), 7.10 (t, $J = 7.3$ Hz, 1H), 7.00 (s, 1H), 5.70 (dt, $J = 15.2, 6.7$ Hz, 1H), 5.57 (ddt, $J = 15.4, 8.5, 1.3$ Hz, 1H), 4.00 (q, $J = 7.6$ Hz, 1H), 3.53 (t, $J = 6.9$ Hz, 2H), 2.59 – 2.41 (m, 2H), 1.89 – 1.66 (m, 2H), 1.00 (t, $J = 7.4$ Hz, 3H); IR (thin film): 3293, 1599, 1440, 1309, 1147, 751 cm^{-1} . HRMS (CI) calcd for $\text{C}_{14}\text{H}_{18}\text{NOS}$: 283.0798, found 283.0795.

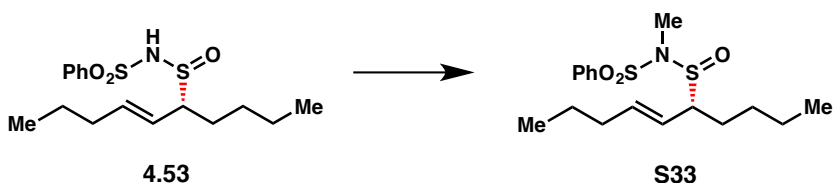
Synthetic Procedures for the Diversification of **4.53**



4.82: Ene adduct **4.53** (0.15 mmol, 92.5:7.5 er) was dissolved in anhydrous toluene (0.2M) within a flame-dried vial set under argon atmosphere. Chlorotitanium(IV) triisopropoxide (30 mL, 1 M hexanes, 20 mol%), was added dropwise, and the solution heated to 60 $^\circ\text{C}$. The reaction mixture was stirred at this temperature for 1.5 h or until TLC indicated complete disappearance of **4.53**, at which time the reaction was cooled to room temperature and diluted in MeOH (1.4 mL). Trimethyl phosphite (88 mL, 5 equiv) was added in and the solution was stirred for 2 h. The reaction was quenched by addition of water (2 mL) and the crude solution was washed with EtOAc (3 x 7 mL). The combined organics were dried over Na_2SO_4 , filtered and concentrated. Purification by flash chromatography (100% hexanes to 20% EtOAc/Hexanes) afforded **4.82** (71% yield, 91.5:8.5 er, 98% es) as a colorless oil:

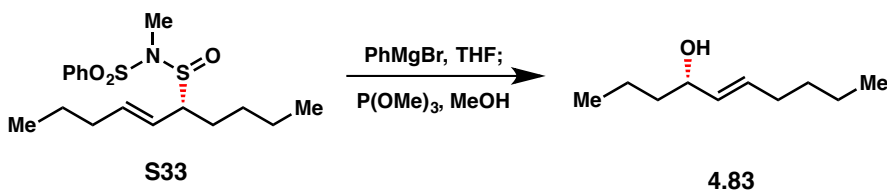
$[\alpha]_D^{23} = -4.2^\circ$ ($c = 0.53$, CH_2Cl_2). ^1H NMR (400 MHz, CDCl_3) δ 7.84 (d, $J = 7.1$ Hz, 2H), 7.54 (t, $J = 7.3$ Hz, 1H), 7.47 (t, $J = 7.3$ Hz, 2H), 5.30 (dt, $J = 14.6, 6.7$ Hz, 1H), 5.02 (dd, $J = 15.3, 7.5$ Hz, 1H), 4.45 (d, $J = 7.8$ Hz, 1H), 3.73 (p, $J = 7.2$ Hz, 1H), 1.78 (q, $J = 6.6, 6.0$ Hz, 2H), 1.53 – 1.32 (m, 2H), 1.34 – 1.06 (m, 8H), 0.83 (t, $J = 6.9$ Hz, 6H); ^{13}C NMR (101 MHz, CDCl_3) δ 141.4, 133.0, 132.4, 129.3, 128.9, 127.3, 56.2, 38.4, 31.8, 31.1,

22.2, 18.8, 14.0, 13.8; IR (thin film): 3273, 2959, 1448, 1325, 1163, 689 cm^{-1} . HRMS (CI) calcd for $[\text{C}_{16}\text{H}_{26}\text{NO}_2\text{S}]^+$ ($[\text{M}+\text{H}]^+$): 296.1684, found 296.1683.



S33: Ene adduct **4.53** (0.093 mmol, 91.5:8.5 er) was dissolved in CH₂Cl₂. Dimethylsulfate (44 μl, 5 equiv) and trimethylamine (39 μl, 3 equiv) were added and the reaction mixture was stirred at room temperature overnight. Upon completion, CH₂Cl₂ (1 mL) was added and the reaction was concentrated to yield a crude viscous oil which was purified by column chromatography (gradient 0-20% EtOAc\ hexanes) to afford **S33** as a clear oil (87% yield).

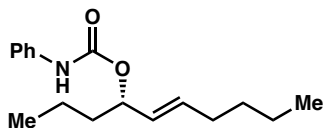
¹H NMR (500 MHz, CDCl₃) (mixture of two diastereomers) δ 7.96 – 7.86 (m, 4H), 7.70 – 7.60 (m, 2H), 7.60 – 7.48 (m, 4H), 5.82 (ddt, J = 36.2, 15.2, 6.8 Hz, 2H), 5.39 (ddt, J = 15.3, 9.2, 1.5 Hz, 1H), 5.27 (ddt, J = 15.4, 9.6, 1.5 Hz, 1H), 3.38 – 3.27 (m, 2H), 2.80 (d, J = 7.5 Hz, 6H), 2.22 – 1.99 (m, 4H), 2.03 – 1.79 (m, 2H), 1.77 – 1.58 (m, 4H), 1.54 – 1.27 (m, 16H), 1.06 – 0.79 (m, 15H). HRMS (ESI-TOF) calcd for [C₁₇H₂₇NO₃S₂] 358.1505, found 358.1504.



4.83: A flame-dried round-bottom flask was charged with anhydrous THF (0.8 mL) and compound **S33** (0.0808 mmol) and the flask was cooled to 0 °C in an ice bath. PhMgBr (0.24 mmol, 3 equiv) was added dropwise to the flask while maintaining the reaction temperature at 0 °C. After the reaction was stirred for additional 2 hours at 0 °C,

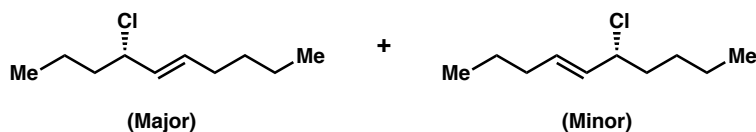
trimethyl phosphite (66 μ l, 5 equiv) and methanol was added and the reaction mixture was allowed to warm up to room temperature and stirred overnight. Upon completion, CH_2Cl_2 was added and the reaction was concentrated to yield a crude product. The crude product was purified by column chromatography (gradient 0-20% EtOAc/ hexanes) to afford **4.83** as clear oil (10.7 mg, 85% yield). The enantiospecificity of this reaction sequence was determined to be 99% after conversion to **S34** (see experimental procedure for **S34**):

^1H NMR (500 MHz, CDCl_3) δ 5.65 (dtd, $J = 15.3, 6.7, 1.0$ Hz, 1H), 5.47 (ddt, $J = 15.4, 7.2, 1.4$ Hz, 1H), 4.07 (q, $J = 6.7$ Hz, 1H), 2.05 (q, $J = 6.8$ Hz, 2H), 1.93 – 1.79 (m, 1H), 1.65 – 1.49 (m, 1H), 1.49 – 1.40 (m, 2H), 1.40 – 1.25 (m, 5H), 0.93 (dt, $J = 14.3, 7.1$ Hz, 6H). ^{13}C NMR (126 MHz, CDCl_3) δ 132.94, 132.24, 73.04, 39.46, 31.89, 31.37, 22.22, 18.72, 14.02, 13.95. IR (thin film): 3399, 2930, 1714, 1458, 969 cm^{-1} . HRMS (CI) calcd for $[\text{C}_{10}\text{H}_{19}\text{O}]^-$ ($[\text{M}-\text{H}]^-$): 155.1436, found 155.1436



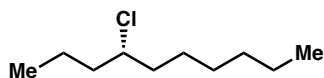
S34: 4.83 (0.17 mmol) was converted to **S34** under the previously described conditions for the synthesis of carbamothioate **S17**. Purification by preparative TLC yielded **S34** as a white solid (62% yield; $R_f = 0.53$ in 15% EtOAc/Hexanes; 91:9 er):

$[\alpha]_D^{23} = -17.7^\circ$ ($c = 0.53$, CH_2Cl_2). ^1H NMR (500 MHz, CDCl_3) δ 7.41 (d, $J = 8.0$ Hz, 2H), 7.37 – 7.30 (m, 3H), 6.59 (s, 1H), 5.79 (dt, $J = 15.7, 6.8$ Hz, 1H), 5.45 (ddt, $J = 15.4, 7.5, 1.5$ Hz, 1H), 5.22 (q, $J = 7.0$ Hz, 1H), 2.31 – 1.96 (m, 2H), 1.78 – 1.53 (m, 2H), 1.49 – 1.25 (m, 6H), 0.96 (t, $J = 7.4$ Hz, 3H), 0.91 (t, $J = 7.1$ Hz, 3H). IR (thin film): 3320, 2958, 1700, 1539, 1050 cm^{-1} . HR-MS (CI) calcd for $[\text{C}_{17}\text{H}_{25}\text{NO}_2]$ ($[\text{M}]$): 275.1885, found 275.1884.



4.85: Ene adduct **4.53** (0.12 mmol, 94:6 er) was diluted in Et₂O (0.6 mL, 0.2 M) within a flame-dried vial set under argon atmosphere. Sulfuryl chloride (11 mL, 1.1 equiv) was added in dropwise at -78°C and the solution warmed to -5°C . After stirring for 30 minutes, the reaction was quenched by addition of water (0.2 mL). The layers were separated and the aqueous layer was washed with Et₂O (3 x 3 mL). The combined organic extracts were dried over MgSO₄ and concentrated under reduced pressure. The resulting residue was suspended in pentane (5 mL) and filtered through a celite plug to afford **4.85** (94% crude yield, 3:1 rr by ¹³C NMR analysis, 95% es). The major regioisomer was assigned after conversion of **4.85** to **S35** (see experimental procedure below). The enantiomeric ratio of the product was determined to be 89:11 after conversion to **S36** (see experimental procedure for **S36**):

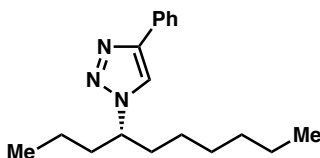
¹H NMR (400 MHz, CDCl₃) δ 5.67 (dtd, $J = 16.0, 6.8, 2.7$ Hz, 1H), 5.51 (ddt, $J = 15.2, 8.8, 1.5$ Hz, 1H), 4.34 (dt, $J = 13.5, 6.2$ Hz, 1H), 2.09 – 1.96 (m, 2H), 1.87 – 1.68 (m, 2H), 1.51 – 1.23 (m, 6H), 0.96 – 0.87 (m, 6H); ¹³C NMR (101 MHz, CDCl₃) δ 133.7, 133.5, 131.4, 131.1, 64.0, 63.7, 41.1, 38.8, 34.1, 31.8, 31.2, 28.9, 22.3, 22.3, 22.2, 20.0, 14.1, 14.1, 13.8, 13.6.



S35: Our procedure was modified from a method reported in the literature for olefin reduction¹⁰⁴: A flame-dried flask was charged with potassium (E)-diazene-1,2-dicarboxylate (254 mg, 12 equiv) and CH₂Cl₂ (2.2 mL, 0.05 M) under argon atmosphere. 4-chloro-5-decene (**4.85**) (0.11 mmol) was added to the suspension followed by dropwise addition of acetic acid (0.88 mL, 0.5M CH₂Cl₂, 4 equiv). The mixture was heated to 30 $^{\circ}\text{C}$ and stirred vigorously for 13.5 h. The resulting suspension was cooled to room

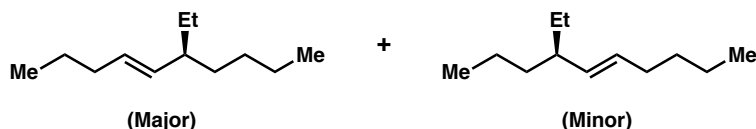
temperature, filtered through a short silica gel plug and concentrated. Purification by flash chromatography (100% pentane) afforded **S35** (71% yield, 2:1 rr by ^{13}C NMR) as a colorless oil. ^1H NMR and ^{13}C NMR spectra were consistent with authentic samples of the corresponding regioisomers prepared by Appel chlorination¹⁰⁵:

$[\alpha]_D^{23} = +1.5^\circ$ ($c = 0.14$, CH_2Cl_2). ^1H NMR (400 MHz, CDCl_3) δ 3.95 – 3.86 (m, 1H), 1.78 – 1.65 (m, 4H), 1.61 – 1.28 (m, 10H), 0.99 – 0.86 (m, 6H); ^{13}C NMR (101 MHz, CDCl_3) δ 64.5, 64.2, 40.7, 38.7, 38.6, 38.4, 31.9, 31.5, 29.0, 28.8, 26.6, 26.3, 22.7, 22.7, 22.4, 19.9, 14.2, 14.2, 14.1, 13.8; IR (thin film): 2932, 2873, 2860, 1466, 1380, 725 cm^{-1} . HRMS (ESI-TOF) calcd for $[\text{C}_{10}\text{H}_{21}\text{Cl}]^+$ ($[\text{M}+\text{Na}]^+$): 199.1224, found 199.9909.



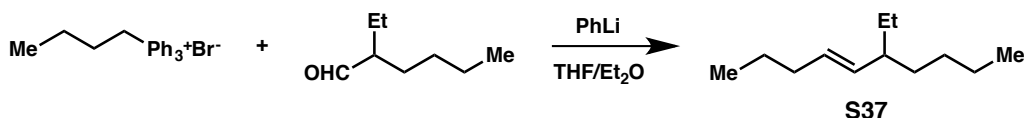
S36: Our procedure was modified from a method reported in the literature for the synthesis of 1,4-disubstituted 1,2,3-triazoles¹⁰⁶: 4-Chlorodecane **S35** (0.28 mmol) was added to a suspension of sodium azide (28 mg, 1.5 equiv) in DMSO (0.56 mL, 0.5 M) and heated to 50 $^\circ\text{C}$. After stirring for 2 h, the reaction was diluted with water (10 mL) and washed with Et_2O (3 x 10 mL). Combined organics were dried over MgSO_4 and concentrated to yield crude 4-azidodecane, which was taken directly on to the next step. $\text{CuSO}_4 \cdot 5\text{H}_2\text{O}$ (7 mg, 10 mol%) and sodium L-ascorbate (11 mg, 20 mol%) were suspended in water/methanol (1:0.5 mL). Phenylacetylene (34 mL, 1.1 equiv) was added in followed by crude 4-azidodecane in 0.5 mL methanol and the heterogenous mixture was stirred overnight. The crude mixture was diluted with water (2 mL) and extracted with CH_2Cl_2 (3 x 5 mL). The organic extracts were dried over Na_2SO_4 and concentrated. Purification by flash chromatography (0-20% EtOAc /hexanes) afforded **S36** as a white solid (18% yield for two steps; $R_f = 0.30$ in 10% EtOAc /Hexanes, 89:11 er):

$[\alpha]_D^{23} = -5.7^\circ$ ($c = 0.07$, CH_2Cl_2). ^1H NMR (400 MHz, CDCl_3) δ 7.86 (dd, $J = 7.2, 2.0$ Hz, 2H), 7.71 (s, 1H), 7.42 (t, $J = 7.7$ Hz, 2H), 7.32 (t, $J = 7.5$ Hz, 1H), 4.56 – 4.47 (m, 1H),



4.86: Our procedure was modified from our method reported in the literature for the alkylation of terminal olefin derived ene adducts⁹⁴: Ene adduct **4.53** (0.2 mmol, 90:10 er) was diluted in 1,2-dimethoxyethane (2 mL, 0.1 M) within a flame-dried vial set under argon atmosphere. Copper(I) bromide dimethyl sulfide (2.1 mg, 5 mol%) was added at –78 °C immediately followed by addition of ethylmagnesium chloride (0.4 mL, 2M THF, 4 equiv). The solution was warmed to 0 °C and stirred vigorously for 3 hours. The resulting mixture was then poured onto wet pentane/Et₂O (20:3 mL) and passed through a silica gel plug, which was subsequently washed with pentane. The filtered organics were concentrated under reduced pressure. Purification by flash chromatography (100% hexanes) afforded **4.86** (73% yield, 3:1 rr, 90:10 er, 100% es) as a colorless oil. The major regioisomer was assigned by comparison to an authentic sample of the major regioisomer (see below **S37**):

[α]_D²³ = +0.99° (0.61, CH₂Cl₂). ¹H NMR (400 MHz, CDCl₃) δ 5.38 – 5.26 (m, 1H), 5.08 (dddd, *J* = 15.2, 8.8, 3.0, 1.6 Hz, 1H), 1.97 (dq, *J* = 7.0, 1.4 Hz, 2H), 1.84 – 1.70 (m, 1H), 1.45 – 1.10 (m, 10H), 0.94 – 0.78 (m, 9H); ¹³C NMR (101 MHz, CDCl₃) δ 135.1, 134.8, 130.4, 130.2, 44.7, 44.5, 37.7, 35.1, 34.9, 32.5, 32.2, 29.9, 29.7, 29.7, 28.4, 23.0, 23.0, 22.3, 20.5, 14.4, 14.3, 14.1, 13.8, 11.9; IR (thin film): 2959, 2926, 2859, 1464, 1378, 968 cm⁻¹.



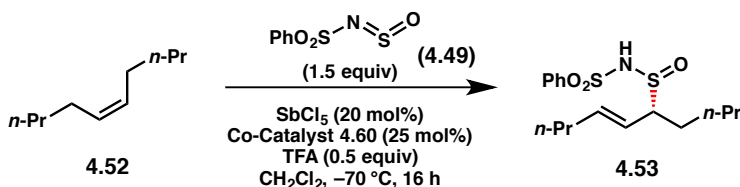
S37: Our procedure was modified from a literature report of a highly E-olefin selective Wittig-Schlosser olefination¹⁰⁷: *n*-Butyltriphenylphosphonium bromide (1.0 mmol) was diluted in THF (1.75 mL) and Et₂O (1 mL) in a flame-dried flask under argon atmosphere. Phenyl lithium (0.56 mL, 1.8 M in Bu₂O, 1 equiv) was added and the solution was stirred for 15 minutes before cooling to – 78 °C. 2-Ethylhexanal 0.156 mL, 1 equiv) was added and the reaction held at –78 °C for 10 minutes before warming to –30 °C. After 30 minutes, a second equivalent of phenyl lithium as added followed by Et₂O (4 mL). After gradually warming the reaction to – 10 °C, the reaction was allowed to warm to room temperature with stirring for 30 minutes. Filtration through celite and purification by flash chromatography (100% pentane) afforded **S37** (43% yield, >>20:1 E/Z) as a colorless oil.

¹H NMR (400 MHz, CDCl₃) δ 5.32 (dt, *J* = 15.0, 6.7 Hz, 1H), 5.09 (ddt, *J* = 15.3, 8.8, 1.4 Hz, 1H), 1.97 (qd, *J* = 7.4, 1.4 Hz, 2H), 1.84 – 1.70 (m, 1H), 1.45 – 1.11 (m, 10H), 0.92 – 0.80 (m, 9H); ¹³C NMR (101 MHz, CDCl₃) δ 135.1, 130.2, 44.8, 35.1, 34.9, 29.7, 28.4, 23.0, 23.0, 14.3, 13.8, 11.9.

Determination of Absolute Stereochemistry of Chiral Allylic Ene Products

A sample of sulfinimide **4.68** was recrystallized from hexanes and chloroform (slow evaporation). The resulting crystals were suitable for X-ray diffraction and the structure was solved (Figure 4.2.3). This structure allowed the assignment of absolute configuration as shown. The absolute configurations of all other allylic ene products were assigned by analogy. We thank Dr. Vincent Lynch (Manager of the X-ray Diffraction Lab at UT Austin) for the X-ray structural analysis. The CIF file is available as a separate file in the appendix.

Linear Correlation Experiment



The (R)- and (S)-enantiomers of diol **4.60** were mixed together to obtain the desired enantiomeric ratio which was checked on HPLC by comparison to a sample of the racemate (see HPLC traces in appendix). The ene reactions were run following the method A of the general procedure. The resulting ene adducts were not isolated but directly converted to **S17** for HPLC analysis.

Entry	Co-Catalyst's ee	product's ee
1	4	4
2	10	10
3	22	16
4	52	48
5	90	76
6	98	85

4.4. References

- (1) Farina, V.; Reeves, J. T.; Senanayake, C. H.; Song, J. J. *Chemical Reviews* **2006**, *106*, 2734.
- (2) Cernak, T.; Dykstra, K. D.; Tyagarajan, S.; Vachal, P.; Krska, S. W. *Chemical Society Reviews* **2016**, *45*, 546.
- (3) Hyneck, M.; Dent, J.; Hook, J. B. In *Chirality in Drug Design and Synthesis*; Academic Press: 1990, p 1.
- (4) Wilson, R. M.; Danishefsky, S. J. *Angewandte Chemie International Edition* **2010**, *49*, 6032.
- (5) Brooks, W.; Guida, W.; Daniel, K. *Current Topics in Medicinal Chemistry*, *11*, 760.
- (6) Davies, H. M. L.; Manning, J. R. *Nature* **2008**, *451*, 417.
- (7) Trost, B. M.; Van Vranken, D. L. *Chemical Reviews* **1996**, *96*, 395.
- (8) Alexakis, A.; Bäckvall, J. E.; Krause, N.; Pàmies, O.; Diéguez, M. *Chemical Reviews* **2008**, *108*, 2796.
- (9) Hartwig, J. F.; Stanley, L. M. *Accounts of Chemical Research* **2010**, *43*, 1461.
- (10) Trost, B. M.; Crawley, M. L. *Chemical Reviews* **2003**, *103*, 2921.
- (11) *Comprehensive Asymmetric Catalysis, Volume 1-3*; Springer, 1999; Vol. 1-3.
- (12) Li, A.-H.; Dai, L.-X.; Aggarwal, V. K. *Chemical Reviews* **1997**, *97*, 2341.
- (13) Sweeney, J. B. *Chemical Society Reviews* **2009**, *38*, 1027.
- (14) *Catalytic Asymmetric Synthesis, Third Edition*; John Wiley & Sons, Inc. , 2010.
- (15) Nasveschuk, C. G.; Rovis, T. *Organic & Biomolecular Chemistry* **2008**, *6*, 240.
- (16) Corey, E. J.; Kurti, L. *Enantioselective Chemical Synthesis: Methods, Logic, and Practice*; Elsevier Science, 2013.
- (17) Liu, G.; Wu, Y. In *C-H Activation*; Yu, J.-Q., Ed.; Springer Berlin Heidelberg: Berlin, Heidelberg, 2010, p 195.
- (18) Andrus, M. B. In *Stereoselective Synthesis 3*; 1st Edition ed.; Evans, P. A., Ed.; Thieme Verlag: Stuttgart, 2011; Vol. Volume 3.
- (19) Grennberg, H.; Bäckvall, J.-E. In *Transition Metals for Organic Synthesis*; Wiley-

VCH Verlag GmbH: 2008, p 243.

- (20) Kharasch, M.; Fono, A. *The Journal of Organic Chemistry* **1958**, 23, 324.
- (21) Kharasch, M. S.; Sosnovsky, G. *Journal of the American Chemical Society* **1958**, 80, 756.
- (22) M. Araki; Nagase, T. *Chemical Abstracts* **1977**, 86, 120886r.
- (23) Denney, D. B.; Napier, R.; Cammarata, A. *The Journal of Organic Chemistry* **1965**, 30, 3151.
- (24) Andrus, M. B.; Argade, A. B.; Chen, X.; Pamment, M. G. *Tetrahedron Letters* **1995**, 36, 2945.
- (25) Gokhale, A. S.; Minidis, A. B. E.; Pfaltz, A. *Tetrahedron Letters* **1995**, 36, 1831.
- (26) Rispen, M. T.; Zondervan, C.; Feringa, B. L. *Tetrahedron: Asymmetry* **1995**, 6, 661.
- (27) Loiseleur, O.; Meier, P.; Pfaltz, A. *Angewandte Chemie International Edition in English* **1996**, 35, 200.
- (28) Södergren, M. J.; Andersson, P. G. *Tetrahedron Letters* **1996**, 37, 7577.
- (29) Andrus, M. B.; Chen, X. *Tetrahedron* **1997**, 53, 16229.
- (30) Kawasaki, K.-i.; Katsuki, T. *Tetrahedron* **1997**, 53, 6337.
- (31) Fahrni, C. J. *Tetrahedron* **1998**, 54, 5465.
- (32) Sekar, G.; DattaGupta, A.; Singh, V. K. *The Journal of Organic Chemistry* **1998**, 63, 2961.
- (33) Muzart, J. *Journal of Molecular Catalysis* **1991**, 64, 381.
- (34) Kawasaki, K.; Tsumura, S.; Katsuki, T. *Synlett* **1995**, 1245.
- (35) Levina, A.; Muzart, J. *Tetrahedron: Asymmetry* **1995**, 6, 147.
- (36) DattaGupta, A.; Singh, V. K. *Tetrahedron Letters* **1996**, 37, 2633.
- (37) Zondervan, C.; Feringa, B. L. *Tetrahedron: Asymmetry* **1996**, 7, 1895.
- (38) Aldea, L.; Delso, I.; Hager, M.; Glos, M.; García, J. I.; Mayoral, J. A.; Reiser, O. *Tetrahedron* **2012**, 68, 3417.
- (39) Andrus, M. B.; Zhou, Z. *Journal of the American Chemical Society* **2002**, 124, 8806.

- (40) Clark, S.; F. Tolhurst, K.; Taylor, M.; Swallow, S. *Journal of the Chemical Society, Perkin Transactions I* **1998**, 1167.
- (41) Kohmura, Y.; Katsuki, T. *Tetrahedron Letters* **2000**, 41, 3941.
- (42) Ramalingam, B.; Neuburger, M.; Pfaltz, A. *Synthesis* **2007**, 2007, 572.
- (43) Malkov, A. V.; Bella, M.; Langer, V.; Kočovský, P. *Organic Letters* **2000**, 2, 3047.
- (44) Hoang, V. D. M.; Reddy, P. A. N.; Kim, T.-J. *Organometallics* **2008**, 27, 1026.
- (45) Zhou, Z.; Andrus, M. B. *Tetrahedron Letters* **2012**, 53, 4518.
- (46) Malkov, A. V.; Pernazza, D.; Bell, M.; Bella, M.; Massa, A.; Teplý, F.; Meghani, P.; Kočovský, P. *The Journal of Organic Chemistry* **2003**, 68, 4727.
- (47) Tan, Q.; Hayashi, M. *Advanced Synthesis & Catalysis* **2008**, 350, 2639.
- (48) Malkov, A. V.; Stewart-Liddon, A. J. P.; Teplý, F.; Kober, L.; Muir, K. W.; Haigh, D.; Kočovský, P. *Tetrahedron* **2008**, 64, 4011.
- (49) Kohmura, Y.; Katsuki, T. *Tetrahedron Letters* **2001**, 42, 3339.
- (50) Clark, J. S.; Roche, C. *Chemical Communications* **2005**, 5175.
- (51) Beletskaya, I. P.; Cheprakov, A. V. *Chemical Reviews* **2000**, 100, 3009.
- (52) Mc Cartney, D.; Guiry, P. J. *Chemical Society Reviews* **2011**, 40, 5122.
- (53) Mata, Y.; Pàmies, O.; Diéguez, M. *Chemistry – A European Journal* **2007**, 13, 3296.
- (54) Mazuela, J.; Pàmies, O.; Diéguez, M. *Chemistry – A European Journal* **2010**, 16, 3434.
- (55) Gilbertson, S. R.; Fu, Z. *Organic Letters* **2001**, 3, 161.
- (56) Wöste, T. H.; Oestreich, M. *Chemistry – A European Journal* **2011**, 17, 11914.
- (57) Hu, J.; Lu, Y.; Li, Y.; Zhou, J. *Chemical Communications* **2013**, 49, 9425.
- (58) Mikami, K.; Shimizu, M. *Chemical Reviews* **1992**, 92, 1021.
- (59) Snider, B. B.; Ron, E. *Journal of the American Chemical Society* **1985**, 107, 8160.
- (60) Evans, D. A.; Burgey, C. S.; Paras, N. A.; Vojkovsky, T.; Tregay, S. W. *Journal of the American Chemical Society* **1998**, 120, 5824.
- (61) Evans, D. A.; Tregay, S. W.; Burgey, C. S.; Paras, N. A.; Vojkovsky, T. *Journal*

- of the American Chemical Society* **2000**, 122, 7936.
- (62) Hao, J.; Hatano, M.; Mikami, K. *Organic Letters* **2000**, 2, 4059.
 - (63) Davies, H. M. L.; Morton, D. *Chemical Society Reviews* **2011**, 40, 1857.
 - (64) Müller, P.; Fruit, C. *Chemical Reviews* **2003**, 103, 2905.
 - (65) Müller, P.; Tohill, S. *Tetrahedron* **2000**, 56, 1725.
 - (66) Davies, H. M. L.; Coleman, M. G.; Ventura, D. L. *Organic Letters* **2007**, 9, 4971.
 - (67) Davies, H. M. L.; Dai, X.; Long, M. S. *Journal of the American Chemical Society* **2006**, 128, 2485.
 - (68) Davies, H. M. L.; Gregg, T. M. *Tetrahedron Letters* **2002**, 43, 4951.
 - (69) Davies, H. M. L.; Ren, P.; Jin, Q. *Organic Letters* **2001**, 3, 3587.
 - (70) Kubiak, R. W.; Mighion, J. D.; Wilkerson-Hill, S. M.; Alford, J. S.; Yoshidomi, T.; Davies, H. M. L. *Organic Letters* **2016**, 18, 3118.
 - (71) Sharpless, K. B.; Hori, T. *The Journal of Organic Chemistry* **1976**, 41, 176.
 - (72) Sharpless, K. B.; Hori, T.; Truesdale, L. K.; Dietrich, C. O. *Journal of the American Chemical Society* **1976**, 98, 269.
 - (73) Singer, S. P.; Sharpless, K. B. *The Journal of Organic Chemistry* **1978**, 43, 1448.
 - (74) Bussas, R.; Muenster, H.; Kresze, G. *The Journal of Organic Chemistry* **1983**, 48, 2828.
 - (75) Muensterer, H.; Kresze, G.; Lamm, V.; Gieren, A. *The Journal of Organic Chemistry* **1983**, 48, 2833.
 - (76) Gadras, A.; Dunogues, J.; Calas, R.; Deleris, G. *The Journal of Organic Chemistry* **1984**, 49, 442.
 - (77) Whitesell, J. K.; Carpenter, J. F. *Journal of the American Chemical Society* **1987**, 109, 2839.
 - (78) Deleris, G.; Dunogues, J.; Gadras, A. *Tetrahedron* **1988**, 44, 4243.
 - (79) Whitesell, J. K.; Carpenter, J. F.; Yaser, H. K.; Machajewski, T. *Journal of the American Chemical Society* **1990**, 112, 7653.
 - (80) Whitesell, J. K.; Yaser, H. K. *Journal of the American Chemical Society* **1991**, 113, 3526.

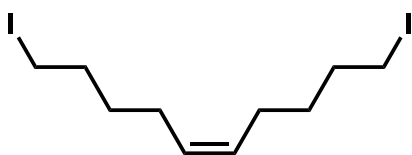
- (81) Katz, T. J.; Shi, S. *The Journal of Organic Chemistry* **1994**, *59*, 8297.
- (82) Salonen, L. M.; Ellermann, M.; Diederich, F. *Angewandte Chemie International Edition* **2011**, *50*, 4808.
- (83) Mahadevi, A. S.; Sastry, G. N. *Chemical Reviews* **2013**, *113*, 2100.
- (84) Collins, K. D.; Glorius, F. *Nat Chem* **2013**, *5*, 597.
- (85) Ishihara, K.; Kaneeda, M.; Yamamoto, H. *Journal of the American Chemical Society* **1994**, *116*, 11179.
- (86) Ishihara, K.; Nakamura, S.; Kaneeda, M.; Yamamoto, H. *Journal of the American Chemical Society* **1996**, *118*, 12854.
- (87) Ishihara, K.; Nakamura, H.; Nakamura, S.; Yamamoto, H. *The Journal of Organic Chemistry* **1998**, *63*, 6444.
- (88) Ishihara, K.; Nakamura, S.; Yamamoto, H. *Journal of the American Chemical Society* **1999**, *121*, 4906.
- (89) Nakamura, S.; Kaneeda, M.; Ishihara, K.; Yamamoto, H. *Journal of the American Chemical Society* **2000**, *122*, 8120.
- (90) Ishihara, K.; Nakashima, D.; Hiraiwa, Y.; Yamamoto, H. *Journal of the American Chemical Society* **2003**, *125*, 24.
- (91) Yamamoto, H.; Futatsugi, K. *Angewandte Chemie International Edition* **2005**, *44*, 1924.
- (92) Surendra, K.; Corey, E. J. *Journal of the American Chemical Society* **2012**, *134*, 11992.
- (93) Hori, T.; Sharpless, K. B. *The Journal of Organic Chemistry* **1979**, *44*, 4204.
- (94) Bao, H.; Bayeh, L.; Tambar, U. K. *Angewandte Chemie International Edition* **2014**, *53*, 1664.
- (95) Bao, H.; Bayeh, L.; Tambar, U. K. *Chemical Science* **2014**, *5*, 4863.
- (96) Qin, D.; Sullivan, R.; Berkowitz, W.; Bittman, R.; Rotenberg, S. *Journal of Medicinal Chemistry* **2000**, *43*, 1413
- (97) Maddox, S.; Nalbandian, C.; Smith, D.; Gustafson, J. *Organic Letters* **2015**, *17*, 1042

- (98) Marton, D.; Tagliavini, G.; Zordan, M.; Wardell, J. *Journal of Organometallic Chemistry* **1990**, *390*, 127
- (99) Ahmed, I.; Clark, D. *Organic Letters* **2014**, *16*, 4332
- (100) Peacock, S.; Walba, D.; Gaeta, F.; Helgeson, R.; Cram, D. J. *Journal of the American Chemical Society* **1980**, *102*, 2043
- (101) Orito, Y.; Hashimoto, S.; Ishizuka, T.; Nakajima, M. *Tetrahedron*, **2006**, *62*, 390
- (102) Le, P. Q.; Nguyen, T.; May, J. *Organic Letters* **2012**, *14*, 6104
- (103) Kresze, G.; Maschke, A.; Albrecht, R.; Bederke, K.; Patzschke, H. P.; Smalla, H.; Trede, A. *Angewandte Chemie* **1962**, *74*, 135
- (104) Biswas, K.; Lin, H.; Njardarson, J. T.; Chappell, M. D.; Chou, T.-C.; Guan, Y.; Tong, W. P.; He, L.; Horwitz, S. B.; Danishefsky, S. J. *Journal of the American Chemical Society* **2002**, *124*, 9825
- (105) Braddock, D. C.; Pouwer, R. H.; Burton, J. W.; Broadwith, P. *The Journal of Organic Chemistry* **2009**, *74*, 6042
- (106) Rostovtsev, V. V.; Green, L. G.; Fokin, V. V.; Sharpless, K. B. *Angewandte Chemie International Edition* **2002**, *41*, 2596
- (107) Johnson, W. S.; DuBois, G. E. *Journal of the American Chemical Society* **1976**, *98*, 1038

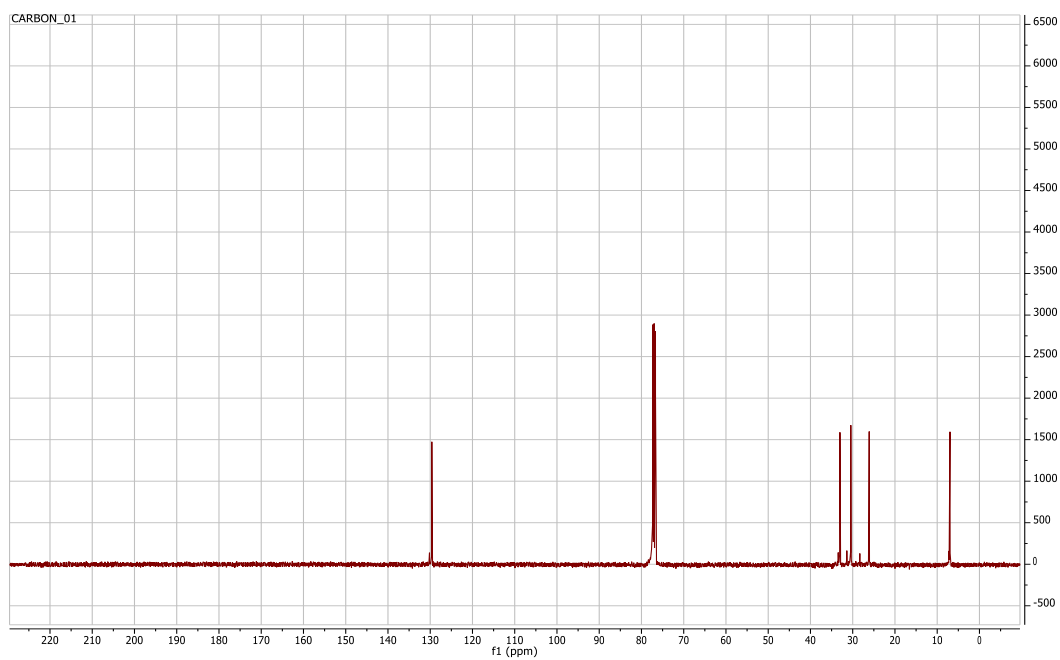
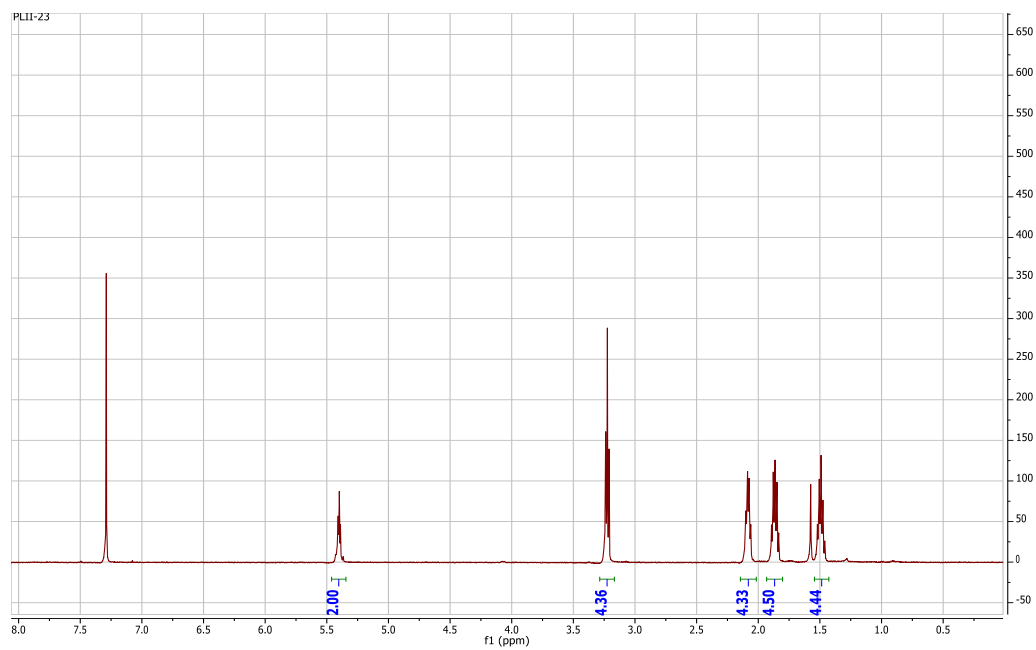
APPENDIX SIX

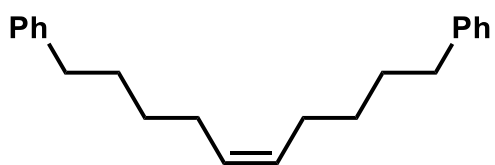
Spectra Relevant to Chapter Four:

**The Development of a General, Highly Selective Method for
the Allylic Functionalization of Unactivated Internal Olefins**

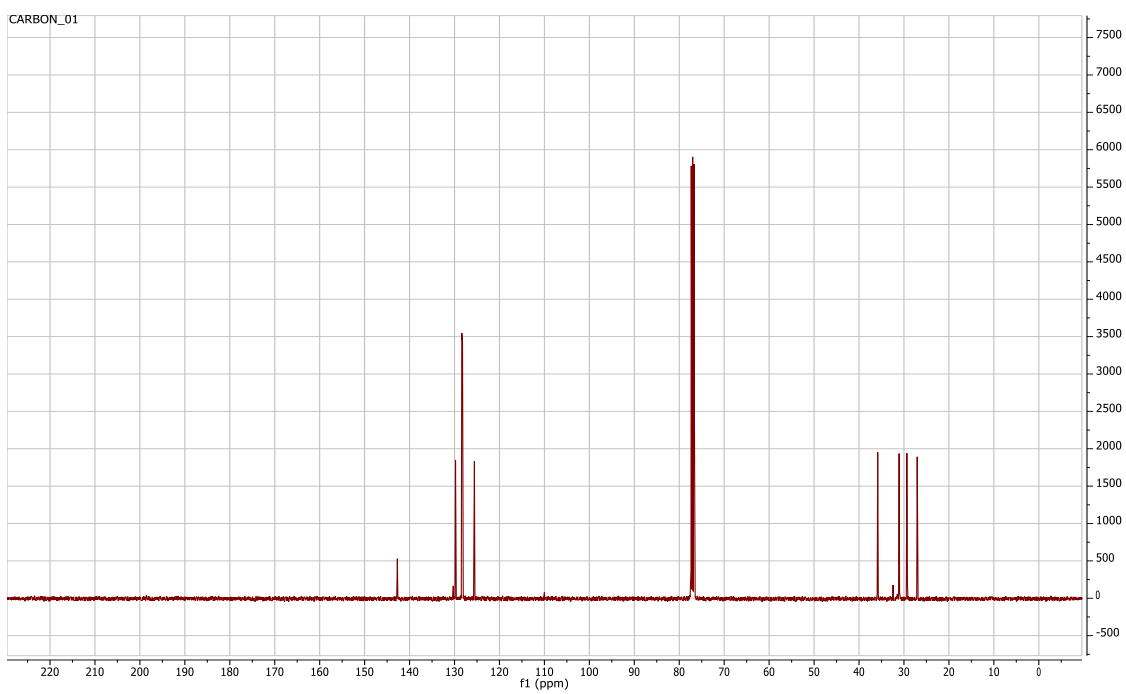
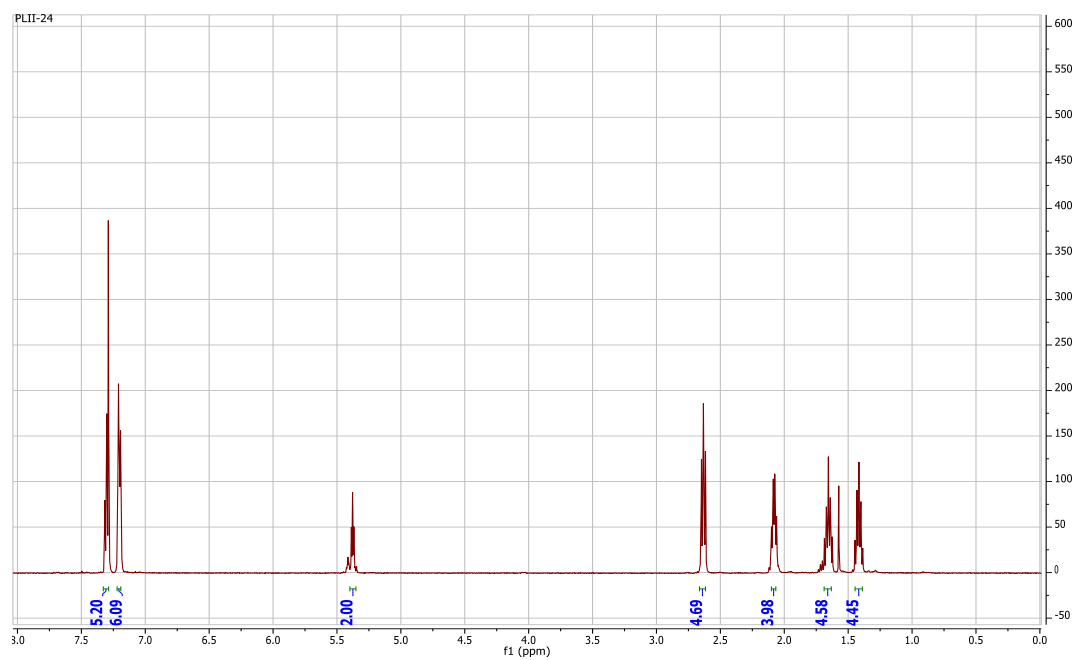


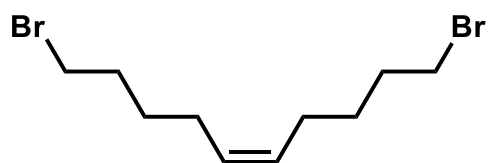
S3 in CDCl_3



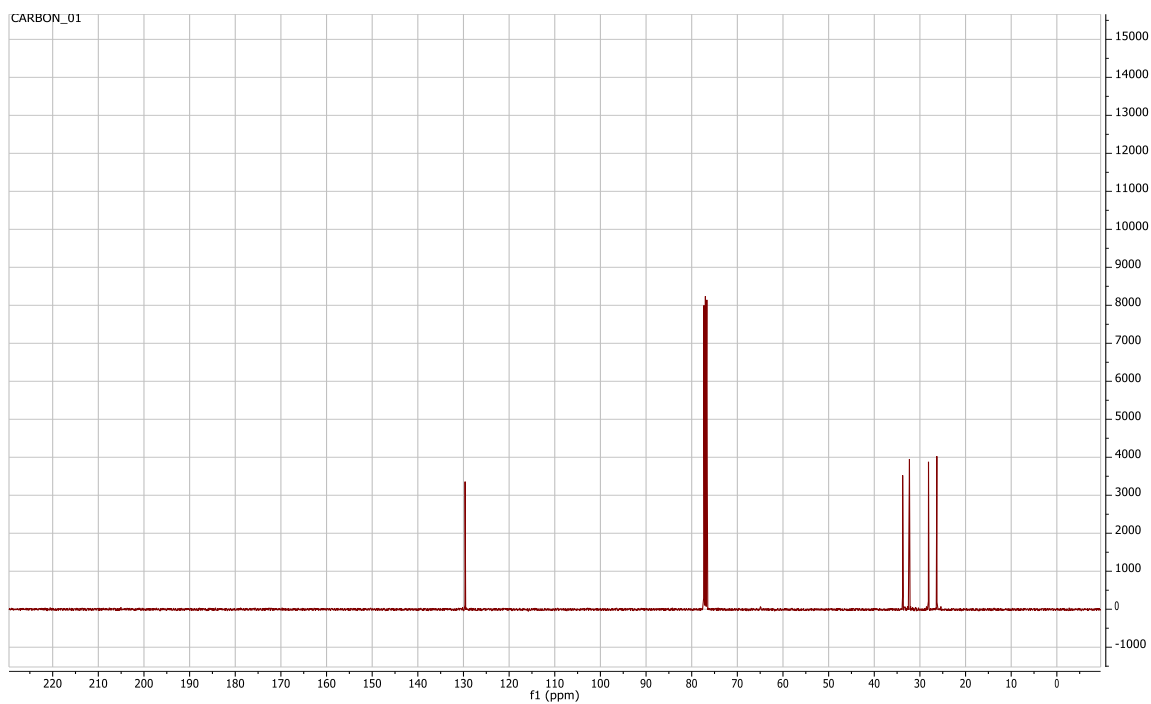
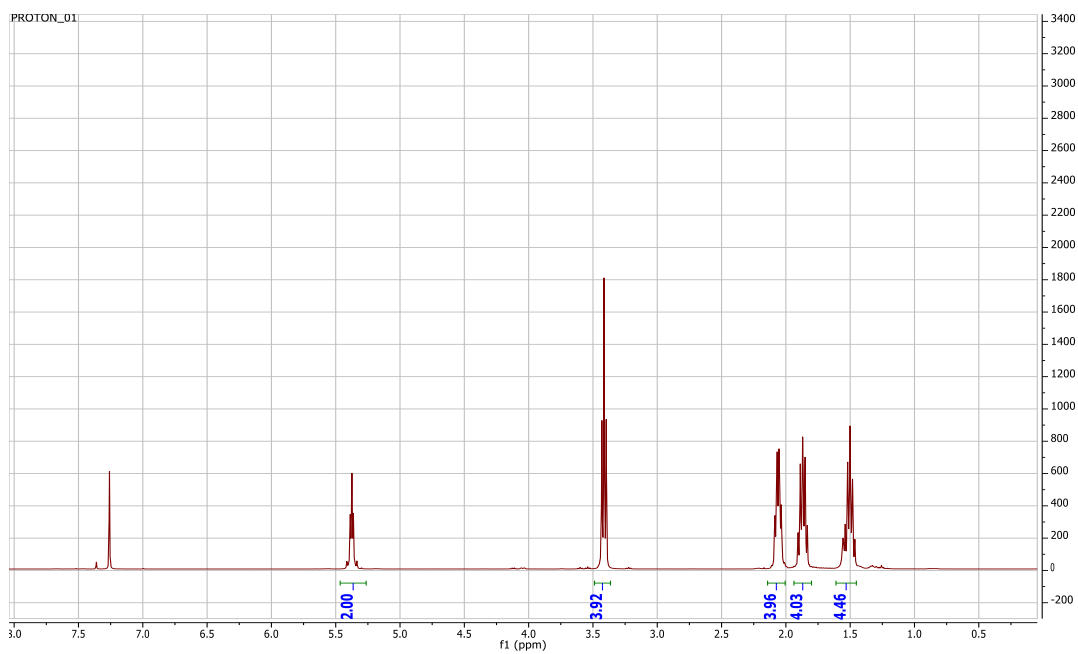


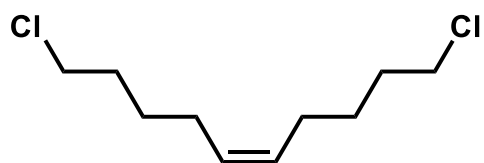
S4 in CDCl₃



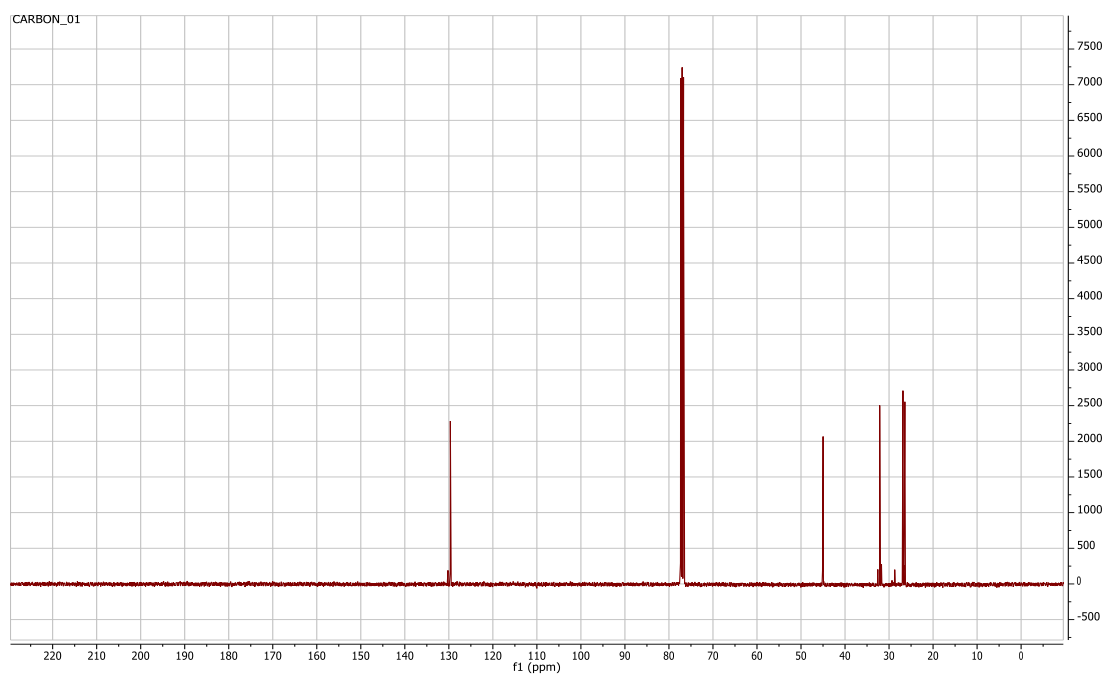
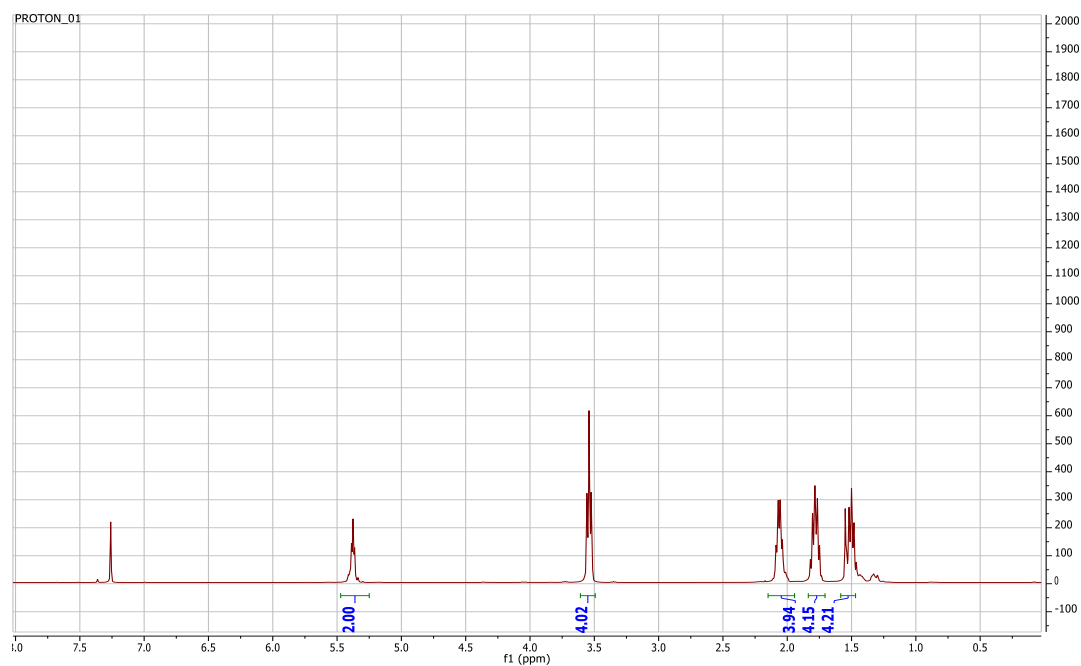


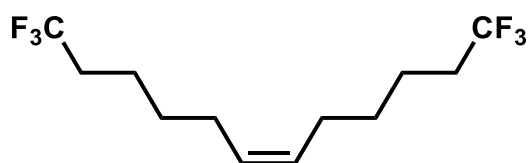
S5 in CDCl_3



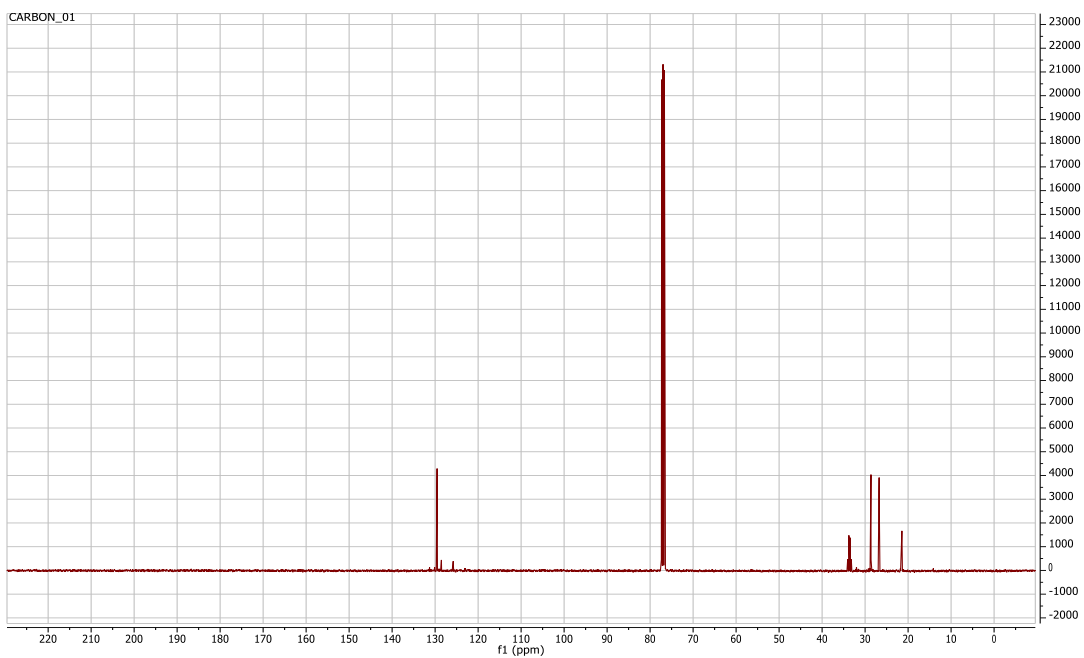
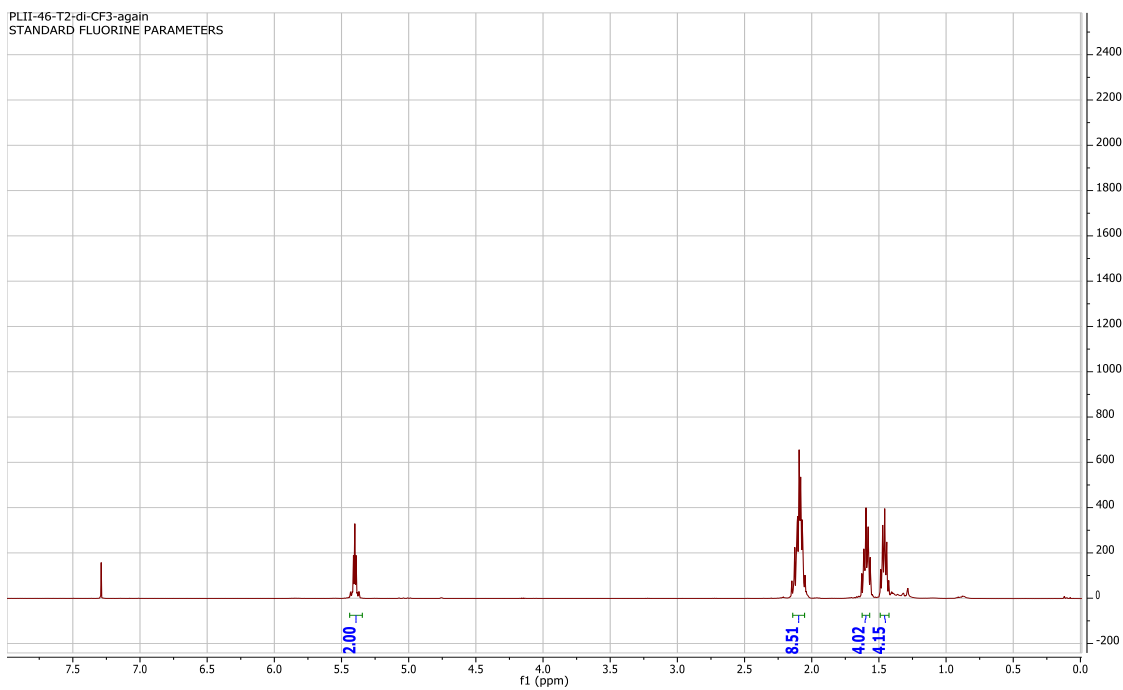


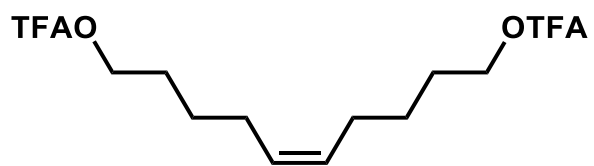
S6 in CDCl₃



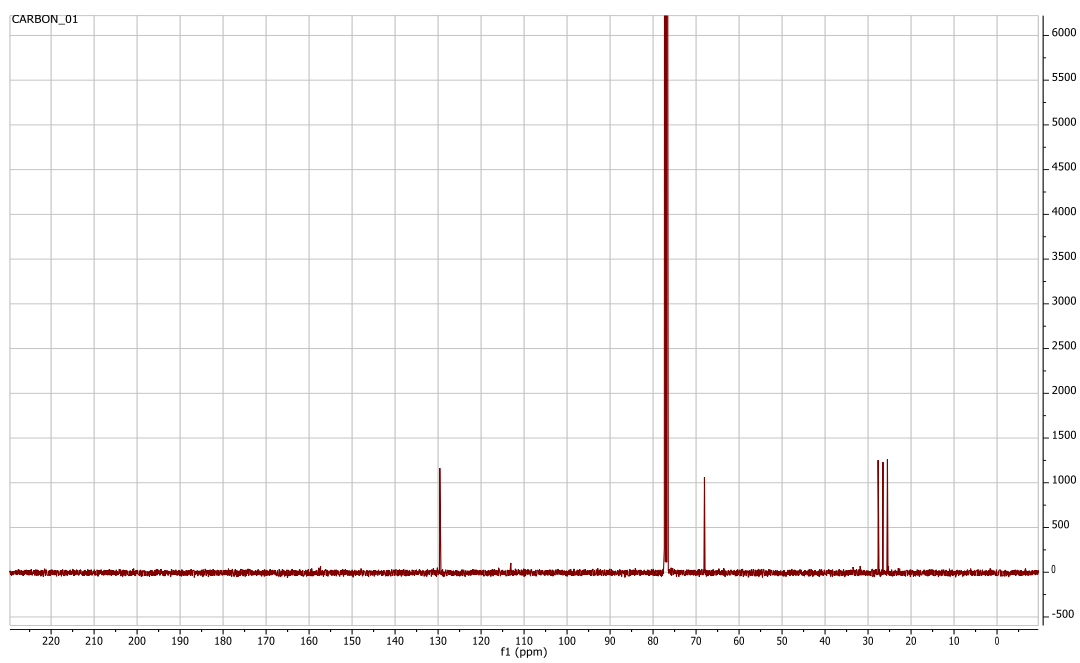
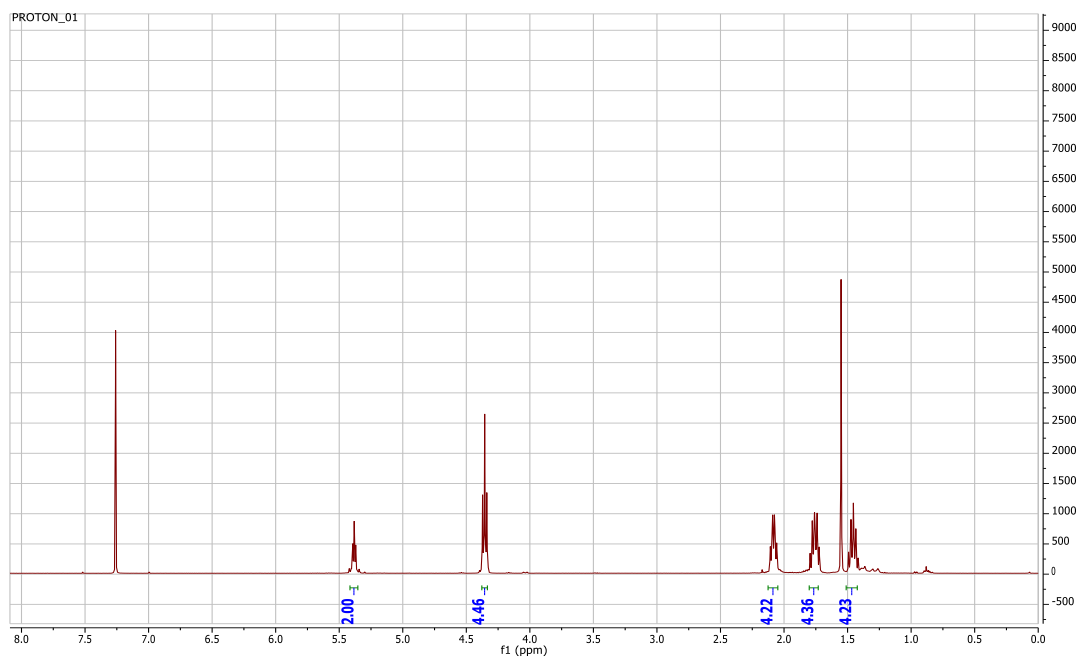


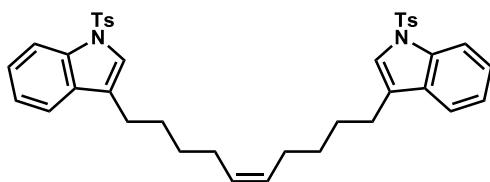
S7 in CDCl₃



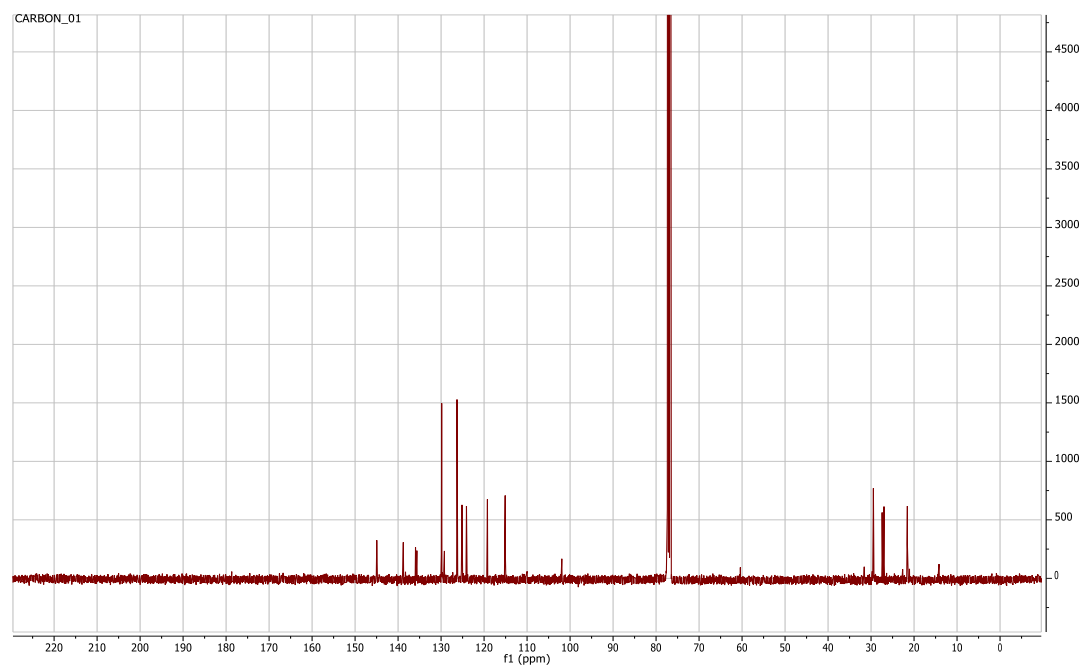
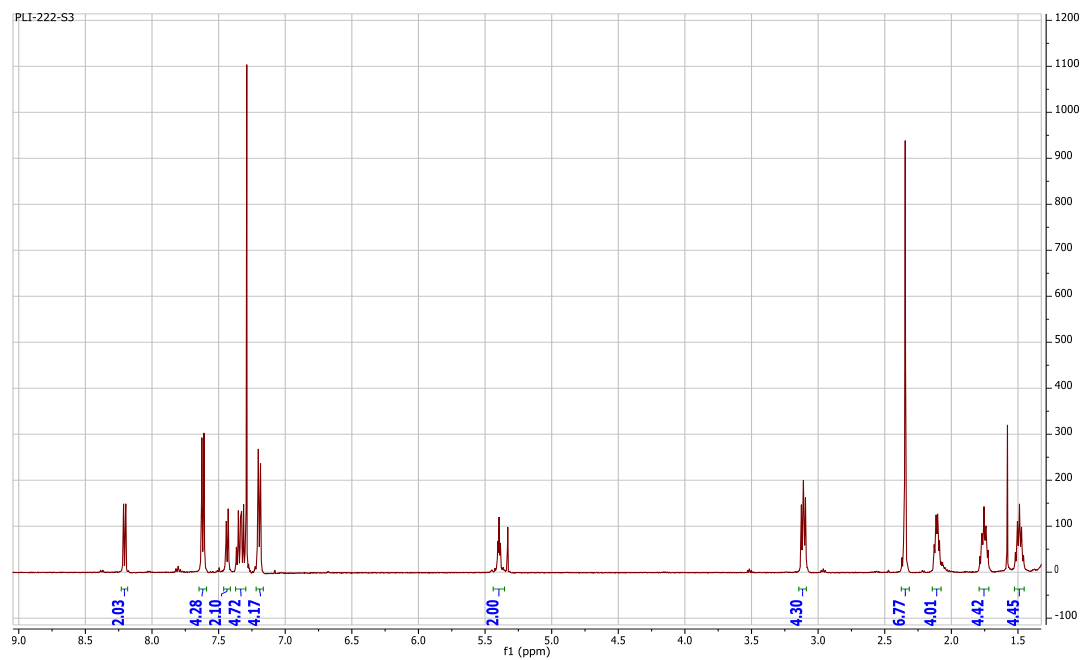


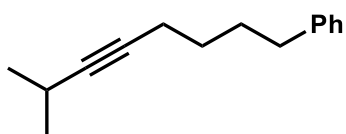
S8 in CDCl₃



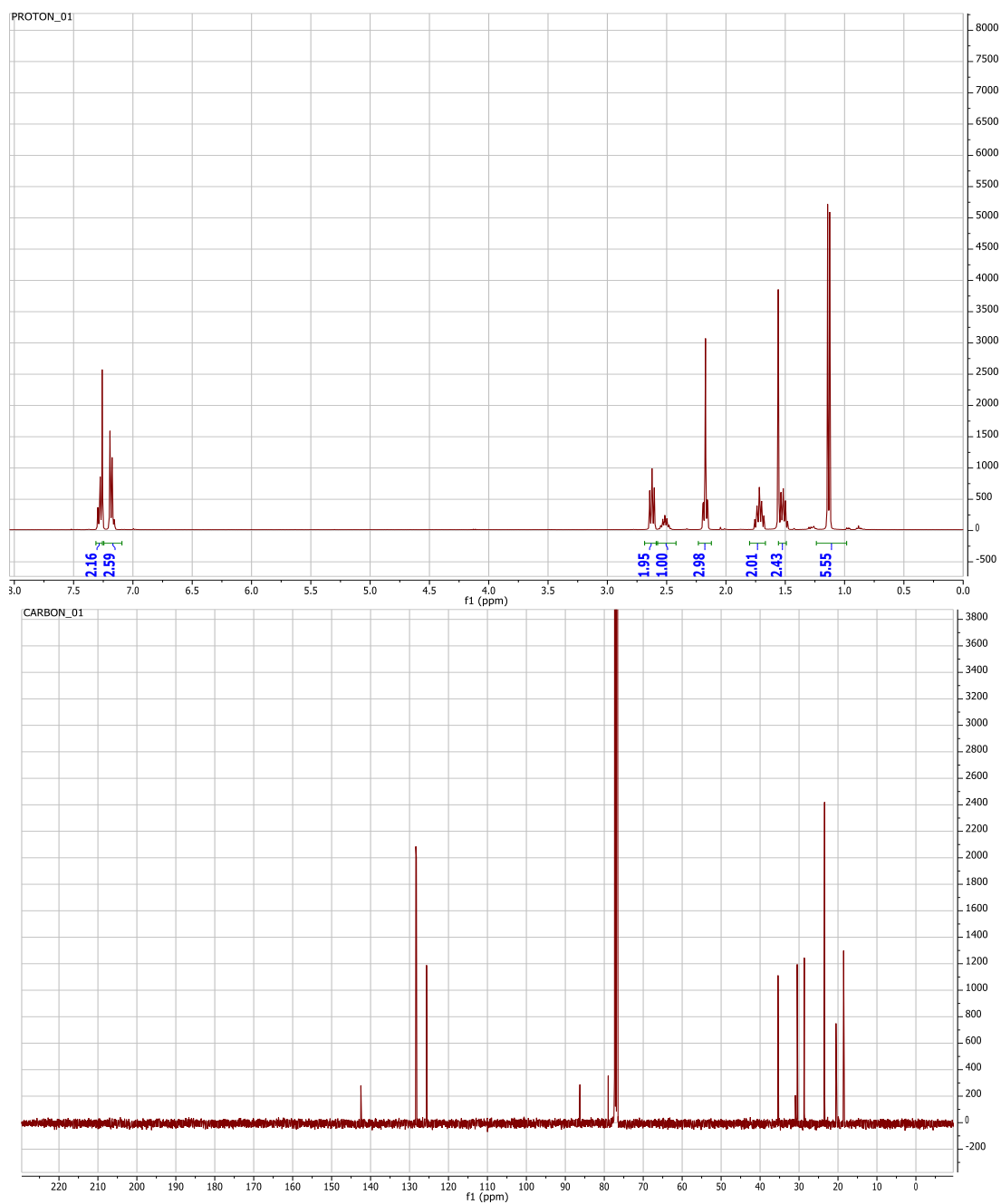


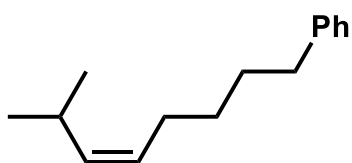
S9 in CDCl₃



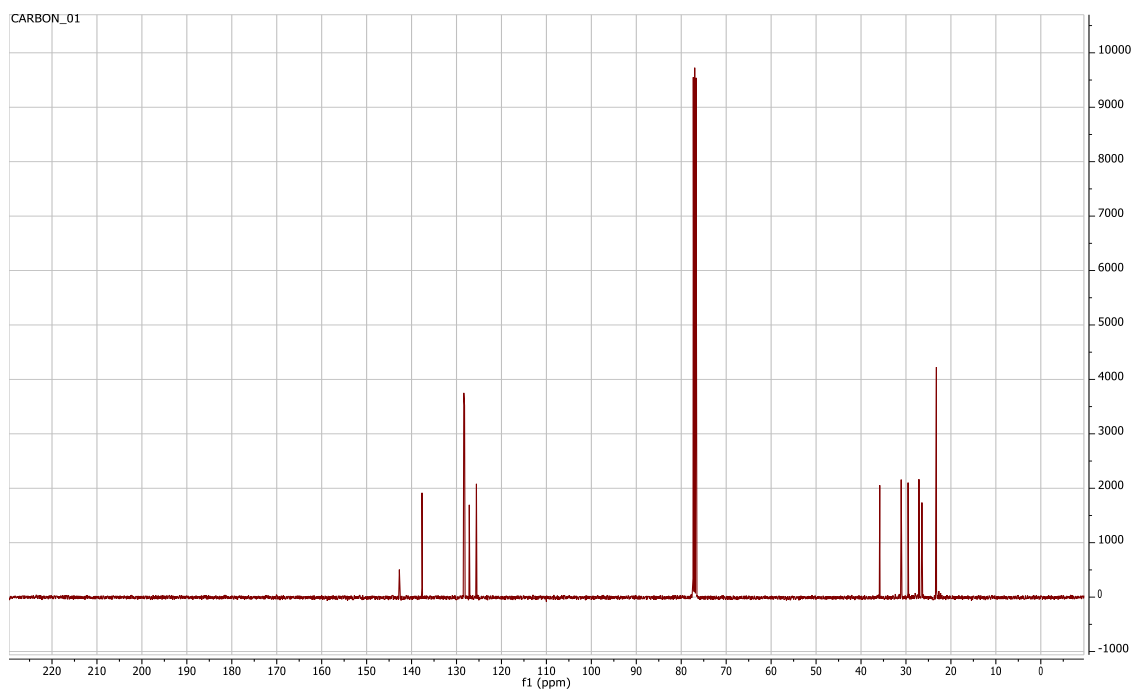
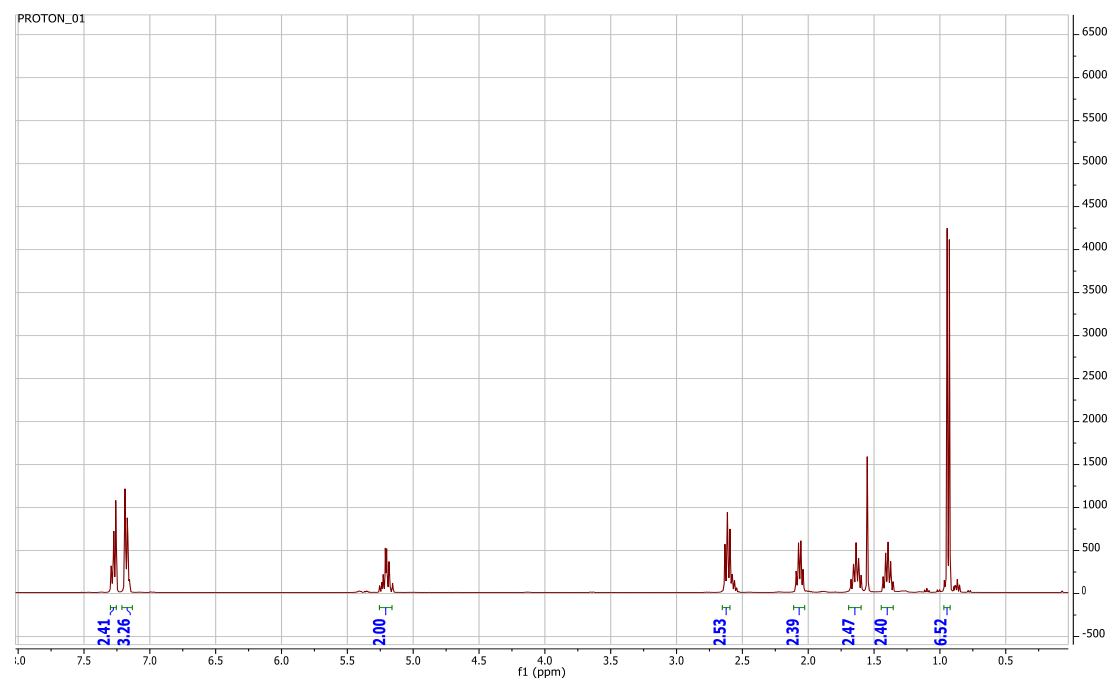


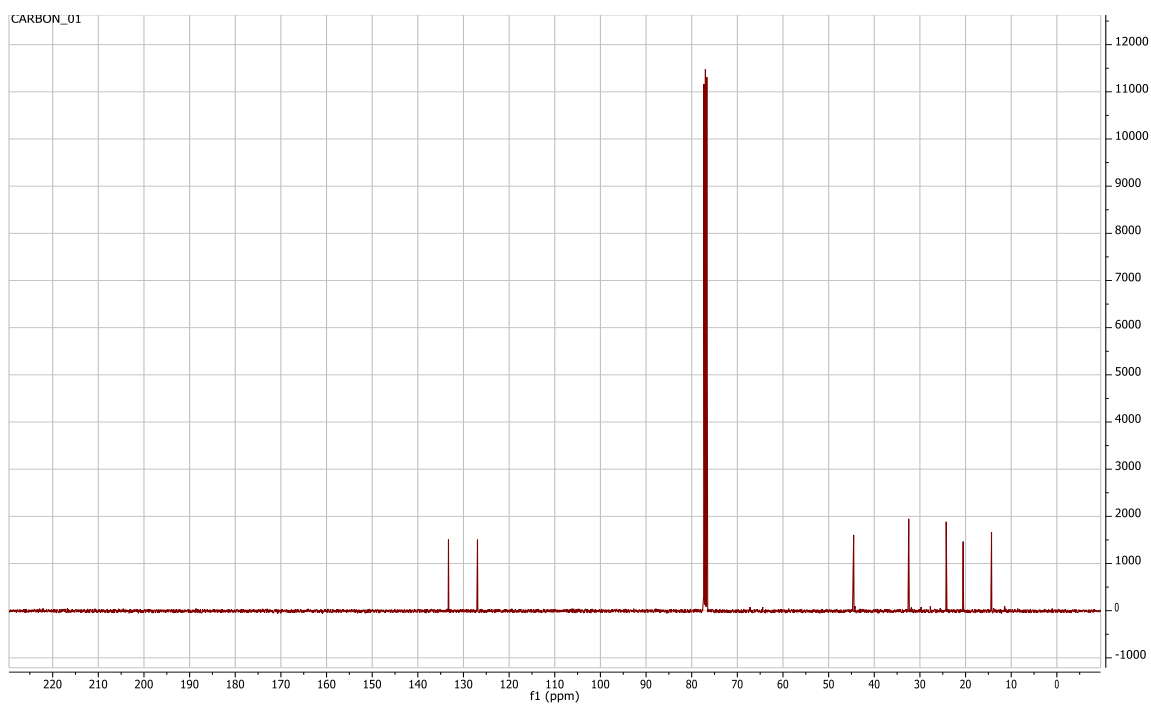
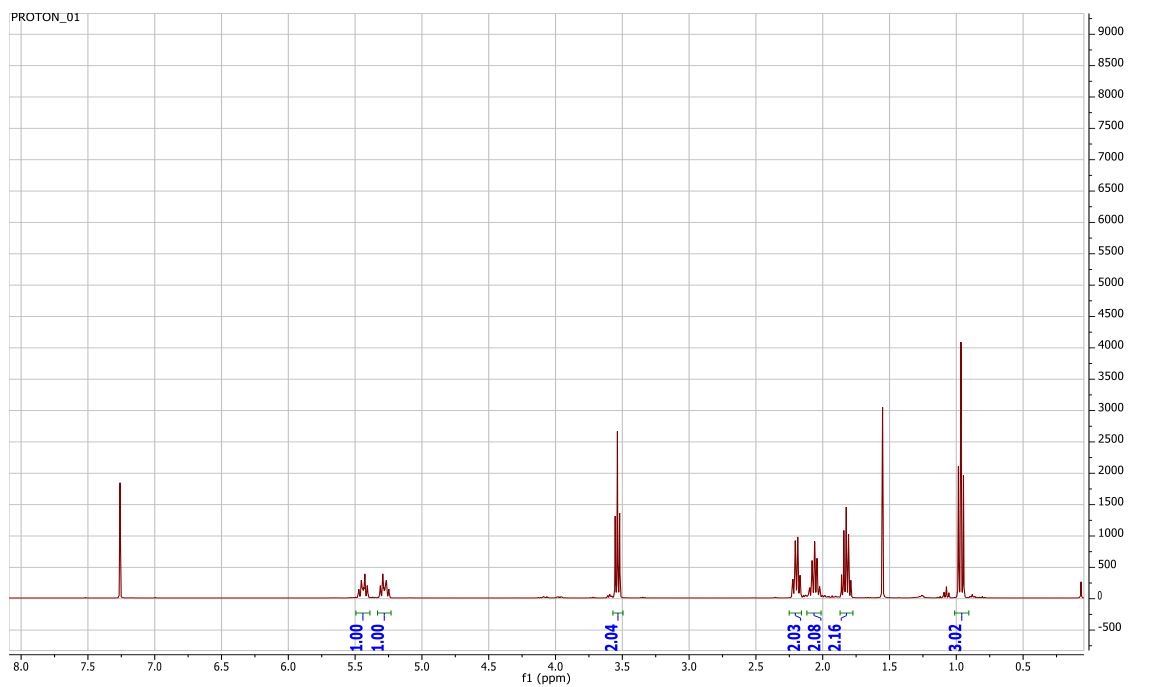
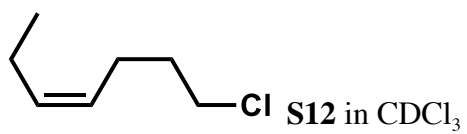
S10 in CDCl₃

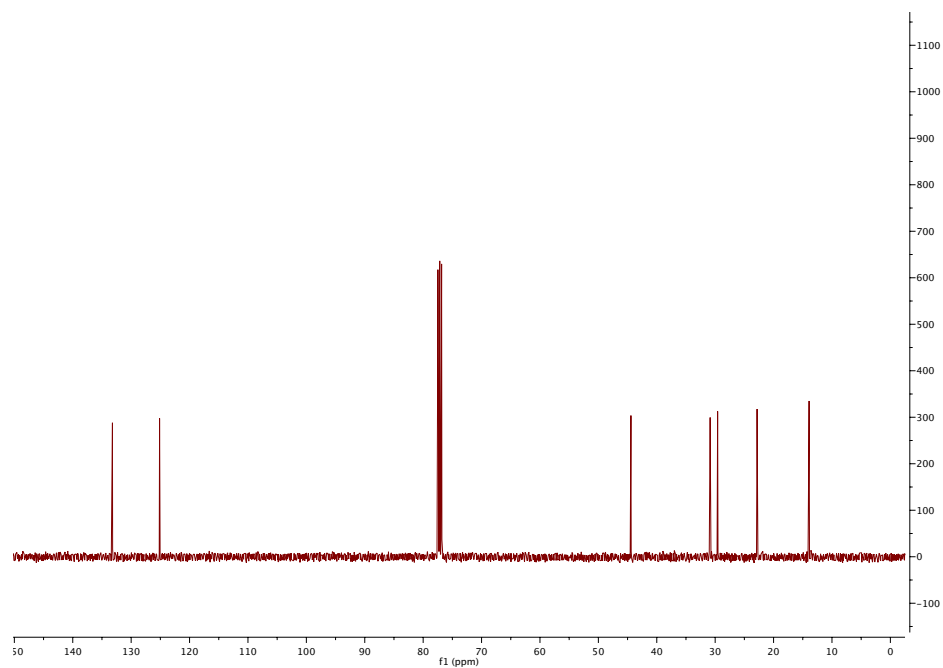
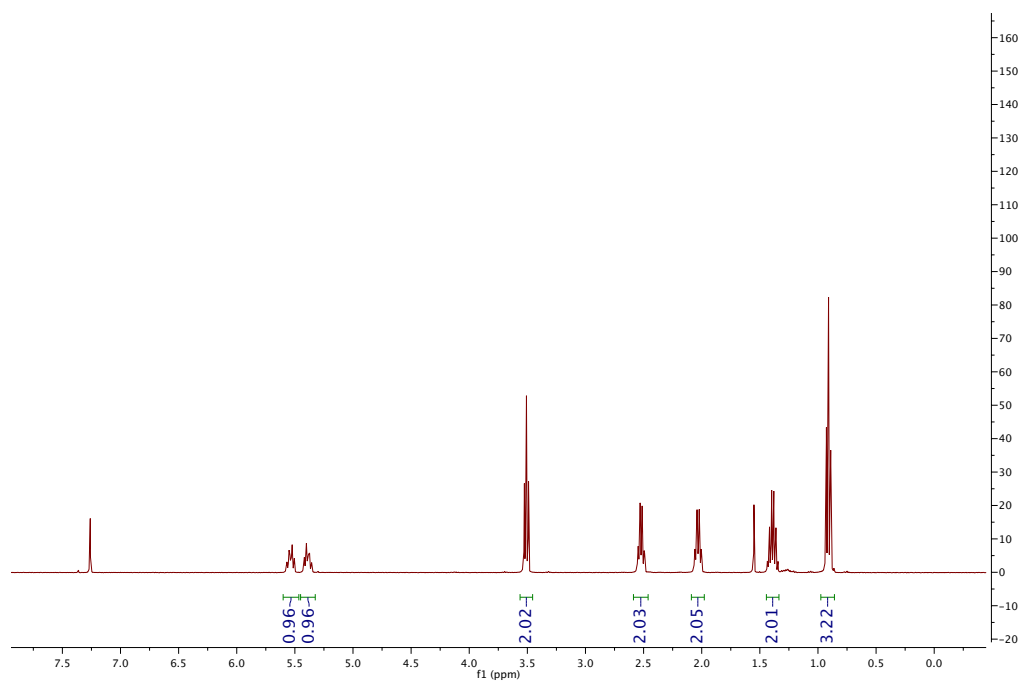
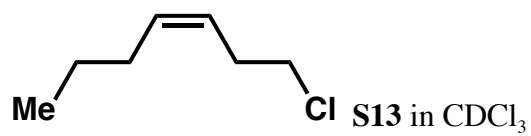


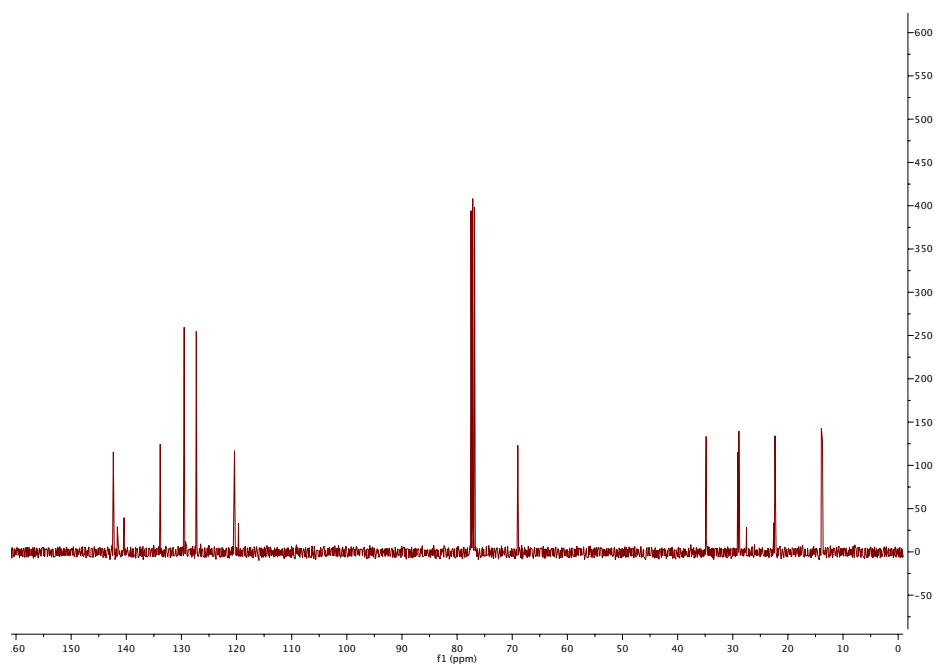
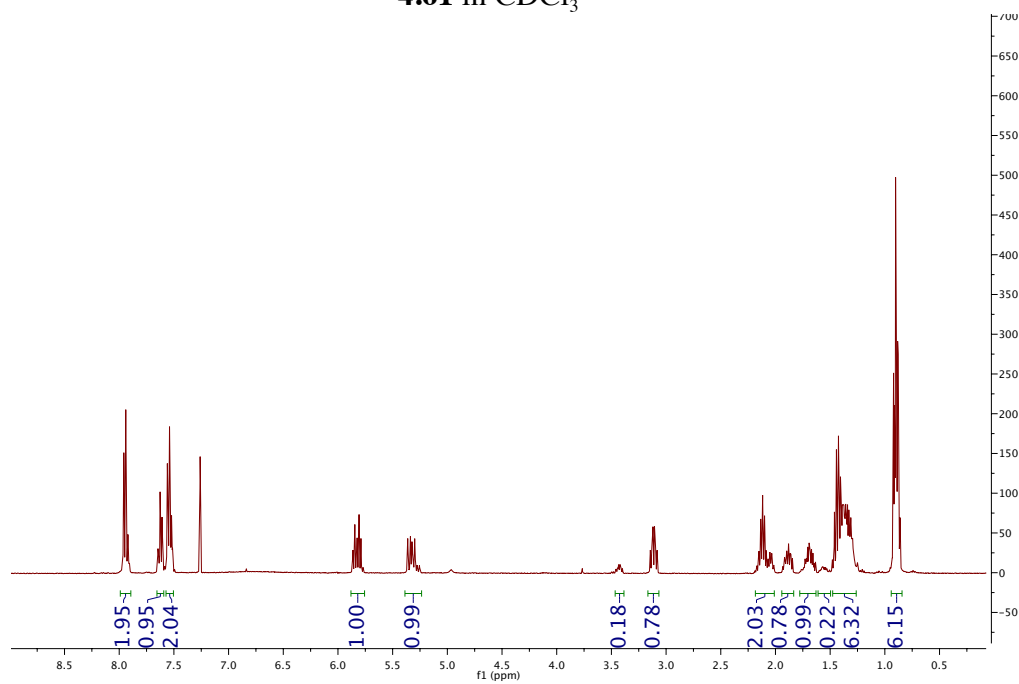
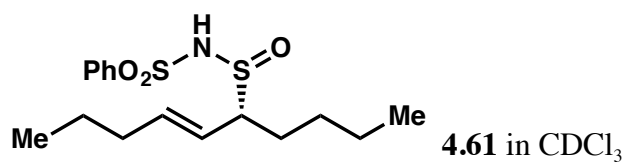


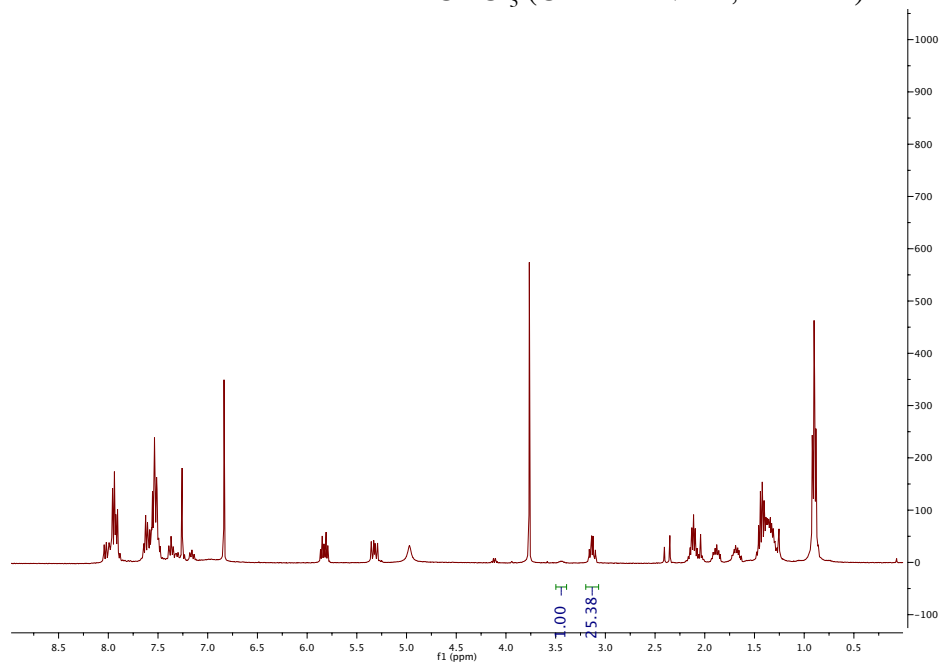
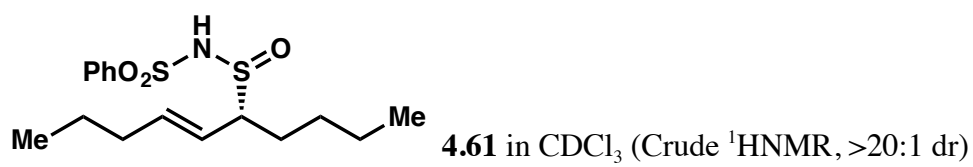
S11 in CDCl₃

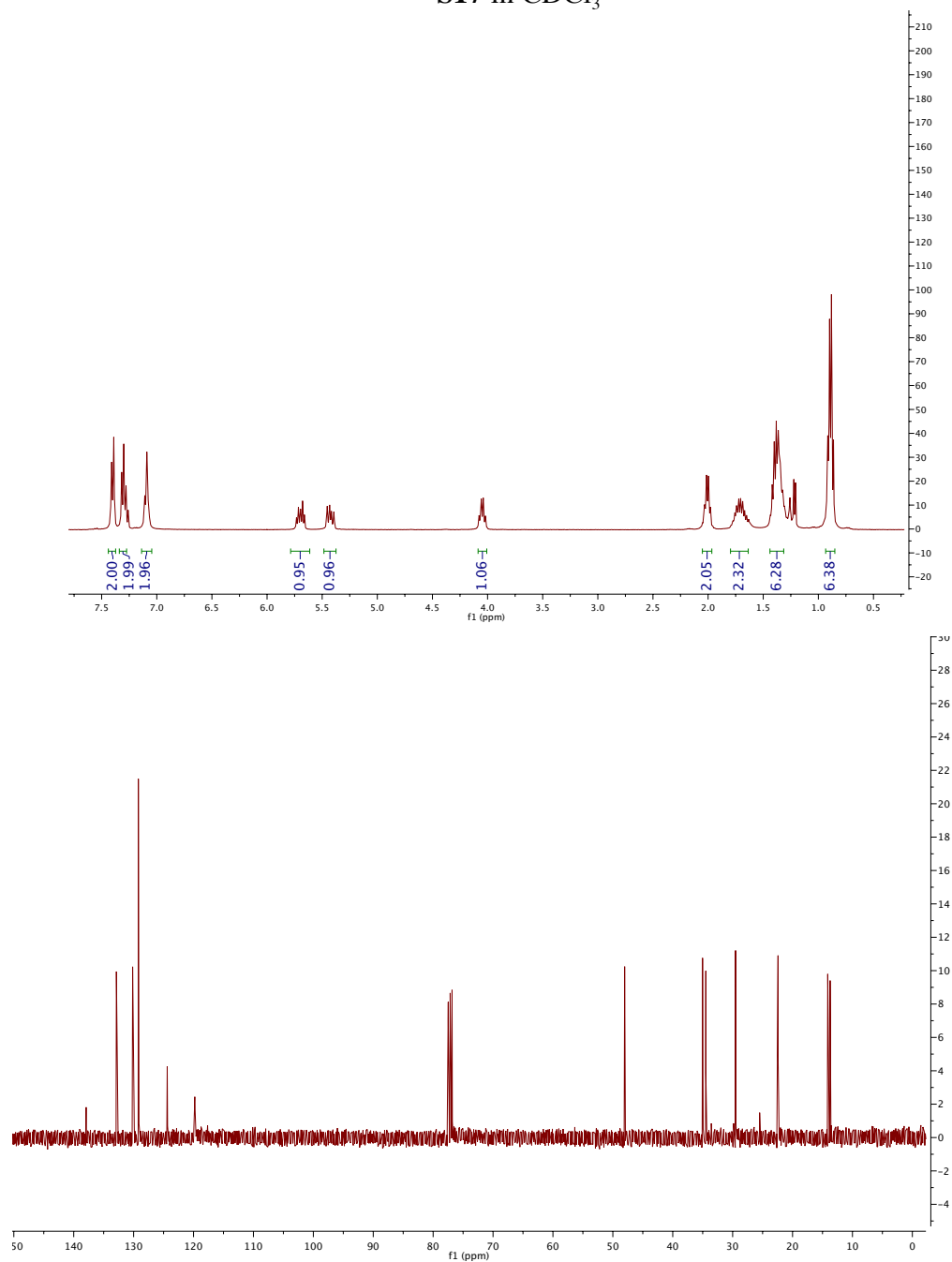
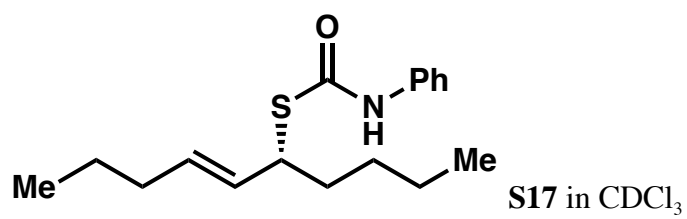


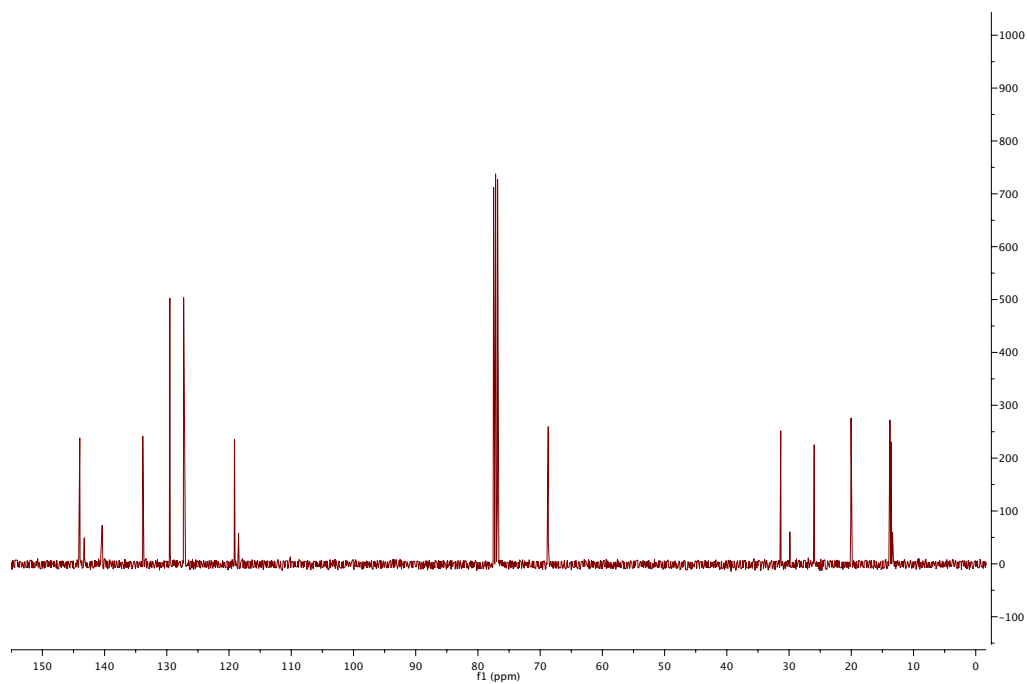
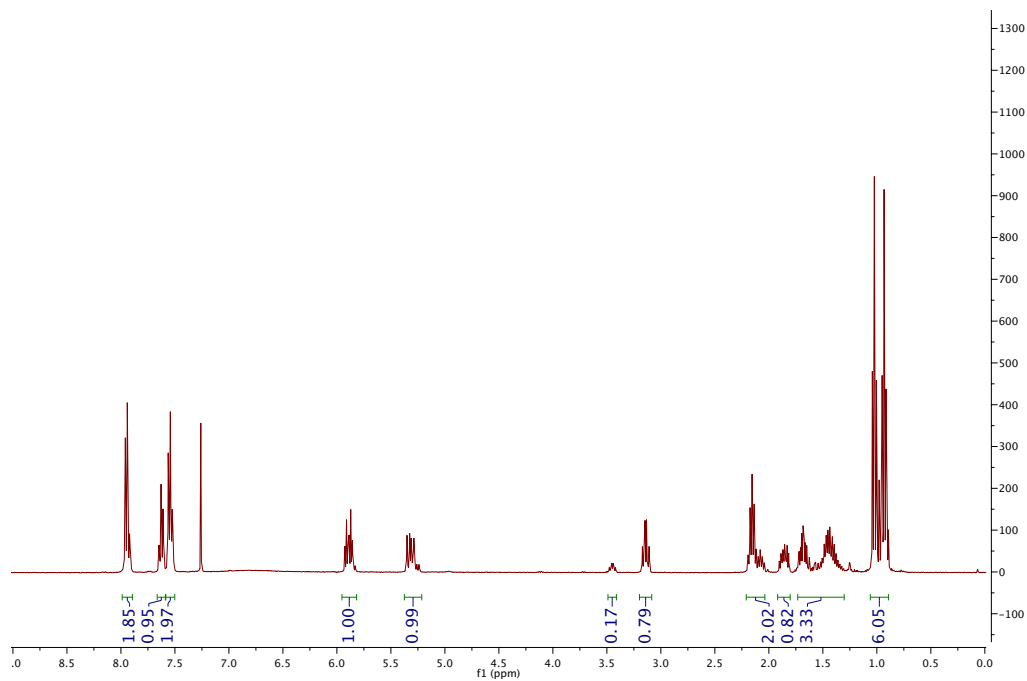
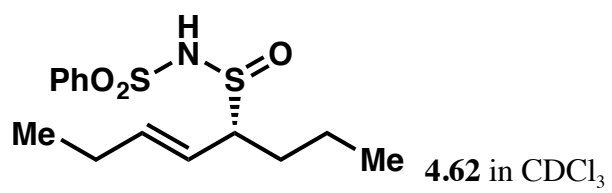


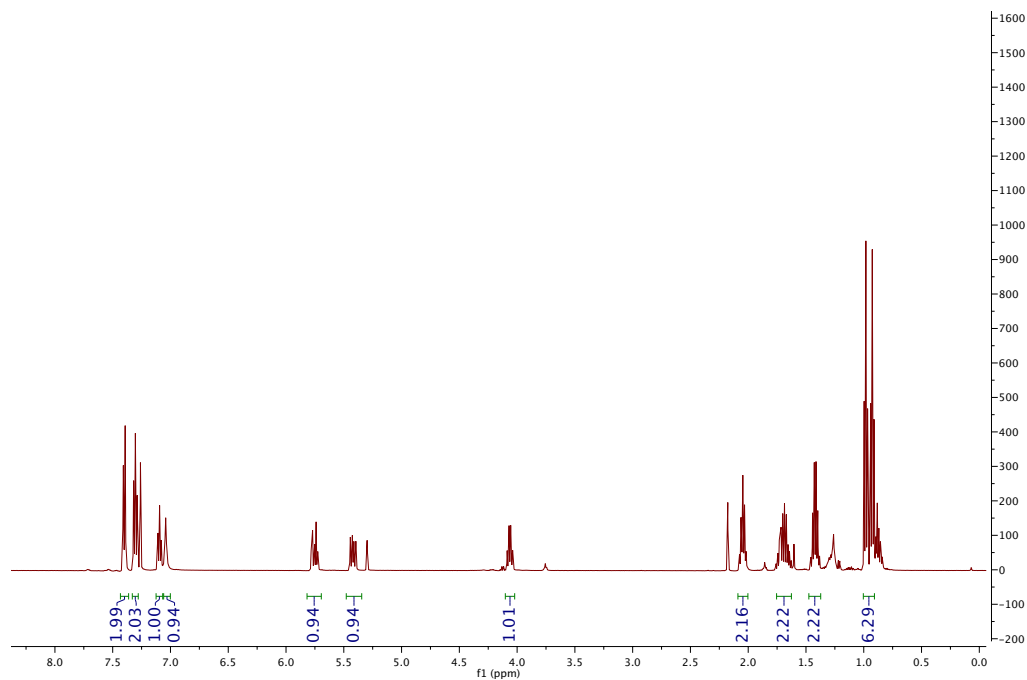
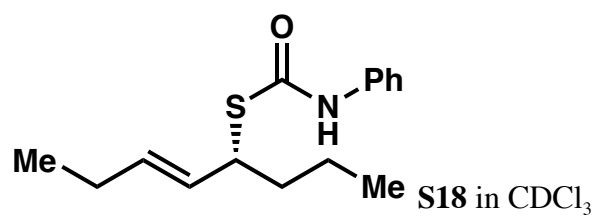


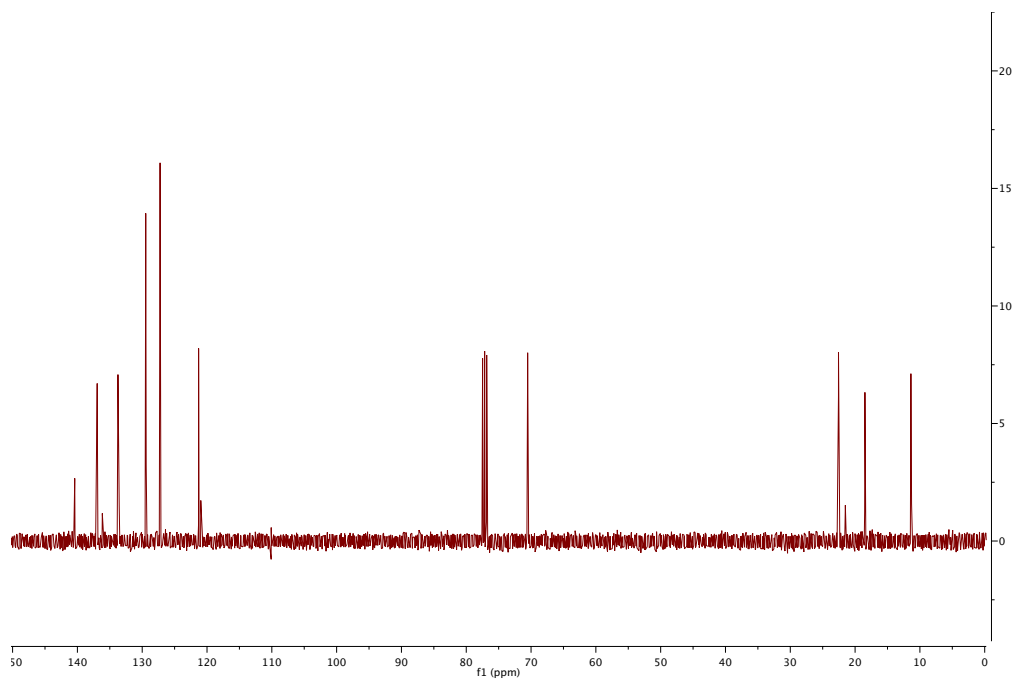
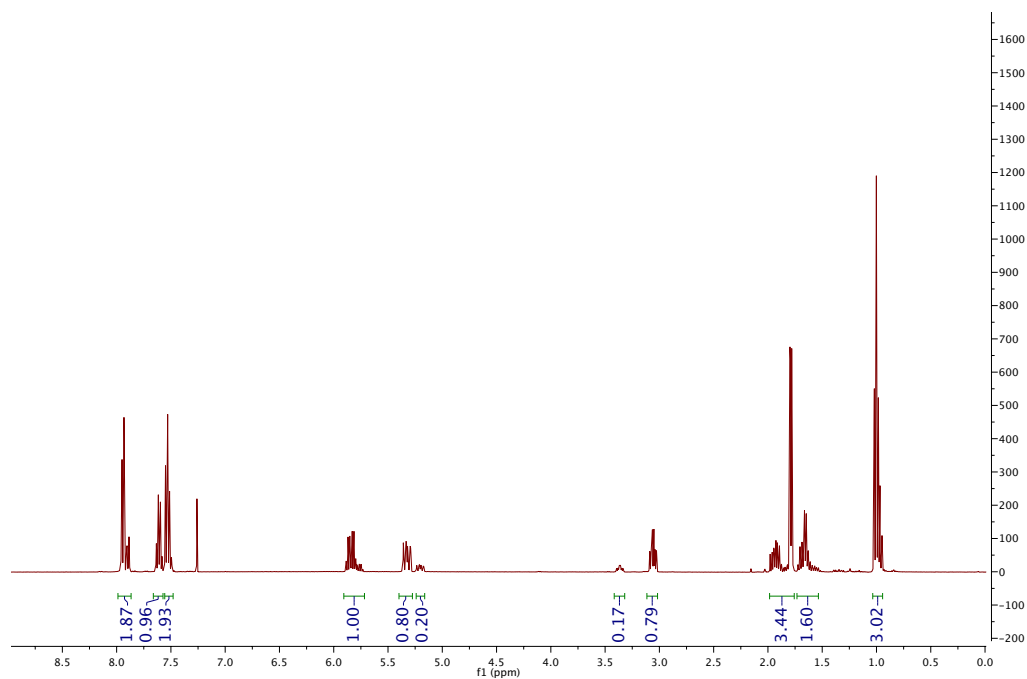
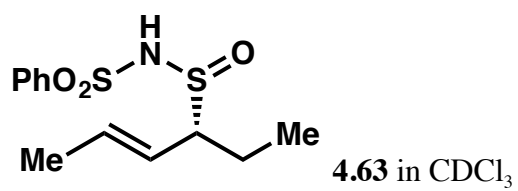


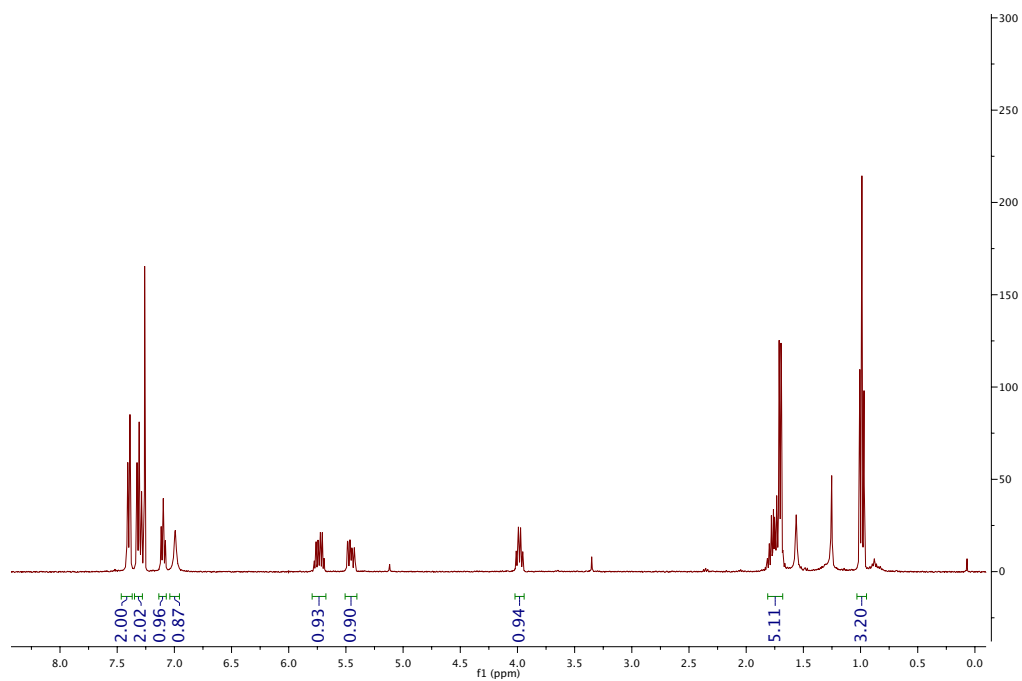
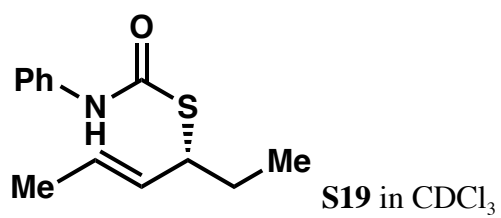


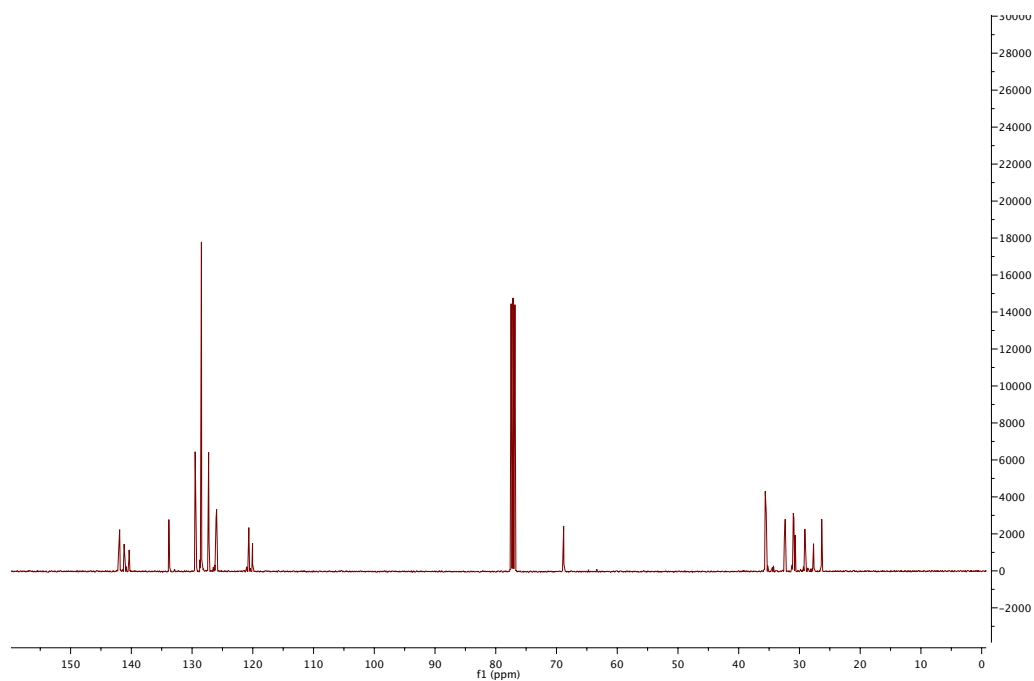
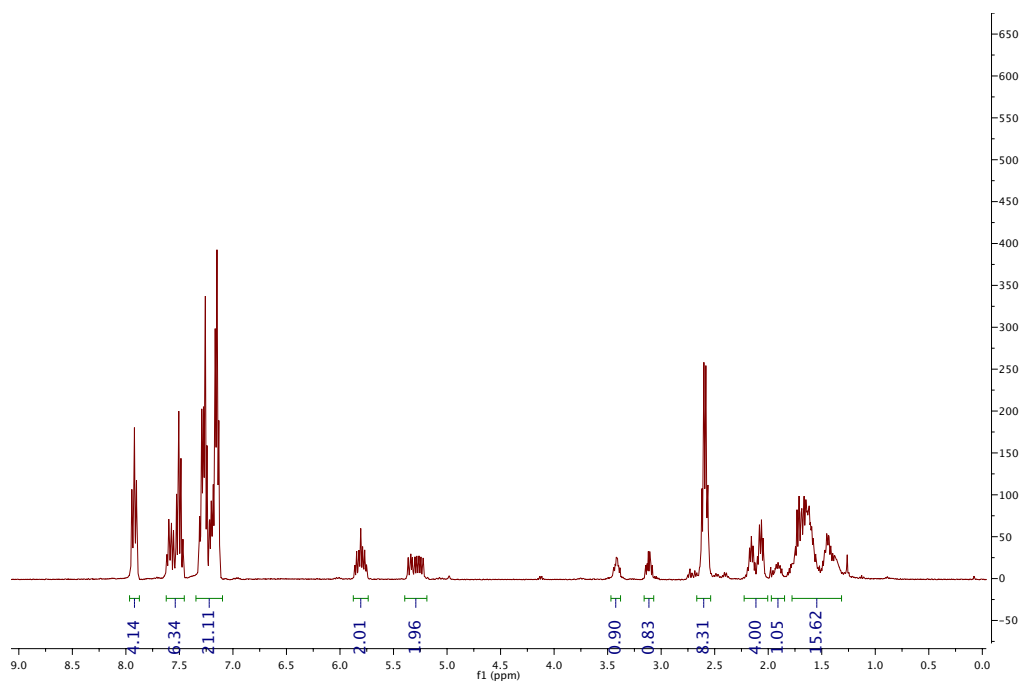
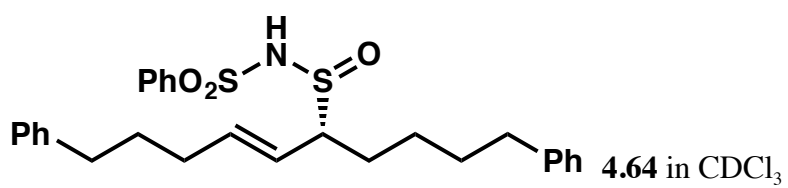


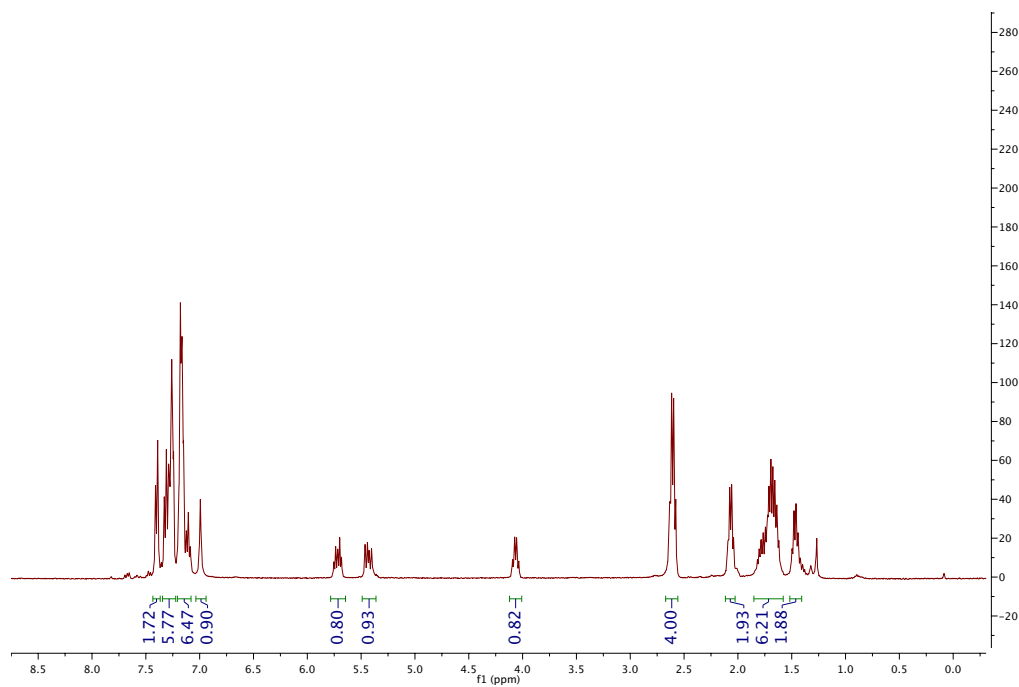
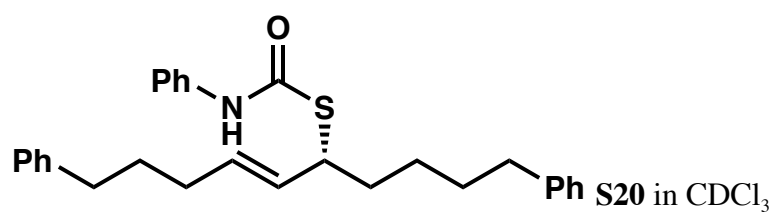


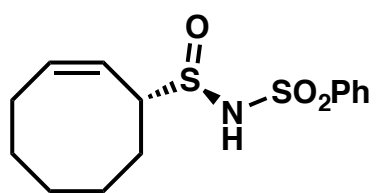




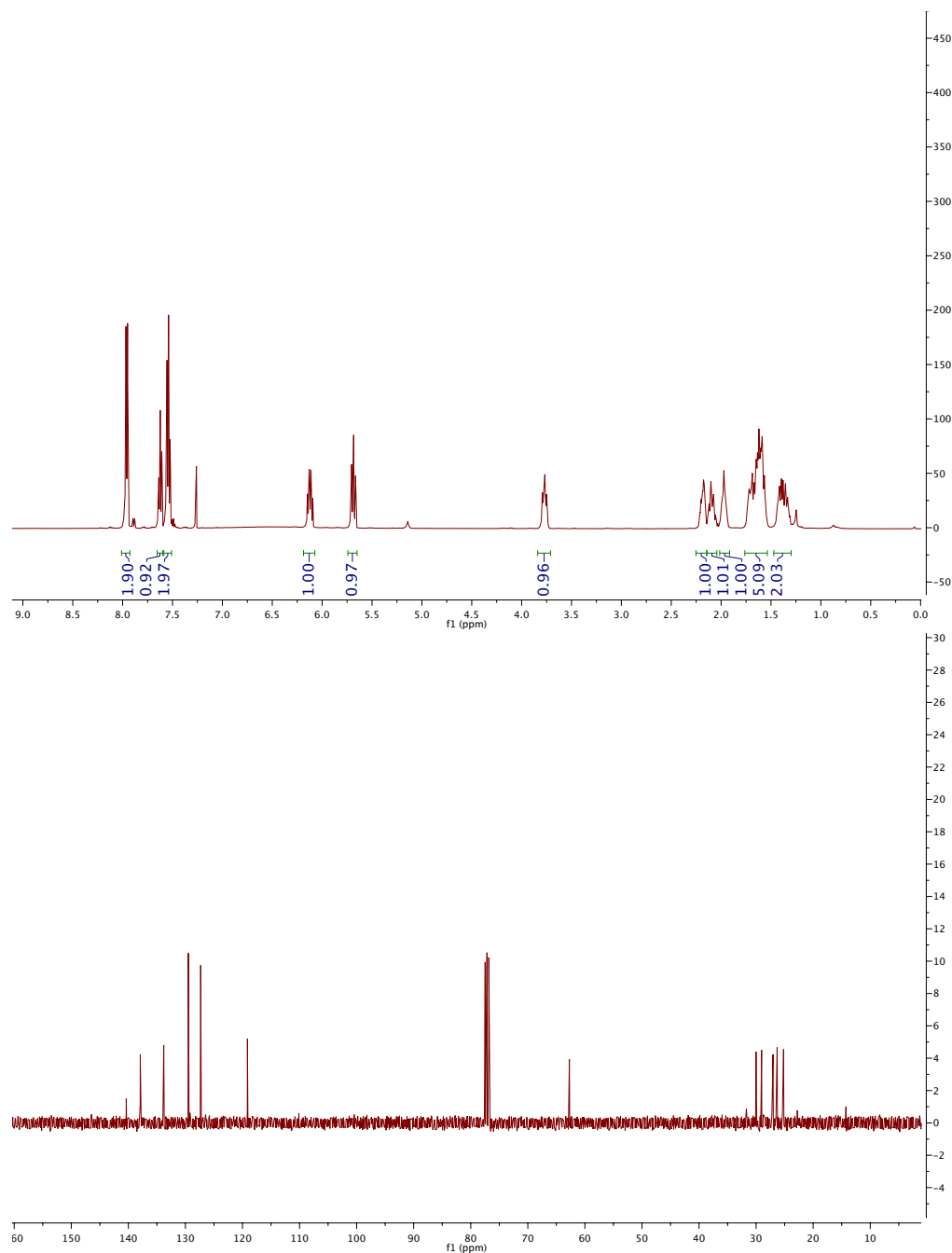


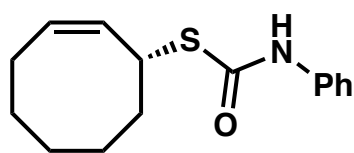




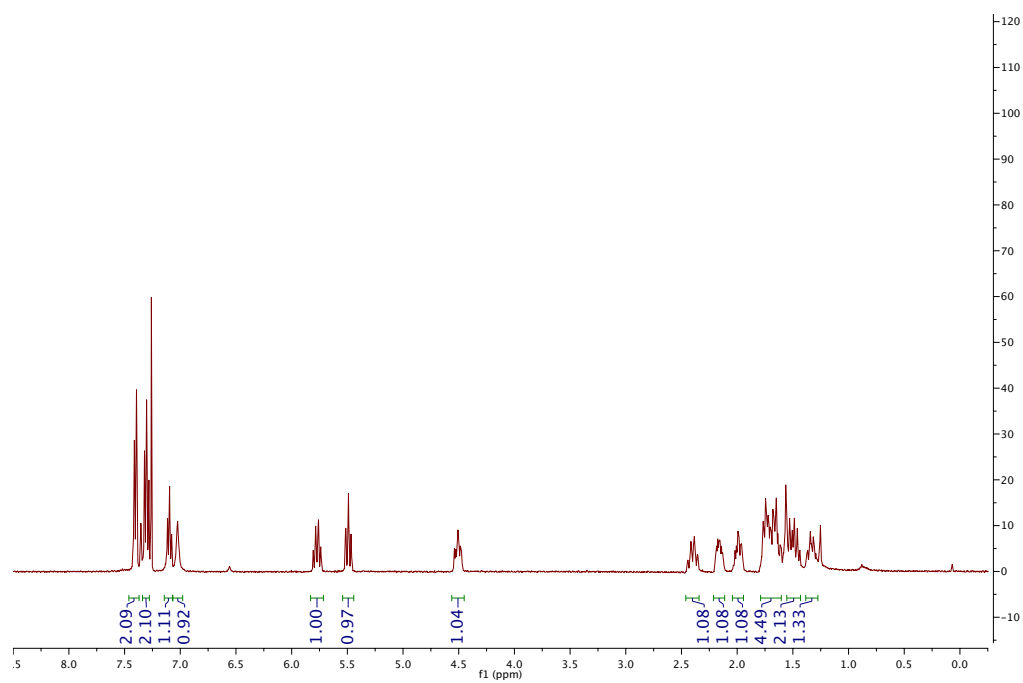


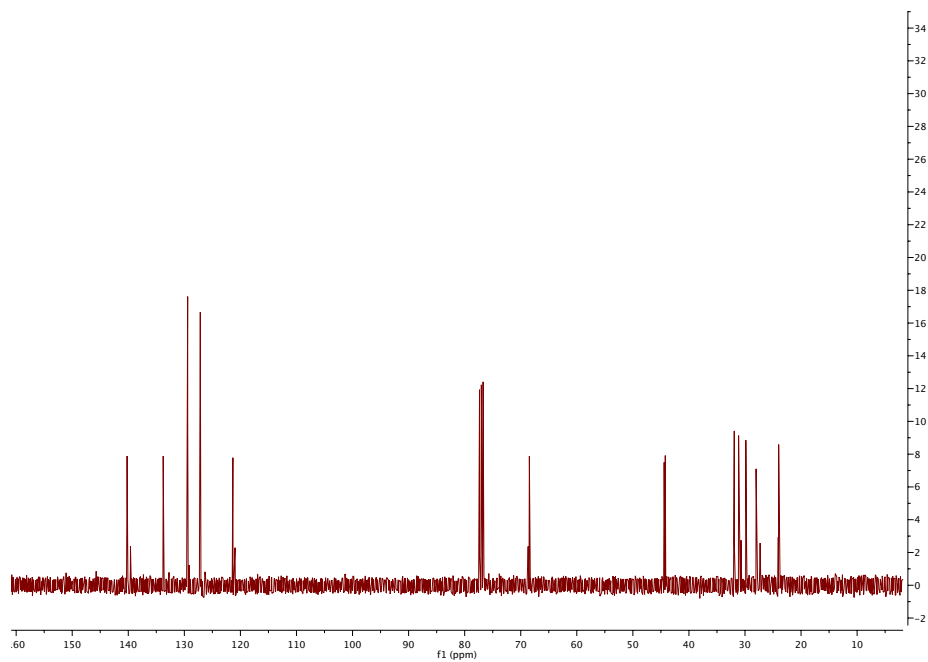
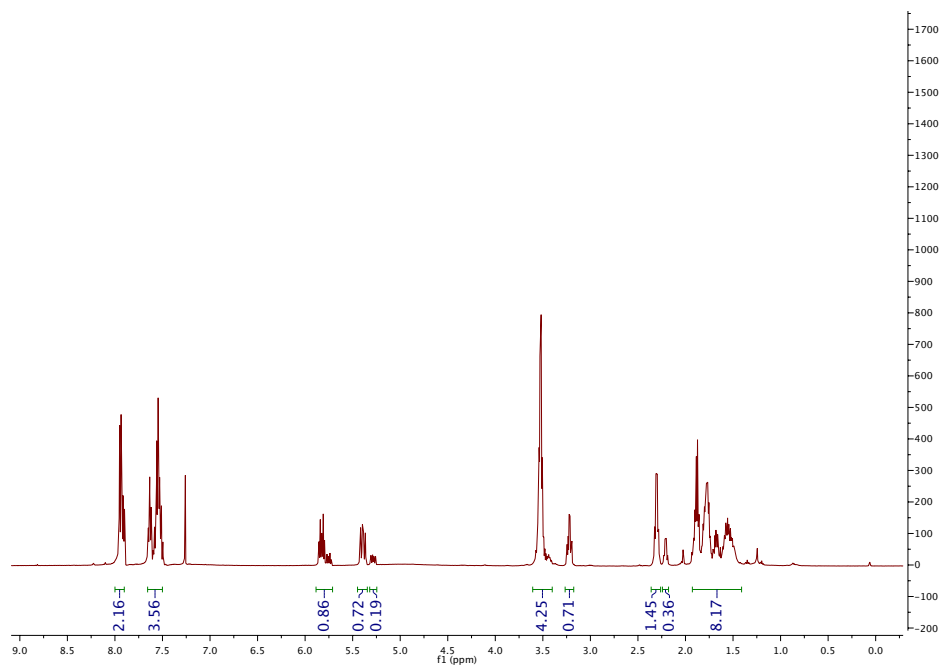
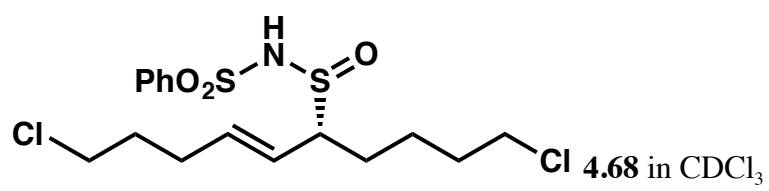
4.65 in CDCl₃

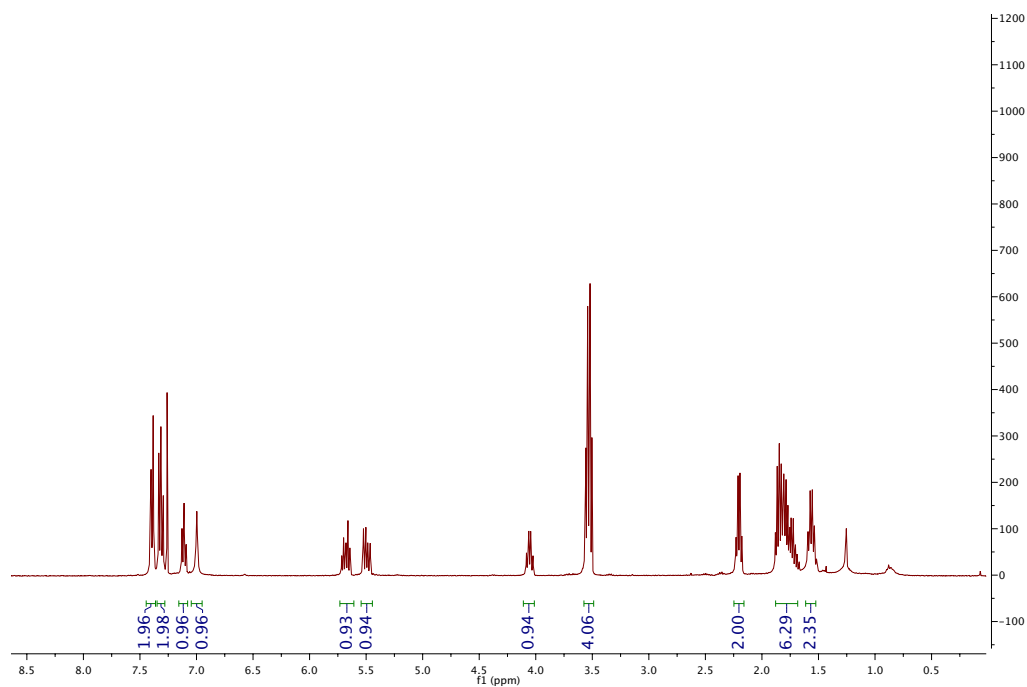
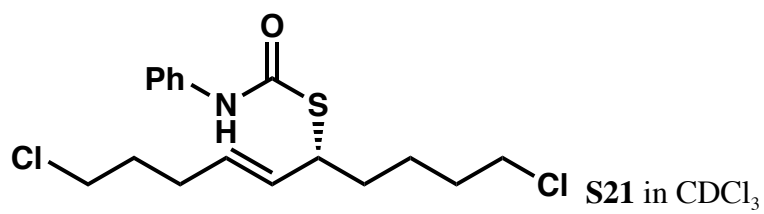


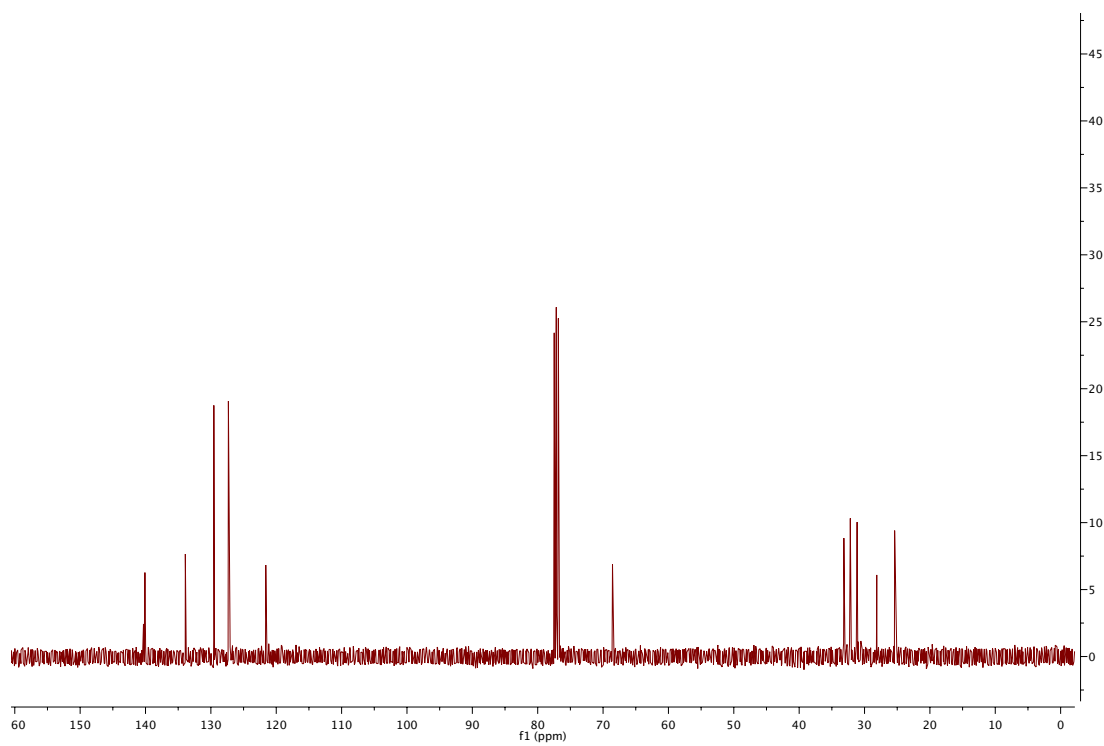
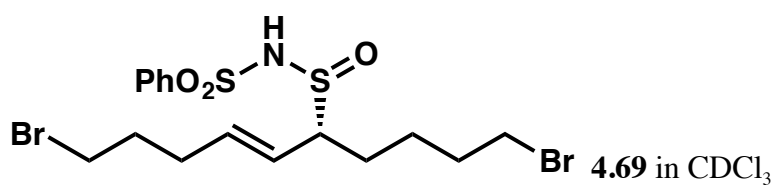


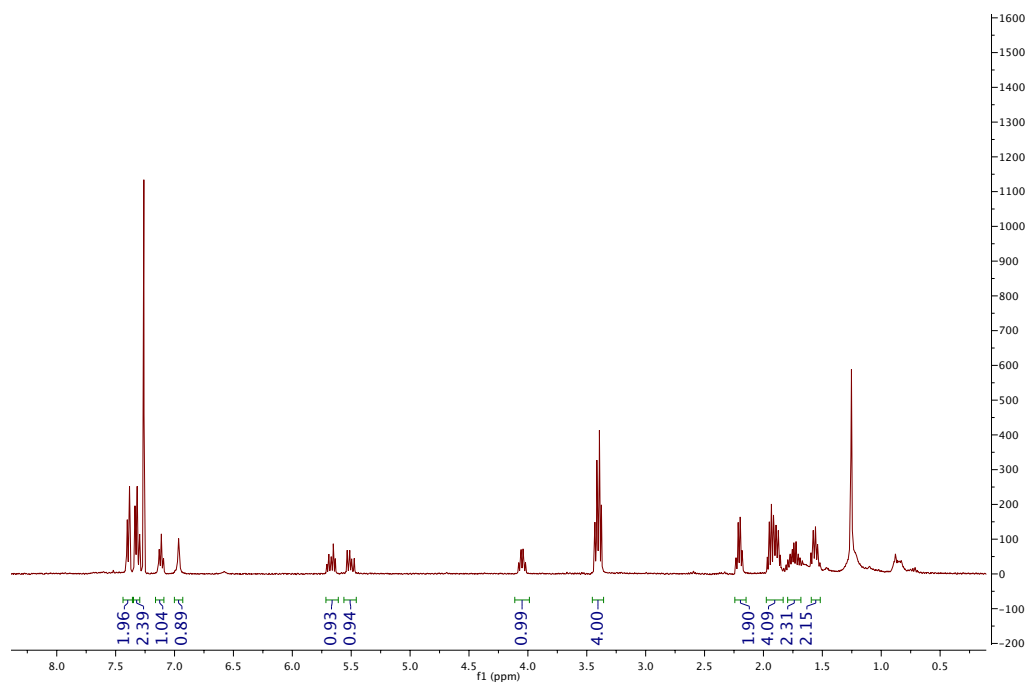
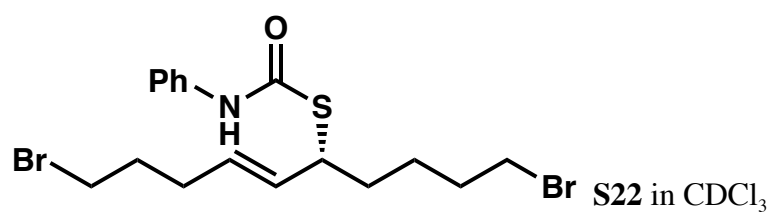
S20 in CDCl₃

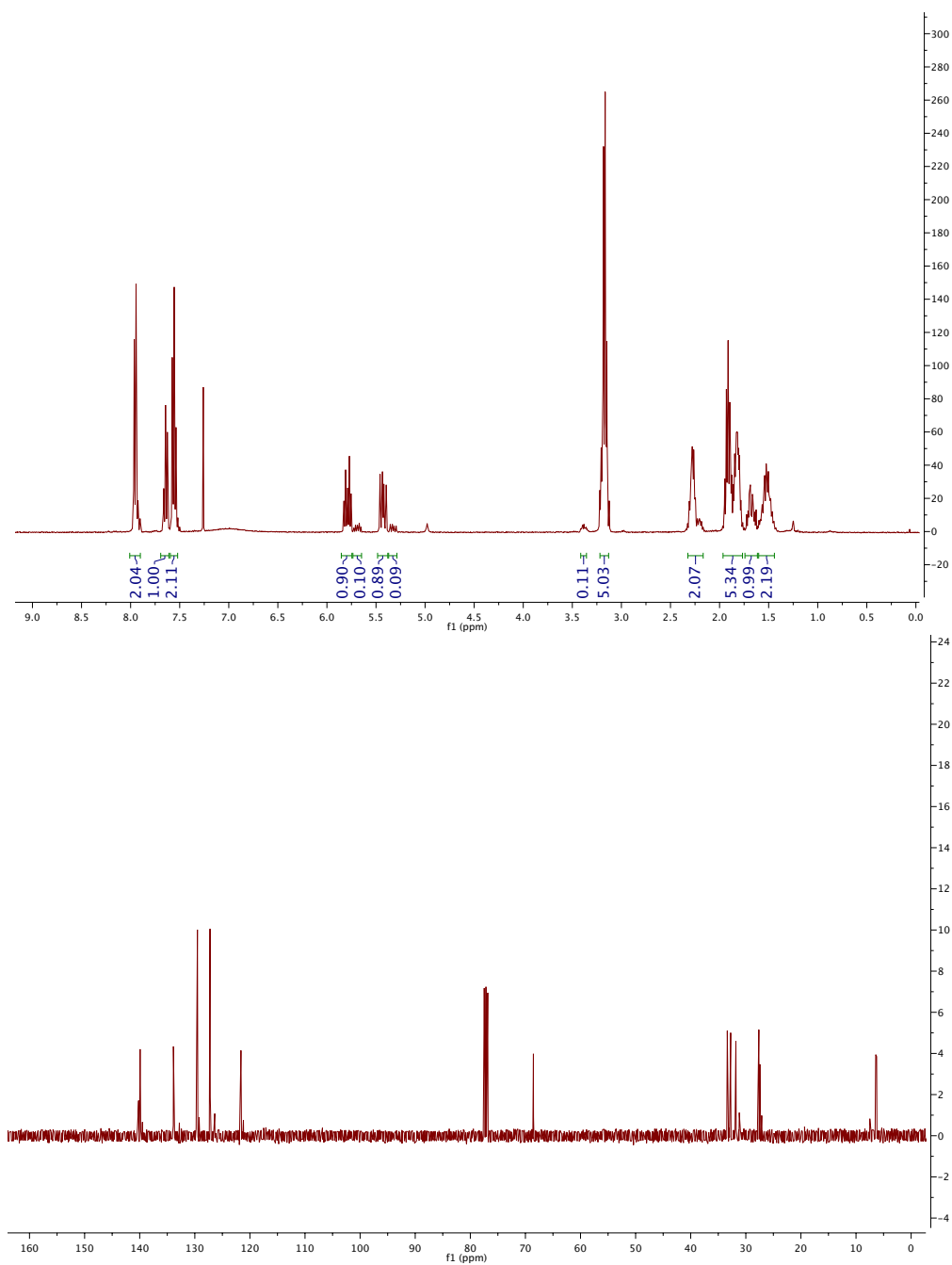
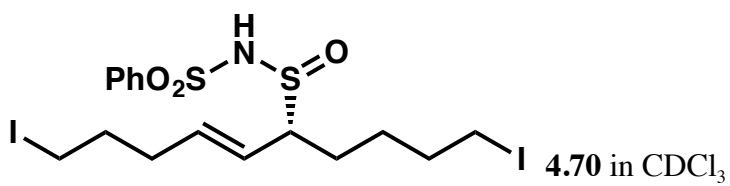


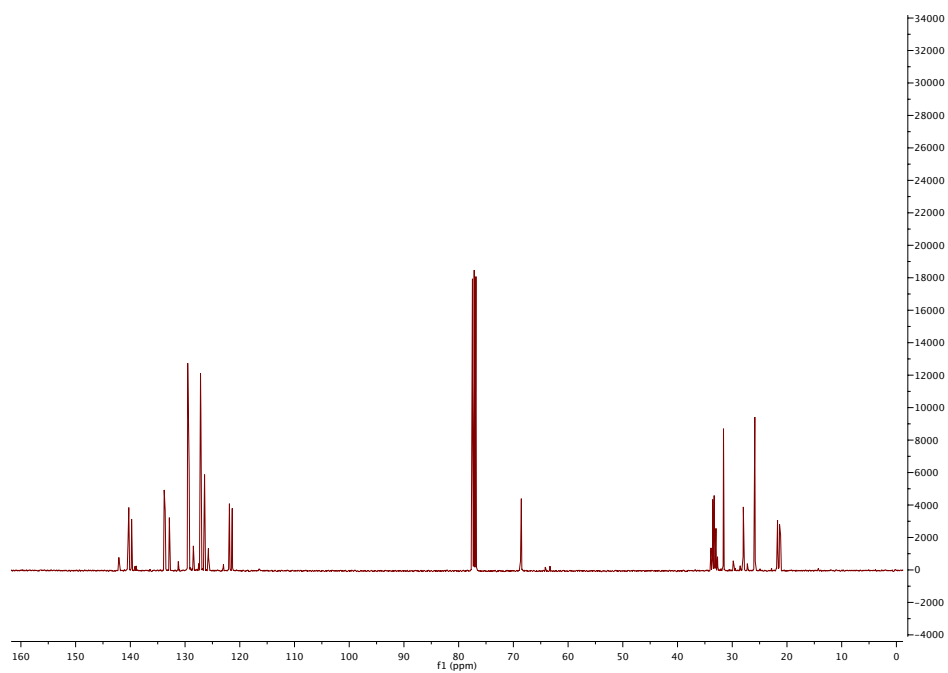
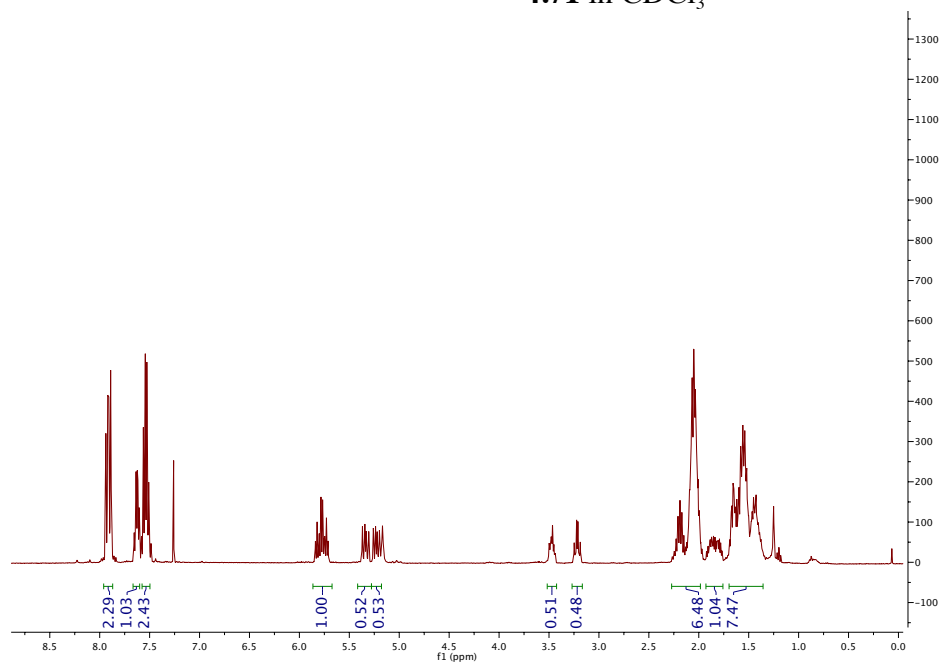
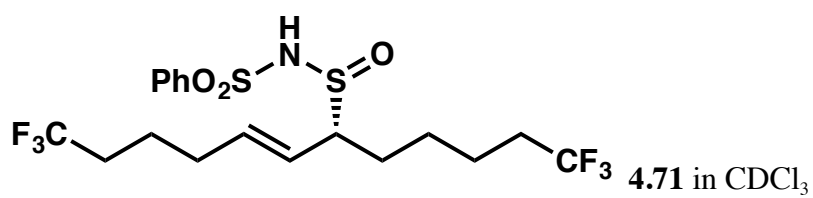


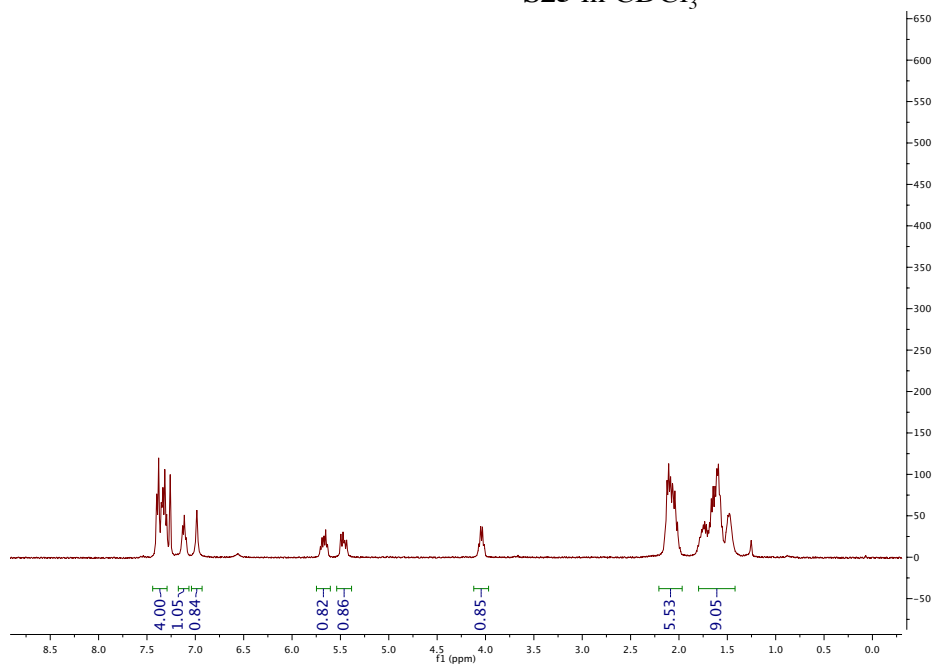
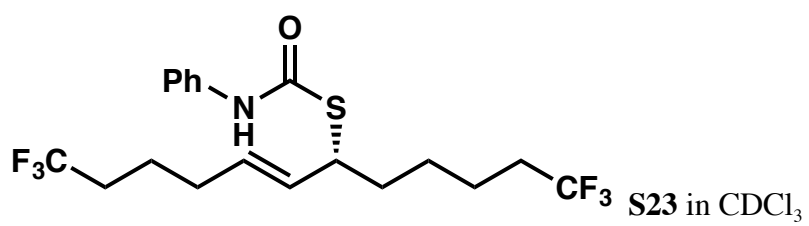


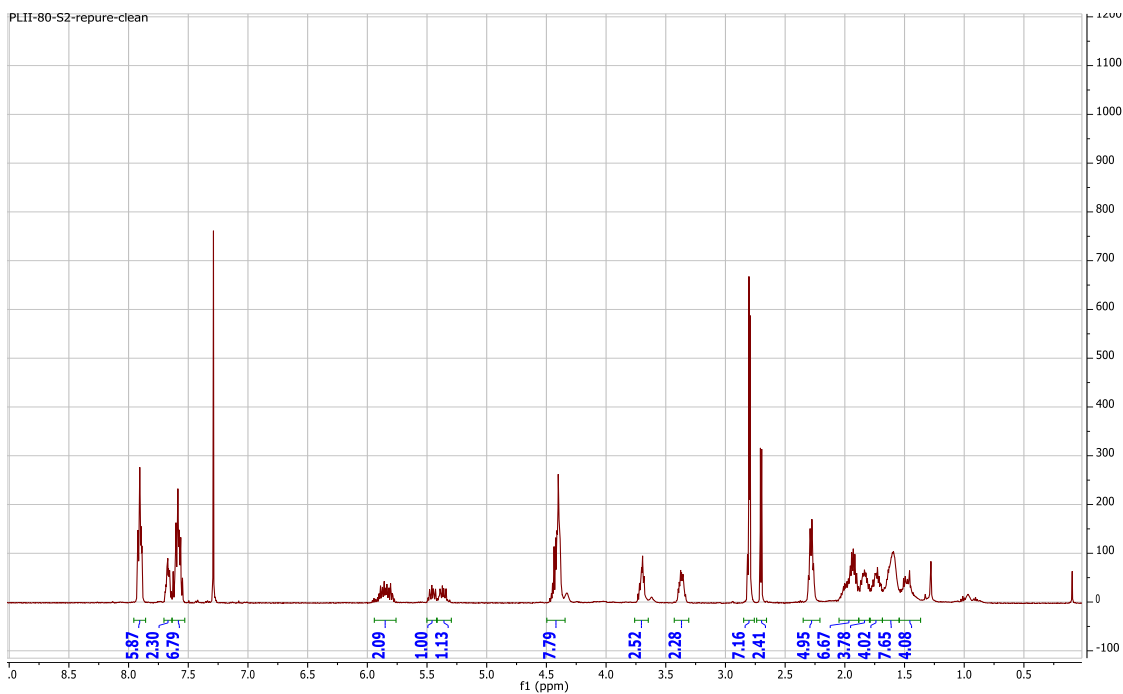
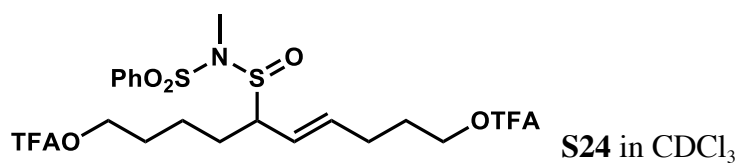


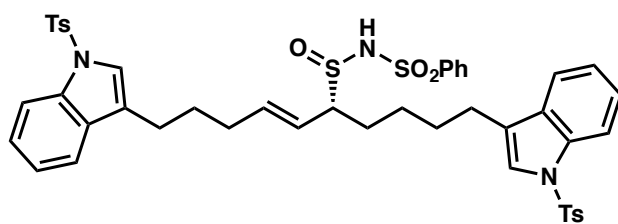




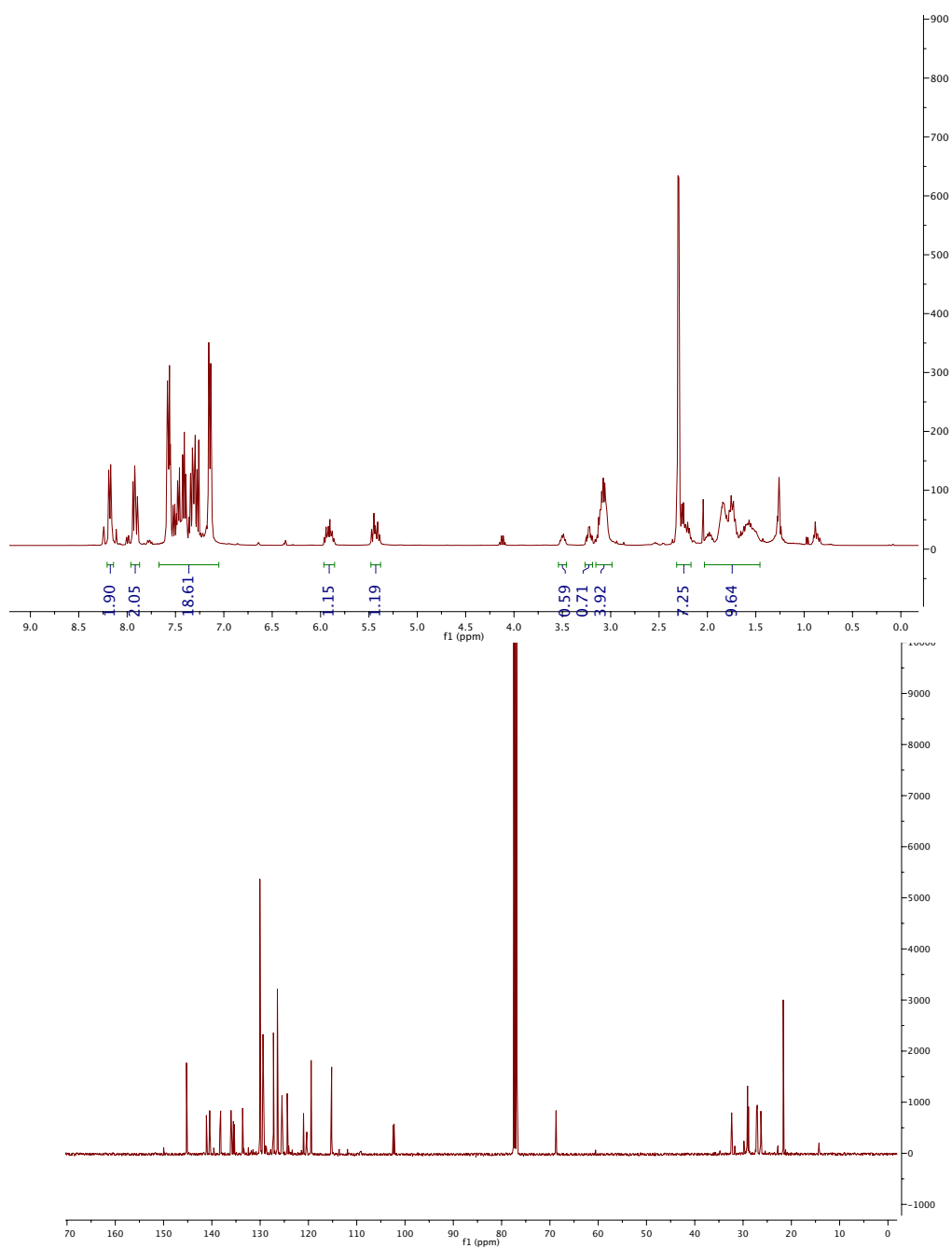


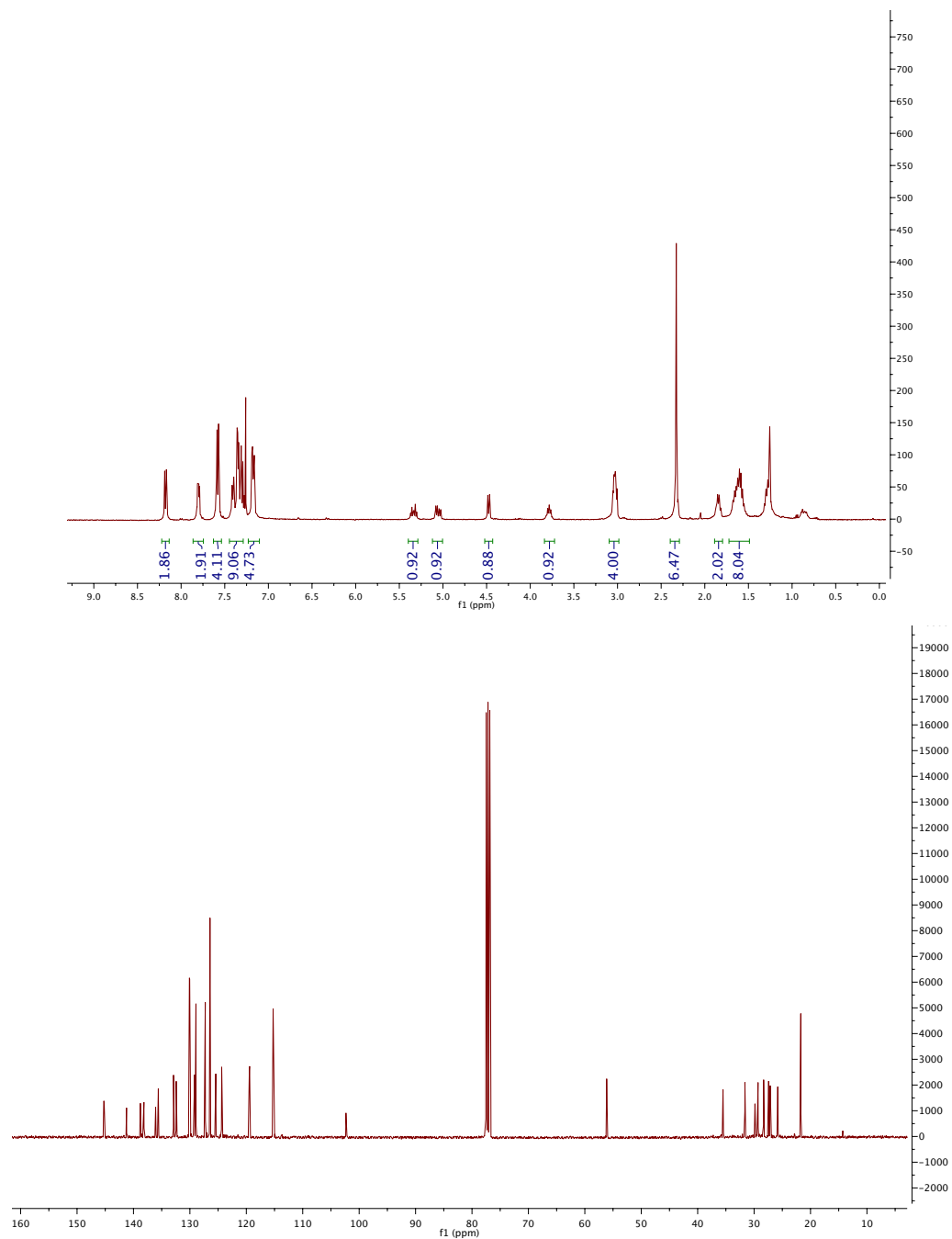
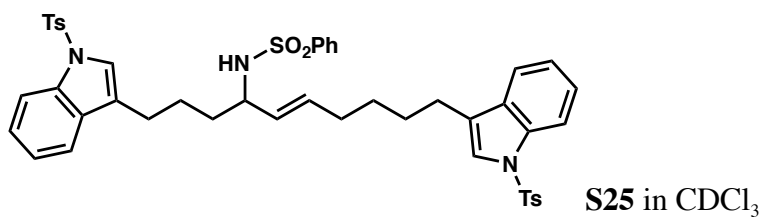


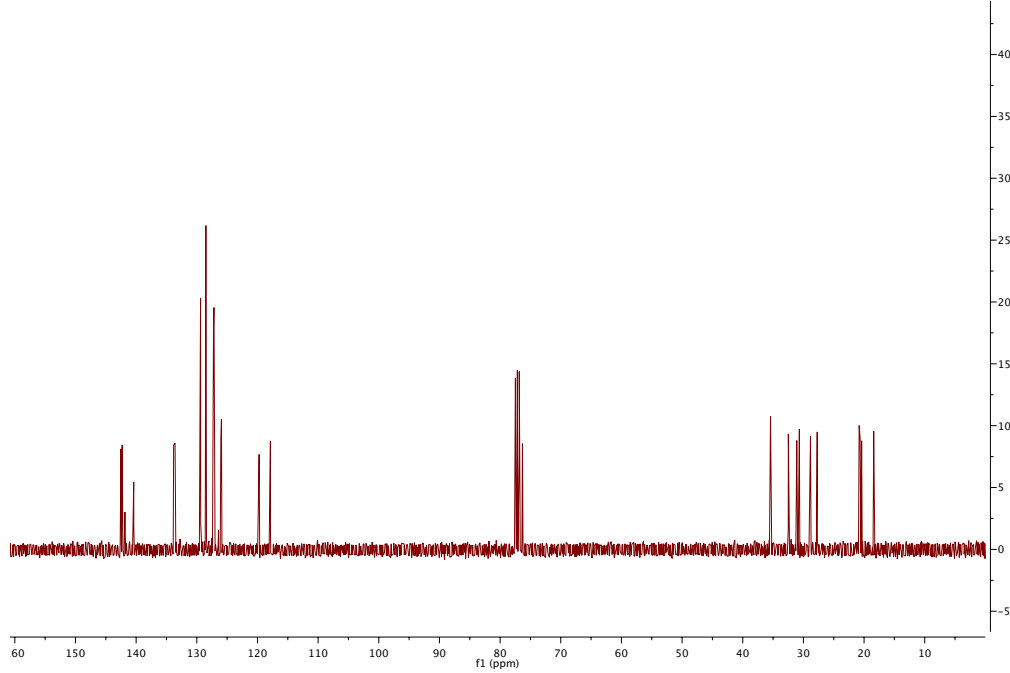
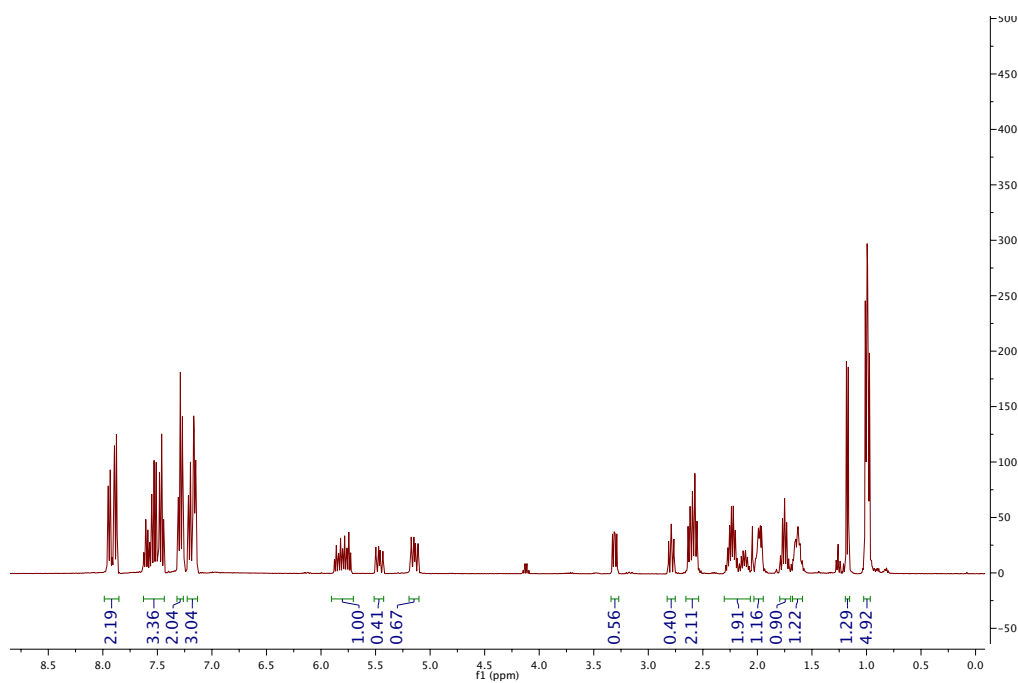
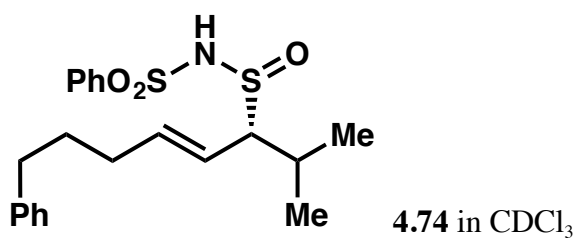


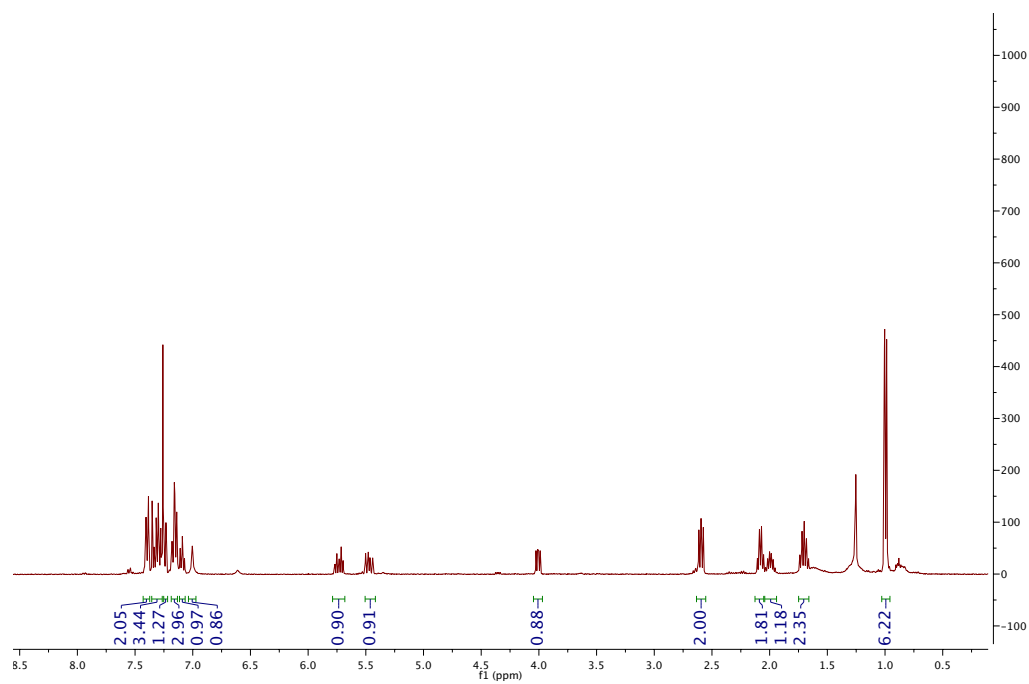
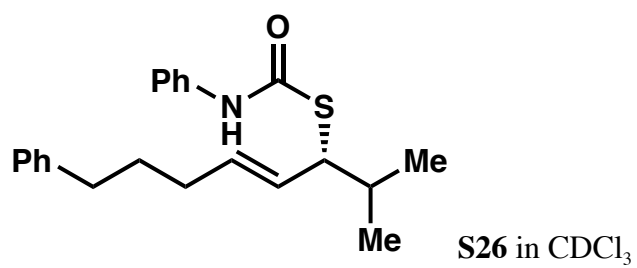


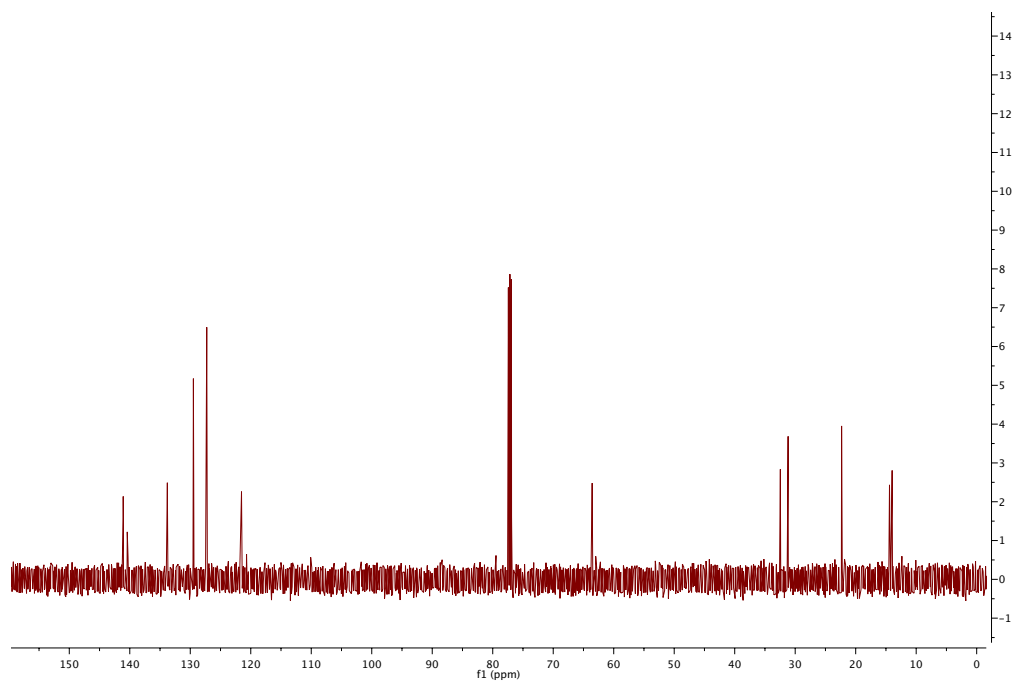
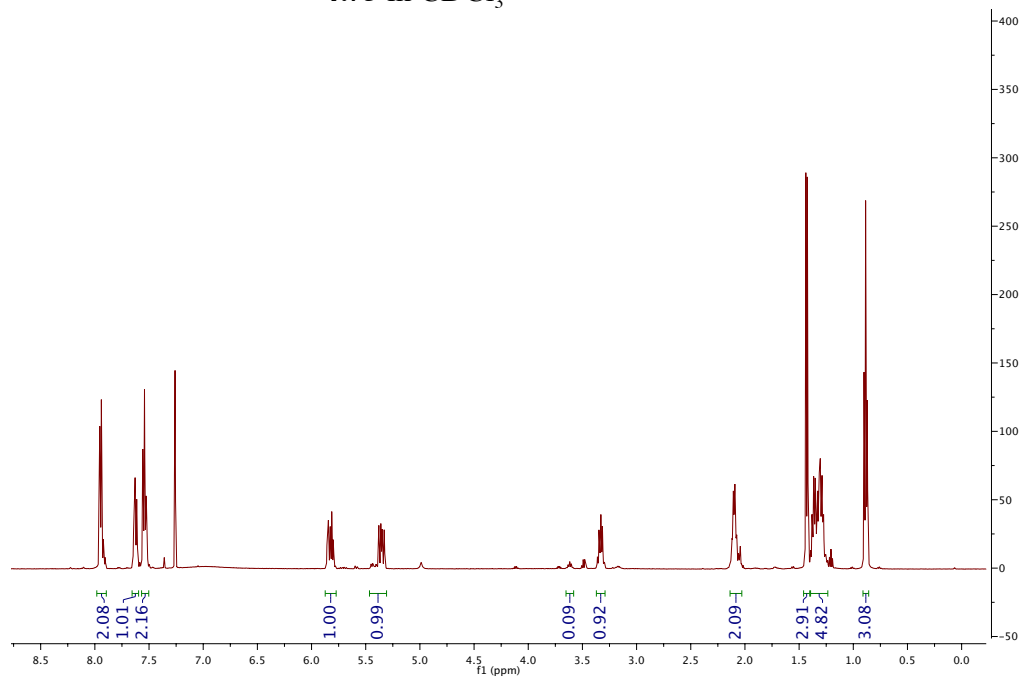
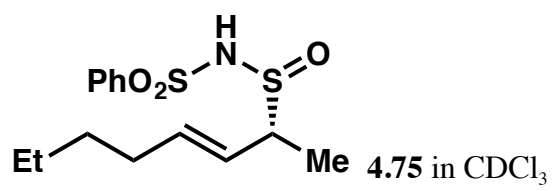
4.73 in CDCl_3

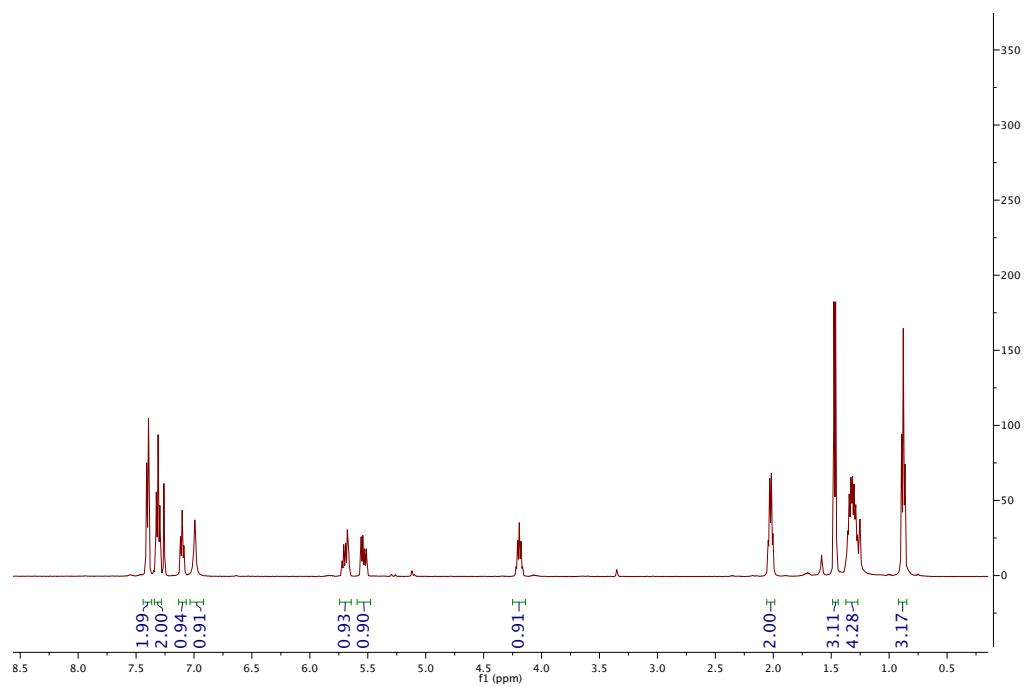
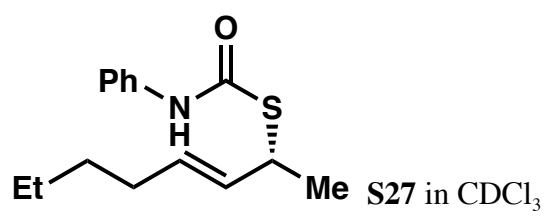


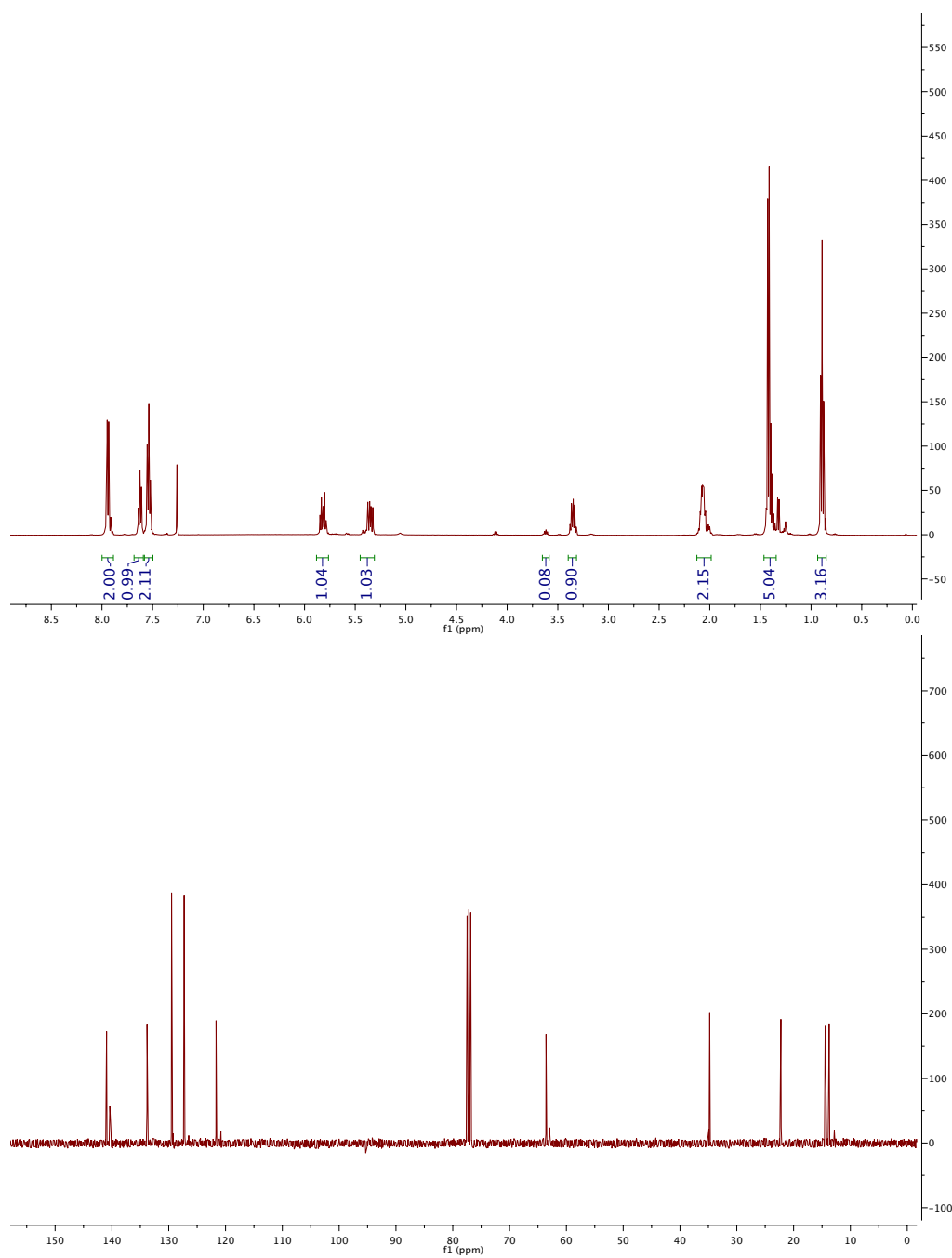
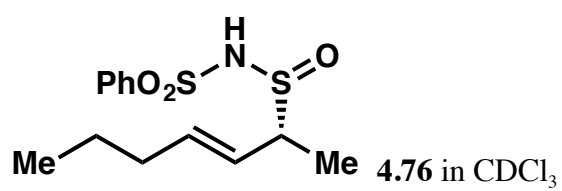


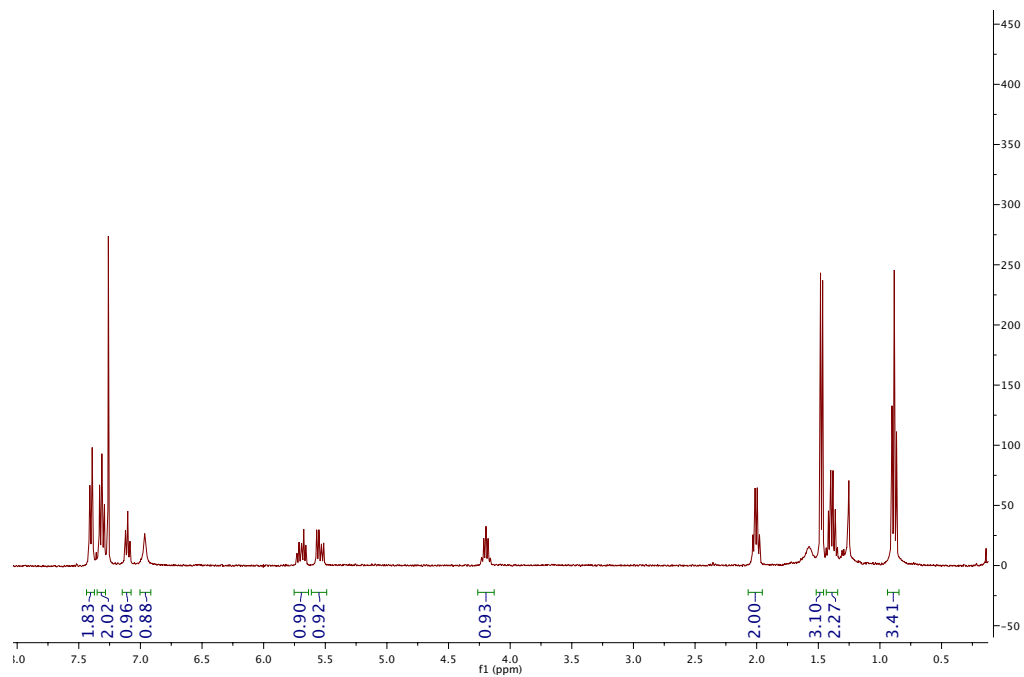
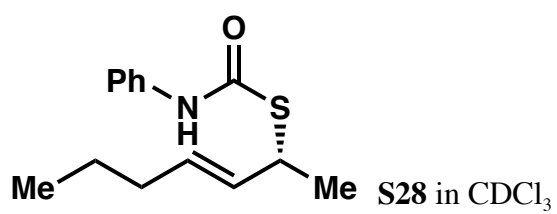


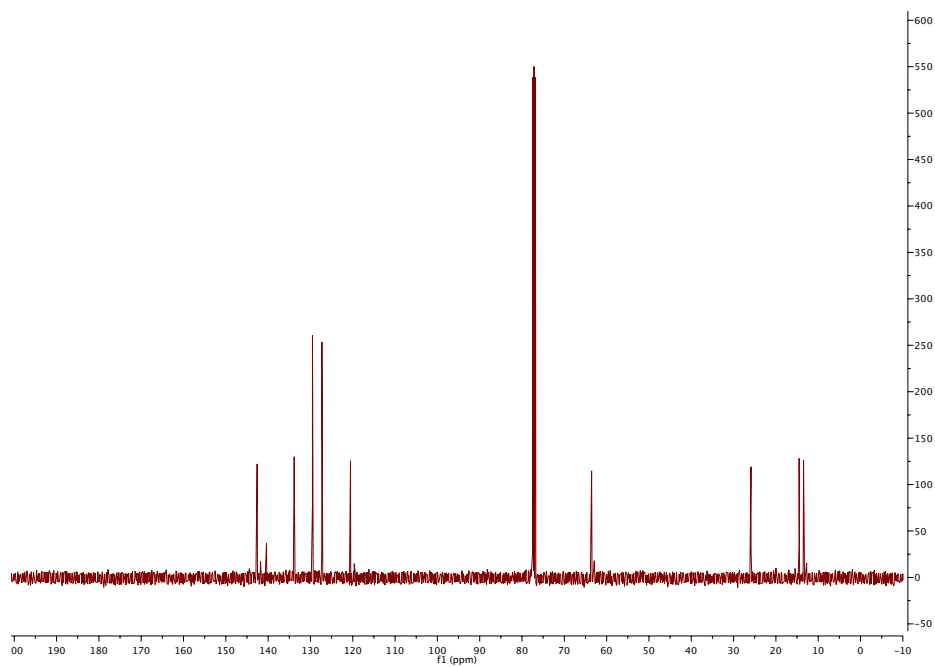
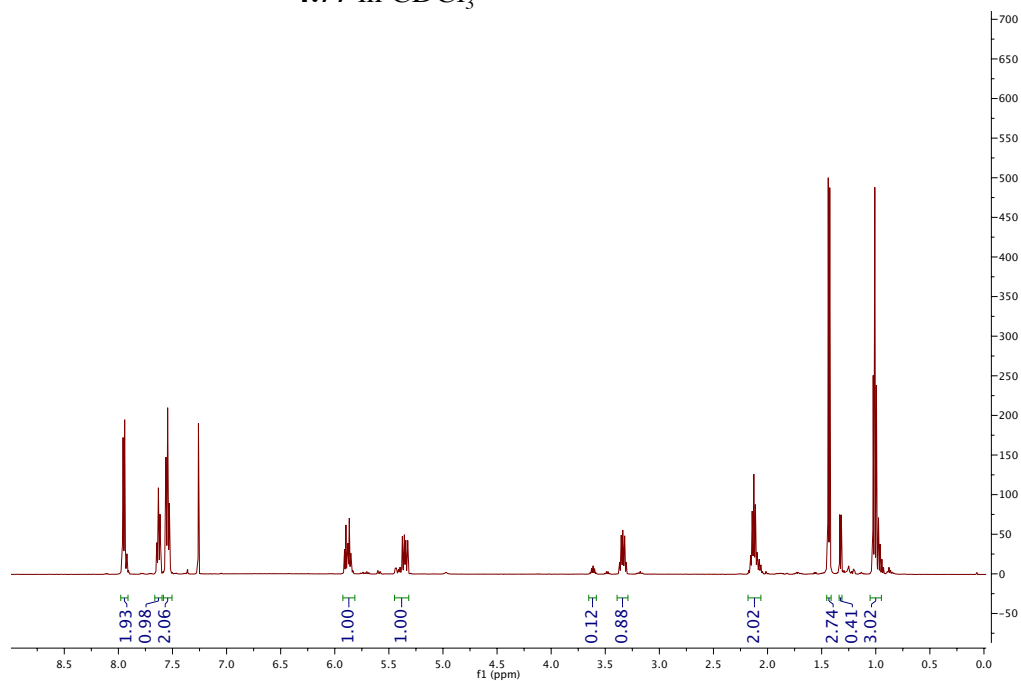
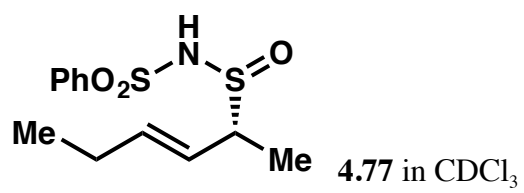


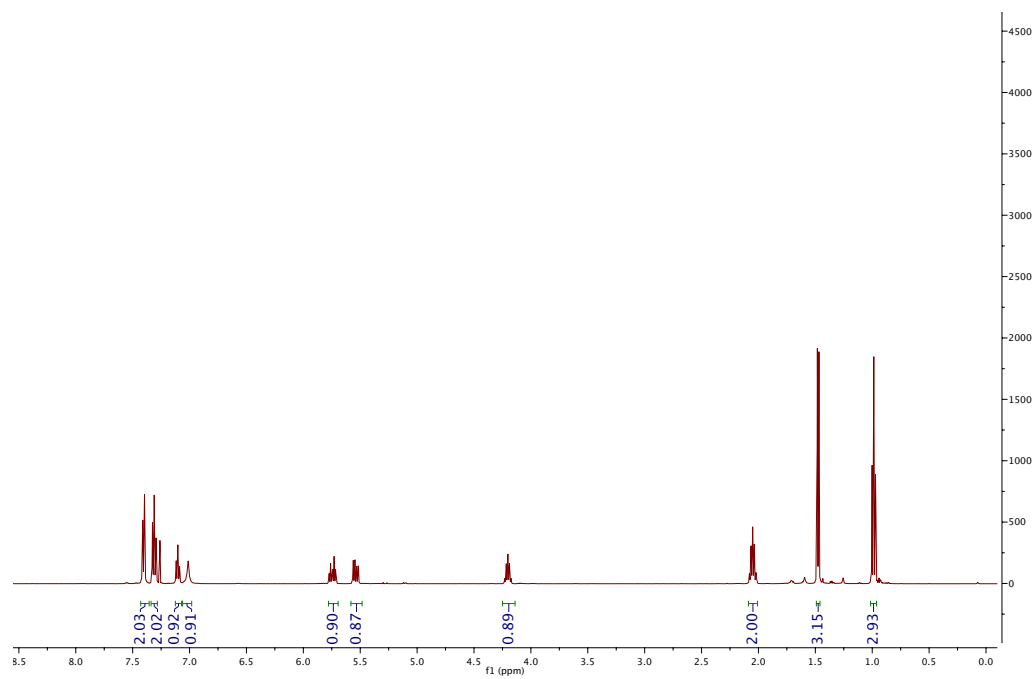
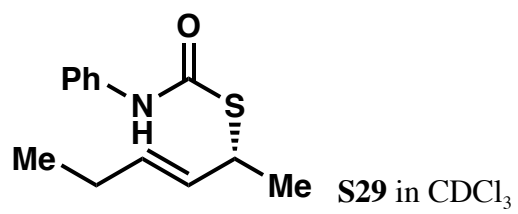


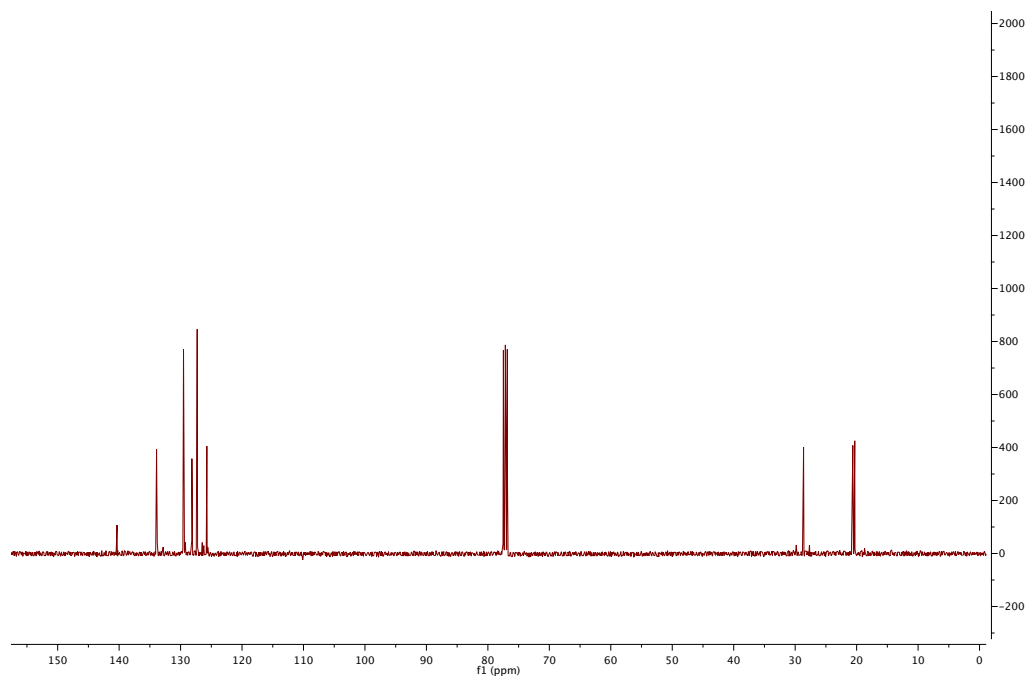
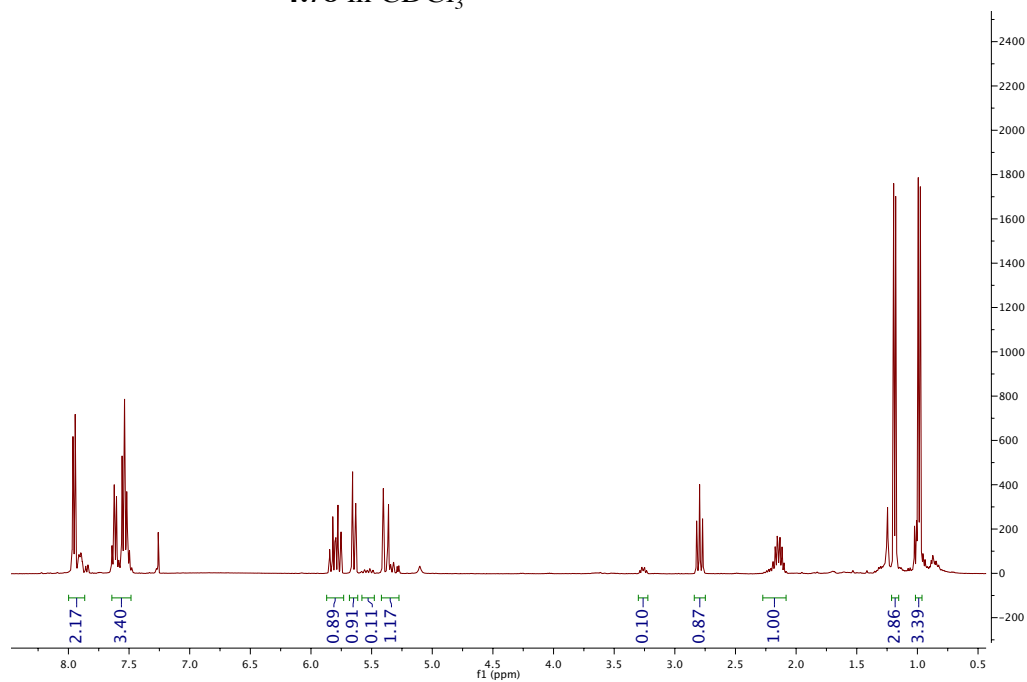
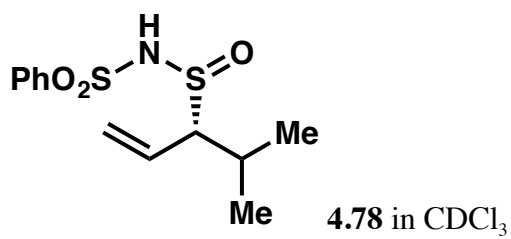


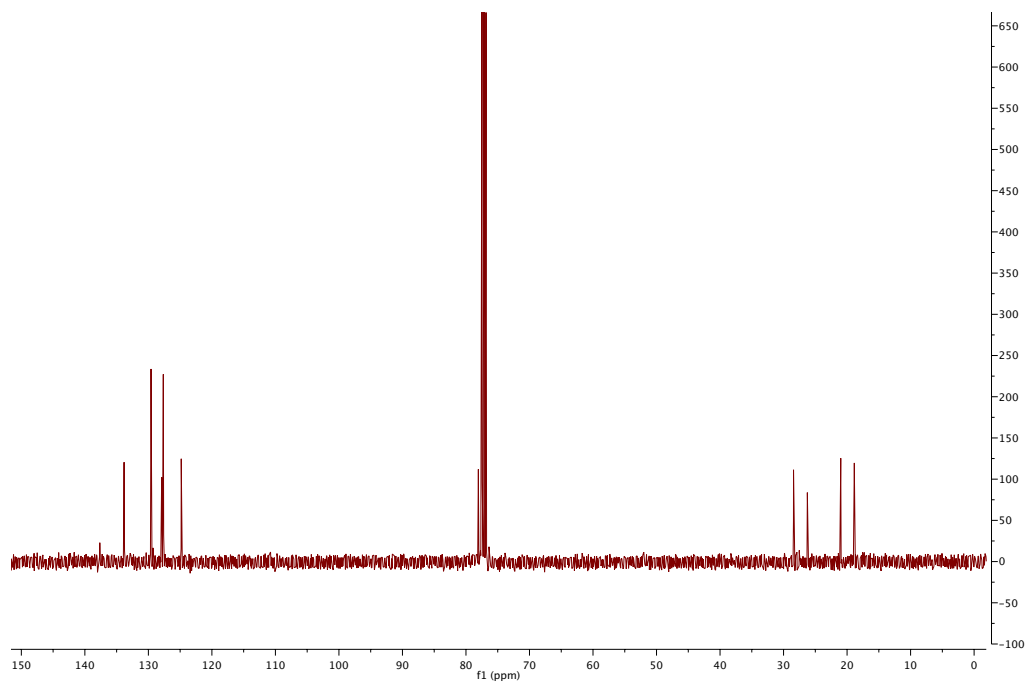
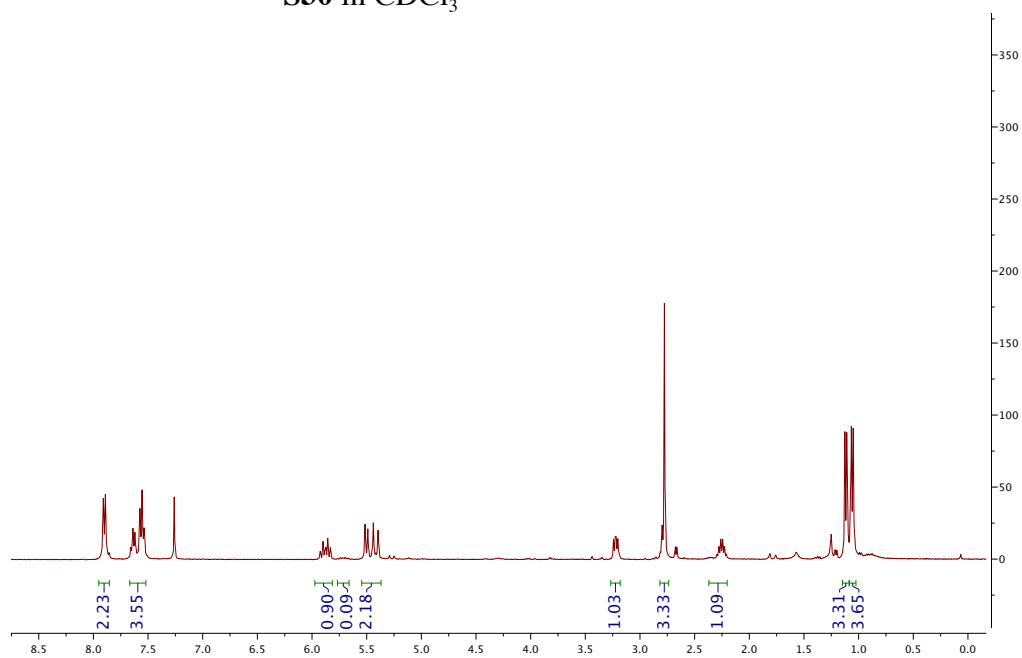
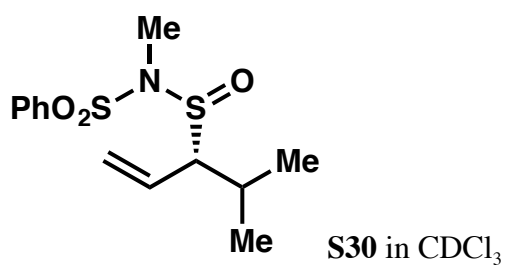


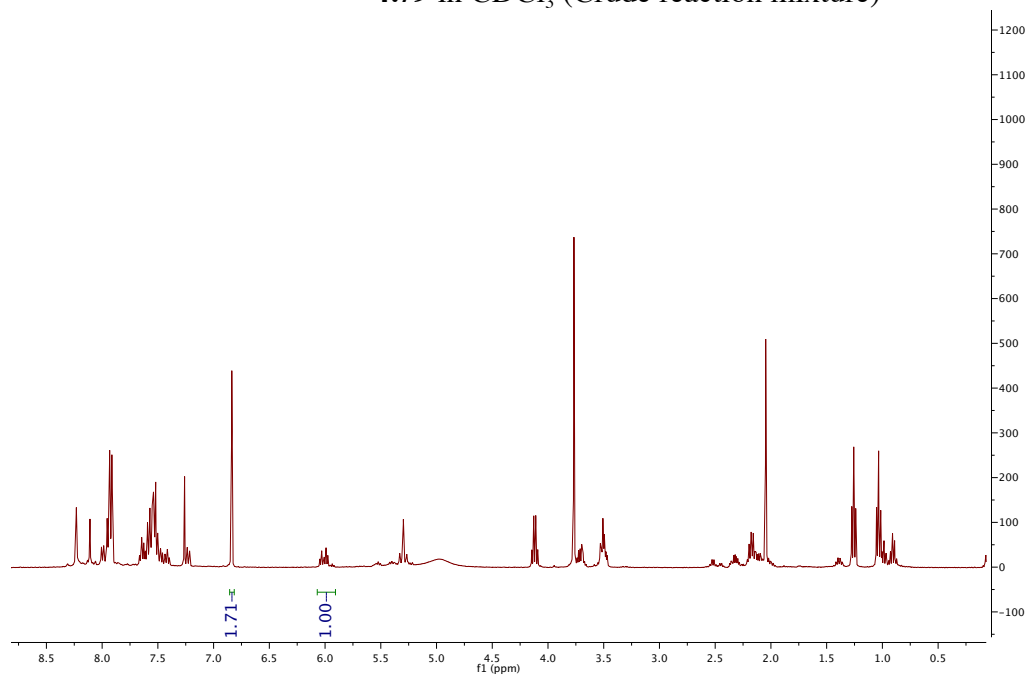
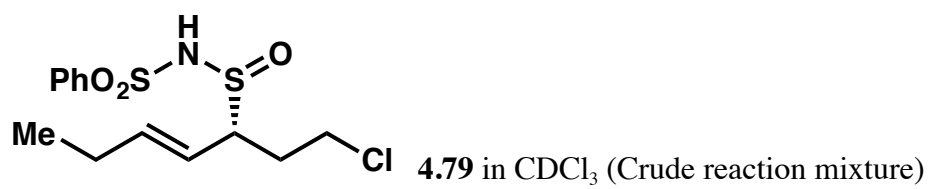


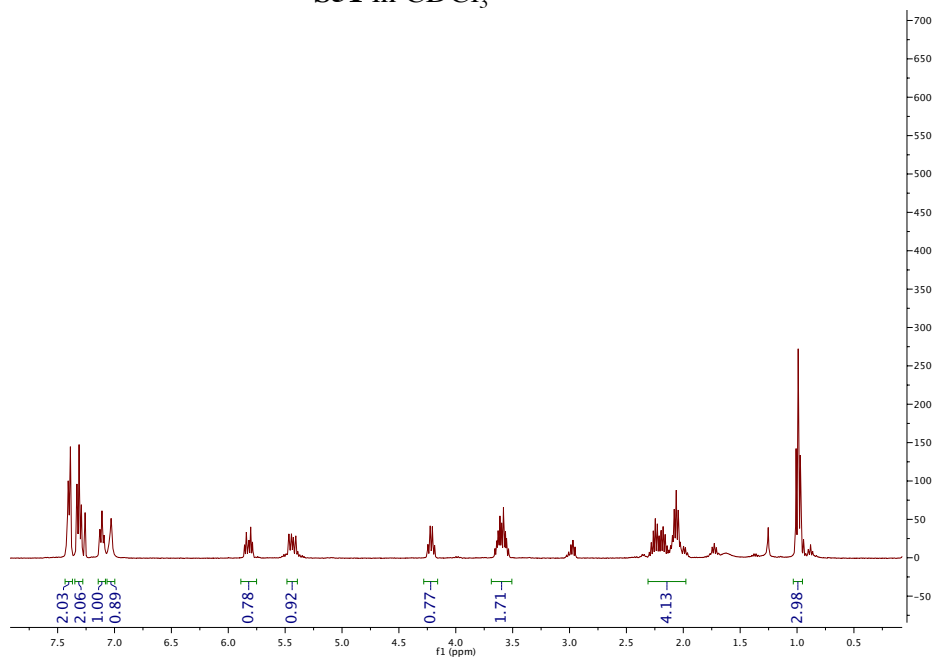
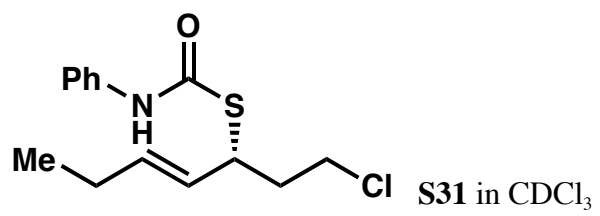


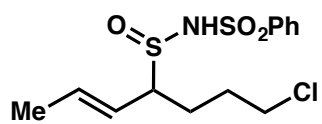






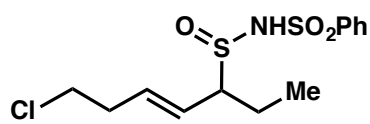






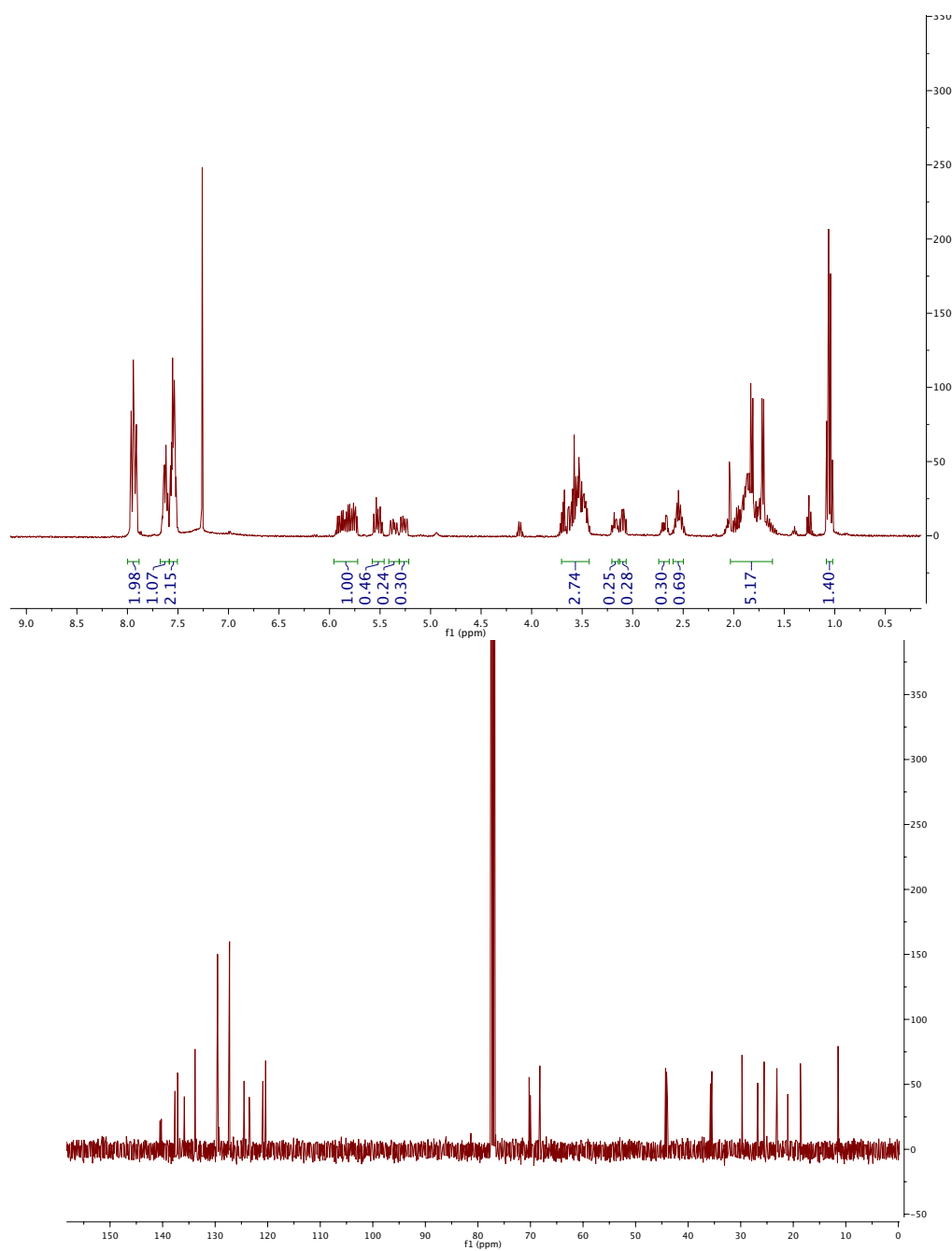
(Major)

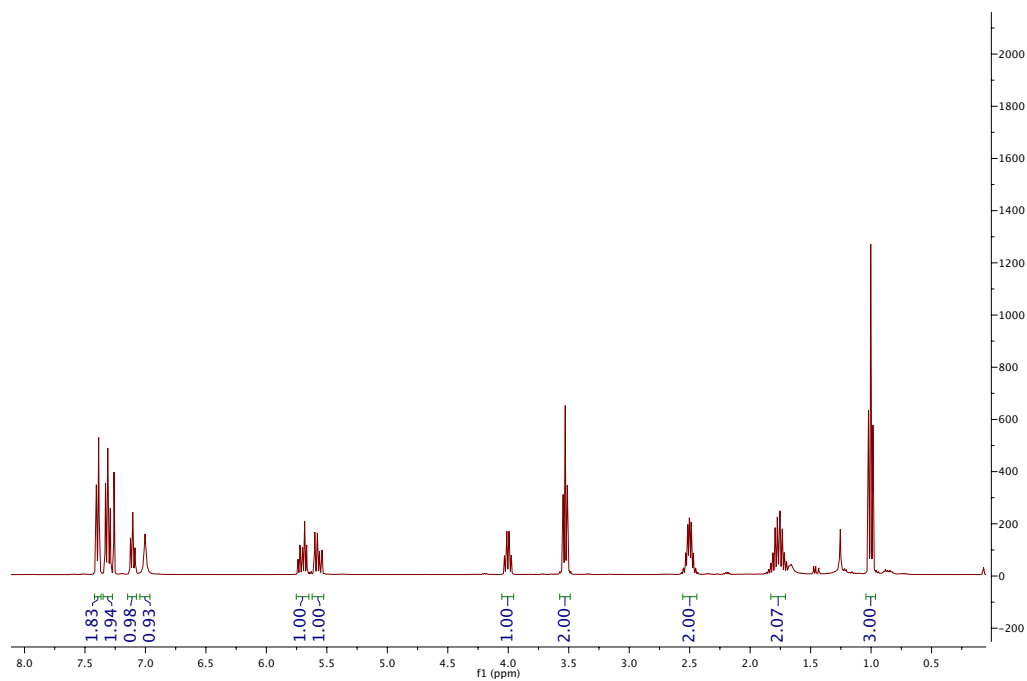
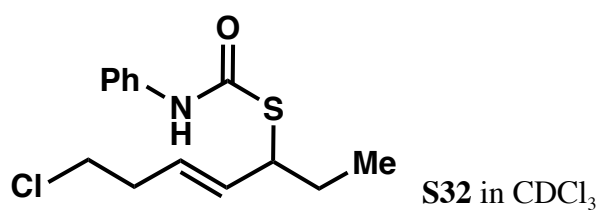
+

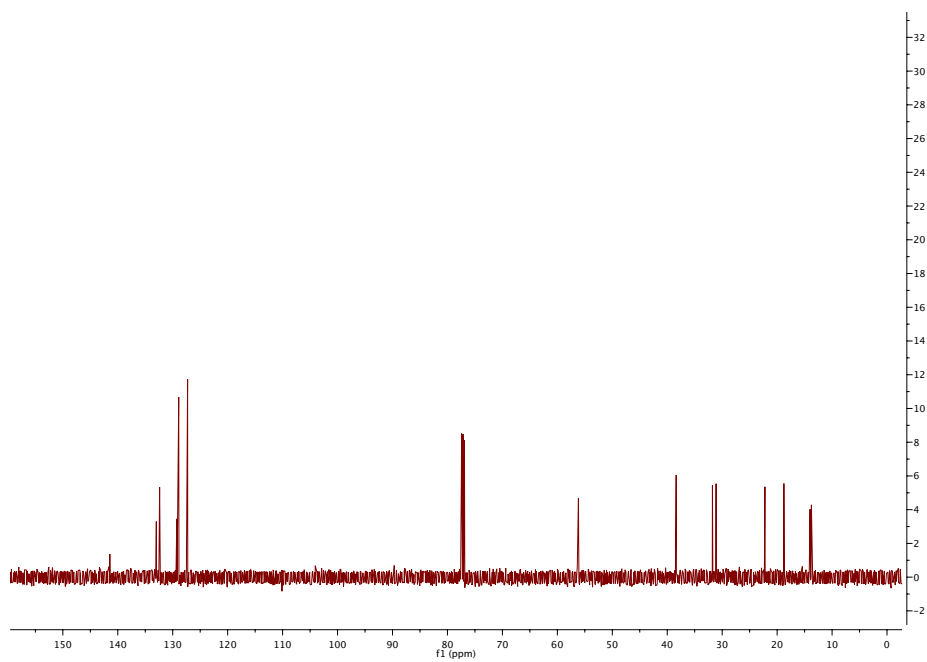
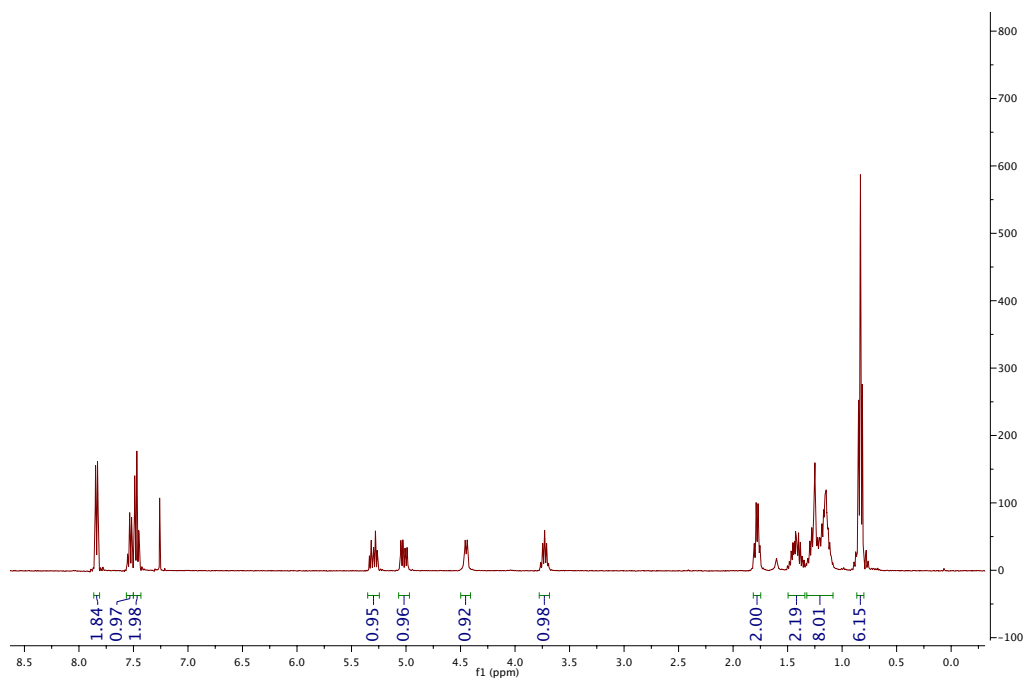
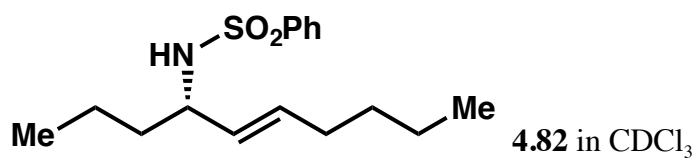


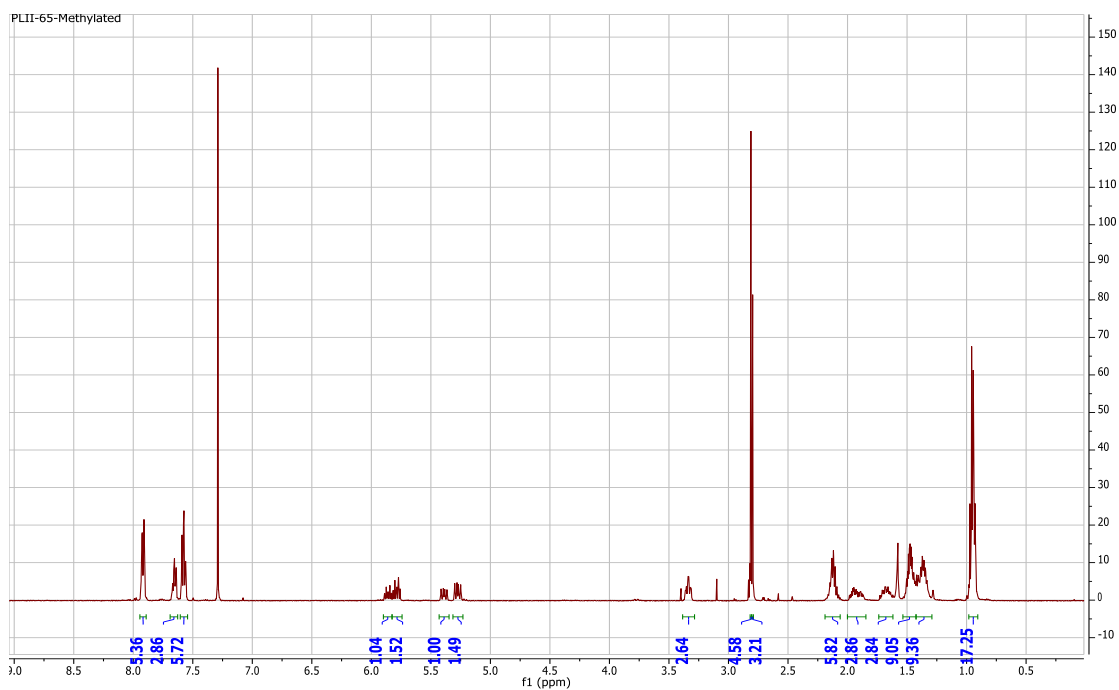
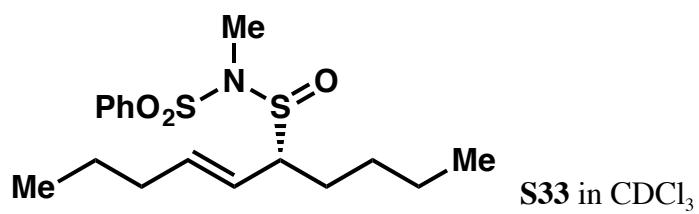
(Minor)

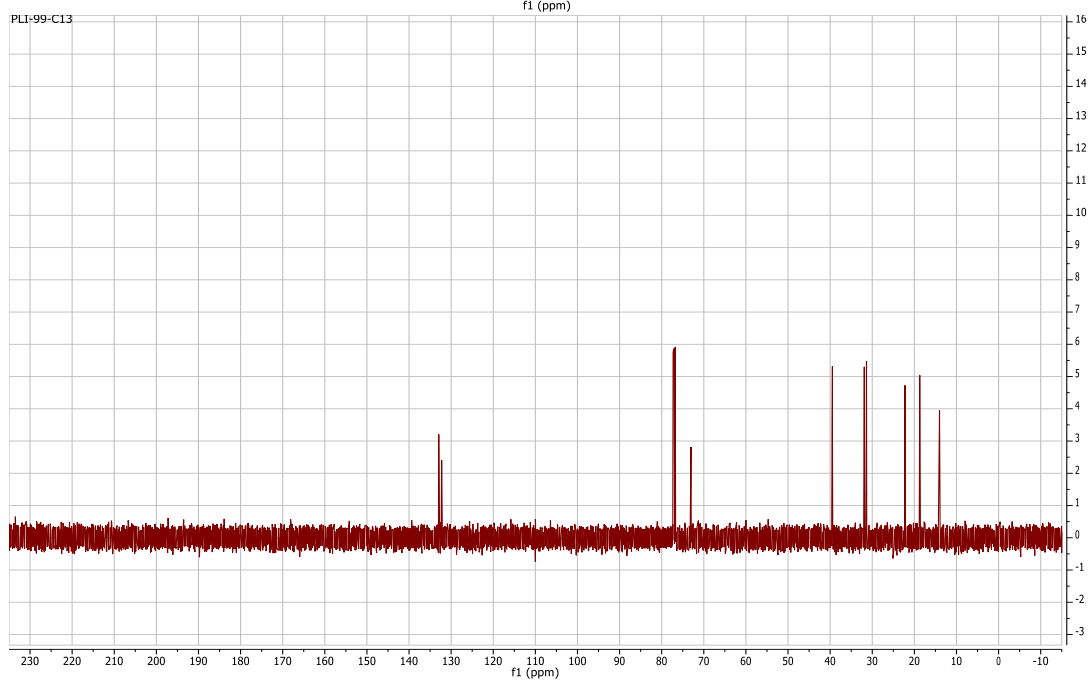
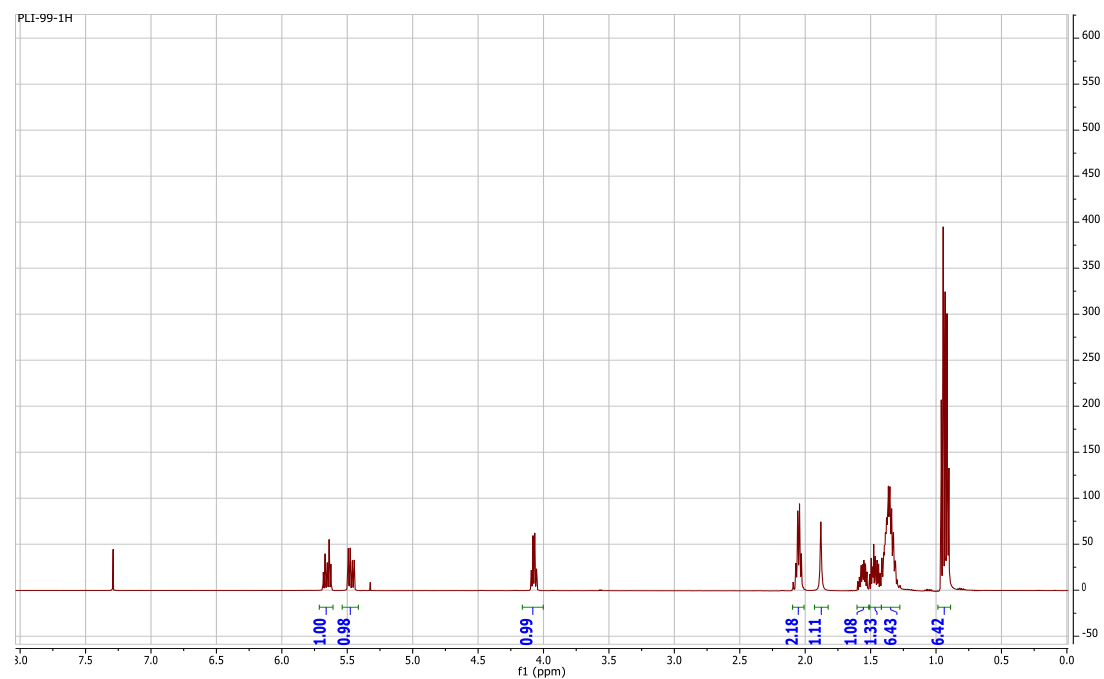
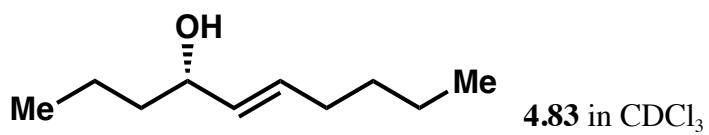
4.80 in CDCl₃

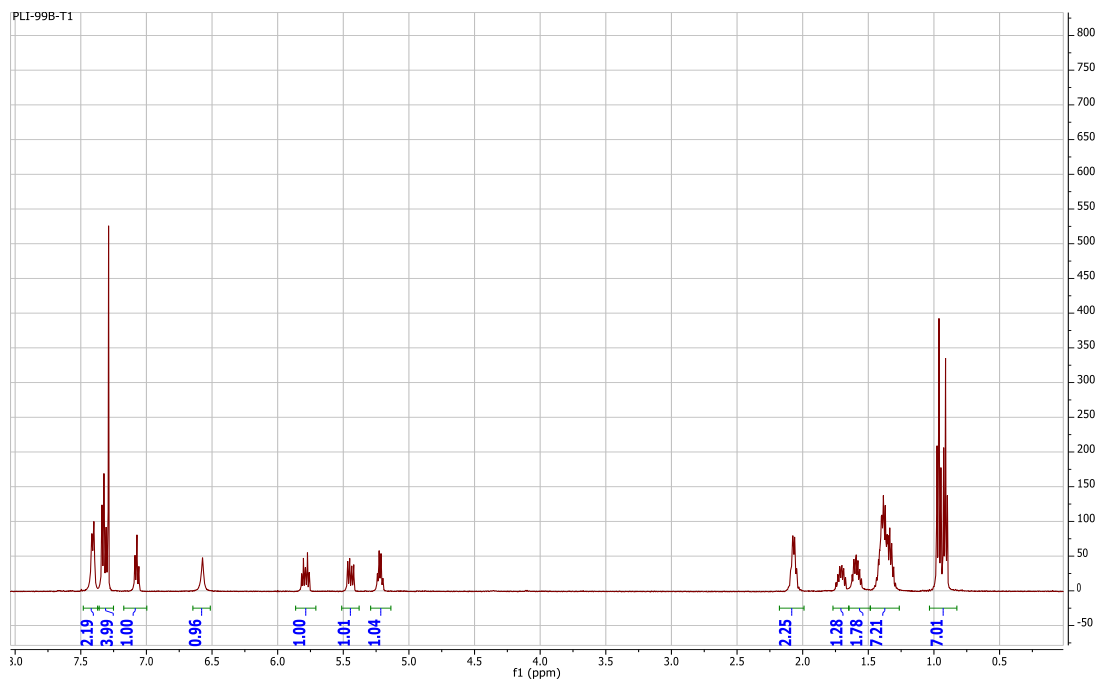
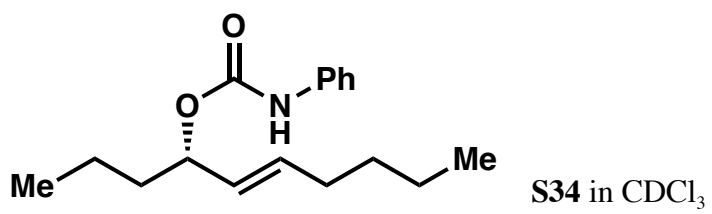


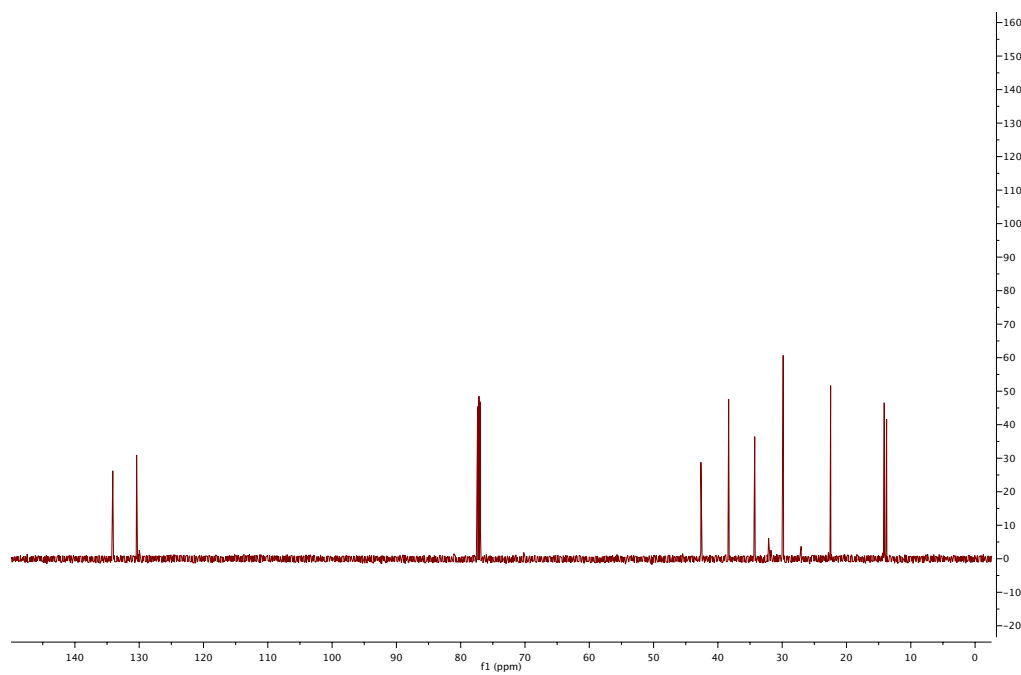
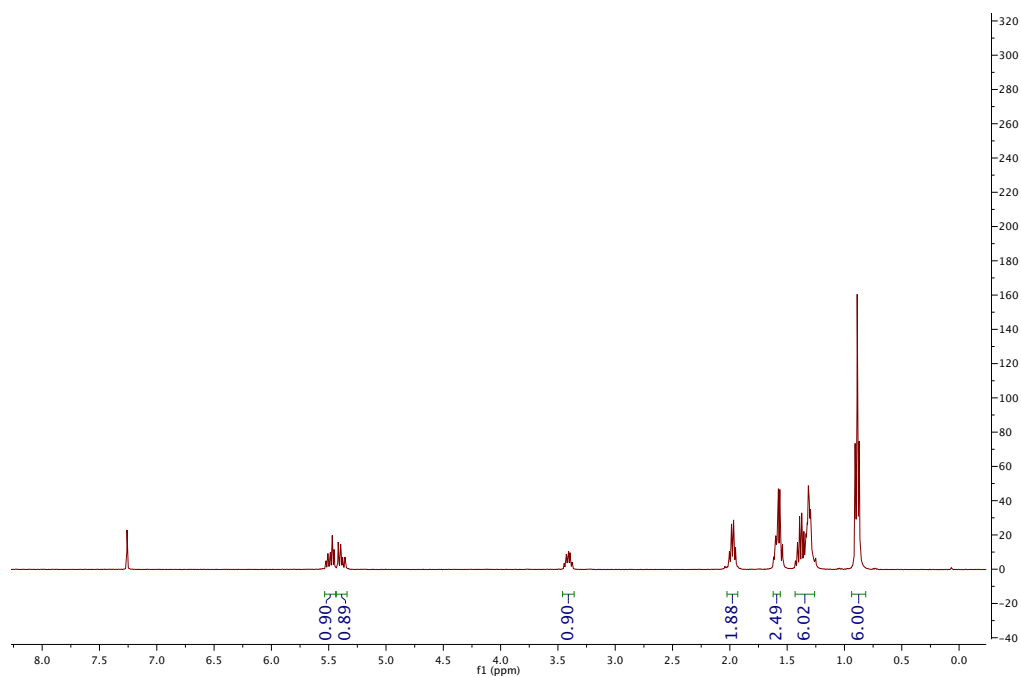
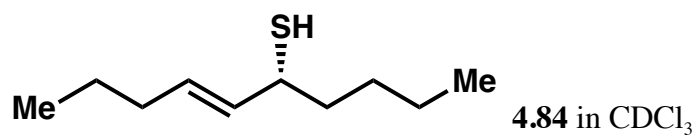


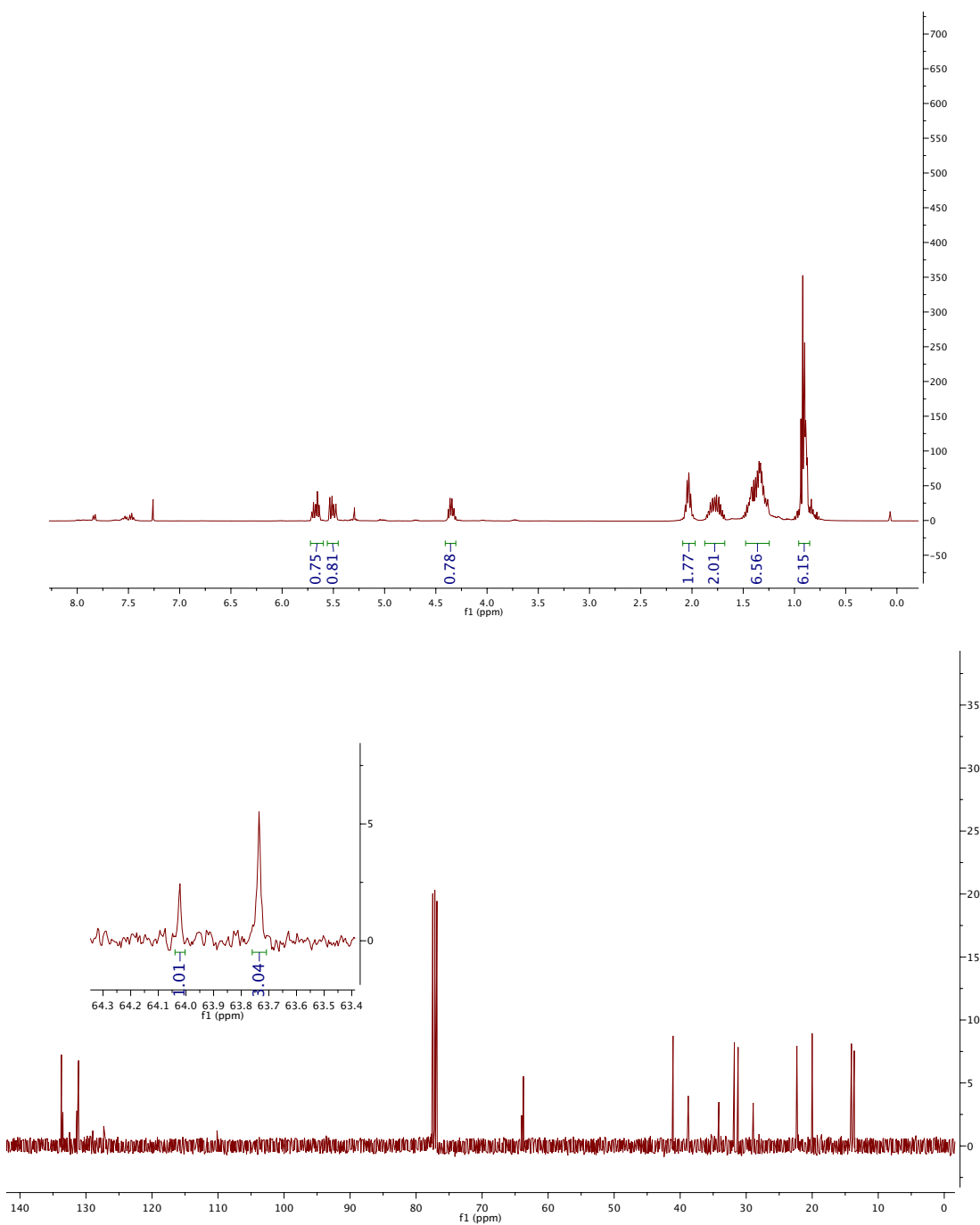
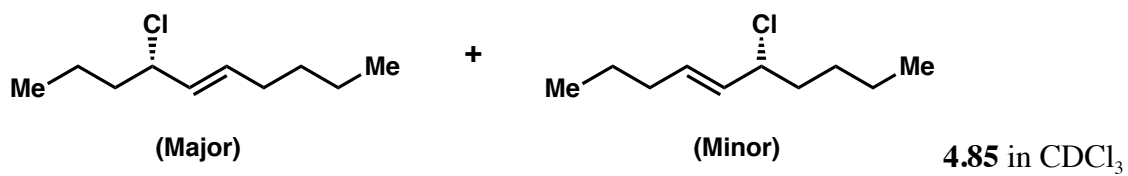


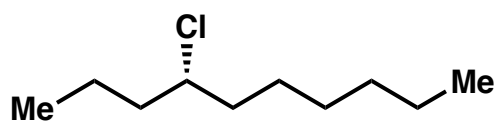




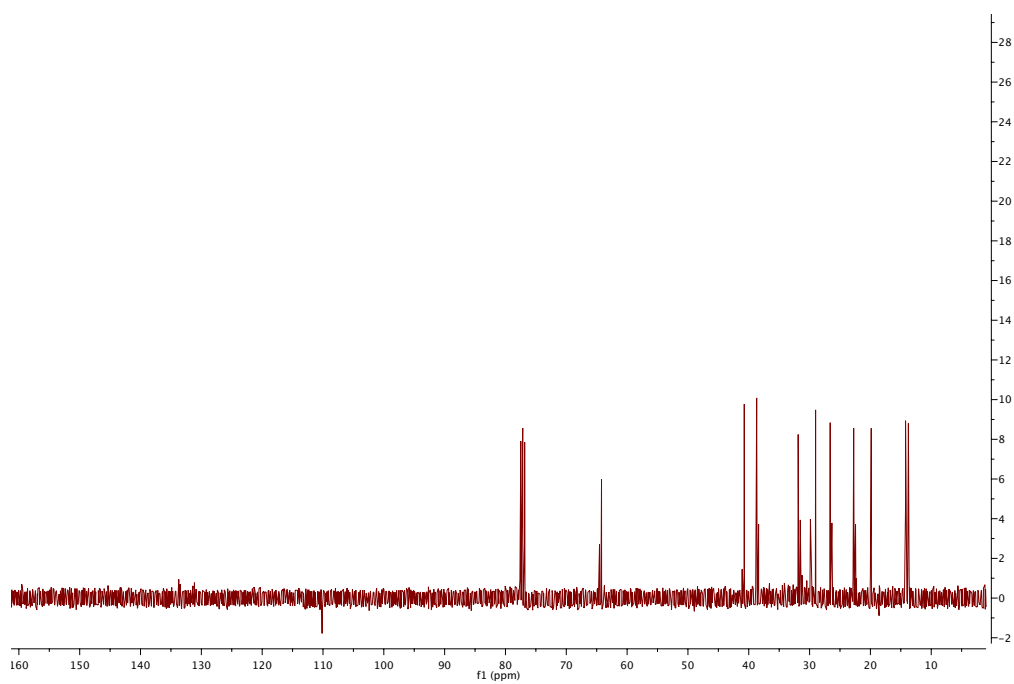
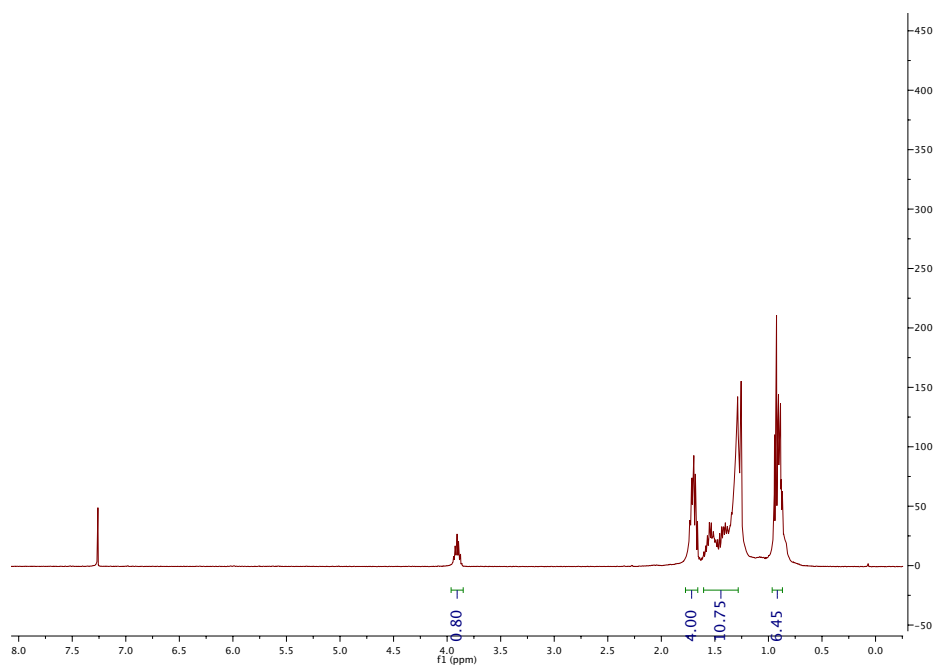


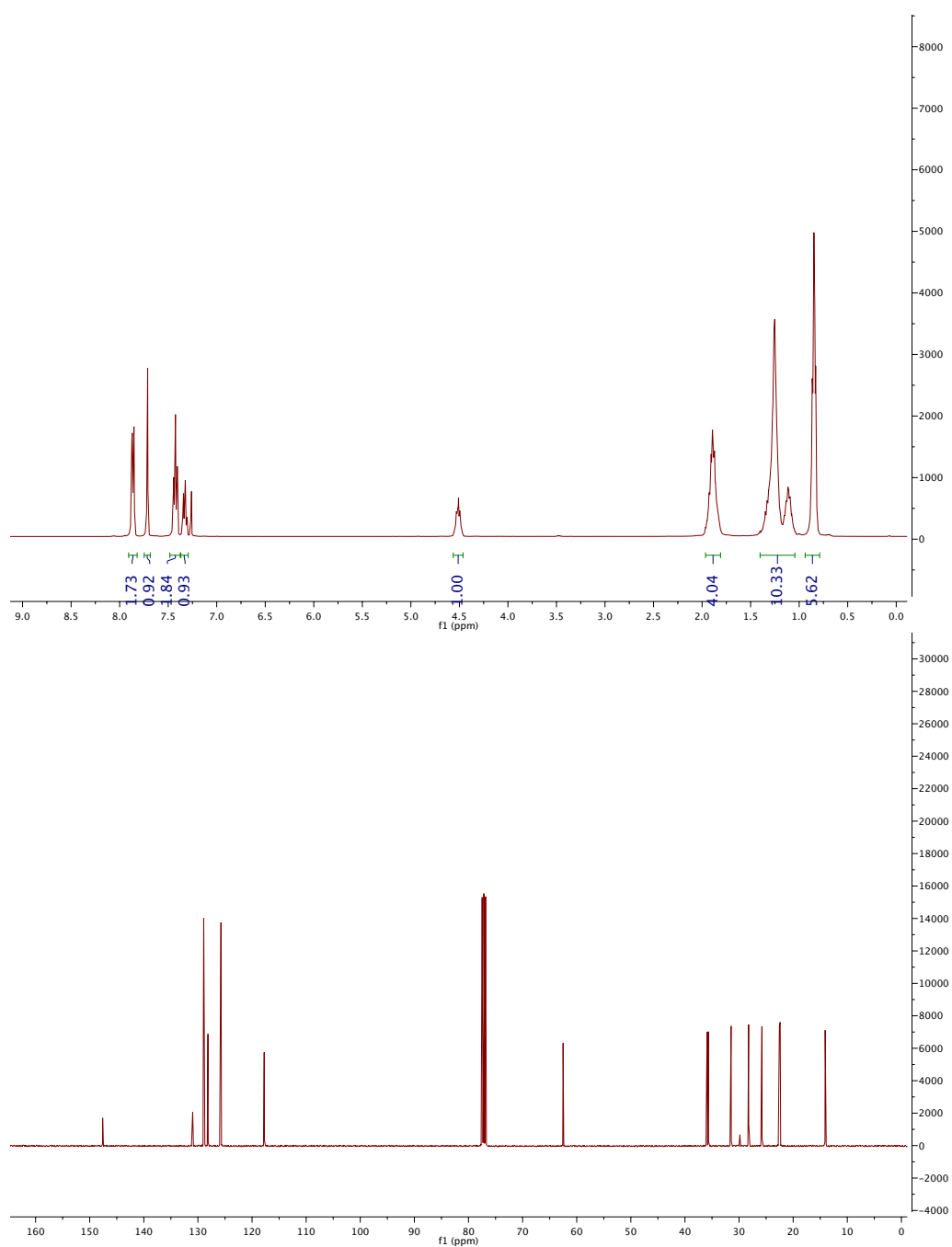
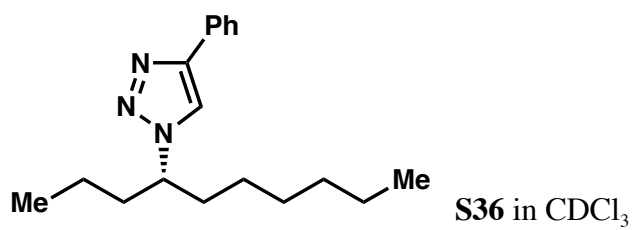


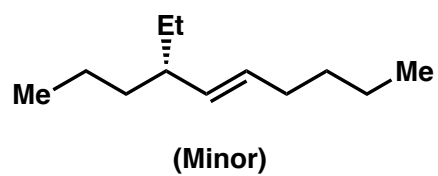
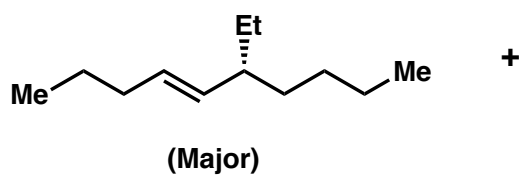




S35 in CDCl₃

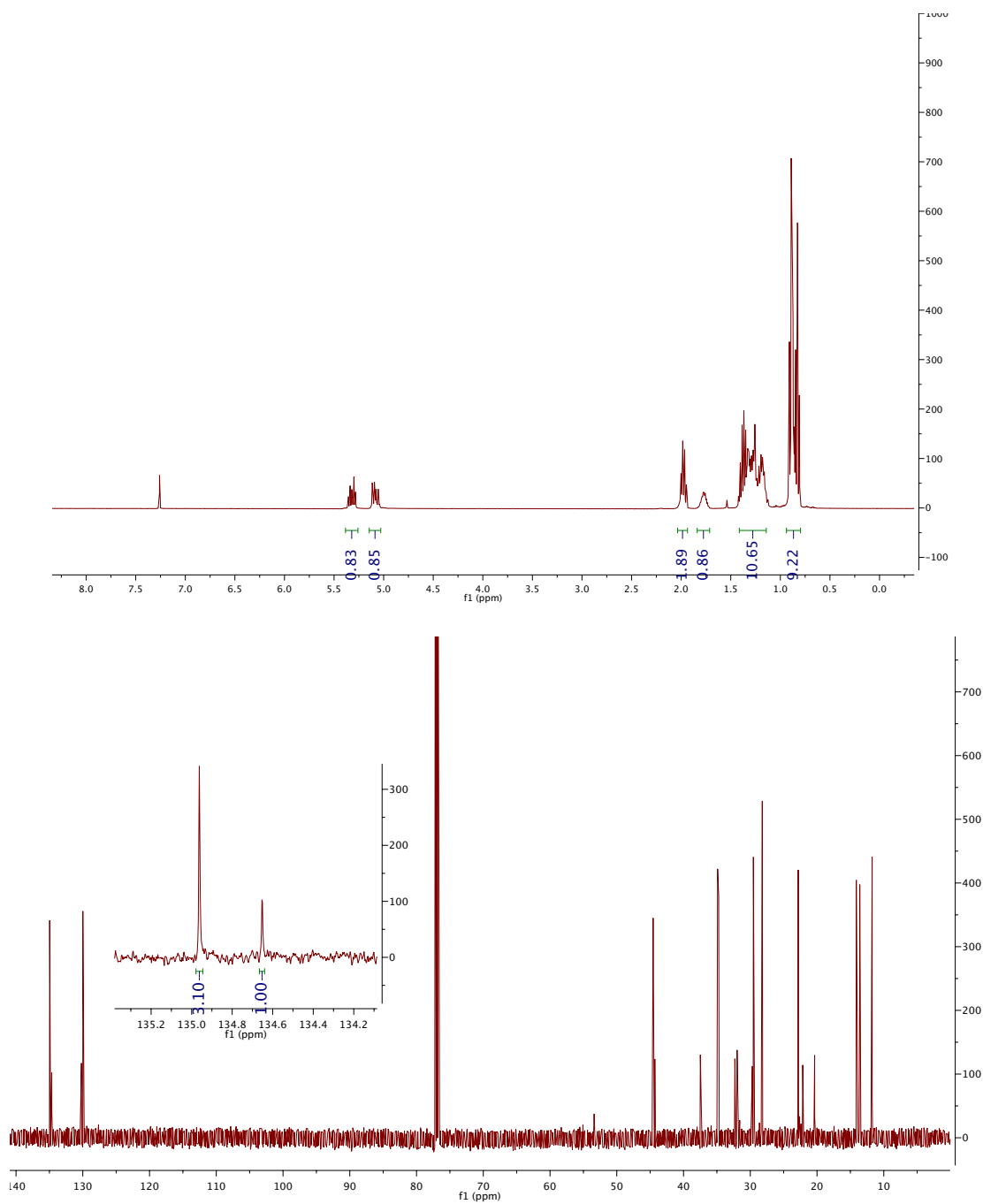


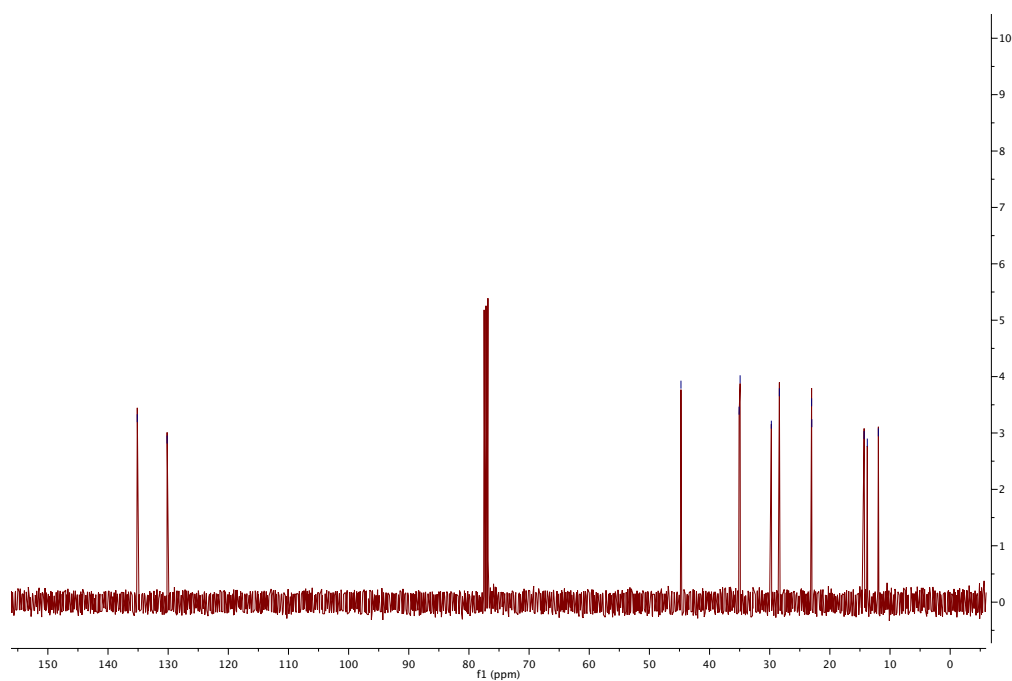
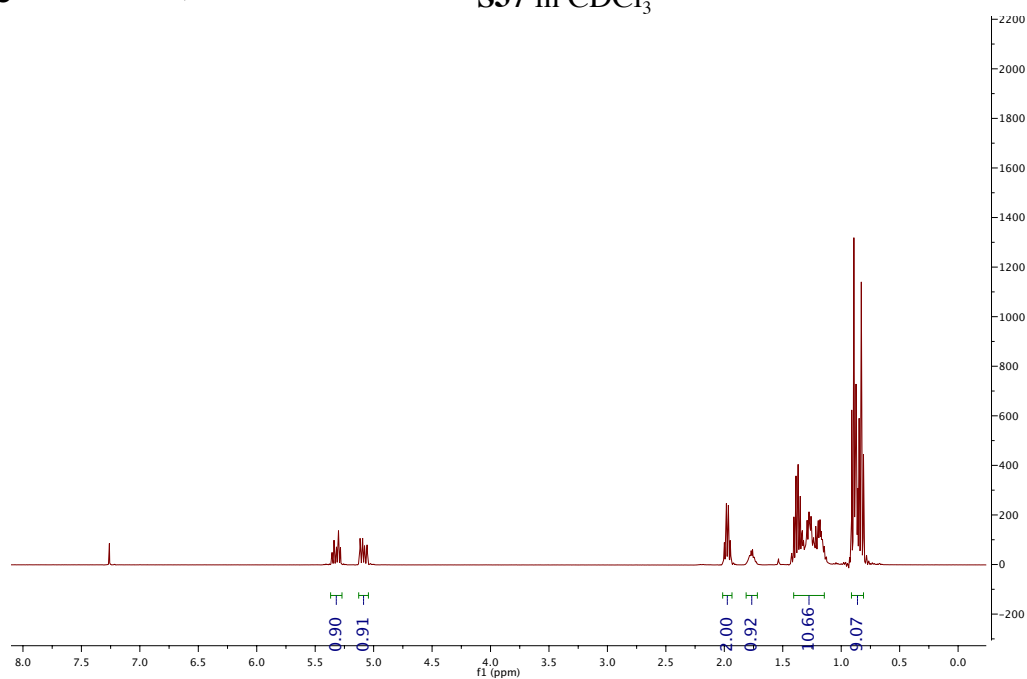
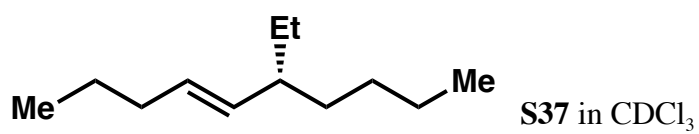




4.86 in

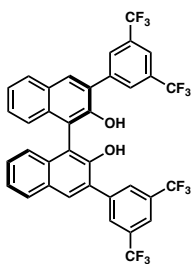
CDCl₃





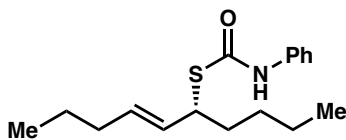
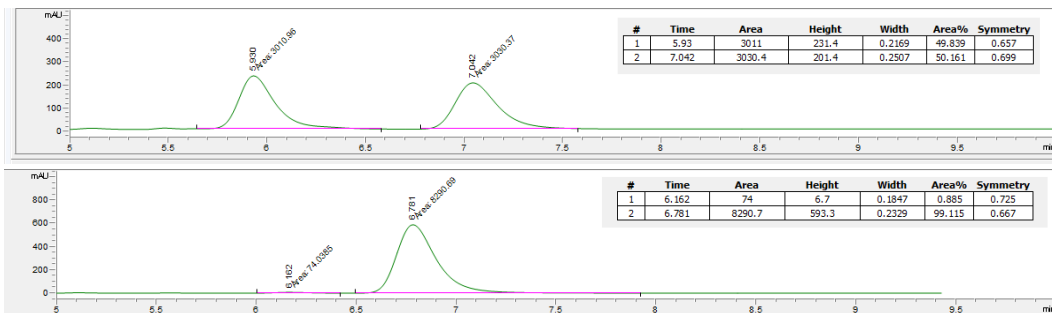
APPENDIX SEVEN

HPLC Traces Relevant to Chapter Four: The Development of a General, Highly Selective Method for the Allylic Functionalization of Unactivated Internal Olefins



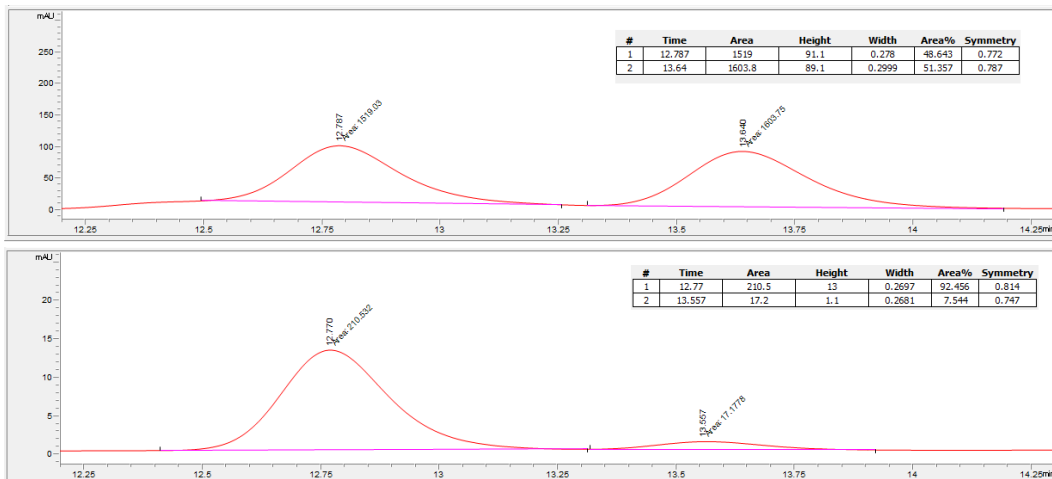
4.60

CHIRALCEL OD-H 97:03 IPA:Hexane 0.6 ml/min

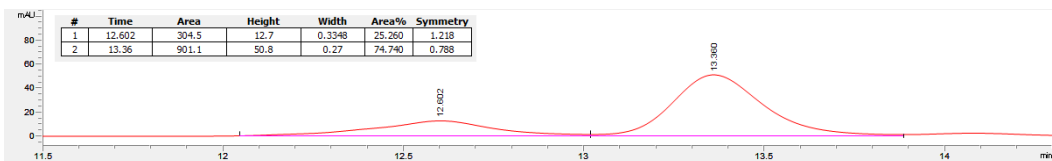


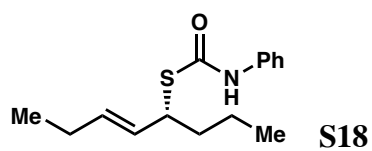
S17

CHIRALCEL OJ-H 95:05 Hex/IPA, 0.5 mL/min, 220 nm

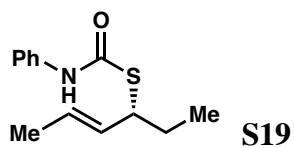
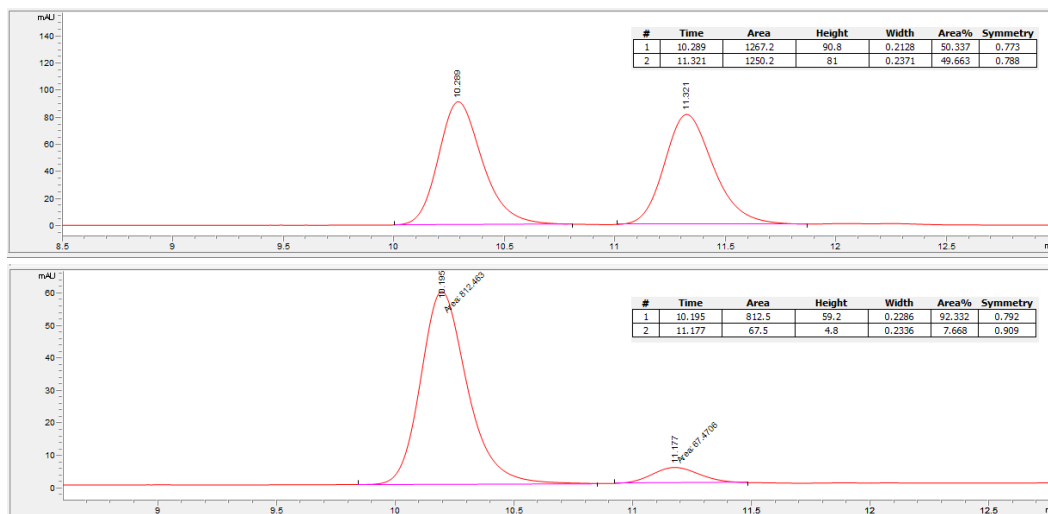


From *trans*-5-decene:

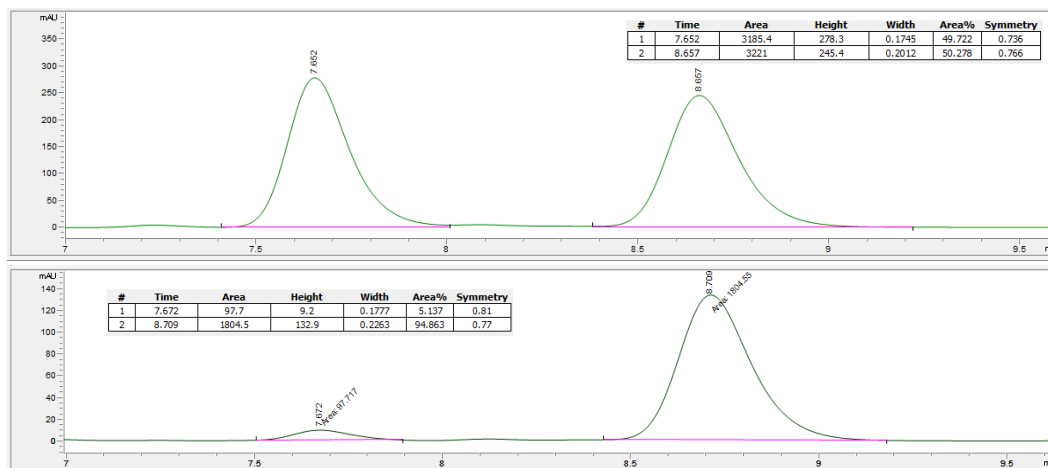


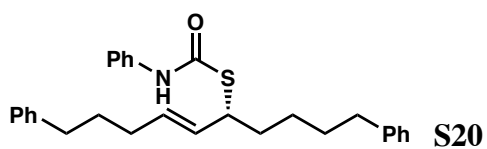


CHIRALCEL OJ-H 95:5 Hex/IPA, 0.5 mL/min, 220 nm

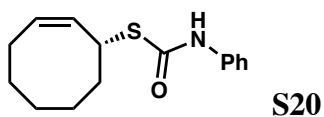
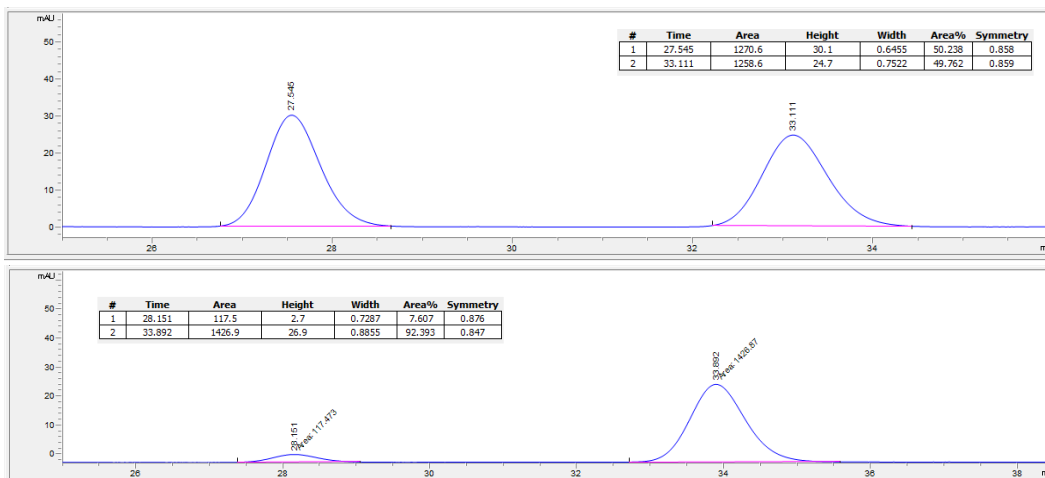


CHIRALCEL OD-H 90:10 Hex/IPA, 0.8 mL/min, 210 nm

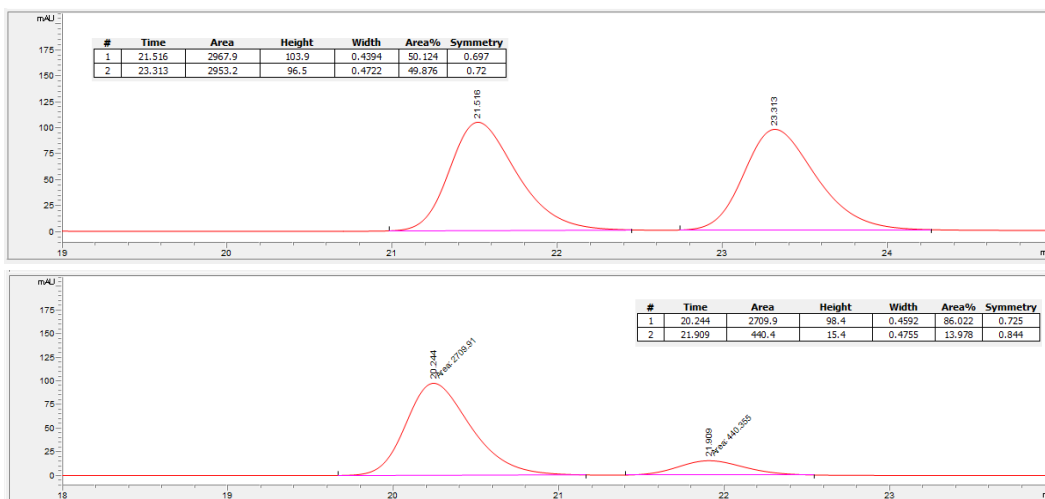


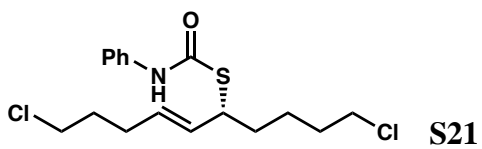


CHIRALPAK AD-H 90:10 Hex/IPA, 0.8 mL/min, 254 nm

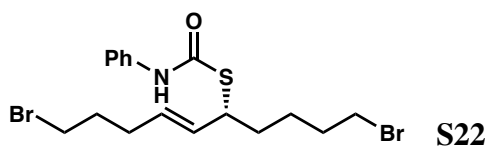
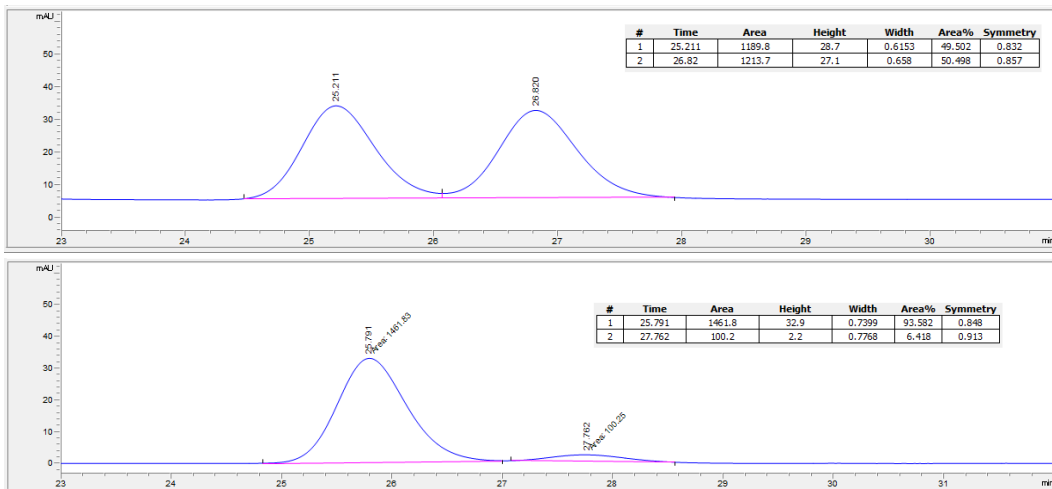


CHIRALCEL OJ-H 95:5 Hex/IPA, 0.8 mL/min, 220 nm

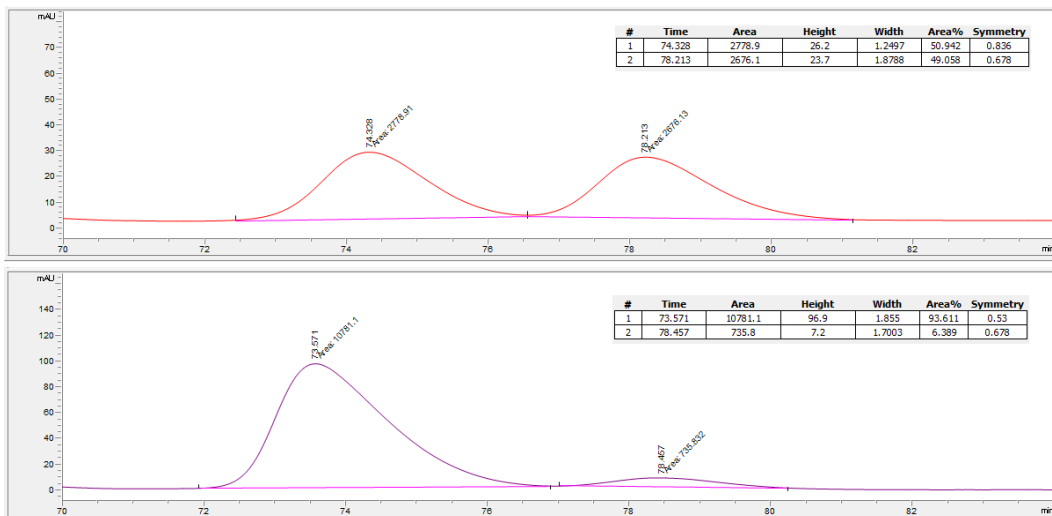


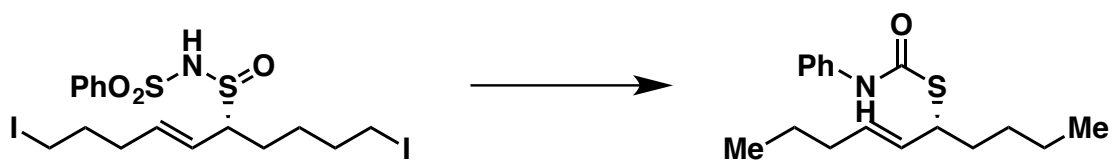


CHIRALCEL OJ-H 90:10 Hex/IPA, 0.8 mL/min, 254 nm



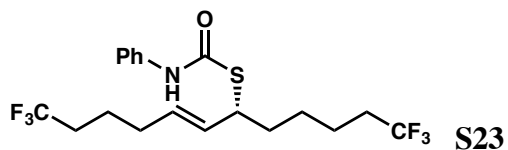
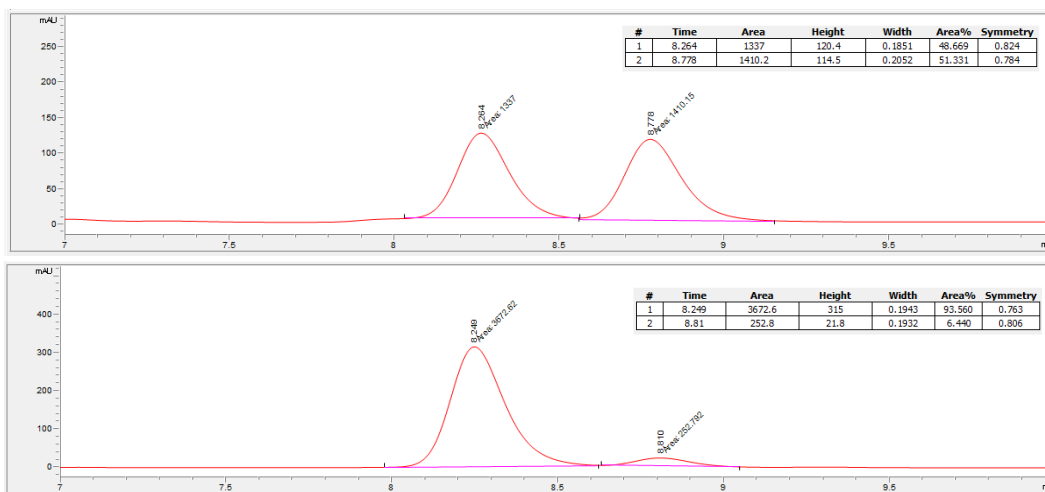
CHIRALPAK AD-H 90:10 Hex/IPA, 0.8 mL/min, 254 nm





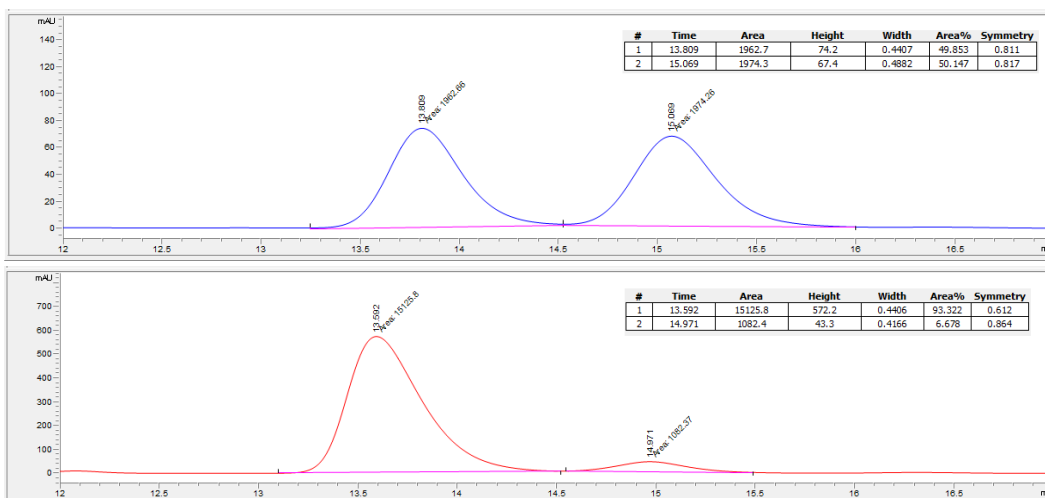
S17

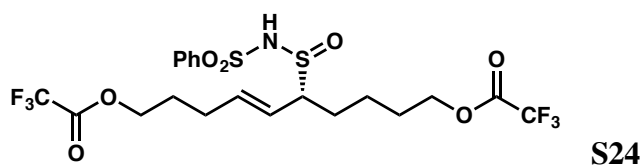
CHIRALCEL OJ-H 95:5 Hex/IPA, 0.8 mL/min, 254 nm



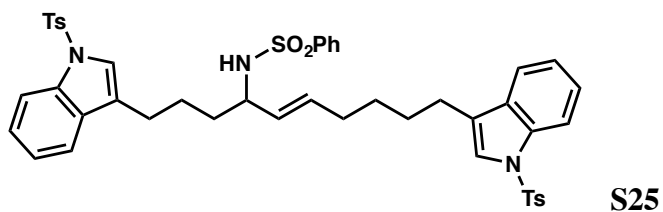
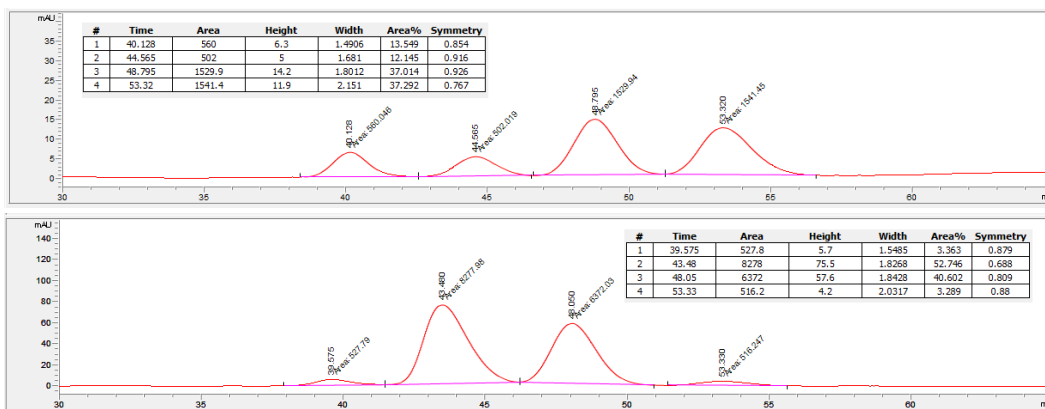
S23

CHIRALCEL OJ-H 90:10 Hex/IPA, 0.6 mL/min, 220 nm

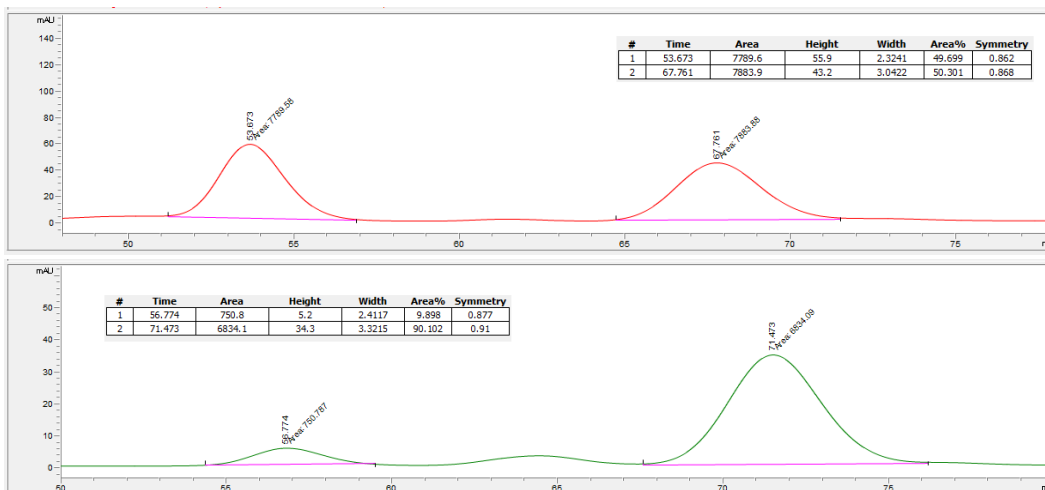


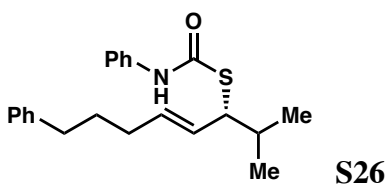


CHIRALPAK AS-H 94:06 Hex/IPA, 0.8 mL/min, 220 nm

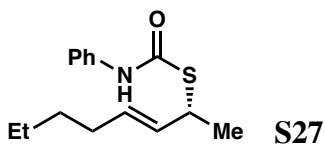
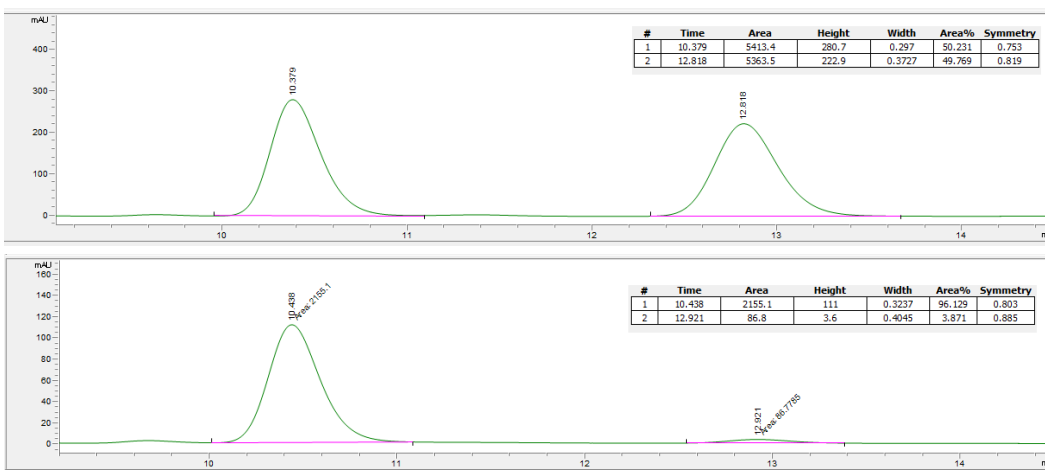


CHIRALPAK AD-H 70:30 Hex/IPA, 0.7 mL/min, 230 nm

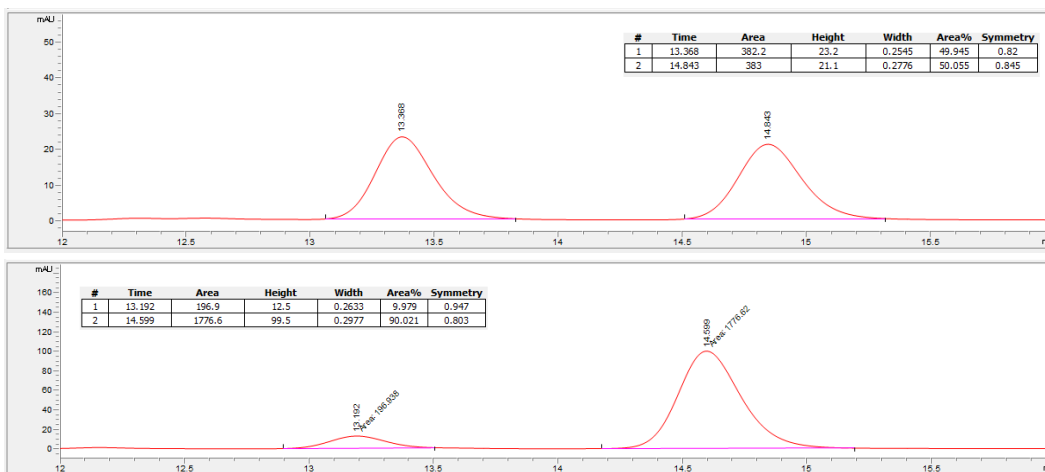


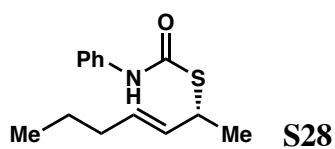


CHIRALCEL OD-H 90:10 Hex/IPA, 0.8 mL/min, 210 nm

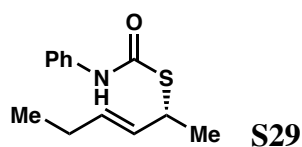
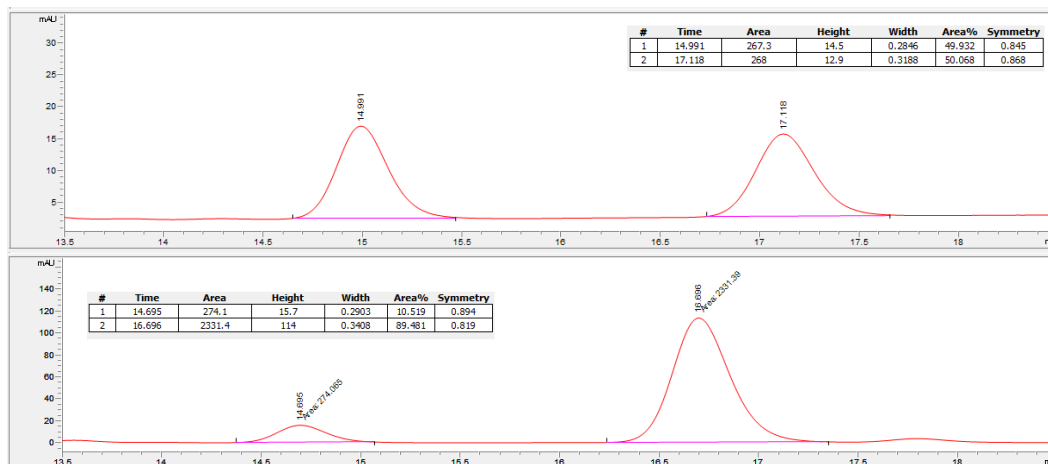


CHIRALCEL OJ-H 95:05 Hex/IPA, 0.8 mL/min, 220 nm

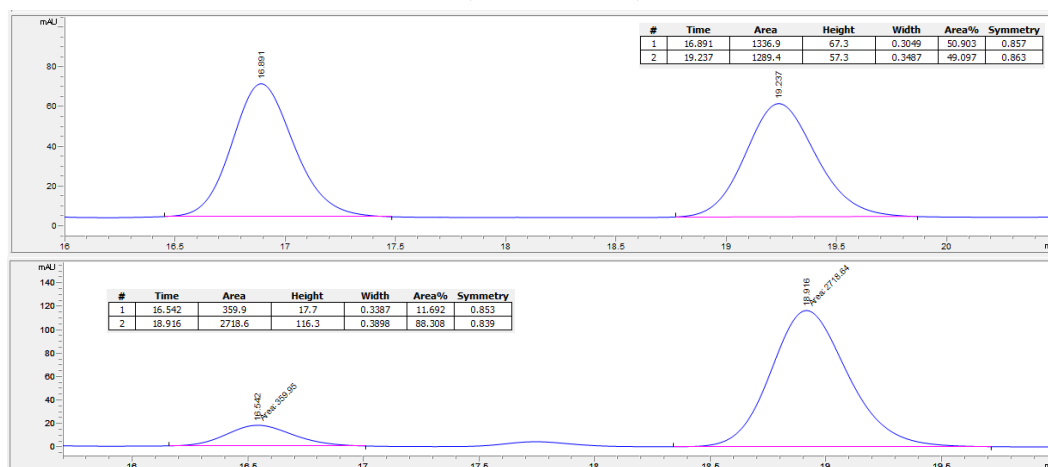


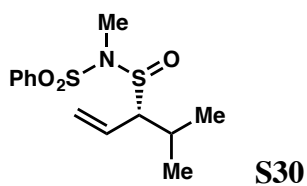


CHIRALCEL OJ-H 95:05 Hex/IPA, 0.8 mL/min, 220 nm

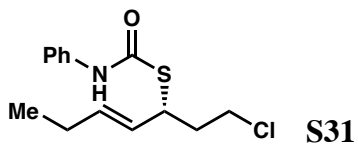
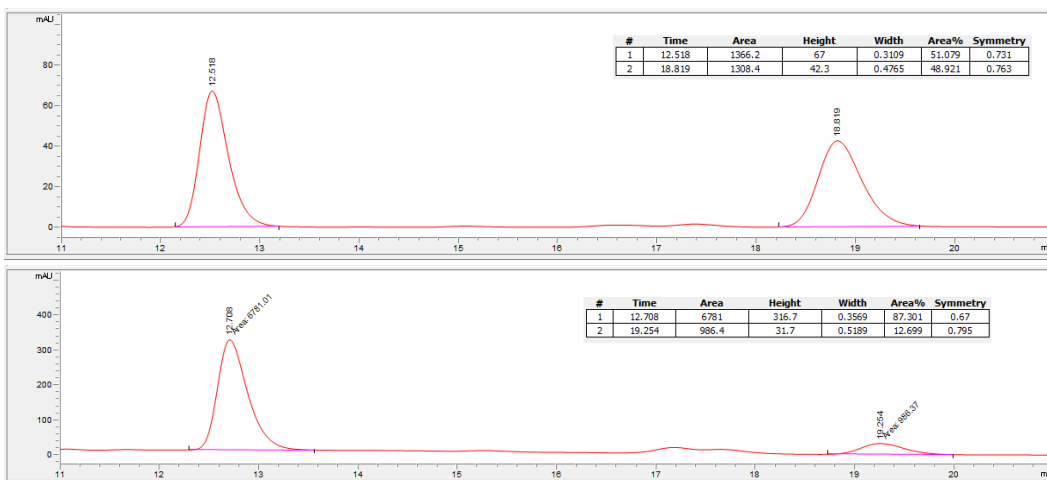


CHIRALCEL OJ-H 95:05 Hex/IPA, 0.8 mL/min, 254 nm

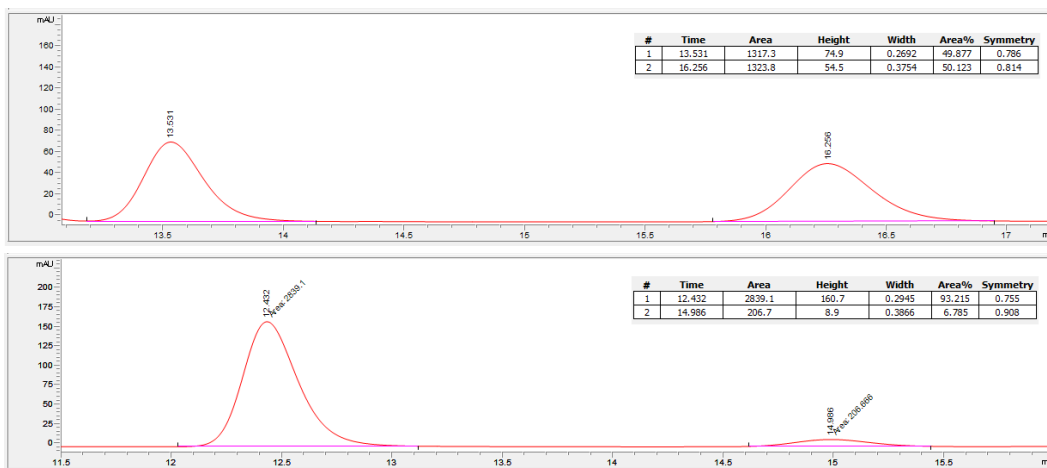


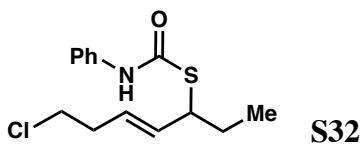


CHIRALCEL OD-H 90:10 Hex/IPA, 0.8 mL/min, 220 nm

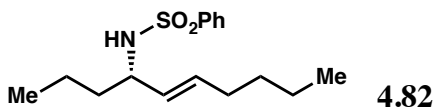
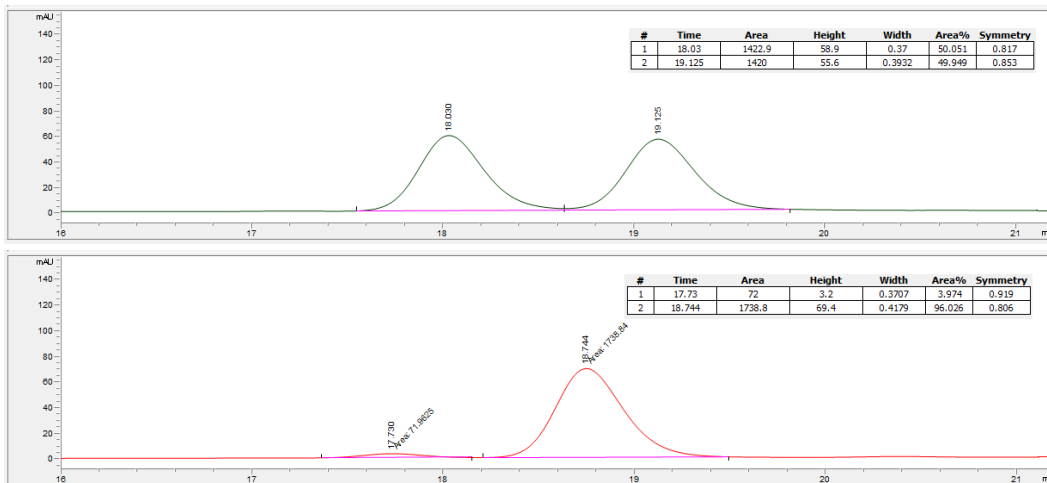


CHIRALCEL OD-H 90:10 Hex/IPA, 0.8 mL/min, 210 nm

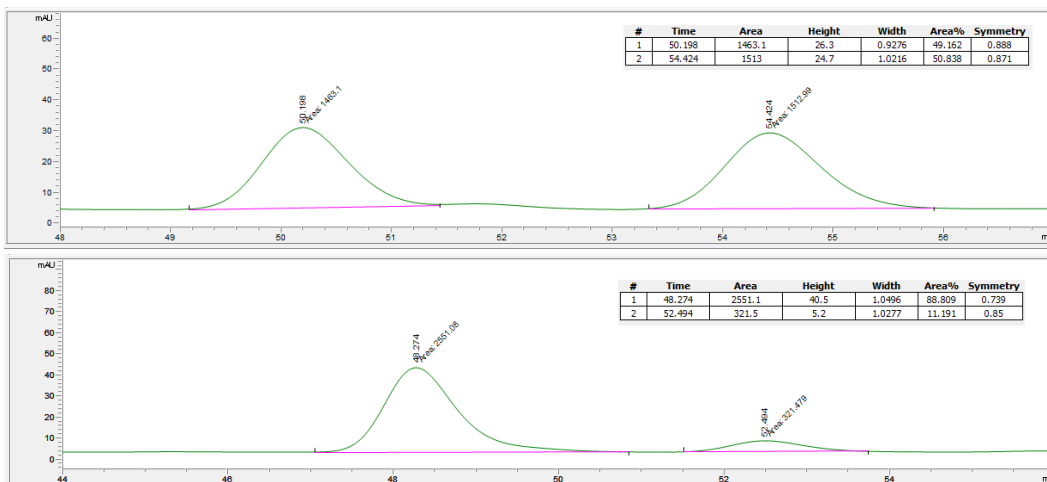


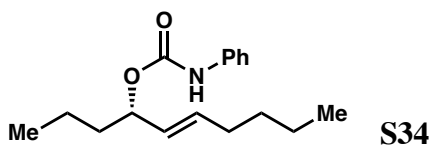


CHIRALCEL OJ-H 90:10 Hex/IPA, 0.8 mL/min, 220 nm

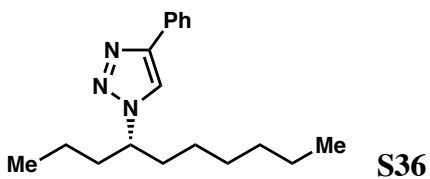
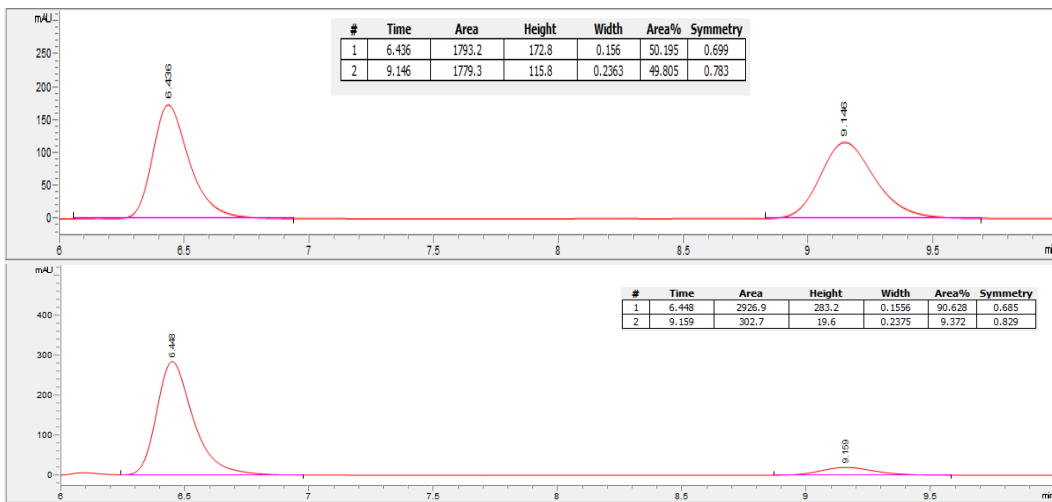


CHIRALPAK AD-H 97:03 Hexanes/IPA, 0.25 mL/min, 230 nm

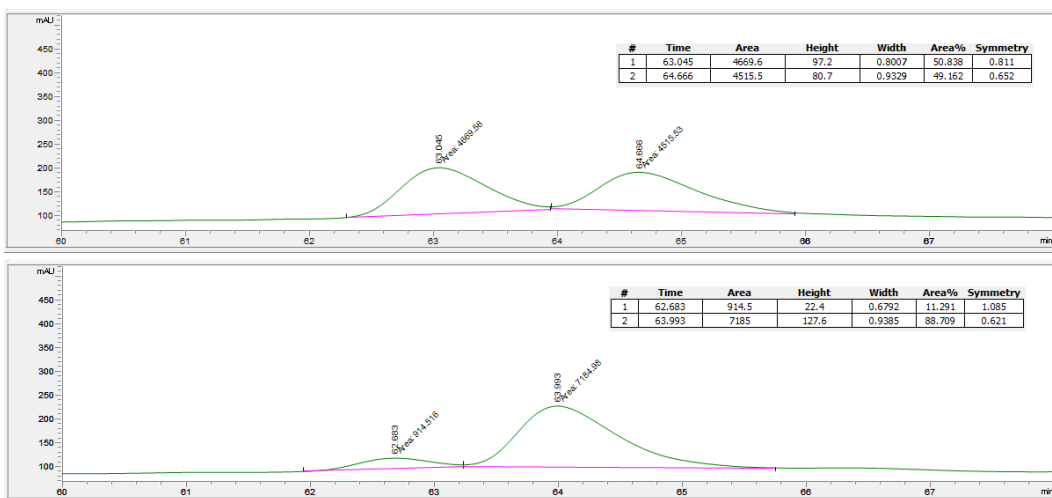


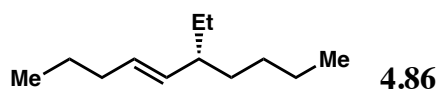


CHIRALCEL OD-H 90:10 IPA/Hexane 0.8 ml/min

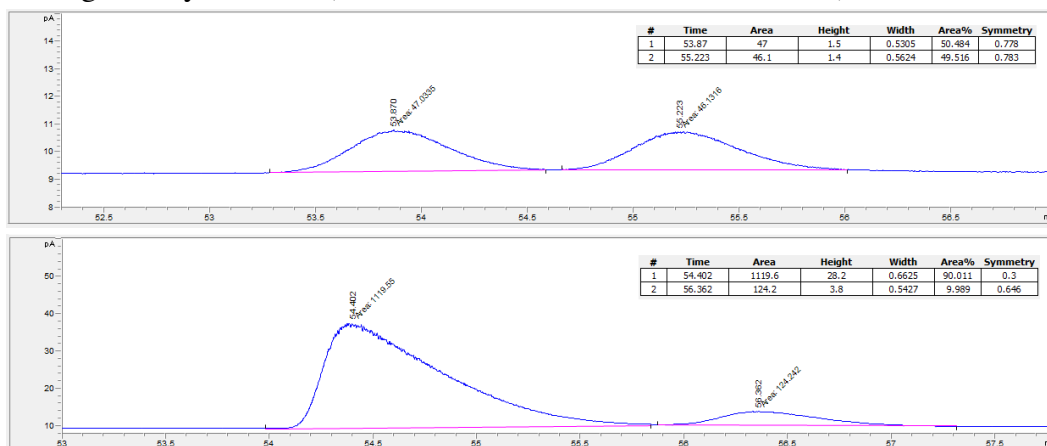


CHIRALCEL OJ-H 100% Hexanes 30 min, gradient to 2% IPA over 20 min, 0.8 mL/min, 210 nm

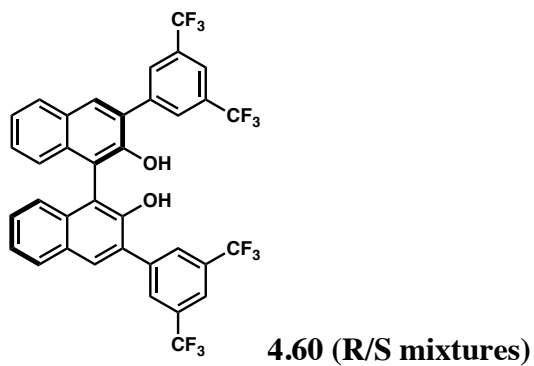




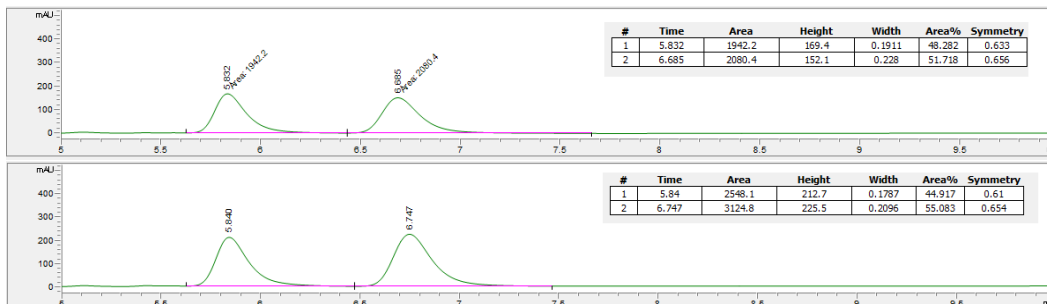
GC Agilent Cyclodex-B (Isothermal, 50 °C; flow rate: 1 mL/min)

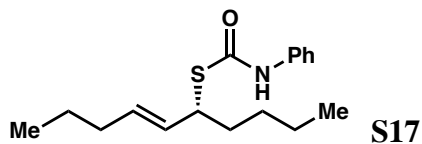
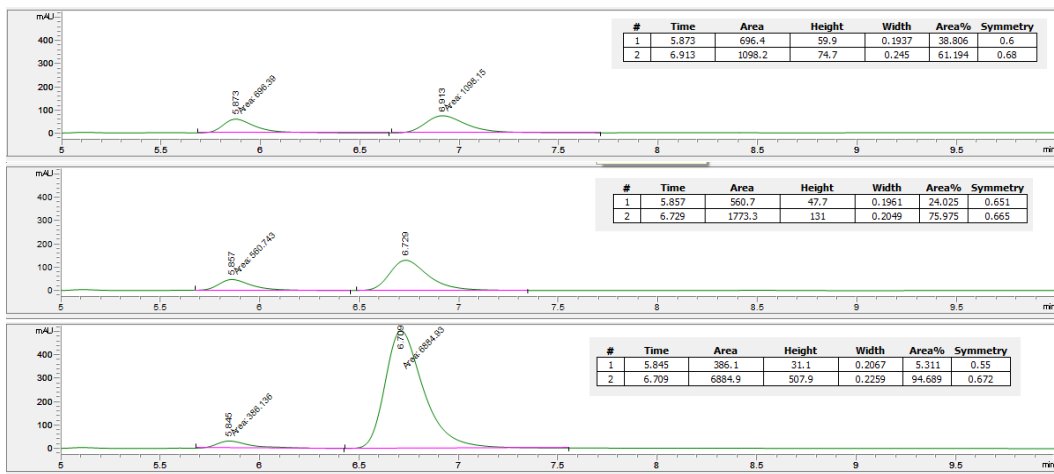


HPLC Traces for Non-Linear Effect Study



CHIRALCEL OD-H 97:03 IPA:Hexane 0.6 ml/min





CHIRALCEL OJ-H 95:05 IPA:Hexane 0.5 ml/min



APPENDIX EIGHT

Crystallography Data: For Chapters One Through Four

A8.1 X-ray Crystallography Reports Relevant to Chapter One:

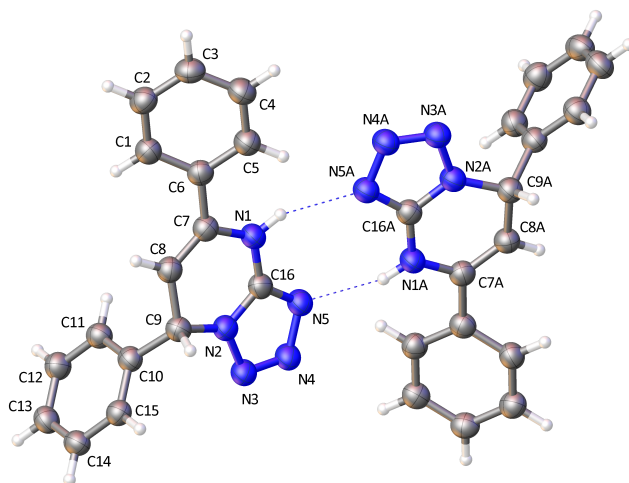


Figure A8.1 Ortep diagram of **1.39** showing ellipsoids at 50% probability and atom labeling scheme.

Experimental Summary

The single crystal X-ray diffraction studies were carried out on a Bruker APEX CCD diffractometer equipped with Cu K α radiation ($\lambda = 1.54178$). A 0.351 x 0.202 x 0.140 mm clear colorless block was mounted on a Cryoloop with Paratone oil. Data were collected in a nitrogen gas stream at 100(2) K using ϕ and ω scans. Crystal-to-detector distance was 40 mm using 1-3 s exposure times with a scan width of 1.0°. Data collection was 100.0% complete to 68.000° in θ . A total of 21873 reflections were collected covering the indices, $-10 \leq h \leq 10$, $-10 \leq k \leq 10$, $-21 \leq l \leq 21$. 4926 reflections were found to be symmetry independent, with a R_{int} of 0.0345. Indexing and unit cell refinement indicated a primitive, monoclinic lattice. The space group was found to be $P2_1$. The data were integrated using the Bruker SAINT software program and scaled

using the SADABS software program. Solution by direct methods (SHELXT) produced a complete phasing model consistent with the proposed structure.

All nonhydrogen atoms were refined anisotropically by full-matrix least-squares (SHELXL). The amine hydrogen atom was found via the difference map and the bond distance was restrained relative to the parent oxygen atom using the appropriate DFIX command in SHELXL. All remaining hydrogen atoms were placed using a riding model. Their positions were constrained relative to their parent atom using the appropriate HFIX command in SHELXL. Crystallographic data are summarized in Table A8.1.1.

Table A8.1.1 Crystal data and structure refinement for 1.39.

Identification code	JEH-1-174-freebase	
Empirical formula	C ₁₆ H ₁₃ N ₅	
Molecular formula	C ₁₆ H ₁₃ N ₅	
Formula weight	275.31	
Temperature	100.0 K	
Wavelength	1.54178 Å	
Crystal system	Monoclinic	
Space group	P 1 21 1	
Unit cell dimensions	a = 8.7736(2) Å	α = 90°.
	b = 8.8396(2) Å	β = 98.8220(9)°.
	c = 17.6810(4) Å	γ = 90°.
Volume	1355.03(5) Å ³	
Z	4	
Density (calculated)	1.350 Mg/m ³	
Absorption coefficient	0.682 mm ⁻¹	
F(000)	576	
Crystal size	0.351 x 0.202 x 0.14 mm ³	

Crystal color, habit	Clear colorless Block
Theta range for data collection	2.529 to 68.238°.
Index ranges	-10<= <i>h</i> <=10, -10<= <i>k</i> <=10, -21<= <i>l</i> <=21
Reflections collected	21873
Independent reflections	4926 [R(int) = 0.0345]
Completeness to theta = 68.000°	100.0 %
Absorption correction	Semi-empirical from equivalents
Max. and min. transmission	0.0818 and 0.0108
Refinement method	Full-matrix least-squares on F ²
Data / restraints / parameters	4926 / 1 / 387
Goodness-of-fit on F ²	1.077
Final R indices [I>2sigma(I)]	R1 = 0.0542, wR2 = 0.1194
R indices (all data)	R1 = 0.0548, wR2 = 0.1206
Absolute structure parameter	0.04(13)
Extinction coefficient	n/a
Largest diff. peak and hole	0.369 and -0.162 e.Å ⁻³

Table A8.1.2 Atomic coordinates ($\times 10^4$) and equivalent isotropic displacement parameters (Å² $\times 10^3$) for 1.39. U(eq) is defined as one third of the trace of the orthogonalized U^{ij} tensor.

	x	y	z	U(eq)
N(1)	1241(2)	7357(3)	2082(1)	44(1)
N(2)	1544(2)	7090(2)	794(1)	43(1)
N(3)	2314(2)	6164(3)	370(1)	47(1)
N(4)	3068(3)	5225(3)	842(1)	48(1)
N(5)	2824(2)	5492(3)	1578(1)	46(1)
C(1)	-730(3)	10885(3)	2498(2)	47(1)
C(2)	-1410(3)	11537(3)	3074(2)	50(1)

C(3)	-1741(3)	10677(4)	3681(2)	51(1)
C(4)	-1382(3)	9151(4)	3714(2)	53(1)
C(5)	-705(3)	8486(3)	3134(2)	49(1)
C(6)	-369(3)	9346(3)	2518(1)	43(1)
C(7)	289(3)	8631(3)	1880(1)	42(1)
C(8)	-12(3)	9102(3)	1151(1)	43(1)
C(9)	427(3)	8252(3)	472(1)	42(1)
C(10)	1090(3)	9162(3)	-127(1)	42(1)
C(11)	2279(3)	10198(3)	67(1)	44(1)
C(12)	2929(3)	10926(3)	-501(2)	47(1)
C(13)	2374(3)	10641(3)	-1267(2)	48(1)
C(14)	1189(3)	9613(3)	-1464(1)	46(1)
C(15)	552(3)	8874(3)	-896(1)	44(1)
C(16)	1852(3)	6651(3)	1524(1)	42(1)
N(1A)	2796(3)	3097(3)	2706(1)	46(1)
N(2A)	1962(2)	2931(3)	3903(1)	44(1)
N(3A)	1134(3)	3784(3)	4332(1)	48(1)
N(4A)	776(3)	5003(3)	3950(1)	48(1)
N(5A)	1334(2)	4997(3)	3269(1)	45(1)
C(1A)	4542(3)	-403(3)	2123(2)	45(1)
C(2A)	5287(3)	-939(3)	1546(2)	48(1)
C(3A)	5921(3)	54(3)	1067(1)	46(1)
C(4A)	5795(3)	1605(3)	1179(1)	46(1)
C(5A)	5040(3)	2156(3)	1756(1)	44(1)
C(6A)	4401(3)	1156(3)	2237(1)	44(1)
C(7A)	3557(3)	1710(3)	2846(1)	43(1)
C(8A)	3471(3)	932(3)	3492(1)	45(1)
C(9A)	2507(3)	1381(3)	4093(1)	44(1)
C(10A)	3383(3)	1305(3)	4906(1)	45(1)
C(11A)	4812(3)	1996(3)	5090(2)	49(1)
C(12A)	5608(3)	1912(3)	5835(2)	54(1)
C(13A)	4957(3)	1140(4)	6393(2)	56(1)
C(14A)	3542(3)	456(4)	6209(2)	56(1)
C(15A)	2745(3)	526(3)	5464(2)	50(1)

C(16A)	2063(3)	3686(3)	3257(1)	42(1)
--------	---------	---------	---------	-------

Table A8.1.3 Bond lengths [Å] and angles [°] for 1.39

N(1)-H(1)	0.84(4)	C(10)-C(15)	1.392(3)
N(1)-C(7)	1.414(3)	C(11)-H(11)	0.9500
N(1)-C(16)	1.346(3)	C(11)-C(12)	1.387(3)
N(2)-N(3)	1.357(3)	C(12)-H(12)	0.9500
N(2)-C(9)	1.473(3)	C(12)-C(13)	1.391(4)
N(2)-C(16)	1.336(3)	C(13)-H(13)	0.9500
N(3)-N(4)	1.287(3)	C(13)-C(14)	1.384(4)
N(4)-N(5)	1.371(3)	C(14)-H(14)	0.9500
N(5)-C(16)	1.326(3)	C(14)-C(15)	1.386(4)
C(1)-H(1A)	0.9500	C(15)-H(15)	0.9500
C(1)-C(2)	1.382(4)	N(1A)-H(1AA)	0.84(4)
C(1)-C(6)	1.396(4)	N(1A)-C(7A)	1.399(4)
C(2)-H(2)	0.9500	N(1A)-C(16A)	1.351(3)
C(2)-C(3)	1.382(4)	N(2A)-N(3A)	1.356(3)
C(3)-H(3)	0.9500	N(2A)-C(9A)	1.473(3)
C(3)-C(4)	1.385(4)	N(2A)-C(16A)	1.338(3)
C(4)-H(4)	0.9500	N(3A)-N(4A)	1.285(3)
C(4)-C(5)	1.392(4)	N(4A)-N(5A)	1.367(3)
C(5)-H(5)	0.9500	N(5A)-C(16A)	1.326(4)
C(5)-C(6)	1.396(4)	C(1A)-H(1AB)	0.9500
C(6)-C(7)	1.485(3)	C(1A)-C(2A)	1.377(4)
C(7)-C(8)	1.341(4)	C(1A)-C(6A)	1.401(4)
C(8)-H(8)	0.9500	C(2A)-H(2A)	0.9500
C(8)-C(9)	1.516(3)	C(2A)-C(3A)	1.394(4)
C(9)-H(9)	1.0000	C(3A)-H(3A)	0.9500
C(9)-C(10)	1.515(3)	C(3A)-C(4A)	1.392(4)
C(10)-C(11)	1.391(4)	C(4A)-H(4A)	0.9500

C(4A)-C(5A)	1.387(4)	C(3)-C(2)-C(1)	120.6(2)
C(5A)-H(5A)	0.9500	C(3)-C(2)-H(2)	119.7
C(5A)-C(6A)	1.401(3)	C(2)-C(3)-H(3)	120.2
C(6A)-C(7A)	1.480(3)	C(2)-C(3)-C(4)	119.7(2)
C(7A)-C(8A)	1.345(4)	C(4)-C(3)-H(3)	120.2
C(8A)-H(8A)	0.9500	C(3)-C(4)-H(4)	120.0
C(8A)-C(9A)	1.510(3)	C(3)-C(4)-C(5)	120.0(3)
C(9A)-H(9A)	1.0000	C(5)-C(4)-H(4)	120.0
C(9A)-C(10A)	1.524(3)	C(4)-C(5)-H(5)	119.7
C(10A)-C(11A)	1.388(4)	C(4)-C(5)-C(6)	120.7(3)
C(10A)-C(15A)	1.390(3)	C(6)-C(5)-H(5)	119.7
C(11A)-H(11A)	0.9500	C(1)-C(6)-C(5)	118.4(2)
C(11A)-C(12A)	1.396(4)	C(1)-C(6)-C(7)	120.6(2)
C(12A)-H(12A)	0.9500	C(5)-C(6)-C(7)	120.9(2)
C(12A)-C(13A)	1.392(4)	N(1)-C(7)-C(6)	115.5(2)
C(13A)-H(13A)	0.9500	C(8)-C(7)-N(1)	120.8(2)
C(13A)-C(14A)	1.374(5)	C(8)-C(7)-C(6)	123.7(2)
C(14A)-H(14A)	0.9500	C(7)-C(8)-H(8)	117.6
C(14A)-C(15A)	1.394(4)	C(7)-C(8)-C(9)	124.8(2)
C(15A)-H(15A)	0.9500	C(9)-C(8)-H(8)	117.6
		N(2)-C(9)-C(8)	105.94(18)
C(7)-N(1)-H(1)	123(2)	N(2)-C(9)-H(9)	107.8
C(16)-N(1)-H(1)	117(3)	N(2)-C(9)-C(10)	109.68(18)
C(16)-N(1)-C(7)	118.1(2)	C(8)-C(9)-H(9)	107.8
N(3)-N(2)-C(9)	124.36(19)	C(10)-C(9)-C(8)	117.5(2)
C(16)-N(2)-N(3)	108.4(2)	C(10)-C(9)-H(9)	107.8
C(16)-N(2)-C(9)	126.9(2)	C(11)-C(10)-C(9)	122.1(2)
N(4)-N(3)-N(2)	106.25(19)	C(11)-C(10)-C(15)	119.4(2)
N(3)-N(4)-N(5)	111.4(2)	C(15)-C(10)-C(9)	118.4(2)
C(16)-N(5)-N(4)	104.9(2)	C(10)-C(11)-H(11)	119.9
C(2)-C(1)-H(1A)	119.7	C(12)-C(11)-C(10)	120.2(2)
C(2)-C(1)-C(6)	120.7(2)	C(12)-C(11)-H(11)	119.9
C(6)-C(1)-H(1A)	119.7	C(11)-C(12)-H(12)	120.0
C(1)-C(2)-H(2)	119.7	C(11)-C(12)-C(13)	120.0(2)

C(13)-C(12)-H(12)	120.0	C(4A)-C(5A)-H(5A)	119.8
C(12)-C(13)-H(13)	120.0	C(4A)-C(5A)-C(6A)	120.3(2)
C(14)-C(13)-C(12)	120.1(2)	C(6A)-C(5A)-H(5A)	119.8
C(14)-C(13)-H(13)	120.0	C(1A)-C(6A)-C(5A)	118.8(2)
C(13)-C(14)-H(14)	120.1	C(1A)-C(6A)-C(7A)	119.7(2)
C(13)-C(14)-C(15)	119.9(2)	C(5A)-C(6A)-C(7A)	121.5(2)
C(15)-C(14)-H(14)	120.1	N(1A)-C(7A)-C(6A)	116.1(2)
C(10)-C(15)-H(15)	119.8	C(8A)-C(7A)-N(1A)	120.7(2)
C(14)-C(15)-C(10)	120.5(2)	C(8A)-C(7A)-C(6A)	123.2(2)
C(14)-C(15)-H(15)	119.8	C(7A)-C(8A)-H(8A)	117.5
N(2)-C(16)-N(1)	121.9(2)	C(7A)-C(8A)-C(9A)	125.0(2)
N(5)-C(16)-N(1)	129.1(2)	C(9A)-C(8A)-H(8A)	117.5
N(5)-C(16)-N(2)	109.0(2)	N(2A)-C(9A)-C(8A)	106.3(2)
C(7A)-N(1A)-H(1AA)	123(3)	N(2A)-C(9A)-H(9A)	108.7
C(16A)-N(1A)-H(1AA)	118(3)	N(2A)-C(9A)-C(10A)	110.8(2)
C(16A)-N(1A)-C(7A)	118.5(2)	C(8A)-C(9A)-H(9A)	108.7
N(3A)-N(2A)-C(9A)	124.9(2)	C(8A)-C(9A)-C(10A)	113.40(19)
C(16A)-N(2A)-N(3A)	108.1(2)	C(10A)-C(9A)-H(9A)	108.7
C(16A)-N(2A)-C(9A)	126.6(2)	C(11A)-C(10A)-C(9A)	120.5(2)
N(4A)-N(3A)-N(2A)	106.32(19)	C(11A)-C(10A)-C(15A)	120.0(2)
N(3A)-N(4A)-N(5A)	111.6(2)	C(15A)-C(10A)-C(9A)	119.5(2)
C(16A)-N(5A)-N(4A)	104.9(2)	C(10A)-C(11A)-H(11A)	120.0
C(2A)-C(1A)-H(1AB)	119.7	C(10A)-C(11A)-C(12A)	120.1(2)
C(2A)-C(1A)-C(6A)	120.5(2)	C(12A)-C(11A)-H(11A)	120.0
C(6A)-C(1A)-H(1AB)	119.7	C(11A)-C(12A)-H(12A)	120.2
C(1A)-C(2A)-H(2A)	119.6	C(13A)-C(12A)-C(11A)	119.7(3)
C(1A)-C(2A)-C(3A)	120.8(2)	C(13A)-C(12A)-H(12A)	120.2
C(3A)-C(2A)-H(2A)	119.6	C(12A)-C(13A)-H(13A)	120.0
C(2A)-C(3A)-H(3A)	120.5	C(14A)-C(13A)-C(12A)	120.1(2)
C(4A)-C(3A)-C(2A)	119.0(2)	C(14A)-C(13A)-H(13A)	120.0
C(4A)-C(3A)-H(3A)	120.5	C(13A)-C(14A)-H(14A)	119.7
C(3A)-C(4A)-H(4A)	119.7	C(13A)-C(14A)-C(15A)	120.6(3)
C(5A)-C(4A)-C(3A)	120.6(2)	C(15A)-C(14A)-H(14A)	119.7
C(5A)-C(4A)-H(4A)	119.7	C(10A)-C(15A)-C(14A)	119.6(2)

C(10A)-C(15A)-H(15A)	120.2
C(14A)-C(15A)-H(15A)	120.2
N(2A)-C(16A)-N(1A)	121.6(2)
N(5A)-C(16A)-N(1A)	129.3(2)
N(5A)-C(16A)-N(2A)	109.1(2)

Table A8.1.4 Anisotropic displacement parameters ($\text{\AA}^2 \times 10^3$) for 1.39. The anisotropic displacement factor exponent takes the form: $-2\pi^2 [h^2 a^{*2} U^{11} + \dots + 2 h k a^* b^* U^{12}]$

	U ¹¹	U ²²	U ³³	U ²³	U ¹³	U ¹²
N(1)	49(1)	44(1)	39(1)	3(1)	9(1)	2(1)
N(2)	47(1)	42(1)	42(1)	2(1)	11(1)	1(1)
N(3)	52(1)	45(1)	45(1)	2(1)	14(1)	2(1)
N(4)	54(1)	45(1)	46(1)	4(1)	17(1)	5(1)
N(5)	49(1)	45(1)	44(1)	4(1)	12(1)	5(1)
C(1)	50(1)	46(1)	44(1)	1(1)	6(1)	1(1)
C(2)	52(1)	47(1)	51(1)	-3(1)	6(1)	6(1)
C(3)	51(1)	58(2)	46(1)	-7(1)	12(1)	4(1)
C(4)	60(1)	56(2)	45(1)	3(1)	15(1)	1(1)
C(5)	54(1)	47(1)	46(1)	1(1)	10(1)	3(1)
C(6)	42(1)	45(1)	42(1)	-2(1)	5(1)	-1(1)
C(7)	41(1)	42(1)	45(1)	0(1)	8(1)	-1(1)
C(8)	43(1)	42(1)	45(1)	1(1)	9(1)	1(1)
C(9)	42(1)	44(1)	41(1)	0(1)	6(1)	0(1)
C(10)	42(1)	41(1)	42(1)	2(1)	8(1)	4(1)
C(11)	45(1)	45(1)	41(1)	0(1)	5(1)	3(1)
C(12)	46(1)	46(1)	50(1)	2(1)	9(1)	-2(1)
C(13)	50(1)	49(1)	45(1)	7(1)	13(1)	2(1)
C(14)	52(1)	48(1)	39(1)	1(1)	6(1)	5(1)
C(15)	46(1)	41(1)	44(1)	-1(1)	7(1)	2(1)
C(16)	44(1)	40(1)	42(1)	2(1)	8(1)	-3(1)
N(1A)	53(1)	45(1)	41(1)	3(1)	13(1)	4(1)
N(2A)	45(1)	47(1)	41(1)	1(1)	8(1)	3(1)
N(3A)	52(1)	50(1)	44(1)	0(1)	11(1)	5(1)
N(4A)	51(1)	50(1)	43(1)	2(1)	10(1)	6(1)
N(5A)	47(1)	46(1)	41(1)	2(1)	9(1)	3(1)
C(1A)	48(1)	45(1)	44(1)	4(1)	9(1)	0(1)

C(2A)	48(1)	46(1)	49(1)	0(1)	7(1)	6(1)
C(3A)	41(1)	54(1)	45(1)	-2(1)	9(1)	4(1)
C(4A)	42(1)	52(1)	45(1)	1(1)	7(1)	-2(1)
C(5A)	44(1)	43(1)	45(1)	0(1)	6(1)	-1(1)
C(6A)	42(1)	48(1)	41(1)	1(1)	4(1)	1(1)
C(7A)	44(1)	43(1)	43(1)	-2(1)	6(1)	-1(1)
C(8A)	49(1)	44(1)	42(1)	0(1)	9(1)	3(1)
C(9A)	47(1)	44(1)	43(1)	1(1)	9(1)	1(1)
C(10A)	49(1)	43(1)	43(1)	1(1)	10(1)	6(1)
C(11A)	54(1)	47(1)	48(1)	3(1)	11(1)	1(1)
C(12A)	53(1)	50(1)	58(1)	-2(1)	2(1)	1(1)
C(13A)	66(2)	56(2)	43(1)	0(1)	3(1)	14(1)
C(14A)	65(2)	59(2)	44(1)	9(1)	13(1)	7(1)
C(15A)	51(1)	53(1)	48(1)	3(1)	11(1)	2(1)
C(16A)	42(1)	44(1)	41(1)	0(1)	6(1)	-1(1)

Table A8.1.5 Hydrogen coordinates ($\times 10^4$) and isotropic displacement parameters ($\text{\AA}^2 \times 10^3$) for 1.39

	x	y	z	U(eq)
H(1)	1280(40)	6900(40)	2500(20)	54(9)
H(1A)	-506	11491	2085	56
H(2)	-1652	12585	3052	60
H(3)	-2212	11131	4074	61
H(4)	-1598	8557	4133	64
H(5)	-469	7436	3157	59
H(8)	-540	10037	1054	52
H(9)	-515	7721	211	51
H(11)	2646	10408	590	53

H(12)	3754	11619	-367	57
H(13)	2808	11151	-1656	57
H(14)	813	9415	-1988	56
H(15)	-258	8165	-1032	52
H(1AA)	2870(40)	3640(50)	2320(20)	54(9)
H(1AB)	4120	-1095	2446	55
H(2A)	5370	-1999	1474	58
H(3A)	6431	-322	669	56
H(4A)	6229	2292	858	56
H(5A)	4956	3217	1826	53
H(8A)	4061	30	3576	54
H(9A)	1593	693	4054	53
H(11A)	5249	2526	4708	59
H(12A)	6589	2379	5961	65
H(13A)	5492	1086	6902	67
H(14A)	3104	-69	6592	67
H(15A)	1771	44	5340	61

Table A8.1.6 Hydrogen bonds for 1.39 [Å and °]

D-H...A	d(D-H)	d(H...A)	d(D...A)	<(DHA)
N(1)-H(1)...N(5A)	0.84(4)	2.16(4)	2.952(3)	157(3)
N(1A)-H(1AA)...N(5)	0.84(4)	2.10(4)	2.912(3)	163(4)

A8.2 X-ray Crystallography Reports Relevant to Chapter Four:

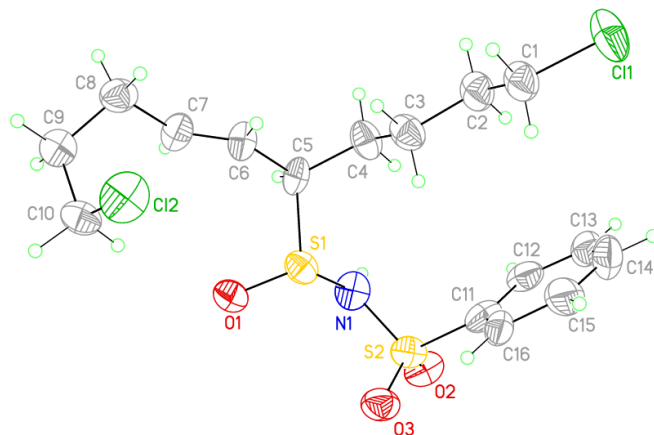


Figure A8.2 View of 4.68 showing the atom labeling scheme. Displacement ellipsoids are scaled to the 50% probability level.

Experimental Summary

X-ray Experimental for $C_{16}H_{23}NO_3S_2Cl_2$: Crystals grew as long, very thin colorless needles by slow evaporation from CH_2Cl_2 . The data crystal had approximate dimensions; 0.34 x 0.13 x 0.05 mm. The data were collected on an Agilent Technologies SuperNova Dual Source diffractometer using a μ -focus Cu $K\alpha$ radiation source ($\lambda = 1.5418\text{\AA}$) with collimating mirror monochromators. A total of 1896 frames of data were collected using ω -scans with a scan range of 1° and a counting time of 7.5 seconds per frame for frames collected with a detector offset of $\pm 41.9^\circ$ and 23.5 seconds per frame with frames collected with a detector offset of $\pm 110.4^\circ$. The data were collected at 100

K using an Oxford Cryostream low temperature device. Details of crystal data, data collection and structure refinement are listed in Table A8.2.1. Data collection, unit cell refinement and data reduction were performed using Agilent Technologies CrysAlisPro V 1.171.37.31.¹ The structure was solved by direct methods using SHELXT² and refined by full-matrix least-squares on F^2 with anisotropic displacement parameters for the non-H atoms using SHELXL-2014/7.³ Structure analysis was aided by use of the programs PLATON98⁴ and WinGX.⁵ The hydrogen atoms were calculated in ideal positions with isotropic displacement parameters set to 1.2xUeq of the attached atom (1.5xUeq for methyl hydrogen atoms). The hydrogen atom bound to N1 was observed in a ΔF map and refined with an isotropic displacement parameter. The absolute configuration was determined using the method of Flack⁶ and confirmed using the Hooft y-parameter method.⁷

The function, $\Sigma w(|F_o|^2 - |F_c|^2)^2$, was minimized, where $w = 1/[(\sigma(F_o))^2 + (0.1012 \cdot P)^2]$ and $P = (|F_o|^2 + 2|F_c|^2)/3$. $R_w(F^2)$ refined to 0.250, with $R(F)$ equal to 0.0917 and a goodness of fit, S , = 1.14. Definitions used for calculating $R(F)$, $R_w(F^2)$ and the goodness of fit, S , are given below.⁸ The data were checked for secondary extinction effects but no correction was necessary. Neutral atom scattering factors and values used to calculate the linear absorption coefficient are from the International Tables for X-ray Crystallography (1992).⁹ All figures were generated using SHELXTL/PC.¹⁰ Tables of positional and thermal parameters, bond lengths and angles, torsion angles and figures are found elsewhere.

Table A8.2.1. Crystal data and structure refinement for 4.68

Empirical formula	C16 H23 Cl2 N O3 S2
Formula weight	412.37
Temperature	100(2) K
Wavelength	1.54184 Å
Crystal system	monoclinic
Space group	P 21

Unit cell dimensions	a = 12.121(2) Å	$\alpha = 90^\circ$.
	b = 6.6569(10) Å	$\beta = 111.94(2)^\circ$.
	c = 13.185(3) Å	$\gamma = 90^\circ$.
Volume	986.8(3) Å ³	
Z	2	
Density (calculated)	1.388 Mg/m ³	
Absorption coefficient	5.059 mm ⁻¹	
F(000)	432	
Crystal size	0.310 x 0.030 x 0.019 mm ³	
Theta range for data collection	6.828 to 57.874°.	
Index ranges	-13 ≤ h ≤ 12, -7 ≤ k ≤ 7, -13 ≤ l ≤ 14	
Reflections collected	8149	
Independent reflections	2712 [R(int) = 0.1908]	
Completeness to theta = 57.874°	99.7 %	
Absorption correction	Semi-empirical from equivalents	
Max. and min. transmission	1.00 and 0.593	
Refinement method	Full-matrix least-squares on F ²	
Data / restraints / parameters	2712 / 1 / 222	
Goodness-of-fit on F ²	1.115	
Final R indices [I > 2sigma(I)]	R1 = 0.0917, wR2 = 0.2216	
R indices (all data)	R1 = 0.1148, wR2 = 0.2498	
Absolute structure parameter	-0.07(8)	
Extinction coefficient	n/a	
Largest diff. peak and hole	0.636 and -0.610 e.Å ⁻³	

Table A8.2.2 Atomic coordinates ($\times 10^4$) and equivalent isotropic displacement parameters ($\text{\AA}^2 \times 10^3$) for 4.68. U(eq) is defined as one third of the trace of the orthogonalized U_{ij} tensor.

	x	y	z	U(eq)
C1	6328(15)	1820(30)	977(12)	50(4)
C2	5931(16)	1520(30)	1899(12)	51(4)
C3	5325(16)	3410(20)	2089(12)	46(4)
C4	4879(15)	3140(30)	3024(13)	47(4)
C5	4207(12)	4950(20)	3232(11)	41(4)
C6	3115(13)	5530(20)	2280(11)	41(4)
C7	2103(14)	6010(20)	2345(13)	45(4)
C8	1026(14)	6630(20)	1366(12)	47(4)
C9	709(15)	8790(20)	1436(12)	43(4)
C10	1677(15)	10310(20)	1528(12)	46(4)
C11	8179(13)	5760(30)	4266(11)	44(4)
C12	8525(14)	3770(20)	4526(13)	47(4)
C13	9047(14)	2760(30)	3901(15)	54(4)
C14	9171(16)	3680(30)	3015(15)	60(5)
C15	8801(16)	5590(30)	2752(14)	56(5)
C16	8299(13)	6680(20)	3394(12)	42(4)
N1	6156(12)	6330(20)	4697(9)	43(3)
O1	4382(11)	8693(16)	3952(9)	51(3)
O2	8105(10)	6508(17)	6179(8)	51(3)
O3	7513(11)	9173(17)	4805(9)	52(3)
S1	5116(3)	7244(6)	3606(2)	40(1)
S2	7544(4)	7089(6)	5080(3)	43(1)
Cl1	7126(5)	-359(8)	786(3)	70(2)
Cl2	2152(4)	10206(7)	390(3)	63(1)

Table A8.2.3 Bond lengths [Å] and angles [°] for 4.68.

C1-C2	1.48(2)	C9-H9A	0.99
C1-Cl1	1.811(15)	C9-H9B	0.99
C1-H1A	0.99	C10-Cl2	1.799(14)
C1-H1B	0.99	C10-H10A	0.99
C2-C3	1.52(2)	C10-H10B	0.99
C2-H2A	0.99	C11-C16	1.36(2)
C2-H2B	0.99	C11-C12	1.39(2)
C3-C4	1.53(2)	C11-S2	1.773(15)
C3-H3A	0.99	C12-C13	1.39(2)
C3-H3B	0.99	C12-H12	0.95
C4-C5	1.53(2)	C13-C14	1.38(2)
C4-H4A	0.99	C13-H13	0.95
C4-H4B	0.99	C14-C15	1.35(3)
C5-C6	1.494(19)	C14-H14	0.95
C5-S1	1.840(16)	C15-C16	1.41(2)
C5-H5	1.0000	C15-H15	0.95
C6-C7	1.30(2)	C16-H16	0.95
C6-H6	0.95	N1-S1	1.635(13)
C7-C8	1.51(2)	N1-S2	1.645(14)
C7-H7	0.95	N1-H1N	0.86(14)
C8-C9	1.50(2)	O1-S1	1.495(11)
C8-H8A	0.99	O2-S2	1.405(11)
C8-H8B	0.99	O3-S2	1.431(12)
C9-C10	1.52(2)		
C2-C1-Cl1	111.2(12)	C1-C2-H2A	109.6
C2-C1-H1A	109.4	C3-C2-H2A	109.6
Cl1-C1-H1A	109.4	C1-C2-H2B	109.6
C2-C1-H1B	109.4	C3-C2-H2B	109.6
Cl1-C1-H1B	109.4	H2A-C2-H2B	108.1
H1A-C1-H1B	108.0	C2-C3-C4	112.0(13)
C1-C2-C3	110.4(13)	C2-C3-H3A	109.2

C4-C3-H3A	109.2	C9-C10-Cl2	112.6(10)
C2-C3-H3B	109.2	C9-C10-H10A	109.1
C4-C3-H3B	109.2	Cl2-C10-H10A	109.1
H3A-C3-H3B	107.9	C9-C10-H10B	109.1
C3-C4-C5	115.1(13)	Cl2-C10-H10B	109.1
C3-C4-H4A	108.5	H10A-C10-H10B	107.8
C5-C4-H4A	108.5	C16-C11-C12	121.2(15)
C3-C4-H4B	108.5	C16-C11-S2	119.8(13)
C5-C4-H4B	108.5	C12-C11-S2	119.0(11)
H4A-C4-H4B	107.5	C13-C12-C11	118.7(15)
C6-C5-C4	114.5(13)	C13-C12-H12	120.7
C6-C5-S1	105.4(10)	C11-C12-H12	120.7
C4-C5-S1	113.1(10)	C14-C13-C12	120.4(16)
C6-C5-H5	107.8	C14-C13-H13	119.8
C4-C5-H5	107.8	C12-C13-H13	119.8
S1-C5-H5	107.8	C15-C14-C13	120.5(16)
C7-C6-C5	124.7(13)	C15-C14-H14	119.8
C7-C6-H6	117.7	C13-C14-H14	119.8
C5-C6-H6	117.7	C14-C15-C16	120.2(16)
C6-C7-C8	123.1(14)	C14-C15-H15	119.9
C6-C7-H7	118.5	C16-C15-H15	119.9
C8-C7-H7	118.5	C11-C16-C15	119.0(16)
C9-C8-C7	111.6(14)	C11-C16-H16	120.5
C9-C8-H8A	109.3	C15-C16-H16	120.5
C7-C8-H8A	109.3	S1-N1-S2	121.4(8)
C9-C8-H8B	109.3	S1-N1-H1N	133(8)
C7-C8-H8B	109.3	S2-N1-H1N	104(8)
H8A-C8-H8B	108.0	O1-S1-N1	108.8(6)
C8-C9-C10	115.9(13)	O1-S1-C5	104.6(7)
C8-C9-H9A	108.3	N1-S1-C5	96.6(7)
C10-C9-H9A	108.3	O2-S2-O3	119.1(7)
C8-C9-H9B	108.3	O2-S2-N1	106.1(6)
C10-C9-H9B	108.3	O3-S2-N1	107.0(7)
H9A-C9-H9B	107.4	O2-S2-C11	109.5(7)

O3-S2-C11 107.8(7) N1-S2-C11 106.7(7)

Table A8.2.4 Anisotropic displacement parameters ($\text{\AA}^2 \times 10^3$) for **1**. The anisotropic displacement factor exponent takes the form: $-2\pi^2 [h^2 a^{*2} U^{11} + \dots + 2 h k a^* b^* U^{12}]$

	U ¹¹	U ²²	U ³³	U ²³	U ¹³	U ¹²
C1	47(10)	48(11)	46(7)	1(8)	8(7)	17(8)
C2	48(10)	51(11)	44(8)	3(7)	7(7)	17(8)
C3	54(11)	38(10)	43(8)	2(7)	15(8)	8(8)
C4	58(11)	37(8)	54(9)	9(7)	30(9)	12(8)
C5	29(8)	50(10)	43(7)	12(7)	11(7)	10(7)
C6	35(9)	52(10)	39(7)	8(7)	15(7)	10(8)
C7	36(9)	43(9)	56(9)	15(8)	16(8)	2(7)
C8	47(10)	52(11)	45(8)	-9(7)	21(8)	-7(8)
C9	48(10)	49(9)	36(7)	2(7)	20(7)	0(8)
C10	58(11)	31(8)	50(8)	0(7)	21(8)	-4(8)
C11	37(9)	59(11)	36(7)	-1(7)	14(7)	-15(8)
C12	37(9)	39(9)	55(9)	6(7)	8(8)	-8(7)
C13	36(10)	38(10)	85(12)	2(8)	19(9)	5(7)
C14	41(11)	68(14)	72(12)	-5(10)	23(10)	15(9)
C15	62(12)	62(12)	56(9)	-16(9)	34(9)	-12(10)
C16	30(8)	42(9)	54(8)	1(7)	15(7)	4(7)
N1	51(8)	55(8)	27(5)	14(6)	18(6)	4(6)
O1	51(7)	46(7)	53(6)	-14(5)	17(6)	0(5)
O2	55(7)	63(8)	36(5)	8(5)	18(5)	-12(6)
O3	59(8)	45(7)	60(6)	-8(5)	32(6)	-13(6)
S1	49(2)	38(2)	36(2)	0(2)	21(2)	2(2)
S2	53(2)	43(2)	38(2)	-2(2)	23(2)	-8(2)

Cl1	86(3)	79(3)	53(2)	-1(2)	33(2)	34(3)
Cl2	67(3)	77(3)	53(2)	12(2)	33(2)	-4(2)

Table A8.2.5 Hydrogen coordinates ($\times 10^4$) and isotropic displacement parameters ($\text{\AA}^2 \times 10^3$) for 4.68.

	x	y	z	U(eq)
H1A	6852	3012	1121	59
H1B	5628	2070	299	59
H2A	6624	1193	2569	61
H2B	5368	377	1736	61
H3A	4645	3750	1411	55
H3B	5895	4543	2262	55
H4A	5571	2857	3704	57
H4B	4349	1958	2864	57
H5	3960	4600	3854	49
H6	3163	5542	1577	50
H7	2039	5975	3041	54
H8A	1190	6421	692	56
H8B	343	5768	1321	56
H9A	481	8943	2078	52
H9B	1	9111	777	52
H10A	2369	10063	2213	56
H10B	1375	11678	1573	56
H12	8406	3123	5118	56
H13	9321	1420	4086	65
H14	9518	2964	2585	72
H15	8880	6212	2133	67
H16	8048	8029	3218	50

H1N	6190(110)	5300(200)	5110(100)	20(30)
-----	-----------	-----------	-----------	--------

Table A8.2.6 Torsion angles [°] for 4.68.

C11-C1-C2-C3	176.7(12)	S2-C11-C16-C15	-179.7(12)
C1-C2-C3-C4	178.9(14)	C14-C15-C16-C11	-1(3)
C2-C3-C4-C5	-177.2(15)	S2-N1-S1-O1	-104.2(9)
C3-C4-C5-C6	59.8(19)	S2-N1-S1-C5	147.8(9)
C3-C4-C5-S1	-61.0(17)	C6-C5-S1-O1	63.4(10)
C4-C5-C6-C7	137.0(17)	C4-C5-S1-O1	-170.8(10)
S1-C5-C6-C7	-98.0(17)	C6-C5-S1-N1	174.8(9)
C5-C6-C7-C8	178.7(15)	C4-C5-S1-N1	-59.3(11)
C6-C7-C8-C9	-113.5(18)	S1-N1-S2-O2	162.5(8)
C7-C8-C9-C10	58.1(16)	S1-N1-S2-O3	34.4(10)
C8-C9-C10-C12	59.1(17)	S1-N1-S2-C11	-80.8(10)
C16-C11-C12-C13	3(2)	C16-C11-S2-O2	-144.7(12)
S2-C11-C12-C13	-178.5(13)	C12-C11-S2-O2	36.5(14)
C11-C12-C13-C14	-3(3)	C16-C11-S2-O3	-13.8(15)
C12-C13-C14-C15	1(3)	C12-C11-S2-O3	167.5(12)
C13-C14-C15-C16	1(3)	C16-C11-S2-N1	100.8(13)
C12-C11-C16-C15	-1(2)	C12-C11-S2-N1	-78.0(14)

Table A8.2.7 Hydrogen bonds for 4.68 [\AA and $^\circ$].

D-H...A	d(D-H)	d(H...A)	d(D...A)	$\angle(\text{DHA})$
N1-H1N...O1#1	0.86(14)	1.95(13)	2.749(16)	153(11)

Symmetry transformations used to generate equivalent atoms:

#1 $-x+1, y-1/2, -z+1$